Annex 7: Working Documents presented to WGWIDE 2020

WD01 PFA self-sampling report for WGWIDE, 2015-2020. M.A. Pastoors and F.J.Quirijns. 53pp.

WD02 Western Horse Mackerel Technical Focus Group On Harvest Control Rule Evaluations 2020. M.A. Pastoors, A. Campbell, V. Trijoulet, D. Skagen, M. Gras, G.I. Lambert, C.R. Sparrevohn and S. Mackinson. 43pp.

WD03 Cruise Report from the International Ecosystem Summer Survey in the Nordic Seas (IESSNS), L.Nøttestad, Valantine Anthonypillai, Are Salthaug, Åge Høines, Anna Heiða Ólafsdóttir, James Kennedy, Eydna í Homrum, Leon Smith, Teunis Jansen, Søren Post and Kai Wieland. 55pp.

WD04 Update of Striped Red Mullet Abundance Indices from Professional Fishing Data (2016-2018). Nathalie Caill-Milly, Muriel Lissardy and Noëlle Bru. 9pp.

WD05 Overview of Spatial Distribution of Catches of Mackerel, Horse Mackerel, Blue Whiting and Herring. M.A.Pastoors 14pp.

WD06 Distribution and Abundance of Norwegian Spring-Spawning Herring during the Spawning Season in 2020. Are Salthaug, Erling Kåre Stenevik, Sindre Vatnehol, Valantine Anthonypillai, Egil Ona and Aril Slotte. 40pp

WD07 Inventory of Industry-Acoustic Data for Potential Application on Blue Whiting Biomass Estimates. Benoit Berges, Serdar Sakanin, Sytse Ybema, Gert-Jan Kooij and Martin Pastoors. 7pp.

WD08 Progress Report on Industry Gonad Research in the Context of the "Year of the Mackerel and Horse Mackerel 2019-2020". Cindy van Damme, Ewout Blom and Martin Pastoors, 24pp.

WD09 NEA Mackerel Alternative Assessment. Höskuldur Björnsson. 9pp.

WD10 International Ecosystem Survey in Nordic Sea (IESNS). Are Salthaug, Erling Kåre Stnevik, Sindre Vatnehol, Åge Høines, Valantine Anthonypillai, Kjell Arne Mork, Cecile Thorsen Broms, Øystein Skagseth, Kai Wieland, Karl-Johan Stæhr, Susan Mærsk Lusseau, Benoit Berges, Sigurvin Bjarnason, Anna Heiða Ólafsdóttir, Sólvá Káradóttir Eliasen, Jan Arge Jacobsen and Leon Smith, 51pp.

WD11 Population Structure of the Atlantic Horse Mackerel (Trachurus trachurus) Revealed by Whole-Genome Sequencing. Angela P. Fuentes-Pardo, Mats Pettersson, C. Grace Sprehn, Leif Andersson and Edward Farrell. 38pp.

REPORT

PELAGIC FREEZER-TRAWLER ASSOCIATION

PFA self-sampling report for WGWIDE, 2015-2020

M.A. Pastoors and F.J. Quirijns

25-8-2020

(Cover image: mackerel self-sampled for gonad analysis, 2019)

Pelagic Freezer-trawler Association (PFA)

Louis Braillelaan 80
2719 EK Zoetermeer
The Netherlands
www.pelagicfish.eu
info@pelagicfish.eu

Please cite as:

Pastoors, M.A. & F.J. Quirijns 2020 PFA self-sampling report for WGWIDE, 2015-2020. PFA report 2020/10

Working document 01, WGWIDE 2020, 26 August-1 September 2020

PFA self-sampling report for WGWIDE, 2015-2020

Martin Pastoors and Floor Quirijns, 25/08/2020

(PFA report 2020_10)

Executive summary

The Pelagic Freezer-trawler Association (PFA) is an association that has nine member companies that together operate 17 (in 2019) freezer trawlers in six European countries (www.pelagicfish.eu). In 2015, the PFA has initiated a self-sampling programme that ex-pands the ongoing monitoring programmes on board of pelagic freezer-trawlers aimed at assessing the quality of fish. The expansion in the self-sampling programme consists of recording of haul information, recording the species compositions by haul and regularly taking length measurements from the catch. The self-sampling is carried out by the vessel quality managers on board of the vessels, who have a long experience in assessing the quality of fish, and by the skippers/officers with respect to the haul information. The scien-tific coordination of the self-sampling programme is carried out by Martin Pastoors (PFA chief science officer) with support of Floor Quirijns (contractor).

The self-sampling programme has been incrementally implemented in the fishery. The increase in the number of vessel, hauls and catch over the years 2015-2017 is due to the build-up of the self-sampling programme. From 2018 onwards, the self-sampling programme has been implemented on all vessels in the fleet.

This report for WGWIDE 2020 presents an overview of the results of the Pelagic Freezer-Trawler Association (PFA) self-sampling program for the fisheries for widely-distributed pelagic stocks: Northeast Atlantic mackerel, Blue whiting, Horse mackerel and Atlanto-scandian herring (herring caught north of 62 degrees). The selection of hauls to be included in the analyses was based on first summing all catches by vessel, trip, species and week. For each vessel-trip-species-week combination, the proportion of the species in the catch were calculated. The following filter criteria have applied to the weekly data:

- for horse mackerel: latitude > 45, proportion in the catch > 10%, catch > 10 tonnes

- for mackerel : latitude > 45, proportion in the catch > 10%, catch > 10 tonnes
- for blue whiting : latitude > 50, proportion in the catch > 10%, catch > 10 tonnes
- for herring : division = 27.2.a, proportion in the catch > 10%, catch > 10 tonnes

The **Mackerel fishery** takes place from October through to March of the subsequent year. Minor bycatches of mackerel may also occur during other fisheries. Overall, the self-sampling activities for the mackerel fisheries during the years 2015 – 2020 (up to August) covered 323 fishing trips with 4,725 hauls, a total catch of 286,957 tonnes and 91,000 individual length measurements. The main fishing areas are ICES division 27.4.a (between 27 and 54% of the catch) and division 27.6.a (between 25 and 44% of the catch). Compared to the previous years, mackerel in the catch have been relatively large in 2020 with median length of 36.4 cm compared to 32.4-35.4 in the preceding years. Also, the median weight has been somewhat higher with median weight of 417 gram compared to 379-400 gram the preceding years. Average annual fat content ranges from 17 to 21% with individual measurements reaching up to 30%

The **horse mackerel fishery** takes place from October through to March of the subsequent year. Overall, the self-sampling activities for the horse mackerel fisheries during the years 2015 – 2020 (up to August) covered 457 fishing trips with 3,454 hauls, a total catch of 140,633 tonnes and 125,000 individual length measurements. The main fishing areas are ICES division 27.6.a (between 21% and 40% of the catch), division 27.7.b (7%-22%) and division 27.7.d (19%-34%, note that this is considered as the North Sea horse mackerel stock). Horse mackerel have a wide range in the length distributions in the catch. Median lengths have fluctuated between 22.8 and 30.0 cm. In 2019 and 2020 there are some indications of a stronger year class being available to the fishery, with a more narrow length distribution. For example, in 27.6.a the mode was 26.6 cm in 2019 and 27.5 cm in 2020. Average annual fat content ranges from 5 to 7.5% with individual measurements reaching up to 15%.

The **blue whiting** fishery takes place from February through to May although some minor fisheries for blue whiting may remain over the other months. Overall, the self-sampling activities for the blue whiting fisheries during the years 2015 – 2020 (up to August) covered 365 fishing trips with 5,836 hauls, a total catch of 561,888 tonnes and 128,000 individual length measurements. The main fishing areas are ICES division 27.6.a (between 41% and 65% of the catch), division 27.7.c (6%-36%) and division 27.7.k (2%-32%). Blue whiting have a wide range in the length distributions in the catch. Median lengths have fluctuated between 23 cm (2016) and 30 cm (2015). During the period 2016 - 2020, the median length is consistently increasing (from 23 to 28 cm), indicating that the fishery is probably concentrating on a strong year class going without new year classes coming in. Fat content for blue whiting is generally low (on average less than 1%).

The fishery for **Atlanto-Scandian herring** (ASH) is a relatively smaller fishery for PFA and takes place mostly in October. Overall, the self-sampling activities for the ASH fisheries during the years 2015 – 2020 (up to August) covered 27 fishing trips with 406 hauls, a total catch of 30,234 tonnes and 8,918 individual length measurements. Only the herring fishery in ICES division 27.2.a is considered for ASH. Note that there are herring catches in other divisions within the selected trips. These are trips where North Sea herring has been fished with some bycatches of mackerel for example. Atlanto-Scandian herring have a narrow range in the length distributions in the catch. Median lengths have fluctuated between 32 and 36 cm. Average annual fat content for ASH has been between 17 and 20% with individual measurements going up to 25%).

1 Introduction

The Pelagic Freezer-trawler Association (PFA) is an association that has nine member companies that together operate 19 freezer trawlers in five European countries (www.pelagicfish.eu). In 2015, the PFA has initiated a self-sampling programme that expands the ongoing monitoring programmes on board of pelagic freezer-trawlers by the specialized crew of the vessels. The primary objective of that monitoring programme is to assess the quality of fish. The expansion in the self-sampling programme consists of recording of haul information, recording the species compositions per haul and regularly taking random length-samples from the catch. The self-sampling is carried out by the vessel quality managers on board of the vessels, who have a long experience in assessing the quality of fish, and by the skippers/officers with respect to the haul information. The scientific coordination of the self-sampling programme is carried out by Martin Pastoors (PFA chief science officer) with support of Floor Quirijns (contractor).

2 Material and methods

The PFA self-sampling programme has been implemented incrementally on many vessels that belong to the members of the PFA. The self-sampling programme is designed in such a way that it follows as closely as possible the working practices on board of the different vessels and that it delivers relevant information for documenting the performance of the fishery and to assist stock assessments of the stocks involved. The following main elements can be distinguished in the self-sampling protocol:

- haul information (date, time, position, weather conditions, environmental conditions, gear attributed, estimated catch, optionally: species composition)
- batch information (total catch per batch=production unit, including variables like species, average size, average weight, fat content, gonads y/n and stomach fill)
- linking batch and haul information (essentially a key of how much of a batch is caught in which of the hauls)
- length information (length frequency measurements, either by batch or by haul)

The self-sampling information is collected using standardized Excel worksheets. Each participating vessel will send in the information collected during a trip by the end of the trip. The data will be checked and added to the database by Floor Quirijns and/or Martin Pastoors, who will also generate standardized trip reports (using RMarkdown) which will be sent back to the vessel within one or two days. The compiled data for all vessels is being used for specific purposes, e.g. reporting to expert groups, addressing specific fishery or biological questions and

supporting detailed biological studies. The PFA publishes an annual report on the self-sampling programme.

A major feature of the PFA self-sampling programme is that it is tuned to the capacity of the vessel-crew to collect certain kinds of data. Depending on the number of crew and the space available on the vessel, certain types of measurements can or cannot be carried out. That is why the programme is essentially tuned to each vessel separately. And that is also the reason that the totals presented in this report can be somewhat different dependent on which variable is used. For example the estimate of total catch is different from the sum of the catch per species because not all vessels have supplied data on the species composition of the catch.

Because the self-sampling programme has been under development over the years, different numbers of vessels have been participating in the programme over different years. Results should not be interpreted as a census of the PFA fleet, but rather as an indicator of relative distributions and samples of catch and catch compositions.

In order to supply relevant information to WGWIDE 2019, the PFA self-sampling data has been filtered using the following approach. First, all catches per vessel, trip and species have been summed by week. For each vessel-trip-species-week combination, the proportion of the species in the catch were calculated. Then the following filter criteria have applied to the weekly data:

- for horse mackerel: latitude > 45, proportion in the catch > 10%, catch > 10 tonnes
- for mackerel : latitude > 45, proportion in the catch > 10%, catch > 10 tonnes
- for blue whiting : latitude > 50, proportion in the catch > 10%, catch > 10 tonnes
- for herring : division = 27.2.a, proportion in the catch > 10%, catch > 10 tonnes

Data have been processed up to 20 August 2020.

3 Results

3.1 General

An overview of all the selected self-sampling hauls between 2015 and (August) 2020 is shown in Table 3.1.1. The increase in the number of vessel, hauls and catch over the years 2015-2017 is due to the build-up of the self-sampling programme. From 2018 onwards, the self-sampling programme has been implemented on all vessels in the fleet.

The percentage non-target catch (defined as the proportion of non-pelagic and unwanted pelagic catch relative to the total catch) has been low (between 0.2 and 1.1%).

year	nvessels	ntrips	ndays	nhauls	catch	catch/day	nontarget	nlength
2015	6	26	390	869	65,899	168	1.10%	69,680
2016	9	47	647	1,456	126,997	196	0.50%	78,708
2017	12	64	887	1,886	184,460	207	0.20%	95,190
2018	16	88	1,330	2,901	272,416	204	0.20%	176,455
2019	16	101	1,423	3,109	252,973	177	0.30%	150,806
2020*	13	65	908	2,092	215,627	237	0.40%	178,114
(all)		391	5,585	12,313	1,118,372			748,953

*Table 3.1.1: PFA selfsampling summary of hauls in widely distributed pelagic fisheries with the number of vessels, trips, days, hauls, catch (tonnes), catch per day (tonnes), %non-target catch and number of fish measured. * denotes incomplete year*

Number of self-sampled hauls in widely distributed pelagic fisheries by year and division

The majority of hauls for widely distributed species have been recorded in division 27.6.a (39%), 27.4.a (12%), 27.7.c (10%) and 27.2.a (7%).

division	2015	2016	2017	2018	2019	2020*	all	perc
27.6.a	242	411	668	1,268	1,281	962	4,832	39.2431%
27.4.a	120	194	191	376	439	191	1,511	12.2716%
27.7.c	32	87	256	243	252	329	1,199	9.7377%
27.2.a	51	148	264	249	174	18	904	7.3418%
27.7.d	99	167	157	190	206	7	826	6.7084%
27.7.b	50	101	140	88	175	205	759	6.1642%
27.7.j	84	62	20	60	138	203	567	4.6049%
27.7.k	56	77	3	59	17	91	303	2.4608%
27.7.e	47	90	45	32	79	4	297	2.4121%
27.5.b	28	57	66	82	38	7	278	2.2578%
27.7.h	5	25	30	96	24	4	184	1.4944%
27.8.a	15	1	1	41	97	9	164	1.3319%
27.4.b	8	15	19	24	53	0	119	0.9665%
27.4.c	5	12	22	16	25	11	91	0.7391%
27.7.g	21	9	0	9	39	5	83	0.6741%
27.6.b	0	0	2	50	10	7	69	0.5604%
27.7.f	3	0	0	4	31	0	38	0.3086%
27.8.b	3	0	0	6	4	24	37	0.3005%
27.8.d	0	0	2	2	13	15	32	0.2599%
27.7.a	0	0	0	6	12	0	18	0.1462%
27.3.a	0	0	0	0	1	0	1	0.0081%
27.8.c	0	0	0	0	1	0	1	0.0081%
(all)	869	1,456	1,886	2,901	3,109	2,092	12,313	100.0000%

*Table 3.1.2: PFA selfsampling summary: number of hauls per year and division in widely distributed pelagic fisheries. * denotes incomplete year*

Number of self-sampled hauls in widely distributed pelagic fisheries by year and month

The overview of number of hauls for widely distributed species by month indicates that the main periods for the fisheries are January until May and October until November. The other months are usually spent on North Sea herring fisheries or repair works.

month	2015	2016	2017	2018	2019	2020*	all	perc
Jan	109	174	315	309	470	374	1,751	14.221%
Feb	127	143	208	333	413	290	1,514	12.296%
Mar	23	161	232	391	413	455	1,675	13.604%
Apr	74	125	201	494	289	580	1,763	14.318%
May	67	105	145	372	251	250	1,190	9.665%
Jun	14	15	0	77	23	103	232	1.884%
Jul	53	26	15	10	75	26	205	1.665%
Aug	0	28	68	39	42	14	191	1.551%
Sep	34	77	153	170	207	0	641	5.206%
Oct	157	240	247	301	410	0	1,355	11.005%
Nov	149	237	271	319	412	0	1,388	11.273%
Dec	62	125	31	86	104	0	408	3.314%
(all)	869	1,456	1,886	2,901	3,109	2,092	12,313	100.000%

*Table 3.1.3: PFA selfsampling summary: number of hauls per year and division in widely distributed pelagic fisheries. * denotes incomplete year*

Catch compositions in widely distributed pelagic fisheries by year and species

Within the widely-distributed pelagic fisheries, as defined in this report, around half of the catch volume has been generated with blue whiting, followed by mackerel (26%), horse mackerel (13%) and herring (8%). Note that the herring catches in 27.2.a are normally only taken in the second part of the year and are therefore not included yet for 2020.

species	english_name	scientific_name	2015	2016	2017	2018	2019	2020*	all	perc
whb	blue whiting	Micromesistius poutassou	15,546	49,378	78,802	162,542	115,672	139,949	561,890	50.2416%
mac	mackerel	Scomber scombrus	26,481	34,298	63,654	57,958	55,055	49,582	287,028	25.6647%
hom	horse mackerel	Trachurus trachurus	10,586	22,966	21,266	30,295	40,899	14,842	140,854	12.5945%
her	herring	Clupea harengus	6,859	7,838	8,621	11,135	23,540	4,323	62,317	5.5721%
her_ash	herring	Clupea harengus	1,369	3,362	7,950	5,278	12,249	26	30,235	2.7035%
arg	argentines	Argentina spp	2,669	1,560	2,596	4,097	4,575	5,453	20,950	1.8732%
pil	pilchard	Sardina pilchardus	1,311	6,134	818	514	169	8	8,953	0.8006%
boc	boarfish	Capros aper	216	234	247	161	351	479	1,688	0.1509%
spr	sprat	Sprattus sprattus	59	539	257	7	32	653	1,547	0.1383%
hke	hake	Merluccius merluccius	392	286	107	274	208	177	1,444	0.1291%
oth	NA	NA	413	401	141	156	224	134	1,469	0.1313%
(all)	(all)	(all)	65,900	126,998	184,460	272,416	252,974	215,627	1,118,375	100.0000%

*Table 3.1.4: PFA selfsampling catch per species in widely distributed pelagic fisheries. OTH refers to all other species that are not the main target species, * denotes incomplete year*

Haul positions

An overview of all self-sampled hauls in PFA widely distributed fisheries.

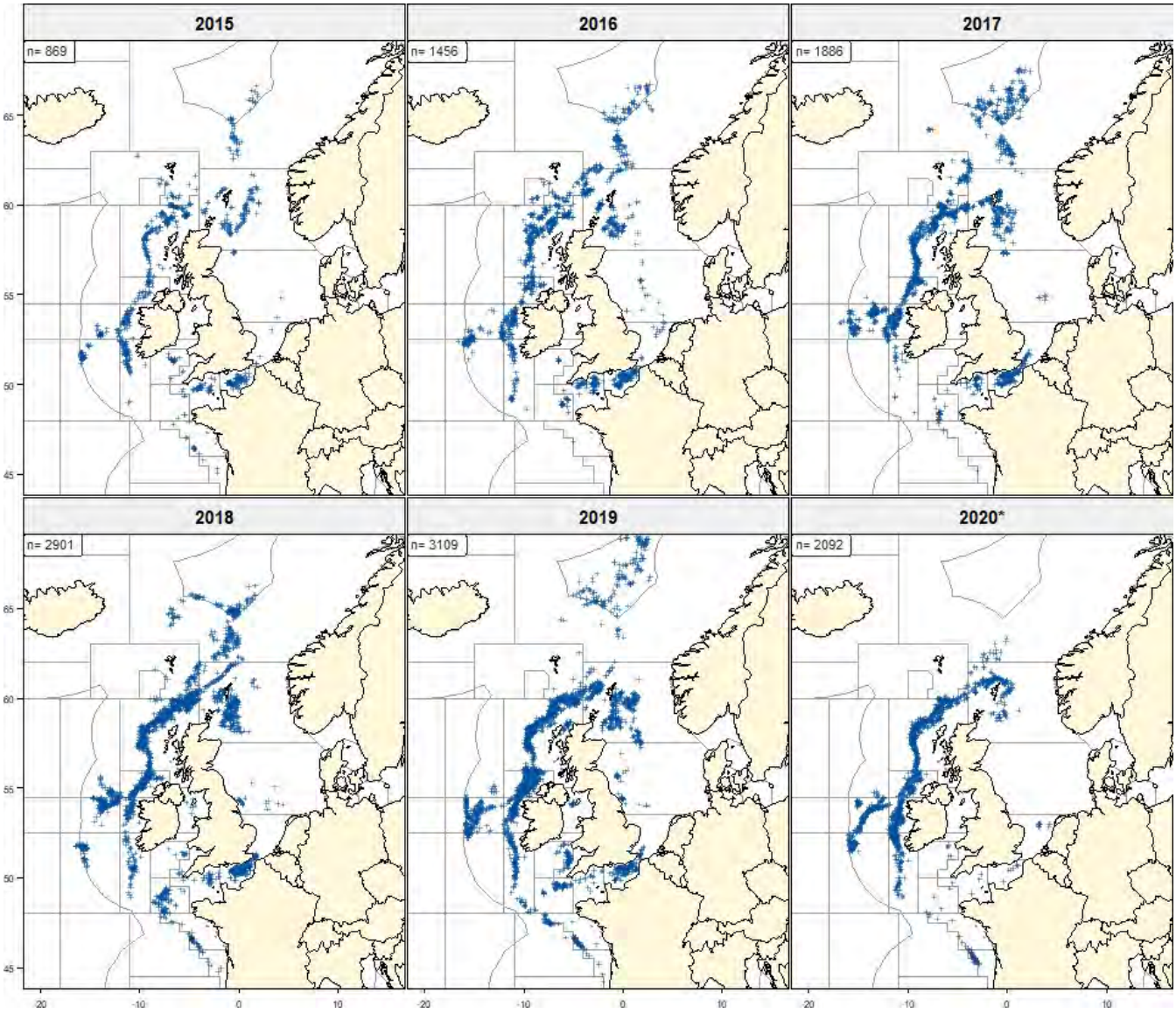

*Figure 3.1.1: Haul positions in PFA self-sampled widely distributed pelagic fisheries. N indicates the number of hauls. * denotes incomplete year*

Total catch per rectangle for the main target species

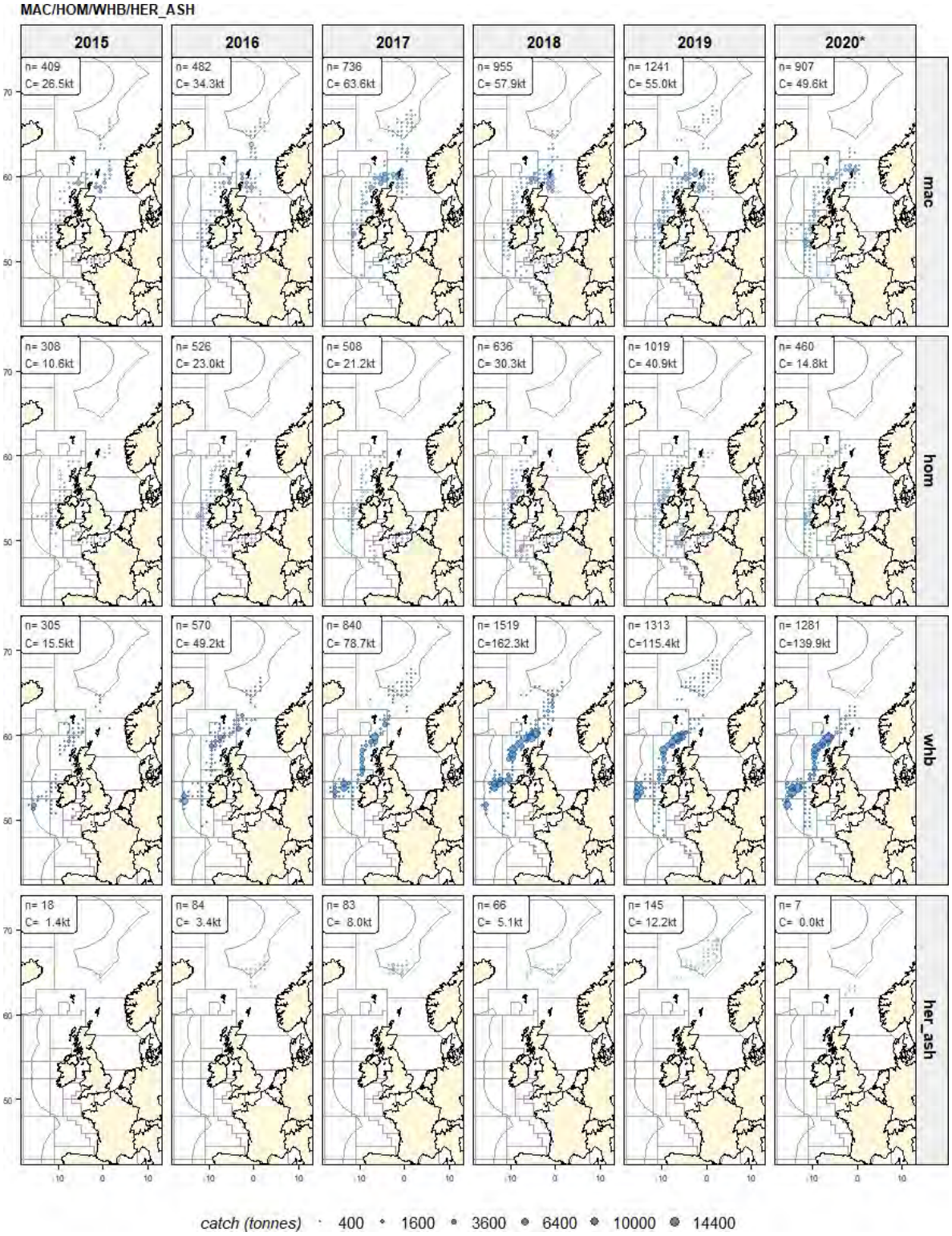

*Figure 3.1.2: Total catch per species and per rectangle in PFA self-sampled widely distributed pelagic fisheries. N indicates the number of hauls; Catch refers to the total catch per year. * denotes incomplete year*

Total catch per rectangle for the main target species

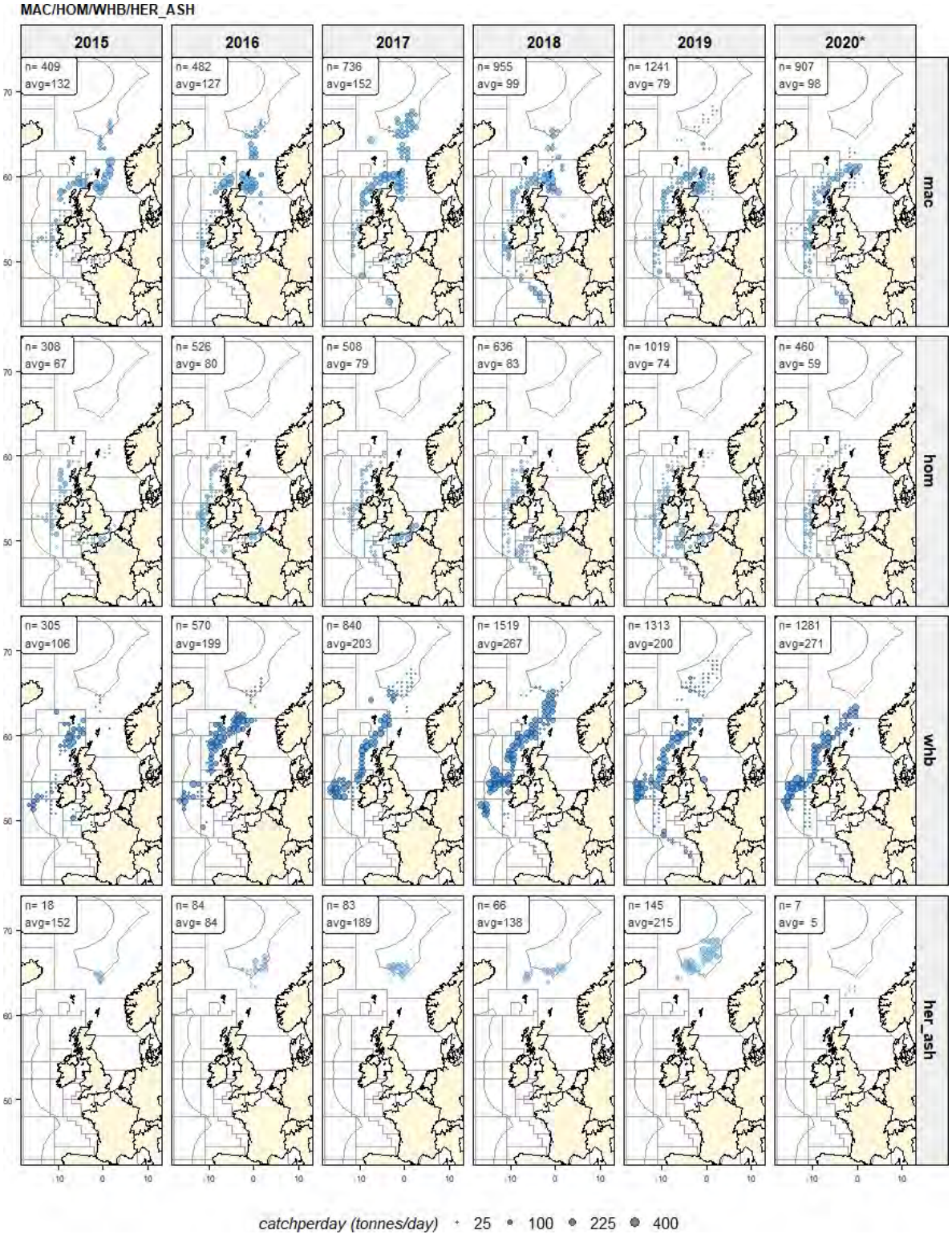

*Figure 3.1.3: Average catch per day, per species and per rectangle in PFA self-sampled widely distributed pelagic fisheries. N indicates the number of hauls; avg refers to the average catch per day; * denotes incomplete year*

Average fishing depth by rectangle

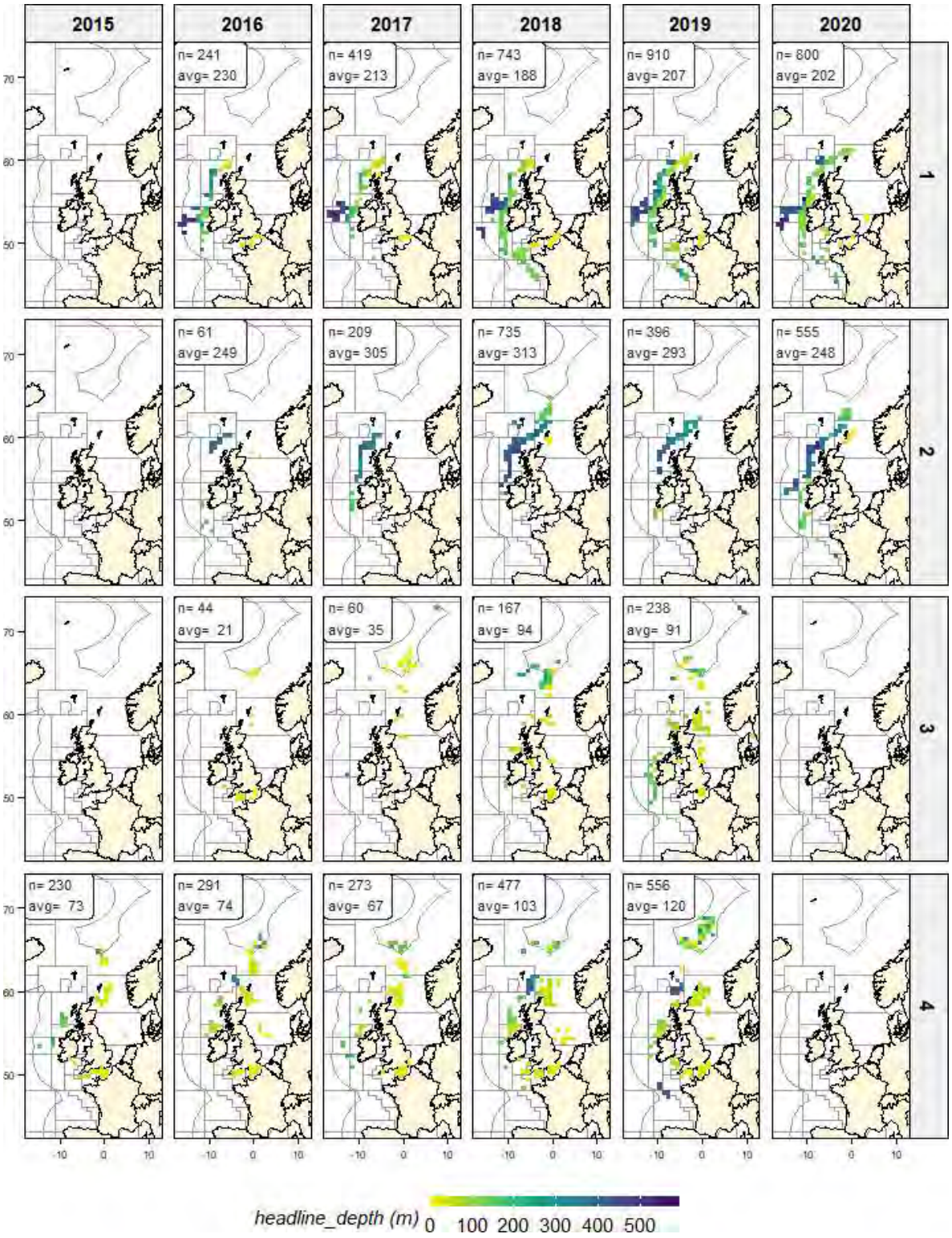

Figure 3.1.4: Average fishing depth (m) in PFA self-sampled widely distributed fisheries, by year and quarter.

Average temperature at fishing depth by rectangle

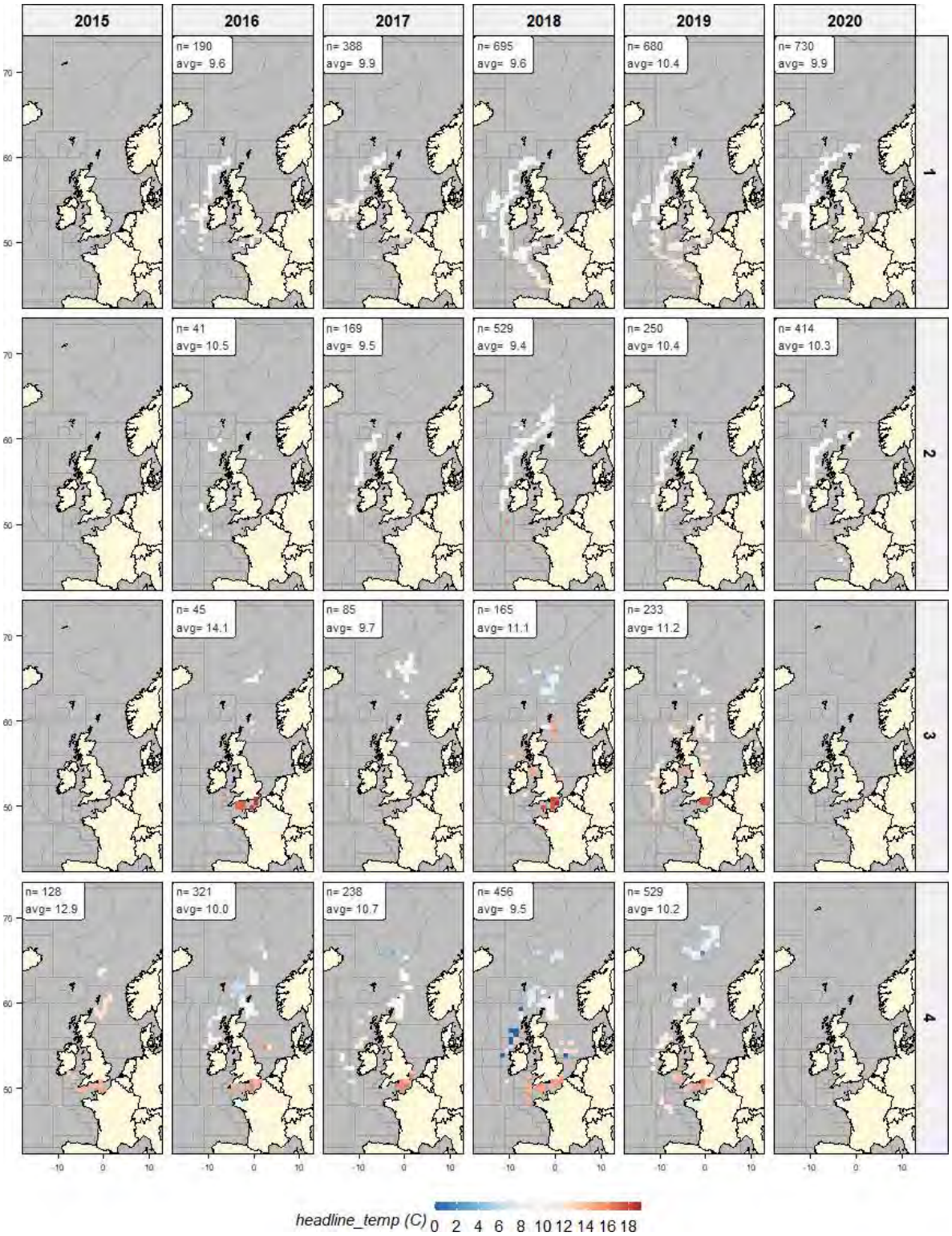

Figure 3.1.5: Average temperature at fishing depth in PFA self-sampled widely distributed fisheries.

Average windspeed by rectangle

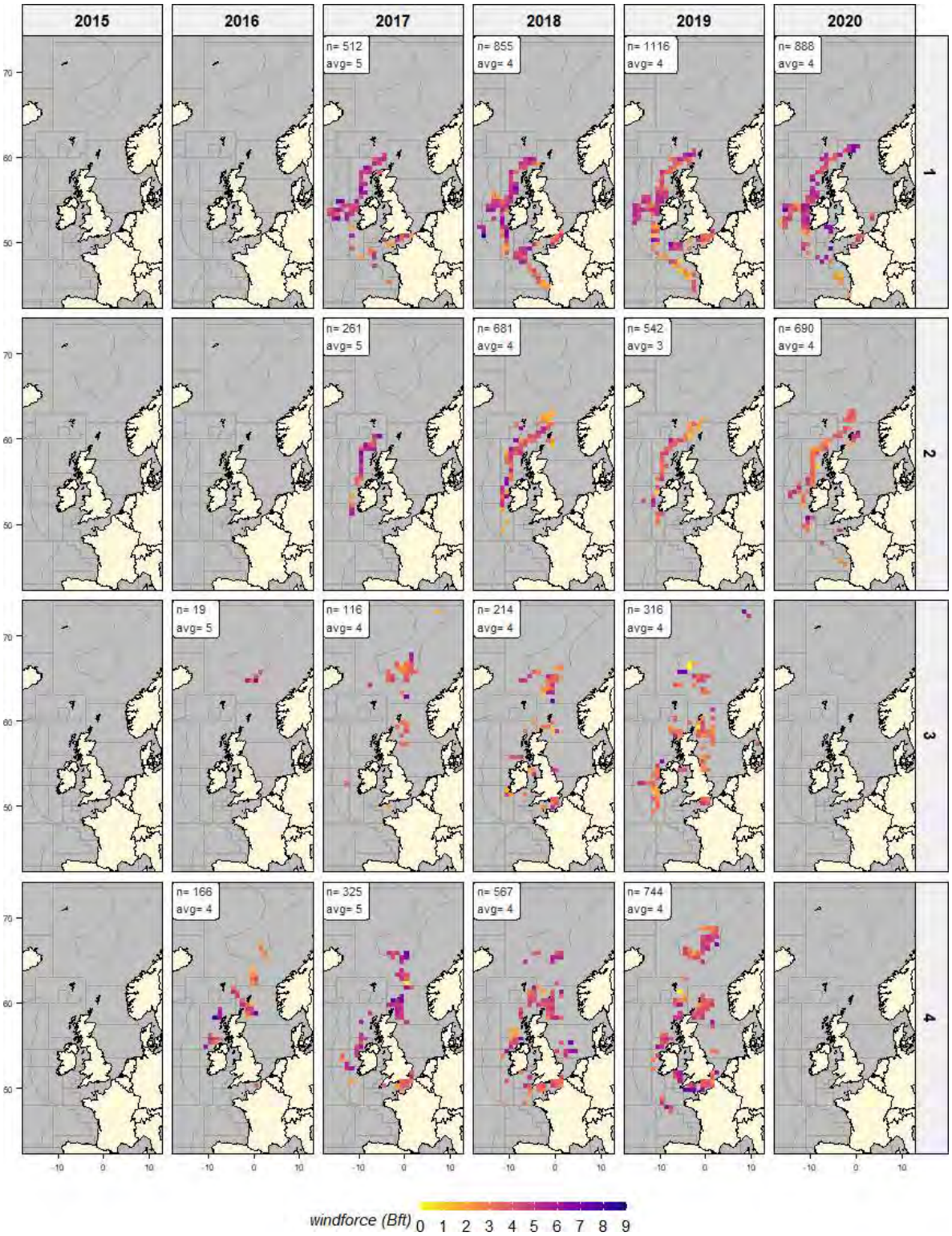

Figure 3.1.6: Average windforce in PFA self-sampled widely distributed fisheries.

3.2 Mackerel (MAC, Scomber scombrus)

The Mackerel fishery takes place from October through to March of the subsequent year. Minor bycatches of mackerel may also occur during other fisheries. Overall, the self-sampling activities for the mackerel fisheries during the years 2015 – 2020 (up to August) covered 323 fishing trips with 4,725 hauls, a total catch of 286,957 tonnes and 91,000 individual length measurements. The main fishing areas are ICES division 27.4.a (between 27 and 54% of the catch) and division 27.6.a (between 25 and 44% of the catch).

species	division	year	nvessels	ntrips	ndays	nhauls	catch	catchperc	catch/day	nlength
mac	27.2.a	2015	3	3	18	35	2,041	8	113	1,561
mac	27.2.a	2016	6	7	48	98	7,442	22	155	2,843
mac	27.2.a	2017	6	9	81	164	13,020	20	161	1,948
mac	27.2.a	2018	5	7	39	66	4,831	8	124	9
mac	27.2.a	2019	4	4	26	45	205	0	8	291
mac	27.2.a	2020*	1	1	4	4	1	0	0	0
mac	27.4.a	2015	5	7	51	111	14,324	54	281	4,926
mac	27.4.a	2016	8	11	66	120	15,705	46	238	1,775
mac	27.4.a	2017	8	17	93	155	17,325	27	186	4,475
mac	27.4.a	2018	13	24	170	296	28,511	49	168	5,651
mac	27.4.a	2019	14	27	182	341	24,300	44	134	7,016
mac	27.4.a	2020*	10	16	83	160	14,979	30	180	13,813
mac	27.6.a	2015	4	7	41	77	7,904	30	193	2,453
mac	27.6.a	2016	6	15	56	94	8,689	25	155	2,647
mac	27.6.a	2017	10	25	156	264	28,288	44	181	5,443
mac	27.6.a	2018	16	31	238	392	18,024	31	76	7,905
mac	27.6.a	2019	15	43	307	517	21,305	39	69	7,691
mac	27.6.a	2020*	13	36	222	407	15,619	32	70	5,553
mac	27.7.b	2015	2	4	19	34	811	3	43	158
mac	27.7.b	2016	5	7	35	68	186	1	5	125
mac	27.7.b	2017	6	9	51	98	3,640	6	71	276
mac	27.7.b	2018	6	9	33	51	1,111	2	34	37
mac	27.7.b	2019	12	22	73	124	5,389	10	74	1,849
mac	27.7.b	2020*	12	22	85	140	6,047	12	71	2,913
mac	27.7.j	2015	4	7	33	69	764	3	23	821
mac	27.7.j	2016	3	6	20	29	1,413	4	71	122
mac	27.7.j	2017	3	4	6	11	496	1	83	170
mac	27.7.j	2018	8	11	26	38	2,662	5	102	314
mac	27.7.j	2019	8	11	47	89	2,357	4	50	1,514
mac	27.7.j	2020*	12	24	78	134	10,705	22	137	2,495
mac	other	2015	5	15	48	83	637	2	13	293
mac	other	2016	6	19	49	74	864	3	18	205
mac	other	2017	8	21	39	52	886	1	23	60
mac	other	2018	8	17	80	114	2,819	5	35	1,083
mac	other	2019	12	27	83	127	1,498	3	18	2,417
mac	other	2020*	10	15	49	63	2,230	4	46	650
mac	(all)	2015		43	210	409	26,481	100	126	10,212
mac	(all)	2016		65	274	483	34,299	101	125	7,717
mac	(all)	2017		85	426	744	63,655	99	149	12,372
mac	(all)	2018		99	586	957	57,958	100	99	14,999
mac	(all)	2019		134	718	1,243	55,054	100	77	20,778
mac	(all)	2020*		114	521	908	49,581	100	95	25,424
mac	(all)	(all)		540	2,735	4,744	287,028		105	91,502

*Table 3.2.1: Mackerel. Self-sampling summary with the number of days, hauls, trips, vessels, catch (tonnes), number of fish measured, catch rates (ton/effort). * denotes incomplete year*

Mackerel (MAC). Catch by month

species	month	2015	2016	2017	2018	2019	2020*	all	perc
mac	Jan	7,557	7,847	18,594	11,592	18,766	20,769	85,125	29.6608%
mac	Feb	1,483	1,189	8,198	7,613	11,872	19,410	49,765	17.3400%
mac	Mar	519	150	4,724	3,307	5,507	7,087	21,294	7.4196%
mac	Apr	240	789	1,025	1,225	1,327	797	5,403	1.8826%
mac	May	70	34	296	191	489	1,218	2,298	0.8007%
mac	Jun	0	179	0	60	96	175	510	0.1777%
mac	Jul	223	194	88	0	327	83	915	0.3188%
mac	Aug	0	147	247	59	431	39	923	0.3216%
mac	Sep	755	1,091	9,388	4,849	3,063	0	19,146	6.6712%
mac	Oct	14,670	14,150	7,972	19,465	11,559	0	67,816	23.6297%
mac	Nov	944	8,358	11,653	9,229	1,613	0	31,797	11.0793%
mac	Dec	15	163	1,463	362	0	0	2,003	0.6979%
mac	(all)	26,476	34,291	63,648	57,952	55,050	49,578	286,995	100.0000%

*Table 3.2.2: Mackerel. Self-sampling summary with the catch (tonnes) by year and month. * denotes incomplete year*

Mackerel (MAC). Catch by rectangle

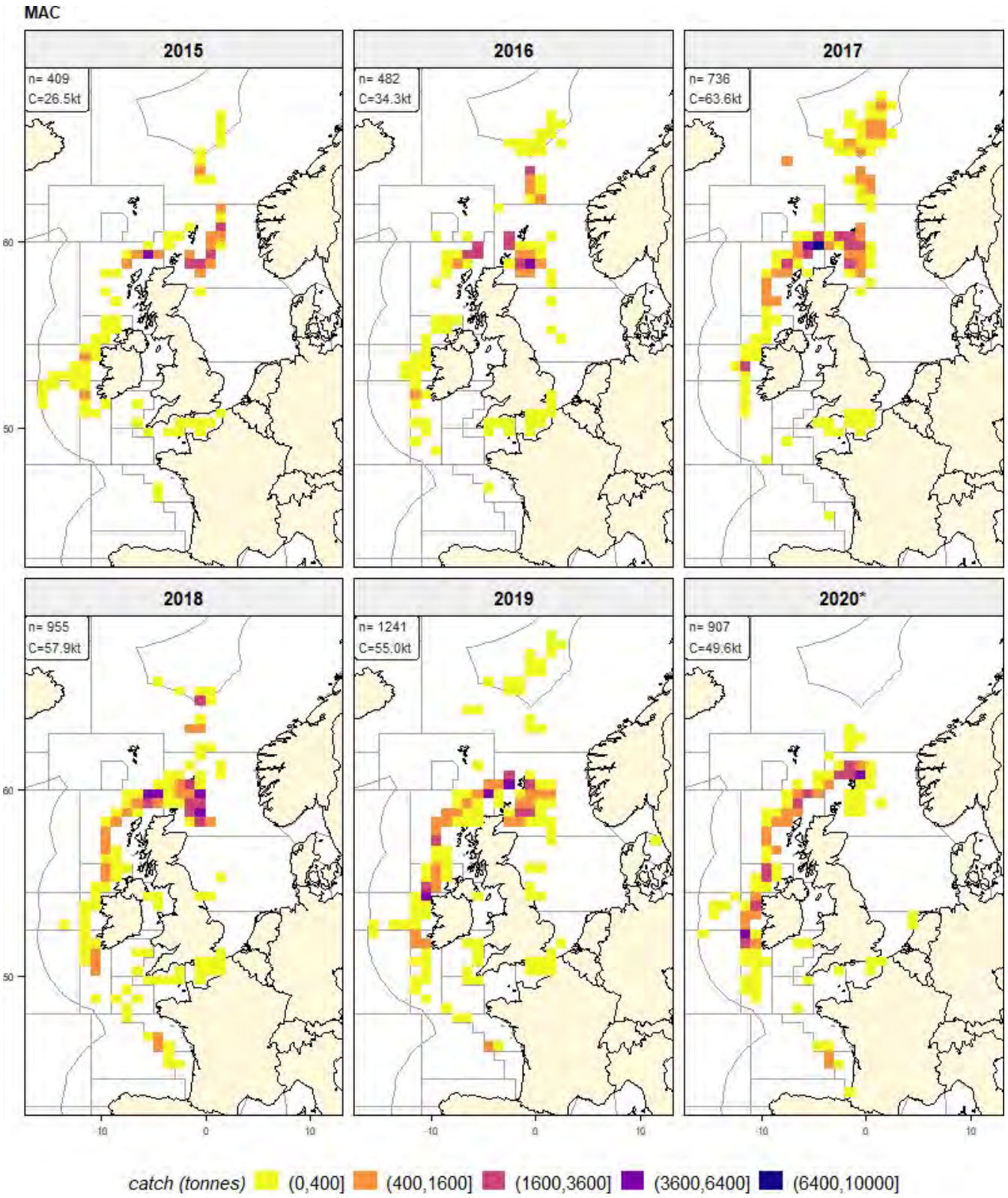

*Figure 3.2.1: Mackerel. Catch per per rectangle. N indicates the number of hauls; Catch refers to the total catch per year. * denotes incomplete year*

Mackerel (MAC). Average catch per day

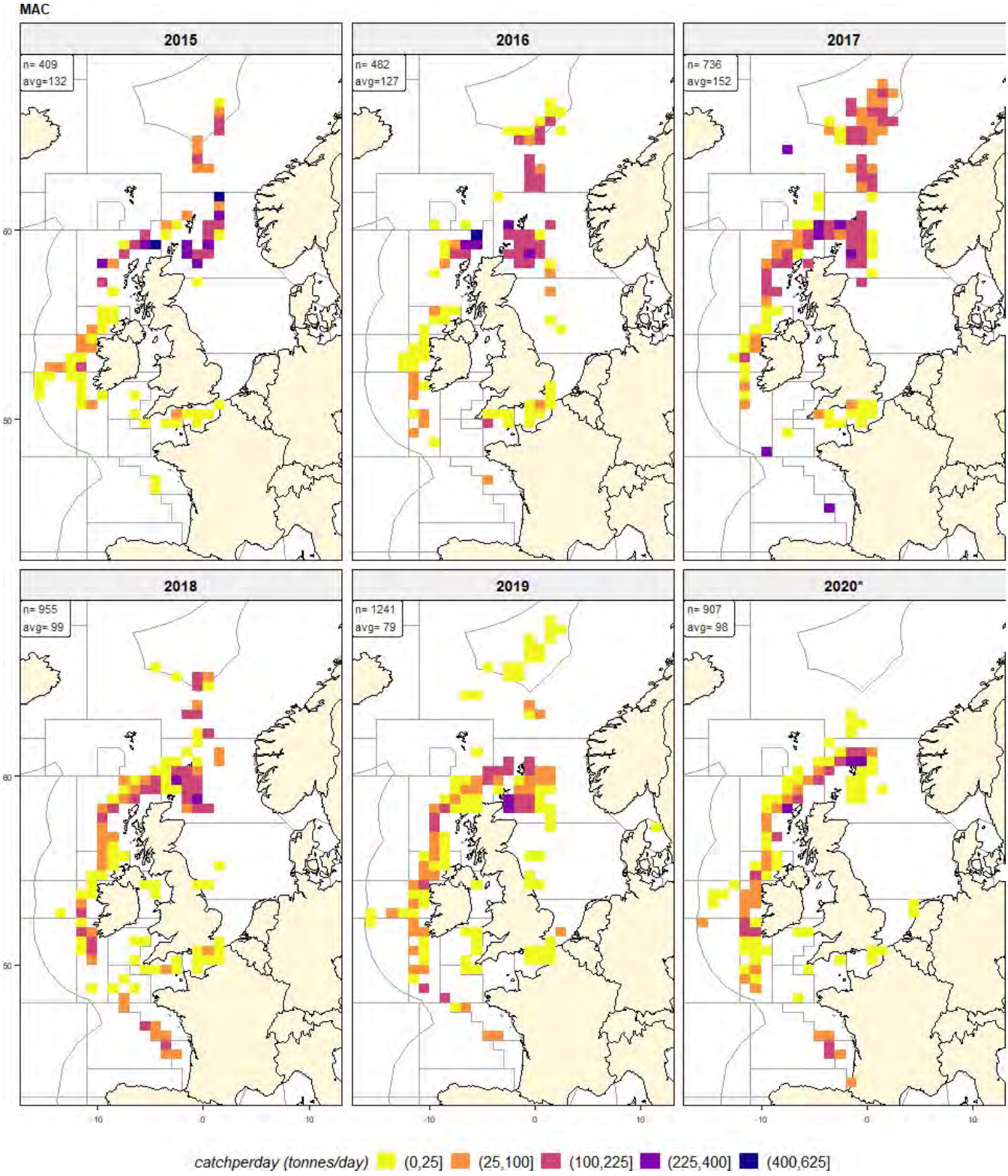

*Figure 3.2.2: Mackerel. Average catch per day per rectangle. N indicates the number of hauls; avg refers to the overall average catch per day. * denotes incomplete year*

Mackerel (MAC). Spatial-temporal evolution of the fishery

Spatial-temporal evolution of the fishery by year and month from the haul-by-haul catch information. Fishing season is from October until March the following year. The midpoint of the distribution is indicated by the blue triangle. The catch has been used as weighting factor in the calculation of the midpoint.

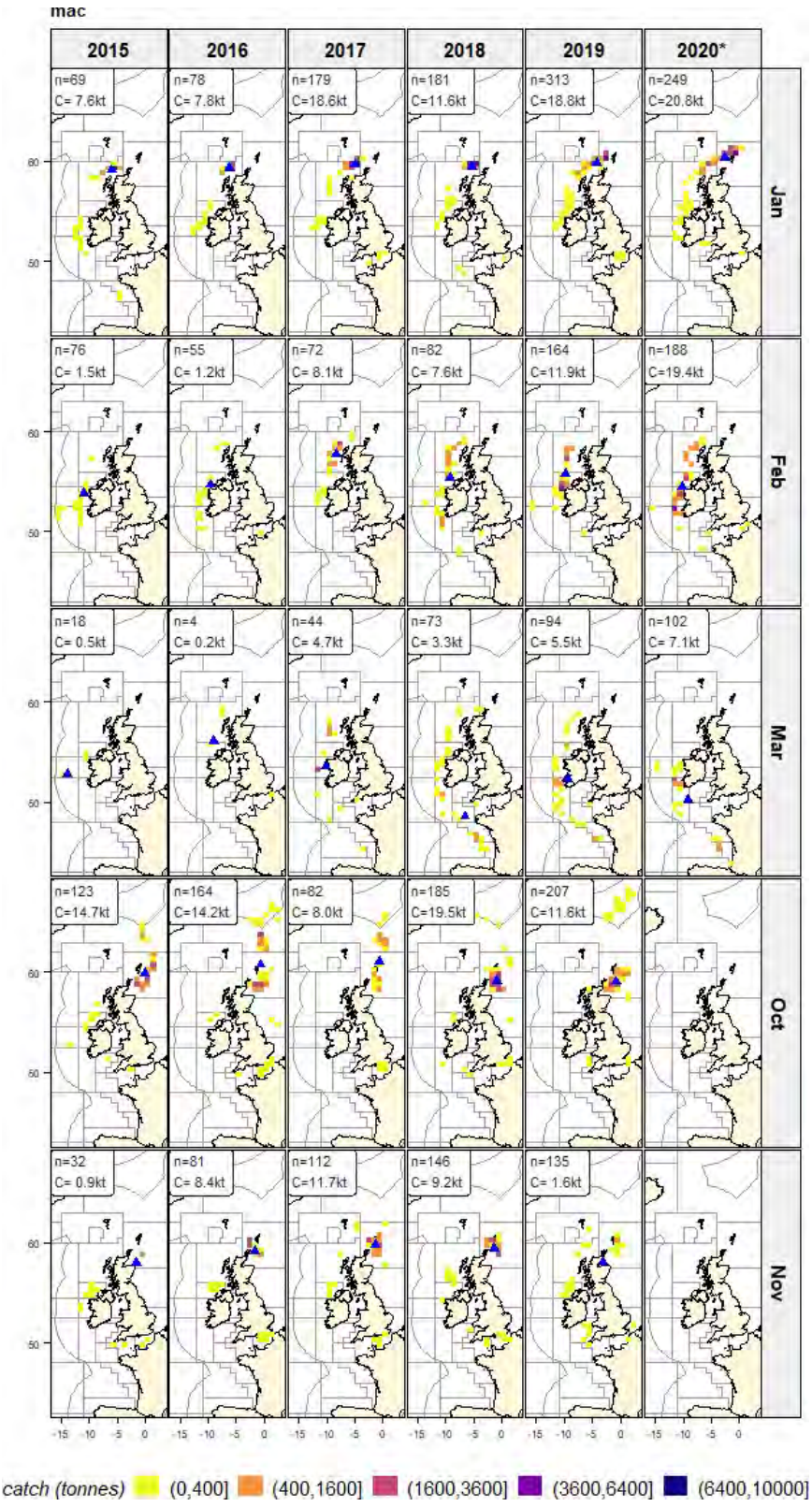

*Figure 3.2.3: Mackerel. Average catch per day per rectangle. N indicates the number of hauls; avg refers to the overall average catch per day. * denotes incomplete year*

Mackerel (MAC). Length distributions of the catch

Compared to the previous years, mackerel in the catch have been relatively large in 2020 with median length of 36.4 cm compared to 32.4-35.4 in the preceding years. Note that the catch in 2020 is only for the first half of the year.

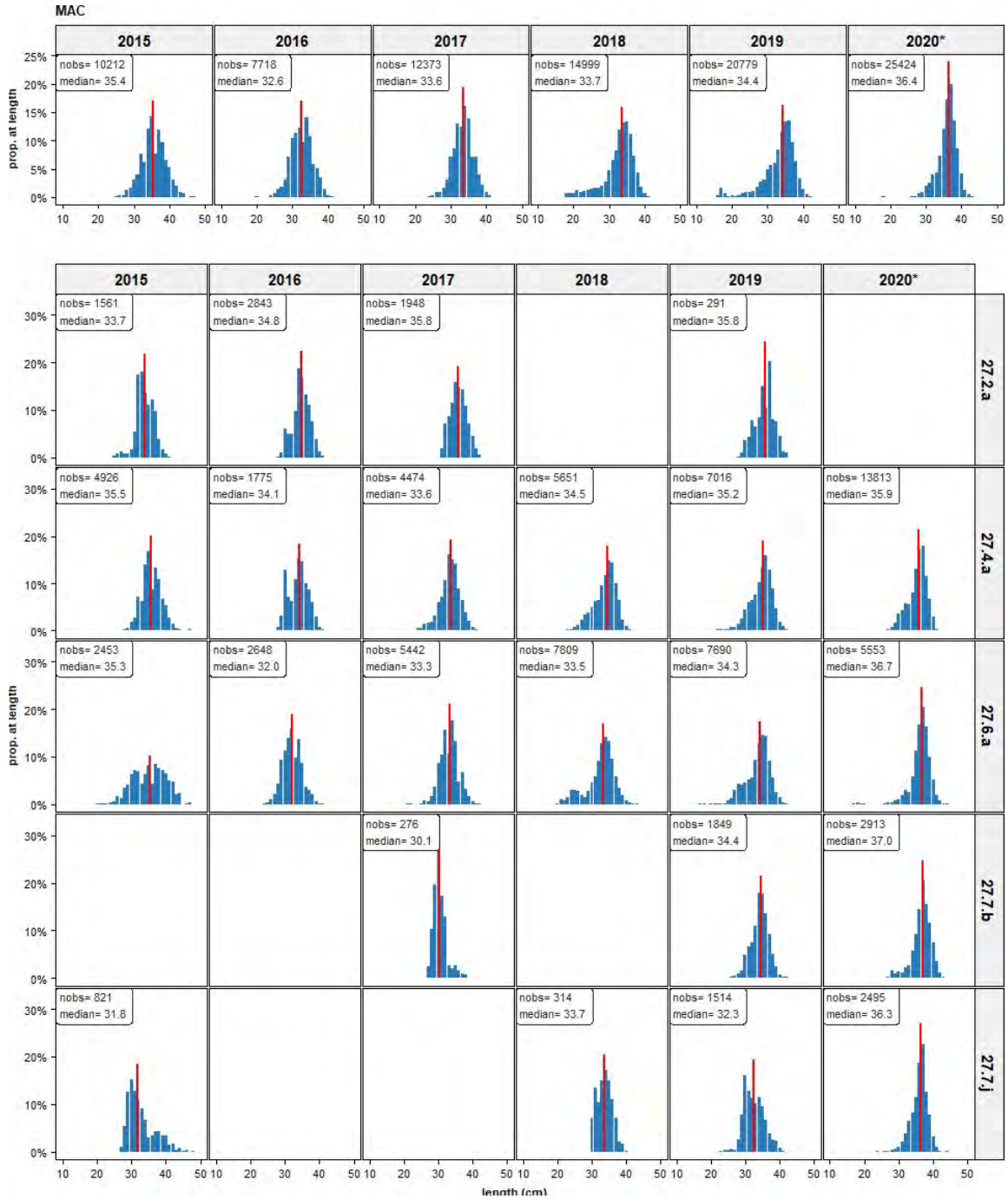

*Figure 3.2.4: Mackerel. Length distributions by year (top) and by year and division (bottom). Nobs refers to the number of observations; median denotes the median length. * denotes incomplete year*

Mackerel (MAC). Length frequencies by year and quarter

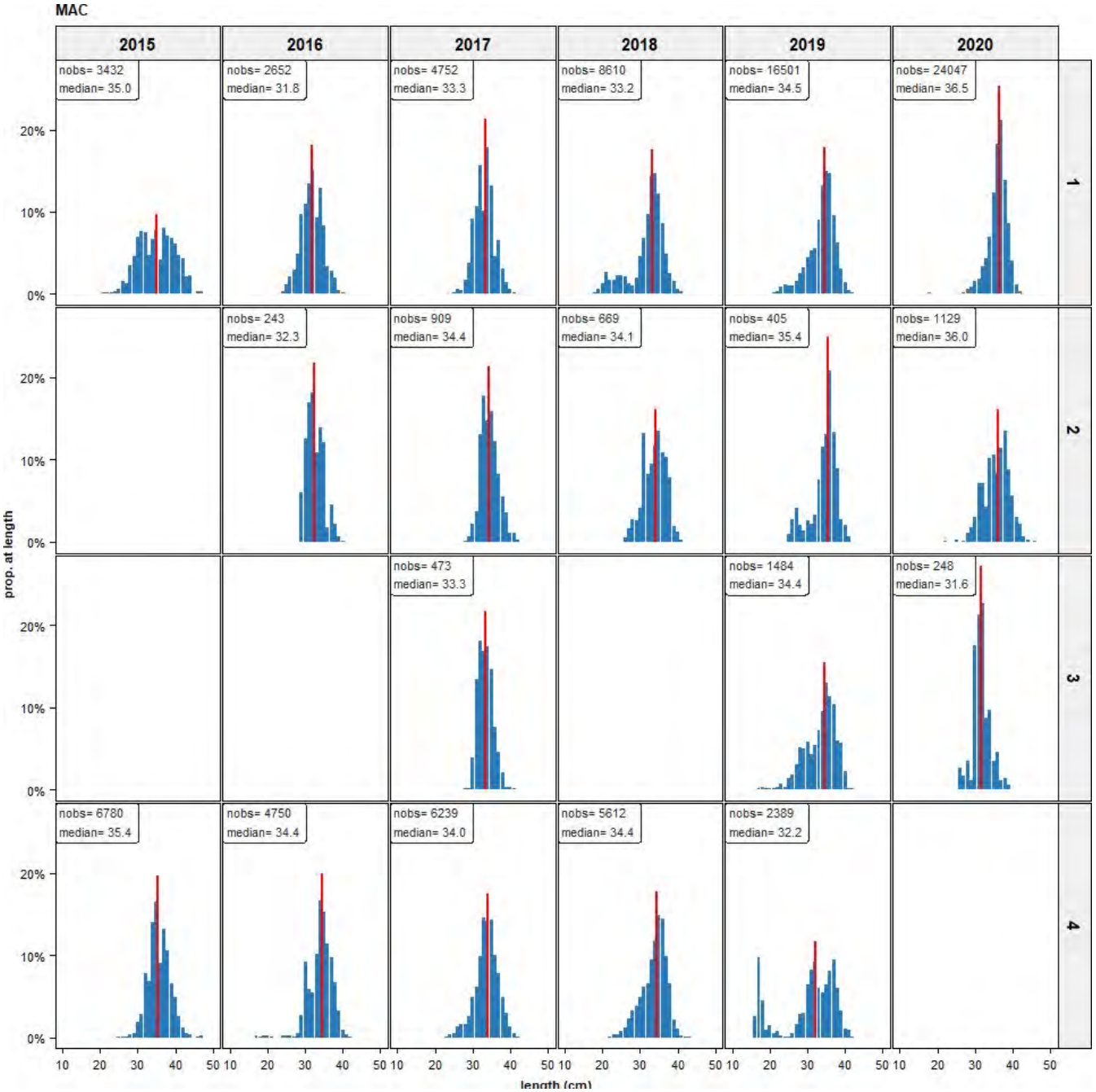

Figure 3.2.5: Mackerel. Length distributions by year (top) and by year and division (bottom). Nobs refers to the number of observations; median denotes the median length

Mackerel (MAC). Weight distributions

In line with the observation that the median length of mackerel in 2020 has been larger than in the preceding years, also the median weight has been somewhat higher with median weight of 417 gram compared to 379-400 gram the preceding years.

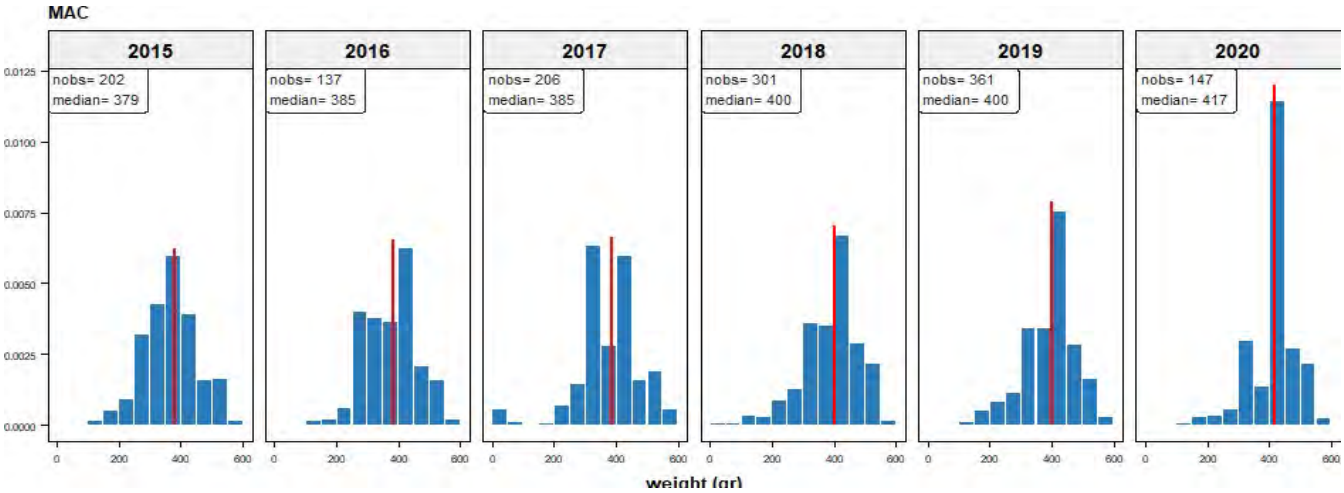

*Figure 3.2.6: Mackerel. Weight distributions (50 gram classes). Nobs refers to the number of batches where average weight was measured; median denotes the median length; * denotes incomplete year*

Mackerel (MAC). Fat percentages by year

Average annual fat content ranges from 17 to 21% with individual measurements reaching up to 30%.

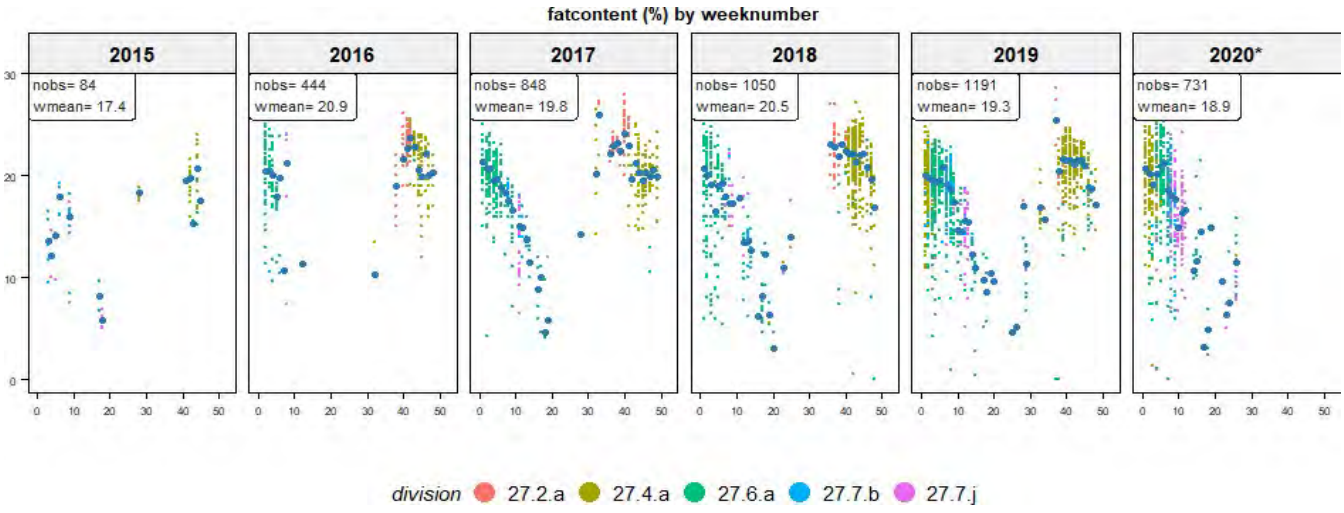

*Figure 3.2.7: Mackerel. Average fat percentage by week. Nobs refers to the number of batches where average fat was measured; blue dots indicate the weekly averages; * denotes incomplete year*

Mackerel (MAC). Fishing depth distributions.

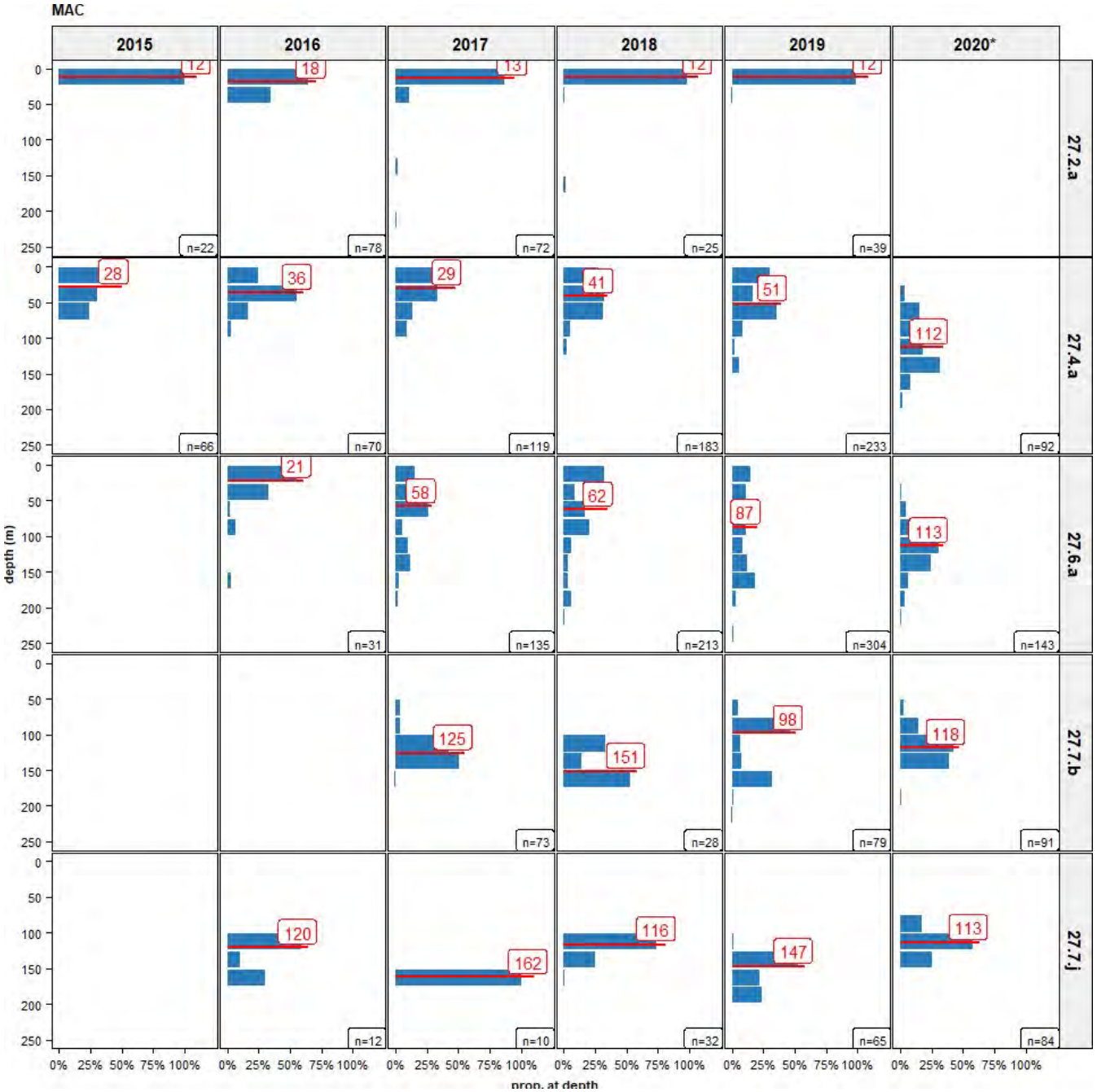

*Figure 3.2.8: Mackerel. Depth distributions by year and division. N is number of observations; median depth in red; * denotes incomplete year*

3.3 Horse mackerel (HOM, Trachurus trachurus)

The horse mackerel fishery takes place from October through to March of the subsequent year. Overall, the self-sampling activities for the horse mackerel fisheries during the years 2015 – 2020 (up to August) covered 457 fishing trips with 3,454 hauls, a total catch of 140,633 tonnes and 125,000 individual length measurements. The main fishing areas are ICES division 27.6.a (between 21% and 40% of the catch), division 27.7.b (7%-22%) and division 27.7.d (19%-34%, note that this is considered as the North Sea horse mackerel stock).

species	division	year	nvessels	ntrips	ndays	nhauls	catch	catchperc	catch/day	nlength
hom	27.6.a	2015	3	6	39	66	2,746	26	70	2,934
hom	27.6.a	2016	6	17	93	153	4,753	21	51	4,983
hom	27.6.a	2017	8	13	82	159	5,343	25	65	5,213
hom	27.6.a	2018	13	23	125	235	12,053	40	96	12,015
hom	27.6.a	2019	14	30	212	384	13,878	34	65	7,443
hom	27.6.a	2020*	8	17	68	112	4,255	29	63	3,668
hom	27.7.b	2015	4	6	27	48	1,483	14	55	927
hom	27.7.b	2016	5	8	47	92	4,313	19	92	3,390
hom	27.7.b	2017	6	12	57	104	4,729	22	83	3,459
hom	27.7.b	2018	9	11	39	60	2,250	7	58	1,663
hom	27.7.b	2019	12	24	78	129	4,268	10	55	2,678
hom	27.7.b	2020*	12	23	84	147	5,231	35	62	5,478
hom	27.7.d	2015	4	6	30	50	2,012	19	67	3,864
hom	27.7.d	2016	5	15	76	130	7,225	31	95	6,313
hom	27.7.d	2017	6	15	75	139	7,202	34	96	1,013
hom	27.7.d	2018	5	13	73	138	6,234	21	85	3,898
hom	27.7.d	2019	8	14	76	141	7,102	17	93	9,123
hom	27.7.d	2020*	3	3	3	4	12	0	4	106
hom	27.7.h	2016	1	1	8	16	1,297	6	162	5,043
hom	27.7.h	2017	2	5	18	30	1,329	6	74	0
hom	27.7.h	2018	9	13	50	89	6,326	21	127	7,804
hom	27.7.h	2019	6	6	13	21	984	2	76	2,663
hom	27.7.h	2020*	2	2	2	2	55	0	28	0
hom	27.7.j	2015	4	6	35	79	3,082	29	88	5,640
hom	27.7.j	2016	4	8	29	55	3,091	13	107	761
hom	27.7.j	2017	3	5	7	13	160	1	23	463
hom	27.7.j	2018	7	10	30	45	813	3	27	519
hom	27.7.j	2019	10	14	58	110	5,076	12	88	1,520
hom	27.7.j	2020*	12	26	92	168	5,067	34	55	4,261
hom	other	2015	6	14	37	65	1,263	12	34	1,005
hom	other	2016	8	16	45	81	2,287	10	51	1,627
hom	other	2017	7	18	41	64	2,503	12	61	1,100
hom	other	2018	7	13	51	70	2,619	9	51	576
hom	other	2019	12	31	131	236	9,590	23	73	14,059
hom	other	2020*	8	14	21	27	222	1	11	438
hom	(all)	2015		38	168	308	10,586	100	63	14,370
hom	(all)	2016		65	298	527	22,966	100	77	22,117
hom	(all)	2017		68	280	509	21,266	100	76	11,248
hom	(all)	2018		83	368	637	30,295	101	82	26,475
hom	(all)	2019		119	568	1,021	40,898	98	72	37,486
hom	(all)	2020*		85	270	460	14,842	99	55	13,951
hom	(all)	(all)		458	1,952	3,462	140,853		72	125,647

*Table 3.3.1: Horse mackerel. Self-sampling summary with the number of days, hauls, trips, vessels, catch (tonnes), number of fish measured, catch rates (ton/effort). * denotes incomplete year*

Horse mackerel (HOM). Catch by month

species	month	2015	2016	2017	2018	2019	2020*	all	perc
hom	Jan	3,053	4,722	9,613	11,518	11,547	7,178	47,631	33.82%
hom	Feb	2,929	6,941	3,112	5,961	5,304	4,804	29,051	20.63%
hom	Mar	145	111	227	3,626	4,083	1,259	9,451	6.71%
hom	Apr	495	256	0	31	45	0	827	0.59%
hom	May	114	175	155	6	41	529	1,020	0.72%
hom	Jun	0	1	0	226	1,357	649	2,233	1.59%
hom	Jul	0	1,733	186	15	5,671	419	8,024	5.70%
hom	Aug	0	15	58	0	8	0	81	0.06%
hom	Sep	71	560	134	1,910	2,343	0	5,018	3.56%
hom	Oct	234	1,838	4,620	1,954	3,555	0	12,201	8.66%
hom	Nov	2,890	5,086	3,027	3,925	5,950	0	20,878	14.83%
hom	Dec	650	1,520	129	1,117	990	0	4,406	3.13%
hom	(all)	10,581	22,958	21,261	30,289	40,894	14,838	140,821	100.00%

*Table 3.3.2: Horse mackerel. Self-sampling summary with the catch (tonnes) by year and month. * denotes incomplete year*

Horse mackerel (HOM). Catch by rectangle

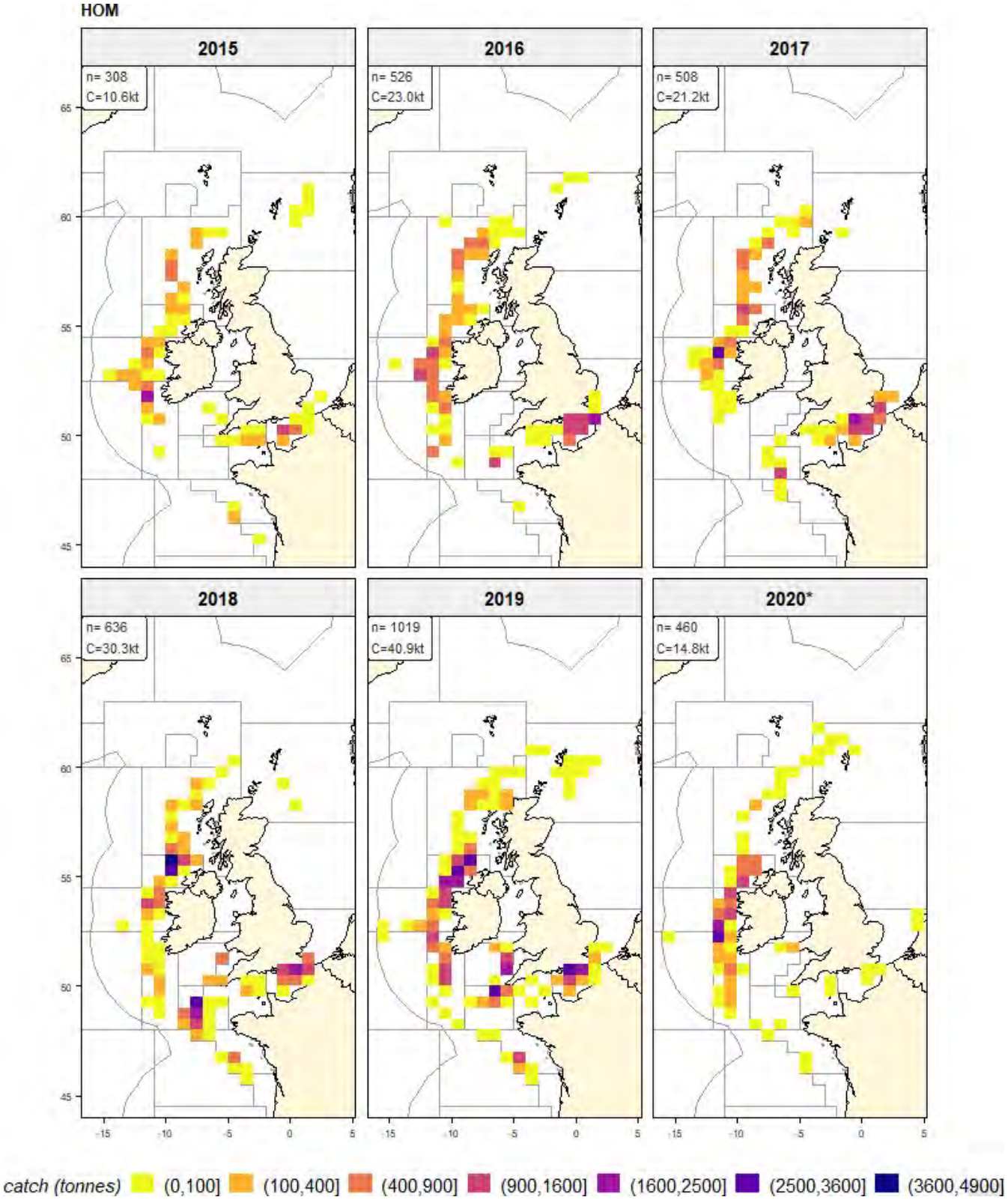

*Figure 3.3.1: Horse mackerel. Catch per per rectangle. N indicates the number of hauls; Catch refers to the total catch per year. * denotes incomplete year*

Horse mackerel (HOM). Average catch per day

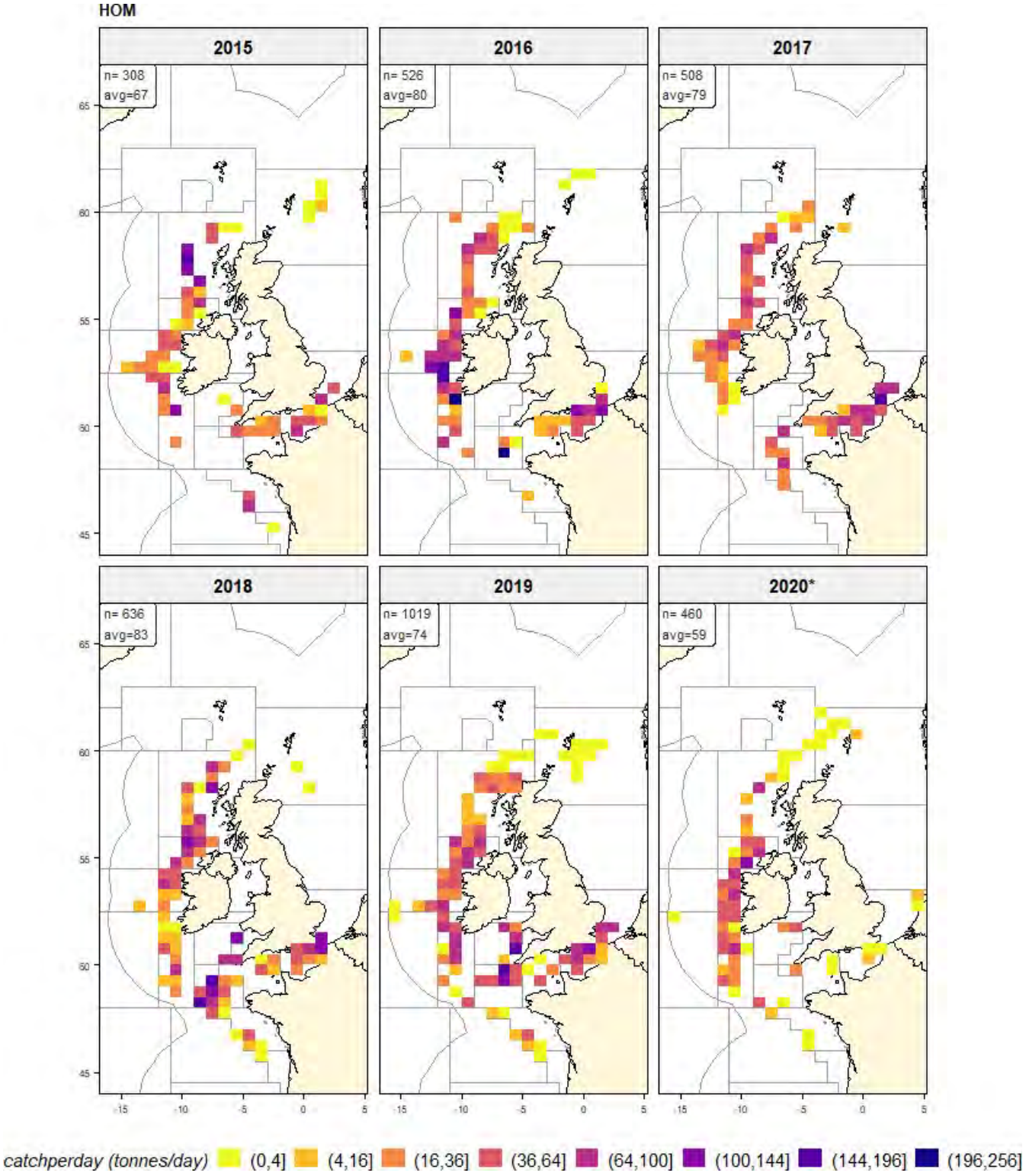

*Figure 3.3.2: Horse mackerel. Average catch per day per rectangle. N indicates the number of hauls; avg refers to the overall average catch per day. * denotes incomplete year*

Horse mackerel (HOM). Spatial-temporal evolution of the fishery

Spatial-temporal evolution of the fishery by year and month from the haul-by-haul catch information. Fishing season is from October until March the following year. The midpoint of the distribution is indicated by the blue triangle. The catch has been used as weighting factor in the calculation of the midpoint.

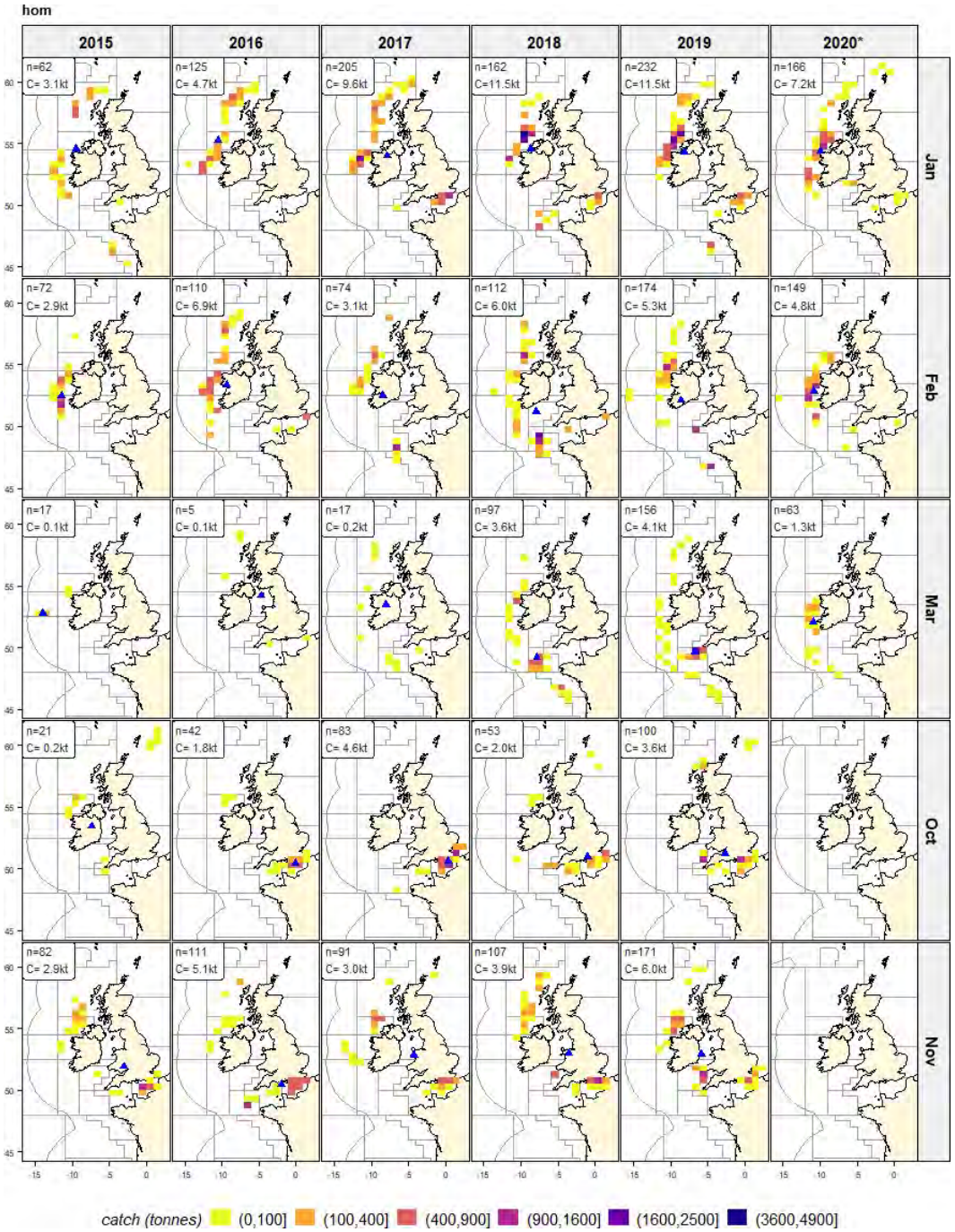

*Figure 3.3.3: Horse mackerel. Average catch per day per rectangle. N indicates the number of hauls; avg refers to the overall average catch per day. * denotes incomplete year*

Horse mackerel (HOM). Length distributions of the catch

Horse mackerel have a wide range in the length distributions in the catch. Median lengths have fluctuated between 22.8 and 30.0 cm.In 2019 and 2020 there are some indications of a stronger year class being available to the fishery, with a more narrow length distribution. For example, in 27.6.a the mode was 26.6 cm in 2019 and 27.5 cm in 2020. Note that the catch in 2020 is only for the first half of the year.

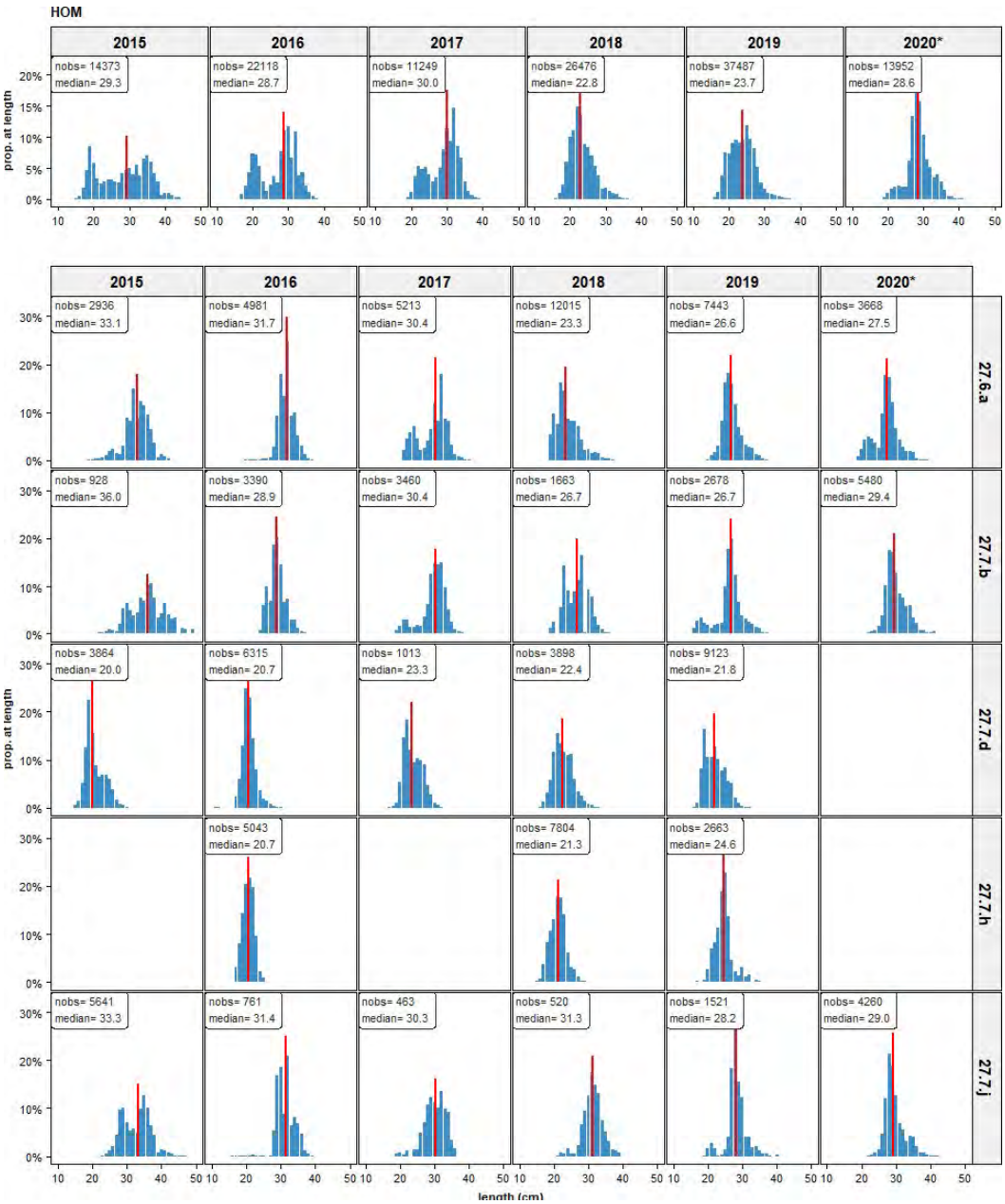

*Figure 3.3.4: Horse mackerel. Length distributions by year (top) and by year and division (bottom). Nobs refers to the number of observations; median denotes the median length. * denotes incomplete year*

Horse mackerel (HOM). Length frequencies by year and quarter

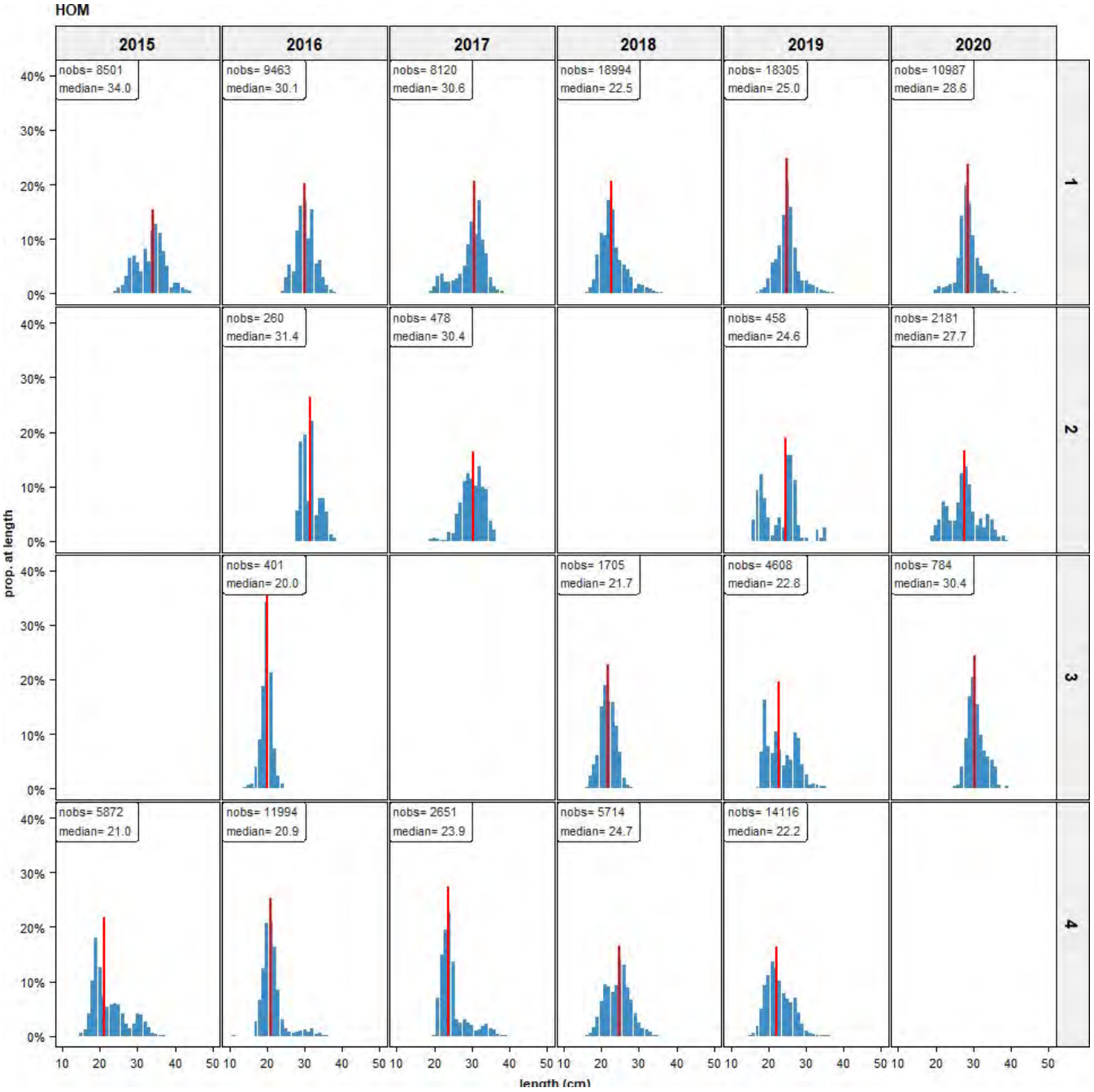

Figure 3.3.5: Horse mackerel. Length distributions by year (top) and by year and division (bottom). Nobs refers to the number of observations; median denotes the median length

Horse mackerel (HOM). Weight distributions

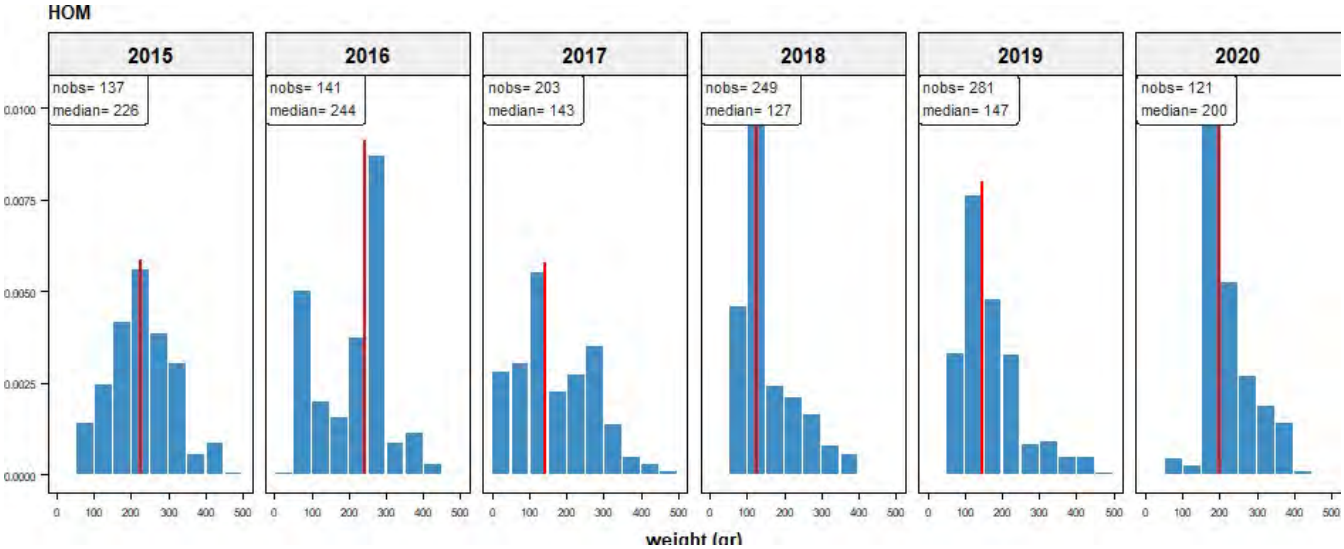

*Figure 3.3.6: Horse mackerel. Weight distributions (50 gram classes). Nobs refers to the number of batches where average weight was measured; median denotes the median length; * denotes incomplete year*

Horse mackerel (HOM). Fat percentages by year

Average annual fat content ranges from 5 to 7.5% with individual measurements reaching up to 15%.

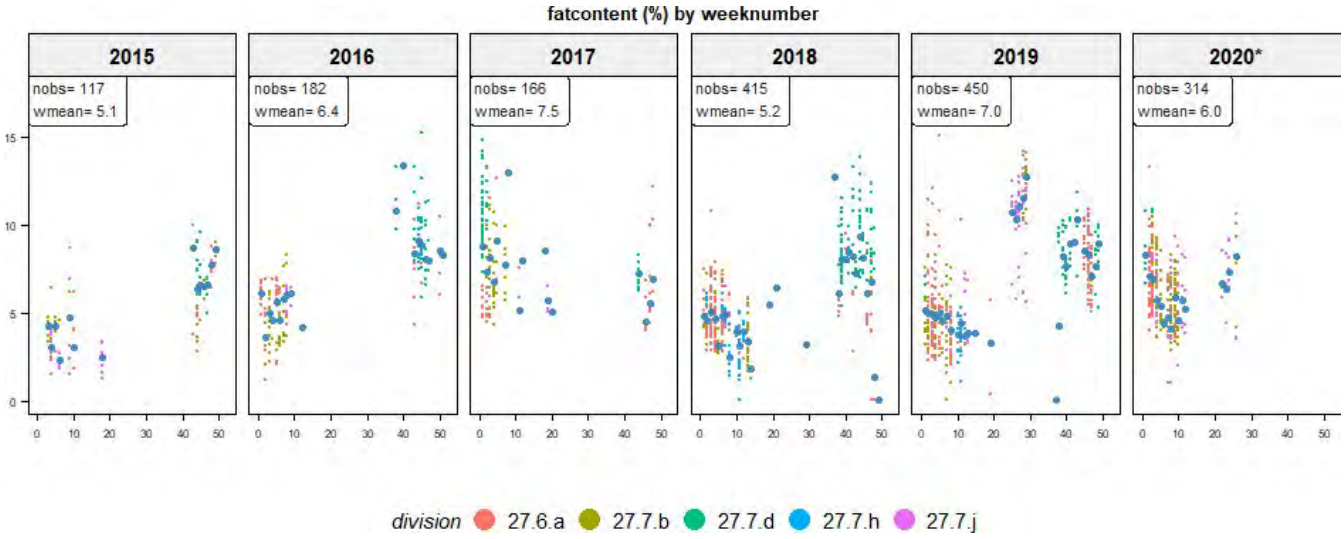

*Figure 3.3.7: Horse mackerel. Average fat percentage by week. Nobs refers to the number of batches where average fat was measured; blue dots indicate the weekly averages; * denotes incomplete year*

Horse mackerel (HOM). Fishing depth distributions.

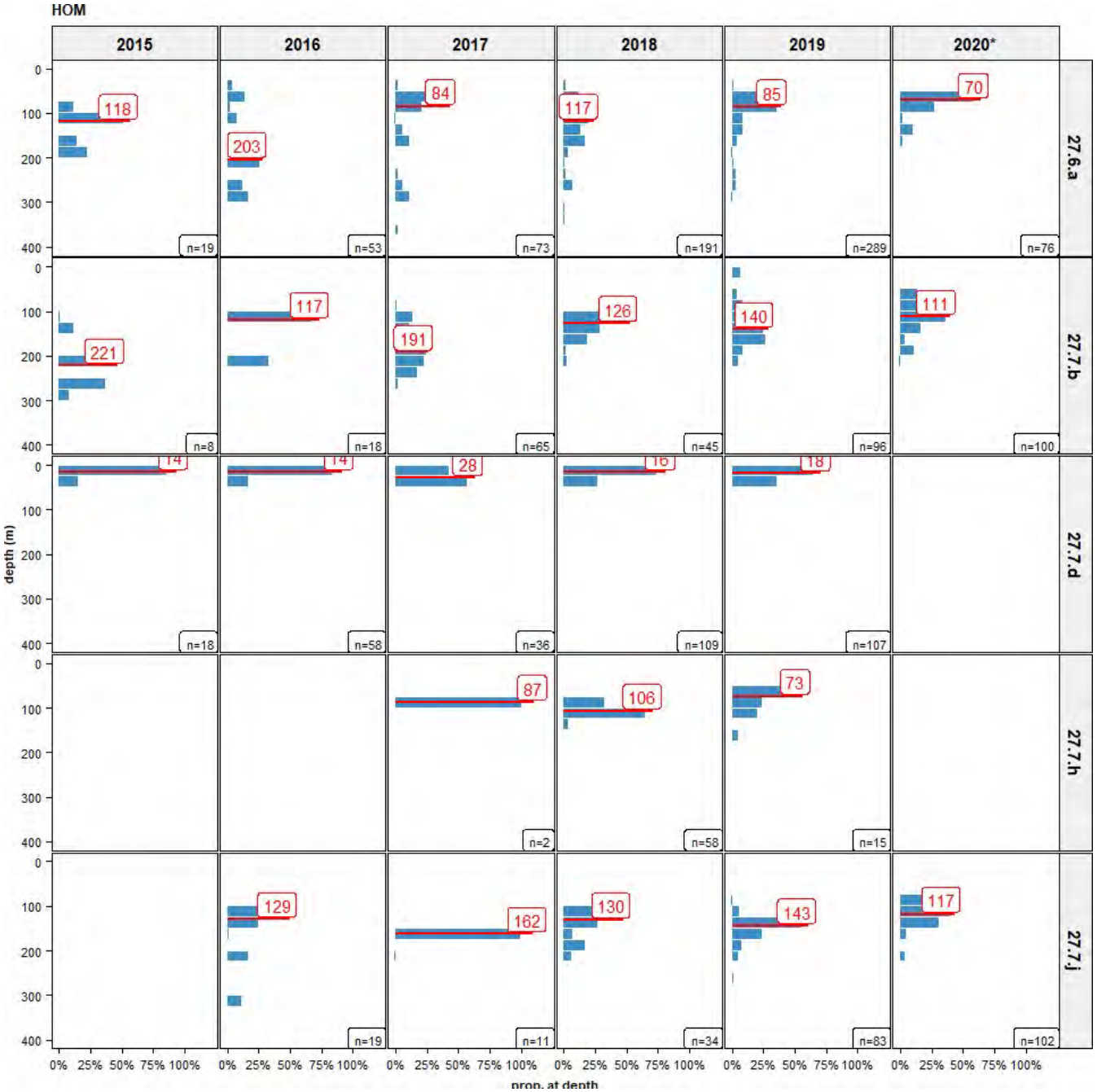

*Figure 3.3.8: Horse mackerel. Depth distributions by year and division. N is number of observations; median depth in red; * denotes incomplete year*

3.4 Blue whiting (WHB, Micromesistius poutassou)

The blue whiting fishery takes place from February through to May although some minor fisheries for blue whiting may remain over the other months. Overall, the self-sampling activities for the blue whiting fisheries during the years 2015 – 2020 (up to August) covered 365 fishing trips with 5,836 hauls, a total catch of 561,888 tonnes and 128,000 individual length measurements. The main fishing areas are ICES division 27.6.a (between 41% and 65% of the catch), division 27.7.c (6%-36%) and division 27.7.k (2%-32%).

species	division	year	nvessels	ntrips	ndays	nhauls	catch	catchperc	catch/day	nlength
whb	27.6.a	2015	3	7	55	127	7,377	47	134	9,384
whb	27.6.a	2016	4	11	89	206	20,300	41	228	13,397
whb	27.6.a	2017	7	16	163	378	39,085	50	240	36,456
whb	27.6.a	2018	12	29	340	860	91,738	56	270	74,164
whb	27.6.a	2019	14	35	310	724	75,757	65	244	37,899
whb	27.6.a	2020*	12	32	287	744	78,067	56	272	66,432
whb	27.7.c	2015	2	4	13	22	889	6	68	0
whb	27.7.c	2016	4	8	37	66	5,472	11	148	6,283
whb	27.7.c	2017	6	10	97	231	28,230	36	291	16,945
whb	27.7.c	2018	6	9	77	235	30,504	19	396	21,392
whb	27.7.c	2019	10	16	99	246	26,587	23	269	14,222
whb	27.7.c	2020*	10	16	128	327	44,639	32	349	42,790
whb	27.7.k	2015	3	3	24	56	4,973	32	207	11,216
whb	27.7.k	2016	3	3	29	77	7,489	15	258	6,993
whb	27.7.k	2018	3	3	20	59	7,646	5	382	3,077
whb	27.7.k	2019	4	4	11	17	2,036	2	185	401
whb	27.7.k	2020*	4	4	34	90	10,961	8	322	10,401
whb	27.5.b	2015	2	3	20	28	1,872	12	94	7,287
whb	27.5.b	2016	3	4	29	57	5,577	11	192	4,685
whb	27.5.b	2017	5	6	40	64	7,960	10	199	8,226
whb	27.5.b	2018	5	7	52	82	7,928	5	152	5,204
whb	27.5.b	2019	4	8	26	34	3,906	3	150	2,331
whb	27.5.b	2020*	2	2	6	7	798	1	133	1,014
whb	27.2.a	2015	3	3	11	20	96	1	9	573
whb	27.2.a	2016	6	6	32	62	2,345	5	73	1,369
whb	27.2.a	2017	5	9	56	92	2,587	3	46	2,597
whb	27.2.a	2018	6	8	90	158	12,032	7	134	12,352
whb	27.2.a	2019	4	7	61	130	1,417	1	23	1,640
whb	27.2.a	2020*	1	1	8	18	2,032	1	254	2,876
whb	other	2015	4	11	32	52	339	2	11	0
whb	other	2016	6	12	55	105	8,196	17	149	6,614
whb	other	2017	6	9	44	76	941	1	21	577
whb	other	2018	11	20	65	128	12,693	8	195	10,087
whb	other	2019	14	25	100	167	5,969	5	60	10,524
whb	other	2020*	9	15	61	95	3,452	2	57	4,958
whb	(all)	2015		31	155	305	15,546	100	100	28,460
whb	(all)	2016		44	271	573	49,379	100	182	39,341
whb	(all)	2017		50	400	841	78,803	100	197	64,801
whb	(all)	2018		76	644	1,522	162,541	100	252	126,276
whb	(all)	2019		95	607	1,318	115,672	99	191	67,017
whb	(all)	2020*		70	524	1,281	139,949	100	267	128,471
whb	(all)	(all)		366	2,601	5,840	561,890		216	454,366

*Table 3.4.1: Blue whiting. Self-sampling summary with the number of days, hauls, trips, vessels, catch (tonnes), number of fish measured, catch rates (ton/effort). * denotes incomplete year*

Blue whiting (WHB). Catch by month

species	month	2015	2016	2017	2018	2019	2020*	all	perc
whb	Jan	24	112	211	956	4,286	9,526	15,115	2.69%
whb	Feb	5,108	1,994	7,693	19,108	17,700	4,050	55,653	9.91%
whb	Mar	867	15,562	24,696	35,934	23,289	42,848	143,196	25.49%
whb	Apr	5,594	13,745	27,316	56,296	26,395	61,755	191,101	34.01%
whb	May	2,202	6,170	9,395	26,731	17,341	20,828	82,667	14.71%
whb	Jun	942	696	0	5,094	13	878	7,623	1.36%
whb	Jul	693	10	0	0	133	61	897	0.16%
whb	Aug	0	0	1,265	4,218	337	0	5,820	1.04%
whb	Sep	13	50	537	413	463	0	1,476	0.26%
whb	Oct	97	316	76	217	1,993	0	2,699	0.48%
whb	Nov	0	3,005	5,934	6,618	14,085	0	29,642	5.28%
whb	Dec	1	7,712	1,674	6,951	9,631	0	25,969	4.62%
whb	(all)	15,541	49,372	78,797	162,536	115,666	139,946	561,858	100.00%

*Table 3.4.2: Blue whiting. Self-sampling summary with the catch (tonnes) by year and month. * denotes incomplete year*

Blue whiting (WHB). Catch by rectangle

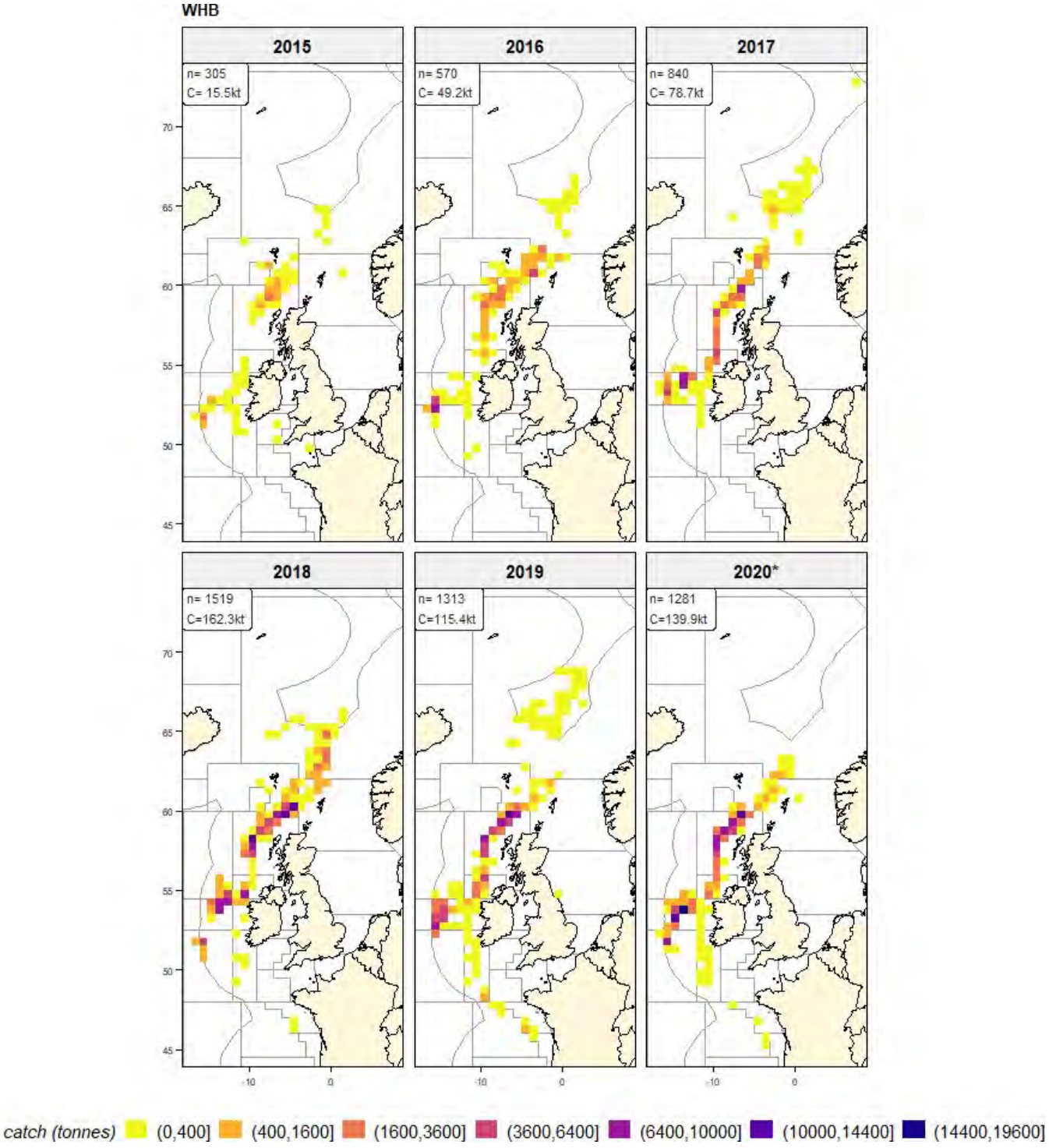

*Figure 3.4.1: Blue whiting. Catch per per rectangle. N indicates the number of hauls; Catch refers to the total catch per year. * denotes incomplete year*

Blue whiting (WHB). Average catch per day

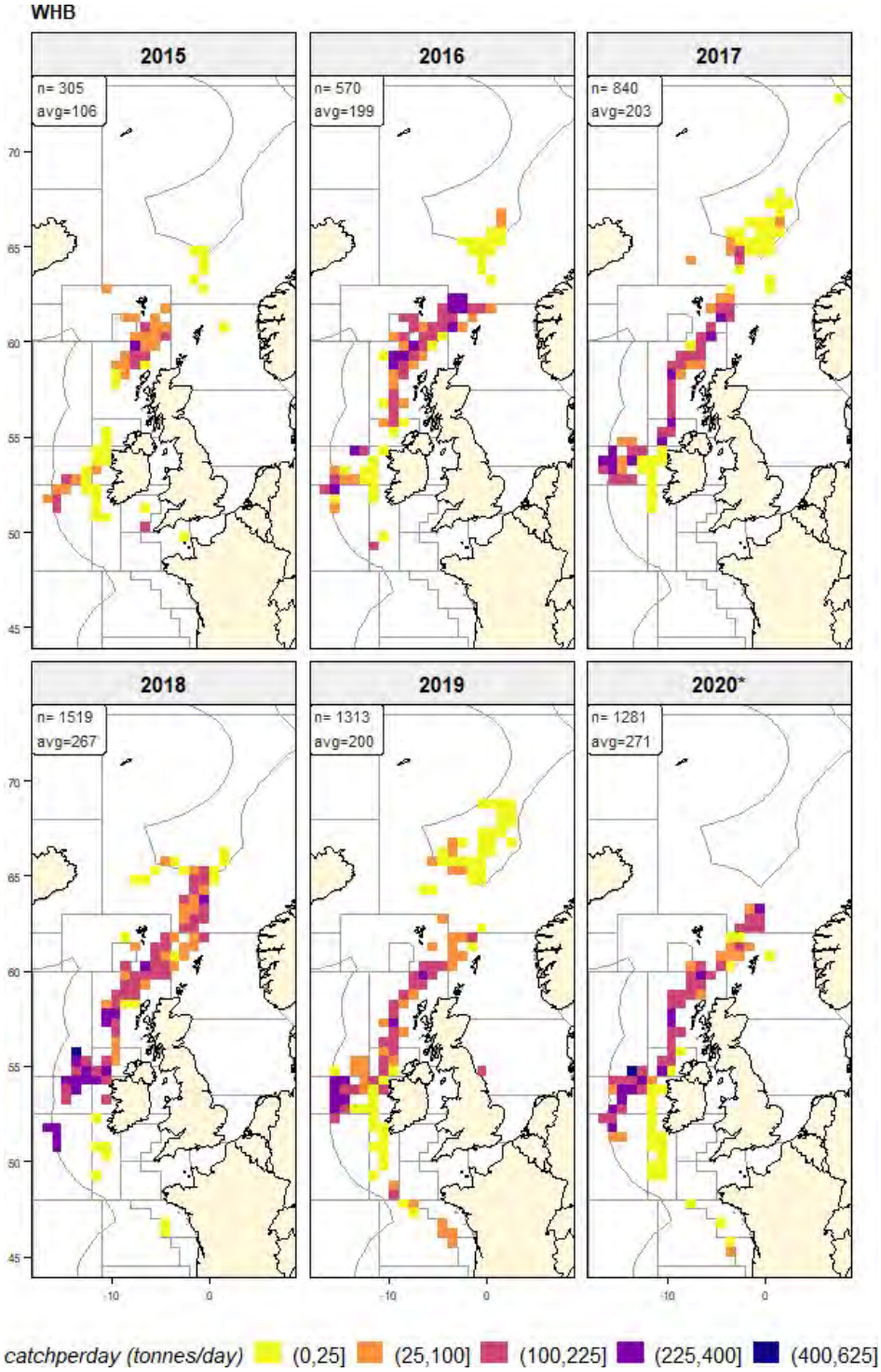

*Figure 3.4.2: Blue whiting. Average catch per day per rectangle. N indicates the number of hauls; avg refers to the overall average catch per day. * denotes incomplete year*

Blue whiting (WHB). Spatial-temporal evolution of the fishery

Spatial-temporal evolution of the fishery by year and month from the haul-by-haul catch information. Fishing season is from February until May. The midpoint of the distribution is indicated by the blue triangle. The catch has been used as weighting factor in the calculation of the midpoint.

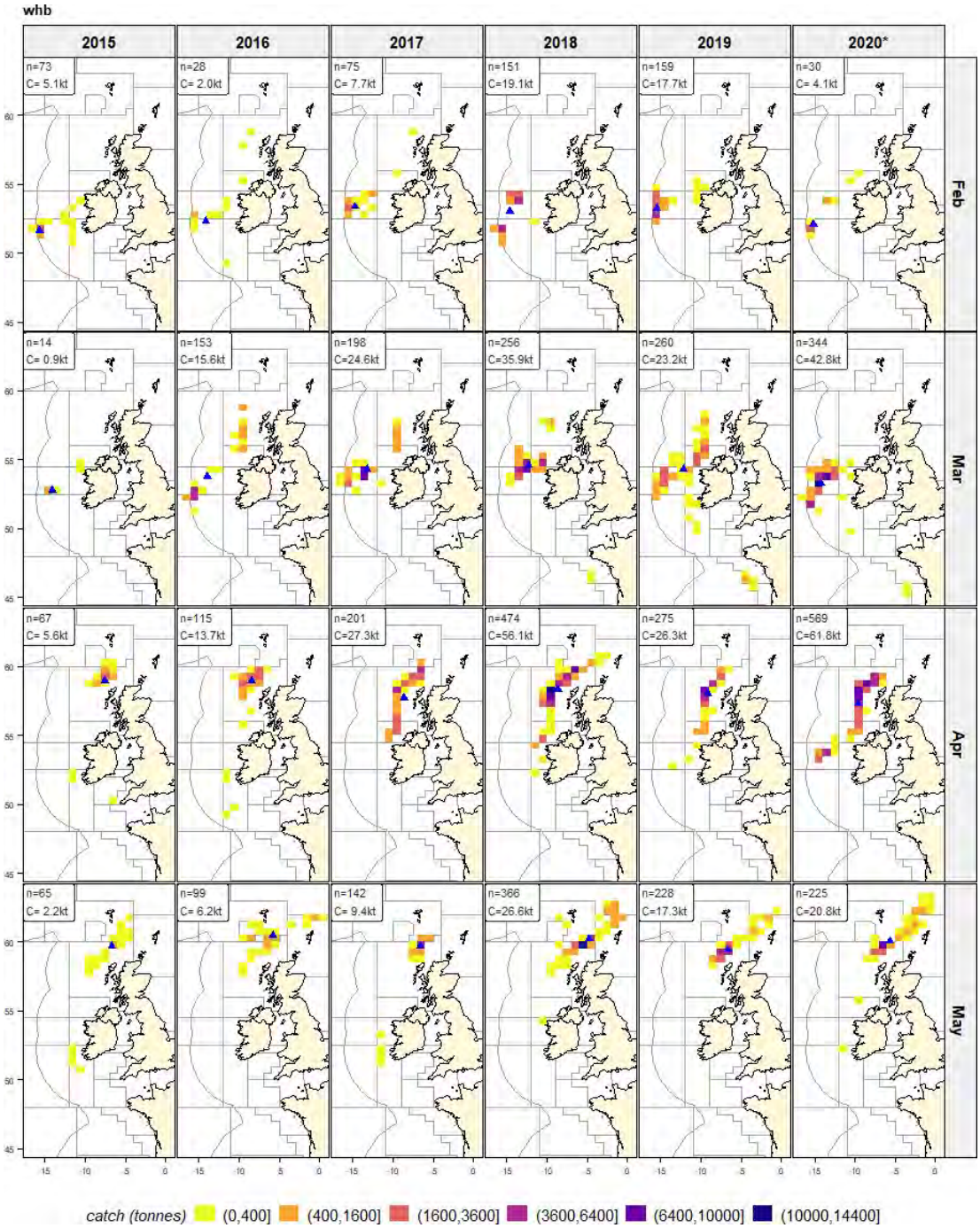

*Figure 3.4.3: Blue whiting. Average catch per day per rectangle. N indicates the number of hauls; avg refers to the overall average catch per day. * denotes incomplete year*

Blue whiting (WHB). Length distributions of the catch

Blue whiting have a wide range in the length distributions in the catch. Median lengths have fluctuated between 23 cm (2016) and 30 cm (2015). During the period 2016 - 2020, the median length is consistently increasing (from 23 to 28 cm), indicating that the fishery is probably concentrating on a strong year class going without new year classes coming in.

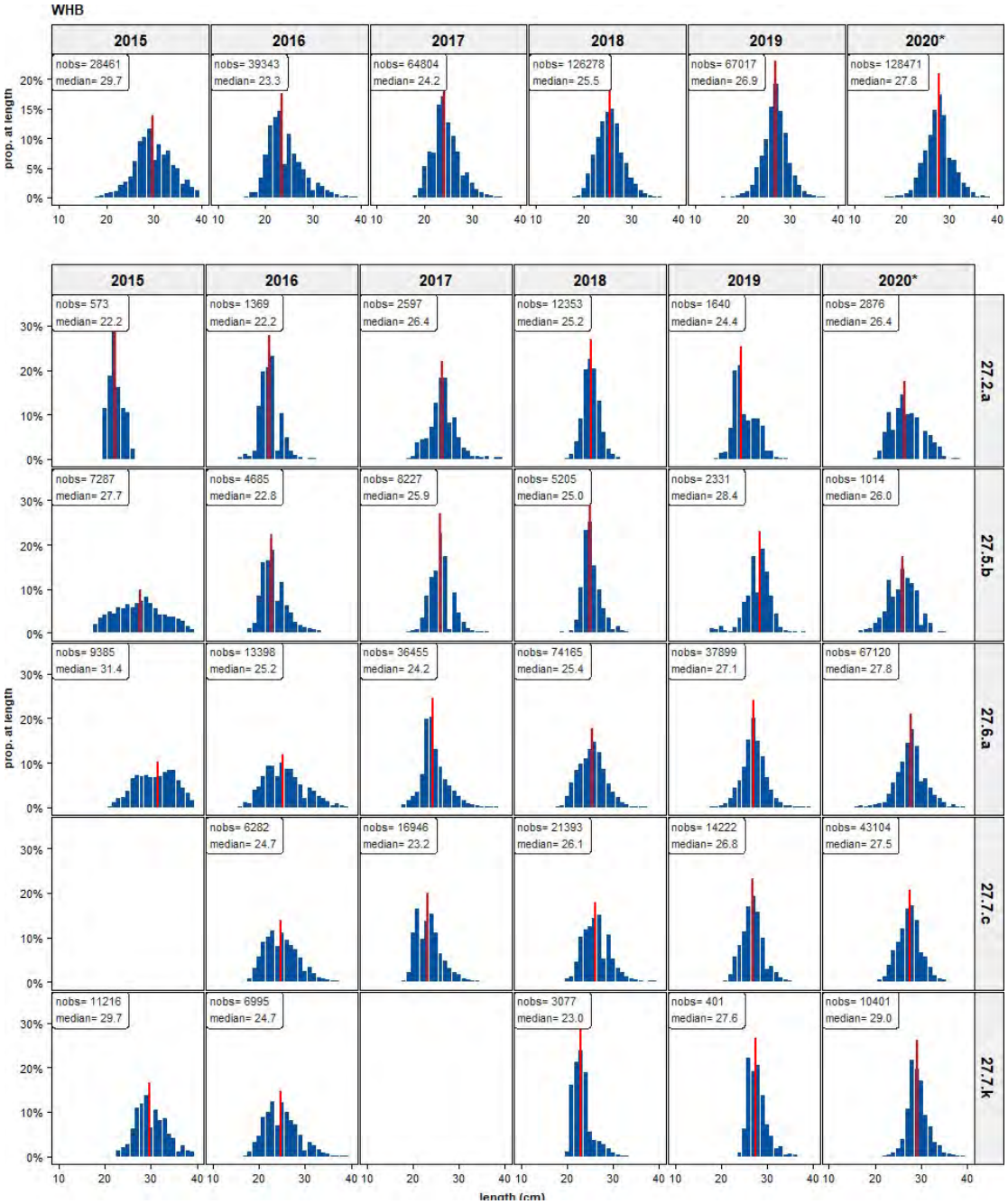

*Figure 3.4.4: Blue whiting. Length distributions by year (top) and by year and division (bottom). Nobs refers to the number of observations; median denotes the median length. * denotes incomplete year*

Blue whiting (WHB). Length frequencies by year and quarter

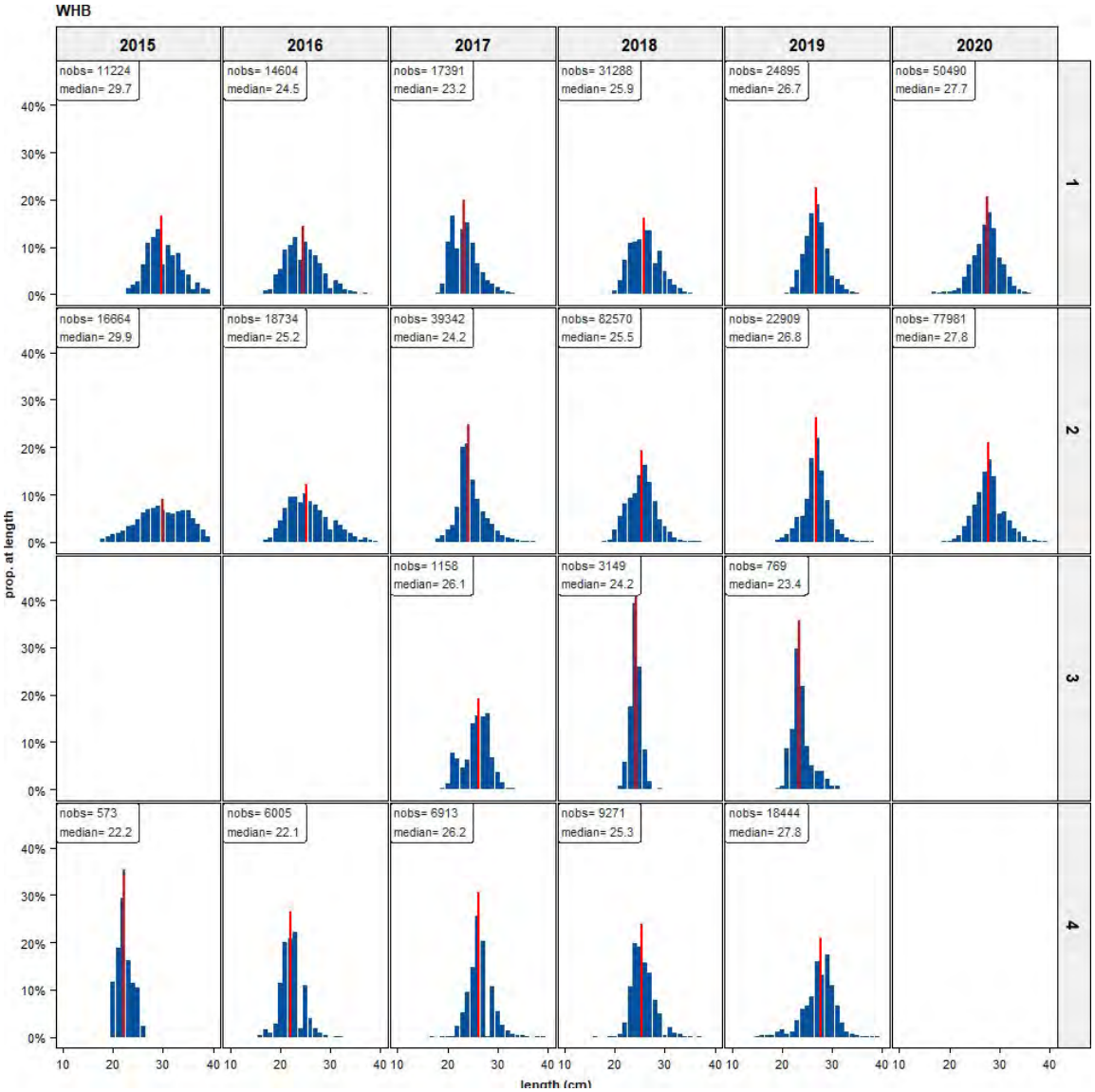

Figure 3.4.5: Blue whiting. Length distributions by year (top) and by year and division (bottom). Nobs refers to the number of observations; median denotes the median length

Blue whiting (WHB). Weight distributions

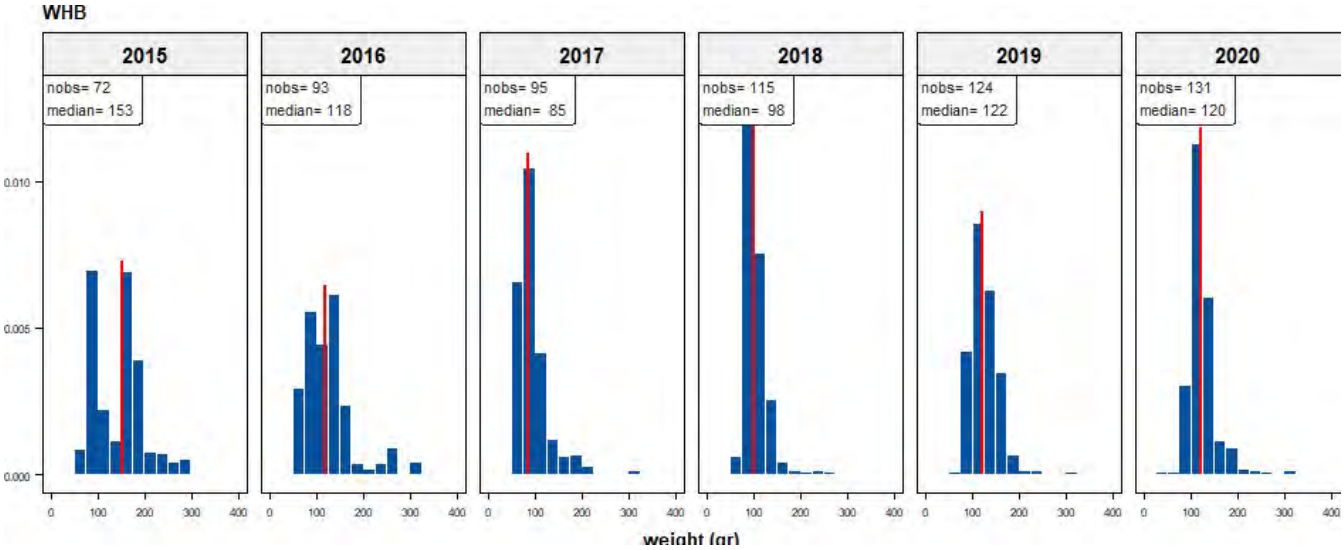

*Figure 3.4.6: Blue whiting. Weight distributions (25 gram classes). Nobs refers to the number of batches where average weight was measured; median denotes the median length; * denotes incomplete year*

Blue whiting (WHB). Fat percentages by year

Fat content for blue whiting is generally low (on average less than 1%)

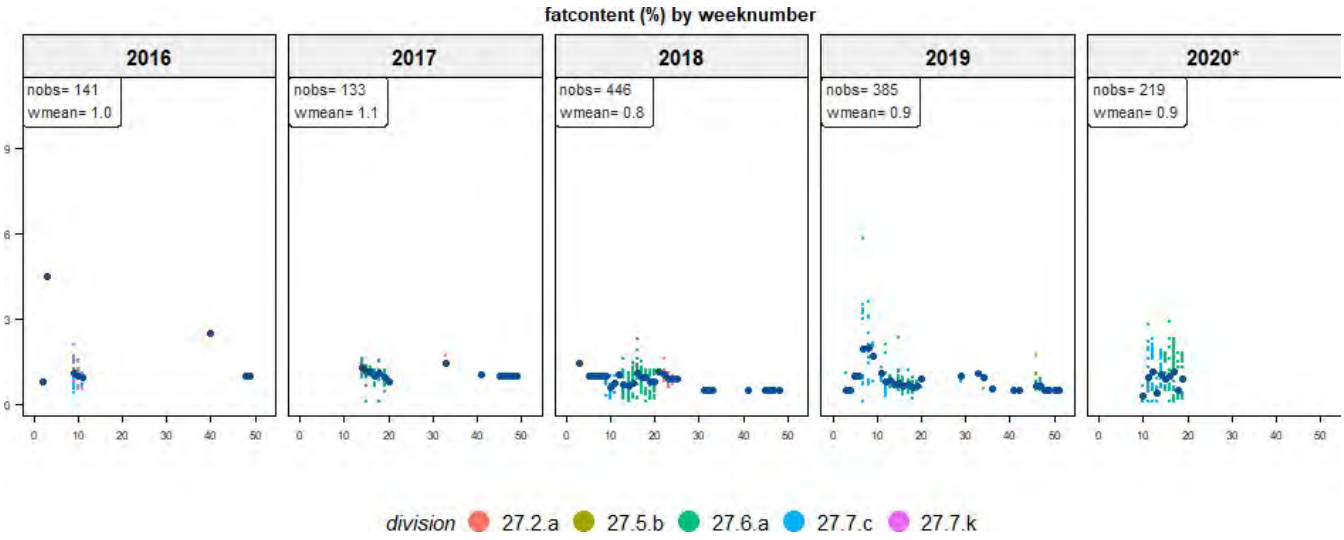

*Figure 3.4.7: Blue whiting. Average fat percentage by week. Nobs refers to the number of batches where average fat was measured; Wmean refers to the weighted mean fat content. Blue dots indicate the weekly averages; * denotes incomplete year*

Blue whiting (WHB). Fishing depth distributions.

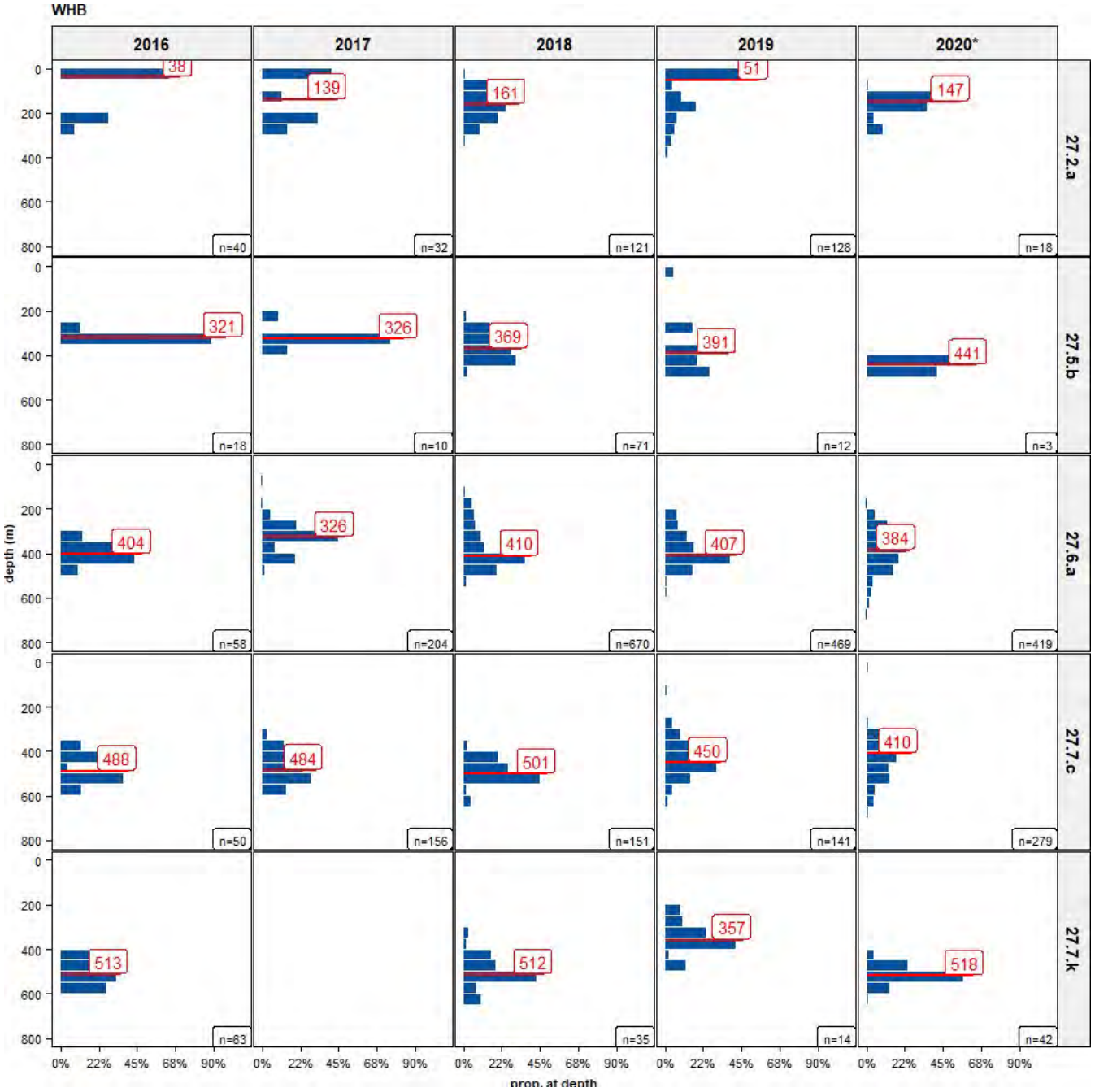

*Figure 3.4.8: Blue whiting. Depth distributions by year and division. N is number of observations; median depth in red; * denotes incomplete year*

3.5 Herring 'Atlanto scandian' (HER_ASH, Clupea harengus)

The fishery for Atlanto-Scandian herring (ASH) is a relatively smaller fishery for PFA and takes place mostly in October. Overall, the self-sampling activities for the ASH fisheries during the years 2015 – 2020 (up to August) covered 27 fishing trips with 406 hauls, a total catch of 30,234 tonnes and 8,918 individual length measurements. Only the herring fishery in ICES division 27.2.a is considered for ASH. Note that there are herring catches in other divisions within the selected trips. These are trips where North Sea herring has been fished with some bycatches of mackerel for example.

species	division	year	nvessels	ntrips	ndays	nhauls	catch	catchperc	catch/day	nlength
her_ash	27.2.a	2015	2	2	9	18	1,369	100	152	1,260
her_ash	27.2.a	2016	6	7	40	85	3,362	100	84	1,206
her_ash	27.2.a	2017	4	7	42	83	7,950	100	189	2,210
her_ash	27.2.a	2018	4	5	37	68	5,278	100	143	490
her_ash	27.2.a	2019	4	5	57	145	12,249	100	215	3,714
her_ash	27.2.a	2020*	1	1	5	7	26	100	5	38
her_ash	(all)	2015		2	9	18	1,369	100	152	1,260
her_ash	(all)	2016		7	40	85	3,362	100	84	1,206
her_ash	(all)	2017		7	42	83	7,950	100	189	2,210
her_ash	(all)	2018		5	37	68	5,278	100	143	490
her_ash	(all)	2019		5	57	145	12,249	100	215	3,714
her_ash	(all)	2020*		1	5	7	26	100	5	38
her_ash	(all)	(all)		27	190	406	30,234		159	8,918

*Table 3.5.1: Herring 'Atlanto scandian'. Self-sampling summary with the number of days, hauls, trips, vessels, catch (tonnes), number of fish measured, catch rates (ton/effort). Top: by year. * denotes incomplete year*

Herring 'Atlanto scandian' (HER_ASH). Catch by month

species	month	2015	2016	2017	2018	2019	2020*	all	perc
her_ash	May	0	0	0	0	0	26	26	0.09%
her_ash	Aug	0	0	118	51	0	0	169	0.56%
her_ash	Sep	0	53	6	405	361	0	825	2.73%
her_ash	Oct	1,369	3,308	7,825	4,820	8,066	0	25,388	83.99%
her_ash	Nov	0	0	0	0	3,821	0	3,821	12.64%
her_ash	(all)	1,369	3,361	7,949	5,276	12,248	26	30,229	100.00%

*Table 3.5.2: Herring 'Atlanto scandian'. Self-sampling summary with the catch (tonnes) by year and month. * denotes incomplete year*

Herring 'Atlanto scandian' (HER_ASH). Catch by rectangle

*Figure 3.5.1: Herring 'Atlanto scandian'. Catch per per rectangle. N indicates the number of hauls; Catch refers to the total catch per year. * denotes incomplete year*

Herring 'Atlanto scandian' (HER_ASH). Average catch per day

*Figure 3.5.2: Herring 'Atlanto scandian'. Average catch per day per rectangle. N indicates the number of hauls; avg refers to the overall average catch per day. * denotes incomplete year*

Herring 'Atlanto scandian' (HER_ASH). Spatial-temporal evolution of the fishery

Spatial-temporal evolution of the fishery by year and month from the haul-by-haul catch information. Fishing season is from September until November. The midpoint of the distribution is indicated by the blue triangle. The catch has been used as weighting factor in the calculation of the midpoint.

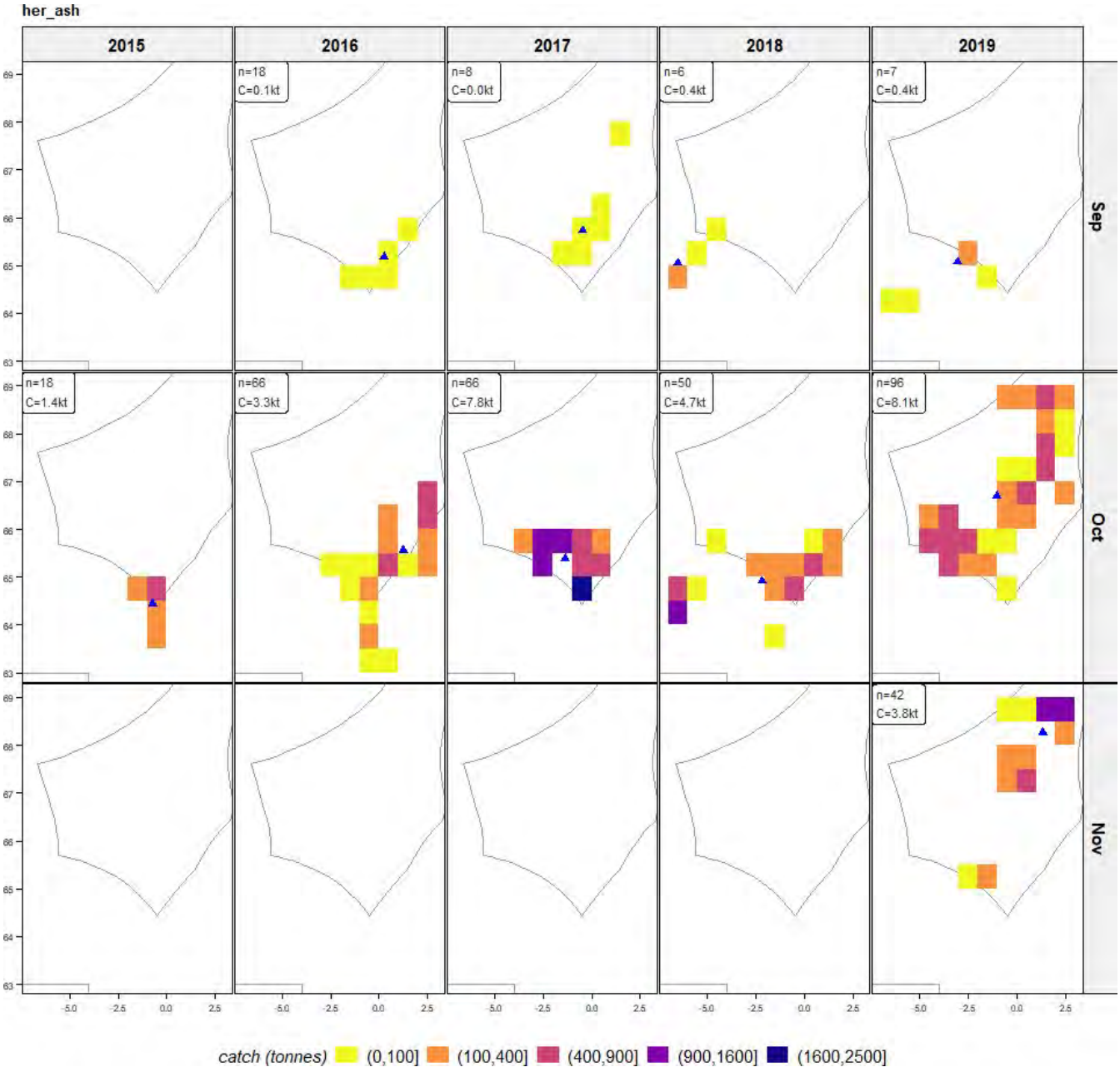

*Figure 3.5.3: Herring 'Atlanto scandian'. Average catch per day per rectangle. N indicates the number of hauls; avg refers to the overall average catch per day. * denotes incomplete year*

Herring 'Atlanto scandian' (HER_ASH). Length distributions of the catch

Atlanto-Scandian herring have a narrow range in the length distributions in the catch. Median lengths have fluctuated between 32 and 36 cm. No data is available yet from the autumn 2020 fishery.

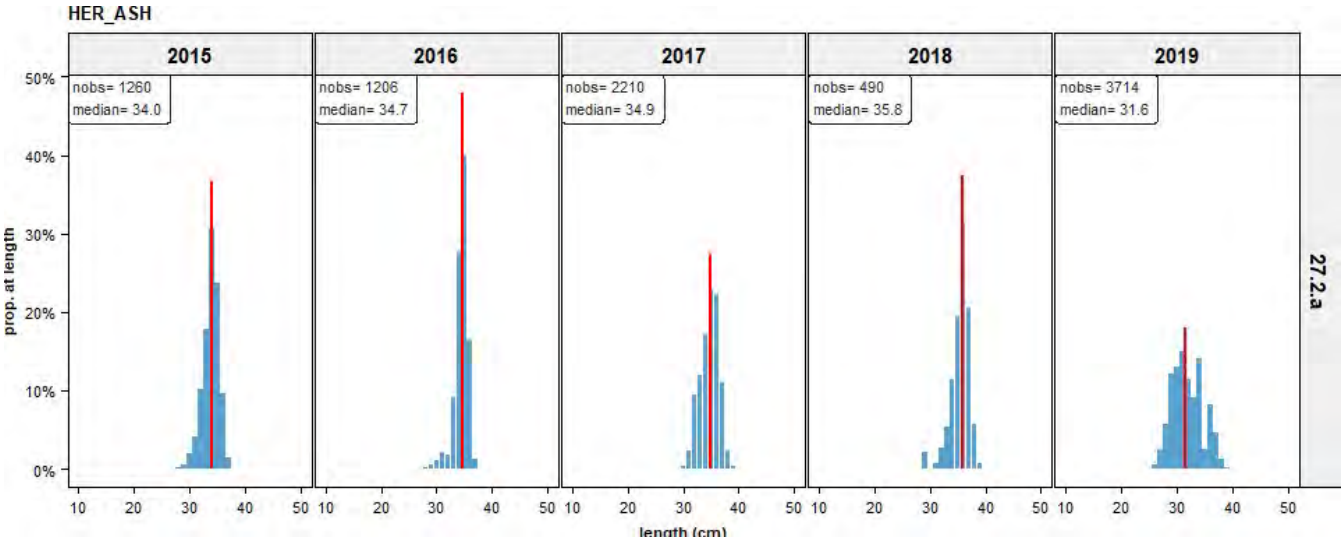

*Figure 3.5.4: Herring 'Atlanto scandian'. Length distributions by year (top) and by year and division (bottom). Nobs refers to the number of observations; median denotes the median length. * denotes incomplete year*

Herring 'Atlanto scandian' (HER_ASH). Length frequencies by year and quarter

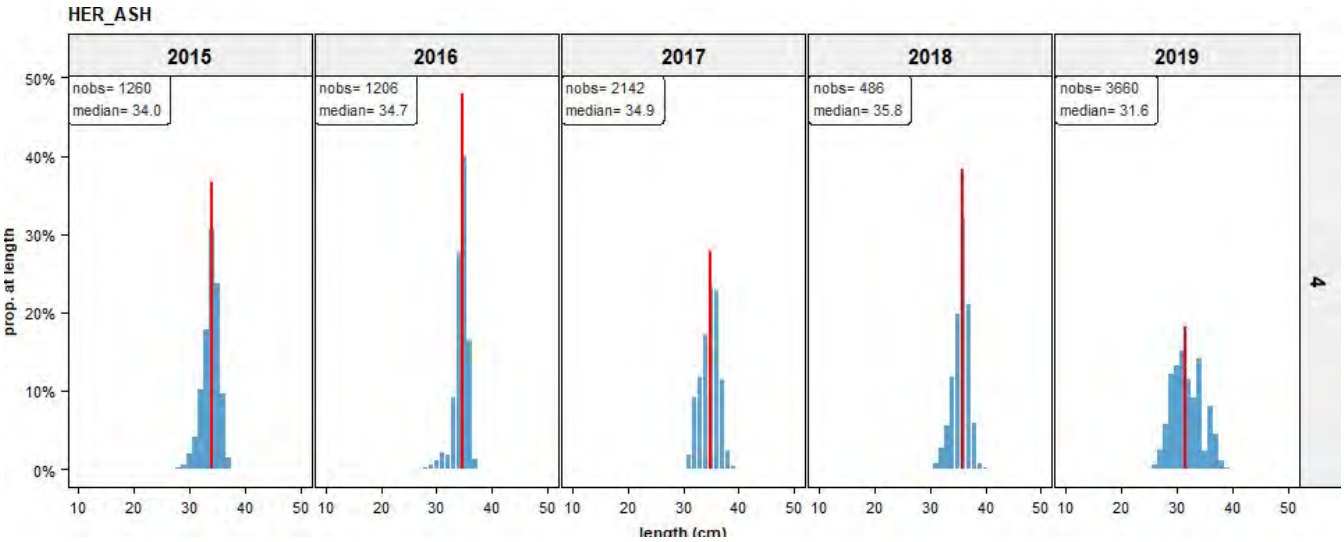

Figure 3.5.5: Herring 'Atlanto scandian'. Length distributions by year (top) and by year and division (bottom). Nobs refers to the number of observations; median denotes the median length

Herring 'Atlanto scandian' (HER_ASH). Weight distributions

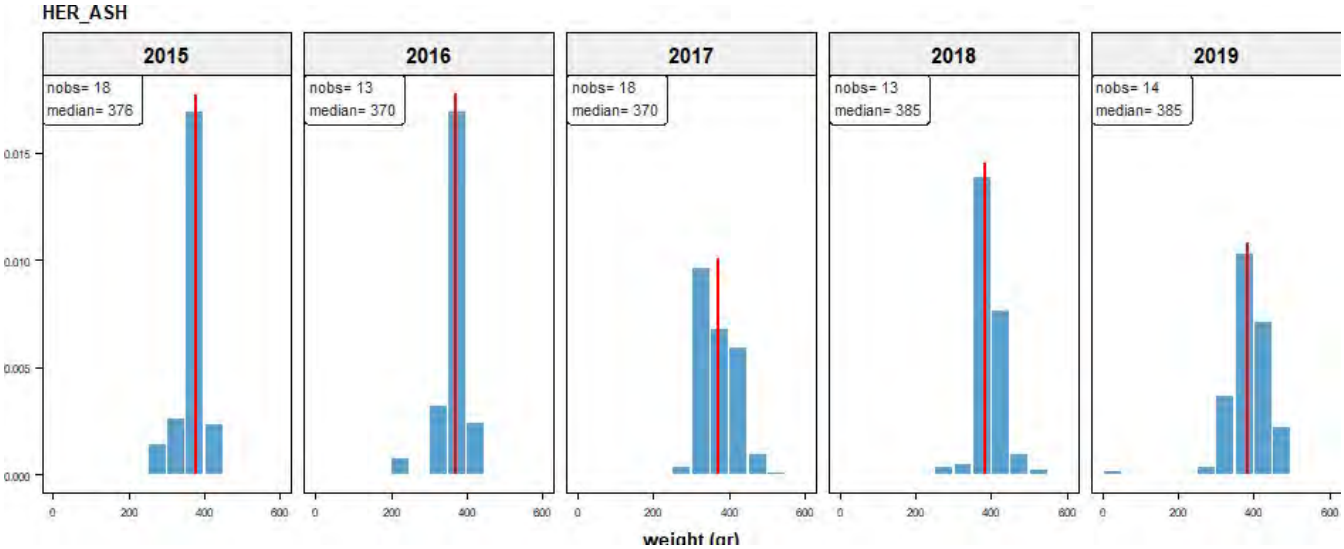

*Figure 3.5.6: Herring 'Atlanto scandian'. Weight distributions (50 gram classes). Nobs refers to the number of batches where average weight was measured; median denotes the median length; * denotes incomplete year*

Herring 'Atlanto scandian' (HER_ASH). Fat percentages by year

Average annual fat content for ASH has been between 17 and 20% with individual measurements going up to 25%)

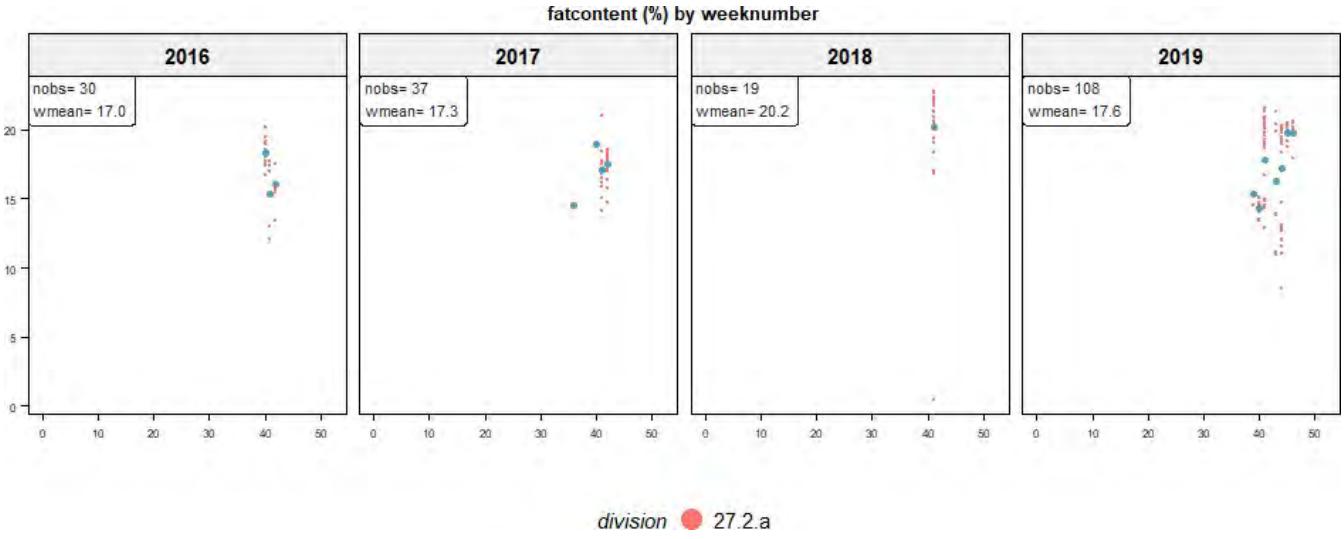

*Figure 3.5.7: Herring 'Atlanto scandian'. Average fat percentage by week. Nobs refers to the number of batches where average fat was measured; blue dots indicate the weekly averages; * denotes incomplete year*

Herring 'Atlanto scandian' (HER_ASH). Fishing depth distributions.

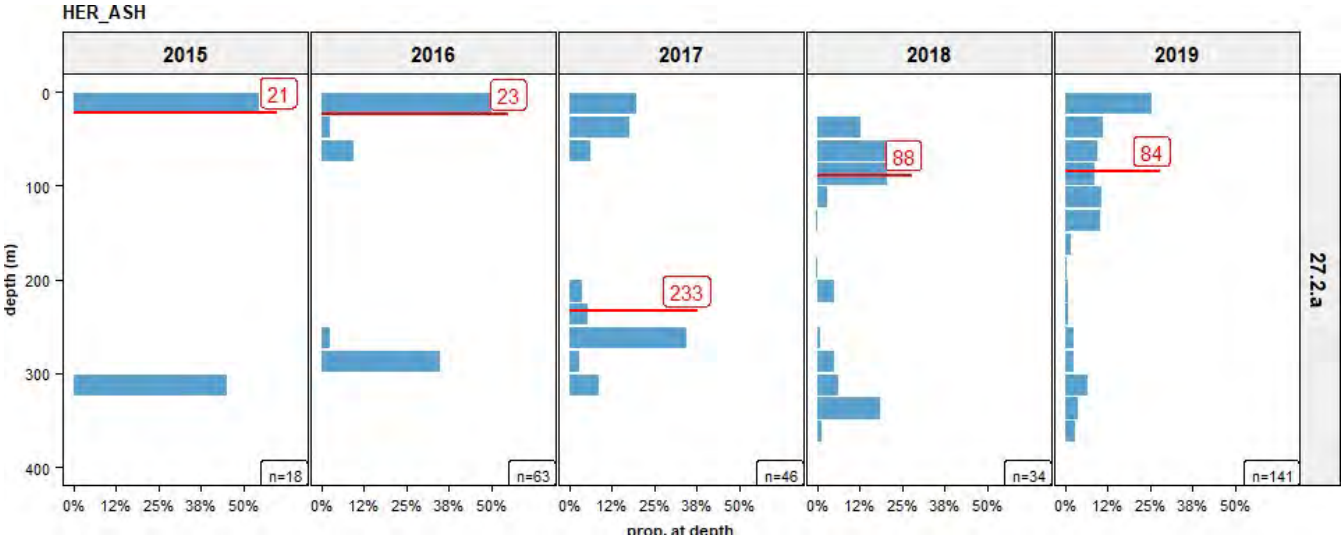

*Figure 3.5.8: Herring 'Atlanto scandian'. Depth distributions by year and division. N is number of observations; median depth in red; * denotes incomplete year*

4 Discussion and conclusions

The PFA self-sampling programme has been carried out for the sixth year in a row (2015-2020). The results are presented in terms of meta-information on the sampling (number of vessels, trips, days and length measurements per area and/or season), in terms of the spatio-temporal distribution of catches and the length and weight compositions by area and/or season.

The definition of what constitutes 'a fishery' for a certain species is still not well specified. In this report we selected all combination of vessel-trip-week where hauls were taken in a certain area and where the catch composition consisted of a minimum percentage of certain species and a minimum catch of 10 tons. Although for herring we aimed to select only trips for Atlanto-scandian herring (in division 27.2.a) some trips with North Sea herring have been included because they were combined with some fishing for mackerel.

The Mackerel fishery takes place from October through to March of the subsequent year. Minor bycatches of mackerel may also occur during other fisheries. Overall, the self-sampling activities for the mackerel fisheries during the years 2015 – 2020 (up to August) covered 323 fishing trips with 4,725 hauls, a total catch of 286,957 tonnes and 91,000 individual length measurements. The main fishing areas are ICES division 27.4.a (between 27 and 54% of the catch) and division 27.6.a (between 25 and 44% of the catch). Compared to the previous years, mackerel in the catch have been relatively large in 2020 with median length of 36.4 cm compared to 32.4-35.4 in the preceding years. Also, the median weight has been somewhat higher with median weight of 417 gram compared to 379-400 gram the preceding years. Average annual fat content ranges from 17 to 21% with individual measurements reaching up to 30%.

The horse mackerel fishery takes place from October through to March of the subsequent year. Overall, the self-sampling activities for the horse mackerel fisheries during the years 2015 – 2020 (up to August) covered 457 fishing trips with 3,454 hauls, a total catch of 140,633 tonnes and 125,000 individual length measurements. The main fishing areas are ICES division 27.6.a (between 21% and 40% of the catch), division 27.7.b (7%-22%) and division 27.7.d (19%-34%, note that this is considered as the North Sea horse mackerel stock). Horse mackerel have a wide range in the length distributions in the catch. Median lengths have fluctuated between 22.8 and 30.0 cm. In 2019 and 2020 there are some indications of a stronger year class being available to the fishery, with a more narrow length distribution. For example, in 27.6.a the mode was 26.6 cm in 2019 and 27.5 cm in 2020. Average annual fat content ranges from 5 to 7.5% with individual measurements reaching up to 15%.

The blue whiting fishery takes place from February through to May although some minor fisheries for blue whiting may remain over the other months. Overall, the self-sampling activities for the blue whiting fisheries during the years 2015 – 2020 (up to August) covered 365 fishing trips with 5,836 hauls, a total catch of 561,888 tonnes and 128,000 individual length measurements. The main fishing areas are ICES division 27.6.a (between 41% and 65% of the catch), division 27.7.c (6%-36%) and division 27.7.k (2%-32%). Blue whiting have a wide range in the length distributions in the catch. Median lengths have fluctuated between 23 cm (2016) and 30 cm (2015). During the period 2016 - 2020, the median length is consistently increasing (from 23 to 28 cm), indicating that the fishery is probably concentrating on a strong year class going without new year classes coming in. Fat content for blue whiting is generally low (on average less than 1%).

The fishery for Atlanto-Scandian herring (ASH) is a relatively smaller fishery for PFA and takes place mostly in October. Overall, the self-sampling activities for the ASH fisheries during the years 2015 – 2020 (up to August) covered 27 fishing trips with 406 hauls, a total catch of 30,234 tonnes and 8,918 individual length measurements. Only the herring fishery in ICES division 27.2.a is considered for ASH. Note that there are herring catches in other divisions within the selected trips. These are trips where North Sea herring has been fished with some bycatches of mackerel for example. Atlanto-Scandian herring have a narrow range in the length distributions in the catch. Median lengths have fluctuated between 32 and 36 cm. Average annual fat content for ASH has been between 17 and 20% with individual measurements going up to 25%).

5 Acknowledgements

The skippers, officers and the quality managers of many of the PFA vessels have put in a lot of effort to make the PFA the self-sampling work. Without their efforts, there would be no self-sampling.

6 More information

Please contact Martin Pastoors (mpastoors@pelagicfish.eu) if you would have any questions on the PFA self-sampling programme or the specific results presented here. Detailed length compositions (e.g. CSV files) can also be made available on request.

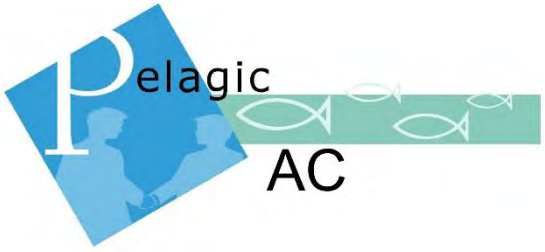

WESTERN HORSE MACKEREL TECHNICAL FOCUS GROUP ON HARVEST CONTROL RULE EVALUATIONS 2020

M.A. Pastoors, A. Campbell, V. Trijoulet, D. Skagen, M. Gras, G.I. Lambert, C.R. Sparrevohn, S. Mackinson

14/8/2020

Contents

The Western horse mackerel technical Focus Group consisted of the following members:

Martin Pastoors, PFA (acting chair)

Andrew Campbell, MI, Ireland

Vanessa Trijoulet, DTU-AQUA, Denmark

Dankert Skagen, Fisheries Science Consultant, Norway

Michael Gras, MI, Ireland

Gwladys Lambert, CEFAS, England

Claus Sparrevohn, DPPO, Denmark

Steve Mackinson, SPFA, Scotland

The group met during the period June 2019 – August 2020 to collate information, carry out analyses and report findings that are embedded in the current report.

Executive summary

This report has brought together many different topics that are related to the western horse mackerel stock in an attempt to develop a potential rebuilding plan for the stock. Even though western horse mackerel was not classified by ICES as in need of rebuilding in their latest advice (ICES, 2019a), the general perception within the fishing industries has been that the stock has been in a poor state but that there have been some positive signals in recent recruitment. Using the new recruitments to improve the stock status requires a careful management approach. The PELAC has been a proponent of developing management plans for all stocks in their remit. In this case, the PELAC has termed the approach a rebuilding plan because of the current stock status of the stock.

Substantial progress has been made over the past few years on horse mackerel stock ID (Farrell et al., 2020). The full genome sequencing of horse mackerel from samples taken all the way from the Skagerrak to the Mediterranean and North Africa, has yielded a suitable panel of SNP markers that can be used to differentiate between the different horse mackerel stocks. The strongest differentiation between populations was between the northern and southern populations, with the boundary being in the middle of Portugal. The North Sea population is clearly distinct from the Western population and it should be possible to tell the difference from mixed samples with a high probability (>93%). This would also allow screening of catches in 7d and 7e on the contribution of western and North Sea populations. The separation between the northern and southern populations could mean that the current division between western and southern horse mackerel is not adequate, as the northern part of 9a is currently included in the southern population. A similar split in the middle of Portugal has also been observed for boarfish (Farrell et al., 2016) and could indicate a biogeographical feature.

Length compositions of the catches are an important element of the assessment approach for western horse mackerel, because Stock Synthesis uses length composition in combination with age-length key to estimate the age compositions within the model. Part of a rebuilding plan for western horse mackerel could be to evaluate differences in length compositions in the catches in certain areas and to take specific measures to protect incoming recruitment. Therefore, we planned to carry out an analysis of length compositions by area and season. However, we found that such data is not currently available for all years. Length data for western horse mackerel is currently not included in the ICES InterCatch database. Instead, length data has been processed on a year by year basis in non-standardized Excel spreadsheets. A time series of length compositions by area and season can therefore only be derived by manually working through the spreadsheets and extracting the required information. This was not feasible as part of the project to develop and evaluate a rebuilding plan for western horse mackerel. We recommend to WGWIDE that the full time series of catch at length by country is recreated from the Excel spreadsheets and input into InterCatch to allow for future interrogations of the data and an underpinning of the input data to the stock assessment.

In order to understand how a stock would respond to recovery measures, it is useful to consider the age composition in the spawning stock which illustrates how recruitment in the previous years contributed to the present spawning stock. To this end, an SSB per recruit analysis has been carried out. As one should expect for a relatively long-lived species with low mortality, the spawning stock is currently rather old. At F =0.075, the mean age is about 9 years, 80% is older than 5 years and 20% older than 12 years. So, an improved recruitment will take some time to materialize as increased SSB.

The current stock assessment method for western horse mackerel is Stock Synthesis 3, as agreed in the WKWIDE benchmark of 2017 (ICES, 2017b). Reference point were also set at WKWIDE 2017 but have subsequently been updated in the IBPWHM 2019 (ICES, 2019b). In addition, an exploratory SAM assessment has been carried out as part of IBPWHM 2019. This was done in order to get a second view on stock trends but also to be able to run the SAM HCR forecast as part of the development of a potential rebuilding plan. The exploratory SAM assessment (https://www.stockassessment.org/setStock.php?stock=WHOM2018) was initiated with the same input data as was used for the Stock Synthesis assessment of WGWIDE 2018 (ICES, 2018) with the exception of the length frequency data, which was not used. The PELACUS survey data was therefore only used as an index of biomass within SAM. The process of fine-tuning the assessment lead to the binding of the observation variances for certain variables and to the application of a fixed selectivity pattern (correlation coefficient ϱ=1 in the F random process (https://github.com/martinpastoors/wgwide/blob/master/R/HOM%20optimization_SAM.R). A comparison of Fbar and SSB between the SS3 assessments of WG2018 and 2019 with the SAM assessment (WG18SAM, WG19SAM), shows that the general trends are the same but that there are some deviations in certain periods (e.g. the SSB in the late 1980s is estimated substantially higher in SAM compared to SS3). The Stock Synthesis results are in general a bit smoother compared to SAM.

In order to be able to use the SAM assessment as an alternative assessment in the rebuilding plan evaluation, we needed to estimate reference point for this assessment. In doing so, we aimed to follow the same procedure as during IBPWHM 2019 (ICES, 2019b). However, one of the elements of the reference point estimation, triggered a more in-depth study: the role of assessment uncertainty parameter Fcv and Fphi. There has been little standardization in how Fcv and Fphi have been calculated in different benchmarks where reference points were estimated. Fcv is expected to capture the assessment error in the advisory year and Fphi is the autocorrelation in assessment error in the advisory year (ICES, 2014a). We documented the method for generating the input data for the calculations and explored the sensitivity of Fcv and Fphi to the assessment that was used (both for western horse mackerel and for Atlantic mackerel). We found that there can be a high dependence of Fphi on the assessment that is used to compare against the Fset (the fishing mortalities that are back-calculated from the observed catches and the annual forecasts). When the assessment that is used has values that are all higher or lower than the Fset values, then Fphi will be close to zero. To our knowledge, this behaviour of Fphi was unknown so far. We also found that the number of years that is used for calculating Fcv and Fphi may have an impact on the values. In the recommendations from WKMSYREF3 it is stated that 10 years (or more) should be taken. A further study should be undertaken to assessment the impacts of using different time periods for estimating Fcv and Fphi.

During the IBPWHM 2019, reference points were estimated for western horse mackerel based on the 2018 WGWIDE assessment and using default values for Fcv and Fphi (0.212 and 0.423) and using a segmented regression through Blim (segregBlim). In order to calculate reference points for the exploratory SAM assessment and to explore the sensitivity to the assessment year, reference points were calculated on the basis of the 2018 or 2019 assessments for SS and SAM. The reference points for the SAM assessment are based on the 2018 assessment. Bpa and Blim are lower than the values for the SS assessment, while the Fmsy is higher. The calculated reference points were not sensitive to the assessmentyear that was used for the calculation for both the SS and SAM assessments.

Note that the calculated value for FMSY_final for the 2018 SS WGWIDE option (0.079) differs slightly from the value in IBPWHM 2019 (0.074). While a full explanation for

this difference could not be arrived at, it is expected that this could have to do with the random seed and the instability of some of the calculations.

RP	WG18	WG18SAM	WG19	WG19SAM
Blim	834480	611814	885341	612635
Flim	0.1107	0.1612	0.1049	0.1756
Fpa	0.07909	0.1152	0.07493	0.1254
MSYBtrigger	1168272	856540	1239478	857689
FMSY	0.09102	0.1262	0.08665	0.1353
FP05	0.08398	0.1255	0.07826	0.1402
FMSY_final	0.07909	0.1152	0.07493	0.1254

HCR evaluations

The HCR analyses represent two different assessment methods (SS3 and SAM) and two different HCR evaluation tools (EqSim and SAM HCR). Both HCR evaluation tools are of the type 'short-cut' with appropriate conditioning of the uncertainties in the assessment based on historical CV and autocorrelation in line with the recommendations from WKMSYREF3 and WKMSYREF4 . The evaluations followed the guidelines from WKGMSE2 (ICES, 2019c) and WKREBUILD (ICES, 2020).

Three different types of harvest control rules were evaluated:

- Constant F strategy: fixed Ftarget independent of biomass level
- ICES Advice Rule: breakpoint at Btrigger and straight decline in F to zero below Btrigger.
- Double Breakpoint rule: breakpoint at Btrigger and straight decline in F to 20% of Ftarget at Blim. Below Blim continued fishing at F = 0.2 * Ftarget.

For each of the HCRs, a number of different target fishing mortalities were explored (0.0, 0.05, 0.075, 0.1, 0.125, 0.15). No evaluation of different Btrigger values was carried out, so that all evaluations used MSY Btrigger as the trigger point. All HCRs where evaluated with three variants:

- Without any additional constraints
- With a minimum TAC of 50 kT
- With a maximum 20% inter-annual variation (IAV) in TAC, but only when the stock is above Btrigger)

Two simulation tools were used: the EqSim simulator and the SAM HCR forecast. The EqSim simulator is a further worked up version of the SimpSIM approach that was used for the blue whiting MSE in 2016 (ICES, 2016). The code was further developed by Andrew Campbell and Martin Pastoors to improve standardization, documentation and visualization of results. EqSim makes use of an Operating Model (OM) and a Management Procedure (MP). The SAM HCR forecast is a simple stochastic forecast with HCR to evaluate management for fish stocks that need rebuilding in the short-term. The stochastic forecasts start from what we believe is the current level of the stock, i.e. the assessment estimates currently used for tactical management advice, with consideration of the uncertainty in these estimates. Rebuilding is evaluated forward for a specified number of years and for different target fishing mortality values.

The EqSim with SS3 results indicate that the constant F strategy is the least cautious rule and the double breakpoint rule is the most cautious rule. Under the F strategy rule with a Ftarget of 0.075, rebuilding to Bpa is only just being achieved (probability just above 50%) by 2025, while in the double breakpoint rule this is expected to be achieved in 2024 with substantially higher probabilities of remaining above Bpa. The first year of rebuilding to Bpa in the double breakpoint rule with target fishing mortalities up to 0.1 is the same as the first year of rebuilding under the zero fishing scenarios.

Similar results have been obtained with the EqSim with SAM evaluations although the levels of SSB are slightly higher and risk to Blim is slightly lower. According to these evaluations, rebuilding to Bpa could be obtained by 2022 in all scenarios.

The SAM HCR with SAM evaluations have only been carried out for the ICES Advice Rule scenario, as this was intended more as a contrasting study rather than a full analysis of HCR evaluation. Again, we find similar patterns in simulated stock trends, but SSB is estimated higher in the SAM evaluation than in the EqSim evaluations and risk to Blim stays below the 0.05 threshold in SAM HCR for all target fishing mortalities that have been explored.

Given that the EqSim with SS3 evaluation is closest to the ICES advisory practice, this was used as the basis for the preferred rebuilding plan by the PELAC. The PELAC preferred options are:

- Target fishing mortality at Fmsy = 0.074 (approximated by 0.075 in the simulations)
- Blim at ICES Blim (834 480 t)
- Btrigger at ICES MSY Btrigger (1 168 272 t)
- Double breakpoint rule with 20% constraint on IAV above Btrigger
- Minimum F when stock is below Blim at 20% of Fmsy = 0.015

The selected rebuilding plan has a 50% probability of rebuilding to Blim by 2021 (similar to zero catch option) and a 50% probability of rebuilding to Bpa/MSY Btrigger by 2024 (similar to the zero-catch option). Furthermore, the probability of being below Blim remains well below 5% for the duration of the simulation.

In this scenario, the average catch in the years 2021-2025 is expected to be lower than recent catches. However, after rebuilding, catches should be able to be maintained around 100 000 tonnes.

1 Introduction

1.1 Challenge

The Western Horse mackerel Focus Group of the Pelagic Advisory Council (PELAC) has been set up in 2015 already to a develop a PELAC proposal for a rebuilding plan or management plan for Western Horse mackerel. After several iterations (see below), the Focus Group initiated a technical working group to develop an operational evaluation tools for management plan evaluation and to evaluate potential Harvest Control Rules, so that PELAC could come to a recommended procedure. Such a recommended procedure, including the evaluation that was carried out, would need to be submitted for review to ICES to establish whether the evaluation procedure is in line with scientific standards and that the results of the HCR are in conformity with the precautionary approach and the MSY approach.

1.2 What happened before

An overview is presented of the attempt to develop a management plan for Western horse mackerel in the ICES area. After an initial egg-survey based management rule had been agreed and evaluated in 2008 (ICES, 2008), the management plan was called into question in 2011 which lead to the statement by ICES in 2013 that the plan was no longer precautionary (ICES, 2013a). In the years 2014-2015, CEFAS and the Marine Institute were commissioned by the Pelagic Regional Advisory Committee to evaluate potential new management plans (Campbell et al., 2015). The SAD assessment that was used to assess the stock in those years, and that underpinned the MSEs for Western horse mackerel, was so uncertain, that the results were that in the case of no-fishing, the stock was expected to increase, but the uncertainty in the stock was also increasing, to the effect that the probability of being below B_{lim} was larger than 5% for the next 40 years to come. Apparently, the framing of those MSEs could not resolve to a meaningful and acceptable management plan.

A second iteration occurred after the stock had been benchmarked in 2017 and was using the Stock synthesis model for the assessment (ICES, 2017). Using the methods described by Cox et al. (Cox and Kronlund, 2008), a proof-of-concept full-feedback MSE[1] was commissioned with Landmark Fisheries Research, Canada (Cox et al., 2018). The evaluations were directed at different fishing strategies, including strategies where fishing would continue when the biomass would be below B_{lim}. The results of the analysis demonstrated a clear recovery potential of the stock under different fishing scenarios, mostly dependent on the recruitment assumptions and the target fishing mortality. However, the starting conditions of the simulated populations did not include uncertainty, and therefore the behaviour of the MSE may have been estimated too positively.

For a final iteration of the management plan evaluation, it was anticipated to use the guidelines from WKGMSE2 (ICES, 2019c) and WKREBUILD (ICES, 2020) to plan for the next step in the development of the management plan. This work is embedded in the current report.

[1] A full-feedback MSE means that the assessment (and forecast) are run within the Management Strategy Evaluation (MSE) framework for each year and for each iteration.

1.3 Approach

The approach during the Focus Group on Western Horse mackerel was to convene a number of physical meetings to identify the main issues and to plan regular updates. In June 2019, a technical subgroup was set up to further carry out the technical analyses that were required. This subgroup was closely affiliated with the ICES WKREBUILD workshop that was going to take place in February 2020.

The first technical subgroup meeting was held on 20-21 June 2019. After presenting the state of affairs during WKREBUILD 2020, a series of online meetings was held during May and June 2020 to finalize the evaluation tools and to carry out the studies and evaluations. Specific focus was paid to the following topics:

- Stock ID (through the genetic work coordinated by Edward Farrell, UCD)
- Analysis of length compositions of catches (Gwladys Lambert, Martin Pastoors)
- Analysis of SSB per recruit (Dankert Skagen)
- Stock assessment (with focus on exploratory SAM assessment; Vanessa Trijoulet and Martin Pastoors)
- Reference points and calculation of Fcv and Fphi (Martin Pastoors)
- Development of HCR evaluation tools
    - EqSim (Andrew Campbell, Martin Pastoors)
    - SAM HCR (Vanessa Trijoulet)
- Application of HCR tools to evaluate different potential rebuilding plan (Andrew Campbell, Vanessa Trijoulet, Martin Pastoors)
- Presentation of results to the PELAC western horse mackerel focus group (Martin Pastoors, Andrew Campbell)

2 Horse mackerel stock ID

Recently, a study has been completed on the population structure of the Atlantic horse mackerel (*Trachurus trachurus*) as revealed by whole-genome sequencing (Farrell et al., 2020). The executive summary of that report is repeated below:

"The Atlantic horse mackerel, Trachurus (Linnaeus, 1758) is a species of jack mackerel distributed in the East Atlantic, from Norway to west Africa and the Mediterranean Sea. It is a pelagic shoaling species found on the continental shelf and it is one of the most widely distributed species in shelf waters in the northeast Atlantic, where it is targeted in pelagic fisheries. In the northeast Atlantic region, the species is assessed and managed as three stocks: the Western, the North Sea and the Southern. Despite the commercial importance of the horse mackerel, the accuracy of alignment of these stock divisions with biological units is still uncertain.

The aims of this study were to identify informative genetic markers for the stock identification of horse mackerel and to estimate the extent of genetic differentiation among populations distributed across the distribution range of the species. For this we used modern sequencing techniques that allowed us to assess genetic variants in the entire genome. We discovered that while the populations differ in a small fraction of their DNA (< 1.5%), such genetic differences are significant as they likely represent natural selection and might be involved in local adaptation. We validated a small fraction of these highly differentiated genetic variants by a SNP assay and demonstrated that they can be used as informative molecular markers for the genetic identification of the main stock divisions of the Atlantic horse mackerel.

The results, based on the analysed samples, indicated that the North Sea horse mackerel are a separate and distinct population. The samples from the Western stock, west of Ireland and the

northern Spanish shelf, and the northern part of the Southern stock, northern Portugal, appear to form a genetically close group. There was significant genetic differentiation between the northern Portuguese samples and those collected in Southern Portuguese waters, with those in the south representing a separate population. The North African and Alboran Sea samples were distinct from each other and from all other samples.

These results indicate that a further large-scale analysis of samples, with a greater temporal and spatial coverage, with the newly identified molecular markers is required to test and reassess the current stock delineations."

The main conclusions of the genetic work can be summarized as follows:

- A suitable panel of SNP markers can be identified to carry out routine population assignments of mixed samples.
- Main differentiation between populations is between northern and southern populations, with the boundary being in the middle of Portugal. Although more work needs to be done on this finding, this could imply that the current division between western and southern horse mackerel is not adequate, as the northern part of 9a is currently included in the southern population.
- The North Sea population is clearly distinct from the Western population and it should be possible to tell the difference from mixed samples with a high probability (>93%?). This allows screening of catches in 7d and 7e on the contribution of western and North Sea populations.

3 Length compositions of catches

A short study was initiated to analyse the length composition of catches by country, area, year and quarter. Length compositions could be informative on selectivity in different areas and fisheries and could therefore also be used to generate specific management measures as part of a rebuilding plan.

In the current SS assessment framework, length compositions are used as the key metric for catches in combination with age-length keys to generate age compositions dynamically. So, while it might be expected that the length information is readily available, this turned out to be not the case. The length data that is submitted by country, is not submitted in a standardized format and not included in the InterCatch database. Historical length data by country has been processed on an annual basis using ad hoc Excel spreadsheets and cannot be easily extracted. Therefore, no real progress has been made on this topic.

Recommendation:

- The Western Horse Mackerel Focus Group recommends to WGWIDE that the full time series of catch at length by country is recreated from the Excel spreadsheets and converted into InterCatch to allow for future interrogations of the data and an underpinning of the input data to the stock assessment.

4 Contribution of recruitment to SSB

Dankert W. Skagen, June 2020

For the understanding of how a stock responds to recovery measures, it is useful to consider the age composition in the spawning stock, to illustrate how recruitment in the previous years contribute to the present spawning stock. When we

calculate SSB per recruit, we do this by calculating the sequence of numbers at age as they are reduced by mortality, starting with one recruit. Then we multiply numbers at each age with weight and maturity at that age to get biomass per recruit of the spawners at each age. The sum of these over all ages is the total SSB per recruit, which is normally what is presented, but the age profile of the SSB per recruit can also be interesting in itself. For example, when we consider a rebuilding strategy, it gives us an indication of how fast SSB can be expected to improve when recruitment improves. The age distribution in the spawning stock of course depends on the fishing mortality level, as does the total SSB per recruit.

The actual SSB at some age is the SSB per recruit at that age, multiplied with the number of recruits born in that cohort. Accordingly, the total SSB in any year is a weighted sum of previous recruitments. The products of cohort recruitment times SSB per recruit at age, summed over all ages. In an equilibrium where all weighting factors are constant, SSB is proportional to the mean recruitment, since it is the sum of SSB per recruit at age, raised by the recruitment.

This simple relation also gives us an easy direct means of calculating how the variation in recruitment carries over to variation in SSB. In probability theory, there is a very simple formula for variance of a weighted sum of independent components. Here the components are annual recruitment, with a presumably known variance, and the weightings are the SSB per recruit at age. Although this only covers the effect of one source of variation in SSB, the recruitment variation is a major source so a direct calculation of the variance, without elaborate bootstrap procedures, can be useful as a proxy in the early phase of management plan developments, and also for understanding the effect of variable recruitment.

Below is a set of age distributions in the SSB per recruit for Western horse mackerel (Figure 2). The data on weights, maturities, natural mortality and selection were those used as input to the short-term prediction by WGWIDE in 2019.

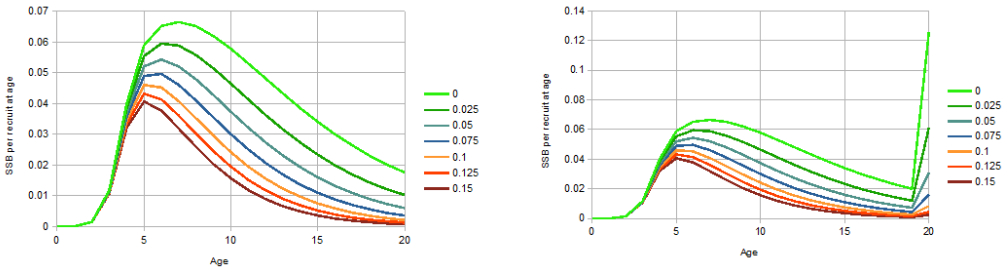

Figure 1 *SSB at age for a range of fishing mortalities (F1-10) With (right) and without (left) regarding age 20 as a plus group.*

Figure 3 shows SSB per recruit as function of F1-10, with the same input data, and in addition the 95 % confidence interval assuming a CV on recruitment of 0.6. which is slightly lower than the CV of the recruitments 1983 – 2018 according to the WGWIDE assessment in 2019, excluding the strong 2001 year class. In the same figure, the mean age in the SSB as function of the F1-10 is also shown.

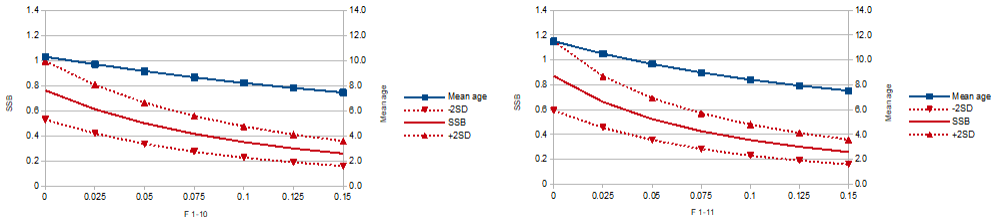

Figure 2 *Mean age (blue) and SSB (Mean ±2SD) for a range of fishing mortalities (1-10). Using only age up to 20 (left, without a plusgroup) and using all ages (right, with a plusgroup at 20). The SDs are the effect of recruitment variation, assuming a CV of 0.6*

As one should expect for a relatively long-lived species with low mortality, the spawning stock is rather old. At F =0.075, the mean age is about 9 years, 80% is older than 5 years and 20% older than 12 years. So, an improved recruitment will take some time to materialize as increased SSB. The results also indicate that with a low F, the plus group still does matter. Finally, the historical variation in recruitment translates into a confidence interval for long term equilibrium SSB that for F=0.075 ranges from approximately 700 to 1400 when the mean recruitment is 2500.

5 Stock assessment of Western horse mackerel

5.1 Stock synthesis assessment

WGWIDE 2019: The SS model with new length and age data from the commercial fleet, and the 2018 information from the 2 surveys available, is presented as the final assessment model. Stock numbers-at-age and fishing mortality-at-age are given in Tables 7.3.1.1 and 7.3.1.2, and a stock-summary is provided in Table 7.3.1.3 and illustrated in Figure 7.2.11.2. SSB peaked in 1988 following the very strong 1982 year class. Subsequently SSB slowly declined till 2003 and then recovered again following the moderate-to-strong year class of 2001 (a third of the size of the 1982 year class). Year classes following 2001 have been weak: 2010 2011, and 2013 recruitments in particular have been estimated as the lowest values in the time-series together with the 1983. The 2008 year class has been estimated to be fairly strong. Recruitment estimates for 2014-2018 are the highest observed since 2008 and are higher than the geometric mean estimated over the years 1983-2018. SSB in 2017 is estimated as the lowest in the time-series. Fishing mortality was increasing after 2007 as a result of increasing catches and decreasing biomass as the 2001 year class was reduced. Since 2012 F has then been decreasing, dropping to low values in 2015-2018 due to lower catches and a reduced proportion of the adult population in the exploited stock.

5.2 SAM assessment

IBPWHM 2019: Since the benchmark in 2017 (ICES, 2017b), the Western horse mackerel assessment has been carried out using the Stock Synthesis method. This method allows for the incorporation of length frequency information and the dynamic estimation of growth. The Stock Synthesis assessment of western horse mackerel utilizes the length distributions of the commercial catch and from the samples obtained during the PELACUS survey, while the other information is provided as biomass (total catch, egg survey) or age specific data (recruitment index). The SS assessments that have been carried

out since the benchmark in 2017 have generally shown narrow confidence intervals, yet the annual revisions in estimated stock size and fishing mortality between subsequent assessments has been substantial. These retrospective revisions are not well understood. In addition, there has been some concern about the complex nature of the input data to the Stock Synthesis method and the ability to adequately quality control the input data and model performance.

As part of the Interbenchmark of Western horse mackerel, it was agreed to explore the possibility of an alternative assessment approach to Stock Synthesis. The intention was to test methods that are more familiar to members of the WGWIDE assessment group. It was decided to use the SAM model as the alternative approach because it is already being used for mackerel and blue whiting and because it will allow for an evaluation of harvest control rules in a similar manner as is currently being applied for Western Baltic Spring Spawning herring.

The exploratory SAM assessment (https://www.stockassessment.org/setStock.php?stock=WHOM2018) was initiated with the same input data as was used for the Stock Synthesis assessment of WGWIDE 2018 (ICES, 2018) with the exception of the length frequency data, which was not used. The PELACUS survey data was therefore only used as an index of biomass within SAM. When using the default SAM configuration, the assessment output displayed a strong retrospective pattern and very large uncertainty in both F and SSB. A process of fine-tuning the assessment lead to the binding of the observation variances for certain variables and the application of a fixed selectivity pattern (correlation coefficient ρ=1 in the F random process, that was originally allowed to change by year (https://github.com/martinpastoors/wgwide/blob/master/R/HOM%20optimization_SAM.R). The only aged-structured observation available for this stock is for the commercial catch. As a result, the model has a tendency to over-fit these observations, notably for the older ages. This induced important variations in fishing selectivity over time that seemed inconsistent and led to very large retrospective patterns in both SSB and F. Fixing the fishing selectivity over time resulted in a significant improvement in these retrospective patterns for only a slightly larger AIC (1217.453 vs. 1212.974 with variable relative fishing mortality). The final exploratory assessment from this exercise was selected on the basis of the trade-off between a low AIC and reduced retrospective pattern.

A comparison of Fbar and SSB between the SS3 assessments of WG2018 and 2019 with the SAM assessment (WG18SAM, WG19SAM).

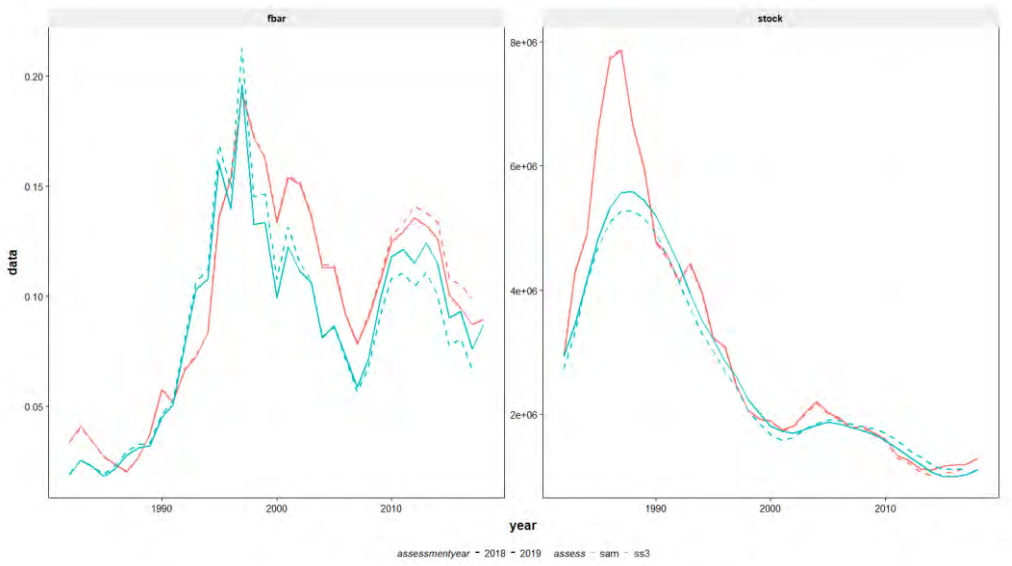

Figure 3 Time trends for Fbar and SSB for the SS3 (red) and SAM (blue) assessments for WG2018 and 2019.

6 Fcv and Fphi uncertainty parameters

The standard approach in ICES for estimating biological reference points is based on the EqSim software conditioned on the most recent assessment. Uncertainties in the assessment are included through two parameters: Fcv and Fphi, where Fcv is expected to capture the assessment error in the advisory year and Fphi is the autocorrelation in assessment error in the advisory year (ICES, 2014a). Methods for deriving Fcv and Fphi are loosely described in the WKMSYREF3 report (ICES, 2014a, p. 11):

"The estimated realised catch and F (Fyr) for the previous 10 years (or more) are taken from the most recent assessment. The annual ICES advice sheets issued in y-1 are consulted to estimate the F_{ya} that would have been advised to obtain the estimated catch. Where the appropriate catch is not available in the catch option table linear interpolation is used to estimate the F_{ya}. The deviation in year y d_y is calculated as $\log_e(F_{yr}/F_{ya})$, the standard deviation σ_m of the log deviations gives the marginal distribution. The conditional standard deviation σ_c is calculated as $\sigma_m \sqrt{(1-\varphi^2)}$, where φ is the autocorrelation of the AR(1) process. Then σ_c [and] φ are input parameters for Eqsim."

The role of Fcv and Fphi in the process of estimating reference points is that they are used to calculate Fp05 which is used as the precautionary buffer on Fmsy, because Fp05 is the value whereby a (less than) 5% annual probability exists that SSB will be below Blim in the long term If the directly estimated Fmsy is larger than Fp05, then Fmsy needs to be reduced to Fp05.

When applying this approach to the western horse mackerel data, we found that there were important sensitivities in calculating the parameters Fcv and Fphi. This initial finding let us to carry out a broader review of the behaviour of Fcv and Fphi for a number of widely distributed pelagic stocks where reference points were recently estimated (western horse mackerel and Atlantic mackerel). The results will be summarized in a working document to ACOM in September 2020. While there has in general been ample attention during benchmark workshops to the estimation of reference point – albeit they are often carried out AFTER the benchmark instead of DURING the benchmark – we found that the documentation of the selection of data and the method to calculate the Fcv and Fphi has been mostly lacking. In most cases it is not clear how many years have been used, nor how the values for the interpolated fishing mortalities have been generated.

Western horse mackerel

Fset and SSBset were calculated from the historical assessment data. Realized catch by year was taken from the most recent advice document. Catch1fcy and Catch2fcy are the two catch options that bracket the actual realized catch in the forecast year and F1fcy and F2fcy are the associated fishing mortalities. Fset is the interpolated fishing mortality that matches the realized catch in a particular forecast.

In the case of horse mackerel, this procedure could not be followed for estimating the SSBset, because only one value of SSB in the forecast year is presented in the forecast tables.

tacyear	catchrealized	catch1fcy	catch2fcy	f1fcy	f2fcy	ssb1fcy	ssb2fcy	fset	ssbset
2011	193268	186433	201312	0.1048	0.1135	-	-	0.108797	1911900
2012	166579	155125	174007	0.0944	0.1064	-	-	0.101679	1879742
2013	165258	155633	170000	0.1638	0.18	-	-	0.174653	1568380
2014	136360	129640	144621	0.1541	0.1734	-	-	0.162757	749334
2015	98419	85820	99304	0.1053	0.1229	-	-	0.121745	601099
2016	98811	98544	99710	0.0997	0.1009	-	-	0.099975	718285
2017	82961	82526	84289	0.1105	0.113	-	-	0.111117	511789
2018	101682	99129	108515	0.081	0.089	-	-	0.083176	818082

The calculation of cv and phi for fishing mortality and SSB is shown below (figure 4). Fassess and SSBassess are taken from the WGWIDE 2019 assessment. The explanations below are only given for fishing mortality, but the same procedures apply to SSB.

The F deviation in year y d_y is calculated as ln(Fassess/Fset). The standard deviation σ_m (=lnSTD) of the log deviations gives the marginal distribution. The autocorrelation in the log deviations φ (=Fphi) is calculated by correlating the deviations 2011-2017 with the deviations 2012-2018 (this is the autocorrelation of the AR(1) process). The conditional standard deviation σ_c (=Fcv) is calculated as $\sigma_m \sqrt{(1-\varphi^2)}$.

In the case of western horse mackerel, Fcv is estimated at 0.2193 and Fphi at the very low value of 0.0212. This can be explained by the almost complete lack of overlap between Fassess and Fset because the most recent assessment estimates a substantially lower fishing mortality than was assumed in the forecasts. The F correlation plot below therefore shows a close to flat line. During IBPWHM 2019, reference points have been calculated using Fcv = 0.212 and Fphi = 0.423 (the default EqSim values) and thus substantially different from the calculated values.

Note that SSBcv and SSBphi have been calculated in the same way, but they are not currently used in the EqSim approach for estimating reference points.

A simulation study on the impact of different values of Fcv and Fphi on the Fmsy for western horse mackerel is shown below (figure 5). Fcv is on the horizontal axis, while the coloured lines indicate the values of Fphi. The five panels demonstrate the five steps in arriving at the final Fmsy.

- Estimate Fmsy without constraints
- Calculate Fpa (has been done previously).
- If Fmsy is larger than Fpa, set Fmsy_interim to Fpa
- Calculate Fp05 with Eqsim using Fcv, Fphi and Blim
- The final Fmsy is the minimum of Fp05 and Fmsy_interim.

The simulation study demonstrates that a larger Fcv leads to a lower Fp05 and also that a larger Fphi leads to the Fp05 being more sensitive to the impact of Fcv. Therefore, the estimated values of Fcv and Fphi can have an important impact on the Fmsy that is calculated in EqSim.

Figure 4 Calculation of Fcv, Fphi, SSBcv and SSBphi for western horse mackerel

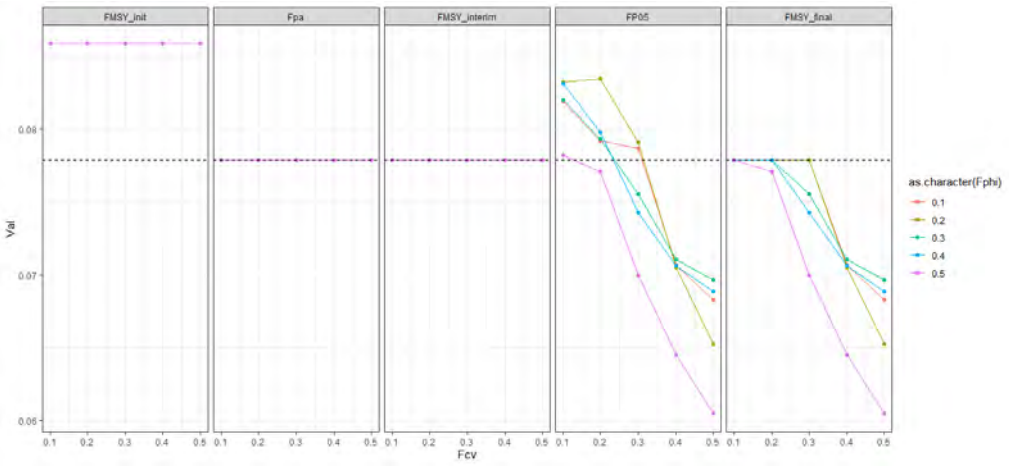

Figure 5 *Simulated values of the impact of Fcv and Fphi on the reference points for western horse mackerel.*

Atlantic mackerel

Following the same procedure as outlined above, we obtained the following values for Fset and SSBset for Atlantic mackerel.

tacyear	catchrealized	catch1fcy	catch2fcy	f1fcy	f2fcy	ssb1fcy	ssb2fcy	fset	ssbset
2009	737969	707000	831000	0.25	0.3	2891000	2842000	0.262488	2878762
2010	875515	726000	996000	0.29	0.42	2397000	2293000	0.361989	2339409
2011	946661	884093	959773	0.31	0.34	2697368	2668541	0.334802	2673535
2012	892353	742000	927000	0.26	0.34	2710000	2638000	0.325018	2651484
2013	931732	930000	1116000	0.41	0.51	2390000	2310000	0.410931	2389255
2014	1393000	1300000	1400000	0.291	0.318	4594000	4573000	0.31611	4574470
2015	1208990	1054000	1396000	0.26	0.36	4344000	4276000	0.305319	4313183
2016	1094066	960009	1235608	0.28	0.38	3766022	3712034	0.328642	3739761
2017	1155944	1067828	1281394	0.28	0.35	4398536	4358095	0.308882	4381850
2018	1026437	977765	1122906	0.405	0.48	3043254	3013235	0.430151	3033187

In the case of mackerel, we were particularly interested in the effect of the assessment year on the calculation of Fcv and Fphi because of the substantial change in perception between the 2018 and the 2019 assessments. Therefore, we calculated Fcv and Fphi for each assessment year separately.

Similar to the observations for Western horse mackerel, the impact of the final assessment year is noticeable here. Due to the revision of the assessment in 2019, there is almost no overlap between the fishing mortalities from the assessment and those derived from the historical forecasts. This impacts on the estimated Fphi (0.3080 using the 2018 assessment, 0.0076 using the 2019 assessment).

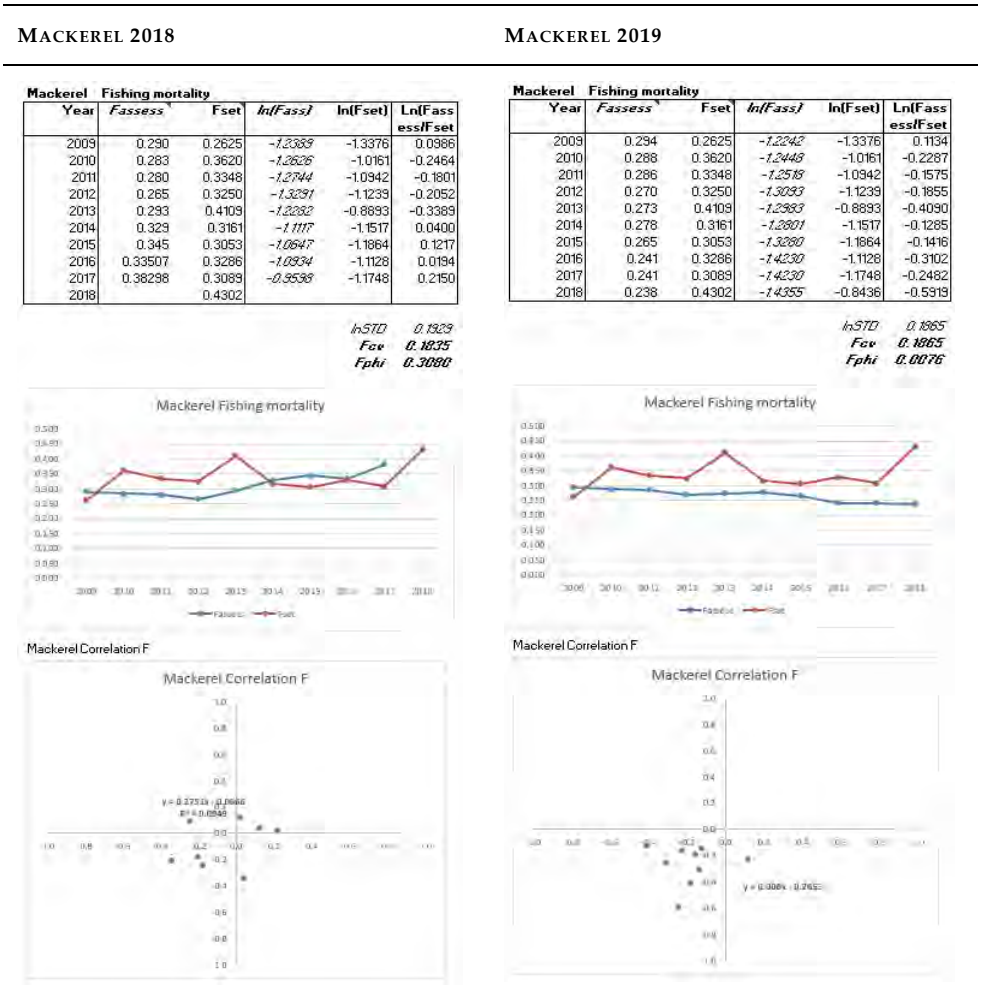

Figure 6 Comparison of Fcv and Fphi for Mackerel based on the assessments of 2018 and 2019.

Conclusions

While an elaborate procedure has been outlined to derive reference points for category 1 and 2 stocks in ICES (ICES, 2017a) based on the work of MSYREF workshops (ICES, 2013b; ICES, 2014a; ICES, 2014b; ICES, 2015), we conclude from our studies on western horse mackerel and Atlantic mackerel that insufficient attention has been given to the method of estimating forecast uncertainty and the impact of that uncertainty on the estimated reference points (notably Fmsy). Here we started with a method for documenting how the Fset is being derived from the historical data, so that at least the estimates of Fcv and Fphi are transparent and can be recreated.

We also note that there can be a high dependence of Fphi on the assessment that is used to compare against the Fset. When the assessment that is used has values that are all higher or lower than the Fset values, then Fphi will be close to zero. To our knowledge, this behaviour of Fphi was unknown so far.

Finally, we note that the number of years that is used for calculating Fcv and Fphi may have an impact on the values. In the recommendations from WKMSYREF3 it is stated that 10 years (or more) should be taken. A further study should be undertaken to assessment the impacts of using different time periods for estimating Fcv and Fphi.

7 Estimation of reference points for SS and SAM assessments

During the IBPWHM 2019, reference points were estimated for western horse mackerel based on the 2018 WGWIDE assessment and using default values for Fcv and Fphi (0.212 and 0.423) and using a segmented regression through Blim (segregBlim). In order to calculate reference points for the exploratory SAM assessment and to explore the sensitivity to the assessment year, reference points were calculated on the basis of the 2018 or 2019 assessments for SS and SAM.

The reference points for the SAM assessment are based on the 2018 assessment. Bpa and Blim are lower than the values for the SS assessment, while the Fmsy is higher. These values will be used in the subsequent evaluations (section 8)

The changes due the assessment year were minor for both the SS and SAM assessments.

RP	WG18	WG18SAM	WG19	WG19SAM
Blim	834480	611814	885341	612635
Flim	0.1107	0.1612	0.1049	0.1756
Fpa	0.07909	0.1152	0.07493	0.1254
MSYBtrigger	1168272	856540	1239478	857689
FMSY	0.09102	0.1262	0.08665	0.1353
FP05	0.08398	0.1255	0.07826	0.1402
FMSY_final	0.07909	0.1152	0.07493	0.1254

8 HCR evaluations

8.1 Type of HCRs evaluated

Three different types of harvest control rules were evaluated:

- Constant F strategy: fixed Ftarget independent of biomass level
- ICES Advice Rule: breakpoint at Btrigger and straight decline in F to zero below Btrigger.
- Double Breakpoint rule: breakpoint at Btrigger and straight decline in F to 20% of Ftarget at Blim. Below Blim continued fishing at F = 0.2 * Ftarget.

For each of the HCRs, a number of different target fishing mortalities were explored (0.0, 0.05, 0.075, 0.1, 0.125, 0.15). No evaluation of different Btrigger values was carried out, so that all evaluations used MSY Btrigger as the trigger point. All HCRs where evaluated with three variants:

- Without any additional constraints
- With a minimum TAC of 50 kT
- With a maximum 20% inter-annual variation (IAV) in TAC, but only when the stock is above Btrigger)

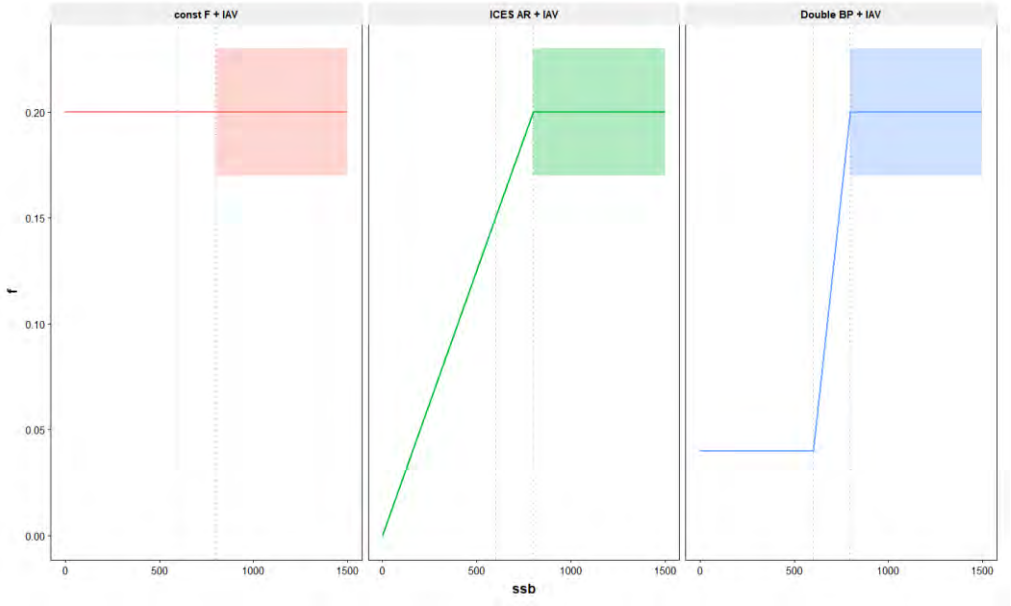

8.2 HCR evaluation tools

The base assessments ("Operating model") of the evaluations were either the WGWIDE 2019 SS3 assessment (ICES, 2019d) or the exploratory SAM assessment that was carried out as part of the IBPWHM 2019 (ICES, 2019b).

As input to the SS3 simulations, 1000 iterations were generated from respective assessments. For SS3 this was done by generating 10000 iterations and then resampling 1000 of them so as to end up with the same starting conditions as in the stock assessment itself.

The 1000 SAM iterations were generated by using the SAM simulate function, based on the IBPWHM 2019 exploratory SAM assessment; these were then converted to FLSAM objects which were again converted to 1000 FLStock objects[2]

The SRR model was the constrained segmented regression (SegRegBlim), similar to the IBPWHM 2019, while leaving out the exceptionally strong 1982 year class.

Two simulation tools were used: the EqSim simulator and the SAM HCR forecast

The EqSim simulator is a further worked up version of the SimpSIM approach that was used for the blue whiting MSE in 2016 (ICES, 2016). The code was further developed by Andrew Campbell and Martin Pastoors to improve standardization, documentation and visualization of results. Some key improvements where:

- the development of standardized codes for Operating Models (OM) a Management Procedures (MP), including new types of HCR elements.
- the development of standardized codes for statistical outputs and visualization thereof.

The SAM HCR forecast is a simple stochastic forecast with HCR to evaluate management for fish stocks that need rebuilding in the short-term. This method enables the investigation of several management strategies without the need of intensive computer power, while still accounting for different sources of uncertainty. The stochastic forecasts start from what we believe is the current level of the stock, i.e. the assessment estimates currently used for tactical management advice, with consideration of the uncertainty in these estimates. Rebuilding is evaluated forward for a specified number of years (here: 23 years) and for different target fishing mortality values (Ftarget)

The method was developed as an extension to the stockassessment R package for the SAM model (Nielsen and Berg, 2014; Berg and Nielsen, 2016) and applied to western horse mackerel[3].

We applied two different assessments to two different evaluation tools as follows:

	WGWIDE19 SS3	WGWIDE19 SAM
EqSim simulator	Yes	Yes
SAM HCR forecast	No	Yes

For each evaluation, we scanned over different F target values: 0, 0.05, 0.075, 0.10, 0.125, 0.15.

Each simulation was run over 23 year, split into the following periods:

[2] https://github.com/ices-eg/wk_WKREBUILD/blob/master/EqSimWHM/Scripts/HOM%20SAM%20simulator.r
Note: running the code required running it in batches of around 200 iterations due to unexplained errors arising when running for larger batches. This issue has not been solved, except by running it in multiple batches.

[3] https://github.com/vtrijoulet/SAM/tree/master2

- Current period (CU): 2018-2020
- Short term (ST): 2021-2025
- Medium term (MT): 2026-2030
- Long term (LT): 2031-2040

8.3 EqSim simulator tool

8.3.1 Eqsim applied to SS3 assessment

The SS3 assessment was run with OM2.2:

```
#WGWIDE2019 Update assessment, IBPWHM reference points, stochastic bio and selection
OM2.2 <- list("code" = "OM2.2",
            "desc" = "WGWIDE19",
            "IM" = NA,
            "SRR" = "SRR.WG19.SegReg_Blim.exterm", "RecAR" = TRUE, maxRecRes = c(3,-3),
            "BioYrs" = c(2008,2017), "BioConst" = FALSE,
            "SelYrs" = c(2008,2017), "SelConst" = FALSE,
            "Obs" = NA,
            refPts = list("Fpa" = 0.074, "Flim" = 0.103, "Fmsy" = 0.074, "Bpa" = 1168272,
                          "Blim" = 834480, "MSYBtrigger" = 1168272, "Bloss" = 761613),
            "pBlim" = 0.05)
```

8.3.1.1 Constant F strategy

- MP5.00 constant F;
- MP5.01 constant F with minimum TAC of 50kT;
- MP5.03 constant F with 20% IAV on TAC constraint above Btrigger.

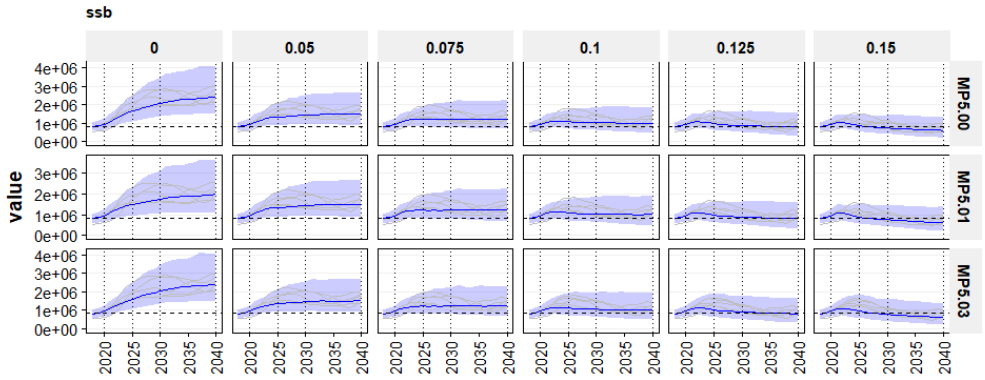

-

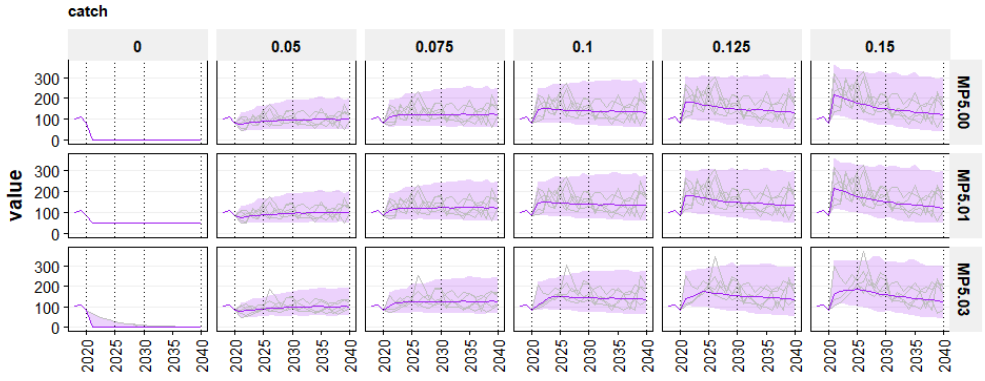

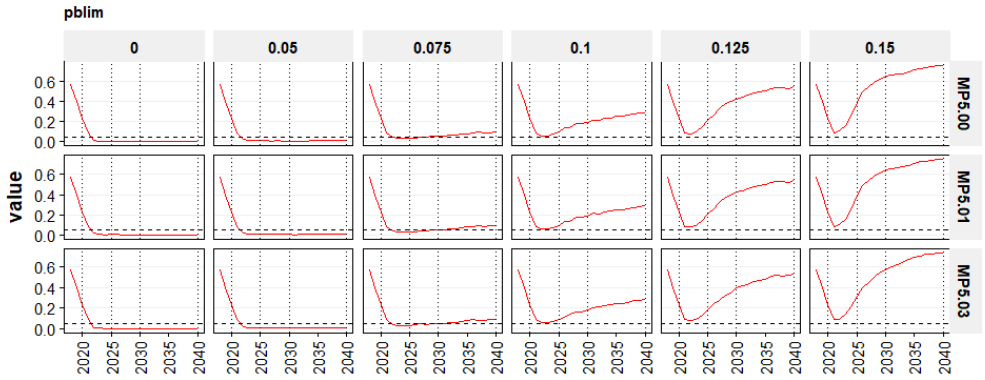

8.3.1.2 ICES Advice Rule

Scenarios 5.1, 5.11 and 5.13 (ICES advice rule variants)

- MP5.10 ICES AR
- MP5.11 ICES AR, min TAC = 50kt
- MP5.13 ICES AR, 20% IAV, only above Btrigger

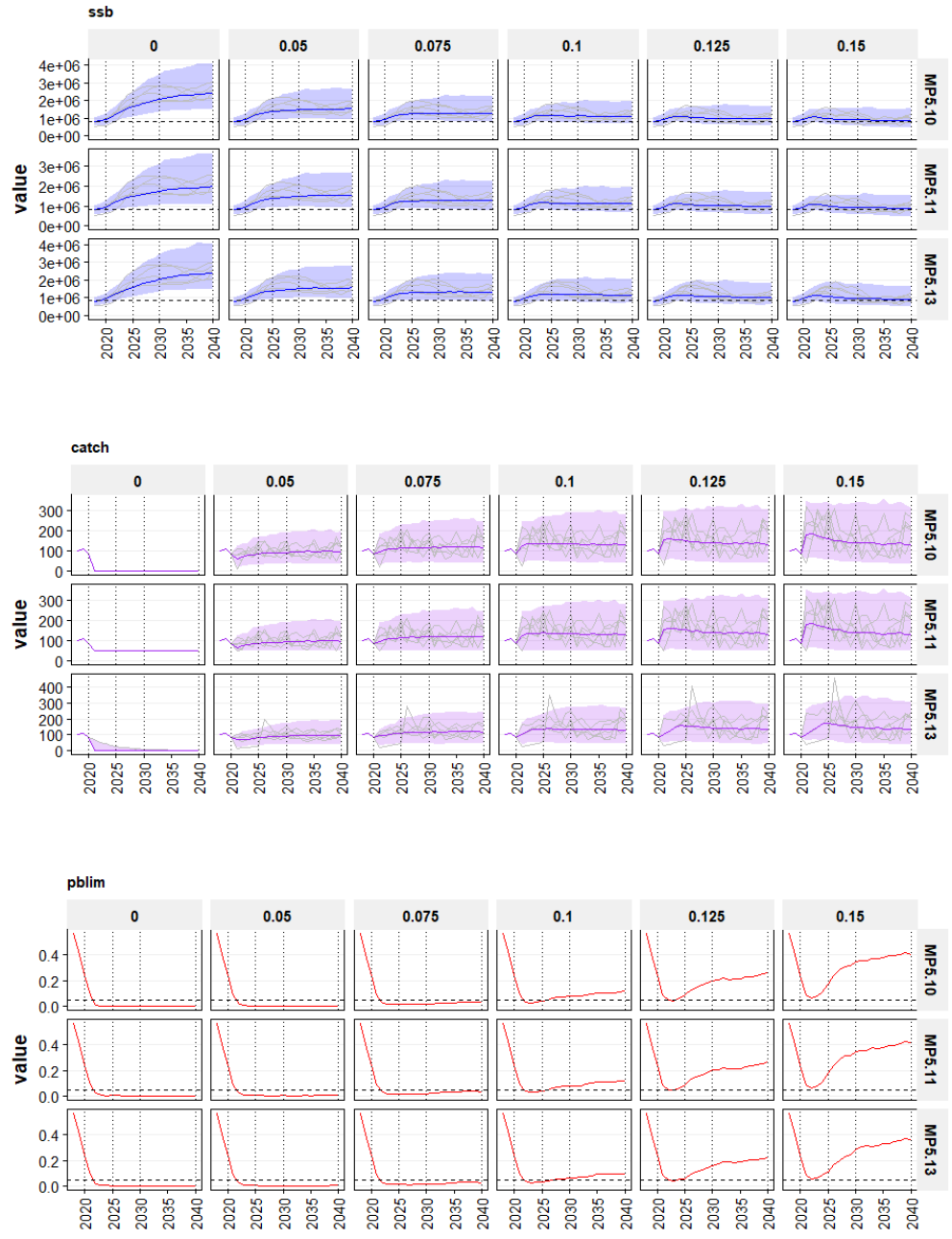

8.3.1.3 Double Breakpoint Rule

This HCR is similar to the blue whiting HCR that was evaluated in 2016 (ICES, 2016).

- MP5.20 Double BP
- MP5.11 Double BP with minimum TAC of 50kT
- MP5.13 Double BP with 20% IAV constraint above Btrigger.

Minimum F in the Double breakpoint rule is 20% of Ftarget.

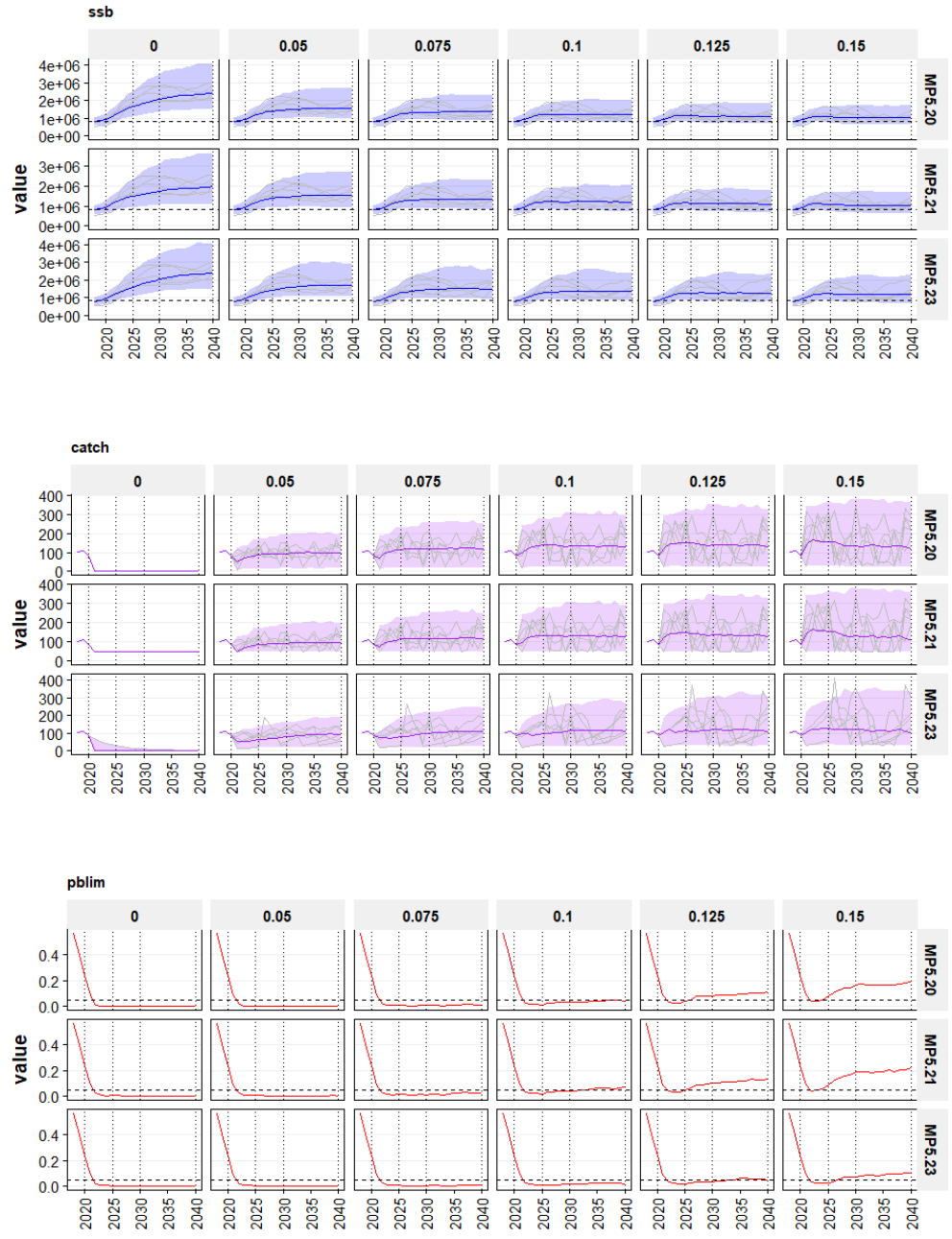

8.3.1.4 First year of achieving rebuilding with 20% IAV constraint scenarios

The first year of achieving rebuilding to Blim and Bpa was calculated as the first year where the probability of being above Blim or Bpa was larger than 50%. The analysis was carried out for the following scenarios:

- MP5.03 constant F with 20% IAV on TAC constraint above Btrigger.
- MP5.13 ICES AR, 20% IAV, only above Btrigger
- MP5.13 Double BP with 20% IAV constraint above Btrigger.

Results indicate that the constant F strategy is the least cautious rule and the double breakpoint rule is the most cautious rule. Under the F strategy rule with a Ftarget of 0.075, rebuilding to Bpa is expected to be achieved is only just being achieved (probability just above 50%) by 2025, while in the double breakpoint rule this is expected to

be achieved in 2024 with substantially higher probabilities of remaining above Bpa. The first year of rebuilding to Bpa in the double breakpoint rule with target fishing mortalities up to 0.1 is the same as the first year of rebuilding under the zero fishing scenarios.

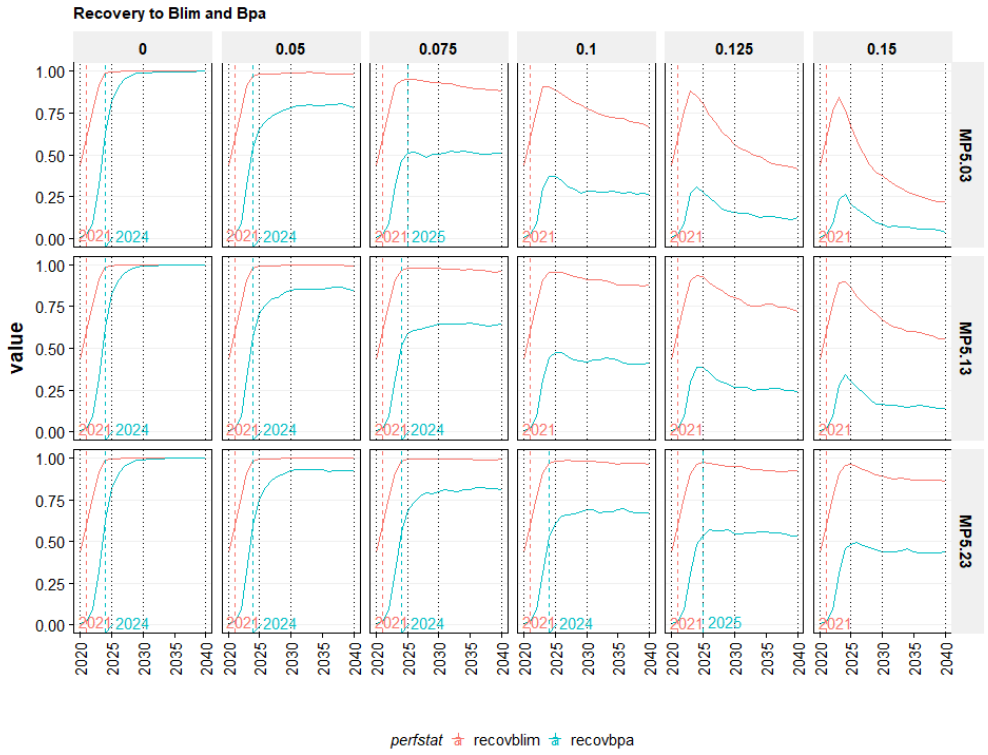

8.3.2 Eqsim applied to SAM assessment

The SS3 assessment was run with OM2.2:

```
#WGWIDE2019 SAM assessment, IBPWHM method for reference points, stochastic bio and selection
OM2.3 <- list("code" = "OM2.3",
              "desc" = "WGWIDE19_sam",
              "IM" = NA,
              "SRR" = "SRR.WG19.SegReg_Blim.exterm", "RecAR" = TRUE, maxRecRes = c(3,-3),
              "BioYrs" = c(2008,2017), "BioConst" = FALSE,
              "SelYrs" = c(2008,2017), "SelConst" = FALSE,
              "Obs" = NA,
              refPts = list("Fpa" = 0.115, "Flim" = 0.161, "Fmsy" = 0.115, "Bpa" = 856540,
                            "Blim" = 611814, "MSYBtrigger" = 856540, "Bloss" = 604476),
              "pBlim" = 0.05)
```

Note that the biomass reference points have been estimated separately for the SAM assessment, and are a bit lower than for the SS assessment (see section 7).

8.3.2.1 Constant F rule with SAM assessment

Results for the constant F rule are not presented because it was clear that this option would not be selected by the PELAC for the potential rebuilding plan.

8.3.2.2 ICES Advice Rule with SAM assessment

Scenarios 5.10, 5.11 and 5.13 (ICES advice rule variants)

- MP5.10 ICES AR;

- MP5.11 ICES AR with minimum TAC of 50kT;
- MP5.13 ICES AR with 20% IAV constraint above Btrigger.

While the probability of being below Blim decreases in the beginning of the simulation period, for all F targets, the probability of being below Blim start to increase again after 2025 when target fishing mortalities are too high (e.g. > 0.075).

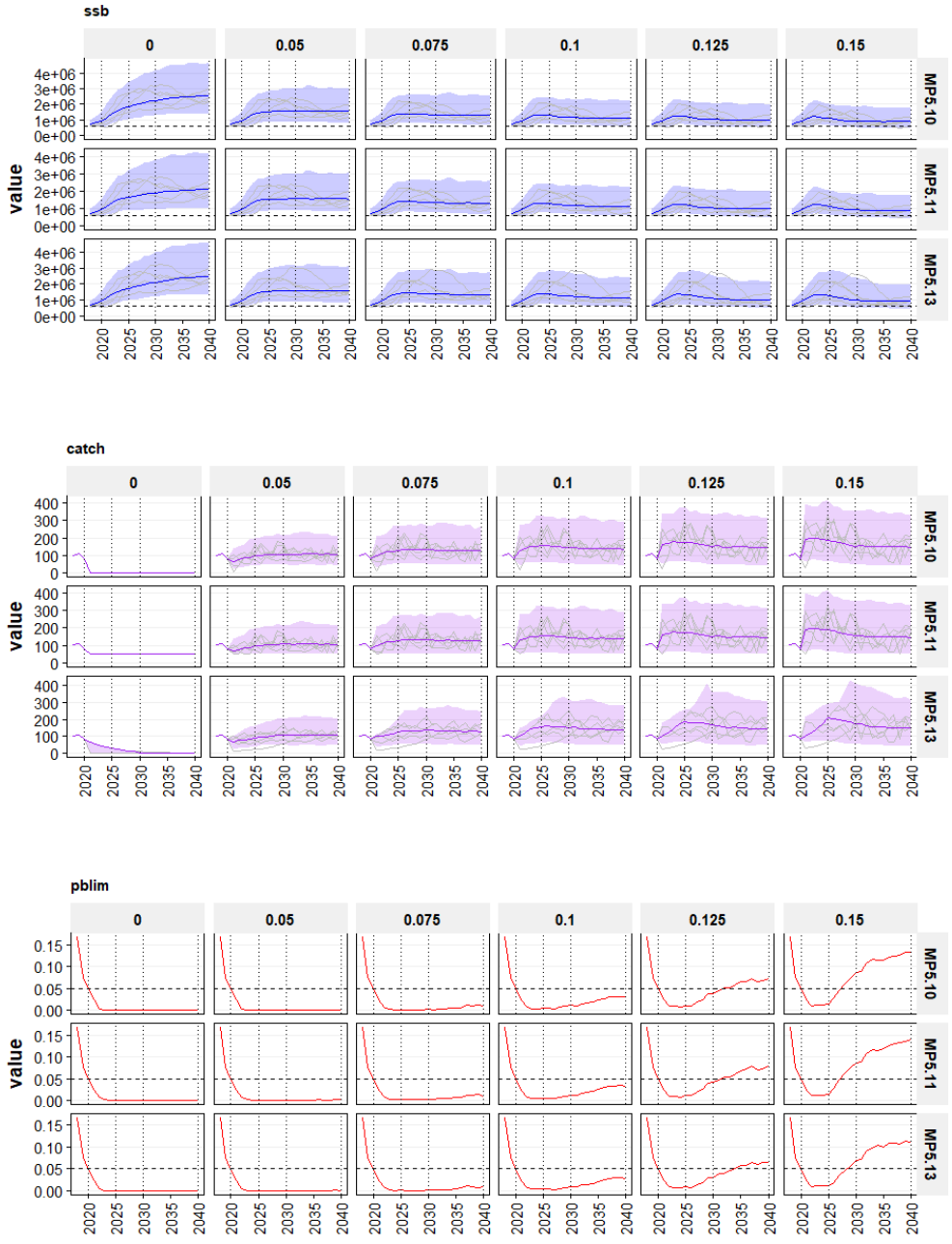

8.3.2.3 Double Breakpoint Rule with SAM assessment

This HCR is similar to the blue whiting HCR that was evaluated in 2016 (ICES, 2016).

- MP5.20 Double BP
- MP5.11 Double BP with minimum TAC of 50kT;

- MP5.13 Double BP with 20% IAV constraint above Btrigger. Minimum F in Double BP is 20% of Fmsy.

Generally, what we find is that the SAM assessment has a somewhat more optimistic view of the stock size in relation to the reference points. This means that the stock is estimated to be above Blim with a high probability in most of the scenarios. It also means that expected recovery to Bpa is in 2022 in all scenarios.

-

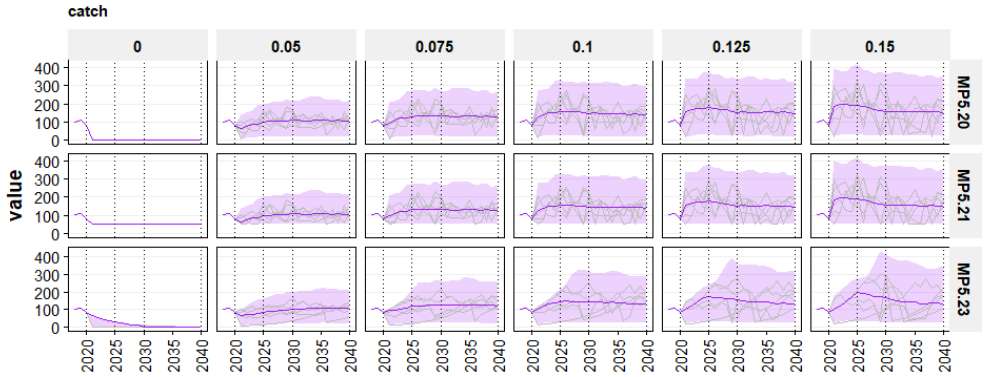

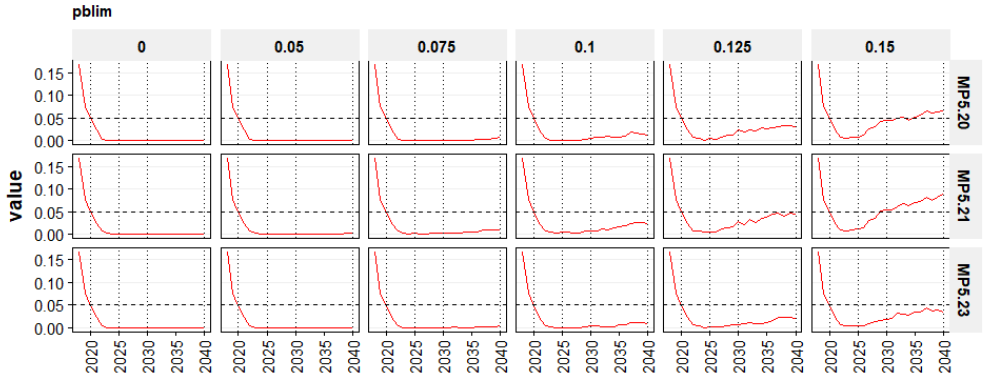

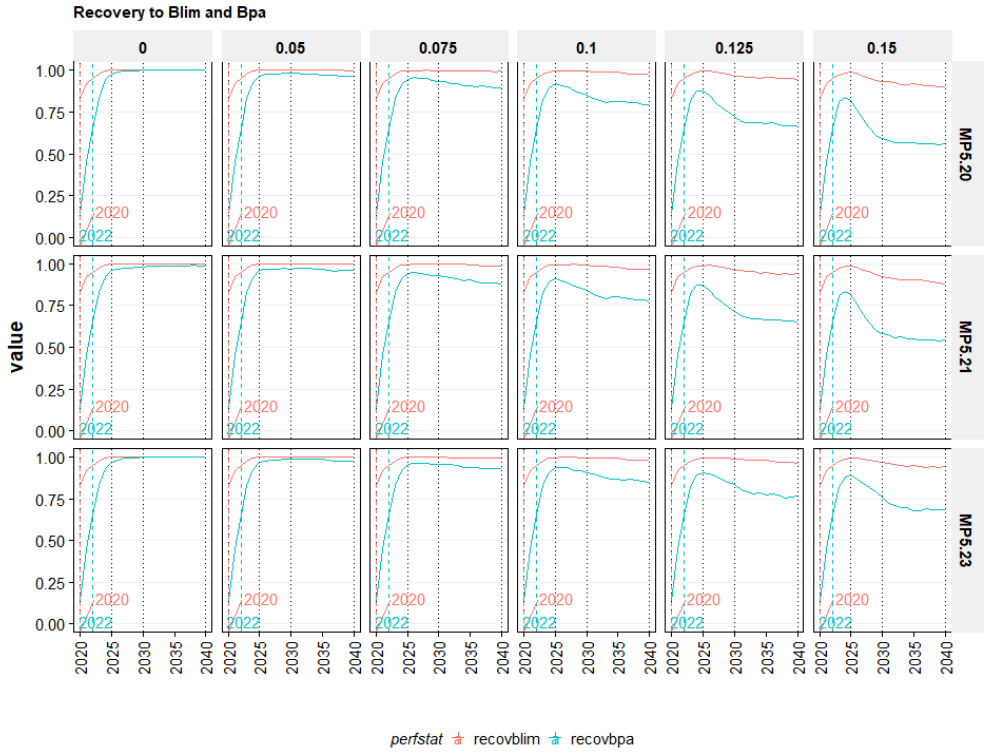

8.4 SAM HCR forecast tool

8.4.1 Description of the method

The SAM HCR was applied to the exploratory SAM assessment (IBPWHM 2019) that was also used for the EqSim with SAM analysis. The SAM HCR forecast can only be run on a SAM assessment[4].

8.4.2 SAM HCR with ICES Advice Rule

Here we only present the simple ICES AR scenario without any additional constraints as the main purpose is only to show the feasibility of using this simple method while generating similar results from more complicated methods.

- MP5.10 ICES AR.

[4] Note that with the SAM HCR it was not possible to run the forecast with F = 0; therefore F = 0.01 has been run for the results denoted below with F = 0 .

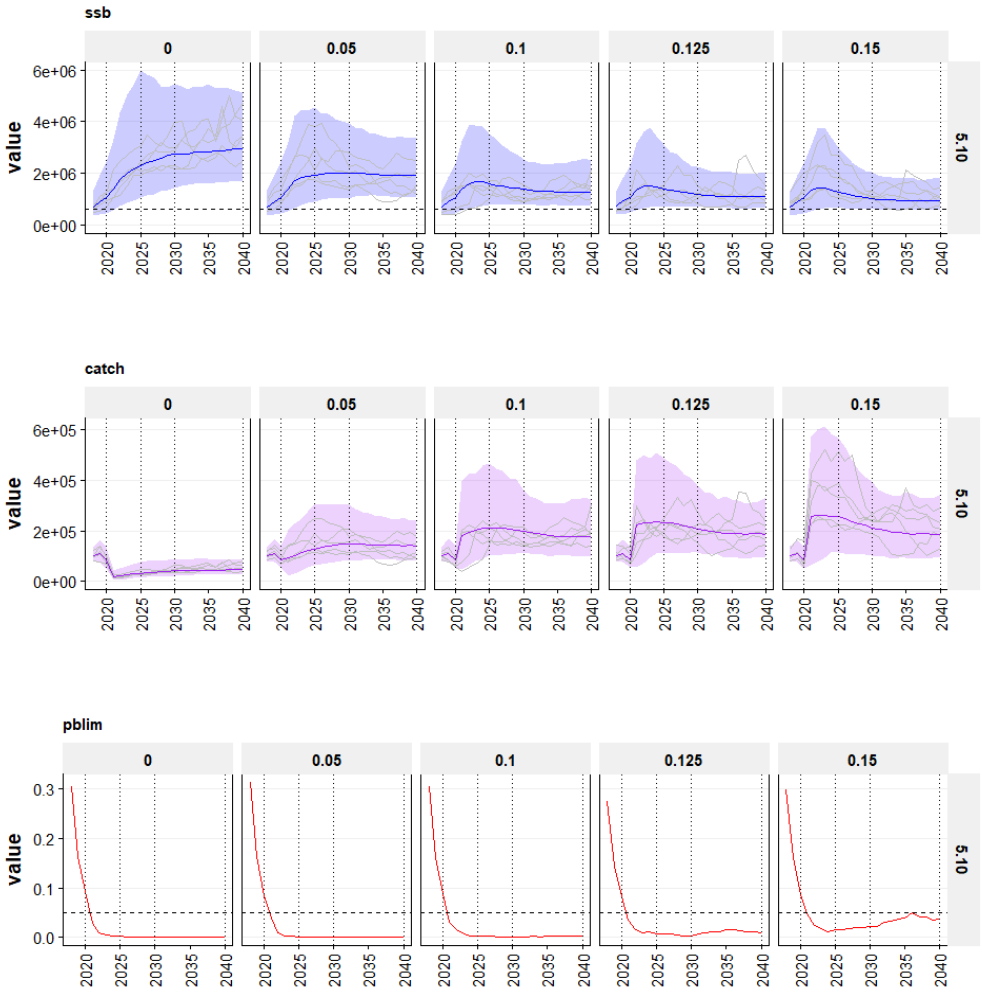

8.5 Comparison of results for different simulation tools and assessments

To compare the behaviour of evaluation tools (EqSim or SAM HCR) and assessment method (SAM or SS3), we compared the simple ICES AR scenarios for the three possible combinations:

- EqSim – SAM – MP5.1 (ICES AR)
- EqSim – SS3 – MP5.1 (ICES AR)
- SAM HCR – SAM – MP5.1 (ICES AR)

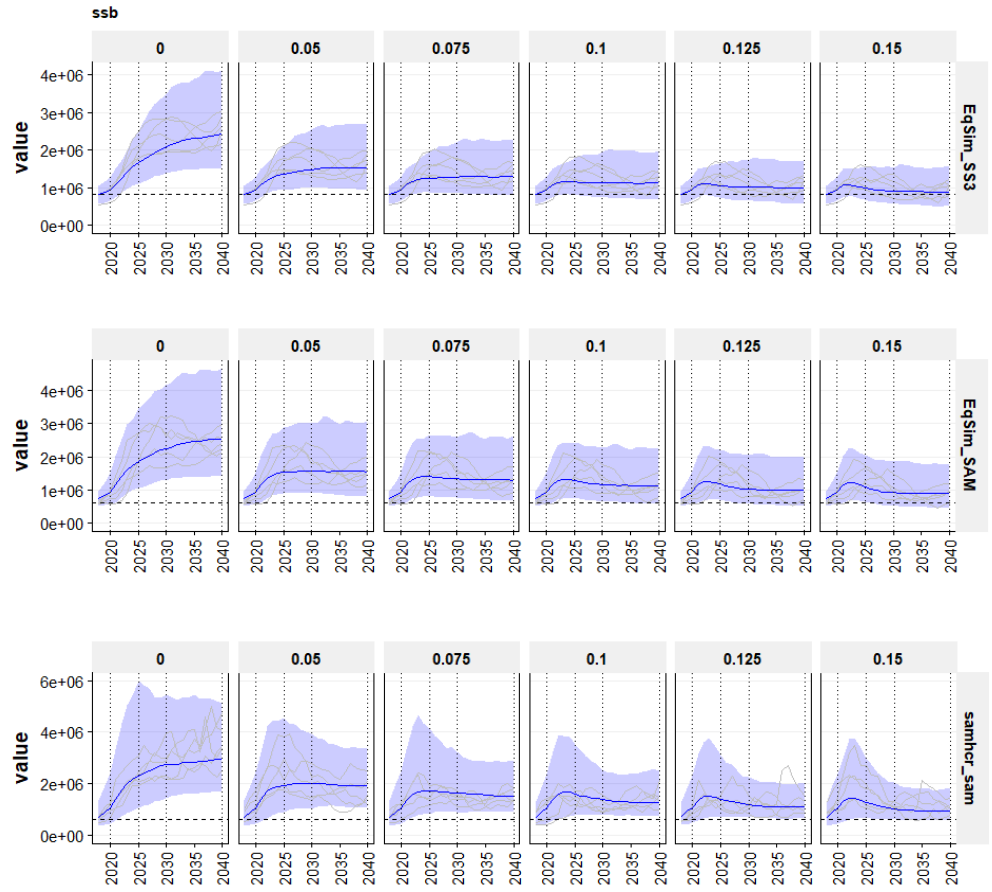
ssb
0
0.05
0.075
0.1
0.125
0.15
value
EqSim_SS3
EqSim_SAM
samhcr_sam
0e+00
1e+06
2e+06
3e+06
4e+06
6e+06
2020
2025
2030
2035
2040

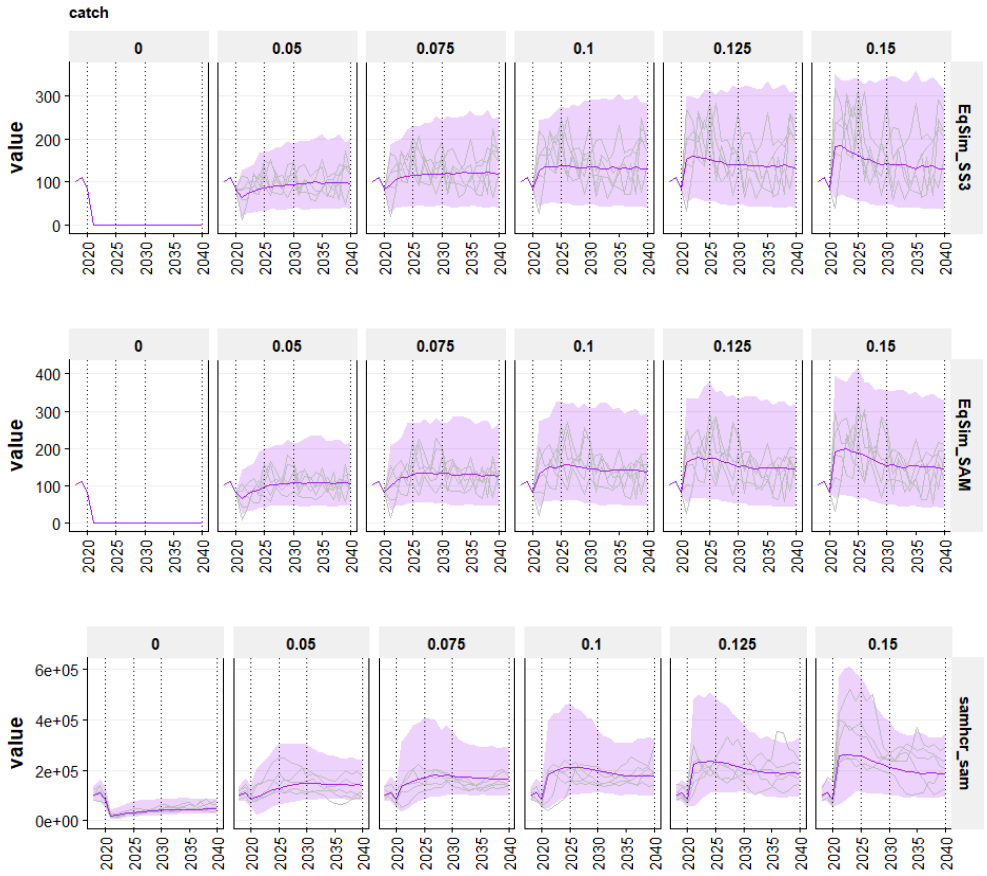
catch
0
0.05
0.075
0.1
0.125
0.15
value
EqSim_SS3
EqSim_SAM
samher_sam
2020
2025
2030
2035
2040

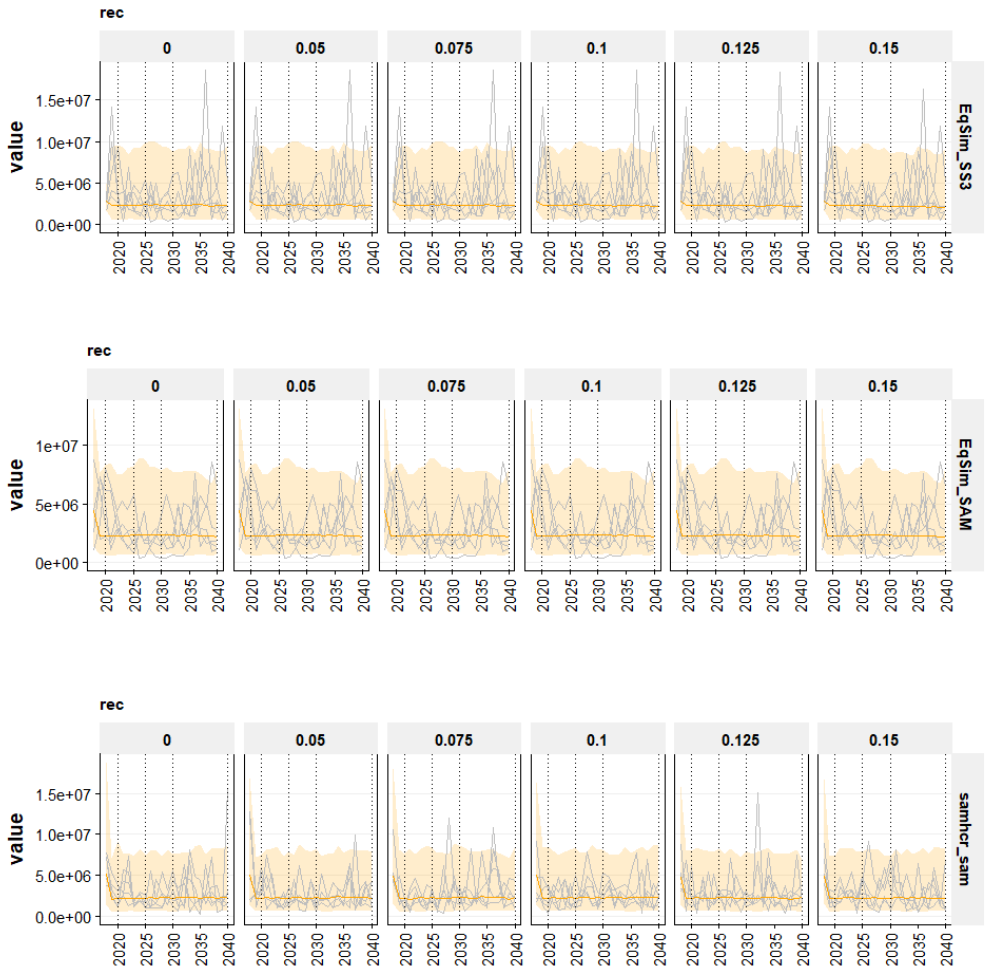
rec
0
0.05
0.075
0.1
0.125
0.15
value
1.5e+07
1.0e+07
5.0e+06
0.0e+00
2020
2025
2030
2035
2040
EqSim_SS3
rec
0
0.05
0.075
0.1
0.125
0.15
value
1e+07
5e+06
0e+00
2020
2025
2030
2035
2040
EqSim_SAM
rec
0
0.05
0.075
0.1
0.125
0.15
value
1.5e+07
1.0e+07
5.0e+06
0.0e+00
2020
2025
2030
2035
2040
samhcr_sam

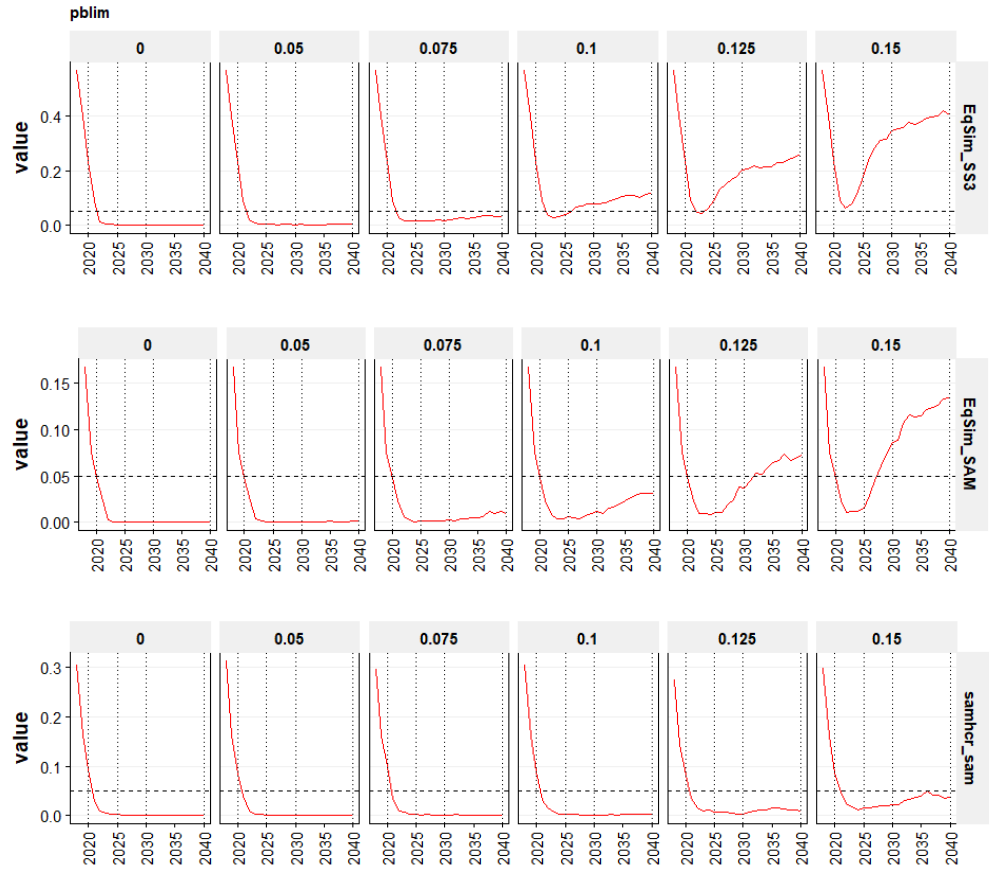

The probability of being below Blim broadly follows the same pattern across the three different evaluation method although the levels do differ between the evaluations. Because the SAM assessment estimates the most recent SSBs higher than year where Bloss was calculated, the probability of currently being below Blim is smaller. The patterns observed for the EqSim_SS and EqSim_SAM runs are qualitatively similar albeit at different levels. The SAMHCR_SAM run exhibits a slightly different pattern because the forecasted SSB is expected to remain above Blim with a high probability in all F scenarios. This may be due to the fact that the SAMHCR is operating as a forecast only and therefore lacks the feature that the management perception of the stock differs from the real stock, so that the implemented HCR in the simulation does not suffer from the mismatch between perception and reality.

9 Selection of preferred HCRs for Western Horse mackerel

The PELAC selected the following preferred option for the Western horse mackerel rebuilding plan:

- Evaluation method: EqSim
- Assessment: Stock Synthesis (WGWIDE 2019), because this is the basis for the assessment and advice.
- Target fishing mortality at Fmsy = 0.074 (approximated by 0.075 in the simulations)
- Blim at ICES Blim (834 480 t)
- Btrigger at ICES MSY Btrigger (1 168 272 t)

- Double breakpoint rule with 20% constraint on IAV above Btrigger
- Minimum F when stock is below Blim at 20% of Fmsy = 0.015

The selected rebuilding plan has a 50% probability of rebuilding to Blim by 2021 (similar to zero catch option) and a 50% probability of rebuilding to Bpa/MSY Btrigger by 2024 (similar to the zero-catch option). Furthermore, the probability of being below Blim remains well below 5% for the duration of the simulation.

In this scenario, the average catch in the years 2021-2025 is expected to be lower than recent catches. However, after rebuilding, catches should be able to be maintained around 100 000 tonnes.

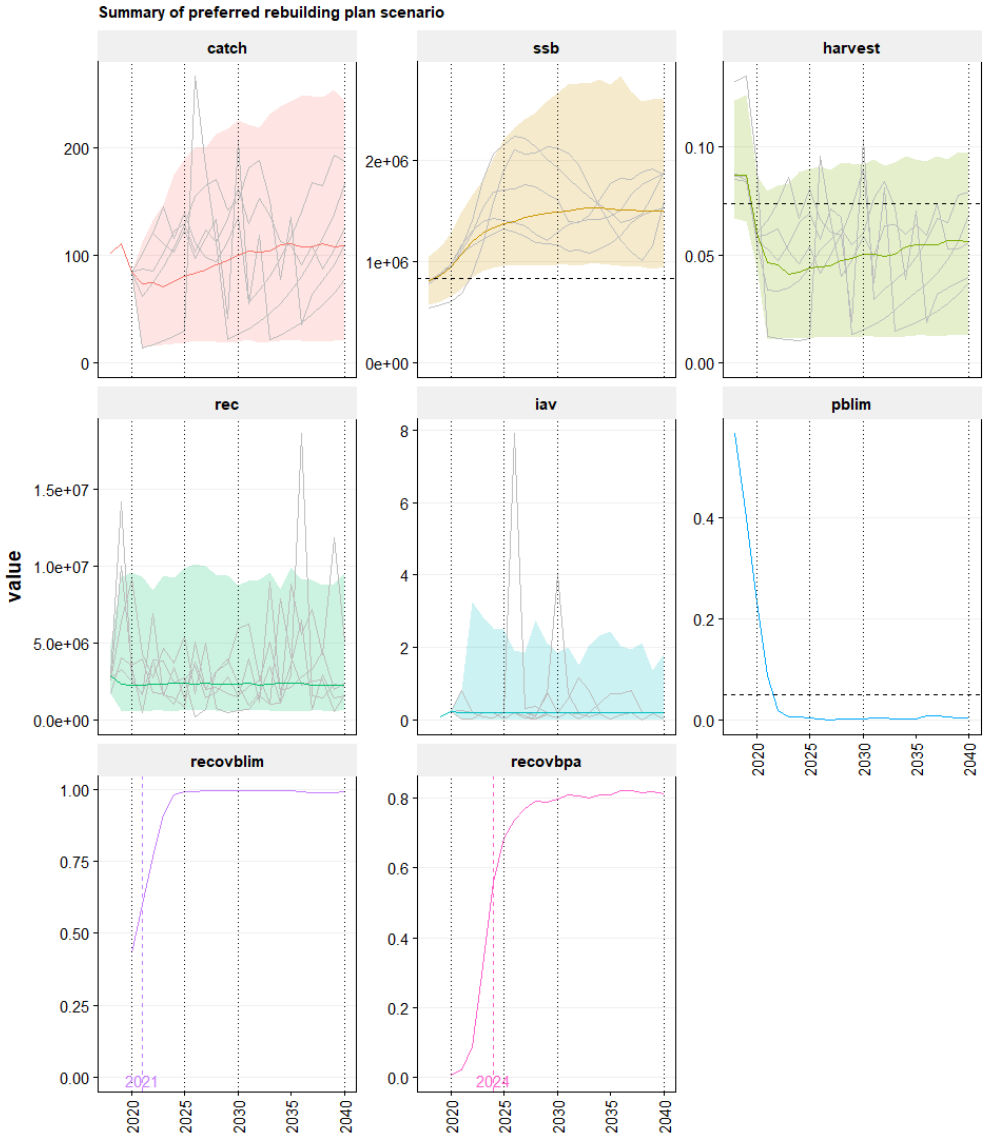

Summary of results of the preferred rebuilding plan

statistic	yearrange	period	median	range	
catch	2018-2020	CU	102	84 - 110	* in kT
catch	2021-2025	ST	75	17 - 167	

catch	2026-2030	MT	92	20 - 210
catch	2031-2040	LT	107	21 - 242
ssb	2018-2020	CU	872,454	608,164 - 1,210,564
ssb	2021-2025	ST	1,249,710	832,465 - 1,902,950
ssb	2026-2030	MT	1,451,882	966,840 - 2,506,102
ssb	2031-2040	LT	1,514,418	958,213 - 2,740,040
harvest	2018-2020	CU	0.080	0.048 - 0.118
harvest	2021-2025	ST	0.044	0.011 - 0.085
harvest	2026-2030	MT	0.047	0.012 - 0.092
harvest	2031-2040	LT	0.054	0.012 - 0.095
rec	2018-2020	CU	2,599,180	696,645 - 7,944,499
rec	2021-2025	ST	2,363,631	606,888 - 9,317,602
rec	2026-2030	MT	2,361,298	599,077 - 9,438,791
rec	2031-2040	LT	2,321,690	612,371 - 9,088,107
iav	2018-2020	CU	0.162	0.086 - 0.239
iav	2021-2025	ST	0.200	0.021 - 2.576
iav	2026-2030	MT	0.200	0.018 - 2.083
iav	2031-2040	LT	0.200	0.017 - 2.032
pblim	2018-2020	CU	0.401	0.243 - 0.560
pblim	2021-2025	ST	0.006	0.005 - 0.082
pblim	2026-2030	MT	0.002	0.001 - 0.003
pblim	2031-2040	LT	0.004	0.002 - 0.009

Table of settings used in the evaluation

class	desc	value
OM	code	OM2.2
OM	desc	WGWIDE19
OM	IM	
OM	SRR	SRR.WG19.SegReg_Blim.exterm
OM	RecAR	TRUE
OM	maxRecRes1	3
OM	maxRecRes2	-3
OM	BioYrs1	2008
OM	BioYrs2	2017
OM	BioConst	FALSE
OM	SelYrs1	2008
OM	SelYrs2	2017
OM	SelConst	FALSE
OM	Obs	
OM	refPts.Fpa	0.074
OM	refPts.Flim	0.103
OM	refPts.Fmsy	0.074
OM	refPts.Bpa	1168272
OM	refPts.Blim	834480
OM	refPts.MSYBtrigger	1168272
OM	refPts.Bloss	761613
OM	pBlim	0.05
MP	code	MP5.23
MP	desc	Double BP HCR
MP	xlab	Double BP IAVBtrig
MP	HCRName	DoubleBP
MP	F_target1	0
MP	F_target2	0.025
MP	F_target3	0.05
MP	F_target4	0.075
MP	F_target5	0.1
MP	F_target6	0.125
MP	F_target7	0.15
MP	B_trigger	MSYBtrigger
MP	minTAC	

```
MP      maxTAC
MP      TAC_IAV1            0.2
MP      TAC_IAV2            0.2
MP      Obs.cvF             0.22
MP      Obs.phiF            0.03
MP      Obs.cvSSB           0.36
MP      Obs.phiSSB          0.51


OTHER   niters              1000
OTHER   nyr                 23
OTHER   CU                  2018-2020
OTHER   ST                  2021-2025
OTHER   MT                  2026-2030
OTHER   LT                  2031-2040
OTHER   flstock             WGWIDE19.RData
OTHER   flstock_sim         MSE_WGWIDE19_FLStocks_1k15PG.RData
```

10 Summary and conclusions

This report has brought together many different topics that are related to the western horse mackerel stock in an attempt to develop a potential rebuilding plan for the stock. Even though western horse mackerel was not classified by ICES as in need of rebuilding in their latest advice (ICES, 2019a), the general perception within the fishing industries has been that the stock has been in a poor state but that there have been some positive signals in recent recruitment. Using the new recruitments to improve the stock status requires a careful management approach. The PELAC has been a proponent of developing management plans for all stocks in their remit. In this case, the PELAC has termed the approach a rebuilding plan because of the current stock status of the stock.

Substantial progress has been made over the past few years on horse mackerel stock ID (Farrell et al., 2020). The full genome sequencing of horse mackerel from samples taken all the way from the Skagerrak to the Mediterranean and North Africa, has yielded a suitable panel of SNP markers that can be used to differentiate between the different horse mackerel stocks. The strongest differentiation between populations was between the northern and southern populations, with the boundary being in the middle of Portugal. The North Sea population is clearly distinct from the Western population and it should be possible to tell the difference from mixed samples with a high probability (>93%). This would also allow screening of catches in 7d and 7e on the contribution of western and North Sea populations. The separation between the northern and southern populations could mean that the current division between western and southern horse mackerel is not adequate, at the northern part of 9a is currently included in the southern population. A similar split in the middle of Portugal has also been observed for boarfish (Farrell et al., 2016) and could indicate a biogeographical feature.

Length compositions of the catches are an important element of the assessment approach for western horse mackerel, because Stock Synthesis uses length composition in combination with age-length key to estimate the age compositions within the model. Part of a rebuilding plan for western horse mackerel could be to evaluate differences in length compositions in the catches in certain areas and to take specific measures to protect incoming recruitment. Therefore, we planned to carry out an analysis of length compositions by area and season. However, we found that such data is not currently available for all years. Length data for western horse mackerel is not included in the ICES InterCatch database. Instead, length data has been processed on a year by year basis in non-standardized Excel spreadsheets. A time series of length compositions by

area and season can therefore only be derived by manually working through the spreadsheets and extracting the required information. This was not feasible as part of the project to develop and evaluate a rebuilding plan for western horse mackerel. We recommend to WGWIDE that the full time series of catch at length by country is recreated from the Excel spreadsheets and converted in a standardized database format to allow for future interrogations of the data and an underpinning of the input data to the stock assessment.

In order to understand how a stock would respond to recovery measures, it is useful to consider the age composition in the spawning stock which illustrates how recruitment in the previous years contributed to the present spawning stock. To this end, an SSB per recruit analysis has been carried out. As one should expect for a relatively long-lived species with low mortality, the spawning stock is currently rather old. At F =0.075, the mean age is about 9 years, 80% is older than 5 years and 20% older than 12 years. So, an improved recruitment will take some time to materialize as increased SSB. The results also indicate that with a low F, the plus group still does matter.

The current stock assessment method for western horse mackerel is Stock Synthesis 3, as agreed in the WKWIDE benchmark of 2017 (ICES, 2017b). Reference point were also set at WKWIDE 2017 but have subsequently been updated in the IBPWHM 2019 (ICES, 2019b). In addition, an exploratory SAM assessment has been carried out as part of IBPWHM 2019. This was done in order to get a second view on stock trends but also to be able to run the SAM HCR forecast as part of the development of a potential rebuilding plan. The exploratory SAM assessment (https://www.stockassessment.org/setStock.php?stock=WHOM2018) was initiated with the same input data as was used for the Stock Synthesis assessment of WGWIDE 2018 (ICES, 2018) with the exception of the length frequency data, which was not used. The PELACUS survey data was therefore only used as an index of biomass within SAM. The process of fine-tuning the assessment lead to the binding of the observation variances for certain variables and to the application of a fixed selectivity pattern (correlation coefficient ϱ=1 in the F random process (https://github.com/martinpastoors/wgwide/blob/master/R/HOM%20optimization_SAM.R). A comparison of Fbar and SSB between the SS3 assessments of WG2018 and 2019 with the SAM assessment (WG18SAM, WG19SAM), shows that the general trends are the same but that there are some deviations in certain periods (e.g. the SSB in the late 1980s is estimated substantially higher in SAM compared to SS3). The Stock Synthesis results are in general a bit smoother compared to SAM.

In order to be able to use the SAM assessment as an alternative assessment in the rebuilding plan evaluation, we needed to estimate reference point for this assessment. In doing so, we aimed to follow the same procedure as during IBPWHM 2019 (ICES, 2019b). However, one of the elements of the reference point estimation, triggered a more in-depth study: the role of assessment uncertainty parameter Fcv and Fphi. There has been little standardization in how Fcv and Fphi have been calculated in different benchmarks where reference points were estimated. Fcv is expected to capture the assessment error in the advisory year and Fphi is the autocorrelation in assessment error in the advisory year (ICES, 2014a). We documented the method for generating the input data for the calculations and explored the sensitivity of Fcv and Fphi to the assessment that was used (both for western horse mackerel and for Atlantic mackerel). We found that there can be a high dependence of Fphi on the assessment that is used to compare against the Fset. When the assessment that is used has values that are all

higher or lower than the Fset values, then Fphi will be close to zero. To our knowledge, this behaviour of Fphi was unknown so far. We also found that the number of years that is used for calculating Fcv and Fphi may have an impact on the values. In the recommendations from WKMSYREF3 it is stated that 10 years (or more) should be taken. A further study should be undertaken to assessment the impacts of using different time periods for estimating Fcv and Fphi.

During the IBPWHM 2019, reference points were estimated for western horse mackerel based on the 2018 WGWIDE assessment and using default values for Fcv and Fphi (0.212 and 0.423) and using a segmented regression through Blim (segregBlim). In order to calculate reference points for the exploratory SAM assessment and to explore the sensitivity to the assessment year, reference points were calculated on the basis of the 2018 or 2019 assessments for SS and SAM. The reference points for the SAM assessment are based on the 2018 assessment. Bpa and Blim are lower than the values for the SS assessment, while the Fmsy is higher. The changes due the assessment year were minor for both the SS and SAM assessments.

RP	WG18	WG18SAM	WG19	WG19SAM
Blim	834480	611814	885341	612635
Flim	0.1107	0.1612	0.1049	0.1756
Fpa	0.07909	0.1152	0.07493	0.1254
MSYBtrigger	1168272	856540	1239478	857689
FMSY	0.09102	0.1262	0.08665	0.1353
FP05	0.08398	0.1255	0.07826	0.1402
FMSY_final	0.07909	0.1152	0.07493	0.1254

HCR evaluations

The HCR analyses represent two different assessment methods (SS3 and SAM) and two different HCR evaluation tools (EqSim and SAM HCR). Both HCR evaluation tools are of the type 'short-cut' with appropriate conditioning of the uncertainties in the assessment based on historical CV and autocorrelation in line with the recommendations from WKMSYREF3 and WKMSYREF4 . The evaluations followed the guidelines from WKGMSE2 (ICES, 2019c) and WKREBUILD (ICES, 2020).

Three different types of harvest control rules were evaluated:

- Constant F strategy: fixed Ftarget independent of biomass level
- ICES Advice Rule: breakpoint at Btrigger and straight decline in F to zero below Btrigger.
- Double Breakpoint rule: breakpoint at Btrigger and straight decline in F to 20% of Ftarget at Blim. Below Blim continued fishing at F = 0.2 * Ftarget.

For each of the HCRs, a number of different target fishing mortalities were explored (0.0, 0.05, 0.075, 0.1, 0.125, 0.15). No evaluation of different Btrigger values was carried out, so that all evaluations used MSY Btrigger as the trigger point. All HCRs where evaluated with three variants:

- Without any additional constraints

- With a minimum TAC of 50 kT
- With a maximum 20% inter-annual variation (IAV) in TAC, but only when the stock is above Btrigger)

Two simulation tools were used: the EqSim simulator and the SAM HCR forecast. The EqSim simulator is a further worked up version of the SimpSIM approach that was used for the blue whiting MSE in 2016 (ICES, 2016). The code was further developed by Andrew Campbell and Martin Pastoors to improve standardization, documentation and visualization of results. EqSim makes use of an Operating Model (OM) and a Management Procedure (MP). The SAM HCR forecast is a simple stochastic forecast with HCR to evaluate management for fish stocks that need rebuilding in the short-term. The stochastic forecasts start from what we believe is the current level of the stock with appropriate uncertainty, i.e. the assessment estimates currently used for tactical management advice, with consideration of the uncertainty in these estimates. Rebuilding is evaluated forward for a specified number of years and for different target fishing mortality values.

The EqSim with SS3 results indicate that the constant F strategy is the least cautious rule and the double breakpoint rule is the most cautious rule. Under the F strategy rule with a Ftarget of 0.075, rebuilding to Bpa is expected to be achieved is only just being achieved (probability just above 50%) by 2025, while in the double breakpoint rule this is expected to be achieved in 2024 with substantially higher probabilities of remaining above Bpa. The first year of rebuilding to Bpa in the double breakpoint rule with target fishing mortalities up to 0.1 is the same as the first year of rebuilding under the zero fishing scenarios.

Similar results have been obtained with the EqSim with SAM evaluations although the levels of SSB are slightly higher and risk to Blim is slightly lower. According to these evaluations, rebuilding to Bpa could be obtained by 2022 in all scenarios.

The SAM HCR with SAM evaluations have only been carried out for the ICES Advice Rule scenario, as this was intended more as a contrasting study rather than a full analysis of HCR evaluation. Again, we find similar patterns in simulated stock trends, but SSB is estimated higher than in the EqSim with SAM evaluations and risk to Blim stays below Blim for all target fishing mortalities that have been explored.

Given that the EqSim with SS3 evaluation is closest to the ICES advisory practice, this was used as the basis for the preferred rebuilding plan by the PELAC. The PELAC preferred options are:

- Target fishing mortality at Fmsy = 0.074 (approximated by 0.075 in the simulations)
- Blim at ICES Blim (834 480 t)
- Btrigger at ICES MSY Btrigger (1 168 272 t)
- Double breakpoint rule with 20% constraint on IAV above Btrigger
- Minimum F when stock is below Blim at 20% of Fmsy = 0.015

The selected rebuilding plan has a 50% probability of rebuilding to Blim by 2021 (similar to zero catch option) and a 50% probability of rebuilding to Bpa/MSY Btrigger by 2024 (similar to the zero-catch option). Furthermore, the probability of being below Blim remains well below 5% for the duration of the simulation.

In this scenario, the average catch in the years 2021-2025 is expected to be lower than recent catches. However, after rebuilding, catches should be able to be maintained around 100 000 tonnes.

11 References

Berg, C. W., and Nielsen, A. 2016. Accounting for correlated observations in an age-based state-space stock assessment model. ICES Journal of Marine Science: Journal du Conseil, 73: 1788-1797.

Campbell, A., De Oliveira, J. A. A., Kelly, C., and Roel, B. 2015. Report on Western Horse mackerel Management Strategy Evaluations (MSE). Report for Pelagic Fishing Industry. .

Cox, S. P., Benson, A. J., Doherty, B., and Johnson, S. 2018. Evaluation of potential rebuilding strategies for the Western Horse Mackerel (Trachurus trachurus) fishery.

Cox, S. P., and Kronlund, A. R. 2008. Practical stakeholder-driven harvest policies for groundfish fisheries in British Columbia, Canada. Fisheries Research, 94: 224-237.

Farrell, E. D., Carlsson, J. E. L., and Carlsson, J. 2016. Next Gen Pop Gen: implementing a high-throughput approach to population genetics in boarfish (Capros aper). Royal Society Open Science, 3.

Farrell, E. D., Fuentes-Pardo, A. P., Pettersson, M., Sprehn, C. G., and Andersson, L. 2020. Population structure of the Atlantic horse mackerel (Trachurus trachurus) revealed by whole-genome sequencing.

ICES. 2008. Western horse mackerel (Trachurus trachurus) (Divisions IIa, IVa, Vb, VIa, VIIa–c,e–k, and VIIIa–e), Section 9.4.3 in Advice 2008. December 2008.

ICES 2013a. EC request to ICES to evaluate possible modifications of the long-term management arrangement for the Western horse mackerel stock. Section 9.3.3.4 in Advice October 2013. *In* Report of the ICES Advisory Committee, 2013, p. 7 pp. ICES advice, 2013.

ICES. 2013b. Report of the Workshop to consider reference points for all stocks (WKMSYREF), 23 - 25 January 2013, Copenhagen, Denmark. ICES C.M. 2013 / ACOM:37. 17 pp. pp.

ICES. 2014a. Report of the Joint ICES-MYFISH Workshop to consider the basis for FMSY ranges for all stocks (WKMSYREF3), 17–21 November 2014, Charlottenlund, Denmark. ICES C.M. 2014 / ACOM:64.

ICES. 2014b. Report of the Workshop to consider reference points for all stocks (WKMSYREF2), 8-10 January 2014, Copenhagen, Denmark. . ICES C.M. 2014 / ACOM:47. 91 pp. pp.

ICES. 2015. Report of the Workshop to consider FMSY ranges for stocks in ICES categories 1 and 2 in Western Waters (WKMSYREF4), 13–16 October 2015, Brest, France. ICES C.M. 2015 / ACOM:58.

ICES. 2016. Report of the Workshop on Blue Whiting Long Term Management Strategy Evaluation (WKBWMS), 30 August 2016, Copenhagen. ICES C.M. 2016 / ACOM: 53.

ICES. 2017a. 12.4.3.1 ICES fisheries management reference points for category 1 and 2 stocks. ices.pub.3036.

ICES. 2017b. Report of the Benchmark Workshop on Widely Distributed Stocks (WKWIDE). ICES C.M. 2017 / ACOM:36.

ICES 2019a. Horse mackerel (Trachurus trachurus) in Subarea 8 and divisions 2.a, 4.a, 5.b, 6.a, 7.a–c, and 7.e–k (the Northeast Atlantic). *In* ICES Advice 2019, p. 7 pp.

ICES. 2019b. Interbenchmark Protocol on reference points for western horse mackerel (Trachurus trachurus) in subarea 8 and divisions 2.a, 4.a, 5.b, 6.a, 7.a-c,e-k (the Northeast Atlantic) (IBPWHM). ICES VOLUME X | ISSUE X (FORTHCOMING).

ICES. 2019c. Report of the Workshop on Guidelines for Management Strategy Evaluations (WKGMSE2). Volume 1, Issue 33.

ICES. 2019d. Working Group on Widely Distributed Stocks (WGWIDE 2019) Volume 1, Issue 36.

ICES. 2020. Workshop on guidelines and methods for the evaluation of rebuilding plans (WKREBUILD).2:55. 79 pp. . Volume 2, Issue 55. 79 pp pp.

Nielsen, A., and Berg, C. W. 2014. Estimation of time-varying selectivity in stock assessments using state-space models. Fisheries Research, 158: 96-101.

Working Document to

ICES Working Group on Widely Distributed Stocks (WGWIDE, No. 5) ICES HQ, Copenhagen, Denmark, (digital meeting) 26. August – 1. September 2020

Cruise report from the International Ecosystem Summer Survey in the Nordic Seas (IESSNS) 1st July – 4th August 2020

Leif Nøttestad, Valantine Anthonypillai, Are Salthaug, Åge Høines
Institute of Marine Research, Bergen, Norway

Anna Heiða Ólafsdóttir, James Kennedy
Marine and Freshwater Research Institute, Hafnarfjörður, Iceland

Eydna í Homrum, Leon Smith
Faroe Marine Research Institute, Tórshavn, Faroe Islands

Teunis Jansen, Søren Post
Greenland Institute of Natural Resources, Nuuk, Greenland

Kai Wieland
National Institute of Aquatic Resources, Denmark

Contents

1 Executive summary

The International Ecosystem Summer Survey in the Nordic Seas (IESSNS) was performed within approximately 5 weeks from July 1st to August 4th in 2020 using six vessels from Norway (2), Iceland (1), Faroe Islands (1), Greenland (1) and Denmark (1). The main objective is to provide annual age-segregated abundance index, with an uncertainty estimate, for northeast Atlantic mackerel (*Scomber scombrus*). The index is used as a tuning series in stock assessment according to conclusions from the 2017 and 2019 ICES mackerel benchmarks. A standardised pelagic swept area trawl method is used to obtain the abundance index and to study the spatial distribution of mackerel in relation to other abundant pelagic fish stocks and to environmental factors in the Nordic Seas, as has been done annually since 2010. Another aim is to construct a new time series for blue whiting (*Micromesistius poutassou*) abundance index and for Norwegian spring-spawning herring (NSSH) (*Clupea harengus*) abundance index. This is obtained by utilizing standardized acoustic methods to estimate their abundance in combination with biological trawling on acoustic registrations. The time series for blue whiting and NSSH have now been conducted for five years (2016-2020).

The mackerel index increased by 7.0% for biomass and 0.3% for abundance (numbers of individuals) compared to the 2019 index. In 2020, the most abundant year classes were 2010, 2016, 2011, 2013 and 2014, respectively. Overall, the cohort internal consistency continues to improve with a longer time series (2010-2020).

The survey coverage area was 2.9 million km^2 in 2020, which is similar as in previous years from 2017 to 2019. Furthermore, 0.26 million km^2 was surveyed in the North Sea in July 2020. Distribution zero boundaries were found in majority of the survey area with an exception of high mackerel abundance in the northwestern region of the Norwegian Sea into the Fram Strait west of Svalbard. The mackerel appeared less patchily distributed within the survey area and had a pronounced distribution in the central and northern Norwegian Sea in 2020 compared to previous years. This major difference in distribution consists of a substantial decline of mackerel in the west and corresponding increase in the central and northern part of the Norwegian Sea.

The total number of Norwegian spring-spawning herring (NSSH) recorded during IESSNS 2020 was 20.3 billion and the total biomass index was 5.93 million tonnes, which is significantly higher than in 2019 (34% and 24%, respectively). The increase was due to the recruiting 2016 year-class coming strongly into the survey area. The herring stock is dominated by 4-year old herring (year class 2016) in terms of numbers (40%) and biomass (33%), but this year class is still mainly in the northeastern part of the Norwegian Sea. The 2013 year class (7 year old) is distributed in all areas with herring in the survey and it contributes 22% and 20% to the total biomass and abundance, respectively.

The total biomass of blue whiting registered during IESSNS 2020 was 1.8 million tons, which is an 11% decrease since 2019. The stock estimate in number of age groups 1+ for 2020 is 16.5 billion compared to 16.2 billion in 2019. Age group 1 is dominating the estimate in 2020 (22% and 35% of the biomass and by numbers, respectively, looking at age groups 1+). A good sign of recruiting year class (0-group) was also seen in the survey this year. Of the older age groups 6 year old blue whiting was most abundant.

As in previous years, there was overlap in the spatio-temporal distribution of mackerel and herring. This overlap occurred in the southern and south-western parts of the Norwegian Sea, and with the strong 2016 year class of NSSH, there was also overlap in the central and north eastern part of the Norwegian Sea. In the eastern Norwegian sea between 62-67°N, mackerel were present but herring were in low abundance, in contrast, in areas north of Iceland, herring were present while mackerel were absent. Older and younger herring were spatially segregated with larger herring distributed to the east and north of Iceland and in the southern Norwegian Sea, while young herring were found in the northeastern Norwegian Sea.

Other fish species also monitored are lumpfish (*Cyclopterus lumpus*) and Atlantic salmon (*Salmo salar*). Lumpfish was caught at 74% of surface trawl stations distributed across the surveyed area from Cape

Farwell, Greenland, to western part of the Barents Sea. Abundance was greater north of latitude 66 °N compared to southern areas. A total of 54 Atlantic salmon were caught in 30 stations both in coastal and offshore areas from 60°N to >77°N in the upper 30 m of the water column. The salmon ranged from 0.084 kg to 2.73 kg in weight, dominated by postsmolt weighing 100-180 grams and 1 sea-winter individuals weighing 1-2 kg.

Satellite measurements of the sea surface temperature (SST) showed that the eastern part of the Norwegian Sea and coastal waters of east Greenland in July 2020 was higher, while the western part of the Norwegian Sea, the waters south of Iceland, in the Irminger Sea and around the Faroe islands in July 2020 was broadly similar, to the average for July 1990-2009. The upper layer (10 m depth) was 1.0-2.0°C colder in 2020 compared to 2019 in most of Icelandic and Greenland waters but along the Norwegian coast, the temperature was 1.0-2.0°C warmer in 2020 compared to 2019.

Zooplankton biomass decreased from 2018-2020 in both Greenlandic and Icelandic waters. Average zooplankton biomass in the Norwegian Sea has been relatively stable over the years of the survey.

2 Introduction

During approximately five weeks of survey in 2020 (1st of July to 4th of August), six vessels; the M/V "Kings Bay" and M/V "Vendla" from Norway, and M/V "Tróndur í Gøtu" operating from Faroe Islands, the R/V "Árni Friðriksson" from Iceland, the M/V "Eros" operating in Greenland waters and M/V "Ceton" operating in the North Sea by Danish scientists, participated in the International Ecosystem Summer Survey in the Nordic Seas (IESSNS).

The main aim of the coordinated IESSNS was to collect data on abundance, distribution, migration and ecology of Northeast Atlantic (NEA) mackerel (*Scomber scombrus*) during its summer feeding migration phase in the Nordic Seas. The resulting abundance index will be used in the stock assessment of NEA mackerel at the annual meeting of ICES working group of widely distributed stocks (WGWIDE). The IESSNS mackerel index time series goes back to 2010. Since 2016, systematic acoustic abundance estimation of both Norwegian spring-spawning herring (*Clupea harengus*) and blue whiting (*Micromesistius poutassou*) have also been conducted. This is considered as potential input for stock assessment, when the time series are sufficiently long. Furthermore, the IESSNS is a pelagic ecosystem survey collecting data on physical oceanography, plankton and other fish species such as lumpfish and Atlantic salmon. Opportunistic whale observations are also recorded. The wide geographical coverage, standardization of methods, sampling on many trophic levels and international cooperation around this survey facilitates research on the pelagic ecosystem in the Nordic Seas, see e.g. Nøttestad et al. (2016), Olafsdottir et al. (2019), Bachiller et al. (2018), Jansen et al. (2016), Nikolioudakis et al. (2019).

The methods have evolved over time since the survey was initiated by Norway in the Norwegian Sea in the beginning of the 1990s. The main elements of standardization were conducted in 2010. Smaller improvements have been implemented since 2010. Faroe Islands and Iceland have participated in the joint mackerel-ecosystem survey since 2009. Greenland since 2013 and Denmark from 2018.

The North Sea was included in the survey area for the third time in 2020, following the recommendations of WGWIDE. This was done by scientists from DTU Aqua, Denmark. The commercial fishing vessels "Ceton S205" was used, and in total 35 stations (CTD and fishing with the pelagic Multpelt 832 trawl) were successfully conducted. No problems applying the IESSNS methods were encountered. Area coverage, however, was restricted to the northern part of the North Sea at water depths deeper than 50 m and no plankton samples were taken (see Appendix 1 for comparison with 2018 and 2019 results).

3 Material and methods

Coordination of the IESSNS 2020 was done during the WGIPS 2020 meeting in January 2020 in Bergen, Norway, and by correspondence in spring and summer 2020. The participating vessels together with their effective survey periods are listed in Table 1.

Overall, the weather conditions were calm with good survey conditions for all six vessels for oceanographic monitoring, plankton sampling, acoustic registrations and pelagic trawling. However, several of the vessels experienced more wind than in previous years. The weather was fairly good and calm for the two Norwegian vessels except for a few days of fog in the northernmost part of the Norwegian Sea influencing the visual observations. The Icelandic vessel, operating in Icelandic waters, the Iceland basin and the Irminger Sea, encounter unusually many stormy days with a total of 6 days where wind conditions hampered plankton sampling and demanded reduced sailing speed for acoustic recordings. The weather was mostly calm for the Faroese vessel operating mainly in Faroese waters. The chartered vessel Ceton had excellent weather throughout the survey.

During the IESSNS, the special designed pelagic trawl, Multpelt 832, has now been applied by all participating vessels since 2012. This trawl is a product of cooperation between participating institutes in designing and constructing a standardized sampling trawl for the IESSNS. The work was lead by trawl gear scientist John Willy Valdemarsen, Institute of Marine Research (IMR), Bergen, Norway (Valdemarsen et al. 2014). The design of the trawl was finalized during meetings of fishing gear experts and skippers at meetings in January and May 2011. Further discussions on modifications in standardization between the rigging and operation of Multpelt 832 was done during a trawl expert meeting in Copenhagen 17-18 August 2012, in parallel with the post-cruise meeting for the joint ecosystem survey, and then at the WKNAMMM workshop and tank experiments on a prototype (1:32) of the Multpelt 832 pelagic trawl, conducted as a sequence of trials in Hirtshals, Denmark from 26 to 28 February 2013 (ICES 2013a). The swept area methodology was also presented and discussed during the WGISDAA workshop in Dublin, Ireland in May 2013 (ICES 2013b). The standardization and quantification of catchability from the Multpelt 832 pelagic trawl was further discussed during the mackerel benchmark in Copenhagen in February 2014. Recommendations and requests coming out of the mackerel benchmark in February 2014, were considered and implemented during the IESSNS survey in July-August 2014 and in the surveys thereafter. Furthermore, recommendations and requests resulting from the mackerel benchmark in January-February 2017 (ICES 2017), were carefully considered and implemented during the IESSNS survey in July-August 2017. In 2018, the Faroese and Icelandic vessels employed new, redesigned cod-ends with the capacity to hold 50 tonnes. This was done to avoid the cod-end from bursting during hauling of large catches as occurred at three stations in the 2017 IESSNS.

Table 1. Survey effort by each of the five vessels during the IESSNS 2020. The number of predetermined ("fixed") trawl stations being part of the swept-area stations for mackerel in the IESSNS are shown after the total number of trawl stations (* including 2 days of capelin study).

Vessel	Effective survey period	Length of cruise track (nmi)	Total trawl stations/ Fixed stations	CTD stations	Plankton stations
Árni Friðriksson	1/7-30/7	5596	65/58	60	48
Tróndur í Gøtu	2-17/7	2600	43/38	38	38
Eros	16/7-4/8	2535*	34/33	37	33
Ceton	1/7-9/7	1720	35/35	35	-
Vendla	3/7-3/8	5346	90/77	78	78
Kings Bay	3/7-3/8	5377	86/74	74	70
Total	1/7-4/8	23174	353/315	322	267

3.1 Hydrography and Zooplankton

The hydrographical and plankton stations by all vessels combined are shown in Figure 1. Árni Friðriksson was equipped with a SEABIRD CTD sensor with a water rosette that was applied during the entire cruise. Tróndur í Gøtu was equipped with a mini SEABIRD SBE 25+ CTD sensor, Kings Bay and Vendla were both equipped with Seabird CTD sensors. Eros used a SEABIRD 19+V2 CTD sensor. Ceton used a Seabird SeaCat 4 CTD. The CTD-sensors were used for recording temperature, salinity and pressure (depth) from the surface down to 500 m, or to the bottom when at shallower depths.

Zooplankton was sampled with a WP2-net on 5 of 6 vessels, Ceton did not take any plankton samples. Mesh sizes were 180 μm (Kings Bay and Vendla) and 200 μm (Árni Friðriksson, Tróndur í Gøtu and Eros). The net was hauled vertically from a depth of 200 m (or bottom depth at shallower stations) to the surface at a speed of 0.5 m/s. All samples were split in two, one half preserved for species identification and enumeration, and the other half dried and weighed. Detailed description of the zooplankton and CTD sampling is provided in the survey manual (ICES 2014a).

Not all planned CTD and plankton stations were taken due to bad weather. The number of stations taken by the different vessels is provided in Table 1.

3.2 Trawl sampling

All vessels used the standardized Multpelt 832 pelagic trawl (ICES 2013a; Valdemarsen et al. 2014; Nøttestad et al. 2016) for trawling, both for fixed surface stations and for trawling at greater depths to confirm acoustic registrations. Standardization of trawl deployment was emphasised during the survey as in previous years (ICES 2013a; ICES 2014b; ICES 2017). Sensors on the trawl doors, headrope and ground rope of the Multpelt 832 trawl recorded data, and allowed live monitoring, of effective trawl width (actually door spread) and trawl depth. The properties of the Multpelt 832 trawl and rigging on each vessel is reported in Table 2.

Trawl catch was sorted to the highest taxonomical level possible, usually to species for fish, and total weight per species recorded. The processing of trawl catch varied between nations as the Norwegian, Icelandic and Greenlandic vessels sorted the whole catch to species but the Faroese vessel sub-sampled the catch before sorting. Sub-sample size ranged from 60 kg (if it was clean catch of either herring or mackerel) to 150 kg (if it was a mixture of herring and mackerel), however, all lumpfish were picked out from the total catch. The biological sampling protocol for trawl catch varied between nations in number of specimens sampled per station (Table 3).

Table 2. Trawl settings and operation details during the international mackerel survey in the Nordic Seas from 1st July to 4th August 2020. The column for influence indicates observed differences between vessels likely to influence performance. Influence is categorized as 0 (no influence) and + (some influence).

Properties	**Kings Bay**	**Árni Friðriksson**	**Vendla**	**Ceton**	**Tróndur í Gøtu**	**Eros**	**Influence**
Trawl producer	Egersund Trawl AS	Hampiðjan new 2017 trawl	Egersund Trawl AS	Egersund Trawl AS	Vónin	Hampiðjan	0
Warp in front of doors	Dynex–34 mm	Dynex-34 mm	Dynex -34 mm	Dynex	Dynema – 30 mm	Dynex-34 mm	+
Warp length during towing	350	350	350	300-350	350	340-347	0
Difference in warp length port/starb. (m)	2-10	16	2-10	10	0-15	10-20	0
Weight at the lower wing ends (kg)	2×400	2×400 kg	2×400	2×400	2×400	2×500	0
Setback (m)	6	14	6	6	6	6	+
Type of trawl door	Seaflex 7.5 m^2 adjustable hatches	Jupiter	Seaflex 7.5 m^2 adjustable hatches	Thybron type 15	Injector F-15	T-20vf Flipper	0
Weight of trawl door (kg)	1700	2200	1700	1970	2000	2000	+
Area trawl door (m^2)	7.5 with 25% hatches (effective 6.5)	6	7.5 with 25% hatches (effective 6.5)	7	6	7 with 50% hatches (effective 6.5)	+
Towing speed (knots) mean (min-max)	4.72 (4.3-5.3)	5.1 (4.5-5.8)	4.89 (4.1-5.5)	4.8 (4.0-5.3)	4.9 (4.4-5.4)	4.9 (4.1-5.9)	+
Trawl height (m) mean (min-max)	28-40	36 (28-45)	28-37	31 (24-39)	45.5 (40.5-49.5)	-	+
Door distance (m) mean (min-max)	118.3 (115-120)	101.3 (90 - 113)	121.8 (118-126)	127 (115-139)	99.1 (94 – 104)	118 (113-121)	+
Trawl width (m)*	65.8	60.6	68.0	70.54	57.2	66.5	+
Turn radius (degrees)	5-10	5	5-12	5-10	5-10 BB turn	6-8 SB turn	+
Fish lock front of cod-end	Yes	Yes	Yes	Yes	Yes	Yes	+
Trawl door depth (port, starboard, m) (min-max)	5-15, 7-18	12-12, 4-31	6-22, 8-23	4-16	4-20, 5-19	(11.4-11)	+
Headline depth (m)	0	0	0	0	0	0-1	+
Float arrangements on the headline	Kite with fender buoy +2 buoys on each wingtip	Kite + 2 buoys on wings	Kite with fender buoy +2 buoys on each wingtip	Kite with fender buoy + 2 buoys on each wingtip	Kite with fender buoy + 1 buoy on each wingtip	Kite + 1 buoy on each wingtips	+
Weighing of catch	All weighted	All weighted	All weighted	All weighted	All weighed	All weighted	+

* calculated from door distance

Table 3. Protocol of biological sampling during the IESSNS 2020. Numbers denote the maximum number of individuals sampled for each species for the different determinations.

	Species	Faroes	Greenland	Iceland	Norway	Denmark
Length measurements	Mackerel	100	100/50*	150	100	≥ 100 (separated in small and large category if appropriate)
	Herring	100	100/50*	200	100	
	Blue whiting	100	100/50*	100	100	
	Lumpfish	All	All	all	all	all
	Salmon	-	All	all	all	-
	Other fish sp.	100	25/25	50	25	As appropriate
Weight, sex and	Mackerel	15-25	25	50	25	***
maturity determination	Herring	15-25	25	50	25	0
	Blue whiting	5-50	25	50	25	0
	Lumpfish	10		1^	25	0
	Salmon	-		0	25	0
	Other fish sp.	0	0	0	0	0
Otoliths/scales collected	Mackerel	15-25	25	25	25	***
	Herring	15-25	25	50	25	0
	Blue whiting	5-50	25	50	25	0
	Lumpfish	0	0	1	0	0
	Salmon	-	0	0	0	0
	Other fish sp.	0	0	0	0	0
Fat content	Mackerel	0	50	10**	0	0
	Herring	0	0	10**	0	0
	Blue whiting	0	50	10	0	0
Stomach sampling	Mackerel	5	20	10**	10	0
	Herring	5	20	10**	10	0
	Blue whiting	5	20	10	10	0
	Other fish sp.	0	0	0	10	0
Tissue for genotyping	Mackerel	0	0	0	0	0
	Herring	0	0	0	0	0

*Length measurements / weighed individuals
**Sampled at every third station
*** One fish per cm-group ≤ 25 cm and two fish > 25 cm from each station was weighed and aged.
^All live lumpfish were tagged and released, only otoliths taken from fish which were dead when brought aboard

Underwater camera observations during trawling

M/V "Kings Bay" and M/V "Vendla" employed an underwater video camera (GoPro HD Hero 4 and 5 Black Edition, www.gopro.com) to observe mackerel aggregation, swimming behaviour and possible escapement from the cod end and through meshes. The camera was put in a waterproof box which tolerated pressure down to approximately 100 m depth. No light source was employed with cameras; hence, recordings were limited to day light hours. Some recordings were also taken during nighttime when there was midnight sun and good underwater visibility. Video recordings were collected at 89 trawl stations. The camera was attached on the trawl in the transition between 200 mm and 400 mm meshes.

3.3 Marine mammals

Opportunistic observations of marine mammals were conducted by scientific personnel and crew members from the bridge between 3rd July and 2nd August 2020 onboard M/V "Kings Bay" and M/V "Vendla". Marine mammal observations were conducted, during the day (weather permitting), by a dedicated whale observer aboard R/V Árni Friðriksson from 1st until 13th July 2020. Opportunistic observations were also done from the bridge by crew members between 1st and 30th July 2020.

3.4 Lumpfish tagging

Lumpfish caught during the survey by vessels R/V "Árni Friðriksson", M/V "Eros", M/V "Kings Bay" and M/V "Vendla" were tagged with Peterson disc tags and released. When the catch was brought aboard, any lumpfish caught were transferred to a tank with flow-through sea water. After the catch of other species had been processed, all live lumpfish larger than ~15 cm were tagged. The tags consisted of a plastic disc secured with a titanium pin which was inserted through the rear of the dorsal hump. Contact details of Biopol (www.biopol.is) were printed on the tag. The fish were returned to the tank until all fish were tagged. The fish were then released, and the time of release was noted which was used to determine the latitude and longitude of the release location.

3.5 Acoustics

Multifrequency echosounder

The acoustic equipment onboard Kings Bay and Vendla were calibrated 2nd July 2020 for 18, 38, 70, 120 and 200 kHz. Onboard Kings Bay there were permanent noise challenges on the multifrequency acoustics including the 38kHz transducer during the entire survey. This noise problem predominantly influenced waters deeper than 200 m and could not be solved during the survey. The noise problem was much less at low speed (<5 knots) compared to high cruising speed (10 knots). Árni Friðriksson was calibrated in early May 2020 for the frequencies 18, 38, 70, 120 and 200 kHz. On Árni, EK80 transceivers were installed recently, there were some unusual noise problems in the backscatter and intermittent technical problems which prevented acoustic recordings a few times when vessel was on transport transect causing lack of acoustic track. Tróndur í Gøtu was calibrated on 26th June 2020 for 38 kHz and due to noise problems the first week; it was again calibrated 8th July after the issue had been resolved. Because of the noise issues, data from Tróndur í Gøtu south of Faroes were only usable down to 150 m. Calibration of the acoustic equipment onboard Eros was done after the cruise on the 2nd of August. All frequencies were calibrated successfully. Ceton did not conduct any acoustic data collection because no calibrated equipment was available. All the other vessels used standard hydro-acoustic calibration procedure for each operating frequency (Foote 1987). CTD measurements were taken in order to get the correct sound velocity as input to the echosounder calibration settings.

Acoustic recordings were scrutinized to herring and blue whiting on daily basis using the post-processing software (LSSS, see Table 4 for details of the acoustic settings by vessel). Acoustic measurements were not conducted onboard Ceton in the North Sea. Species were identified and partitioned using catch information, characteristic of the recordings, and frequency between integration on 38 kHz and on other frequencies by a scientist experienced in viewing echograms.

To estimate the abundance from the allocated NASC-values the following target strengths (TS) relationships were used.

Blue whiting: $TS = 20 \log(L) - 65.2$ dB (rev. acc. ICES CM 2012/SSGESST:01)
Herring: $TS = 20.0 \log(L) - 71.9$ dB

Table 4. Acoustic instruments and settings for the primary frequency (38 kHz) during IESSNS 2020.

	M/V Kings Bay	R/V Árni Friðriksson	M/V Vendla	M/V Tróndur í Gøtu 250620	M/V Tróndur í Gøtu 080720	Eros
Echo sounder	Simrad EK80	Simrad EK 80	Simrad EK 60	Simrad EK 60	Simrad EK 60	Simrad EK 80
Frequency (kHz)	18, 38, 70, 120, 200	18, 38, 70, 120, 200	18, 38, 70, 120, 200	38,120, 200	38,120, 200	18, 38, 70, 120, 200, 333
Primary transducer	ES38-7	ES38-7	ES38B	ES38B	ES38B	ES38B
Transducer installation	Drop keel	Drop keel	Drop keel	Hull	Hull	Hull
Transducer depth (m)	9	8	9	7	7	8
Upper integration limit (m)	15	15	15	Not used	Not used	15
Absorption coeff. (dB/km)	9.6	10.0	10.1	9.7	9.7	9.3
Pulse length (ms)	1.024	1.024	1.024	1.024	1.024	1.024
Band width (kHz)	2.43		2.43	2.43	2.43	2.43
Transmitter power (W)	2000	2000	2000	2000	2000	2000
Angle sensitivity (dB)	21.90	18	21.90	21.9	21.9	21.9
2-way beam angle (dB)	-20.70	-20.3	-20.70	-20.6	-20.6	-20.7
TS Transducer gain (dB)	26.33	26.9	25.46	23.44	24.09	25.50
s_A correction (dB)	-0.03	-0.02	-0.02	-0.65	-0.65	-0.6
alongship:	-0.28	6.53	0.19	7.42	7.20	6.86
athw. ship:	0.00	6.5	0.08	7.09	7.03	7.05
Maximum range (m)	500	500	500	500	500	750 for 18 and 38 kHz 500 for 70, 120 and 200 kHz
Post processing software	LSSS v.2.8.1	LSSS v.2.8	LSSS v.2.8.1	LSSS 2.8.0	LSSS 2.8.0	LSSS v.2.8

* No acoustic data collection

Multibeam sonar

Both M/V Kings Bay and M/V Vendla were equipped with the Simrad fisheries sonar SH90 (frequency range: 111.5-115.5 kHz), with a scientific output incorporated which allow the storing of the beam data for post-processing. Acoustic multibeam sonar data was stored continuously onboard Kings Bay and Vendla for the entire survey.

Cruise tracks

The six participating vessels followed predetermined survey lines with predetermined surface trawl stations (Figure 1). Calculations of the mackerel index are based on swept area approach with the survey area split into 13 strata, permanent and dynamic strata (Figure 2). Distance between predetermined surface trawl stations is constant within stratum but variable between strata and ranged from 35-90 nmi. The survey design using different strata is done to allow the calculation of abundance indices with uncertainty estimates, both overall and from each stratum in the software program StoX (see Salthaug et al. 2017). Temporal survey progression by vessel along the cruise tracks in July-August 2020 is shown in Figure 3. The cruising speed was between 10-12 knots if the weather permitted otherwise the cruising speed was adapted to the weather situation.

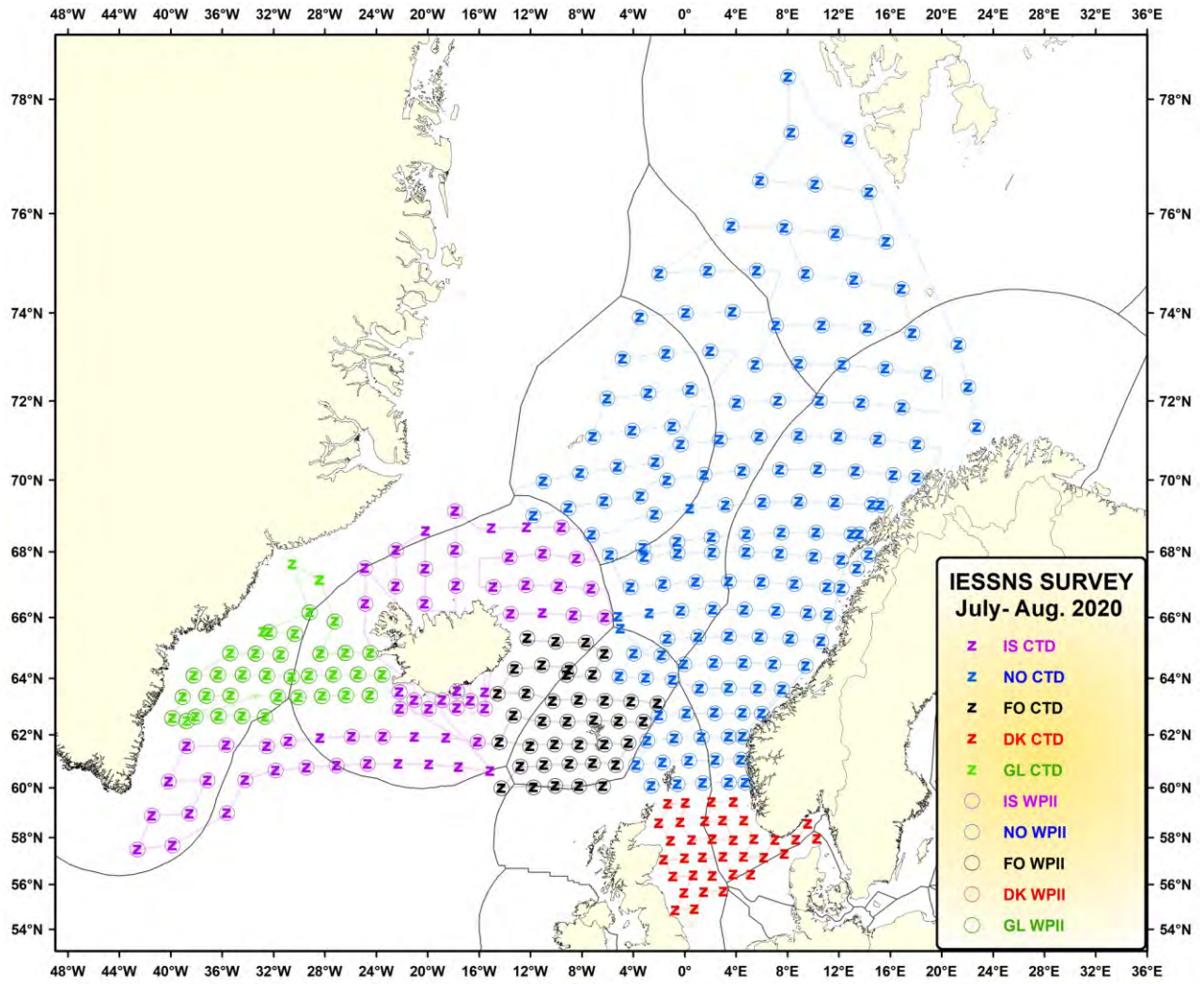

Figure 1. Fixed predetermined trawl stations (shown for CTD and WP2) included in the IESSNS 1st July – 4th August 2020. At each station a 30 min surface trawl haul, a CTD station (0-500 m) and WP2 plankton net samples (0-200 m depth) was performed. The colour codes, Árni Friðriksson (purple), Tróndur í Gøtu (black), Kings Bay and Vendla (blue), Eros (green) and Ceton (red).

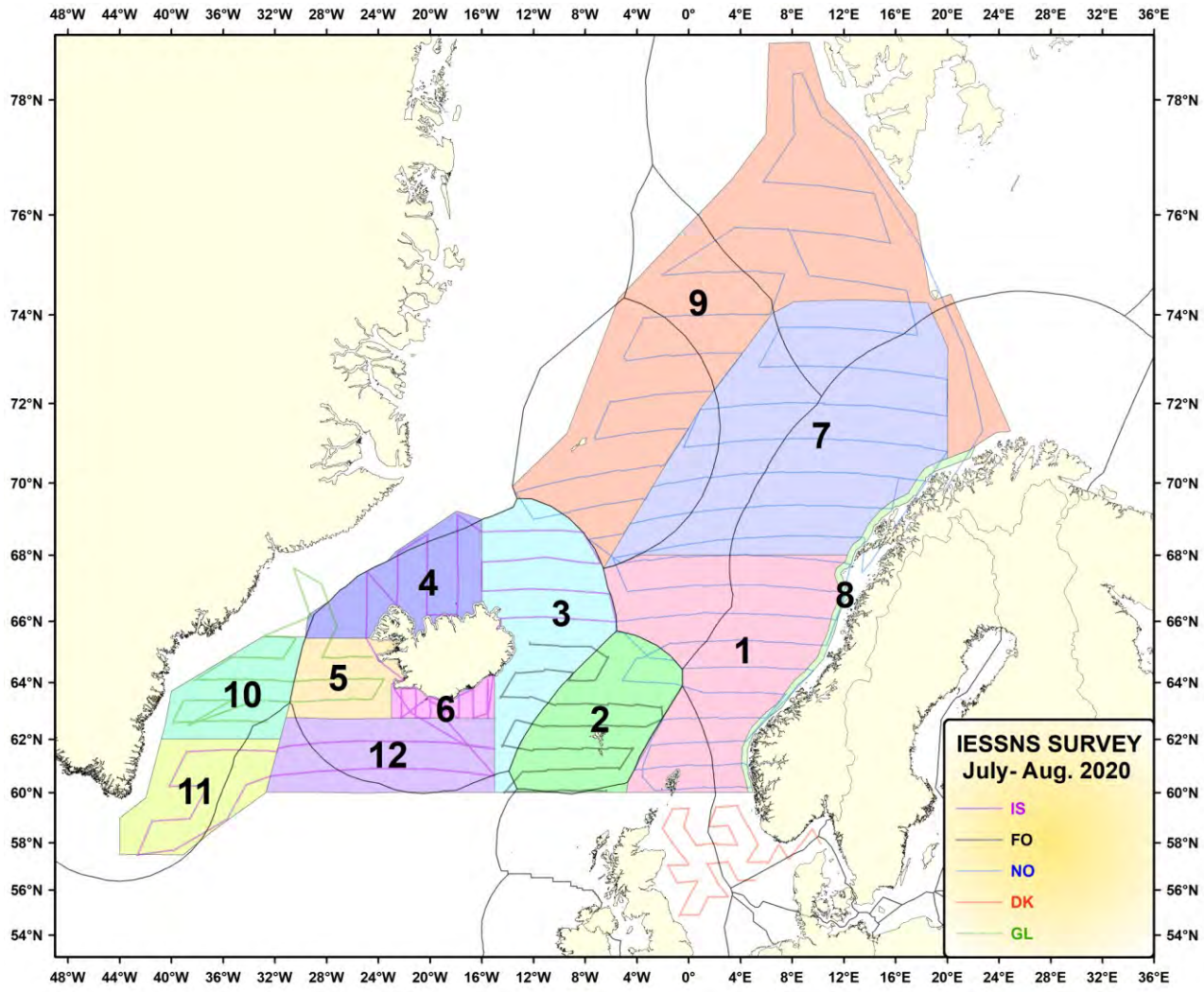

Figure 2. Permanent and dynamic strata used in StoX for IESSNS 2020. The dynamic strata are: 4, 9 and 11.

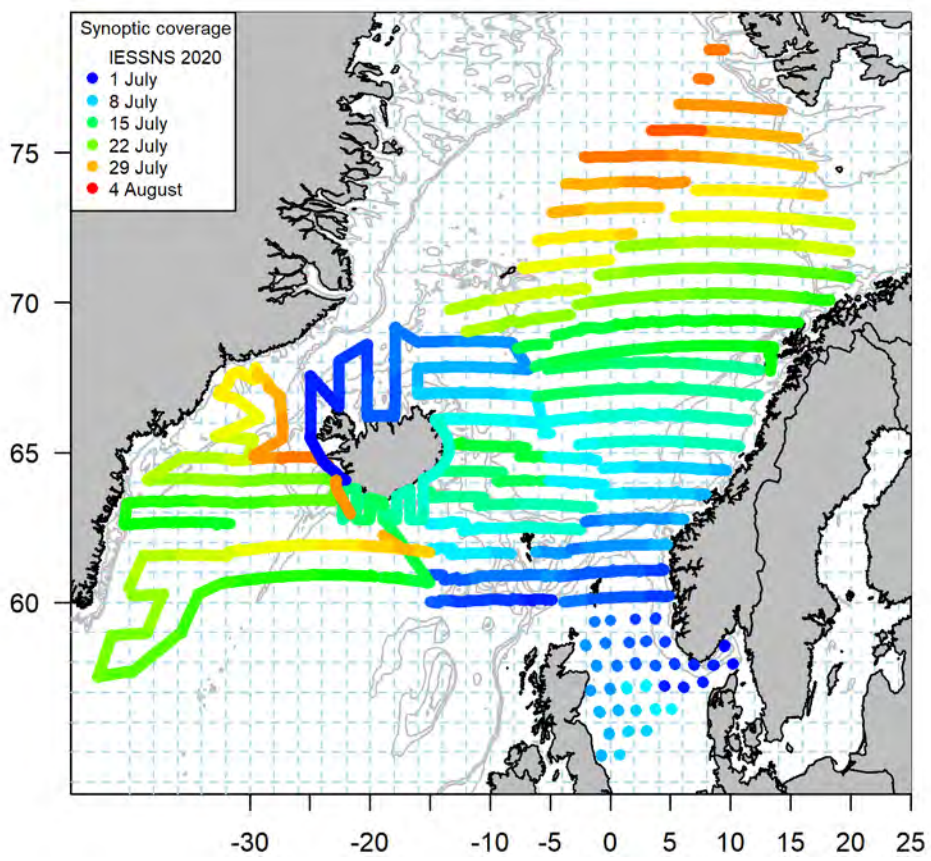

Figure 3. Temporal survey progression by vessel along the cruise tracks during IESSNS 2020: blue represents effective survey start (1st of July) progressing to red representing a five-week span (survey ended 4th of August). As Ceton did not record acoustics, they have been represented by station positions.

3.6 StoX

Stox is open source software developed at IMR, Norway to calculate survey estimates from acoustic and swept area surveys. A description of Stox can be found in Johnsen et al. (2019). The software, with examples and documentation, can be found at: http://www.imr.no/forskning/prosjekter/stox/nb-no. The program is a stand-alone application built with Java for easy sharing and further development in cooperation with other institutes. The underlying high-resolution data matrix structure ensures future implementations of e.g. depth dependent target strength and high-resolution length and species information collected with camera systems. Despite this complexity, the execution of an index calculation can easily be governed from user interface and an interactive GIS module, or by accessing the Java function library and parameter set using external software like R. Various statistical survey design models can be implemented in the R-library, however, in the current version of StoX the stratified transect design model developed by Jolly and Hampton (1990) is implemented. Mackerel, herring and blue whiting indices were calculated using the StoX software package (version 2.7).

3.7 Swept area index and biomass estimation

The swept area age segregated index is calculated separately for each stratum (see stratum definition in Figure 2). Individual stratum estimates are added together to get the total estimate for the whole survey area which is approximately defined by the area between 55°N and 79°N and 43°W and 23°E in 2020. The

density of mackerel on a trawl stations is calculated by dividing the total number caught by the assumed area swept by the trawl. The area swept is calculated by multiplying the towed distance by the horizontal opening of the trawl. The horizontal opening of the trawl is vessel specific, and the average value across all hauls is calculated based on door spread (Table 5 and Table 6). An estimate of total number of mackerel in a stratum is obtained by taking the average density based on the trawl stations in the stratum and multiplying this with the area of the stratum.

Table 5. Descriptive statistics for trawl door spread, vertical trawl opening and tow speed for each vessel during IESSNS 2020. Number of trawl stations used in calculations is also reported. Horizontal trawl opening was calculated using average vessel values for trawl door spread and tow speed (details in Table 6).

	Tróndur í Gøtu	RV Árni Friðriksson	Kings Bay	Vendla	Eros	Ceton
Trawl doors horizontal spread (m)						
Number of stations	37	58	74	78	33	35
Mean	99.1	101.3	118.3	121.8	115.2	127
max	104	113	135	129	134	139
min	94	90	110	107	100	114
st. dev.	2.2	5.1	2.84	4.6	5.2	5.7
Vertical trawl opening (m)						
Number of stations	37	58	74	78	33	35
Mean	45.5	36.4	33.6	30.3	34.9	31
max	49.5	45.0	40	40	44.8	39
min	40.5	27.5	29	25	29.2	24
st. dev.	2.0	3.8	2.9	3.0	3.2	3.9
Horizontal trawl opening (m)						
mean	57.2	60.6	65.8	68.0	67.4	70.5
Speed (over ground, nmi)						
Number of stations	38	58	74	78	33	35
mean	4.55	5.1	4.72	4.89	4.9	4.8
max	4.8	4.5	5.7	5.7	5.4	5.3
min	4.3	5.8	4.1	4.4	4.4	4.0
st. dev.	0.1	0.2	0.30	0.29	0.3	0.3

Horizontal trawl opening was calculated using average vessel values for trawl door spread and tow speed (Table 6). The estimates in the formulae were based on flume tank simulations in 2013 (Hirtshals, Denmark) where formulas were developed from the horizontal trawl opening as a function of door spread, for two towing speeds, 4.5 and 5 knots:

Towing speed 4.5 knots: Horizontal opening (m) = 0.441 * Door spread (m) + 13.094

Towing speed 5.0 knots: Horizontal opening (m) = 0.3959 * Door spread (m) + 20.094

Table 6. Horizontal trawl opening as a function of trawl door spread and towing speed. Relationship based on simulations of horizontal opening of the Multpelt 832 trawl towed at 4.5 and 5 knots, representing the speed range in the 2014 survey, for various door spread. See text for details. In 2017, the towing speed range was extended from 5.0 to 5.2, and in 2020 the door spread was extended to 122 m.

	Towing speed							
Door spread(m)	4.5	4.6	4.7	4.8	4.9	5.0	5.1	5.2
100	57.2	57.7	58.2	58.7	59.2	59.7	60.2	60.7
101	57.6	58.1	58.6	59.1	59.6	60.1	60.6	61.1
102	58.1	58.6	59.0	59.5	60.0	60.5	61.0	61.4
103	58.5	59.0	59.5	59.9	60.4	60.9	61.3	61.8
104	59.0	59.4	59.9	60.3	60.8	61.3	61.7	62.2
105	59.4	59.9	60.3	60.8	61.2	61.7	62.1	62.6
106	59.8	60.3	60.7	61.2	61.6	62.1	62.5	62.9
107	60.3	60.7	61.2	61.6	62.0	62.5	62.9	63.3
108	60.7	61.1	61.6	62.0	62.4	62.9	63.3	63.7
109	61.2	61.6	62.0	62.4	62.8	63.2	63.7	64.1
110	61.6	62.0	62.4	62.8	63.2	63.6	64.1	64.5
111	62.0	62.4	62.8	63.2	63.6	64.0	64.4	64.8
112	62.5	62.9	63.3	63.7	64.0	64.4	64.8	65.2
113	62.9	63.3	63.7	64.1	64.4	64.8	65.2	65.6
114	63.4	63.7	64.1	64.5	64.9	65.2	65.6	66.0
115	63.8	64.2	64.5	64.9	65.3	65.6	66.0	66.3
116	64.3	64.6	65.0	65.3	65.7	66.0	66.4	66.7
117	64.7	65.0	65.4	65.7	66.1	66.4	66.8	67.1
118	65.1	65.5	65.8	66.1	66.5	66.8	67.1	67.5
119	65.6	65.9	66.2	66.6	66.9	67.2	67.5	67.9
120	66.0	66.3	66.6	67.0	67.3	67.6	67.9	68.2
121	66.5	66.8	67.1	67.4	67.7	68.0	68.3	68.6
122	66.9	67.2	67.5	67.8	68.1	68.4	68.7	69.0

4 Results and discussion

4.1 Hydrography

Satellite measurements of sea surface temperature (SST) in the eastern part of the Norwegian Sea in July 2020 was slightly higher (0.5-1°C) compared to the average for July 1990-2009 based on SST anomaly plot (Figure 4). Surface temperature in the western part of the Norwegian Sea in July 2020 was broadly similar compared to the average (Figure 4). The coastal regions of Greenland were 1-2°C warmer than the average while in the waters south of Iceland, in the Irminger Sea and around the Faroe islands, the SST was similar to the average for July 1990-2009 (Figure 4). This contrasts with the situation in 2019 when SST in the coastal areas of Greenland were 2-3°C warmer and the waters south of Iceland, in the Irminger Sea and around the Faroe islands were 1-2°C warmer than the average. The pattern of anomalies of Sea Surface Temperature in July 2020 was quite different from the other years in the time series from 2010 to 2019.

It must be mentioned that the NOAA SST are sensitive to the weather condition (i.e. wind and cloudiness) prior to and during the observations and do therefore not necessarily reflect the oceanographic condition of the water masses in the areas, as seen when comparing detailed in situ features of SSTs between years (Figures 5-8). However, since the anomaly is based on the average for the whole month of July, it should give representative results of the surface temperature.

In situ measurements showed the upper layer (10 m depth) was 1.0-2.0°C colder in 2020 compared to 2019 in most of Icelandic and Greenland waters but 1.0-2.0°C warmer in 2020 compared to 2019 along the Norwegian coast (Figure 5). The temperature in the upper layer was higher than 8°C in most of the surveyed area, except along the north-western fringes of the surveyed areas north of Iceland where it was lower. In the deeper layers (50 m and deeper; Figure 6-8), the hydrographical features in the area were similar to the last four years (2014-2018) except around the Faroe Islands where temperature at 100 m depth was about 1°C warmer. At all depths there were a clear signal from the cold East Icelandic Current, which originates from the East Greenland Current.

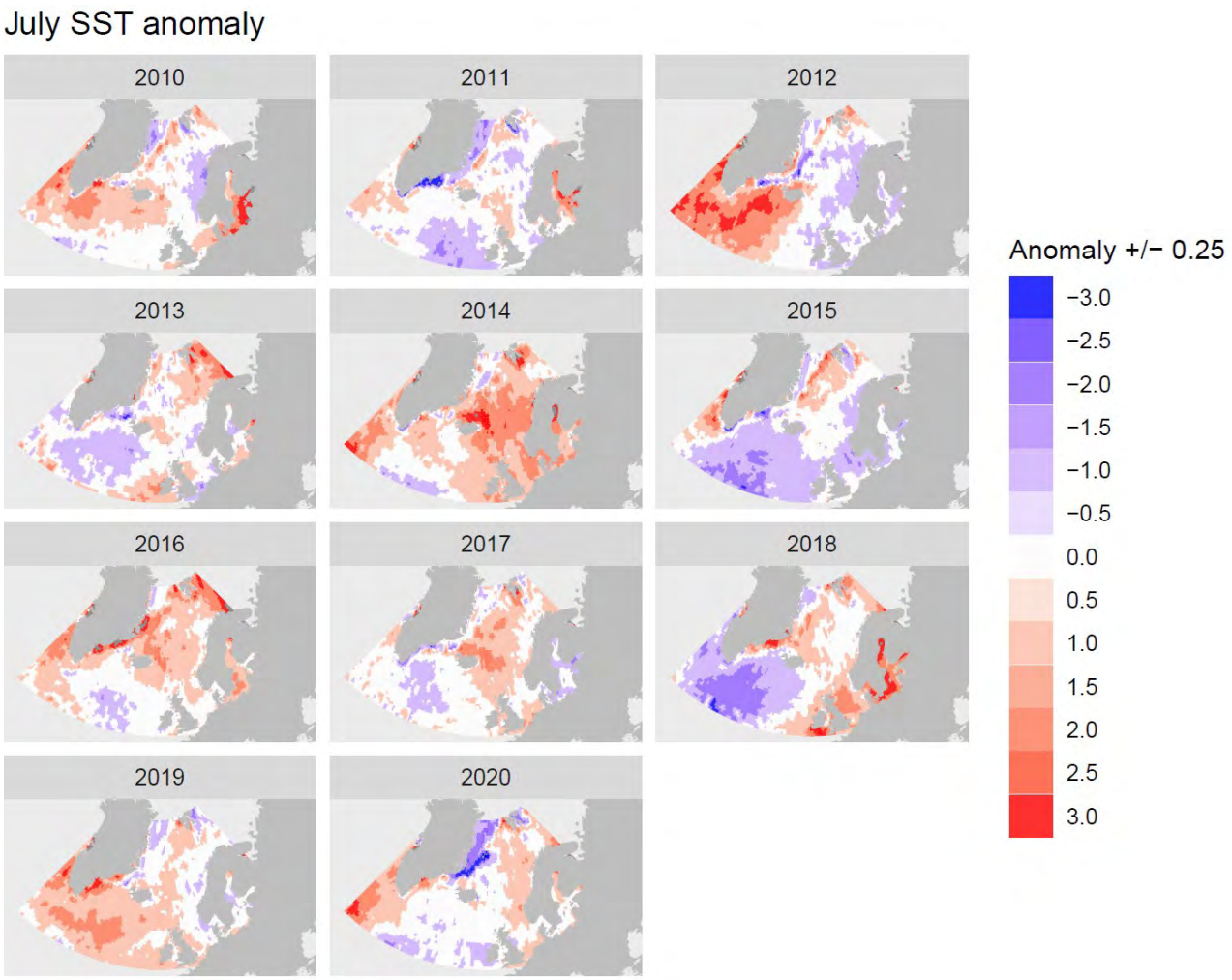

Figure 4. Annual sea surface temperature anomaly (°C) in Northeast Atlantic for the month of July from 2010 to 2020 showing warm and cold conditions in comparison to the average for July 1990-2009. Based on monthly averages of daily Optimum Interpolation Sea Surface Temperature (OISST, AVHRR-only, Banzon et al. 2016, https://www.ncdc.noaa.gov/oisst).

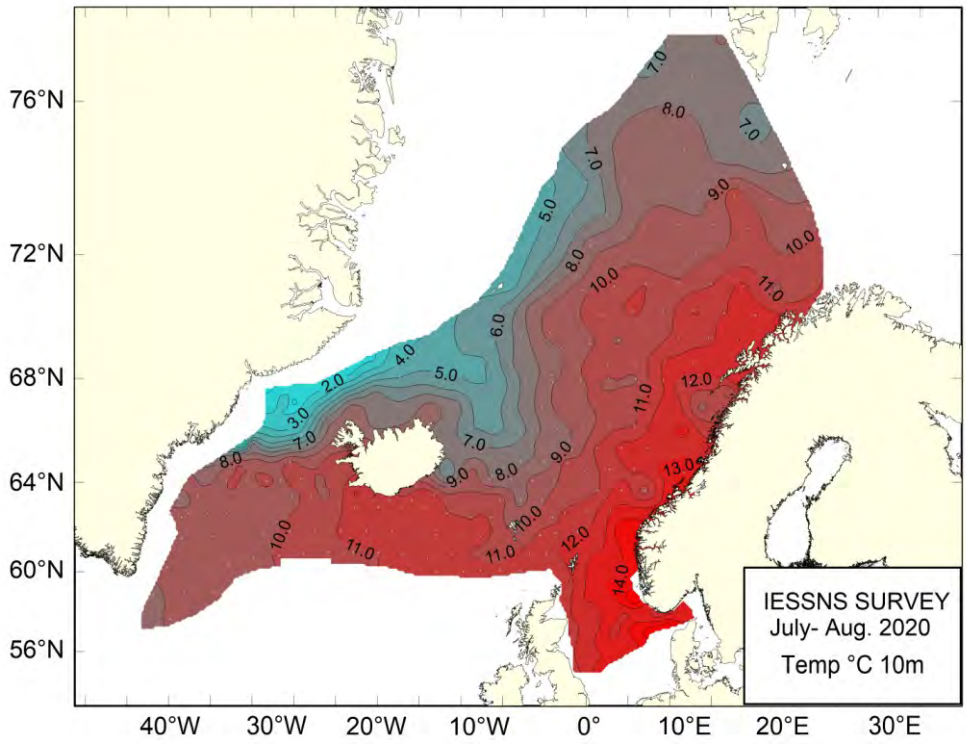

Figure 5. Temperature (°C) at 10 m depth in Nordic Seas and the North Sea in July-August 2020.

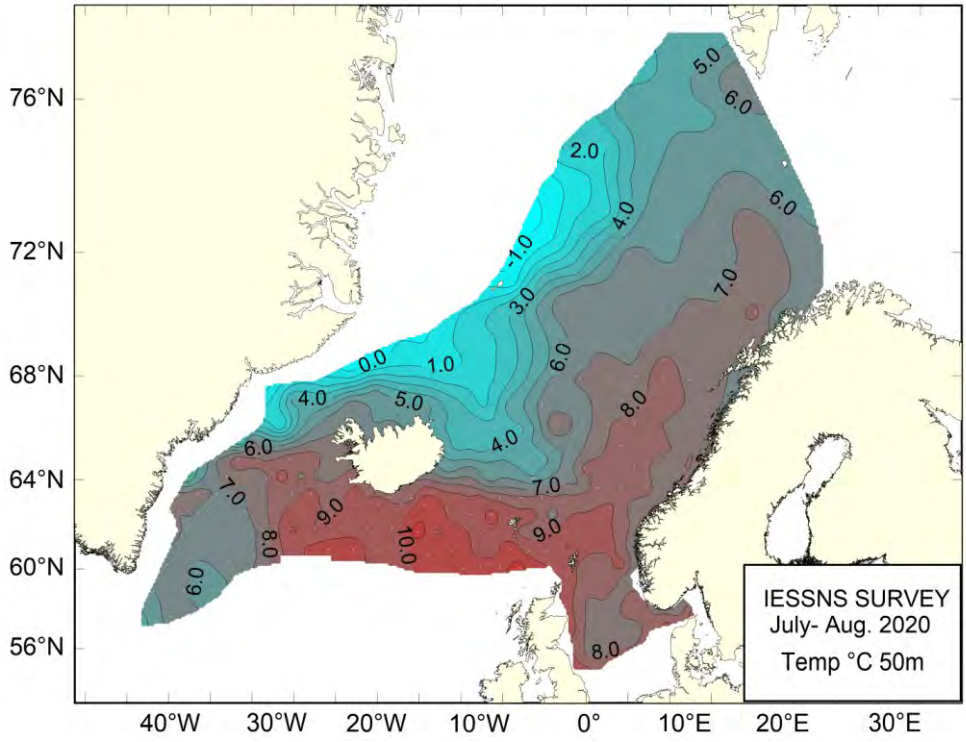

Figure 6. Temperature (°C) at 50 m depth Nordic Seas and the North Sea in July-August 2020.

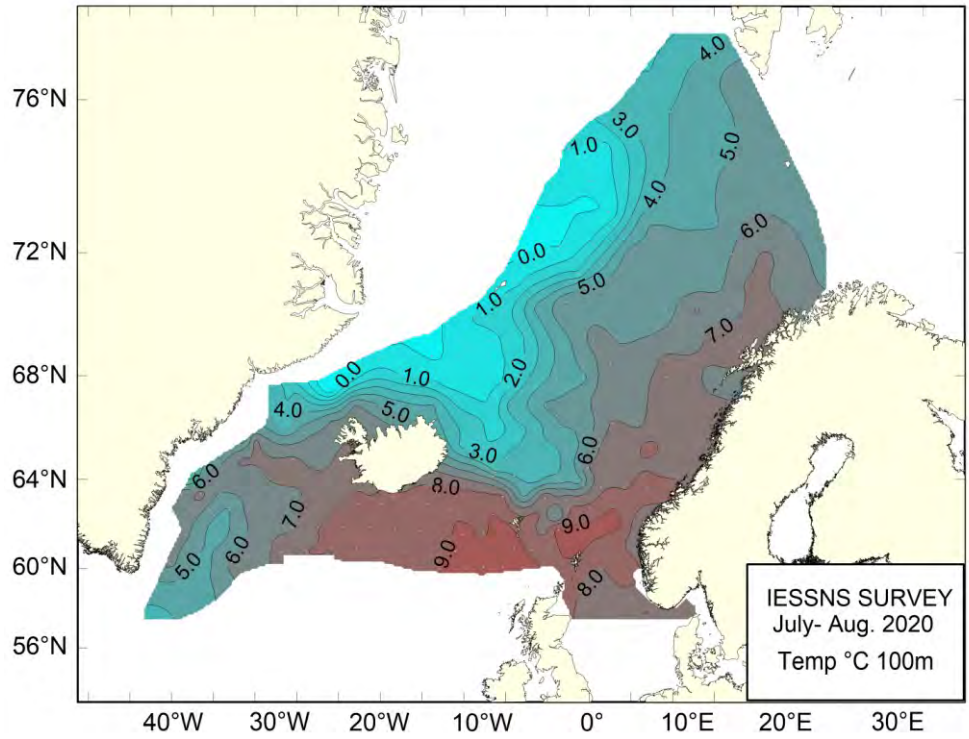

Figure 7. Temperature (°C) at 100 m depth in Nordic Seas and the North Sea in July-August 2020.

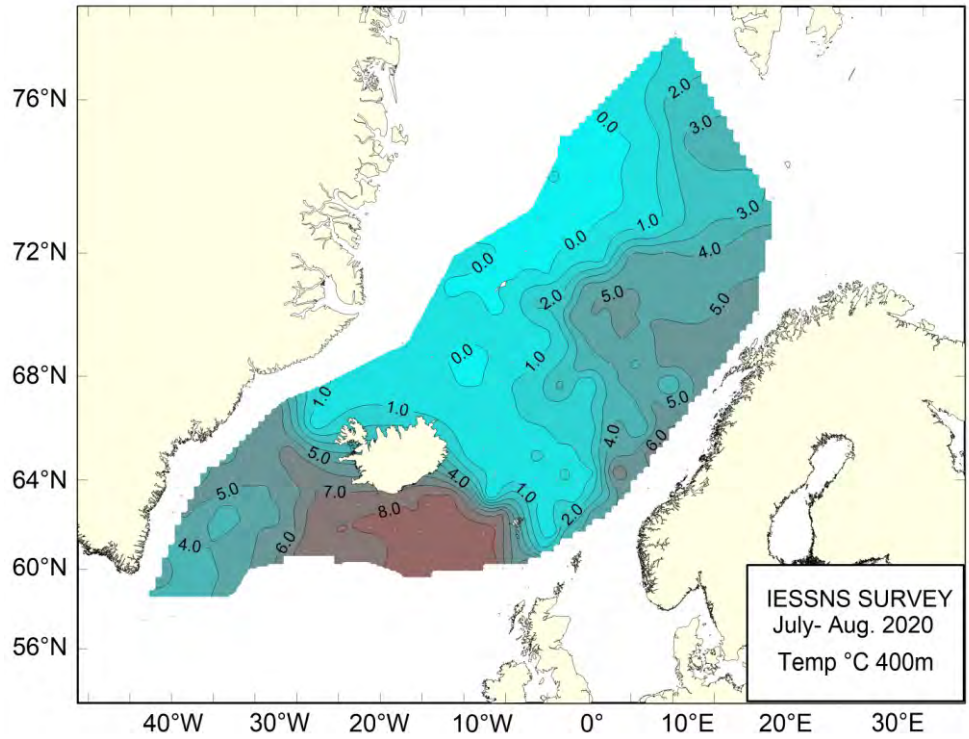

Figure 8. Temperature (°C) at 400 m depth in Nordic Seas and the North Sea in July-August 2020.

4.2 Zooplankton

Zooplankton biomass varied between areas and was lowest in Greenland waters, which contrasts with the previous 3 years where zooplankton biomass was the highest of the three areas (Figure 9a). In Greenland waters in 2020, the average zooplankton biomass has decreased substantially from 2018, it was 5.5 g m^{-2} in 2020 compared to 10.0 g m^{-2} in 2019 and 16.4 g m^{-2} in 2018. Average zooplankton biomass in Icelandic waters also showed a decrease from 2018 through to 2020, respectively declining from 10.8 g m^{-2} to 6.1 g m^{-2}. Through the time series from 2012-2020, the average zooplankton biomass is correlated in Icelandic and Greenlandic waters ($R^2 = 0.73$).

The average zooplankton biomass in Norwegian waters was similar to the average biomass in 2019. In this relatively short time-series, there is greater fluctuations and year-to-year variability (cyclical patterns) in Icelandic and Greenlandic waters compared to the Norwegian Sea. This might in part be explained by both more homogeneous oceanographic conditions in the area defined as Norwegian Sea.

These plankton indices should be treated with some caution as it is only a snapshot of the standing stock biomass, not of the actual production in the area, which complicates spatio-temporal comparisons.

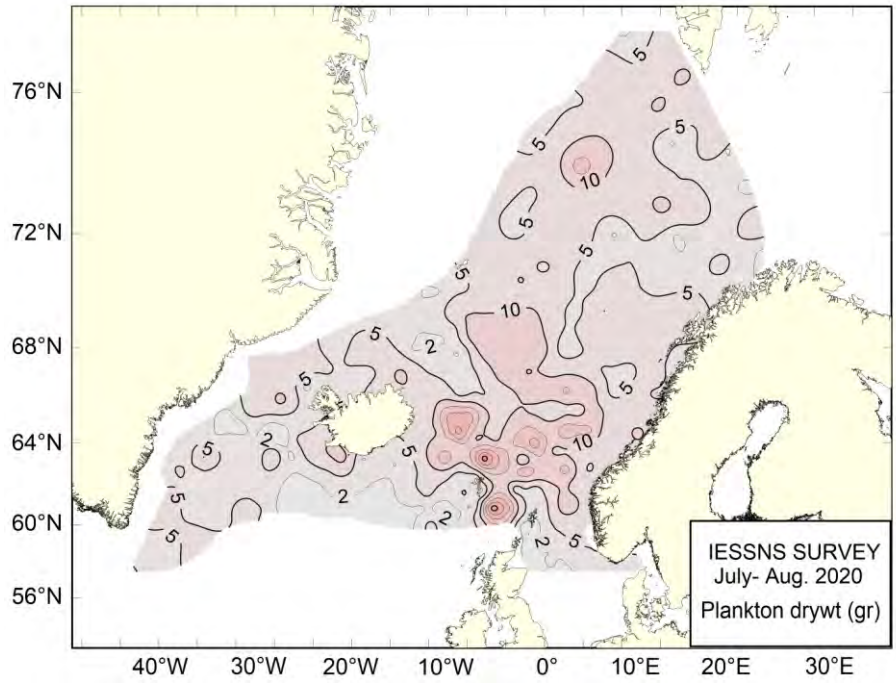

Figure 9a. Zooplankton biomass indices (g dw/m^2, 0-200 m) in Nordic Seas in July-August.

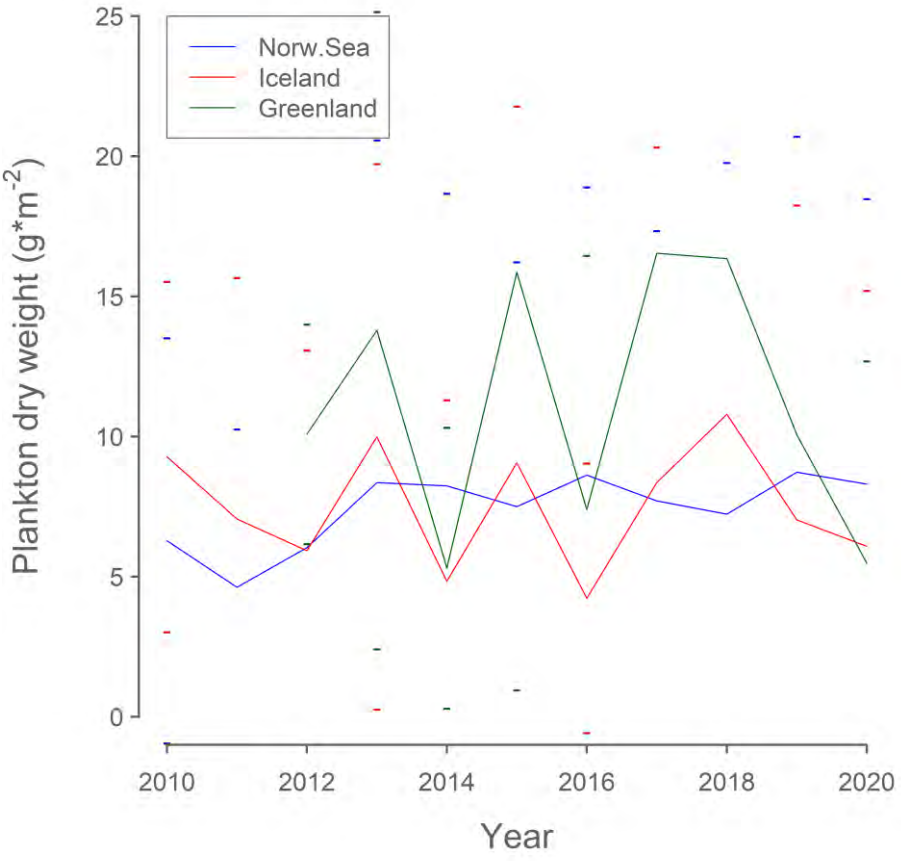

Figure 9b. Zooplankton biomass indices (g dw/m², 0-200 m). Time-series of mean zooplankton biomass for three subareas within the survey range: Norwegian Sea (between 14°W-17°E & north of 61°N), Icelandic waters (14°W-30°W) and Greenlandic waters (west of 30°W).

4.3 Mackerel

The mackerel biomass index i.e. catch rates by trawl station (kg/km²) measured at predetermined surface trawl stations is presented in Figure 10 together with the mean catch rates per 2° lat. x 4° lon. rectangles. The map shows large variations in trawl catch rates throughout the survey area from zero to 62 tonnes/km² (mean = 4.0). High density areas were found in the central and northern Norwegian Sea in 2020, with very small concentrations of mackerel in the western part compared to previous years (Figure 11 & 12). This was both apparent in Greenland waters with no mackerel catches taken and a large decline of mackerel catches in Icelandic waters.

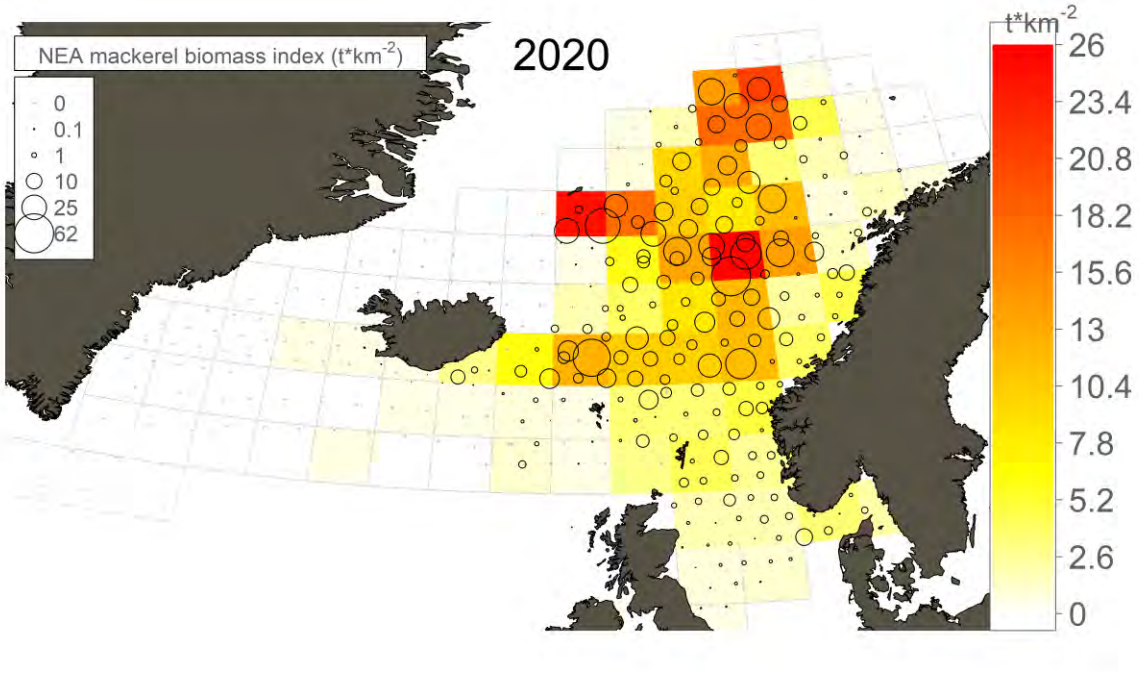

Figure 10. Mackerel catch rates by Multpelt 832 pelagic trawl haul at predetermined surface trawl stations (circle areas represent catch rates in kg/km²) overlaid on mean catch rates per standardized rectangles (2° lat. x 4° lon.).

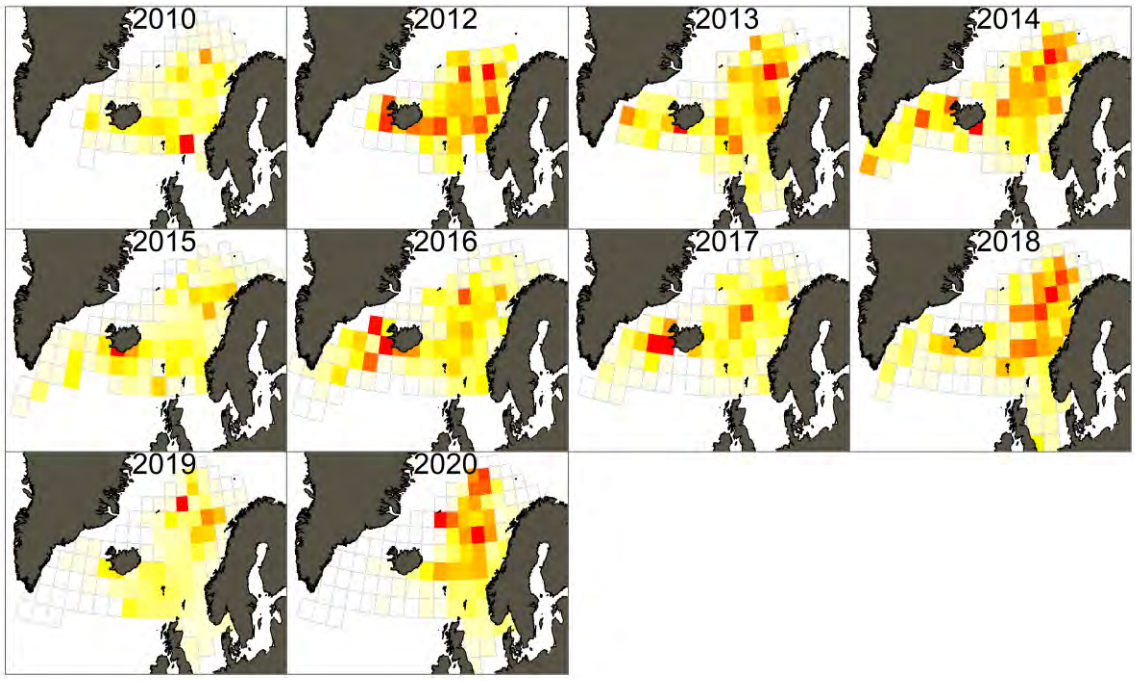

Figure 11. Annual distribution of mackerel proxied by the absolute distribution of mean mackerel catch rates per standardized rectangles (2° lat. x 4° lon.), from Multpelt 832 pelagic trawl hauls at predetermined surface trawl stations. Colour scale goes from white (= 0) to red (= maximum value for the highest year).

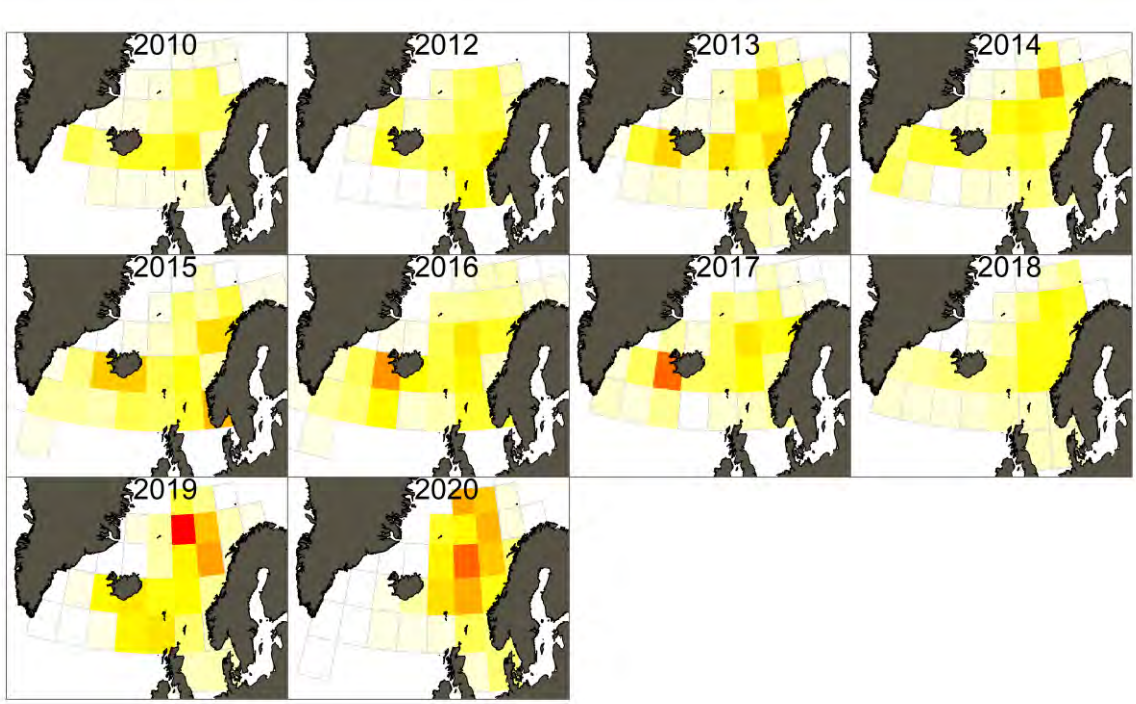

Figure 12. Annual distribution of mackerel proxied by the relative distribution of mean mackerel catch rates per standardized rectangles (4° lat. x 8° lon.), from Multpelt 832 pelagic trawl hauls at predetermined surface trawl stations. Colour scale goes from white (= 0) to red (= maximum value for the given year).

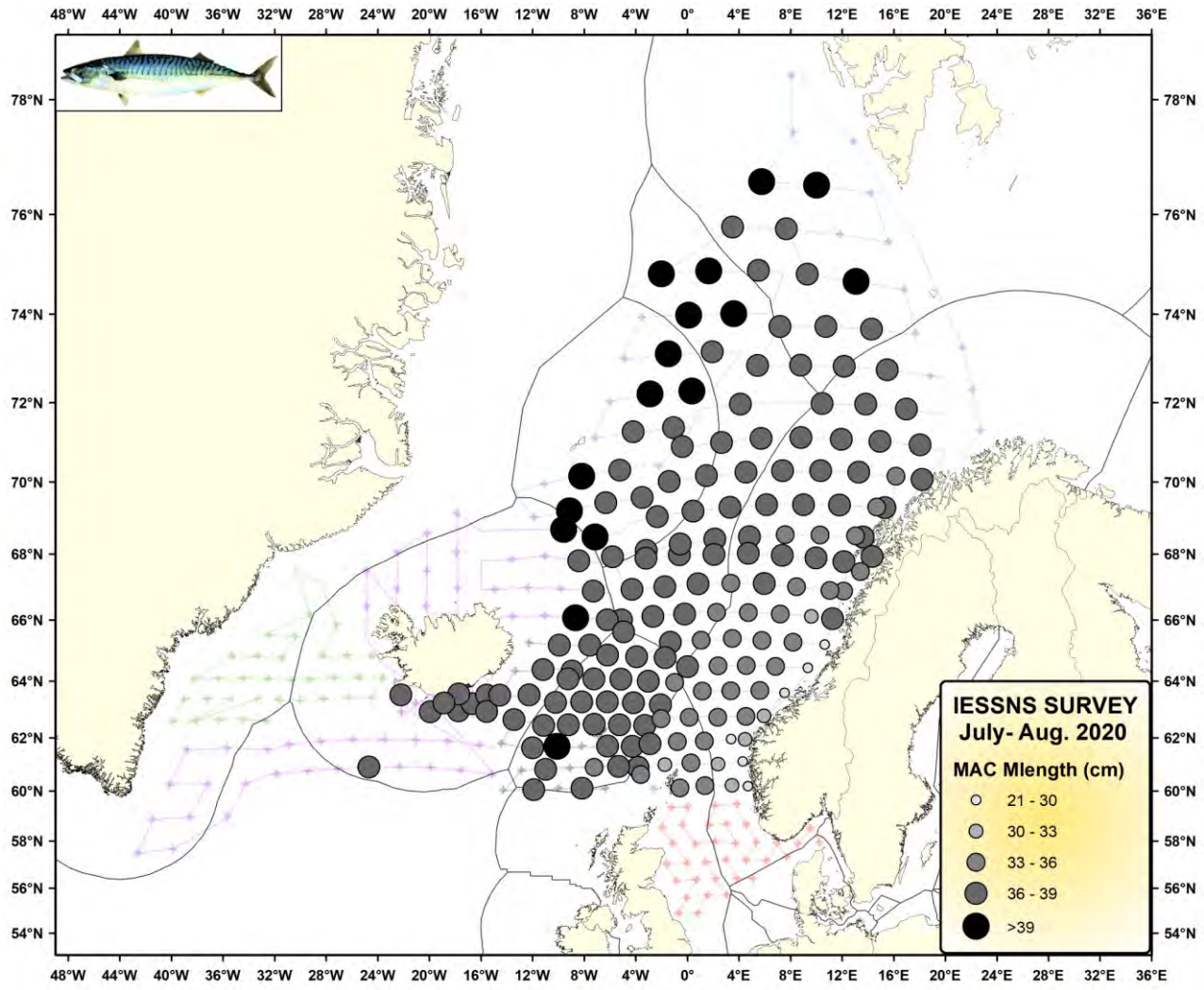

Figure 13. Average length of mackerel at predetermined surface trawl stations during IESSNS 2020.

The length of mackerel caught in the pelagic trawl hauls onboard the six vessels varied from 24.4 to 39.8 cm, with an average of 36.3 cm. Individuals in the length range 33–37 cm dominated in numbers and biomass. The mackerel weight varied between 123 to 642 g with an average of 456 g. Mackerel length distribution followed the same overall pattern as previous years in the Norwegian Sea, with increasing size towards the distribution boundaries in the north and the north-west (Figure 13). The spatial distribution and overlap between the major pelagic fish species (mackerel, herring, blue whiting, salmon and lumpfish) in 2020 according to the catches are shown in Figure 14.

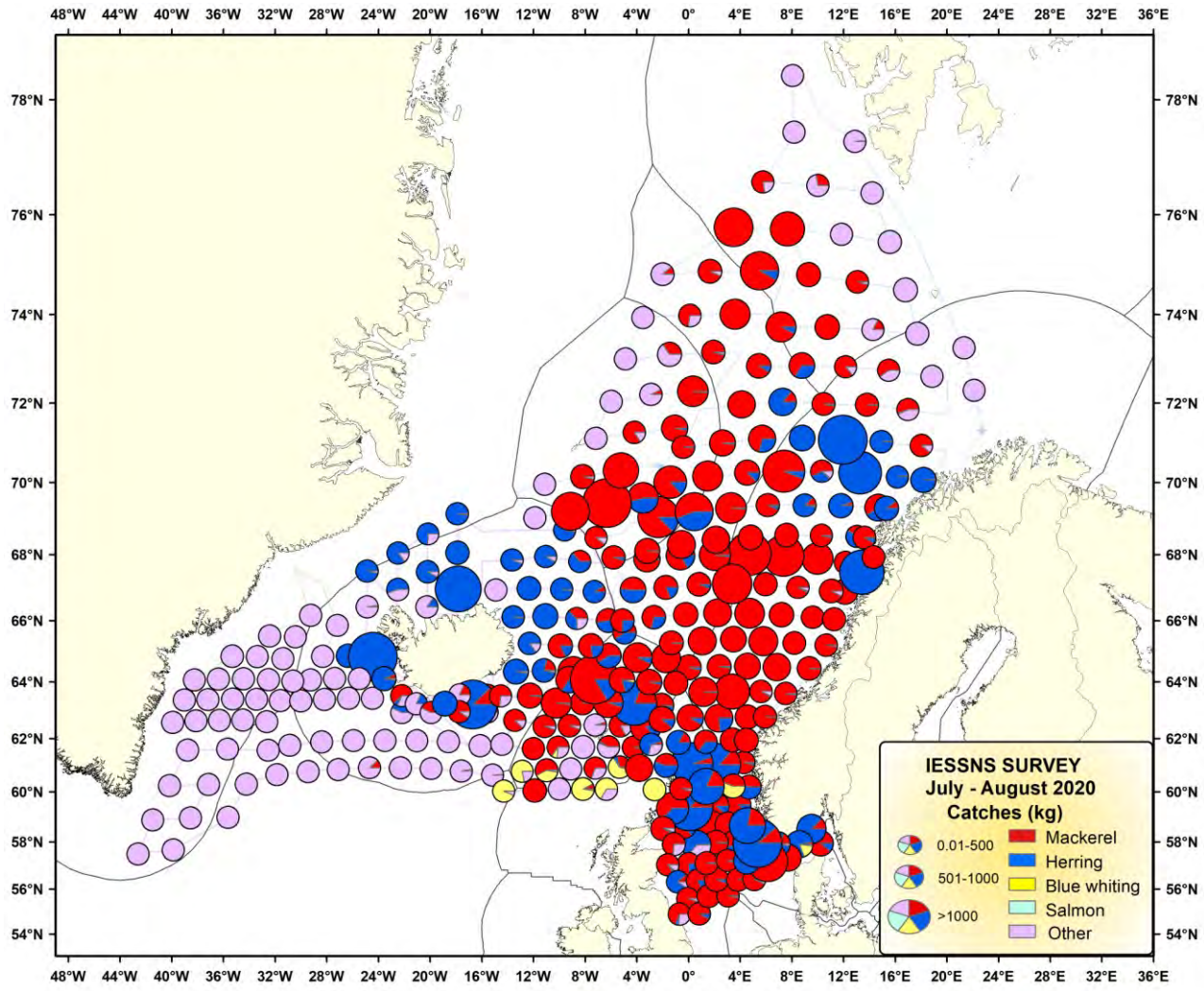

Figure 14. Distribution and spatial overlap between various pelagic fish species (mackerel, herring, blue whiting, salmon, and other (lumpfish)) in 2020 at all surface trawl stations. Vessel tracks are shown as continuous lines.

Swept area analyses from standardized pelagic trawling with Multpelt 832

The swept area estimates of mackerel biomass from the 2020 IESSNS were based on abundance of mackerel per stratum (see strata definition in Figure 2) and calculated in StoX. The mackerel biomass and abundance indices in 2020 were the highest in the time series that started in 2010 (Table 7, Figure 15). Comparing the 2020 estimate to the 2019 estimate shows a 0.3% increase in abundance and 7.0% increase in biomass. The survey coverage area (excl. the North Sea, 0.27 million km^2) was 2.9 million km^2 in 2020, which is similar to the years 2017-2019. The most abundant year classes were 2010, 2016, 2011, 2013 and 2014 (Figure 16). Mackerel of age 1, 2 and to some extent also age 3 are not completely recruited to the survey (Figure 18), information on recruitment is therefore uncertain. However, the abundance of 1-3 year olds from the 2016 and 2017 year classes have consistently been high suggesting that these year classes are large. The 2018 year class appears to be closer to average. Variance in age index estimation is provided in Figure 17.

The overall internal consistency plot for age-disaggregated year classes is improved compared to last year (Figure 19), especially for the ages older than 8 years. There is a good to strong internal consistency for the younger ages (1-5 years) and older ages (8-14+ years) with r between 0.73 and 0.93. However, the internal consistency is poor to moderate (0.10 < r < 0.63) between age 5 to 8 as in previous years. The reason for this poor consistency is not clear.

Mackerel index calculations from the catch in the North Sea (stratum 13 in Figure 2) were excluded from the index calculations presented in the current chapter to facilitate comparison to previous years and because the 2017 mackerel benchmark stipulated that trawl stations south of latitude 60 °N be excluded from index calculations (ICES 2017). Results from the mackerel index calculations for the North Sea are presented in Appendix 1.

The indices used for NEA mackerel stock assessment in WGIWIDE are the number-at-age indices for age 3 to 11 year (Table 7a).

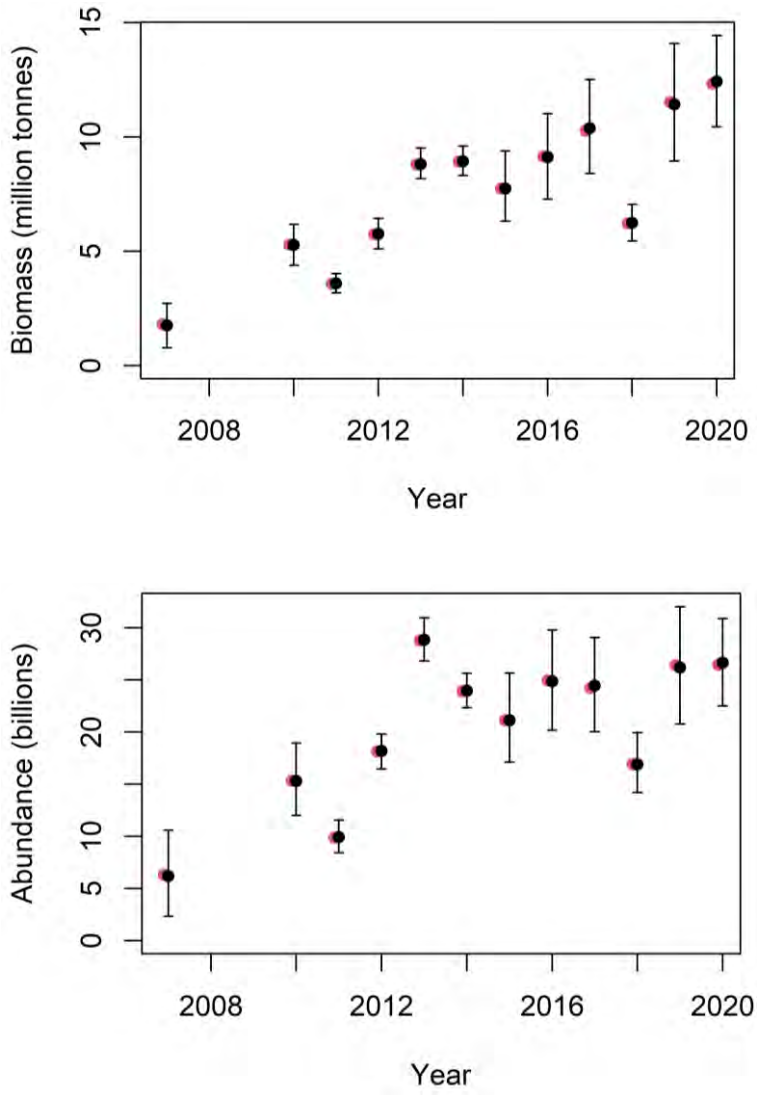

Figure 15. Estimated total stock biomass (upper panel) and total stock numbers (lower panel) of mackerel from StoX . The red dots are baseline estimates, the black dots are mean of 1000 bootstrap replicates while the error bars represent 90 % confidence intervals based on the bootstrap.

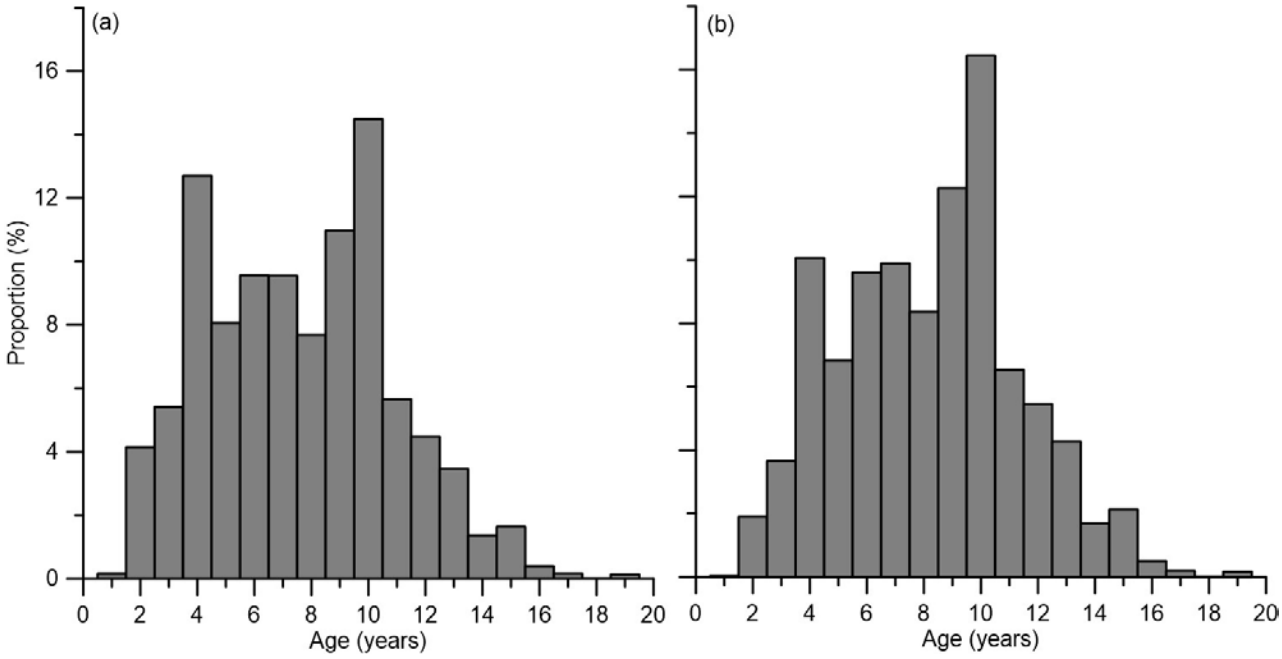

Figure 16. Age distribution in proportion represented as a) % in numbers and b) % in biomass of Northeast Atlantic mackerel in 2020.

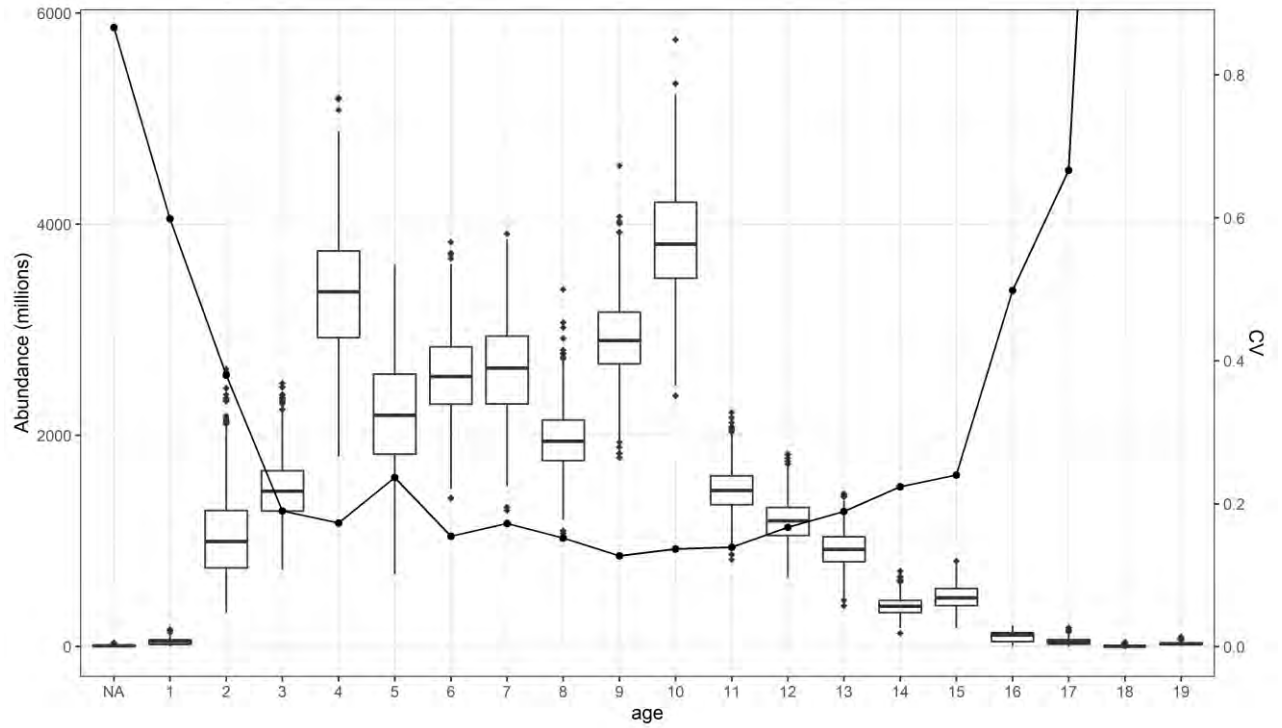

Figure 17. Number by age for mackerel. Boxplot of abundance and relative standard error (CV) obtained by bootstrapping with 500 replicates using the StoX software.

Table 7. a-d) StoX baseline time series of the IESSNS showing (a) age-disaggregated abundance indices of mackerel (billions), (b) mean weight (g) per age and (c) estimated biomass at age (million tonnes) from 2007 to 2020. d) Output from StoX.

a)

Year\Age	1	2	3	4	5	6	7	8	9	10	11	12	13	14(+)	Tot N
2007	1.33	1.86	0.90	0.24	1.00	0.16	0.06	0.04	0.03	0.01	0.01	0.00	0.01	0.00	5.65
2010	0.03	2.80	1.52	4.02	3.06	1.35	0.53	0.39	0.20	0.05	0.03	0.02	0.01	0.01	13.99
2011	0.21	0.26	0.87	1.11	1.64	1.22	0.57	0.28	0.12	0.07	0.06	0.02	0.01	0.00	6.42
2012	0.50	4.99	1.22	2.11	1.82	2.42	1.64	0.65	0.34	0.12	0.07	0.02	0.01	0.01	15.91
2013	0.06	7.78	8.99	2.14	2.91	2.87	2.68	1.27	0.45	0.19	0.16	0.04	0.01	0.02	29.57
2014	0.01	0.58	7.80	5.14	2.61	2.62	2.67	1.69	0.74	0.36	0.09	0.05	0.02	0.00	24.37
2015	1.20	0.83	2.41	5.77	4.56	1.94	1.83	1.04	0.62	0.32	0.08	0.07	0.04	0.02	20.72
2016	<0.01	4.98	1.37	2.64	5.24	4.37	1.89	1.66	1.11	0.75	0.45	0.20	0.07	0.07	24.81
2017	0.86	0.12	3.56	1.95	3.32	4.68	4.65	1.75	1.94	0.63	0.51	0.12	0.08	0.04	24.22
2018	2.18	2.50	0.50	2.38	1.20	1.41	2.33	1.79	1.05	0.50	0.56	0.29	0.14	0.09	16.92
2019	0.08	1.35	3.81	1.21	2.92	2.86	1.95	3.91	3.82	1.50	1.25	0.58	0.59	0.57	26.4
2020	0.04	1.10	1.43	3.36	2.13	2.53	2.53	2.03	2.90	3.84	1.50	1.18	0.92	0.98	26.47

b)

Year\Age	1	2	3	4	5	6	7	8	9	10	11	12	13	14(+)
2007	133	233	323	390	472	532	536	585	591	640	727	656	685	671
2010	133	212	290	353	388	438	512	527	548	580	645	683	665	596
2011	133	278	318	371	412	440	502	537	564	541	570	632	622	612
2012	112	188	286	347	397	414	437	458	488	523	514	615	509	677
2013	96	184	259	326	374	399	428	445	486	523	499	547	677	607
2014	228	275	288	335	402	433	459	477	488	533	603	544	537	569
2015	128	290	333	342	386	449	463	479	488	505	559	568	583	466
2016	95	231	324	360	371	394	440	458	479	488	494	523	511	664
2017	86	292	330	373	431	437	462	487	536	534	542	574	589	626
2018	67	229	330	390	420	449	458	477	486	515	534	543	575	643
2019	153	212	325	352	428	440	472	477	490	511	524	564	545	579
2020	99	213	315	369	394	468	483	507	520	529	539	567	575	593

c)

Year\Age	1	2	3	4	5	6	7	8	9	10	11	12	13	14(+)	Tot B
2007	0.18	0.43	0.29	0.09	0.47	0.09	0.03	0.02	0.02	0.01	0.01	0.00	0.01	0.00	1.64
2010	0.00	0.59	0.44	1.42	1.19	0.59	0.27	0.20	0.11	0.03	0.02	0.01	0.01	0.00	4.89
2011	0.03	0.07	0.28	0.41	0.67	0.54	0.29	0.15	0.07	0.04	0.03	0.01	0.01	0.00	2.69
2012	0.06	0.94	0.35	0.73	0.72	1.00	0.72	0.30	0.17	0.06	0.03	0.01	0.00	0.00	5.09
2013	0.01	1.43	2.32	0.70	1.09	1.15	1.15	0.56	0.22	0.10	0.08	0.02	0.01	0.01	8.85
2014	0.00	0.16	2.24	1.72	1.05	1.14	1.23	0.80	0.36	0.19	0.05	0.03	0.01	0.00	8.98
2015	0.15	0.24	0.80	1.97	1.76	0.87	0.85	0.50	0.30	0.16	0.04	0.04	0.02	0.01	7.72
2016	<0.01	1.15	0.45	0.95	1.95	1.72	0.83	0.76	0.53	0.37	0.22	0.10	0.04	0.04	9.11
2017	0.07	0.03	1.18	0.73	1.43	2.04	2.15	0.86	1.04	0.33	0.28	0.07	0.05	0.03	10.29
2018	0.15	0.57	0.16	0.93	0.50	0.63	1.07	0.85	0.51	0.26	0.30	0.16	0.08	0.05	6.22
2019	0.01	0.29	1.24	0.43	1.25	1.26	0.92	1.86	1.87	0.77	0.65	0.33	0.32	0.32	11.52
2020	<0.01	0.23	0.45	1.24	0.84	1.18	1.22	1.03	1.51	2.03	0.81	0.67	0.53	0.58	12.33

Table 7d) IESSNS 2020. StoX baseline estimates of mackerel abundance, mean weight and mean length.

Variable: Abundance
EstLayer: 1
Stratum: TOTAL
SpecCat: makrell

LenGrp \ age	1	2	3	4	5	6	7	8	9	10	11	12	13	14	15	16	17	18	19	Unknown	Number (1E3)	Biomass (1E3kg)	Mean W (g)
17-18	-	-	-	-	-	-	-	-	-	-	-	-	-	-	-	-	-	-	-	393	393	19.6	50.00
18-19	-	-	-	-	-	-	-	-	-	-	-	-	-	-	-	-	-	-	-	393	393	21.2	54.00
19-20	-	-	-	-	-	-	-	-	-	-	-	-	-	-	-	-	-	-	-	909	909	57.1	62.84
20-21	4052	-	-	-	-	-	-	-	-	-	-	-	-	-	-	-	-	-	-	-	4052	282.8	69.81
21-22	8023	7247	-	-	-	-	-	-	-	-	-	-	-	-	-	-	-	-	-	-	15270	1165.8	76.35
22-23	10030	22198	-	-	-	-	-	-	-	-	-	-	-	-	-	-	-	-	-	-	32228	2962.1	91.91
23-24	7565	111117	-	-	-	-	-	-	-	-	-	-	-	-	-	-	-	-	-	-	118681	11701.7	98.60
24-25	7310	183431	-	1008	336	-	-	-	-	-	-	-	-	-	-	-	-	-	-	-	192085	22156.8	115.35
25-26	2690	123171	11765	-	1669	-	-	-	-	-	-	-	-	-	-	-	-	-	-	-	139295	17949.6	128.86
26-27	1862	65554	-	-	-	-	-	-	-	-	-	-	-	-	-	-	-	-	-	-	67416	9474.6	140.54
27-28	881	3699	-	-	-	-	-	-	-	-	-	-	-	-	-	-	-	-	-	-	4580	757.6	165.41
28-29	-	17564	-	-	-	-	-	-	-	-	-	-	-	-	-	-	-	-	-	-	17564	3501.4	199.35
29-30	-	25790	53653	-	-	-	-	-	-	-	-	-	-	-	-	-	-	-	-	-	79444	17383.5	218.82
30-31	-	103227	72012	115359	-	-	-	-	-	-	-	-	-	-	-	-	-	-	-	-	290598	74688.6	257.02
31-32	-	83435	292521	246781	1141	2324	-	-	-	-	-	-	-	-	-	-	-	-	-	-	626201	177386.6	283.27
32-33	-	215024	542203	572880	107105	-	9922	-	-	-	-	-	-	-	-	-	-	-	-	-	1447134	454841.9	314.31
33-34	-	84119	257712	724062	649131	7306	26677	-	4140	-	-	-	15167	-	-	-	-	-	-	-	1768314	609438.2	344.64
34-35	-	47238	96933	751455	505451	121005	78200	23241	-	-	-	-	-	-	-	-	-	-	-	-	1623524	616341.5	379.63
35-36	-	4399	79195	524047	472886	382463	166463	49074	51302	11993	2579	-	-	-	-	-	-	-	-	-	1744401	731706.0	419.46
36-37	-	-	3654	351209	262547	712252	696102	484937	147595	295261	42807	19532	-	3932	-	-	-	-	-	-	3019827	1386576.9	459.16
37-38	-	-	21347	54617	122176	866143	814695	573593	949691	1013723	296145	96365	10683	12836	-	-	-	-	-	-	4832014	2377172.0	491.96
38-39	-	-	-	13638	8232	398085	624742	597232	1086693	1305787	539570	261743	243535	100280	39644	17118	2952	144	-	-	5239394	2766655.1	528.05
39-40	-	-	-	141	3737	39029	53003	191022	562466	850989	375653	426225	252322	98605	85067	55565	31515	-	36000	-	3061339	1725434.6	563.62
40-41	-	-	-	6581	-	43	55389	111204	88355	291356	192351	269252	263156	63588	185140	13199	1128	-	-	-	1540743	920775.2	597.62
41-42	-	-	-	-	-	-	203	2251	13923	52584	38870	103846	77423	53161	96072	9620	5888	-	-	-	453840	292985.8	645.57
42-43	-	-	-	-	-	-	64	228	-	10518	5611	7922	18106	26678	10654	42	1571	-	-	-	81394	55052.9	676.38
43-44	-	-	-	-	-	-	-	-	73	1022	2064	-	29226	-	15338	8177	-	1898	-	-	57798	42299.0	731.84
44-45	-	-	-	-	-	-	-	-	-	2249	-	-	-	-	-	-	-	-	-	-	2249	1652.2	734.80
45-46	-	-	-	-	-	-	-	-	-	-	-	-	6013	-	-	-	-	-	-	-	6013	4875.6	810.79
46-47	-	-	-	-	-	-	-	-	-	-	-	-	-	-	-	-	-	-	-	-	-	-	-
48-49	-	-	-	-	-	-	-	-	-	-	-	-	-	-	-	-	-	-	-	1500	1500	1524.5	1016.00
TSN(1000)	42414	1097212	1430995	3361778	2134411	2528651	2525460	2032783	2904239	3835479	1495649	1184884	915631	359080	431915	103721	43054	2041	36000	3195	26468594	-	-
TSB(1000 kg)	4214.6	233291.1	451303.1	1240926.0	841504.4	1183109.7	1219891.1	1029686.5	1510848.4	2027319.3	806035.6	671778.4	526625.0	208291.0	261661.8	62120.9	24499.0	1458.5	20653.9	1622.5	-	12326840.6	-
Mean length (cm)	22.87	28.37	32.35	33.81	34.54	36.69	37.04	37.51	37.97	38.21	38.53	39.15	39.47	39.51	40.18	39.72	39.60	42.70	39.36	32.52	-	-	-
Mean weight (g)	99.37	212.62	315.38	369.13	394.26	467.88	483.04	506.54	520.22	528.57	538.92	566.96	575.15	580.07	605.82	598.92	569.03	714.50	573.71	507.79	-	-	465.72

Table 8. Bootstrap estimates from StoX (based on 1000 replicates) of mackerel. Numbers by age and total number (TSN) are in millions and total biomass (TSB) in million tons.

Age	5th percentile	Median	95th percentile	Mean	SD	CV
1	7.8	47.2	93.4	45.7	27.4	0.60
2	533.0	994.5	1835.8	1054.7	400.3	0.38
3	1068.7	1468.2	1994.3	1491.9	282.5	0.19
4	2401.5	3359.1	4298.3	3351.8	578.5	0.17
5	1358.1	2189.3	3031.9	2193.4	517.6	0.24
6	1923.0	2556.7	3194.6	2558.8	394.7	0.15
7	1837.6	2635.6	3363.3	2626.8	451.6	0.17
8	1468.6	1942.4	2434.8	1950.1	295.8	0.15
9	2337.5	2897.5	3543.4	2919.9	369.5	0.13
10	3048.3	3811.0	4752.4	3858.5	526.0	0.14
11	1175.6	1476.2	1824.7	1483.6	206.0	0.14
12	861.8	1189.3	1511.5	1187.9	198.0	0.17
13	645.9	917.4	1214.9	921.8	174.0	0.19
14	240.2	379.6	517.3	380.6	84.9	0.22
15	292.5	459.7	660.7	468.3	112.3	0.24
16	19.9	106.2	157.6	93.2	46.4	0.50
17	4.7	42.8	98.4	45.8	30.5	0.67
18	0.0	0.4	16.7	2.7	5.7	2.10
19	0.0	15.3	44.0	16.3	16.4	1.01
Unknown	0.5	4.9	19.7	6.8	5.9	0.87
TSN	22513.1	26682.4	30875.5	26658.6	2511.3	0.09
TSB	10.45	12.41	14.43	12.42	1.23	0.10

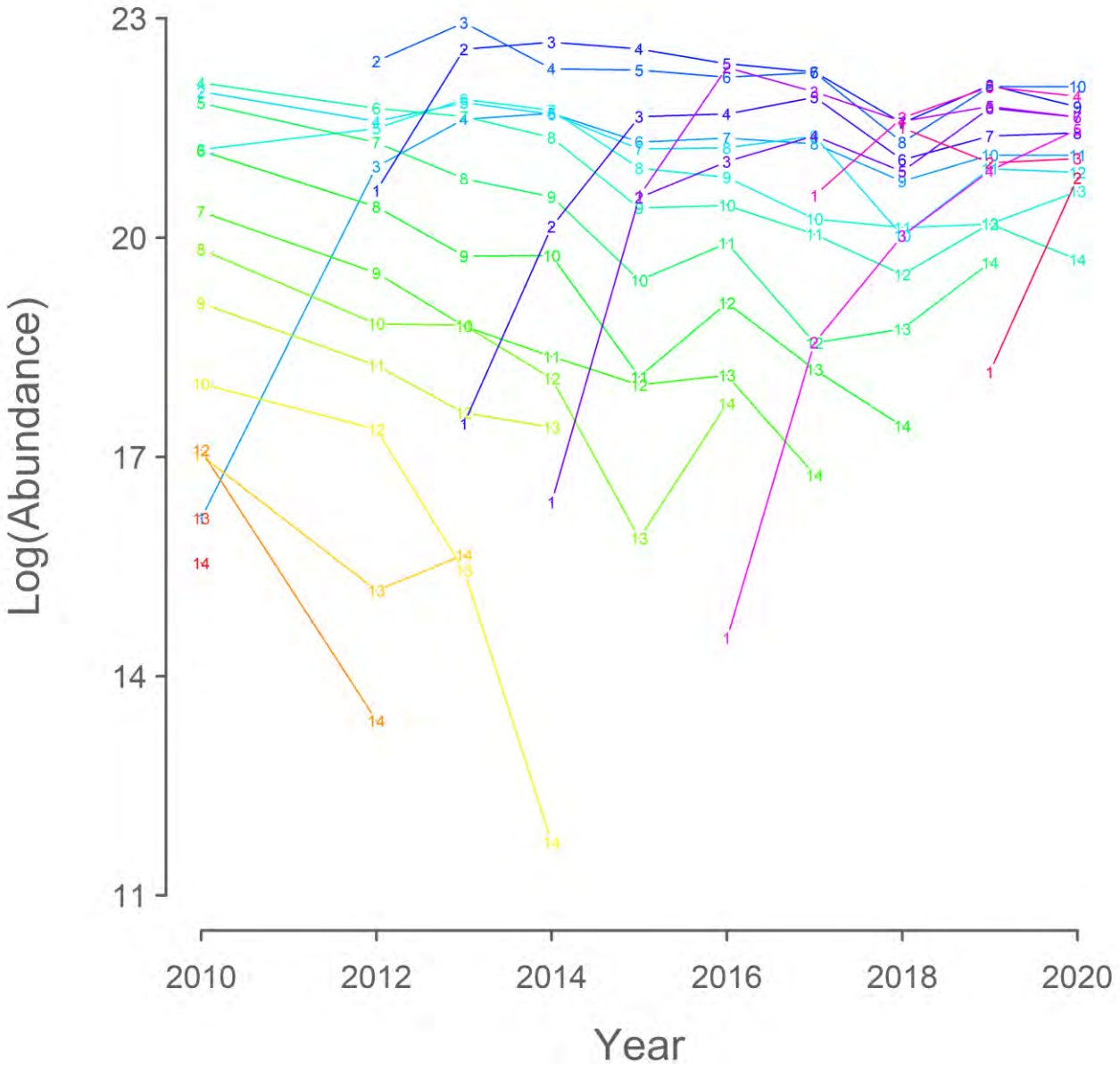

Figure 18. Catch curves. Each cohort is marked by a uniquely coloured line that connects the estimates indicated by the respective ages.

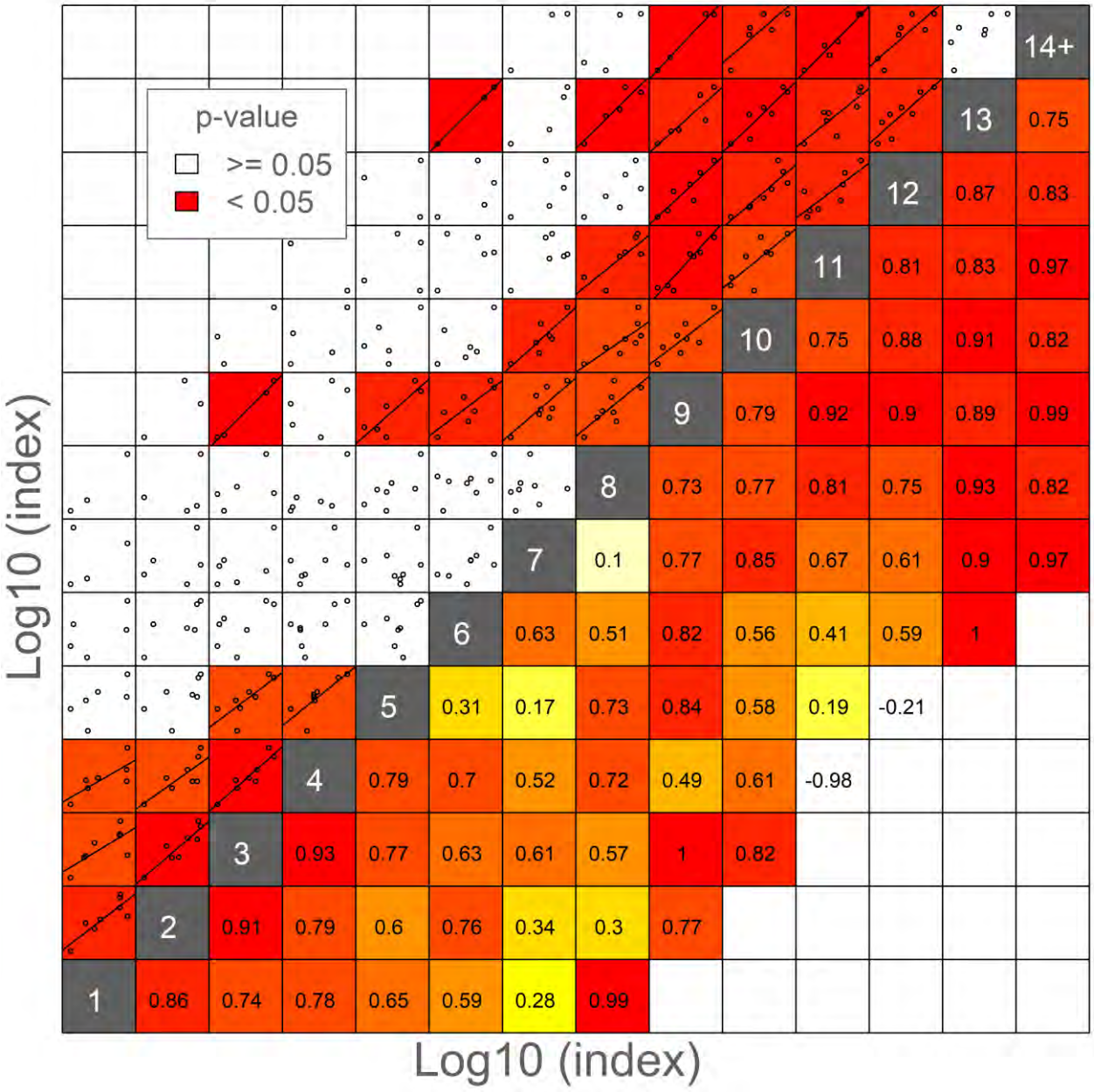

Figure 19. Internal consistency of the of mackerel density index from 2012 to 2020. Ages indicated by white numbers in grey diagonal cells. Statistically significant positive correlations ($p<0.05$) are indicated by regression lines and red cells in upper left half. Correlation coefficients (r) are given in the lower right half.

Distribution zero boundaries were found in majority of survey area with a notable exception of high mackerel abundance in the north-western region towards the Fram Strait west of Svalbard.

The mackerel appeared less patchily distributed within the survey area and was distributed more in the central and northern Norwegian Sea in 2020 compared to 2018 and 2019. This difference in distribution primarily consists of a marked biomass decline in the west and an increase in the central and northern part of the Norwegian Sea. Furthermore, there was also a northerly and north-westerly shift in densities of mackerel within the Norwegian Sea.

The marked decrease since 2017 and now even disappearance of mackerel in major western areas in 2020 likely has several causes. In 2019 there were practically no mackerel in Greenland waters during the survey, and in 2020 the mackerel had disappeared altogether from Greenland waters according to our survey results. A similar pattern has also taken place in Icelandic waters, where the abundance of mackerel has declined substantially during the last few years from 2017 to 2020. Why is this happening? First of all, we measured lower mesozooplankton biomasses in both Icelandic and Greenland waters in 2020 compared to previous years, which may have reduced mackerel feeding opportunities in the western area. The temperature was 1-2°C lower in parts of Icelandic and Greenland waters in summer 2020 compared to 2019. This accounts for both the sea surface temperatures (SSTs) and in situ temperature measurements from 10 m depth. However, there should be warm enough for the mackerel to migrate to and feed in these areas. The increase of mackerel in the Norwegian Sea, particularly in the central and northern part of the Norwegian Sea, cannot be explained by improved feeding conditions, as the zooplankton biomasses in summer (at the time of IESSNS) have varied little among the recent years. Neither can it be explained by reduced abundance, as the present survey estimate is the highest on record.

The swept area method assumes that potential distribution of mackerel outside the survey area – both vertically and horizontally – is a constant percentage of the total biomass. In some years, this assumption may be violated, e.g. when mackerel may be distributed below the lower limit of the trawl or if the proportion of mackerel outside the survey coverage varies among years. In order to improve the precision of the swept-area estimate it would be beneficial to extend the survey coverage further south covering the southwestern waters south of 60°N.

As in previous years, there was overlap in the spatio-temporal distribution of mackerel and herring. This overlap occurred in the southern and south-western parts of the Norwegian Sea, and with the strong 2016 year class of NSSH, there was also overlap in the central and north eastern part of the Norwegian Sea. In the eastern Norwegian Sea between 62-67°N, mackerel were present but herring were in low abundance, in contrast, in areas north of Iceland, herring were present while mackerel were absent.

The swept-area estimate was, as in previous years, based on the standard swept area method using the average horizontal trawl opening by each participating vessel (ranging 57.2.5-70.5.4m; Table 5), assuming that a constant fraction of the mackerel inside the horizontal trawl opening are caught. Further, that if mackerel is distributed below the depth of the trawl (footrope), this fraction is assumed constant from year to year.

Results from the survey expansion southward into the North Sea is analysed separately from the traditional survey grounds north of latitude 60°N as per stipulations from the 2017 mackerel benchmark meeting (ICES 2017). We have now available IESSNS survey data from 2018, 2019 and 2020 for the northern part of the North Sea.

This year's survey was well synchronized in time and was conducted over a relatively short period (less than 5 weeks) given the large spatial coverage of around 2.9 million km^2 (Figure 1). This was in line with recommendations put forward in 2016 that the survey period should be around four weeks with mid-point around 20. July. The main argument for this time period was to make the survey as synoptic as possible in space and time, and at the same time be able to finalize data and report for inclusion in the assessment for the same year.

4.4 Norwegian spring-spawning herring

Norwegian spring-spawning herring (NSSH) was recorded in the southern (north of the Faroes and east and north of Iceland) and northern part of the Norwegian Sea basin (Figure 20). The fish in the northeast consisted of young adults (mainly 4 year olds) while the fish further southwest are a range of age groups, although also in this southwestern area significant amounts of the 4- year old as well as 7- year old herring were present. Herring registrations south of 62°N in the eastern part were allocated to a different stock, North Sea herring while the herring closer to the Faroes south of 62°N were Faroese autumn spawners.

Also, herring to the west in Icelandic waters (west of 14°W south of Iceland) were allocated to Icelandic summer-spawners. The abundance and biomass of NSSH was distributed with slightly more than half of the biomass in the north-eastern part (mainly young herring) and slightly less than half in the south-western area. The 0-boundary of the distribution of the adult part of NSSH was considered to be reached in all directions. However, the most abundant year class in the survey estimate, the 2016- year class (4- year olds) may not be fully covered in this survey. Some of this young year class may still not be fully recruited to the survey area.

The NSSH stock is dominated by 4 and 7-year old herring (year classes 2016 and 2013) in terms of numbers and biomass (Table 9). The 2013 year class is distributed in all areas with herring in the survey whereas the 2016 year class was mainly found in the north-eastern part. The 2013 year-class contributed 22% and 20% to the total biomass and total abundance, respectively, whereas the 2016 year-class contributed 33% and 40% to the total biomass and total abundance, respectively. The total number of herring recorded in the Norwegian Sea was 20.3 billion and the total biomass index was 5.93 million tonnes in 2020, in comparison to 15.2 billion and a total biomass index of 4.78 million tonnes in 2019. The increase was due to the recruiting 2016 year-class coming strongly into the survey area. Number by age, with uncertainty estimates, for NSSH is shown in Figure 21. The group considered the acoustic biomass estimate of herring to be of good quality in the 2020 IESSNS as in the previous survey years.

Bootstrap estimates of numbers by age of herring are shown in table 10 and the baseline point estimates from 2016-2020 are shown in table 11. The internal consistency among year classes is shown in Figure 22.

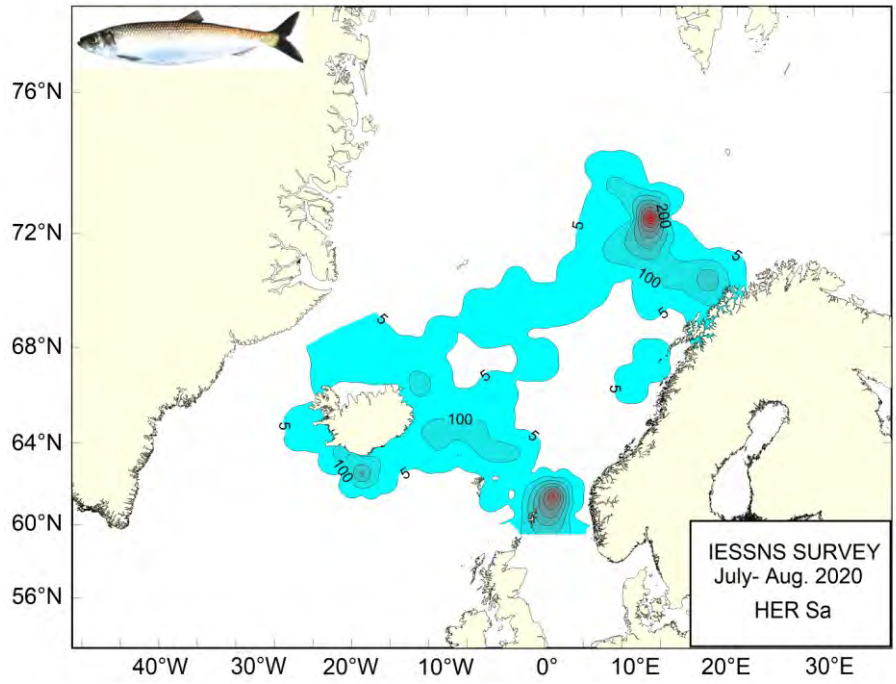

Figure 20a. The s_A/Nautical Area Scattering Coefficient (NASC) values of herring along the cruise tracks in 2020. Presented as contour lines. Values north of 62ºN, and east of 14ºW, are considered to be Norwegian spring-spawning herring. South and west of this area the herring observed are other stocks, *i.e.* Faroese autumn spawners, North Sea herring and Icelandic summer spawning herring.

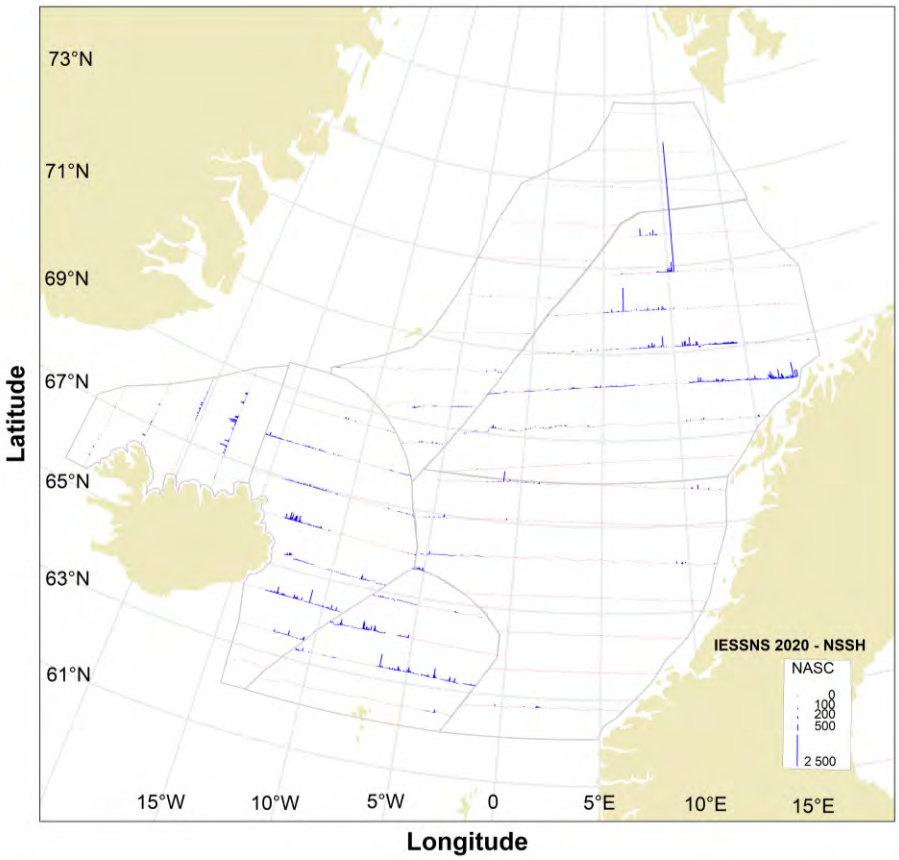

Figure 20b. The SA/Nautical Area Scattering Coefficient (NASC) values of herring along the cruise tracks in 2020. Presented as bar plot. Values north of 62ºN, and east of 14ºW, are considered to be Norwegian spring-spawning herring. South and west of this area the herring observed are other stocks, *i.e.* Faroese autumn spawners, North Sea herring and Icelandic summer spawning herring.

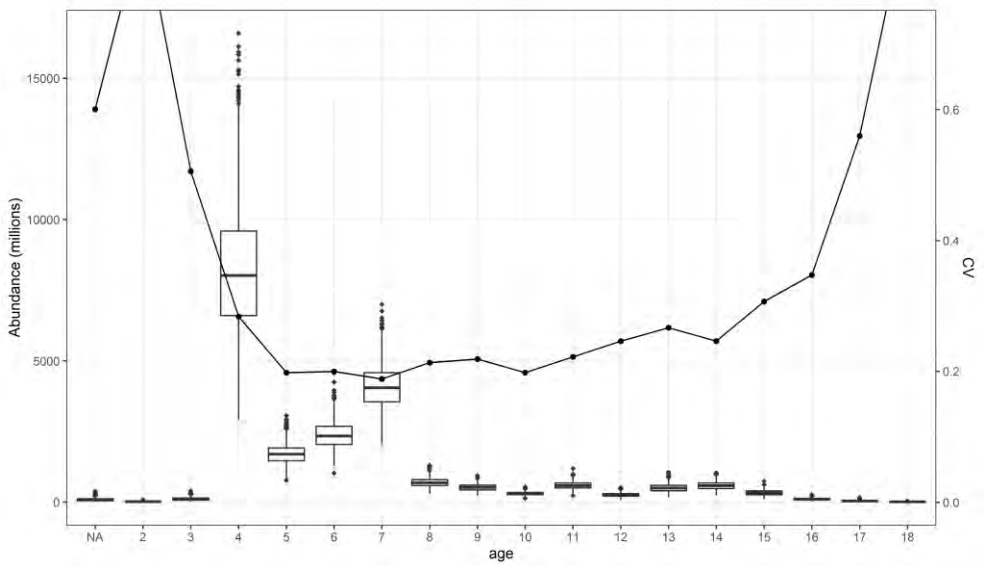

Figure 21. Number by age for Norwegian spring-spawning herring during IESSNS 2020. Boxplot of abundance and relative standard error (CV) obtained by bootstrapping with 500 replicates using the StoX software.

Table 9. Estimates of abundance, mean weight and mean length of Norwegian spring-spawning herring based on calculation in StoX for IESSNS 2020.

	age																				
LenGrp	2	3	4	5	6	7	8	9	10	11	12	13	14	15	16	17	18	Unknown	Number (1E3)	Biomass (1E3kg)	Mean W (g)
23-24	-	-	-	-	-	-	-	-	-	-	-	-	-	-	-	-	-	8096	8096	1214.4	150.00
24-25	-	8096	1245	-	-	-	-	-	-	-	-	-	-	-	-	-	-	-	9341	1213.7	129.93
25-26	-	-	-	-	-	-	-	-	-	-	-	-	-	-	-	-	-	78567	78567	12099.8	154.01
26-27	3375	27307	351715	-	11208	-	-	-	-	-	-	-	-	-	-	-	-	-	393604	68895.1	175.04
27-28	-	24446	836562	99166	3492	-	-	-	-	-	-	-	-	-	-	-	-	-	963667	181071.1	187.90
28-29	3379	16894	1117284	63398	-	25315	3361	6758	7283	-	-	-	-	-	-	-	-	-	1243672	258390.6	207.76
29-30	-	27259	1659886	40066	7109	13661	5715	-	11105	-	-	-	-	-	-	-	-	-	1764802	412482.5	233.73
30-31	-	7425	2265337	210515	57260	24416	30560	3439	3595	17197	-	-	3595	-	-	-	-	-	2623338	672023.4	256.17
31-32	-	-	1490880	466629	293454	133664	19253	2627	6213	2102	2627	-	-	-	525	-	-	-	2417976	667635.7	276.11
32-33	-	-	256258	656657	1062980	820021	49599	25652	2447	9536	15645	979	1958	3789	3789	-	-	-	2909309	867854.8	298.30
33-34	-	-	51102	141466	649300	1796292	167355	22699	9237	18390	5873	-	-	-	-	-	-	-	2861712	910369.8	318.12
34-35	-	-	39963	5198	182740	1064853	186269	87278	9070	56884	10899	598	465	3859	-	-	-	-	1648074	553397.8	335.78
35-36	-	-	-	12888	59750	213889	219024	134632	37843	92581	8328	52787	20612	32823	-	11277	-	-	896432	321715.6	358.88
36-37	-	-	-	1485	7364	9469	29872	134729	126028	200909	66365	190091	201609	68316	2763	-	-	-	1039001	394231.3	379.43
37-38	-	-	11302	-	-	-	1295	65134	63493	156242	106558	182404	228486	58252	54793	2182	-	-	930141	370334.6	398.15
38-39	-	-	-	-	-	-	2049	7654	17207	35751	30464	66722	107175	100662	37800	29396	5000	-	439879	185616.9	421.97
39-40	-	-	-	-	-	-	-	-	-	-	1368	12316	28053	48916	12316	-	-	-	102969	46454.8	451.15
40-41	-	-	-	-	-	-	-	-	-	-	-	-	5170	-	4579	654	-	-	10402	5147.3	494.83
TSN(1000)	6754	111426	8081535	1697468	2334655	4101580	714352	490601	293521	589590	248127	505896	597123	316616	116565	43509	5000	86663	20340981	-	-
TSB(1000 kg)	1263.0	21354.6	1942260.4	465900.3	711503.7	1307705.0	236374.2	174051.4	108720.0	222214.0	93474.7	199884.1	234966.8	129554.8	47528.2	17760.3	2319.5	13314.2	-	5930149.1	-
Mean length (cm)	27.25	27.60	29.56	31.29	32.52	33.24	33.87	35.09	35.50	35.84	36.24	36.64	36.87	37.19	37.53	37.33	38.00	25.08	-	-	-
Mean weight (g)	187.01	191.65	240.33	274.47	304.76	318.83	330.89	354.77	370.40	376.90	376.72	395.11	393.50	409.19	407.74	408.20	463.95	153.63	-	-	291.54

Table 10. Bootstrap estimates of Norwegian spring-spawning herring in IESSNS 2020 from StoX based on 1000 replicates. Numbers by age and total number (TSN) are in millions and total biomass (TSB) in thousand tonnes.

Age	5th percentile	Median	95th percentile	Mean	SD	CV
2	0.0	11.9	42.7	15.5	13.7	0.89
3	40.7	106.5	232.6	117.2	59.3	0.51
4	4841.3	8022.4	12501.3	8280.3	2350.6	0.28
5	1182.0	1698.4	2276.3	1709.8	338.7	0.20
6	1633.7	2336.4	3144.4	2367.2	472.7	0.20
7	2938.4	4043.9	5406.8	4087.3	770.0	0.19
8	475.2	687.4	950.7	695.9	148.4	0.21
9	348.8	516.0	711.3	520.1	113.9	0.22
10	213.1	301.1	402.8	304.9	60.4	0.20
11	400.2	581.6	823.4	593.7	131.8	0.22
12	157.6	256.3	364.3	259.1	63.8	0.25
13	293.1	494.7	734.7	502.6	134.1	0.27
14	354.6	578.0	831.3	580.5	142.9	0.25
15	174.4	320.2	496.4	327.3	100.4	0.31
TSN	14655.8	20497.9	27132.4	20611.4	3829.6	0.19
TSB	4353.7	5981.3	7740.8	5990.8	1028.2	0.17

Table 11. IESSNS baseline time series from 2016 to 2020. StoX abundance estimates of Norwegian spring-spawning herring (millions).

	Age												
Year	1	2	3	4	5	6	7	8	9	10	11	12+	TSB(1000 t)
2016	41	146	752	604	1 637	1 559	2 010	1 614	1 190	2 023	2 151	6 467	6 753
2017	1 216	248	1 285	4 586	1 056	1 188	816	1 794	1 022	1 131	1 653	4 119	5 885
2018	0	577	722	879	3 078	931	1 264	734	948	1 070	694	2 792	4 465
2019	0	153	1 870	590	1 067	3 475	859	702	520	700	463	4 808	4 780
2020	0	7	111	8 082	1 697	2 335	4 102	714	491	294	590	1 833	5 930

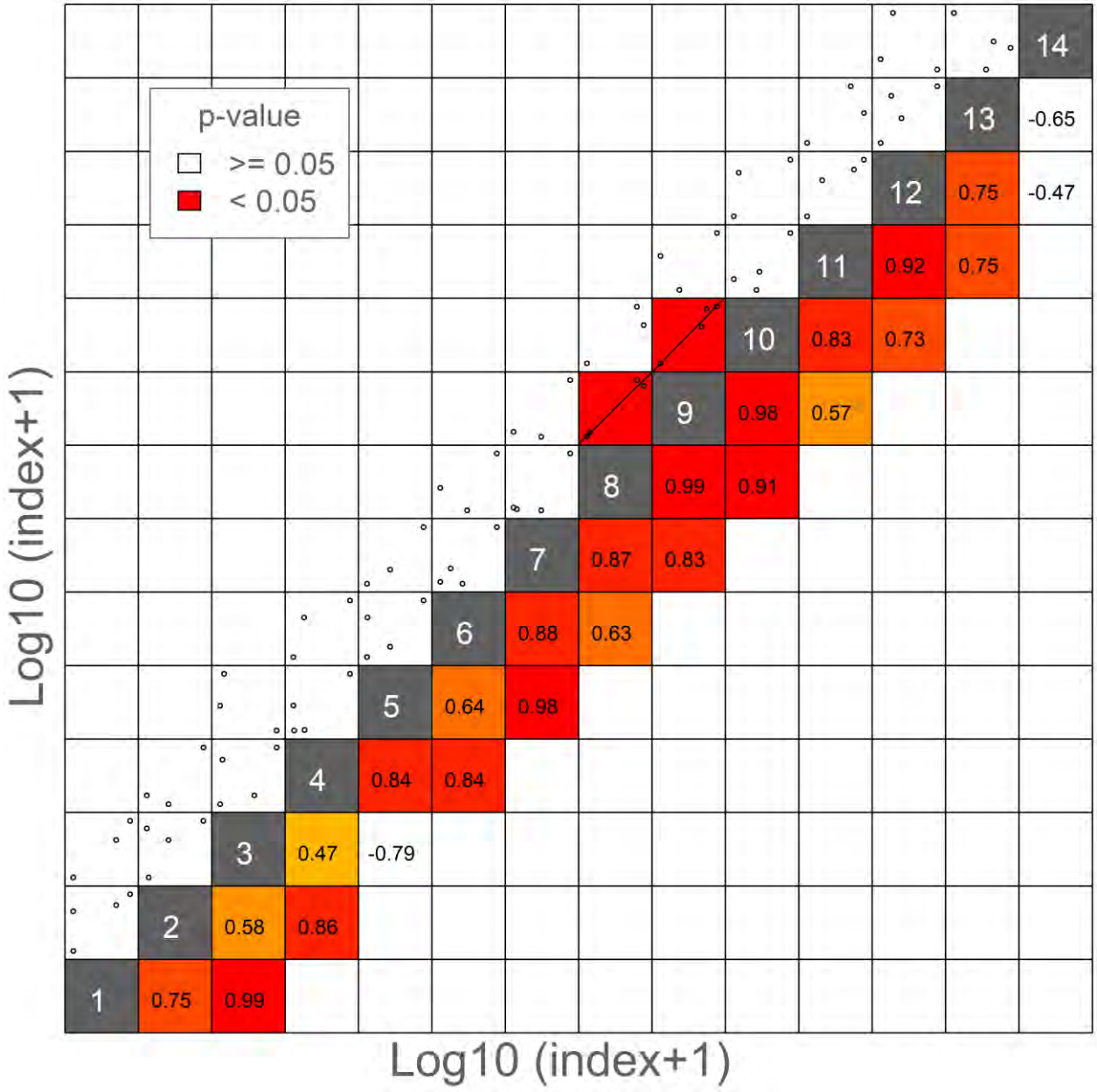

Figure 22. Internal consistency for Norwegian spring-spawning herring within the IESSNS. The upper left part of the plots shows the relationship between log index-at-age within a cohort. Linear regression line shows the best fit to the log-transformed indices. The lower-right part of the plots shows the correlation coefficient (r) for the two ages plotted in that panel. The background colour of each panel is determined by the r value, where red equates to r=1 and white to r<0.

4.5 Blue whiting

Blue whiting was distributed in the central and eastern part of the survey area. The area around Iceland, influenced by the cold East Icelandic Current, southern Iceland and in the East Greenland area had very little blue whiting. The highest sA-values were observed in the eastern and southern part of the Norwegian Sea, along the Norwegian continental slope and around the Faroe Islands. The distribution in 2020 is somewhat changed compared to the 2019 distribution since the area to the west had less blue whiting. The main concentrations of older fish were observed in connection with the continental slopes, both in the eastern and the southern part of the Norwegian Sea (Figure 23). The largest fish were found in the central and northern part of the survey area.

The total biomass of blue whiting registered during IESSNS 2020 was 1.8 million tons (Table 12), a decrease compared to 2019 (2.0 mill tons). The stock estimate in number for 2019 is 16.5 billion compared to 16.2 billion of age groups 1+ in 2019. Age group 1 is dominating the estimate in 2020 (22% and 35% of the biomass and by numbers, respectively, looking at age groups 1+). A good sign of recruiting year class (0-group) was also seen in the survey this year.

Number by age, with uncertainty estimates, for blue whiting during IESSNS 2020 is shown in Figure 24.

The group considered the acoustic biomass estimate of blue whiting to be of good quality in the 2020 IESSNS as in the previous survey years.

Bootstrap estimates of numbers by age of blue whiting are shown in table 13 and the baseline point estimates from 2016-2020 are shown in table 14. The internal consistency among year classes is shown in Figure 25.

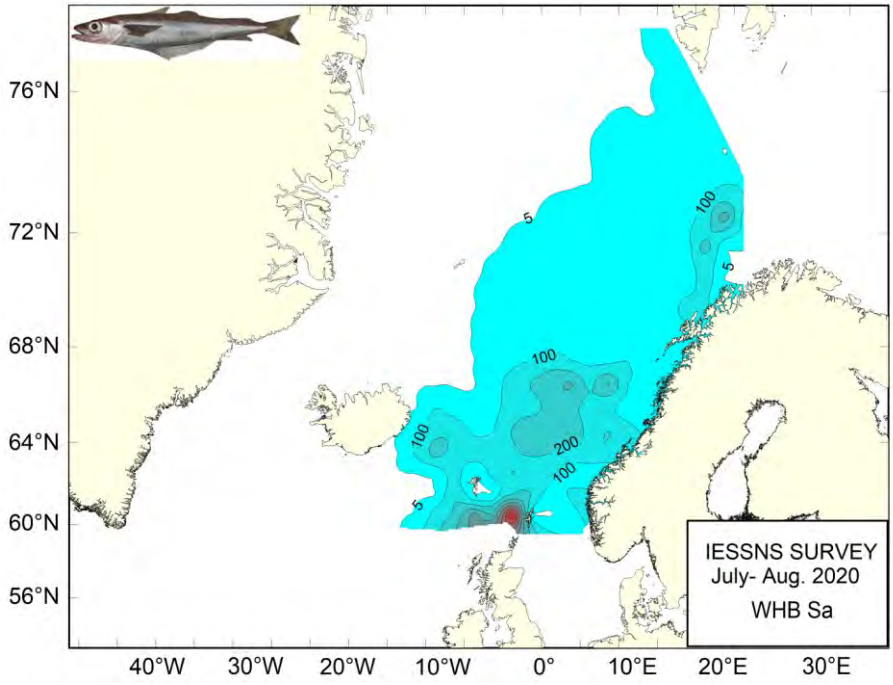

Figure 23a. The s_A/Nautical Area Scattering Coefficient (NASC) values of blue whiting along the cruise tracks in IESSNS 2020. Presented as contour lines.

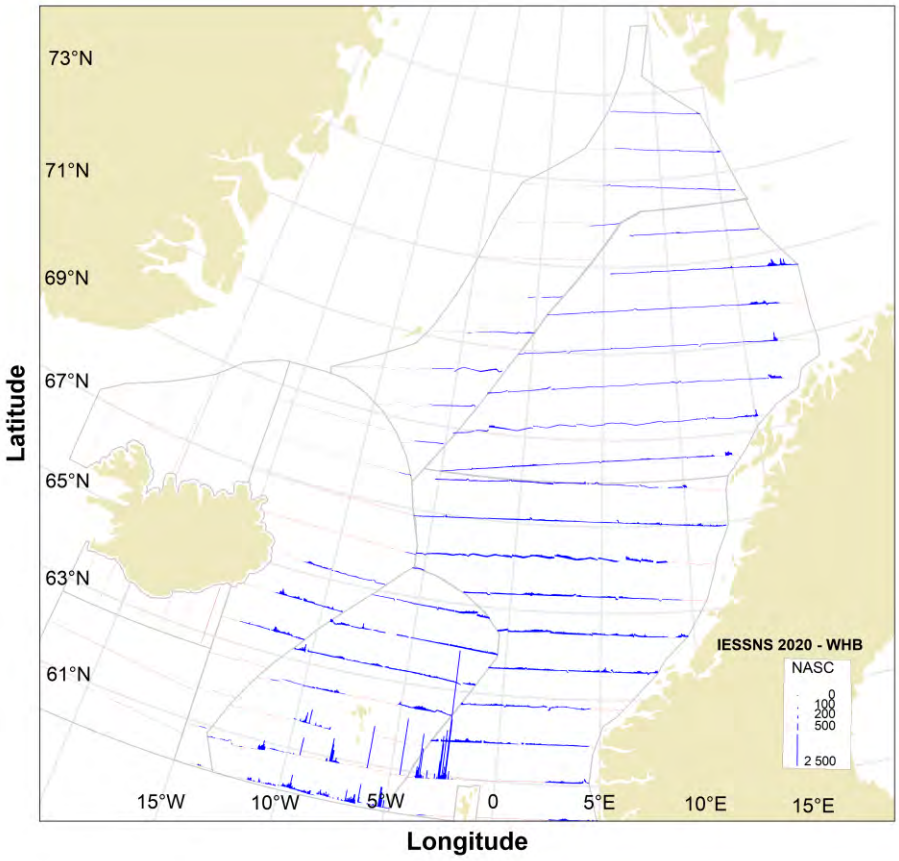

Figure 23b. The s_A/Nautical Area Scattering Coefficient (NASC) values of blue whiting along the cruise tracks in IESSNS 2020. Presented as bar plot.

Table 12. Estimates of abundance, mean weight and mean length of blue whiting based on calculation in StoX for IESSNS 2020.

	age															
LenGrp	0	1	2	3	4	5	6	7	8	9	10	11	Unknown	Number (1E3)	Biomass (1E3kg)	Mean W (g)
5-6	-	-	-	-	-	-	-	-	-	-	-	-	475244	475244	712.9	1.50
6-7	-	-	-	-	-	-	-	-	-	-	-	-	143824	143824	287.6	2.00
7-8	-	-	-	-	-	-	-	-	-	-	-	-	-	-	-	-
8-9	-	-	-	-	-	-	-	-	-	-	-	-	-	-	-	-
9-10	-	-	-	-	-	-	-	-	-	-	-	-	-	-	-	-
10-11	-	-	-	-	-	-	-	-	-	-	-	-	8818	8818	-	-
11-12	563743	-	-	-	-	-	-	-	-	-	-	-	-	563743	5035.3	8.93
12-13	1397043	-	-	-	-	-	-	-	-	-	-	-	-	1397043	14951.9	10.70
13-14	1144766	-	-	-	-	-	-	-	-	-	-	-	-	1144766	15260.0	13.33
14-15	708720	-	-	-	-	-	-	-	-	-	-	-	-	708720	12718.3	17.95
15-16	204667	-	-	-	-	-	-	-	-	-	-	-	-	204667	4388.4	21.44
16-17	47482	-	-	-	-	-	-	-	-	-	-	-	-	47482	1288.3	27.13
17-18	-	3418	-	-	-	-	-	-	-	-	-	-	-	3418	88.9	26.00
18-19	-	64303	-	-	-	-	-	-	-	-	-	-	-	64303	1888.1	29.36
19-20	-	284101	-	-	-	-	-	-	-	-	-	-	-	284101	9739.1	34.28
20-21	-	587975	-	-	-	-	-	-	-	-	-	-	-	587975	24124.0	41.03
21-22	-	545134	47261	-	-	-	-	-	-	-	-	-	-	592395	32192.9	54.34
22-23	-	1398559	107462	37309	-	-	-	-	-	-	-	-	-	1543330	100316.9	65.00
23-24	-	1711675	308186	38983	-	-	-	-	-	-	-	-	-	2058844	153721.1	74.66
24-25	-	940084	647953	10125	10125	-	-	-	-	-	-	-	-	1608287	137805.7	85.68
25-26	-	236626	976587	187545	13539	-	-	-	-	-	-	-	-	1414296	139747.6	98.81
26-27	-	25266	630904	542256	117736	6493	12986	12986	-	-	-	-	-	1348629	144673.9	107.27
27-28	-	-	225161	499183	242781	286923	227906	82001	35726	-	-	-	-	1599680	184243.3	115.18
28-29	-	6671	29683	146062	307749	407455	442685	242832	46698	-	-	-	-	1629835	202332.8	124.14
29-30	-	-	3603	103964	357715	325435	424059	123417	17867	7132	-	-	-	1363192	185760.3	136.27
30-31	-	-	19072	-	35630	319960	432661	241792	51531	-	-	-	-	1100647	172701.0	156.91
31-32	-	-	-	42429	109970	230538	173418	61271	18805	-	7979	-	-	644410	115474.0	179.19
32-33	-	-	-	21413	10255	84793	163006	52500	5510	-	-	-	-	337476	66983.8	198.48
33-34	-	-	-	-	-	53440	76612	45387	-	3143	-	-	-	178582	37721.3	211.23
34-35	-	-	-	-	-	3265	17964	73978	4902	4902	-	3265	-	108277	24233.5	223.81
35-36	-	-	-	-	-	-	15450	2572	11583	6000	2572	-	-	38177	9852.7	258.08
36-37	-	-	-	-	-	-	3428	-	8719	-	-	15899	-	28047	7717.8	275.17
TSN(1000)	4066422	5803812	2995873	1629269	1205499	1718303	1990176	938736	201341	21177	10551	19165	627886	21228210	-	-
TSB(1000 kg)	53642.3	389957.9	286417.5	187223.1	156139.2	250393.4	297906.6	141121.8	30522.9	4034.1	2102.3	5499.9	1000.5	-	1805961.5	-
Mean length (cm)	12.93	22.54	25.10	26.86	28.42	29.36	29.60	29.92	29.86	32.51	32.35	36.07	5.55	-	-	-
Mean weight (g)	13.19	67.19	95.60	114.91	129.52	145.72	149.69	150.33	151.60	190.49	199.25	286.98	1.62	-	-	85.11

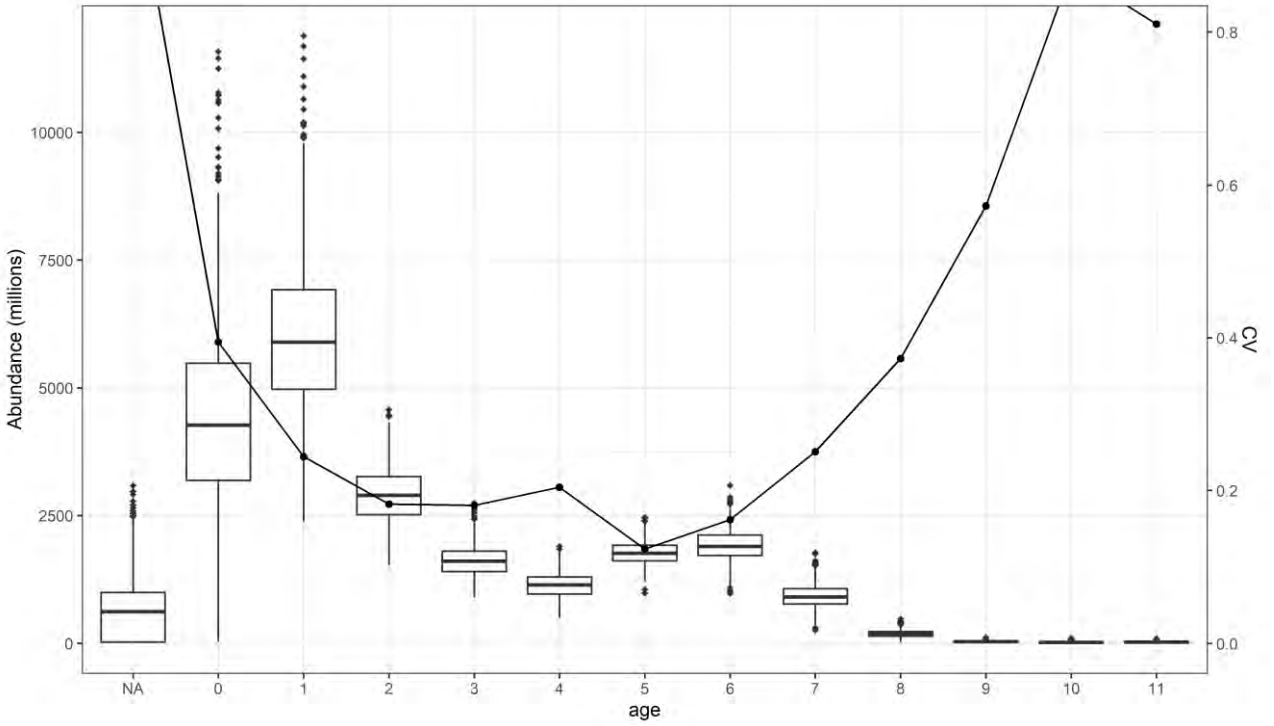

Figure 24. Number by age with uncertainty for blue whiting during IESSNS 2020. Boxplot of abundance and relative standard error (CV) obtained by bootstrapping with 500 replicates using the StoX software.

Table 13. Bootstrap estimates of blue whiting in IESSNS 2020 from StoX based on 1000 replicates. Numbers by age and total number (TSN) are in millions and total biomass (TSB) in thousand tonnes.

Age	5th percentile	Median	95th percentile	Mean	SD	CV
0	2022.3	4267.3	7716.5	4460.7	1760.1	0.39
1	3897.4	5891.6	8780.3	6027.3	1473.2	0.24
2	2083.9	2896.4	3787.5	2903.3	529.4	0.18
3	1138.0	1602.8	2081.1	1607.7	290.3	0.18
4	755.5	1140.6	1502.4	1134.9	231.8	0.20
5	1411.6	1761.9	2114.7	1762.2	217.3	0.12
6	1431.1	1894.8	2453.9	1923.9	311.4	0.16
7	563.8	907.5	1350.8	928.6	232.9	0.25
8	73.5	184.5	305.9	186.0	69.3	0.37
9	9.1	30.9	68.8	33.4	19.2	0.57
10	0.0	14.9	42.1	16.3	14.4	0.88
TSN	17416.6	21333.9	26740.9	21611.2	2850.5	0.13
TSB	1524.4	1787.7	2102.1	1798.8	177.9	0.10

Table 14. IESSNS baseline time series from 2016 to 2020. StoX abundance estimates of blue whiting (millions).

	Age											
Year	0	1	2	3	4	5	6	7	8	9	10+	TSB(1000 t)
2016	3 869	5 609	11 367	4 373	2 554	1 132	323	178	177	8	233	2 283
2017	23 137	2 558	5 764	10 303	2 301	573	250	18	25	0	25	2 704
2018	0	915	1 165	3 252	6 350	3 151	900	385	100	52	41	2 039
2019	2 153	640	1 933	2 179	4 348	5 434	1 151	209	229	5	8	2 028
2020	4 066	5 804	2 996	1 629	1 205	1 718	1 990	939	201	21	30	1 806

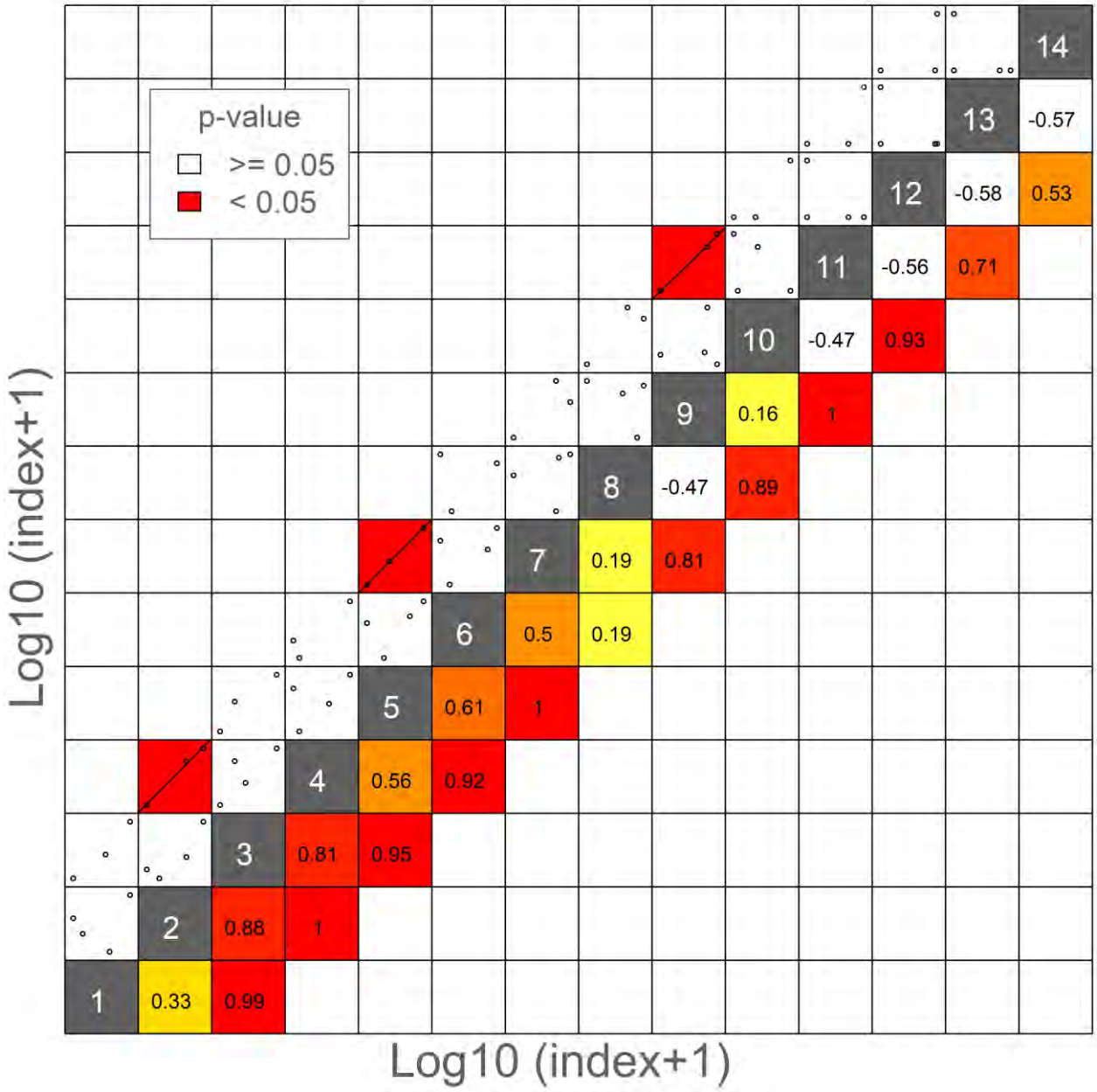

Figure 25. Internal consistency for blue whiting within the IESSNS. The upper left part of the plots shows the relationship between log index-at-age within a cohort. Linear regression line shows the best fit to the log-transformed indices. The lower-right part of the plots shows the correlation coefficient (r) for the two ages plotted in that panel. The background colour of each panel is determined by the r value, where red equates to r=1 and white to r<0.

4.6 Other species

Lumpfish (*Cyclopterus lumpus*)

Lumpfish was caught in approximately 74% of trawl stations across the six vessels (Figure 26) and where lumpfish was caught, 72% of the catches were ≤10kg. Lumpfish was distributed across the entire survey area, from west of Cape Farwell in Greenland in the southwest to the central Barents Sea in the northeast part of the covered area. Of note, in previous years aboard the Faroese vessel, a subsample of 50 kg to 200 kg of the total catch was processed. Therefore, small catches (<10 kg) of lumpfish may have been missed, however in 2020, all lumpfish were sorted from the catch and weighed.

Abundance was greatest north of 66°N, and lowest directly south of Iceland, and western side of the North Sea. The zero line was not hit to the north, northwest and southwest of the survey so it is likely that the distribution of lumpfish extends beyond the survey coverage. The length of lumpfish caught varied from 2 to 50 cm with a bimodal distribution with the left peak (5-20 cm) likely corresponding to 1-group lumpfish and the right peak consisting of a mixture of age groups (Figure 27). For fish ≥20 cm in which sex was determined, the males exhibited a unimodal distribution with a peak around 25-27 cm. The females also exhibited a unimodal distribution but with a peak around 27-30 cm which was positively skewed. Aboard the Norwegian vessels, of the fish which were sexed, the ratio of females to males was approximately 4.4:1. Generally, the mean length and mean weight of the lumpfish was highest in Faroese waters and the coastal waters and along the shelf edges of Norway and lowest in the central and northern Norwegian Sea.

A total of 715 fish (370 by R/V "Árni Friðriksson", 159 by M/V "Eros", 93 by M/V Vendla and 95 by M/V King's Bay) between 10 and 48 cm were tagged during the survey (Figure 28).

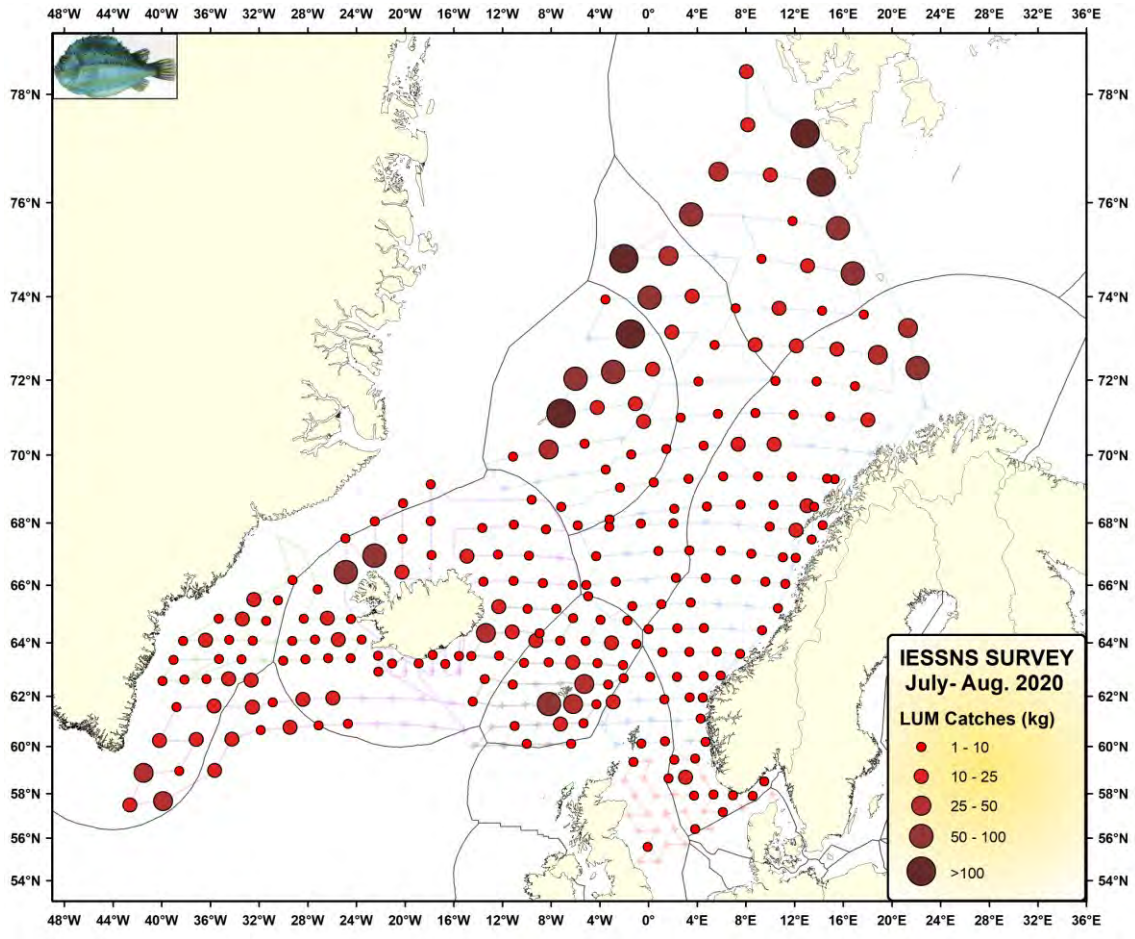

Figure 26. Lumpfish catches at surface trawl stations during IESSNS 2020.

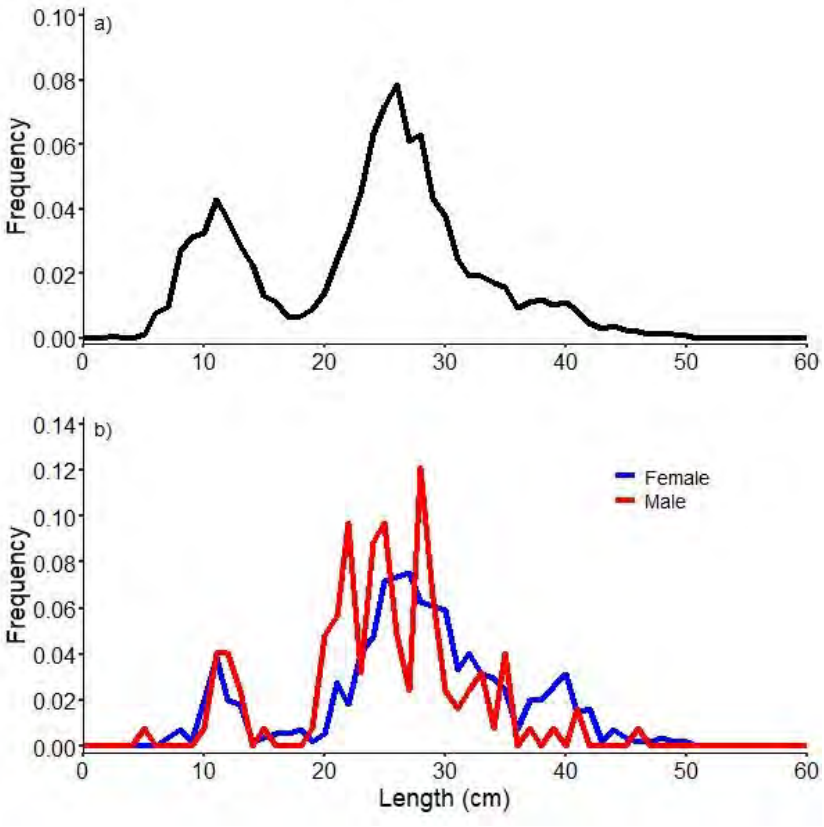

Figure 27. Length distribution of a) all lumpfish caught during the survey and b) length distribution of fish in which sex was determined.

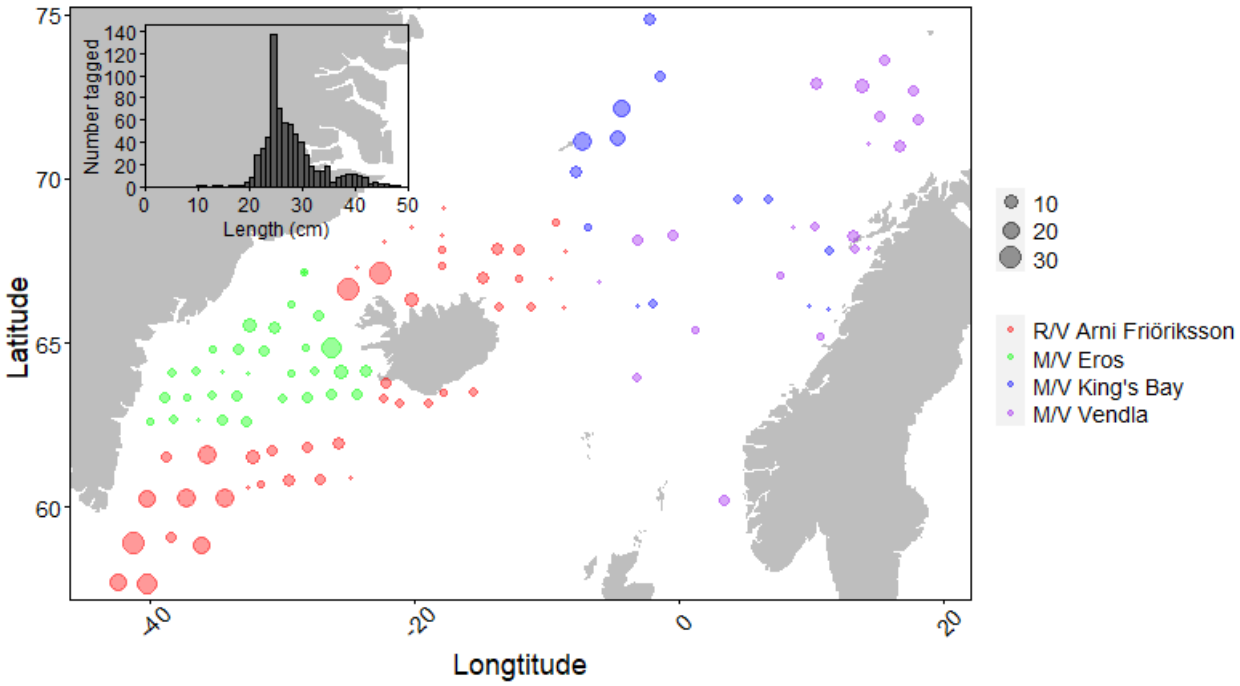

Figure 28. Number tagged, and release location, of lumpfish. Insert shows the length distribution of the tagged fish. Location of fish tagged aboard King's Bay was not available at time of writing.

Salmon (*Salmo salar*)

A total of 54 North Atlantic salmon were caught in 30 stations both in coastal and offshore areas from 60°N to >77°N in the upper 30 m of the water column during IESSNS 2020 (Figure 29). The salmon ranged from 0.084 kg to 2.73 kg in weight, dominated by postsmolt weighing 100-180 grams and individuals weighing 1-2 kg. We caught from 1 to 8 salmon (small shoals) during individual surface trawl hauls. The length of the salmon ranged from 20.5 cm to 61 cm, with a pronounced bimodal distribution of <30 cm and >45 cm long salmon.

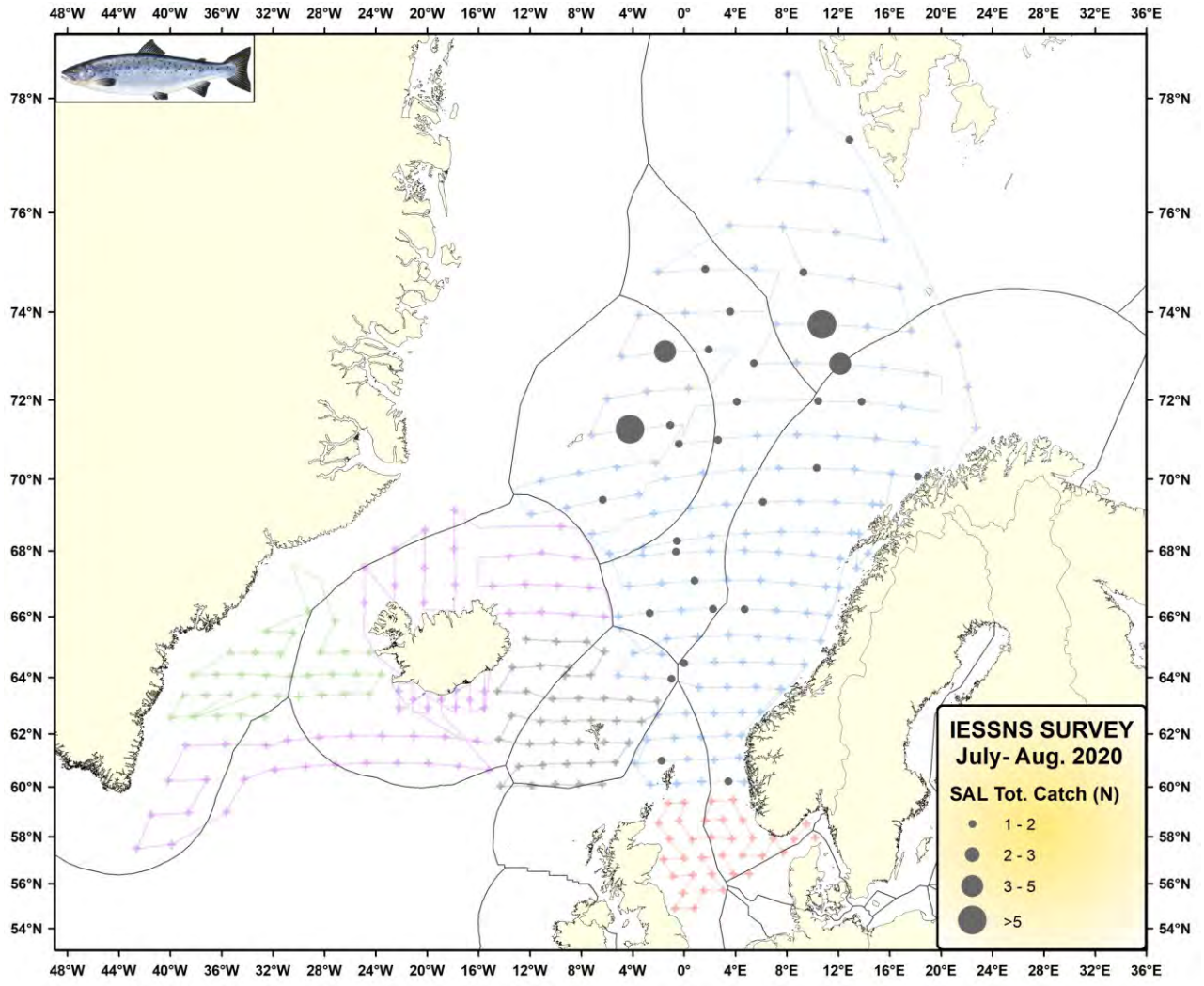

Figure 29. Catches of salmon at surface trawl stations during IESSNS 2020.

Capelin (*Mallotus villosus*)

Capelin was caught in the surface trawl on 42 stations primarily along the cold fronts: In East Greenland from Cape Farewell to Ittoqqertoormiit, Denmark Strait, North of Iceland, North-East of Jan Mayen and at the entrance to the Barents Sea (Figure 30).

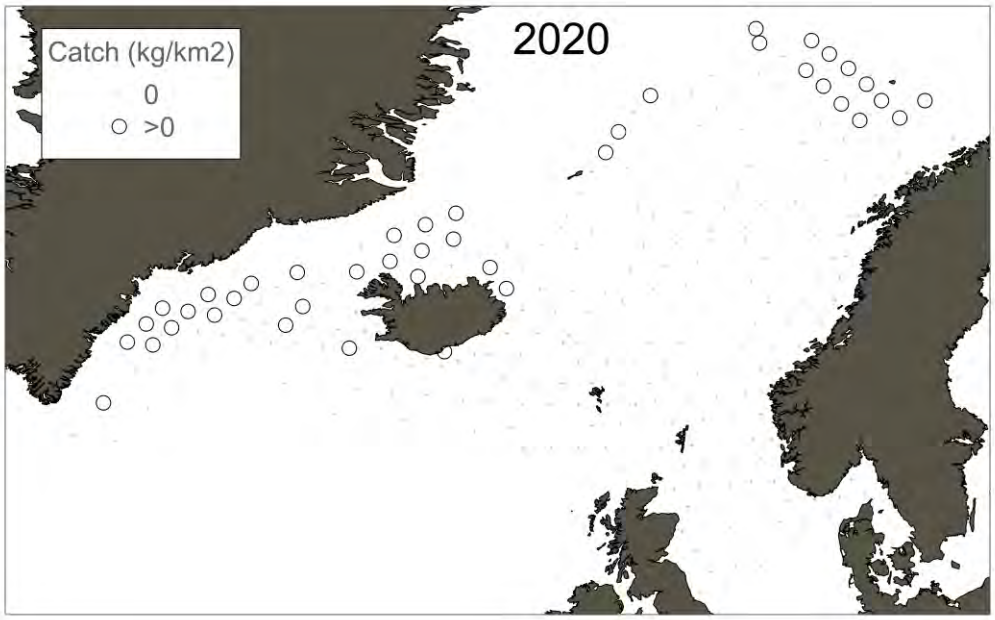

Figure 30. Presence of capelin in surface trawl stations.

4.7 Marine Mammals

Opportunistic whale observations were done by M/V "Kings Bay" and M/V "Vendla" from Norway in addition to R/V "Árni Friðriksson" from Iceland in 2020 (Figure 31). Overall, 802 marine mammals of 10 different species were observed, which was an increase from 521 marine mammals in 2019, 600+ in 2018 and 700+ in 2017 observed individuals. R/V "Árni Friðriksson" dedicated whale observers were onboard in 2017 and for the 1st leg in 2020, which was not the case from 2018-2019 and the 2nd leg in 2020. Kings Bay and Vendla conducted only opportunistic whale observations for all years including the years 2017-2020. The increase in number of marine mammals came even though both Kings Bay and Vendla had several days with fog and very reduced visibility in the north-western region (Jan Mayen area) and northernmost areas between Bear Island and Svalbard. This has possibly influenced the low number of marine mammals observed on these two vessels in the normally abundant marine mammal habitats within the northernmost parts of our surveyed areas during IESSNS 2020. R/V "Árni Friðriksson" had also occasional periods with fog north of Iceland.

The species that were observed included; blue whales (*Balaenoptera musculus),* fin whales (*Balaenoptera physalus*), minke whales (*Balaenoptera acutorostrata*), humpback whales (*Megaptera novaeangliae*), bottlenose whales (*Hyperoodon ampullatus)*, pilot whales (*Globicephala sp.*), killer whales (*Orcinus orca*), sperm whales (*Physeter macrocephalus*), white beaked dolphins (*Lagenorhynchus albirostris*) and harbour porpoise (*Phocoena phocoena*). The dominant number of marine mammal observations were found around Iceland, along the continental shelf between the north-eastern part of the Norwegian Sea and in a line between Finnmark to southwest of Svalbard. Fin whales (n = 117, group size = 1-20 (average groups size = 4.7)) and humpback whales (n = 89, group size = 1-60 (average groups size = 5.1)) dominated among the large whale species, and

they were particularly abundant northwest of Iceland and from Norwegian coast outside Finnmark stretching north/northwest via Bear Island to southwest of Svalbard. Fin whales also appeared to be present in the northeastern part of the Norwegian Sea feeding on NSS herring. Killer whales (n = 71, group size = 1-12 (average groups size = 5.1)) dominated in the southern, northern and north-eastern part of the Norwegian Sea, mostly overlapping and feeding on NES mackerel in the upper water masses. Dolphins (n = 134, group size = 3-20 (average groups size = 8.9)) were present in the northern part of the Norwegian Sea. Minke whales (n = 37, group size = 1-4 (average groups size = 1.4)) dominated in the north-eastern part of the Norwegian Sea, primarily overlapping and feeding on NSS herring in the upper 40 m of the water column. Altogether 3 individual observations of blue whale were done north and northwest of Iceland, whereas 2 northern bottlenose whales were observed south of Iceland. There were generally low numbers of marine mammal observations made of marine mammals in the southern and central parts of the Norwegian Sea in 2020 compared to previous years.

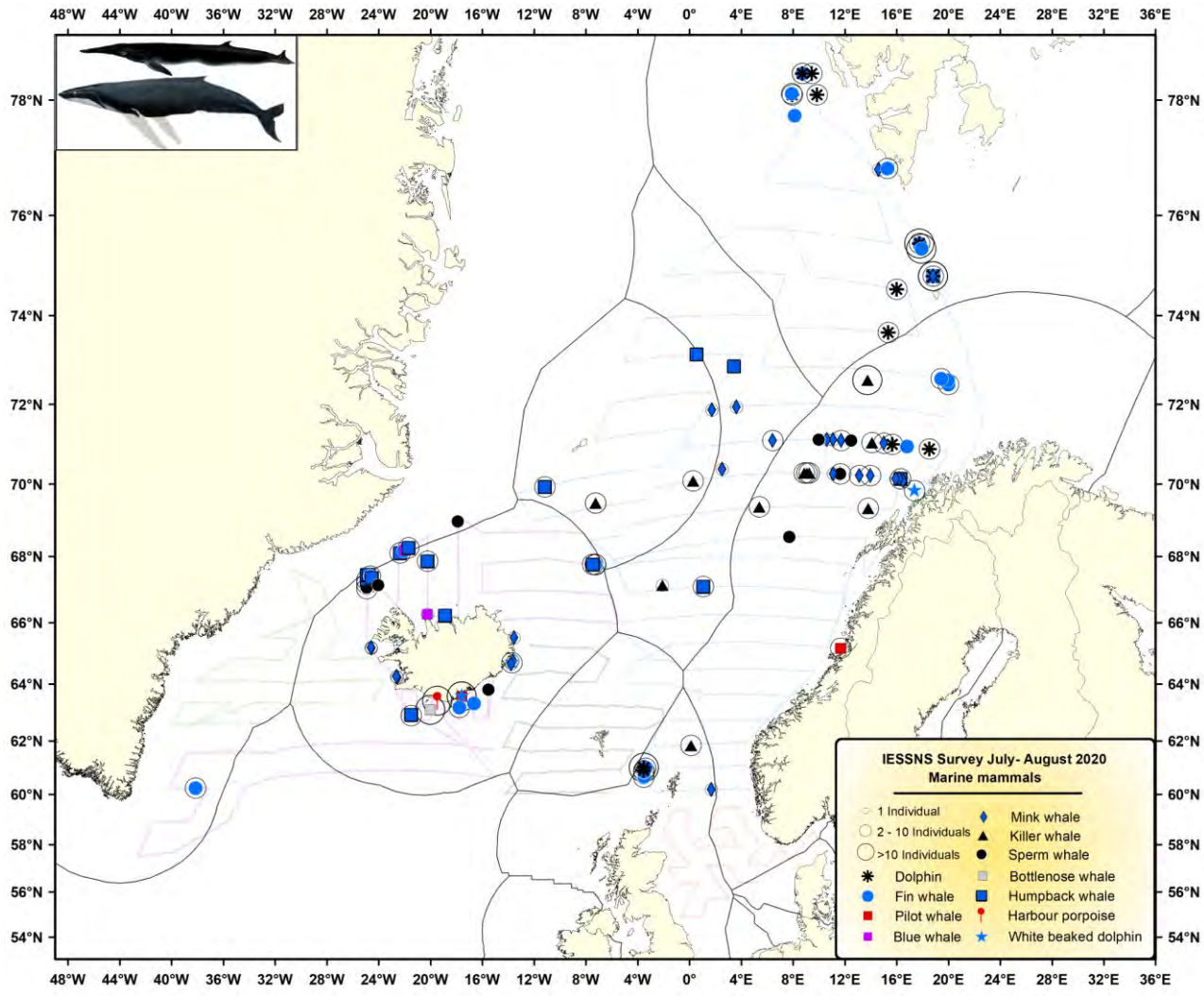

Figure 31. Overview of all marine mammals sighted during IESSNS 2020.

5 Recommendations

Recommendation	To whom
WGIPS recommends that the IESSNS extension to the North Sea should continue for establishing a time series suitable for assessing the part of the NE Atlantic Mackerel stock in the North Sea. The surveys conducted by Denmark in 2018, 2019 and 2020 have demonstrated that the IESSNS methodology works also for the northern North Sea (i.e. north and west from Doggerbank) and the Skagerrak for the area that is deeper than 50 m. The survey provides essential fishery-independent information on the stock during its feeding migration in summer and WGIPS recommends that the Danish survey should continue as a regular annual survey.	WGWIDE, RCG NANSEA

6 Action points for survey participants

Action points
The guidelines for trawl performance should be revised to reflect realistic manoeuvring of the Multpelt832 trawl.
Criteria and guidelines should be established for discarding substandard trawl stations using live monitoring of headline, footrope and trawl door vertical depth, and horizontal distance between trawl doors. For predetermined surface trawl station, discarded hauls should be repeated until performance is satisfactory. Explicit guideline for incomplete trawl hauls is to repeat the station or exclude it from future analysis. It is not acceptable to visually estimate mackerel catch, it must be hauled onboard and weighed. If predetermined trawl hauls are not satisfactory according to criteria the station will be excluded from mackerel index calculations, i.e. treated as it does not exist, but not as a zero mackerel catch station.
Tagging of lumpfish should be initiated or continue on all vessels.
We recommend that observers collect sighting information of marine mammals on all vessels.
Table 3 – biological sampling - needs to be changed to reflect what is sampled on the different vessels.
We should consider calculating the zooplankton index from annually gridded field polygons to extract area-mean time-series.
For next year's survey, the group should consider having the strata Greenland South and Iceland south offshore (Strata numbers 11 and 12) as dynamic Strata given the absence of mackerel in these strata the last two years.
For next year's survey, the group should consider distributing transects differently among vessels, such that synoptic coverage becomes better than this year and survey time is optimally used.

7 Survey participants

M/V "Vendla":
Arne Johannes Holmin (cruise leader), Institute of Marine Research, Bergen, Norway
Åge Høines (cruise leader), Institute of Marine Research, Bergen, Norway
Lage Drivenes, Institute of Marine Research, Bergen, Norway
Benjamin Marum, Institute of Marine Research, Bergen, Norway
Valantine Anthonypillai, Institute of Marine Research, Bergen, Norway
Thassya Christina dos Santos Schmidt, Institute of Marine Research, Bergen, Norway
Vilde Regine Bjørdal, Institute of Marine Research, Bergen, Norway
Lea Marie Hellenbrecht, , Institute of Marine Research, Bergen, Norway
Frøydis Tousgaard Rist Bogetveit, Institute of Marine Research, Bergen, Norway
Susanne Tonheim, Institute of Marine Research, Bergen, Norway

M/V "Kings Bay":
Leif Nøttestad (International coordinator and cruise leader), Institute of Marine Research, Bergen, Norway
Are Salthaug (cruise leader), Institute of Marine Research, Bergen, Norway
Jarle Kristiansen, Institute of Marine Research, Bergen, Norway
Olav j. Sørås, Institute of Marine Research, Bergen, Norway
Guosong Zhang, Institute of Marine Research, Bergen, Norway
Eilert Hermansen, Institute of Marine Research, Bergen, Norway
Ørjan Sørensen, Institute of Marine Research, Bergen, Norway
Erling Boge, Institute of Marine Research, Bergen, Norway
Astrid Fuglseth Rasmussen, Institute of Marine Research, Bergen, Norway
Herdis Langøy Mørk, Institute of Marine Research, Bergen, Norway
Inger Henriksen, Institute of Marine Research, Bergen, Norway
Adam Custer, Institute of Marine Research, Bergen, Norway
Christine Djønne, Institute of Marine Research, Bergen, Norway

R/V "Árni Friðriksson":
Anna Heiða Ólafsdóttir (cruise leader and coordinator), Marine and Freshwater Research Institute, Reykjavík, Iceland
Arnþór B. Kristjánsson, Marine and Freshwater Research Institute, Reykjavík, Iceland
Ása Hilmarsdóttir, Marine and Freshwater Research Institute, Reykjavík, Iceland
Ástþór Gíslason, Marine and Freshwater Research Institute, Reykjavík, Iceland
Birkir Bárðarson, Marine and Freshwater Research Institute, Reykjavík, Iceland
Enrique G. A. Garcia, DTU Aqua, Denmark
Freyr Arnaldsson, Marine and Freshwater Research Institute, Reykjavík, Iceland
Georg Haney, Marine and Freshwater Research Institute, Reykjavík, Iceland
Guðrún Finnbogadóttir, Marine and Freshwater Research Institute, Reykjavík, Iceland
Halldór Tyrfingsson, Marine and Freshwater Research Institute, Reykjavík, Iceland
Jacek Sliwinski, Marine and Freshwater Research Institute, Reykjavík, Iceland
James Kennedy (cruise leader), Marine and Freshwater Research Institute, Reykjavík, Iceland
Klara Jakobsdóttir, Marine and Freshwater Research Institute, Reykjavík, Iceland
Martina Blumel, Geomar, Germany
Ragnhildur Ólafsdóttir, Marine and Freshwater Research Institute, Reykjavík, Iceland
Sigurlína Gunnarsdóttir, Marine and Freshwater Research Institute, Reykjavík, Iceland
Sólrún Sigurgeirsdóttir, Marine and Freshwater Research Institute, Reykjavík, Iceland

Svanhildur Egilsdóttir, Marine and Freshwater Research Institute, Reykjavík, Iceland
Sverrir Daníel Halldórsson, Marine and Freshwater Research Institute, Reykjavík, Iceland
Teresa S. G. Silva, Marine and Freshwater Research Institute, Reykjavík, Iceland

M/V "Tróndur í Gøtu":
Eydna í Homrum, Faroe Marine Research Institute, Torshavn, Faroe
Ebba Mortensen, Faroe Marine Research Institute, Torshavn, Faroe
Poul Vestergaard, Faroe Marine Research Institute, Torshavn, Faroe
Ragnar Karlsson, Faroe Marine Research Institute, Torshavn, Faroe

M/V "Eros":
On-board cruise leader: Søren L. Post, Greenland Institute of Natural Resources, Nuuk, Greenland
Jørgen Sethsen, Greenland Institute of Natural Resources, Nuuk, Greenland
Alexander Damkjær, Greenland Institute of Natural Resources, Nuuk, Greenland
Frederik Fuda Bjare, Greenland Institute of Natural Resources, Nuuk, Greenland
Svandís Eva Aradóttir, Marine and Freshwater Research Institute, Reykjavík, Iceland
Land based coordinator: Teunis Jansen, Greenland Institute of Natural Resources, Nuuk, Greenland

M/V "Ceton"
At sea:
Kai Wieland (cruise leader), National Institute of Aquatic Resources, Denmark
Per Christensen, National Institute of Aquatic Resources, Denmark
Dirk Tijssen, National Institute of Aquatic Resources, Denmark
Lab team:
Jesper Knudsen, National Institute of Aquatic Resources, Denmark
Søren Eskildsen, National Institute of Aquatic Resources, Denmark
Gert Holst, National Institute of Aquatic Resources, Denmark
Maria Jarnum, National Institute of Aquatic Resources, Denmark

8 Acknowledgements

We greatly appreciate and thank skippers and crew members onboard M/V "Kings Bay", M/V "Vendla", M/V "Eros", M/V "Tróndur í Gøtu", R/V "Árni Friðriksson" and M/V "Ceton" for outstanding collaboration and practical assistance during the joint mackerel-ecosystem IESSNS cruise in the Nordic Seas from 1st of July to 4th of August 2020.

9 References

Bachiller E, Utne KR, Jansen T, Huse G. 2018. Bioenergetics modeling of the annual consumption of zooplankton by pelagic fish feeding in the Northeast Atlantic. PLOS ONE 13(1): e0190345. https://doi.org/10.1371/journal.pone.0190345

Banzon, V., Smith, T. M., Chin, T. M., Liu, C., and Hankins, W., 2016. A long-term record of blended satellite and in situ sea-surface temperature for climate monitoring, modelling and environmental studies. Earth System Science Data. 8, 165–176, doi:10.5194/essd-8-165-2016.

Foote, K. G., 1987. Fish target strengths for use in echo integrator surveys. Journal of the Acoustical Society of America. 82: 981-987.

ICES. 2012. Report of the International Bottom Trawl Survey Working Group (IBTSWG), 27–30 March 2012, Lorient, France. ICES CM 2012/SSGESST:03. 323 pp.

ICES 2013a. Report of the Workshop on Northeast Atlantic Mackerel monitoring and methodologies including science and industry involvement (WKNAMMM), 25–28 February 2013, ICES Headquarters, Copenhagen and Hirtshals, Denmark. ICES CM 2013/SSGESST:18. 33 pp.

ICES. 2013b. Report of the Working Group on Improving Use of Survey Data for Assessment and Advice (WGISDAA), 19-21 March 2013, Marine Institute, Dublin, Ireland. ICES CM 2013/SSGESST:07.22 pp.

ICES 2014a. Manual for international pelagic surveys (IPS). Working document of Working Group of International Surveys (WGIPS), Version 1.02 [available at ICES WGIPS sharepoint] 98 pp.

ICES 2014b. Report of the Benchmark Workshop on Pelagic Stocks (WKPELA), 17–21 February 2014, Copenhagen, Denmark. ICES CM 2014/ACOM: 43. 341 pp

ICES. 2017. Report of the Benchmark Workshop on Widely Distributed Stocks (WKWIDE), 30 January-3 February 2017, Copenhagen, Denmark. ICES CM 2017/ACOM:36. 196 pp.

Jansen, T., Post, S., Kristiansen, T., Oskarsson, G.J., Boje, J., MacKenzie, B.R., Broberg, M., Siegstad, H., 2016. Ocean warming expands habitat of a rich natural resource and benefits a national economy. Ecol. Appl. 26: 2021–2032. doi:10.1002/eap.1384

Johnsen, E., Totland, A., Skålevik, Å., Holmin, A.J., Dingsør, G.E., Fuglebakk, E., Handegard, N.O. 2019. StoX: An open source software for marine survey analyses. Methods Ecol Evol. 2019; 10:1523–1528.

Jolly, G. M., and I. Hampton. 1990. A stratified random transect design for acoustic surveys of fish stocks. Canadian Journal of Fisheries and Aquaculture Science. 47: 1282-1291.

Nikolioudakis, N., Skaug, H. J., Olafsdottir, A. H., Jansen, T., Jacobsen, J. A., and Enberg, K. 2019. Drivers of the summer-distribution of Northeast Atlantic mackerel (Scomber scombrus) in the Nordic Seas from 2011 to 2017; a Bayesian hierarchical modelling approach. ICES Journal of Marine Science. 76(2): 530-548. doi:10.1093/icesjms/fsy085

Nøttestad, L., Utne, K.R., Óskarsson, G. J., Jónsson, S. Þ., Jacobsen, J. A., Tangen, Ø., Anthonypillai, V., Aanes, S., Vølstad, J.H., Bernasconi, M., Debes, H., Smith, L., Sveinbjörnsson, S., Holst, J.C., Jansen, T. and Slotte, A. 2016. Quantifying changes in abundance, biomass and spatial distribution of Northeast Atlantic (NEA) mackerel (*Scomber scombrus*) in the Nordic Seas from 2007 to 2014. ICES Journal of Marine Science. 73(2): 359-373. doi:10.1093/icesjms/fsv218.

Ólafsdóttir, A., Utne, K.R., Jansen, T., Jacobsen, J.A., Nøttestad, L., Óskarsson, G.J., Slotte, A., Melle, W. 2019. Geographical expansion of Northeast Atlantic mackerel (Scomber scombrus) in the Nordic Seas from 2007 - 2014 was primarily driven by stock size and constrained by temperature. Deep-Sea Research Part II. 159, 152-168.

Salthaug, A., Aanes, S., Johnsen, E., Utne, K. R., Nøttestad, L., and Slotte, A. 2017. Estimating Northeast Atlantic mackerel abundance from IESSNS with StoX. Working Document (WD) for WGIPS 2017 and WKWIDE 2017. 103 pp.

Valdemarsen, J.W., J.A. Jacobsen, G.J. Óskarsson, K.R. Utne, H.A. Einarsson, S. Sveinbjörnsson, L. Smith, K. Zachariassen and L. Nøttestad 2014. Swept area estimation of the North East Atlantic mackerel stock using a standardized surface trawling technique. Working Document (WD) to ICES WKPELA. 14 pp.

1 Appendix 1:

Denmark joined the IESSNS in 2018 for the first time extending the original survey area into the North Sea. The commercial fishing vessels "Ceton S205" was used, and in total 39 stations (CTD and fishing with the pelagic Multipelt 832 trawl) had successfully been conducted. No problems applying the IESSNS methods were encountered. Area coverage, however, was restricted to the northern part of the North Sea at water depths larger 50 m. No plankton samples were taken and no acoustic data were recorded because this is covered by the HERAS survey in this area.

Denmark joined the IESSNS again in 2020 using the same vessel. 35 stations were taken (PT and CTD, no plankton and no appropriate acoustic equipment available). The locations of stations differed slightly from the previous year focussing on the area north and west of Doggerbank and extended into the eastern Skagerrak.

Average mackerel catch in 2020 was higher than in 2019 (1318 kg/km² compared to 1009 kg/km² in 2019 and 1743 kg/km² in 2018). The length and age composition indicate a relative high amount of small (< 25 cm) individuals (Tab. A.1) whereas the abundance of older (≥ age 6) mackerel was similar to the two previous years (Fig. A.1.).

StoX baseline estimate of mackerel abundance in the North Sea was 257 079 tonnes (Table A1-1.)

Table A1-1. StoX baseline estimate of age segregated and length segregated mackerel index for the North Sea in 2020. Also provided is average length and weight per age class.

	age																	
LenGrp	1	2	3	4	5	6	7	8	9	10	11	12	13	14	16	Number (1E3)	Biomass (1E3kg)	Mean W (g)
17-18	-	-	-	-	-	-	-	-	-	-	-	-	-	-	-	-	-	-
18-19	-	-	-	-	-	-	-	-	-	-	-	-	-	-	-	-	-	-
19-20	290	-	-	-	-	-	-	-	-	-	-	-	-	-	-	290	16.2	56.00
20-21	658	-	-	-	-	-	-	-	-	-	-	-	-	-	-	658	46.0	69.86
21-22	14362	-	-	-	-	-	-	-	-	-	-	-	-	-	-	14362	1095.1	76.25
22-23	89711	-	-	-	-	-	-	-	-	-	-	-	-	-	-	89711	7814.2	87.10
23-24	243191	-	-	-	-	-	-	-	-	-	-	-	-	-	-	243191	24255.8	99.74
24-25	221620	-	-	-	-	-	-	-	-	-	-	-	-	-	-	221620	24426.8	110.22
25-26	70558	-	-	-	-	-	-	-	-	-	-	-	-	-	-	70558	8987.5	127.38
26-27	20143	30	-	-	-	-	-	-	-	-	-	-	-	-	-	20173	3056.0	151.49
27-28	14250	755	-	-	-	-	-	-	-	-	-	-	-	-	-	15005	2587.2	172.43
28-29	16512	10895	30	-	-	-	-	-	-	-	-	-	-	-	-	27438	5589.7	203.72
29-30	41904	45292	-	118	-	-	-	-	-	-	-	-	-	-	-	87314	20048.0	229.61
30-31	12433	105414	10511	149	-	-	-	-	-	-	-	-	-	-	-	128506	32163.8	250.29
31-32	9337	87232	18023	8	56	-	-	-	-	-	-	-	-	-	-	114656	30945.2	269.90
32-33	-	44072	29681	2938	273	-	33	33	-	-	-	-	-	-	-	77031	23036.7	299.06
33-34	-	6172	33006	24828	3610	17	-	33	-	-	-	-	-	-	-	67667	21906.0	323.73
34-35	-	104	18866	8811	27909	2740	10	-	-	-	-	-	-	-	-	58440	19251.6	329.43
35-36	-	-	2525	2680	24833	8721	-	-	-	71	-	-	-	-	-	38830	14652.9	377.36
36-37	-	-	-	8	6446	14148	1943	271	-	-	-	-	-	-	-	22816	9291.2	407.22
37-38	-	-	-	-	420	4214	3603	1294	31	765	61	-	-	-	-	10388	4638.9	446.57
38-39	-	-	-	-	138	215	273	982	403	16	-	-	-	-	-	2026	966.3	476.93
39-40	-	-	-	-	-	-	891	194	800	-	-	-	-	-	-	1885	956.1	507.11
40-41	-	-	-	-	-	-	-	635	8	246	689	125	-	157	-	1860	963.2	517.87
41-42	-	-	-	-	-	-	-	-	-	48	224	-	-	-	-	272	170.5	626.65
42-43	-	-	-	-	-	-	-	-	-	212	-	-	18	-	61	291	207.7	714.65
43-44	-	-	-	-	-	-	-	-	-	8	-	-	-	-	-	8	6.3	807.00
44-45	-	-	-	-	-	-	-	-	-	-	-	-	-	-	-	-	-	-
45-46	-	-	-	-	-	-	-	-	-	-	-	-	-	-	-	-	-	-
46-47	-	-	-	-	-	-	-	-	-	-	-	-	-	-	-	-	-	-
TSN(1000)	754967	299966	112643	39540	63685	30054	6754	3442	1242	1366	974	125	18	157	61	1314994	-	-
TSB(1000 kg)	91063.5	76959.2	34212.6	13320.1	22366.7	12552.2	2985.1	1575.9	592.4	711.0	542.8	68.5	11.4	81.0	36.4	-	257078.9	-
Mean length (cm)	24.13	30.42	32.35	33.26	34.55	35.68	36.99	37.79	38.63	38.40	40.04	40.00	42.00	40.00	42.00	-	-	-
Mean weight (g)	120.62	256.56	303.73	336.88	351.21	417.66	441.98	457.84	476.86	520.68	557.39	550.00	649.00	516.00	596.00	-	-	195.50

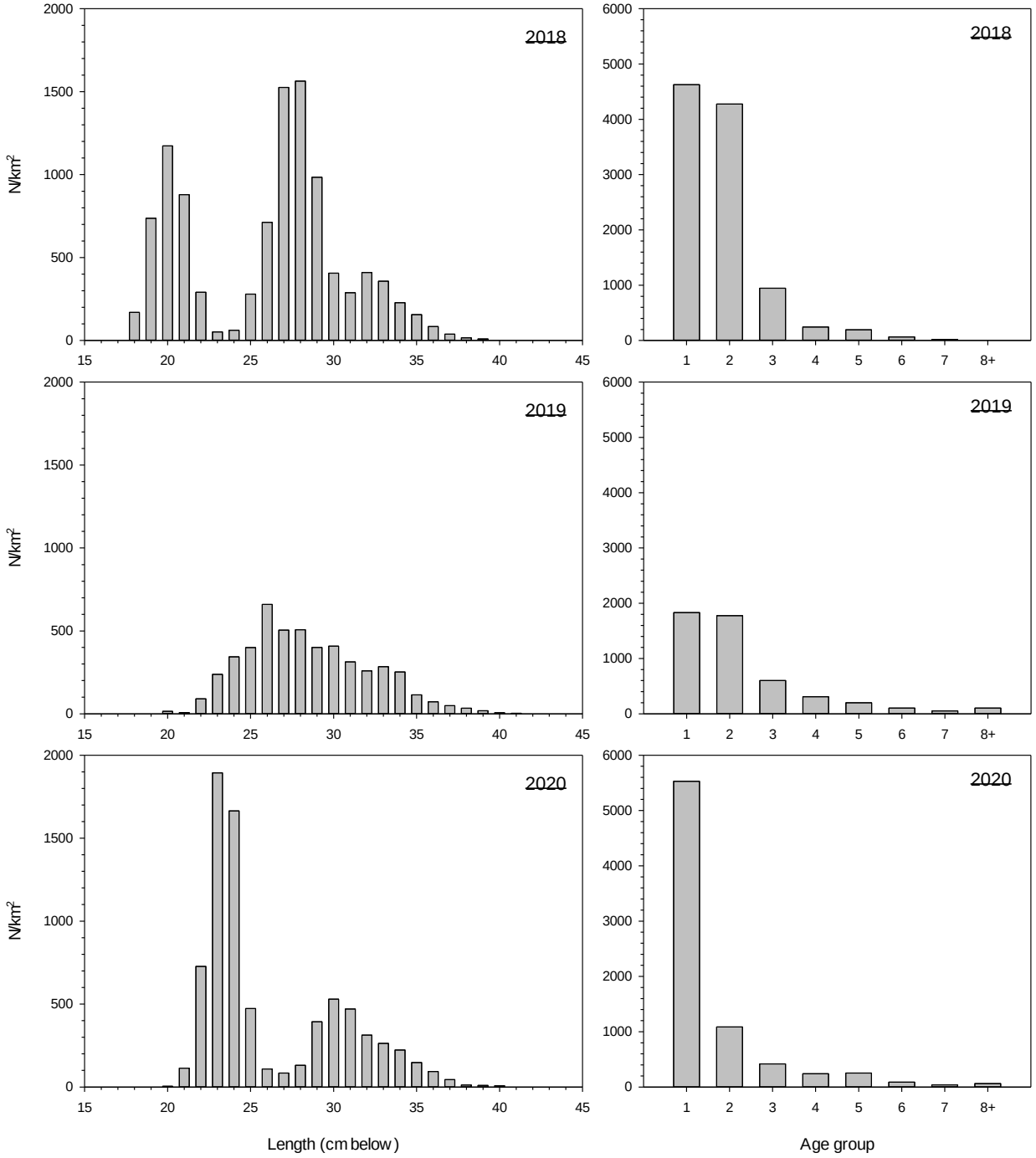

Fig. A1. Comparison of length and age distribution of mackerel in the North Sea 2018, 2019 and 2020.

2 Annex 2:

The mackerel index is calculated on all valid surface stations. That means, that invalid and potential extra surface stations and deeper stations need to be excluded. Below is the exclusion list used when calculating the mackerel abundance index for IESSNS 2020.

Table A2-1: Trawl station exclusion list for IESSNS 2020 for calculating the mackerel abundance index.

Vessel	Country	Exclusion list	
		Cruise	Stations
Kings Bay	Norway	2020814	15,21,28,33,38,46,50,57,61,64,69,81,94
Vendla	Norway	2020813	41,46,54,61,71,77,85,88,89,91,96,99,101,104,125
Árni Friðriksson	Iceland	A7-2020	393,401,414,417,424,427,433
Tróndur í Gøtu	Faroe Islands	2052	7,14,25,42,49,70,73 *
Eros	Greenland	CH-2020-01	122,128
Ceton	EU (Denmark)	IESSNS2020	none

* Observe that in PGNAPES and the national database station numbers are 4-digit numbers preceded by 2052 (e.g. ‘20520025’)

Working Group for the Working Group on Widely Distributed Stocks (WGWIDE)
26 August – 1 September 2020, Copenhagen (Denmark)

Update of striped red mullet abundance indices from professional fishing data (2016-2018)

Nathalie Caill-Milly[1], Muriel Lissardy[1], Noëlle Bru[2]

[1] Ifremer, LITTORAL, 1, allée du Parc Montaury, F-64600 Anglet, France

[2] Université de Pau et des Pays de l'Adour, E2S UPPA, CNRS, LMAP, Anglet, France

Context

The ROMELIGO project (2015-2018) aimed to contribute to the improvement of the knowledge on three stocks (mur-west, whg-89a and pol-89a – see Table 1) on the basis of the available data (landings data, sampling data for the French fleet, data from scientific campaigns...) or specific data collected during the project.

Table 1: Stocks considered by the ROMELIGO project for red mullet, whiting and pollack.

Species	Stock name	Stock code
Striped red mullet	Striped red mullet areas VI, VIII et sub-areas VIIa-c, e-k et IXa (West area)	mur-west
Whiting	Whiting area VIII et sub-area IXa	whg-89a
Pollack	Pollack area zone VIII et sub-area IXa	pol-89a

The project was organized in the same way in three parts and applied for each of the three stocks:

- Part 1 - Analyses of catches and activity of the French professional fishery (composition and evolution of catches, seasonality, spatial distribution, gear used and discards);
- Part 2 - Analyses of the size composition of the catches on professional and scientific vessels, analyses of the discards, proposition of abundance indicators using professional fishing data and analyses of CPUE from available scientific surveys;
- Part 3 - Collection of basic biological data relying on various samplings and calculation of biological parameters (length / weight relationships, growth curves, length at first maturity (L50) or maturity ogive...).

The contract report is available online (Léauté et al., 2018[1]). A paper on the methodology used to select the reference fleets for the calculation of red mullet LPUE was also published (Caill-Milly et al., 2019).

In relation to this work and regarding **striped red mullet**, two WDs were already sent and presented to the WGWIDE respectively in 2017 and 2018:

- One dedicated to part 1 integrating as a preamble a bibliographic review on the biology of the species (Caill-Milly et al., 2017);
- One dedicated to parts 2 and 3 (Caill-Milly et al., 2018).

This WD provides the update of striped red mullet abundance indices from professional fishing data (2016-2018).

[1] https://archimer.ifremer.fr/doc/00440/55126/

A reminder of the previous results (Caill-Milly et al., 2018)

For this species and for the Bay of Biscay, Table 2 describes the characteristics of the fleets selected to build abundance indices from professional fishing data. The selection was based on gears, technical characteristics of the vessels (defined by clusters), characteristics of the gears (mesh class) and time. No space specification within the Bay of Biscay were defined for this species. For red mullet, the retained gears and clusters are:

- "Bottom otter trawls" (OTB) and cluster 1. Cluster 1 corresponds to small vessels (7.9 to 15.8 m) with small tonnage (2.0 to 43.9 grt) and an engine power comprised between 44 and 256 kW. The full year was considered;
- "Set gillnets (anchored)" (GNS) and cluster 2. This second cluster corresponds to medium vessels (8.2 to 14.8) with medium tonnage (2.0 to 30.2 grt) and an engine power comprised between 70 and 331 kW. Depending of the mesh class, quarters 2 and/or 3 were selected because the activity is marked by a strong seasonality.

Table 2: Characteristics of the selected fleets regarding whiting.

Retained gear	Cluster	Gear mesh class	Period	Specific spatial delimitation
Bottom otter trawls (1 vessel) "OTB"	Cluster 1	70 to 79 mm	Annual	No (whole Bay of Biscay)
Set gillnets (anchored) "GNS"	Cluster 2	50 to 59 mm	Quarter 2	No (whole Bay of Biscay)
			Quarter 3	
		60 to 69 mm	Quarter 2	
		Sup to 90 mm	Quarter 2	

Gear "OTB"

For the selected mesh class (70 - 79 mm), the evolutions of the LPUE mean level and of its use over time were considered for the entire year and the whole Bay of Biscay.

The number of uses shows a decrease during the study period, however this decrease is not significant. Like uses, LPUE decreases over the period of study but significantly in this case (Figure 1).

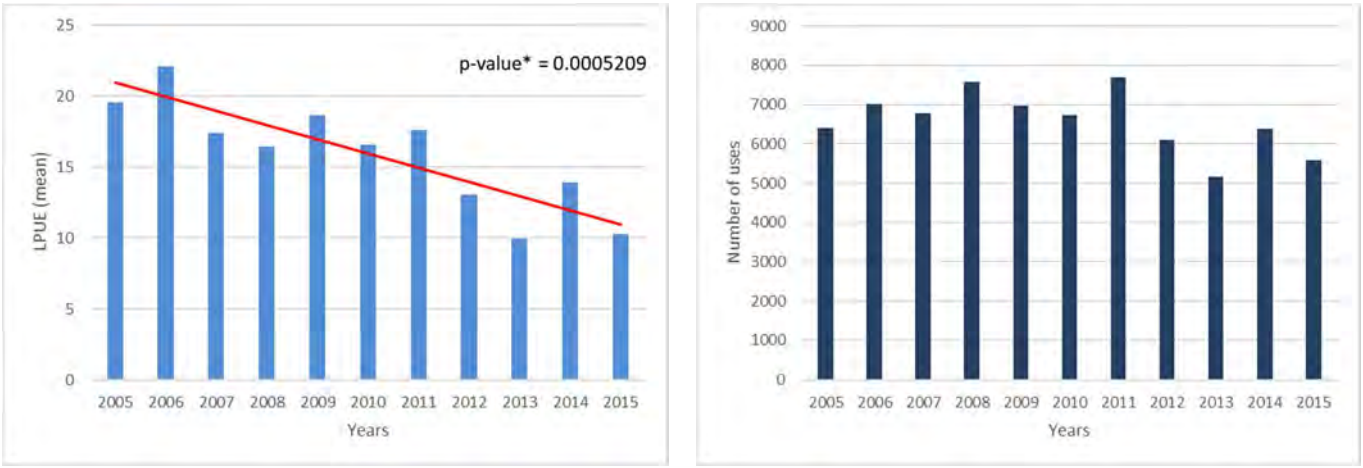

Figure 1: Levels of LPUE and number of uses - Bottom otter trawls - Cluster 1 - Mesh class 70 - 79 mm - Annual – Bay of Biscay

Gear "GNS"

For each of the combinations mesh / quarter of cluster 2 - GNS, the evolutions of their use over time and of their LPUEs for the entire Bay of Biscay were considered.

Gear meshes 50 - 59 mm and 60 - 69 mm have their use levels of gear that decrease significantly for the second quarter (Figures 2 and 4). For the gear mesh 60 - 69 mm, this decrease is in conjunction with a significant decrease of the LPUEs over the period. For the other couples of gear mesh classes / quarter, the number of uses and the LPUEs seem to decrease but it is not significant (Figures 3 and 5).

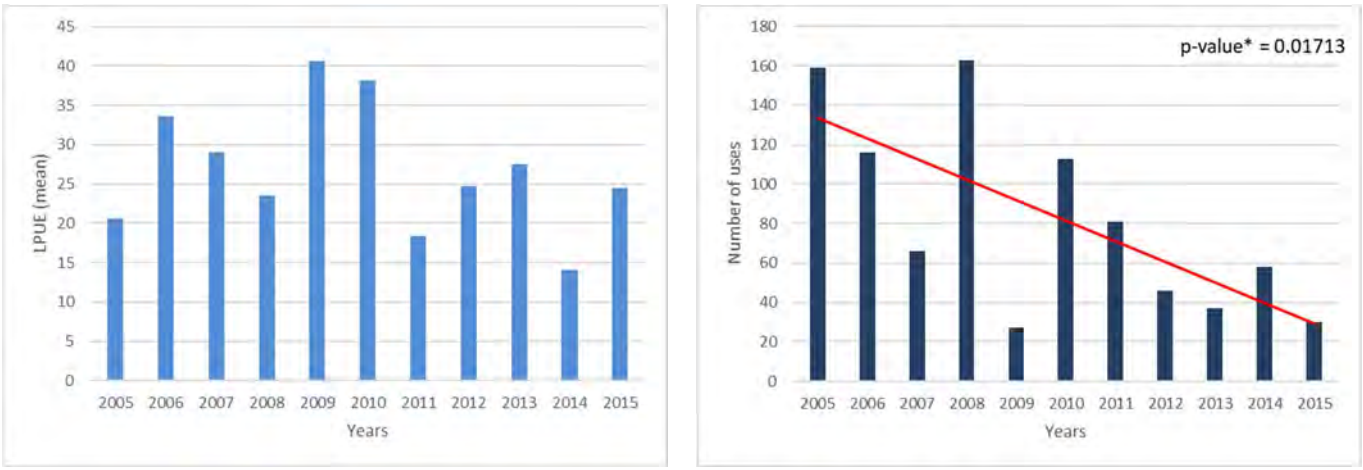

Figure 2: Levels of LPUE and number of uses - Set gillnets - Cluster 2 - Mesh class 50 - 59 mm - Quarter 2 – Bay of Biscay

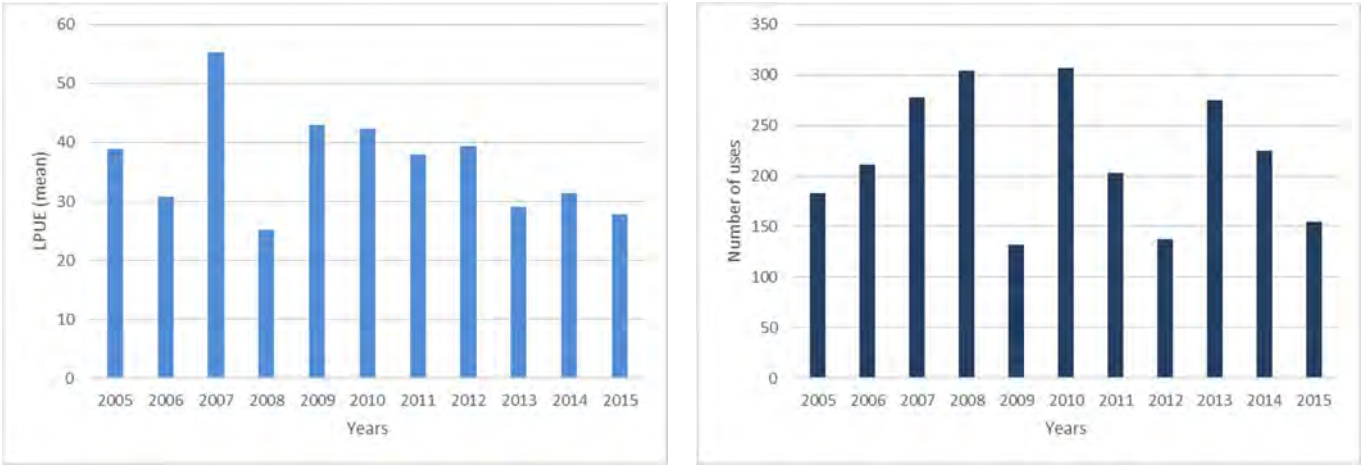

Figure 3: Levels of LPUE and number of uses - Set gillnets - Cluster 2 - Mesh class 50 - 59 mm - Quarter 3 – Bay of Biscay

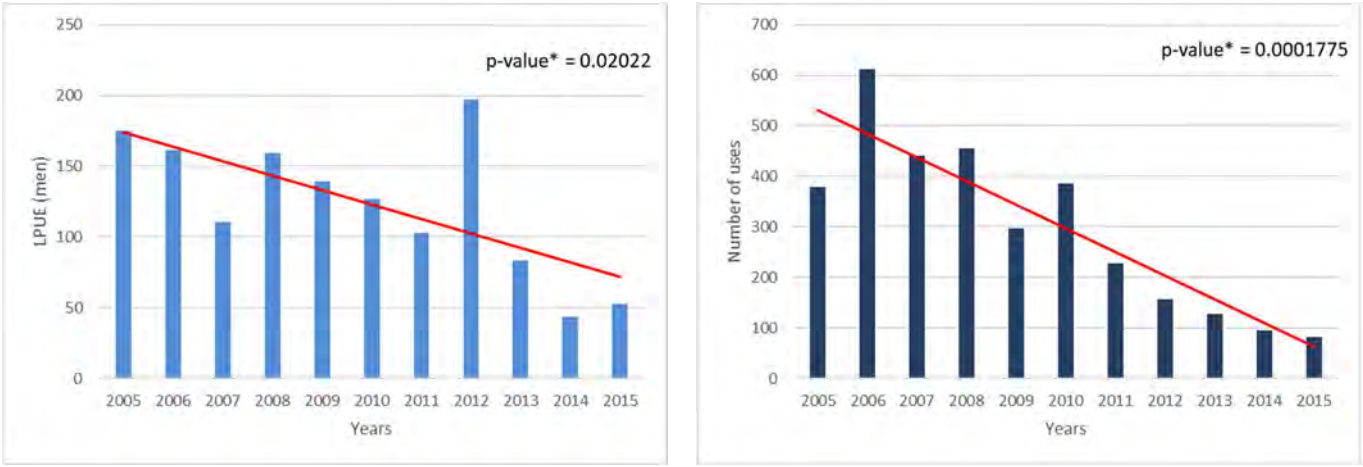

Figure 4: Levels of LPUE and number of uses - Set gillnets - Cluster 2 - Mesh class 60 - 69 mm - Quarter 2 – Bay of Biscay

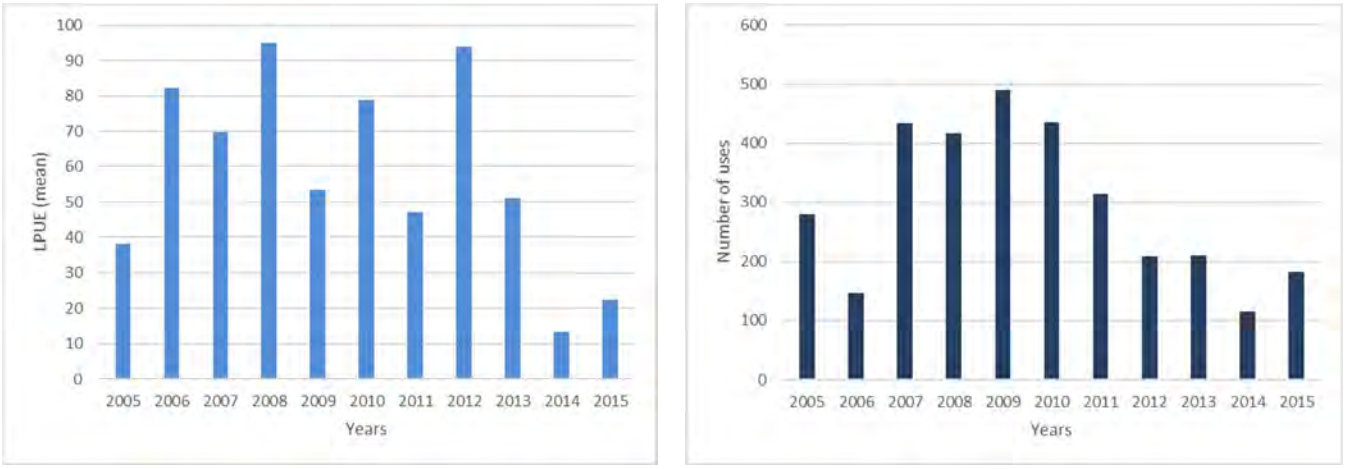

Figure 5: Levels of LPUE and number of uses - Set gillnets - Cluster 2 - Mesh class higher than 90 mm - Quarter 2 – Bay of Biscay

Method used to update the abundance indices from professional fishing data

The proposed method allows an update of the LPUEs of the selected fleets after 2015. It requires the assignment of new vessels in one of the clusters defined in the project beforehand. This is to be done at the level of the selected gear for the species (*i.e.* OTB and GNS for striped red mullet).

Clusters are the result of a hierarchical classification of vessels based on their technical characteristics (length, tonnage and engine power). The vessels were grouped according to their degree of similarity for these three variables using Hierarchical Aggregation Clustering (HAC) with Ward aggregation criterion and Euclidean distance.

When grouping with a clustering method such as the above one, it is difficult to identify clearly the bounds allowing to affect one vessel in a specified cluster (because of possible overlaps of some of the characteristics from one cluster to another). A method of assigning vessels was therefore developed for the selected gear.

To do this, conditional decision trees were built for each selected gear (OTB and GNS for striped red mullet). In each case, the targeted variable was the variable “cluster”. Based on the existing classification, each decision tree provides the rules fixing the values that must take the different technical variables for a vessel to belong to a given cluster for a given gear. The leaves (of the tree) not selected are either because they do not concern the targeted cluster or because the risk of classification error is considered too high.

Once this step has been completed, updating of the data (number of uses of the selected gears and average levels of LPUE) was carried out. It concerned the years 2016, 2017 and 2018. This update was sent to the professional structures involved in the former "CPUE Working Group" of the Romeligo project. The objective was to identify regulatory or other elements that could potentially disturb the LPUE index constructed for 2016, 2017 and 2018.

Results

Decision criteria for the assignment of new vessels appearing in 2016, 2017 or 2018

Regarding striped red mullet and for OTB, the retained tree (Fig. 6) is the one which setting minimizes the prediction error for cluster 1 and for all the data (cluster 1 prediction error: 0.4%; total prediction error: 1.1%).

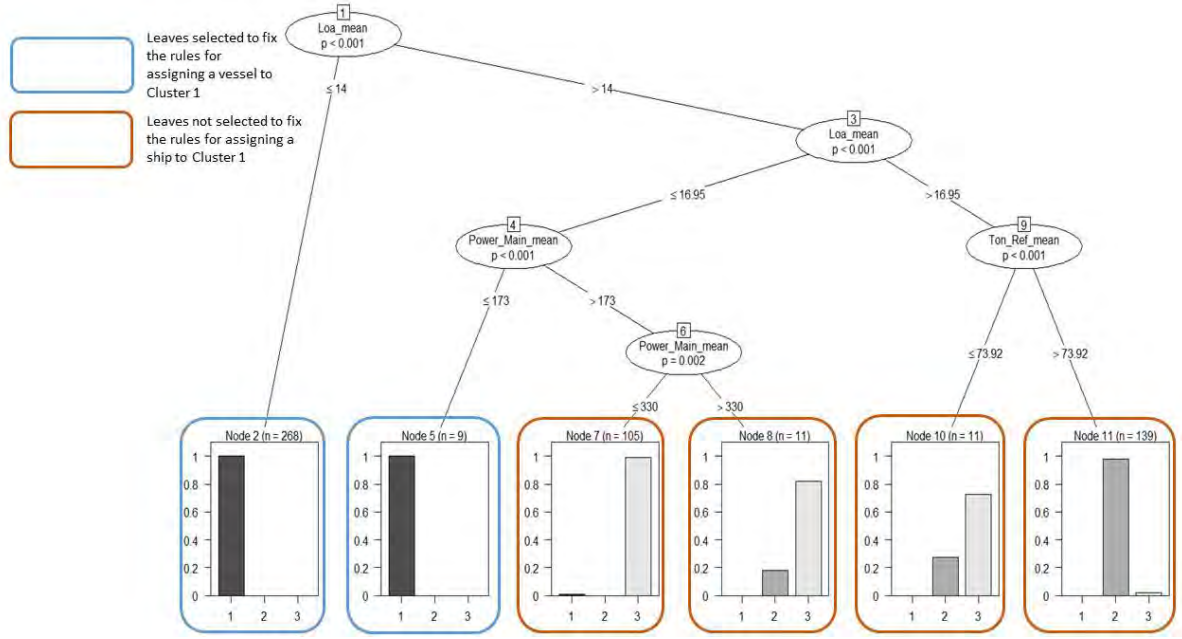

Figure 6: Conditional regression tree on cluster 1 variable (for striped red mullet / OTB) with technical characteristics [Loa: Length (m); Ton_Ref: tonnage (grt); Power_Main: engine power (kW)].

Consequently, a vessel falls into the cluster 1 if:

• Its length is less or equal to 14 m;

• Or if its length is greater than 14 m and less than 16.95 m with an engine power less or equal to 173 kW.

Regarding striped red mullet and for GNS, the retained tree (Fig. 7) is the one which setting minimizes the prediction error for cluster 2 and for all the data (cluster 2 prediction error: 0.8%; total prediction error: 1.3%).

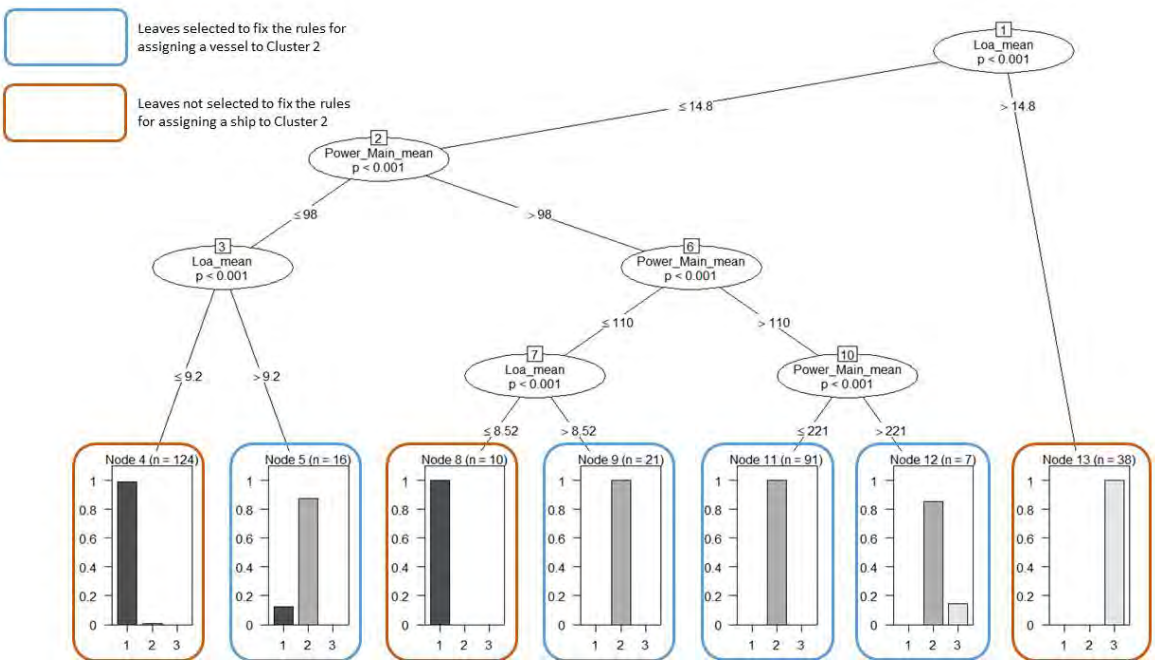

Figure 7: Conditional regression tree on cluster 2 variable (for striped red mullet / GNS) with technical characteristics [Loa: Length (m); Ton_Ref: tonnage (grt); Power_Main: engine power(kW)].

Consequently, a vessel falls into the cluster 2 if its length is less than 14.8 m and:

• If its engine power is less or equal to 98 kW and its length greater than 9.2 m;

• Or if its engine power is greater than 98 kW and lower than 100 kW with a length greater than 8.52 m;

• Or if its engine power is greater than 110 kW.

Update of data and evolution of the indices

For OTB

The evolution of the number of uses and of the mean level of LPUE are shown for the entire year and the whole Bay of Biscay (Figure 8).

Figure 8: Numbers of uses and levels of LPUE - Bottom otter trawls - Cluster 1 - Mesh class 70 - 79 mm – Annual – Bay of Biscay

The number of uses shows little variation during the period. In recent years, the LPUEs calculated for the Bay of Biscay show low levels which remain low compared to the whole series. The end of the series seems to be marked by an upward recovery which will remain to be confirmed in the following years.

For GNS

The evolution of the number of uses and of the mean level of LPUE for each couples of gear mesh classes / quarter are shown for the selected quarters and for the whole Bay of Biscay (Figures 9 to 12).

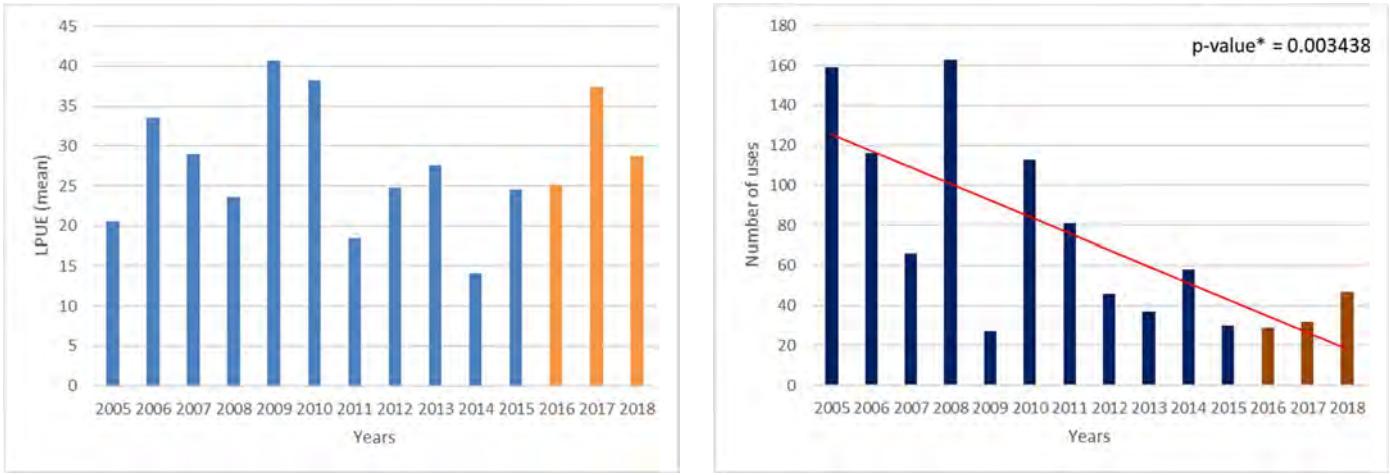

Figure 9: Numbers of uses and levels of LPUE - Set gillnets - Cluster 2 - Mesh class 50 - 59 mm – Quarter 2 – Bay of Biscay

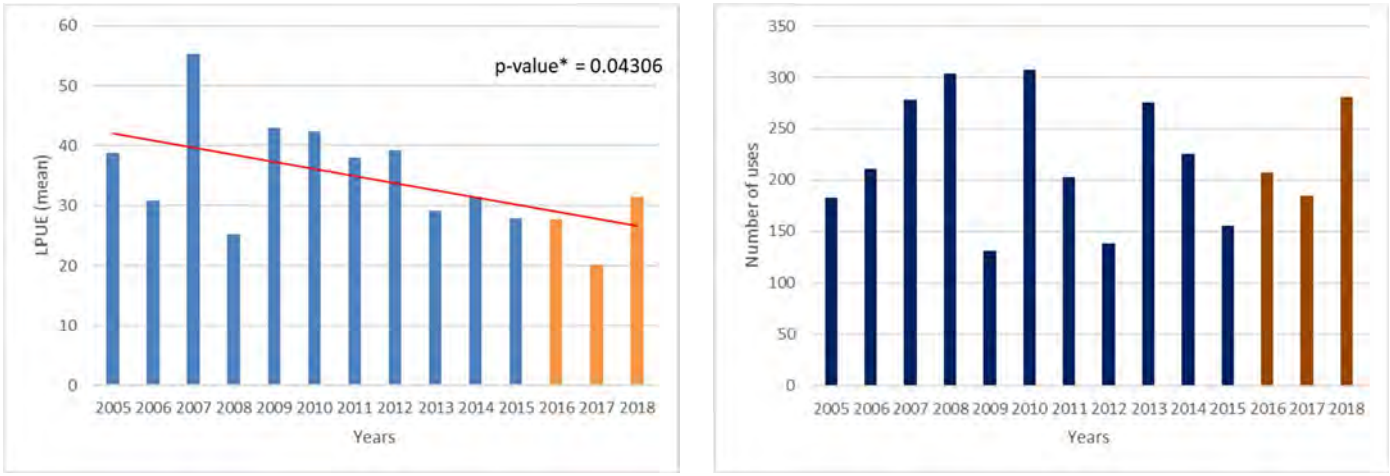

Figure 10: Numbers of uses and levels of LPUE - Set gillnets - Cluster 2 - Mesh class 50 - 59 mm – Quarter 3 – Bay of Biscay

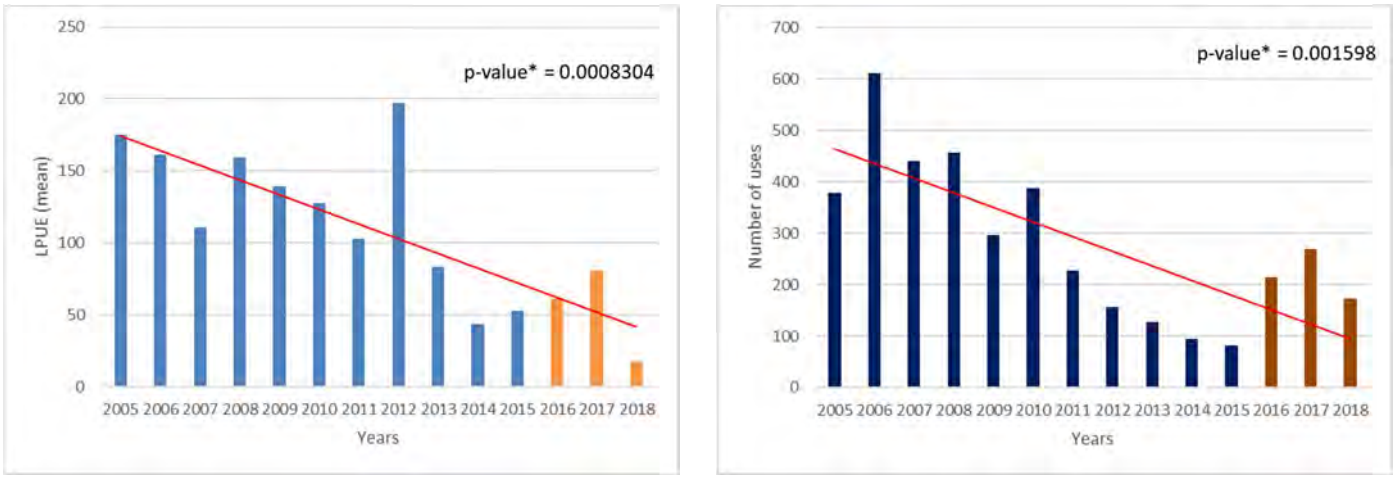

Figure 11: Numbers of uses and levels of LPUE - Set gillnets - Cluster 2 - Mesh class 60 - 69 mm – Quarter 2 – Bay of Biscay

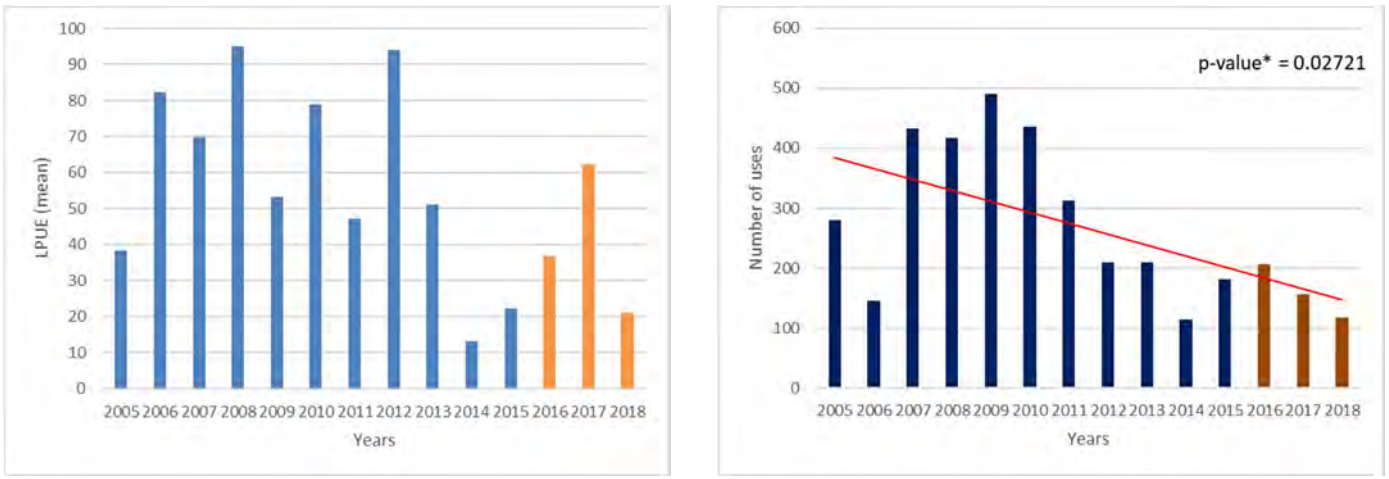

Figure 12: Numbers of uses and levels of LPUE - Set gillnets - Cluster 2 - Mesh class higher than 90 mm – Quarter 2 – Bay of Biscay

Over the whole period, a downward trend is observed in three out of four cases for the number of fishing sequences and in two out of four cases for the average LPUE.

In recent years, only LPUEs for the 50-59 mm class in the second quarter have shown high levels compared to the rest of the series, but for a low number of sequences. The LPUE level for the 60-69 mm mesh class in the second quarter was particularly low in 2018.

Information from the consultation of professional structures

For OTB

The consultation identified one regulatory element that could potentially have disturbed the LPUE indices built for 2016, 2017 and 2018: the decree concerning trawlers over 12 m which have a European Fishing Authorization (EFA) to fish common sole in the Bay of Biscay[2].

The list of these vessels was not recovered. We only looked at the evolution of the number of fishing sequences by vessels over 12 m and their associated LPUE. This number of sequences is marked by a sharp drop in 2016 and remained at a low level in 2017 and 2018. It was accompanied by a drop in the average LPUE for these vessels (longer than 12 m), a drop already recorded before.

⇨ Considering all the available data and assuming that all things are equal, it is estimated that the levels of LPUE between 2016 and 2018 could have been impacted by the measurement management, but without changing the trend of the indicator.

For GNS

The consultation did not identify regulatory element that could potentially have disturbed the LPUE / GNS indices built for 2016, 2017 and 2018.

Conclusion

Currently five fleets are selected for the Bay of Biscay:

- OTB - Cluster 1 - Mesh size 70 - 79 mm - Annual - Bay of Biscay;
- GNS - Cluster 2 - Class mesh 50 - 59 mm - Quarter 2 - Bay of Biscay;
- GNS - Cluster 2 - Class mesh 50 - 59 mm - Quarter 3 - Bay of Biscay;
- GNS - Cluster 2 - Class mesh 60 - 69 mm - Quarter 2 - Bay of Biscay;
- GNS - Cluster 2 - Class mesh greater than 90 mm - Quarter 2 - Bay of Biscay.

For the GNS indicators, the number of uses decreases in three out of four cases, that concerning the mesh class 50 - 59 mm in the 2nd quarter reaching a very low level (around 40 sequences in 2018). It is proposed to no longer use this last indicator because we consider that it is no longer representative. For the others, more in-depth work should be able to be carried out in the project ACOST (submitted to the FFP call). At the same time, the interest of considering the Danish seine gear could be posed because the length of the series is now sufficient.

[2] Since January 1st, 2016, this decree imposes a mandatory minimum mesh size of 80 mm for the vessels concerned (having this authorization), out of derogation period from June 1st to September 30th each year. This latter period makes it possible to practice specific metiers (for example bottom trawls targeting wedge sole). This decree was modified at the end of 2018, with the possibility of shifting the derogation period of 4 consecutive months.

References

Caill-Milly N., Lissardy M., Léauté J.-P., 2017. Improvement of the fishery knowledge of striped red mullet of the Bay of Biscay. Working Document for the Working Group on Widely Distributed Stocks (WGWIDE). 30 August - 5 September 2017, Copenhagen (Denmark). https://archimer.ifremer.fr/doc/00399/51057/

Caill-Milly N., Lissardy M., Bru N., Dutertre M.-A., Saguet C., 2018. Reference fleets identification by LPUE data filtering applied to the striped red mullet (*Mullus surmulletus*) in the Bay of Biscay. Working Document for the Working Group on Widely Distributed Stocks (WGWIDE). 28 August - 3 September 2018, The Faroe Islands. https://w3.ifremer.fr/archimer/doc/00466/57750/

Caill-Milly N., Lissardy M., Bru N., Dutertre M.-A., Saguet C., 2019. A methodology based on data filtering to identify reference fleets to account for the abundance of fish species: Application to the Striped red mullet (*Mullus surmulletus*) in the Bay of Biscay. Continental Shelf Research, 183, 51-72. https://doi.org/10.1016/j.csr.2019.06.004

Léauté J.-P., Caill-Milly N., Lissardy M., Bru N., Dutertre M.-A., Saguet C., 2018. ROMELIGO. Amélioration des connaissances halieutiques du ROuget-barbet, du MErlan et du LIeu jaune du GOlfe de Gascogne. RBE/HGS/LRHLR et ODE/UL/LERAR/18-001. https://archimer.ifremer.fr/doc/00440/55126/

Sacrois versions used for the update: V.3.3.7 for the 2016 to 2017 data and V.3.3.8 for the 2018 data (extraction November 2019)

Working document 05, WGWIDE 2020

Overview of spatial distribution of catches of mackerel, horse mackerel, blue whiting and herring

Martin Pastoors, 31/08/2020

Abstract

An overview is presented of the catch per rectangle data that is available at WGWIDE 2020 for mackerel, horse mackerel, blue whiting and Atlanto-scandian herring.

Introduction

WGWIDE and its precursors WGMHSA and WGNPBW have been publishing catch per rectangle plots in their reports for many years already. Catch by rectangle has been compiled by WG members and generally provide a WG estimate of catch per rectangle. In most cases the information is availalble by quarter whereas most recently, the data has been requested by month. So far, the catch by rectangle has only been presented for one single year in the WG reports. Here, we collated all the catch by rectangle data that is available for herring, blue whiting, mackerel and horse mackerel for as many years as available.

Results

An overview of the available catches by rectangle, species and year is shown in the text table below. For horse mackerel and mackerel, a long time series is available, starting in 2001 (HOM) and 1998 (MAC). The time series for herring and blue whiting are shorter (starting in 2011) although additional information could be derived from earlier WG reports.

species	1998	1999	2000	2001	2002	2003	2004	2005	2006	2007
HOM	.	.	.	242971	220889	226642	204409	218002	182172	162691
MAC	634501	573960	614831	664986	648890	568184	579449	505956	447288	550033

species	2008	2009	2010	2011	2012	2013	2014	2015	2016	2017
HER	.	.	.	993001	819755	684723	461383	328679	383081	715545
HOM	111071	261563	252455	211305	181505	220870	141685	108136	113592	122009
MAC	584410	713180	861394	936099	874986	920066	1374495	1166138	1083641	1151726
WHB	.	.	.	103861	377079	616511	1139737	1389447	1175687	1540077

species	2018	2019
HER	592555	776193
HOM	118276	144149
MAC	1016924	831564
WHB	1698078	1507471

For each species an overview table is presented of catch by country and year and a figure with catch by rectangle and year. Catches by rectangle have been grouped in logarithmic classes (1-10, 10-100 etc).

Discussion

While the aggregation and presentation of the catch per rectangle data for mackerel, horse mackerel, blue whiting and atlanto-scandian herring does not constitute rocket-science, it does provide us with meaningful insights into the changes of catching areas over time. This could be relevant also in understanding the impacts of climate change on fisheries and in relating changes in the distribution of prey or predator species (e.g. bluefin tuna). As such, these graphical representations of catching areas provide a useful addition to the WG report.

One important check that still needs to be carried out is the check on data availability by country and year that may not be consistent over the time series. Making the time-series complete would improve the useability of the information.

Mackerel

country	1998	1999	2000	2001	2002	2003	2004	2005	2006	2007
DEU	21490	19956	22977	25323	26532	24059	23368	19123	16599	18221
DNK	28157	30208	32693	31133	32180	27198	25311	22921	24230	24877
ESP	44607	45914	38320	44143	31845	23858	34968	53192	54569	63235
FRA	.	.	.	.	.	.	.	.	15968	14997
FRO	11229	11620	21023	24004	19768	14014	13029	9769	12066	13393
GBR	179710	159321	164069	189809	191100	170575	174728	152702	95816	133686
IRL	69171	59578	71226	70443	72173	63588	58929	42530	38563	46675
ISL	.	.	.	.	.	.	.	.	4220	36496
NLD	46127	28070	32403	49815	42254	34263	35680	41432	24007	23912
NOR	158179	160728	174098	180595	184291	163404	157363	119680	121981	131697
POL	.	.	.	.	.	.	.	.	.	977
PRT	2846	1981	2253	3049	2934	2749	2143	1479	2591	2598
RUS	67837	51348	50772	41568	45811	40026	49489	39922	33462	35408
SWE	5146	5233	4995	5099	.	4447	4437	3202	3210	3858
(ALL)	634499	573957	614829	664981	648888	568181	579445	505952	447282	550030

country	2008	2009	2010	2011	2012	2013	2014	2015	2016	2017
BEL	.	.	.	.	38	60	.	51	142	128
BES	.	.	.	.	.	.	10509	.	8165	.
DEU	15503	22703	19055	24082	18974	20933	28451	28207	23411	24857
DNK	26726	23228	41045	29213	36503	33261	41903	45015	40655	37899
ESP	64785	114141	53350	23988	17735	13069	33734	33744	21426	34425
EST	.	.	.	.	.	1366	.	.	.	.
FRA	15454	9740	12108	12393	17859	14642	21695	.	20171	22920
FRO	11289	14061	70987	122049	107629	143001	150419	107993	93266	99499
GBR	113945	157012	160419	181629	169733	163303	287418	246962	216819	225404
GRL	.	.	.	162	5319	52796	78672	30410	36194	46498
GUY	.	.	.	.	.	8	8	4	.	.
IMN	.	.	.	11	.	7	3	4	7	.
IRL	44318	61086	57993	63188	63058	56611	103178	88738	76523	84914
ISL	112220	116157	122337	159008	149584	151326	172960	169257	170374	166601
JEY	7	7	.	6	.	.	6	2	2	.
LTU	.	.	.	.	.	.	.	553	2539	.
NLD	19933	23355	25062	34500	32554	21159	46665	39807	37752	43765
NOR	121470	121225	233941	208077	176031	164602	277724	242233	210569	222397
POL	.	.	.	.	.	.	.	.	0	0
PRT	2367	1742	2355	938	821	253	636	928	619	633
RUS	32728	41413	59310	73601	74578	80756	116086	128292	121336	138077
SWE	3660	7303	3428	3247	4563	2906	4421	3930	3662	3700
(ALL)	584405	713173	861390	936092	874979	920059	1374488	1166130	1083632	1151717

country	2018	2019
BEL	167	66
DEU	19882	16904
DNK	29865	30401
ESP	28196	21056
FRA	21370	17855
FRO	81078	62663
GBR	189999	151803
GRL	63024	30469
IMN	3	2
IRL	66743	53311
ISL	168328	128076
NLD	30392	22697
NOR	187030	159107

POL	4056	3706
PRT	4564	3941
RUS	118254	126543
SWE	3965	2957
(ALL)	1016916	831557

Table 1: Catch of mackerel (tonnes) included in the rectangle data by year and country

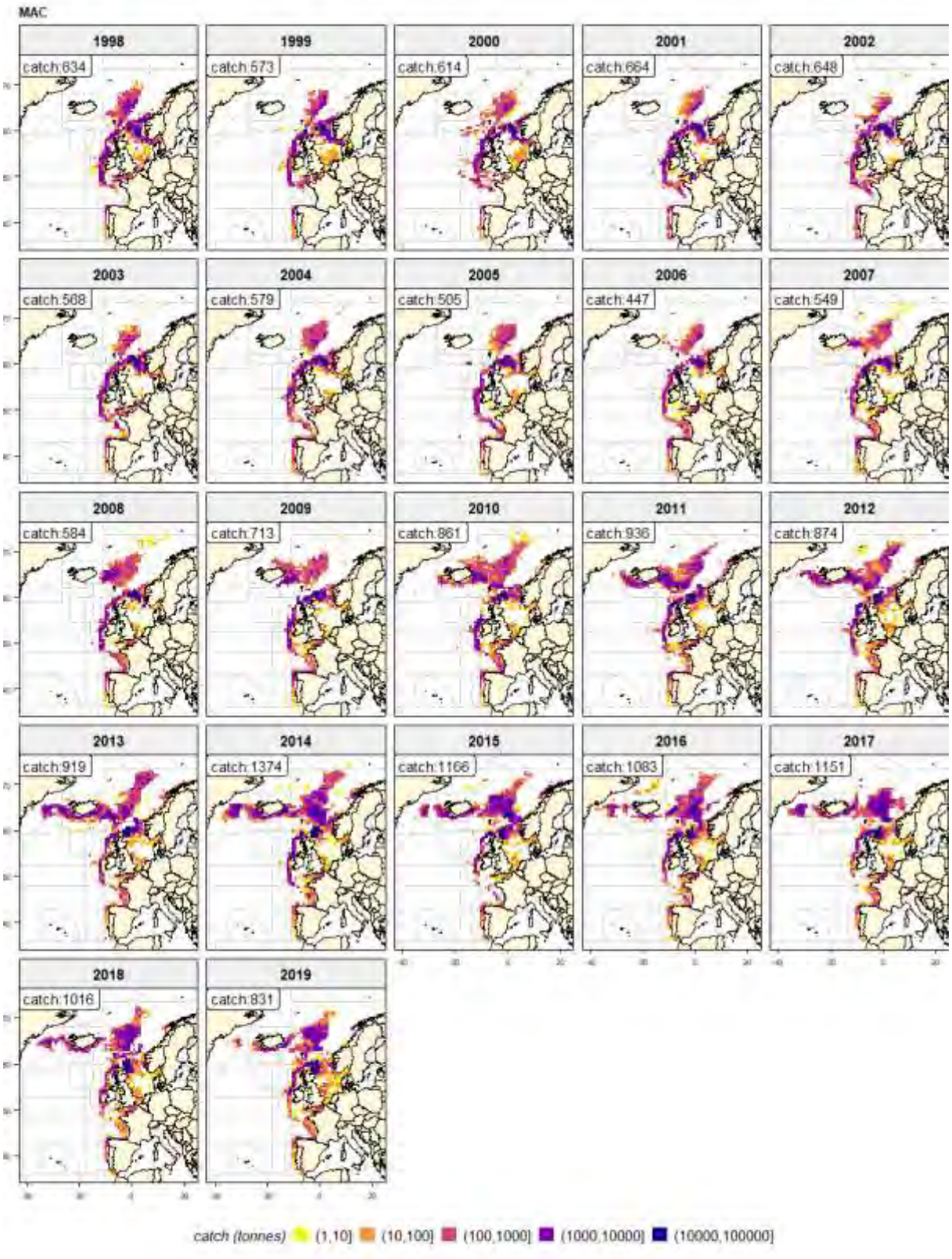
MAC
1998
catch:634
1999
catch:573
2000
catch:614
2001
catch:664
2002
catch:648
2003
catch:568
2004
catch:579
2005
catch:505
2006
catch:447
2007
catch:549
2008
catch:584
2009
catch:713
2010
catch:861
2011
catch:936
2012
catch:874
2013
catch:919
2014
catch:1374
2015
catch:1166
2016
catch:1083
2017
catch:1151
2018
catch:1016
2019
catch:831
catch (tonnes) (1,10] (10,100] (100,1000] (1000,10000] (10000,100000]

Figure 1.1: Catch of mackerel (tonnes) by year and rectangle. Catch by rectangle data do not represent the official catches and cannot be used for management purposes. In general, the total annual catches by rectangle are within 10 % from the official catches.

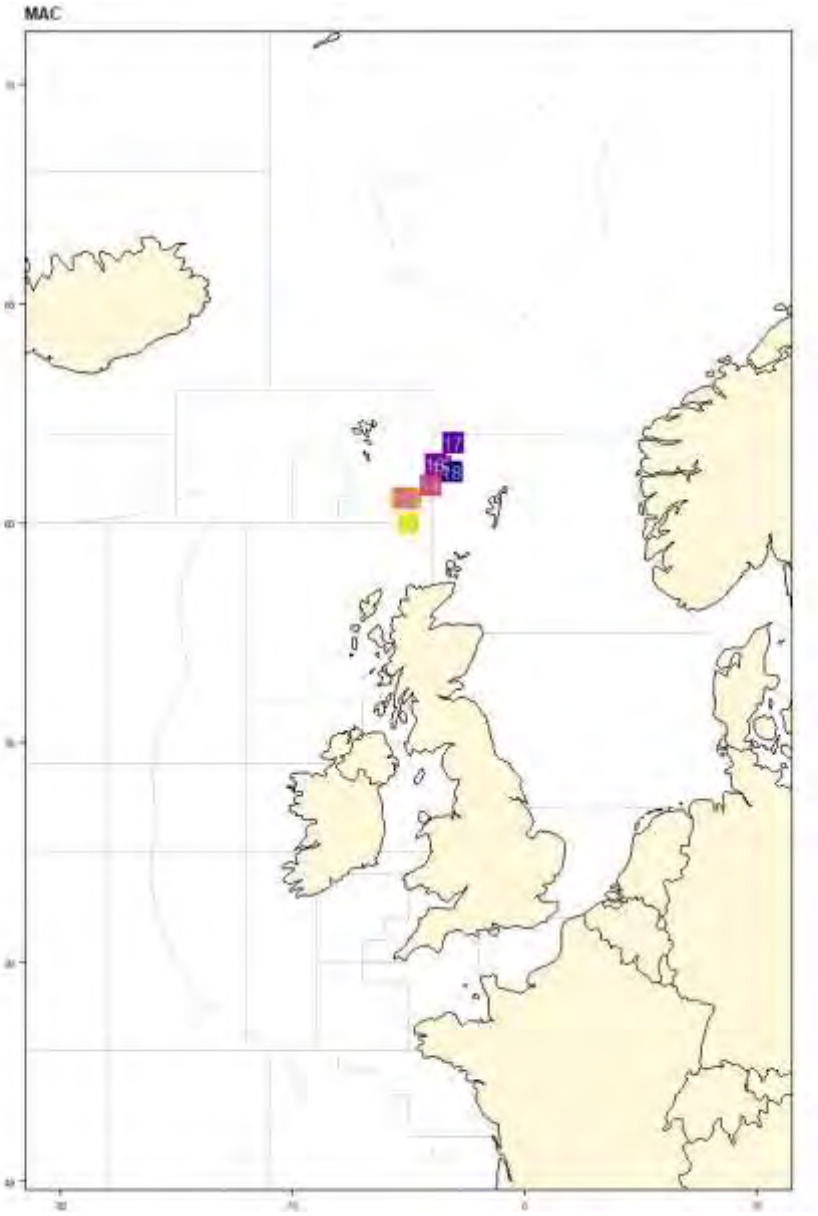

Figure 1.2: Centre of gravity of mackerel catches by year. Only latitudes between 46 and 70 have been used for the calculations.

Horse Mackerel

country	2001	2002	2003	2004	2005	2006	2007	2008	2009	2010
DEU	12510	15925	18762	22792	18978	12453	5871	12882	16420	21482
DNK	.	12478	14636	20256	14135	9794	7885	.	6097	5935
ESP	34688	34258	32926	27947	26435	23829	27319	34169	36722	54230
FRO	.	.	808	3846	3695	.	477	477	.	.
GBR	18459	11201	6405	11775	7845	993	13807	5508	17627	17063
IRL	52212	36482	35854	26432	35359	28856	30091	36508	40779	44475
NLD	103349	59585	86162	68733	73130	64413	61433	.	60459	85042
NOR	7992	36689	20515	10749	25115	27225	5425	12247	72615	12500
PRT	13759	14269	10571	11874	13307	14607	10380	9278	10840	11726
(ALL)	242969	220887	226639	204404	217999	182170	162688	111069	261559	252453

country	2011	2012	2013	2014	2015	2016	2017	2018	2019
BEL	.	.	.	.	63	.	67	44	.
DEU	21114	22588	27959	19056	10061	13293	8121	8121	8462
DNK	6100	4674	.	.	.	.	.	.	.
ESP	32942	12373	39507	32907	37896	32851	33860	37109	44473
FRA	.	.	.	.	.	.	5785	3443	1869
FRO	.	.	.	.	.	.	50	.	.
GBR	26932	14631	48307	12426	737	970	.	190	9666
IRL	38464	45306	35783	32660	21647	27606	23559	25347	28899
NLD	71981	78552	62519	29975	28150	27685	19906	19906	31862
NOR	13770	3378	6791	14658	9560	11184	11184	10742	11274
PRT	.	.	.	.	.	.	19473	13370	7641
SWE	.	.	1	1	18	.	.	.	.
(ALL)	211303	181502	220867	141683	108132	113589	122005	118272	144146

Table 2: Catch of horse mackerel (tonnes) included in the rectangle data by year and country

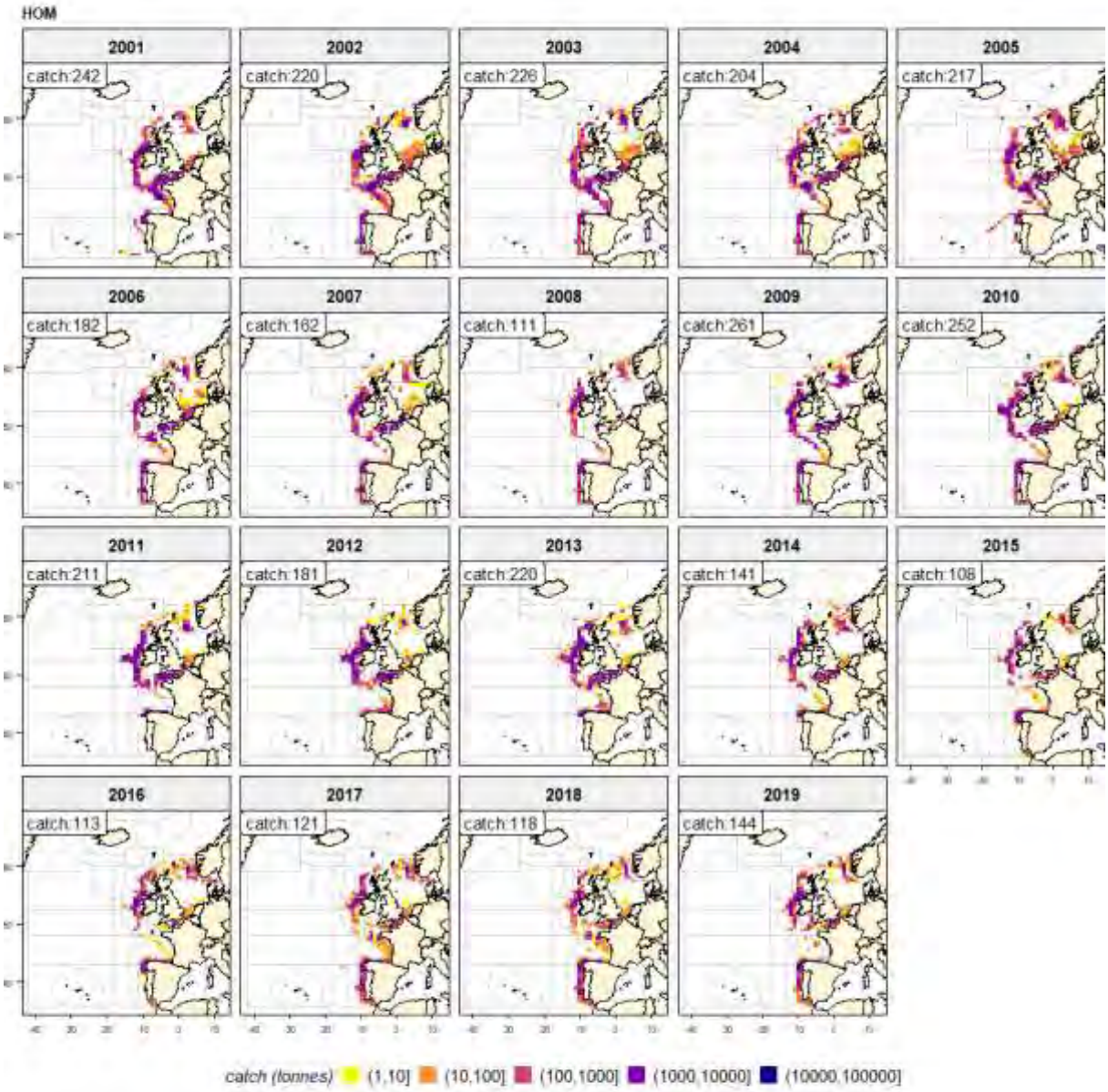
HOM
2001
catch:242
2002
catch:220
2003
catch:226
2004
catch:204
2005
catch:217
2006
catch:182
2007
catch:162
2008
catch:111
2009
catch:261
2010
catch:252
2011
catch:211
2012
catch:181
2013
catch:220
2014
catch:141
2015
catch:108
2016
catch:113
2017
catch:121
2018
catch:118
2019
catch:144
catch (tonnes)
(1,10]
(10,100]
(100,1000]
(1000,10000]
(10000,100000]

Figure 2.1: Catch of horse mackerel (tonnes) by year and rectangle. Catch by rectangle data do not represent the official catches and cannot be used for management purposes. In general, the total annual catches by rectangle are within 10 % from the official catches.

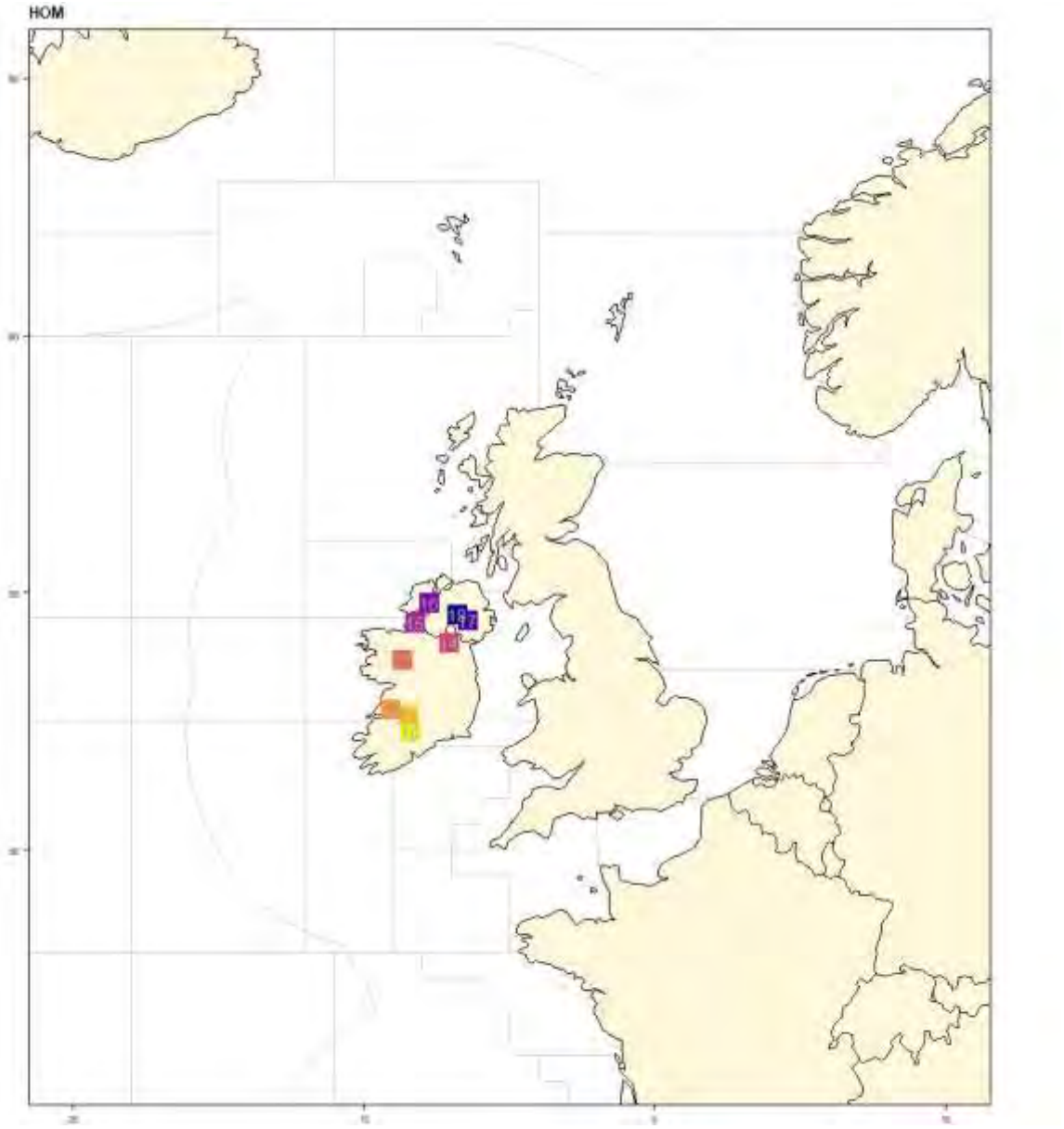

Figure 2.2: Centre of gravity of horse mackerel catches by year. Only latitudes between 46 and 65 have been used for the calculations.

Blue whiting

country	2011	2012	2013	2014	2015	2016	2017	2018	2019
ALL	.	377079	.	.	.	.	.	.	.
DEU	266	.	11528	24487	24106	20024	45555	47797	38243
DNK	.	.	.	27945	45047	39134	60866	83564	64169
ESP	2416	.	13388	25140	24967	27493	27433	21059	20621
FRA	4337	.	8978	10410	9657	10345	13221	16409	16095
FRO	16404	.	85767	224699	282477	282364	356501	349837	336568
GBR	1331	.	8166	26835	30508	38270	68132	68375	60757
GRL	.	.	.	.	.	.	20212	23333	19753
IRL	1194	.	13205	21467	24785	26329	43237	49902	38568
ISL	5887	.	104912	182873	214868	186907	228934	292951	268351
LTU	.	.	.	4718	.	1129	5299	.	.
NLD	4595	.	51634	38524	56397	58148	81155	121864	75020
NOR	20539	.	196246	399520	489438	310412	399363	438426	351428
POL	.	.	.	.	.	.	.	12152	27184
PRT	.	.	2014	1303	1429	1429	1625	1497	2659
RUS	46888	.	120669	151810	185763	173655	188449	170891	188006
SWE	.	.	.	1	.	42	89	15	43
(ALL)	103857	377079	616507	1139732	1389442	1175681	1540071	1698072	1507465

Table 3: Catch of blue whiting (tonnes) included in the rectangle data by year and country

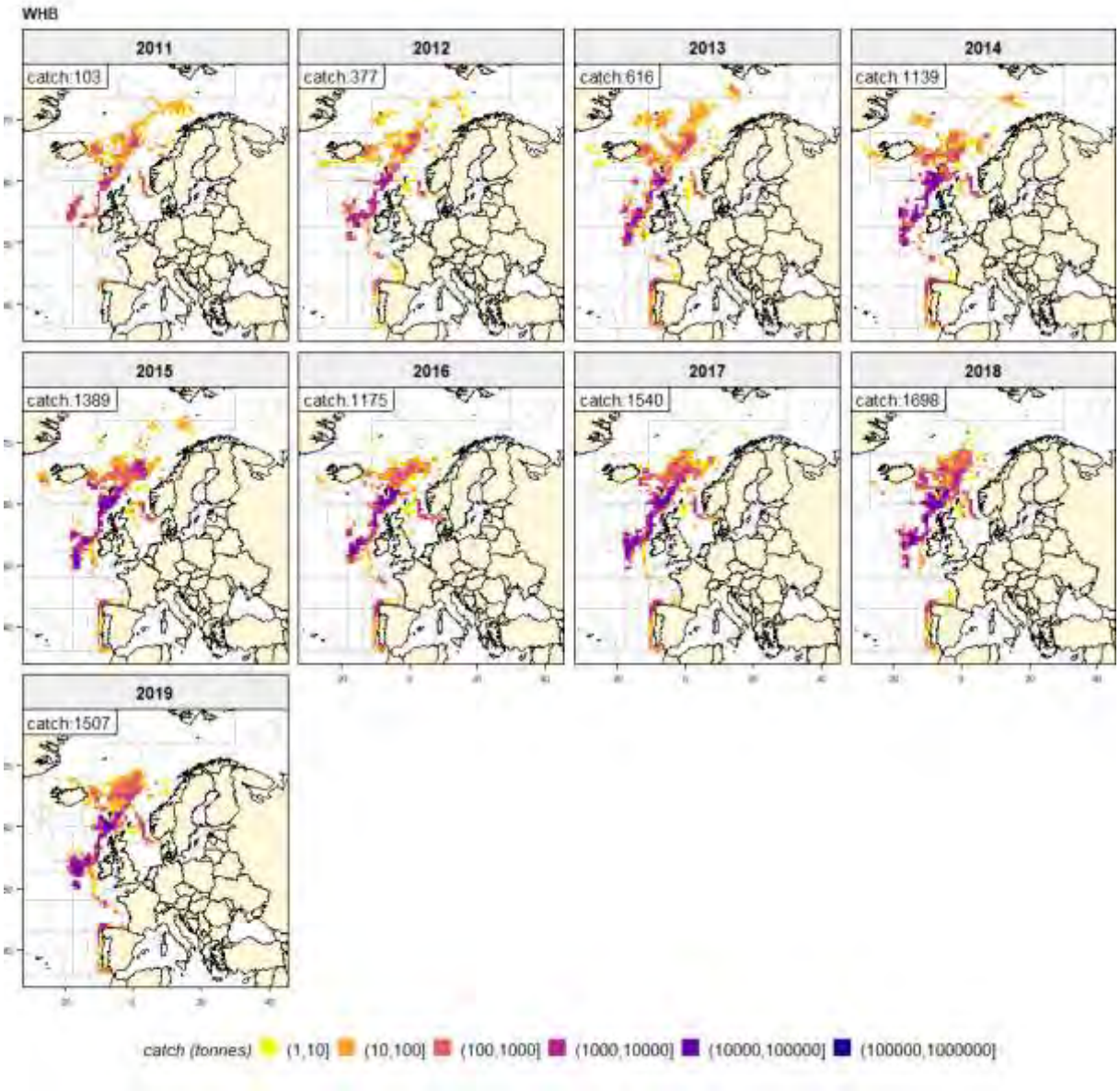

Figure 3.1: Catch of blue whiting (tonnes) by year and rectangle. Catch by rectangle data do not represent the official catches and cannot be used for management purposes. In general, the total annual catches by rectangle are within 10 % from the official catches.

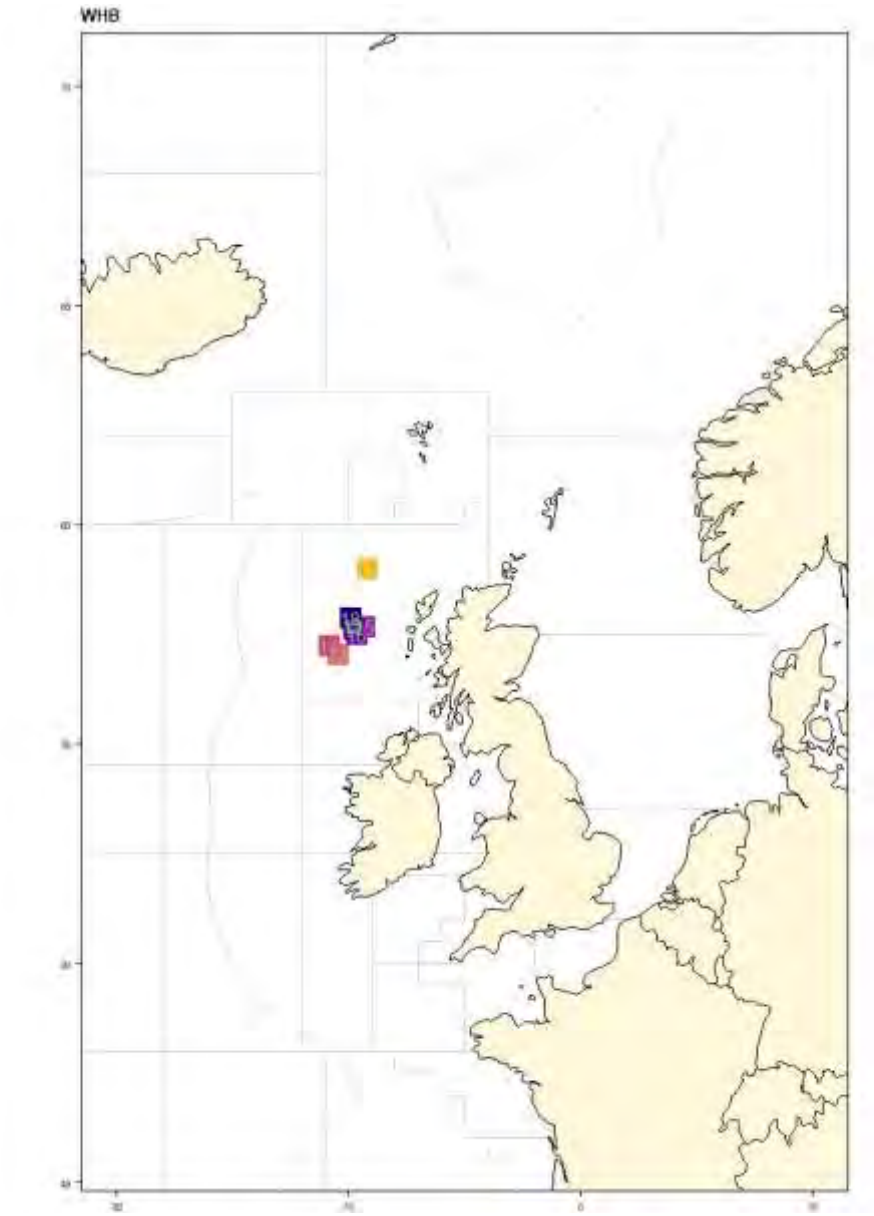

Figure 3.2: Centre of gravity of blue whiting catches by year. Only latitudes between 46 and 70 have been used for the calculations.

Atlanto-scandian herring

country	2011	2012	2013	2014	2015	2016	2017	2018	2019
ALL	.	819755	.	.	.	.	.	.	.
DEU	13295	.	4243	668	2660	2582	5201	1994	4188
DNK	26732	.	17159	12513	9105	10384	17373	17051	20247
FRO	53270	.	105037	38527	33030	44726	98170	82062	113940
GBR	14045	.	8342	4233	.	3899	.	2581	1800
GRL	3426	.	11787	13187	12434	17507	12569	2465	3190
IRL	5738	.	3814	705	1399	2048	3494	2428	2775
ISL	151078	.	90729	58827	42626	50457	90400	83392	108044
NLD	8348	.	5625	9175	5248	3519	6678	4289	5110
NOR	572637	.	359458	263252	176321	197500	389383	331717	430501
POL	.	.	.	.	.	.	.	.	1327
RUS	144429	.	78501	60291	45853	50454	91119	64147	84362
SWE	.	.	23	.	.	.	1155	425	705
(ALL)	992998	819755	684718	461378	328676	383076	715542	592551	776189

Table 4: Catch of Atlanto-scandian herring (tonnes) included in the rectangle data by year and country

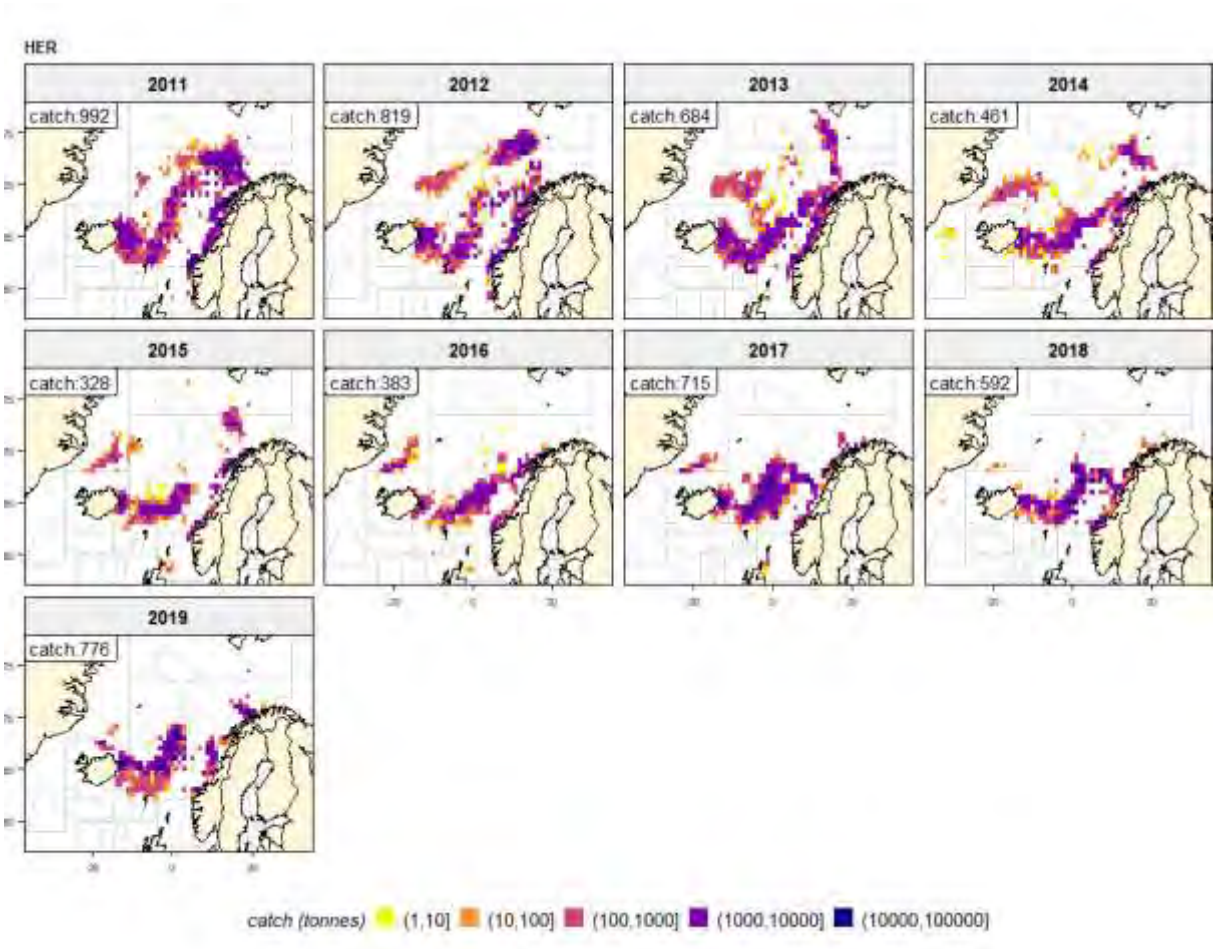

Figure 4.1: Catch of Atlanto-scandian herring (tonnes) by year and rectangle. Catch by rectangle data do not represent the official catches and cannot be used for management purposes. In general, the total annual catches by rectangle are within 10 % from the official catches.

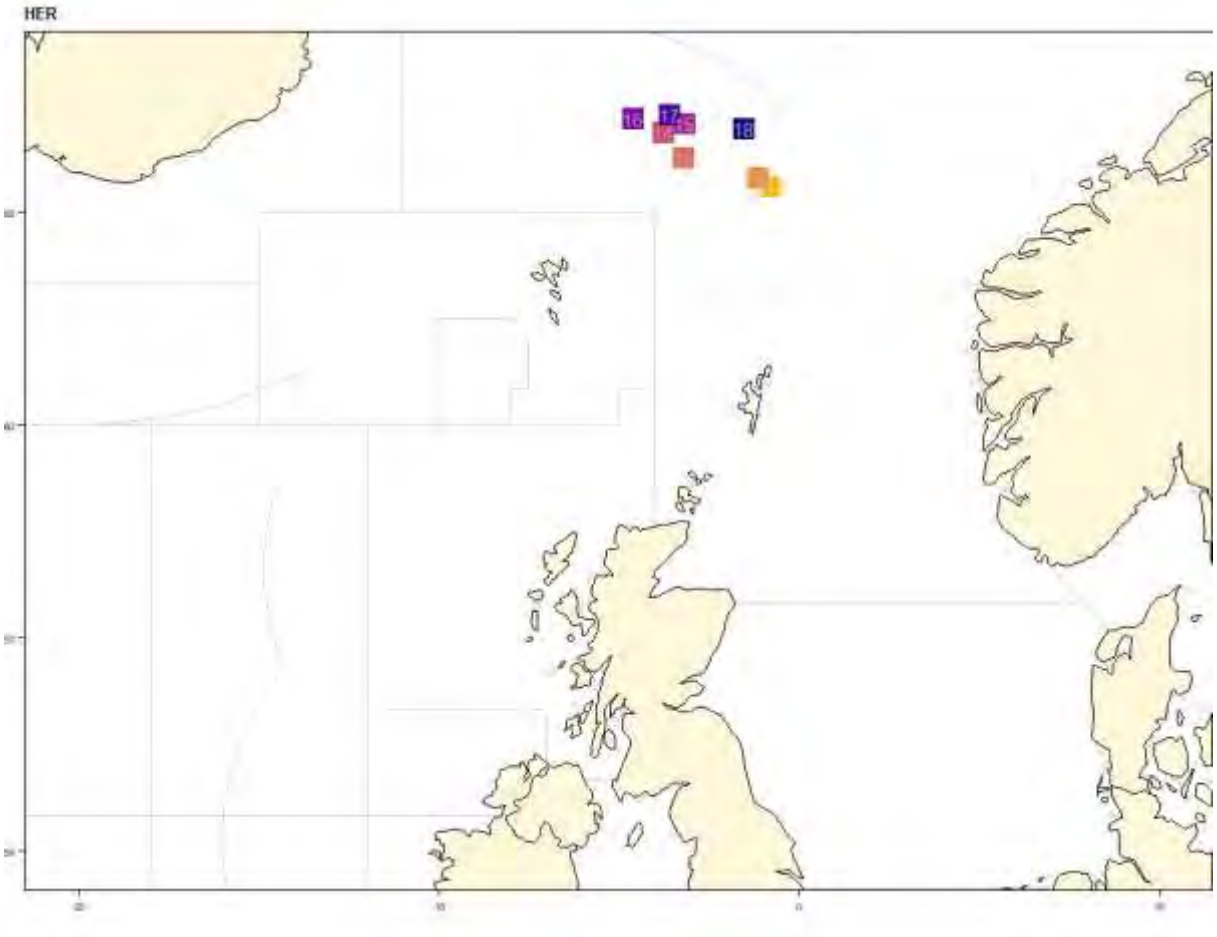

Figure 1.2: Centre of gravity of herring catches by year.

Survey report

MS *Eros*, MS *Kings Bay* MS *Vendla* 14.-26.02.2020

Distribution and abundance of Norwegian spring-spawning herring during the spawning season in 2020

By Are Salthaug, Erling Kåre Stenevik, Sindre Vatnehol, Valantine Anthonypillai, Egil Ona and Aril Slotte

Institute of Marine Research (IMR), P. O. Box 1870 Nordnes, N-5817 Bergen, Norway

Summary

During the period 14-26th of February 2020 the spawning grounds of Norwegian spring-spawning herring from Møre (62º20´N) to Nordvestbanken (70º40´N) were covered acoustically by the commercial vessels MS *Eros*, MS *Kings Bay* and MS *Vendla.* The survey was carried out under challenging weather conditions, however, the collected acoustic and biological data are considered to be of good quality. The estimated biomass was around 24 % lower and the estimated total number was about 10 % lower this year than in the 2019 survey. The uncertainty of the estimate in 2020 was estimated to be higher compared with 2019. The surveyed population was dominated by the 2013 and 2016 year classes. The 2016 year class is estimated to be around three times more abundant than the 2013 year class was as 4 year olds in 2017 (in this survey). The spatial distribution of the spawning stock was similar to earlier years; close to the coast south of Træna and on the slope around the banks outside Lofoten and Vesterålen, with the youngest and smallest herring in the north and older and larger herring in the south. The estimates of relative abundance from the survey in 2020 are recommended to be used in this year's ICES stock assessment of Norwegian spring-spawning herring.

Survey participants 14-26.02.2019:

MS *Eros*	
Erling Kåre Stenevik	Survey leader
Lage Drivenes	Instrument/Acoustics
Guosong Zhang	Instrument /Acoustics
Inger Henriksen	Biology
Jostein Røttingen	Biology
Egil Ona	Head of acoustics
MS *Kings Bay*	
Sindre Vatnehol	Survey leader
Reidar Johannesen	Instrument/Acoustics
Sture Vatnehol	Instrument/Acoustics
Adam Custer	Biology
Ørjan Sørensen	Biology
MS *Vendla*	
Are Salthaug	Survey coordinator
Benjamin Marum	Instrument/Acoustics
Magnar Polden	Instrument/Acoustics
Valantine Anthonypillai	Biology
Justine Diaz	Biology

Introduction

Acoustic surveys on Norwegian spring-spawning herring during the spawning season has been carried out regularly since 1988, with some breaks (in 1992-1993, 1997, 2001-2004 and 2009-2014). In 2015 the survey was initiated again partly based on the feedback from fishermen and fishermen's organizations that IMR should conduct more surveys on this commercially important stock. Since then this has continued with a survey design using three commercial vessels, and IMR has contracted the same vessels to run this survey during the period 2017-2020. The ICES WKPELA benchmark in 2016 decided to use the data from this time series as input to the stock assessment, together with the ecosystem survey in the Norwegian Sea in May and catch data, meaning that the results of the survey have significant influence on ICES catch advice.

Hence, the objective of the NSS spawning survey 2020 was to continue the relative abundance estimates for use in the ICES WGWIDE stock assessment, more specifically to estimate indices of abundance and biomass at age during the period of spawning migration from wintering areas

at/off the northern Norwegian coast and in the Norwegian Sea towards the coastal spawning ground further south. Finally, it was also a purpose that the results of the survey should be compared with recent surveys with comparable effort and design during 2015-2019.

Material and methods

Survey design

During the period 14-26th of February 2020 (same period as in 2017-2019) the spawning grounds from Møre (62º20´N) to Troms (70º40´N) were covered acoustically by the commercial fishing vessels *MS Eros, MS Kings Bay* and MS *Vendla*.

The survey was planned based on information from the previous spawning cruises and the distribution of the herring fishery during the autumn 2019 up to the survey start February 14 2020 (Figure 1). The fishery prior to the survey start in 2020 indicated that the herring wintering in the Norwegian Sea were entering the coast in the Træna deep south of Røst and following the eastern shelf edge 200 m depth southwards from Træna as also observed in 2016-2019. This information also suggested that smaller and younger herring recruiting to the spawning stock initiated their spawning migration from wintering grounds further north of 70ºN west of Tromsøflaket and in the Kvænangen fjord area, which was the basis for the planned survey coverage this far north. As seen from Figure 1, the fishery had already started at Buagrunnen (63°N) at the onset of survey in 2020.

The survey design followed a standard stratified design (Jolly and Hampton 1990), where the survey area was stratified before the survey start according to the expected density and age structures of herring (Figure 2). With exception of stratum 13, all strata this year were covered with a zigzag design instead of parallel transects. The introduction of a zigzag design started in 2018. Compared with parallel transects, zigzag design is more efficient since a higher proportion of the sailed distance is used for coverage (Harbitz 2019). In 2015-2017, a significant part of the survey time was used as transport between transects, whereas in 2018-2020 insignificant time was used on transport. Each straight line in the zigzag design were considered as transects and primary sampling units (Simmonds and MacLennan 2008), with fairly uniform coverage of strata and a random starting position in the start of each stratum. In order to investigate potential herring aggregations west of Buagrunnen (it has previously been stated by

some fishermen that herring arrives on the Buagrunnen directly from the Norwegian Sea, i.e. from west) two parallel transects were covered extending approximately 80 nautical miles west of Buagrunnen (63°N).

Biological sampling

Trawl sampling was carried out on a regular basis during the survey to confirm the acoustic observations and to be able to give estimates of abundance for different size and age groups. All three vessels used commercial herring trawls with small meshed (20 mm) inner net in the codend, and with a slit (so called "splitt") close to the codend to avoid too large catches. The positions of the trawl hauls are shown in Figure 3. The following variables of individual herring were analysed for each station with herring catch: Total weight (W) in grams and total length (L_T) in cm (rounded down to the nearest 0.5 cm) of up to 100 individuals per sample. In addition, age from scales, sex, maturity stage, stomach fullness and gonad weight (W_G) in grams were measured in up to 50 individuals per sample. The maturation stages were determined by visual inspection of gonads as recommended by ICES: immature = 1 and 2, early maturing = 3, late maturing = 4, ripe = 5, spawning = 6, spent = 7 and resting/recovering = 8. Data from the subjective evaluation of maturation stages were used to split between immature and mature herring in the estimation of spawning stock biomass (SSB), as well as to demonstrate spatial differences in maturation. The gonadosomatic index (GSI=gonad weight/total weight x100) was also used to demonstrate spatial differences in maturation along the coast.

Environmental sampling

CTD casts (using Seabird 911 systems) were taken by Eros and Vendla, spread out in the survey area (Figure 3).

Echo sounder data

Multifrequency (18, 38, 70, 120, 200 kHz) acoustic data were recorded with a SIMRAD EK 60 echo sounder and echo integrator on board Eros and Vendla, and SIMRAD EK 80 on board Kings Bay. Continuous Wave (CW) pulse, i.e. single frequency, was transmitted from all sounders. All three vessels were calibrated at the tip of the fishing pier in Ålesund prior to the survey according to standard methods (Foote et al., 1987), adjusted for split beam methods as described in Ona (1999) and (Demer et al. 2015). The calibration reports of each vessel are shown in Annex 1. The low frequency sonars were not calibrated. The intention was only to use the sonar data for studies of potential issues with herring in the echo sounder blind zone

close to the surface or avoidance, not for biomass estimations of schools. Hence, a new calibration of the sonars was not considered necessary.

LSSS, Large Scale Survey System (Korneliussen et al., 2006) was applied for the interpretation of the multi-frequency data. The recorded area echo abundance, i.e. the nautical area backscattering coefficient (NASC) (MacLennan et al. 2002), was interpreted and distributed to herring and 'other' species at 38 kHz. Various characteristics of the acoustic recordings like frequency response (Korneliussen and Ona 2002) and visual appearance were used to identify herring from other targets.

In 2020 the survey suffered from relatively bad weather condition, like last year. During conditions where the vessels had to survey against strong winds, acoustic registrations on some transects were significantly influenced by air bubble attenuation. This was corrected for during the scrutinization of the data in LSSS, and the problems and methods used to adjust is described in Annex 3 in last year's cruise report (Slotte et al. 2019). However, only a small fraction of the acoustic values had to be corrected in this year's survey.

Abundance estimation methods

The acoustic density values were stored by species category in nautical area scattering coefficient (NASC) [m^2 $n.mi.^{-2}$] units (MacLennan et al. 2002) in a database with a horizontal resolution of 0.1 nmi and a vertical resolution of 10 m, referenced to the sea surface. To estimate the mean and variance of NASC, we use the methods established by Jolly and Hampton (1990) and implemented in the software StoX (Johnsen et al. 2019). The primary sampling unit is the sum of all elementary NASC samples of herring along the transect multiplied with the resolution distance. The transect (*t*) has NASC value (*s)* and distance length *L*. The average NASC (S) in a stratum (*i*) is then:

$$\hat{S}_i = \frac{1}{n_i} \cdot \sum_{i=1}^{n_i} w_{it} s_{it} \quad (1)$$

where $w_{it} = L_{it} / \overline{L}_t$ (t= 1,2,.. n_i) are the lengths of the n_i sample transects, and

$$\overline{L}_i = \frac{1}{n_i} \sum_{t=1}^{n_i} L_{it} \quad (2)$$

The final mean NASC is given by weighting by stratum area, A;

$$\hat{S} = \frac{\sum_i A_i \hat{S}_i}{\sum_i A_i} \quad (3)$$

Variance by stratum is estimated as:

$$\hat{V}\left(\hat{S}_i\right) = \frac{n}{n_i - 1} \sum_{t=1}^{n} w_{it}^2 \left(s_t - \bar{s}\right)^2 \quad \text{with } \bar{s}_i = \frac{1}{n_i} \cdot \sum_{t=1}^{n_i} s_t \quad (4)$$

Where $w_{it} = L_{it} / \bar{L}_t$ (t= 1,2,.. n_i) are the lengths of the n_i sample transects.

The global variance is estimated as

$$\hat{V}(\hat{S}) = \frac{\sum_i A_{i=1}^2 \hat{V}(\hat{S})}{\left(\sum_i A\right)^2} \quad (5)$$

The global relative standard error of NASC

$$RSE = 100 \sqrt{\frac{\hat{V}(\hat{S})}{N}} \Big/ \hat{S} \quad (6)$$

where N is number of strata.

In order to verify acoustic observations and to analyse year class structure over the surveyed area, trawling was carried out regularly along the transects (Figure 3). All trawl stations with herring were used to derive a common length distribution for all transect within the respective strata. All stations had equal weight.

Relative standard error by number of individuals by age group was estimated by combining Monto Carlo selection from estimated NASC distributions by stratum with bootstrapping techniques of the assigned trawl stations.

The acoustic estimates presented in this report use the 38 kHz NASC, and the mean was calculated for data scrutinized as herring and collected along the transects (acoustic recordings taken during trawling, and for experimental activity are excluded). The number of herring (*N*) in each length group (*l*) within each stratum (*i*) is then computed as:

$$N_l = \frac{f_l \cdot \hat{S}_i \cdot A_i}{\langle \sigma \rangle}$$

Where

$$f_l = \frac{n_l L_i^2}{\sum_{l=1}^{m} n_l L_l}$$

is the ”acoustic contribution” from the length group L_l to the total energy and $\langle s_i \rangle$is the mean nautical area scattering coefficient [m^2/nmi^2] (NASC) of the stratum. A is the area of the stratum [nmi^2] and σ is the mean backscattering cross section at length L_l. The conversion from number of fish by length group (*l)* to number by age is done by estimating an age ratio from the individuals of length group *(l)* with age measurements. Similar, the mean weight by length and age grouped is estimated.

The mean target strength (TS) is used for the conversion where $\sigma = 4\pi\ 10^{(TS/10)}$ is used for estimating the mean backscattering cross section. Traditionally, TS = 20logL – 71.9 (Foote 1987) has been used for mean target strength of herring during the spawning surveys, however, several papers question this mean target strength. Ona (2003) describes how the target strength of herring may change with changes with depth, due to swimbladder compression. He measured the mean target strength of herring to be TS = 20logL – 2.3 log(1 + z/10) – 65.4 where z is depth in meters. Given that previous surveys were estimated using Foote (1987), the estimation this year was also done with this TS, for direct comparison and possible inclusion in the stock assessment by ICES WGWIDE 2020 as another year in the time series.

The StoX software developed by IMR were used in the abundance estimation in 2020, just as in 2015-2019. StoX is an open source software developed at IMR, Norway (Johnsen et al. 2019) to calculate survey estimates from acoustic and swept area surveys. The program is a stand-alone application build with Java for easy sharing and further development in cooperation with other institutes. The underlying high resolution data matrix structure ensures future implementations of e.g. depth dependent target strength and high resolution length and species information collected with camera systems. Despite this complexity, the execution of an index calculation can easily be governed from user interface and an interactive GIS module, or by accessing the Java function library and parameter set using external software like R. Accessing

StoX from external software may be an efficient way to process time series or to perform bootstrapping on one dataset, where for each run, the content of the parameter dataset is altered. Various statistical survey design models can be implemented in the R-library, however, in the current version of StoX the stratified transect design model developed by Jolly and Hampton (1990) is implemented.

Sonar data and analyses

Data from Simrad low-frequency sonars were logged on board all vessels with the objective to measure the presence and magnitude of potential bias related to vertical distribution (fish in blind zone above the echo sounder transducer) and avoidance behaviour of the herring relative to the presence of the vessel. Data from fisheries sonars have been collected from all participating vessels since 2015. Methods to quantify or evaluate the extent of these biases are presently being developed.

Results and discussion

Estimates of abundance

The abundance estimates from this survey are viewed as relative, i.e. as indices of abundance, since there are highly uncertain scaling parameters like acoustic target strength and compensation for herring migrating in the opposite direction of the survey (the latter issue is discussed in Appendix 2). In StoX, there are two types of point estimates of (relative) abundance at age and total abundance: baseline estimate and mean or median based on 1000 bootstrap replications. The baseline estimates are shown in Table 1 and the bootstrap estimates are shown in Table 2. The baseline estimate of biomass from the survey is 3.24 million tonnes while the bootstrap mean estimate is 3.27 million tonnes. The decline in estimated biomass from the survey in 2019 is 24 % based on the baseline estimates and 23 % based on the bootstrap estimates. The relative standard error (CV) of the biomass estimate for 2020 based on the bootstrap replicates is 17 % which is higher than in 2019 (CV = 10 %). The survey time series of stock biomass based on bootstrap replicates from the period 2015 to 2020 is shown in Figure 4. The level of the biomass has not changed significantly during 2016-2020. The baseline estimate of total number of individuals from the survey is 12.57 billion while the bootstrap mean estimate is 12.75 billion. The decline in estimated total numbers from the survey in 2019 is 11 % based on the baseline estimates and 10 % based on the bootstrap estimates. The estimated relative standard error (CV) of the total number in 2020 based on the bootstrap replicates is 16 % which is higher than in 2019 (CV = 10 %). The survey time series of total number based on bootstrap replicates from the period 2015 to 2020 is shown in Figure 5. The level of total number has not changed significantly during 2016-2020. The estimated stock number is dominated by 4 and 7 year old herring, which is the 2016 and 2013 year classes (Table 1-2 and Figure 6). The uncertainty is high for the very young and old year classes and moderate for the most abundant ages in the survey (Table 2 and Figure 6), which is the normal pattern observed in surveys and samples from commercial catches. Estimated numbers per year class from the surveys in 2015-2020 are shown in Figure 7. The estimated numbers from the survey in 2020 seems to decline as excepted for the year classes that are fully recruited to the survey, and it now seems like the survey in 2019 slightly over-estimated numbers at age (Figure 7). The 2016 year class is estimated more than three times more abundant than the 2013 year class was as 4 year olds in 2017.

Spatial distribution of the stock

The distribution and densities of herring in the area covered in 2020 was quite similar to that observed in 2017-2019, relatively evenly distributed along the coast 63-70º39´N, yet with some high density areas close to the coast from Buagrunnen to Træna (63°-66°30´N) and around the continental slope outside Lofoten, the Vesterålen banks and further north (66°30´N-70º39´N) (Figure 8 and 9). The relative distribution of the estimated biomass per stratum is shown in Figure 10. Most of the biomass was found in stratum 4, 6, 7, 9 and 10, i.e. close to the coast south of Træna and on the slope around the banks outside Lofoten and Vesterålen. This distribution is fairly similar to the distribution in 2019 but a bit more uniform in 2020 with more of the biomass in the north due to the incoming 2016 year class. Age compositions per stratum are shown in Figure 11. The southernmost strata (1-4) were dominated by herring older than 6 years and the age distributions are fairly uniform. In the middle strata from Træna to Lofoten (strata 5-9) 7 year olds (2013 year class) was the most numerous while the 4 year olds (2016 year class) dominated in the northernmost strata (10-13). The 2016 year class also appears clearly in stratum 8 and 9 (outside Lofoten). Mean length and mean weight per trawl station are shown in Figure 12 and 13. These figures show that the largest herring is found in the southern part of the covered area while smaller fish dominates in the north. The observed size dependent distribution pattern in 2020 is similar to what was observed in 2015-2019 (Slotte et al 2015, 2016, 2017, 2018, 2019). It is also in accordance with the observations in earlier years, which has been thoroughly discussed in Slotte and Dommasnes, 1997, 1998, 1999, 2000; Slotte, 1998b; Slotte, 1999a, Slotte 2001, Slotte et al. 2000, Slotte & Tangen 2005, 2006).. The main hypothesis is that this could be due to the high energetic costs of migration, which is relatively higher in small compared to larger fish (Slotte, 1999b). Large fish and fish in better condition will have a higher migration potential and more energy to invest in gonad production and thus the optimal spawning grounds will be found farther south (Slotte and Fiksen, 2000), due to the higher temperatures of the hatched larvae drifting northwards and potentially better timing to the spring bloom (Vikebø et al. 2012).

Geographical variation in temperatures experienced by the herring

Temperatures experienced by herring from close to the surface and down to deeper waters than 200 m varied from 4°-8°C (Figure 14). At typical spawning depths of herring 100-200 m temperature varied more this year than in 2017-2019 (Slotte et al. 2017, 2018, 2019), with warm water in the southern part of the covered area (around 8°C), colder water west of Lofoten (4-5°C) and warmer water again furthest north (6-7°C).

Quality of the survey

In 2020 all vessels were equipped with multifrequency equipment on a drop keel. Even though the weather conditions were challenging with strong wind during most of the survey period, acoustic data with good quality was recorded and trawling on registrations could be carried out most of the time. There were some periods where the survey speed had to be reduced to ensure acceptable quality of the acoustic data. Correction for air bubble attenuation had to be done in only a few instances so most of the NASC values were not adjusted. As in earlier years, the young fish in the north was sometimes found close to the surface and it is therefore assumed that some herring was "lost" in the blind zone, especially during the night. Moreover, an unknown fraction of the 2016 year class was distributed outside the survey area (Norwegian Sea and Barents Sea). This is not unexpected as it is assumed in the ICES stock assessment that 4 year olds are not fully recruited in this survey (this information is contained in the catchability parameters). Regarding the older and larger herring in the southern part of the survey area there are no observations this year or earlier years which indicate that significant amounts of herring has been distributed outside the area covered by the survey. This issue has been extensively discussed and analysed in previous survey reports and this year it was also carried out two additional "oceanic" transect west of Buagrunnen where no herring was observed. Also, the distribution of the commercial fishery indicates that most of the spawning stock was contained in the area covered by the survey. To conclude, the acoustic and biological data recorded in 2020 were of satisfactory quality and the estimates from the survey are recommended to be used in the stock assessment of Norwegian spring-spawning herring.

References

Demer, D.A., Berger, L., Bernasconi, M., Bethke, E., Boswell, K., Chu, D., Domokos, R., *et al*. 2015. Calibration of acoustic instruments. ICES Cooperative Research Report No. 326. 133 pp.

Foote, K. 1987. Fish target strengths for use in echo integrator surveys. J. Acoust. Soc. Am. 82: 981-987.

Harbitz, A. 2019.A zigzag survey design for continuous transect sampling with guaranteed equal coverage probability. Fisheries Research 213, 151-159.

Johnsen, E., Totland, A., Skålevik, Å., Holmin, A.J., Dingsør, G.E., Fuglebakk, E., Handegard, N.O. 2019. StoX: An open source software for marine survey analyses. Methods in Ecology and Evolution 10:1523–1528.

Jolly, G.M., and Hampton, I. 1990. A stratified random transect design for acoustic surveys of fish stocks. Canadian Journal of Fisheries and Aquatic Sciences 47: 1282-1291.

Korneliussen, R. J., and Ona, E. 2002. An operational system for processing and visualizing multi-frequency acoustic data. ICES Journal of Marine Science, 59: 293–313.

Korneliussen, R. J., Ona, E., Eliassen, I., Heggelund, Y., Patel, R., Godø, O.R., Giertsen, C., Patel, D., Nornes, E., Bekkvik, T., Knudsen, H.P., Lien, G. The Large Scale Survey System - LSSS. Proceedings of the 29th Scandinavian Symposium on Physical Acoustics, Ustaoset 29 January– 1 February 2006.

MacLennan, D.N., Fernandes, P., and Dalen, J. 2002. A consistent approach to definitions and symbols in fisheries acoustics. ICES J. Mar. Sci., 59: 365-369.

Ona, Egil. 1999.An expanded target-strength relationship for herring."ICES Journal of Marine Science: Journal du Conseil 60: 493-499.

Ona, E. (Ed). 1999. Methodology for target strength measurements (with special reference to *in situ* techniques for fish and mikro-nekton. ICES Cooperative ResearchReport No. 235. 59 pp.

Simmonds, J, and David N. MacLennan. 2005. Fisheries acoustics: theory and practice. John Wiley & Sons, 2008.

Slotte, A. 1998*a*. Patterns of aggregation in Norwegian spring spawning herring (*Clupea harengus* L.) during the spawning season. ICES C. M. 1998/J:32.

Slotte, A. 1998*b*. Spawning migration of Norwegian spring spawning herring (*Clupea harengus* L.) in relation to population structure. Ph. D. Thesis, University of Bergen, Bergen, Norway. ISBN : 82-7744-050-2.

Slotte, A. 1999*a*. Effects of fish length and condition on spawning migration in Norwegian spring spawning herring (*Clupea harengus* L). *Sarsia* **84**, 111-127.

Slotte, A. 1999*b*. Differential utilisation of energy during wintering and spawning migration in Norwegian spring spawning herring. *Journal of Fish Biology* **54**, 338-355.

Slotte, A. 2001. Factors Influencing Location and Time of Spawning in Norwegian Spring Spawning Herring: An Evaluation of Different Hypotheses. In: F. Funk, J. Blackburn, D. Hay, A.J. Paul, R. Stephenson, R. Toresen, and D. Witherell (eds.), Herring: Expectations for a New Millennium. University of Alaska Sea Grant, AK-SG-01-04, Fairbanks, pp. 255-278.

Slotte, A. and Dommasnes, A. 1997. Abundance estimation of Norwegian spring spawning at spawning grounds 20 February-18 March 1997. Internal cruise reports no. 4. Institute of Marine Research, P.O. Box. 1870. N-5024 Bergen, Norway.

Slotte, A. and Dommasnes, A. 1998. Distribution and abundance of Norwegian spring spawning herring during the spawning season in 1998. *Fisken og Havet* 5, 10 pp.

Slotte, A. and Dommasnes, A. 1999. Distribution and abundance of Norwegian spring spawning herring during the spawning season in 1999. *Fisken og Havet* **12**, 27 pp.

Slotte, A and Dommasnes, A. 2000. Distribution and abundance of Norwegian spring spawning herring during the spawning season in 2000. *Fisken og Havet* 10, 18 pp.

Slotte, A. and Fiksen, Ø. 2000. State-dependent spawning migration in Norwegian spring spawning herring (*Clupea harengus* L.). Journal of Fish Biology 56, 138-162.

Slotte, A. & Tangen, Ø. 2005. Distribution and abundance of Norwegian spring spawning herring in 2005. Institute of Marine Research, P. O. Box 1870 Nordnes, N-5817 Bergen (www.imr.no). ISSN 1503-6294/Cruise report no. 4 2005.

Slotte, A. and Tangen, Ø. 2006. Distribution and abundance of Norwegian spring spawning herring in 2006. Institute of Marine Research, P. O. Box 1870 Nordnes, N-5817 Bergen (www.imr.no). ISSN 1503-6294/Cruise report no. 1. 2006.

Slotte, A, Johannessen, A and Kjesbu, O. S. 2000. Effects of fish size on spawning time in Norwegian spring spawning herring (*Clupea harengus* L.). Journal of Fish Biology 56: 295-310.

Slotte A., Johnsen, E., Pena, H., Salthaug, A., Utne, K. R., Anthonypillai, A., Tangen , Ø and Ona, E. 2015. Distribution and abundance of Norwegian spring spawning herring during the spawning season in 2015. Survey report / Institute of Marine Research/ISSN 1503 6294/Nr. 5 – 2015

Slotte, A., Salthaug, A., Utne, KR, Ona, E., Vatnehol, S and Pena, H. 2016. Distribution and abundance of Norwegian spring spawning herring during the spawning season in 2016. Survey report / Institute of Marine Research/ /ISSN 1503 6294/Nr. 17–2016

Slotte, A., Salthaug, A., Utne, KR, Ona, E. 2017. Distribution and abundance of Norwegian spring spawning herring during the spawning season in 2017. Survey report / Institute of Marine Research/ ISSN 15036294/Nr. 8 – 2017

Slotte A., Salthaug, A., Høines, Å., Stenevik E. K., Vatnehol, S and Ona, E. 2018. Distribution and abundance of Norwegian spring spawning herring during the spawning season in 2018. Survey report / Institute of Marine Research/ISSN 15036294/Nr. 5– 2018.

Slotte, A., Salthaug, A., Stenevik, E.K., Vatnehol, S. and Ona, E. 2019 Distribution and abundance of Norwegian spring spawning herring during the spawning season in 2019. Survey report / Institute of Marine Research/ISSN 15036294/Nr. 2– 2018.

Vikebø, F., Korosov, A., Stenevik, E.K., Husebø, Å. Slotte, A. 2012. Spatio-temporal overlap of hatching in Norwegian spring spawning herring and spring phytoplankton bloom at available spawning substrates – observational records from herring larval surveys and SeaWIFS. ICES Journal of Marine Science, 69: 1298-1302.

Tables

Table 1. Baseline estimates from StoX of Norwegian spring-spawning herring during the spawning season 14.-26. February 2020.

	age																			
Length (cm)	2	3	4	5	6	7	8	9	10	11	12	13	14	15	16	17	18	Unknown	Number	Biomass	MeanW
21-22	4401	-	-	-	-	-	-	-	-	-	-	-	-	-	-	-	-	-	4401	264	60
22-23	-	-	-	-	-	-	-	-	-	-	-	-	-	-	-	-	-	-	-	-	-
23-24	-	-	-	-	-	-	-	-	-	-	-	-	-	-	-	-	-	5970	5970	501	83.9
24-25	-	-	24672	-	-	-	-	-	-	-	-	-	-	-	-	-	-	-	24672	2143	86.8
25-26	-	3349	79838	-	-	-	-	-	-	-	-	-	-	-	-	-	-	-	83187	8304	99.8
26-27	-	6738	226706	8151	-	-	-	-	-	-	-	-	-	-	-	-	-	-	241595	28037	116.1
27-28	-	16462	560050	2246	-	-	-	-	-	-	-	-	-	-	-	-	-	-	578758	74175	128.2
28-29	-	4401	1042950	78583	15729	38580	-	-	-	-	-	-	-	-	-	-	-	-	1180245	172641	146.3
29-30	-	8803	851130	57312	23250	-	-	-	34397	-	-	-	-	-	-	-	-	-	974892	160763	164.9
30-31	-	-	412161	124936	62859	-	-	-	-	-	-	-	-	-	-	-	-	-	599956	113719	189.6
31-32	-	-	124488	136422	323548	272276	2332	2896	-	-	-	-	-	-	-	-	-	-	861962	194614	225.8
32-33	-	-	52436	51801	485479	947774	47440	3088	-	-	-	-	-	-	-	-	-	-	1588018	403094	253.8
33-34	-	-	20670	55790	283548	1221070	176018	76803	-	-	-	-	-	-	-	-	-	-	1833899	505588	275.7
34-35	-	-	-	24537	33764	607968	174940	202273	19902	23515	4666	9854	9903	-	20635	-	-	-	1131956	340265	300.6
35-36	-	-	33467	-	22277	207402	72637	191609	63650	193184	24543	35361	117013	58179	89862	-	2399	-	1111581	371008	333.8
36-37	-	-	-	-	-	20699	35799	57267	124742	350808	66818	143322	311285	51094	224322	39112	8180	-	1433447	510053	355.8
37-38	-	-	-	-	1714	10637	7449	31916	65666	99504	20180	50587	210310	21927	166959	36004	1253	-	724106	276079	381.3
38-39	-	-	-	-	-	-	-	6200	7978	3720	6628	30840	40734	9932	27522	1845	29247	-	164645	66541	404.2
39-40	-	-	-	-	-	-	-	-	-	-	-	-	-	-	6586	-	10496	-	17081	7374	431.7
40-41	-	-	-	-	-	-	-	-	-	-	-	-	2079	-	5669	-	-	-	7748	3893	502.4
TSN (1000)	4401	39752	3428570	539777	1252169	3326407	516615	572050	316334	670730	122835	269964	691324	141131	541554	76960	51575	5970	12568119	-	-
TSB (t)	264	5428	532007	109415	304172	917088	153727	184640	106128	237339	44483	97099	249981	51076	197450	28077	20182	501	-	3239055	-
Mean L (cm)	21.5	27.4	28.6	30.7	32.2	33.1	34.1	34.9	35.4	36.0	36.2	36.4	36.5	36.1	36.5	36.8	38.0	23.5	-	-	-
Mean W (g)	60.0	136.5	155.2	202.7	242.9	275.7	297.6	322.8	335.5	353.9	362.1	359.7	361.6	361.9	364.6	364.8	391.3	83.9	-	-	257.7
% mature	0	72	97	100	100	100	100	100	100	100	100	100	100	100	100	100	100	-	-	-	-
SSB (t)	0	3908	516047	109415	304172	917088	153727	184640	106128	237339	44483	97099	249980	51076	197450	28077	20182	-	-	3220811	-

Table 2. Bootstrap estimates from StoX (based on 1000 replicates) of Norwegian spring-spawning herring during the spawning season 14. -26. February 2020. Numbers by age and total number (TSN) are in millions and total biomass (TSB) in thousand tons.

Age	5th percentile	Median	95th percentile	Mean	SD	CV
2	0.0	4.0	19.3	5.7	6.7	1.17
3	9.7	38.6	104.5	44.4	29.7	0.67
4	2385.5	3427.1	4808.1	3502.4	741.0	0.21
5	354.9	552.4	840.6	571.1	152.8	0.27
6	847.4	1202.5	1602.0	1212.4	225.7	0.19
7	2363.1	3329.1	4307.9	3336.7	584.4	0.18
8	349.3	523.9	729.3	530.2	116.2	0.22
9	406.4	599.6	850.5	609.1	135.1	0.22
10	201.8	355.4	553.2	364.1	109.5	0.30
11	415.7	641.6	919.5	649.7	154.0	0.24
12	80.2	127.9	192.7	131.4	34.9	0.27
13	177.6	273.8	393.1	279.5	67.2	0.24
14	384.6	669.7	987.6	676.6	187.1	0.28
15	64.2	152.3	258.9	154.9	59.3	0.38
16	330.6	520.8	843.4	541.4	153.8	0.28
17	42.8	76.2	134.9	81.0	27.2	0.34
18	10.9	46.7	95.6	48.1	26.9	0.56
TSN	9375.3	12756.7	16221.0	12750.4	2068.2	0.16
TSB	2376.8	3269.2	4212.5	3273.7	543.9	0.17

Figures

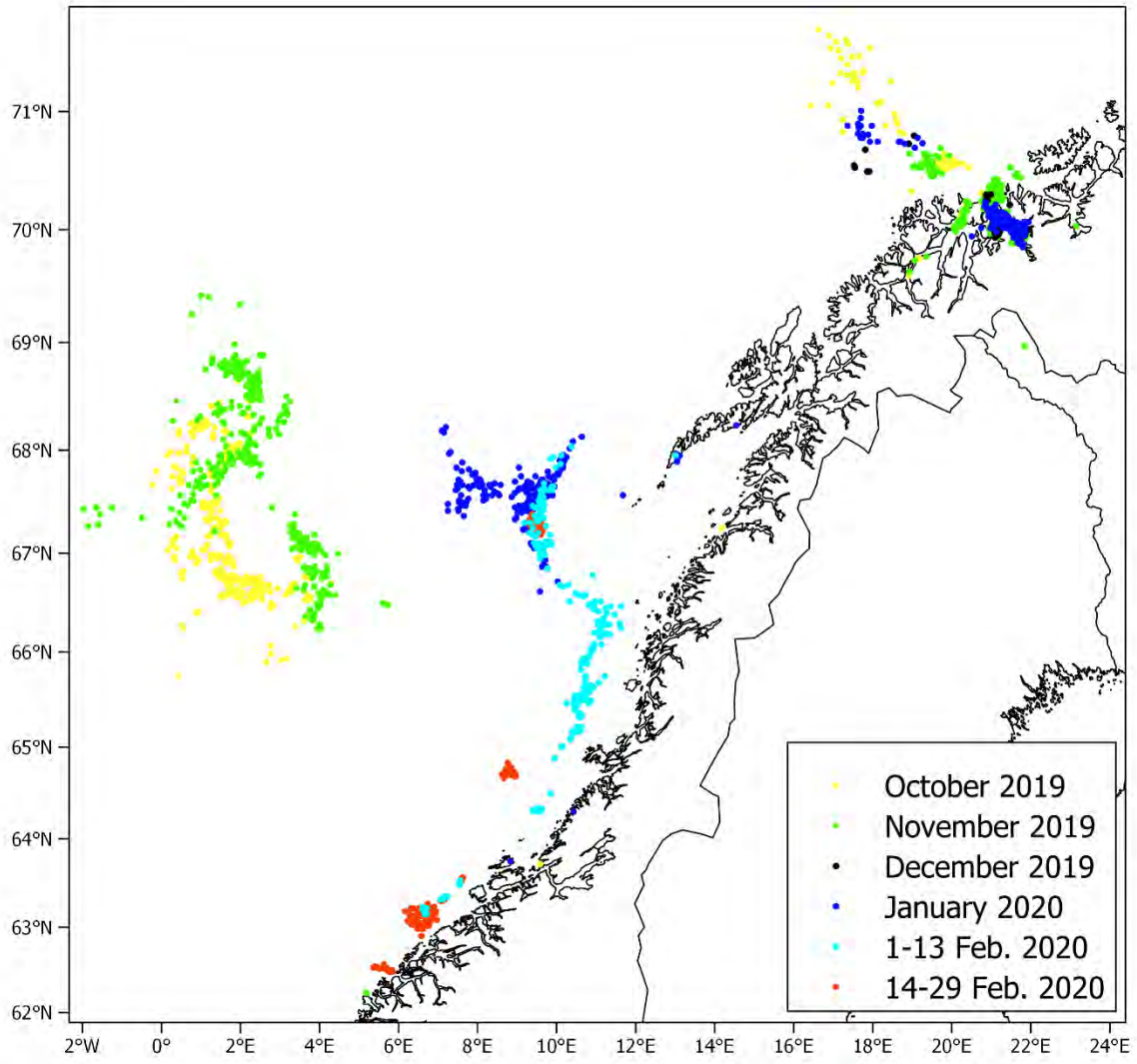

Figure 1. Distribution of commercial catches of Norwegian Spring-spawning herring from October 2019 until February 2020, based on electronic logbooks. Each point represent one catch, only catches larger than 10 tons are shown.

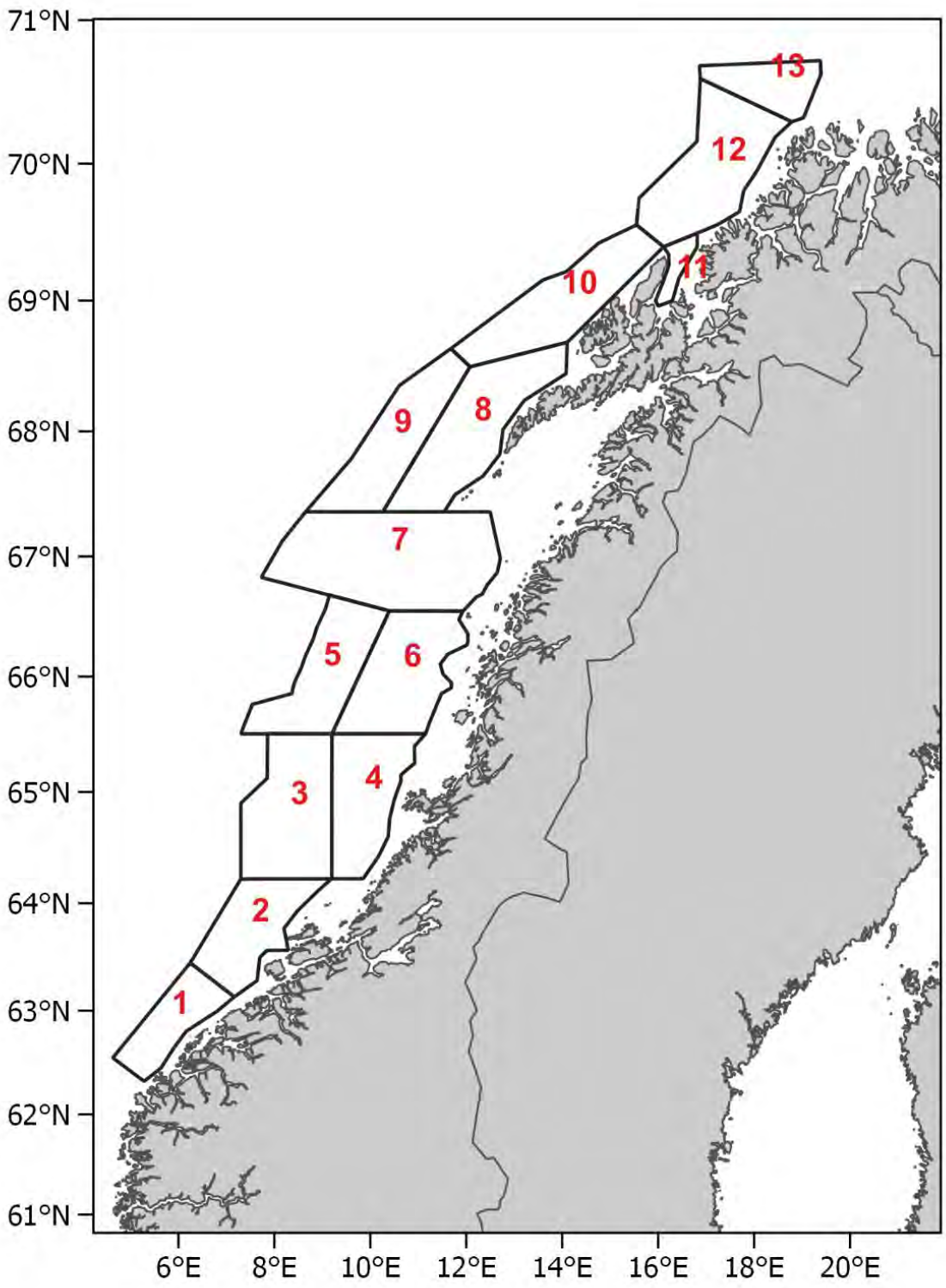

Figure 2. Strata covered during 14.-26. February 2020 with MS *Eros, Kings Bay* and *Vendla*

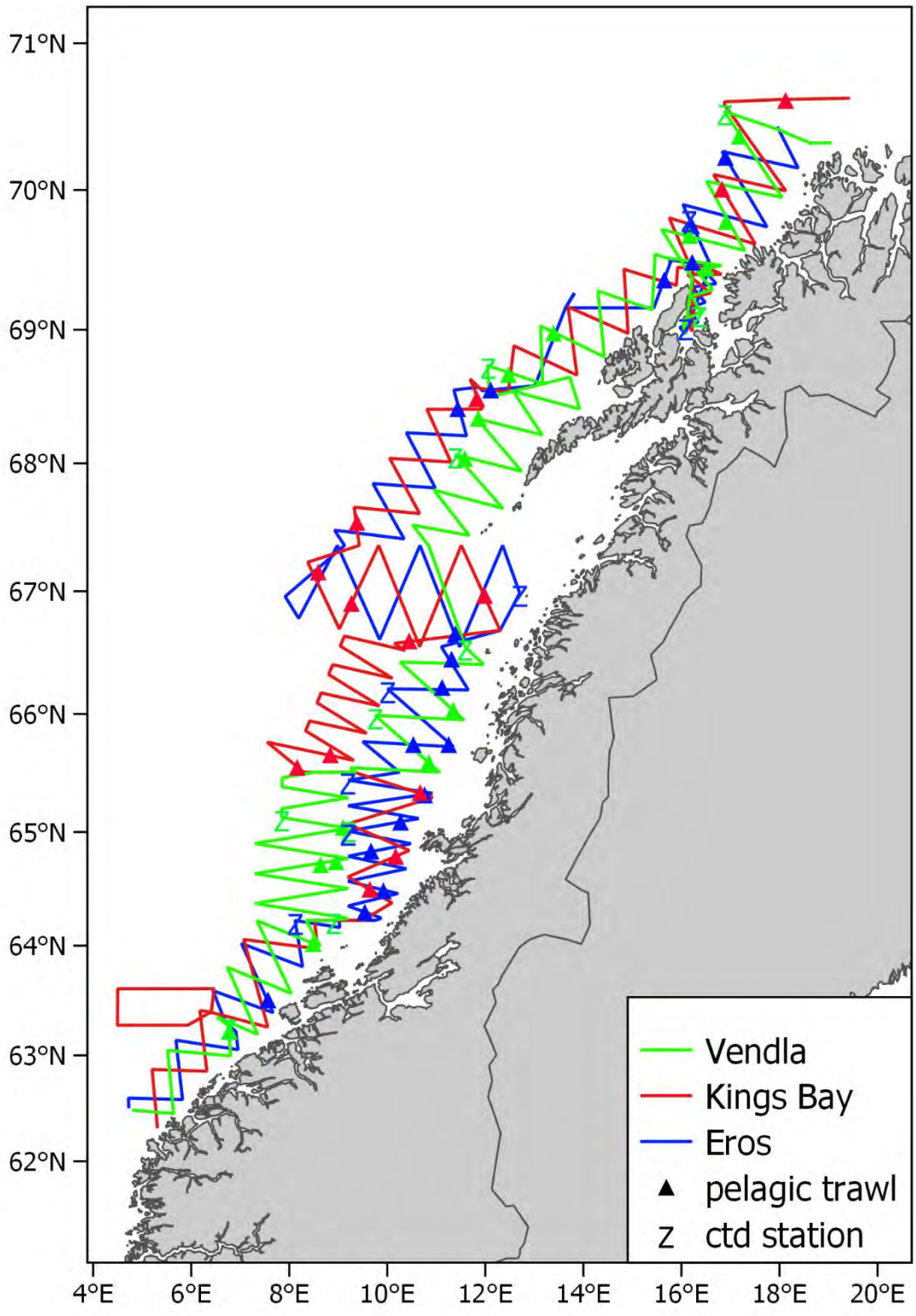

Figure. 3. Acoustic transects, pelagic trawl stations (triangles), and CTD stations (Z) covered with *Eros, Kings Bay* and *Vendla* 14.-26. February 2020.

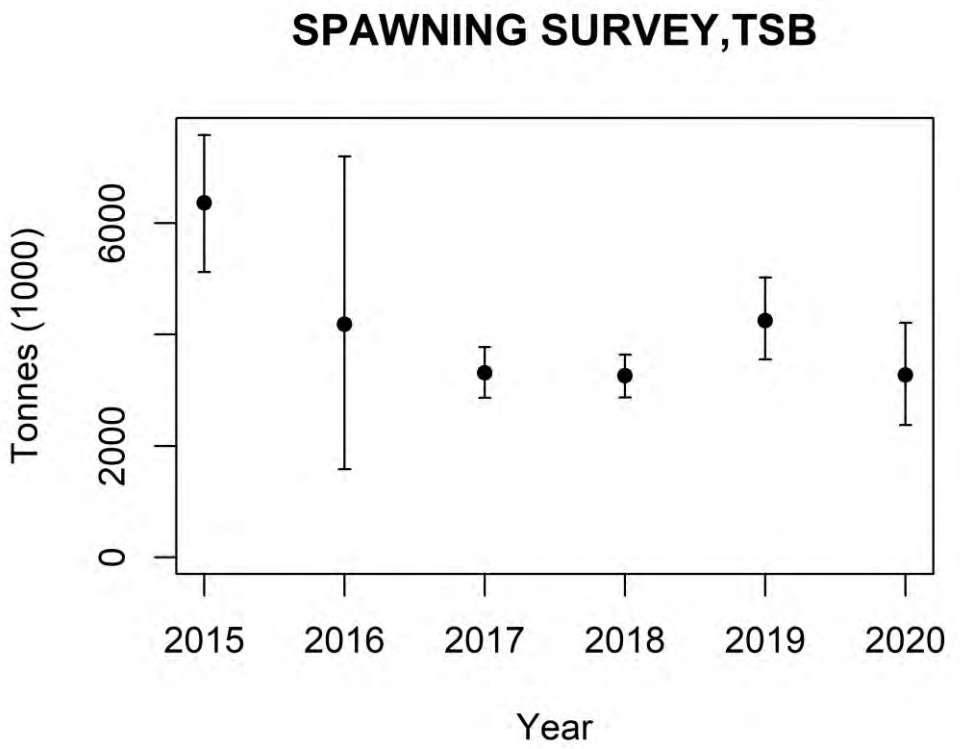

Figure 4. Estimates of total biomass from the Norwegian spring-spawning herring spawning surveys 2015-2020. The estimates are mean of 1000 bootstrap replicates in StoX and the error bars represent 90 % confidence intervals.

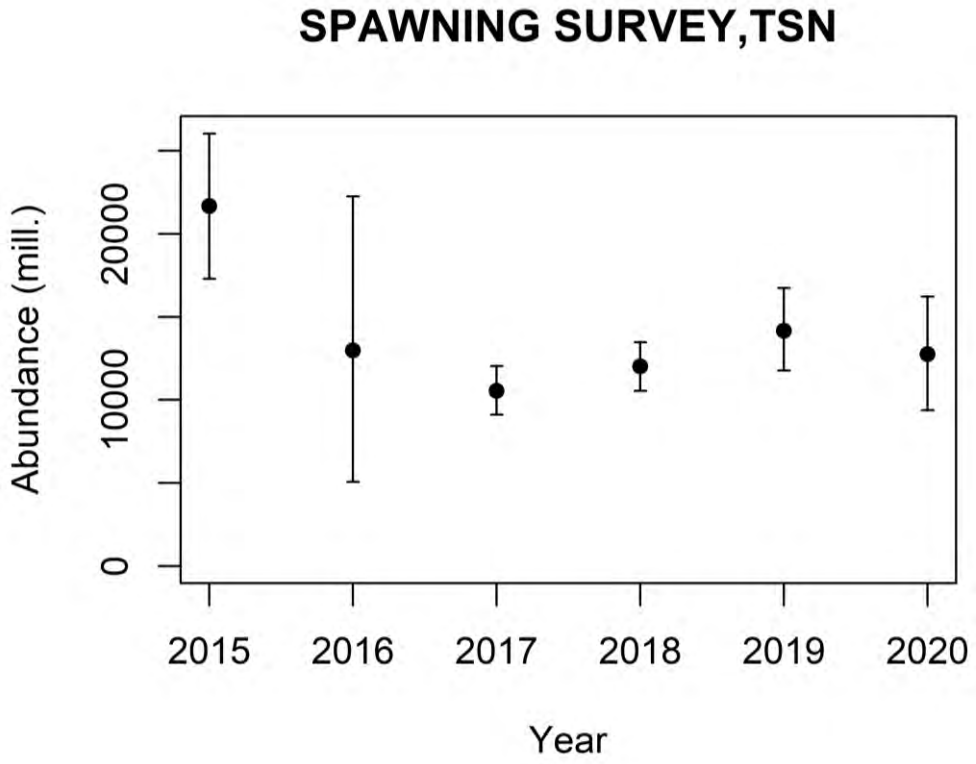

Figure 5. Estimates of total number from the Norwegian spring-spawning herring spawning surveys 2015-2020. The estimates are mean of 1000 bootstrap replicates in StoX and the error bars represent 90 % confidence intervals.

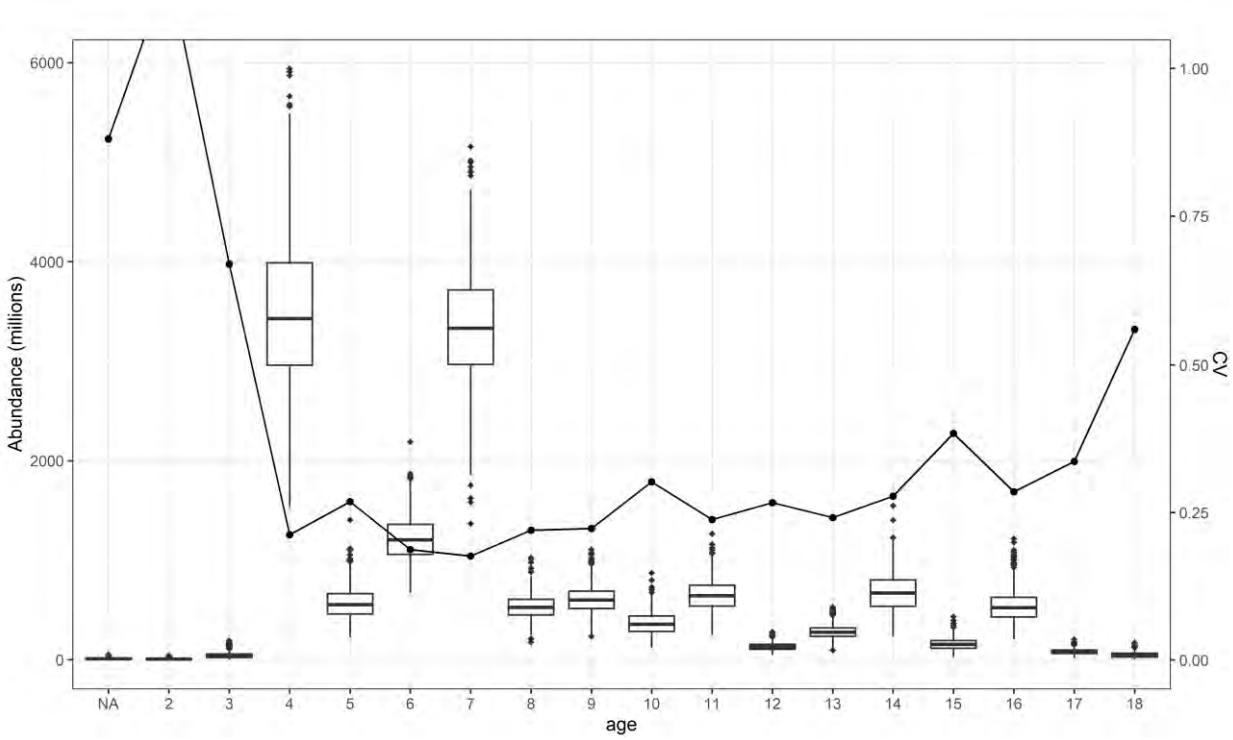

Figure 6. Standard box plot of abundance by age with uncertainty (CV) as estimated during 14.-26. February 2020. The Uncertainty estimates were based on 1000 bootstrap replicates in StoX.

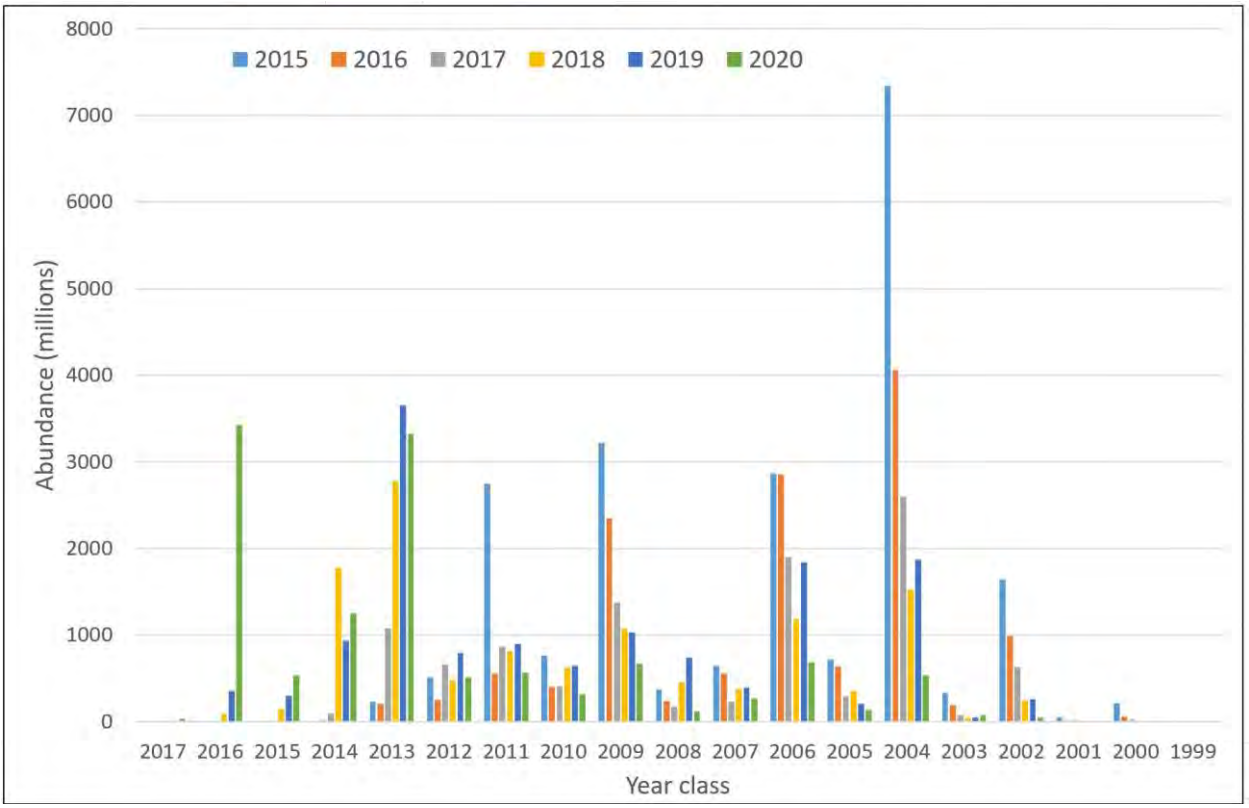

Figure 7. Abundance by year class estimated during the Norwegian spring-spawning herring surveys 2015-2020 (baseline estimates from StoX). Legend: Separate colour for each survey year.

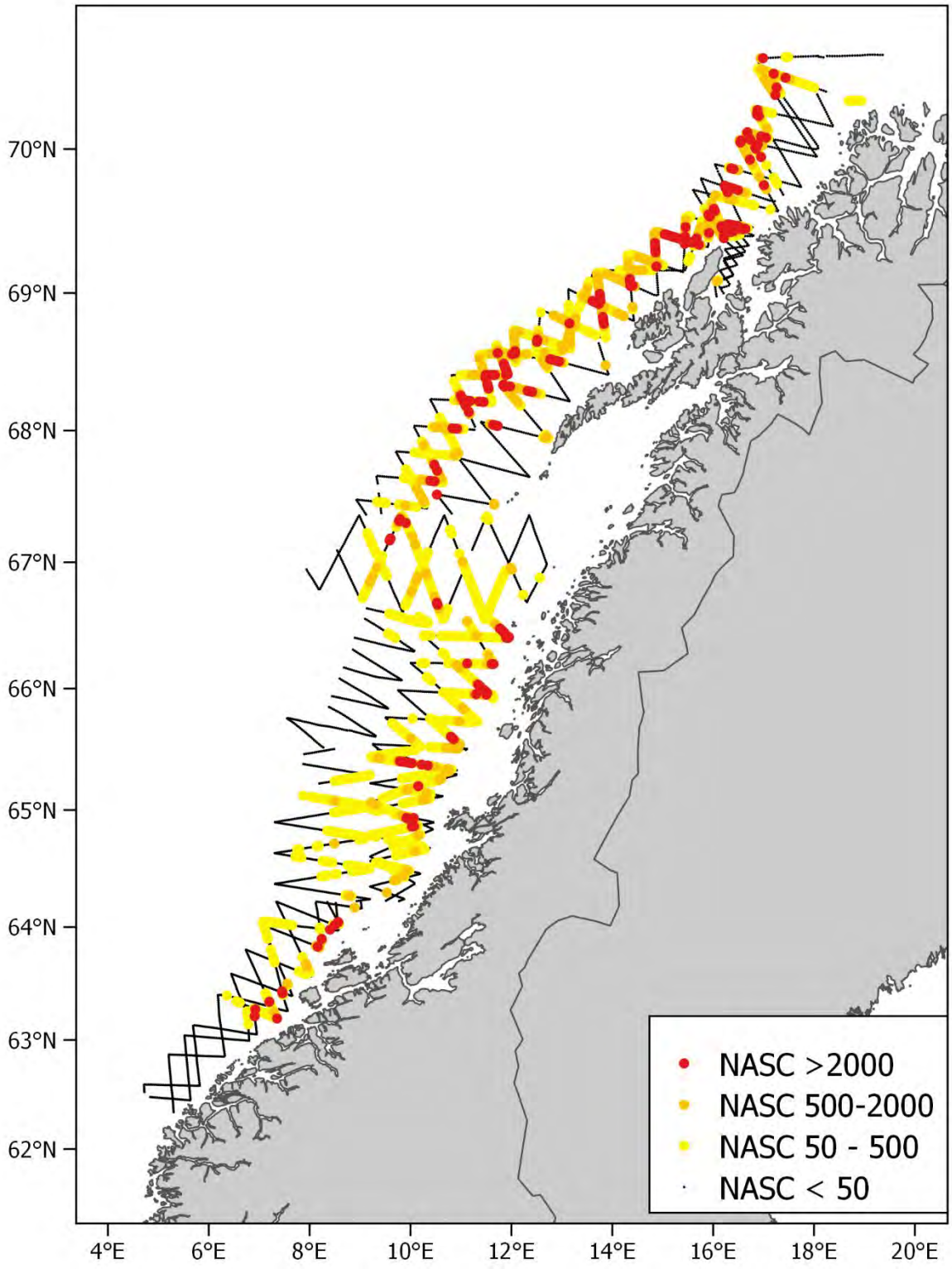

Figure 8. Acoustic density (NASC) of herring recorded during 14.-26. February 2020. Points represent NASC values per nautical mile.

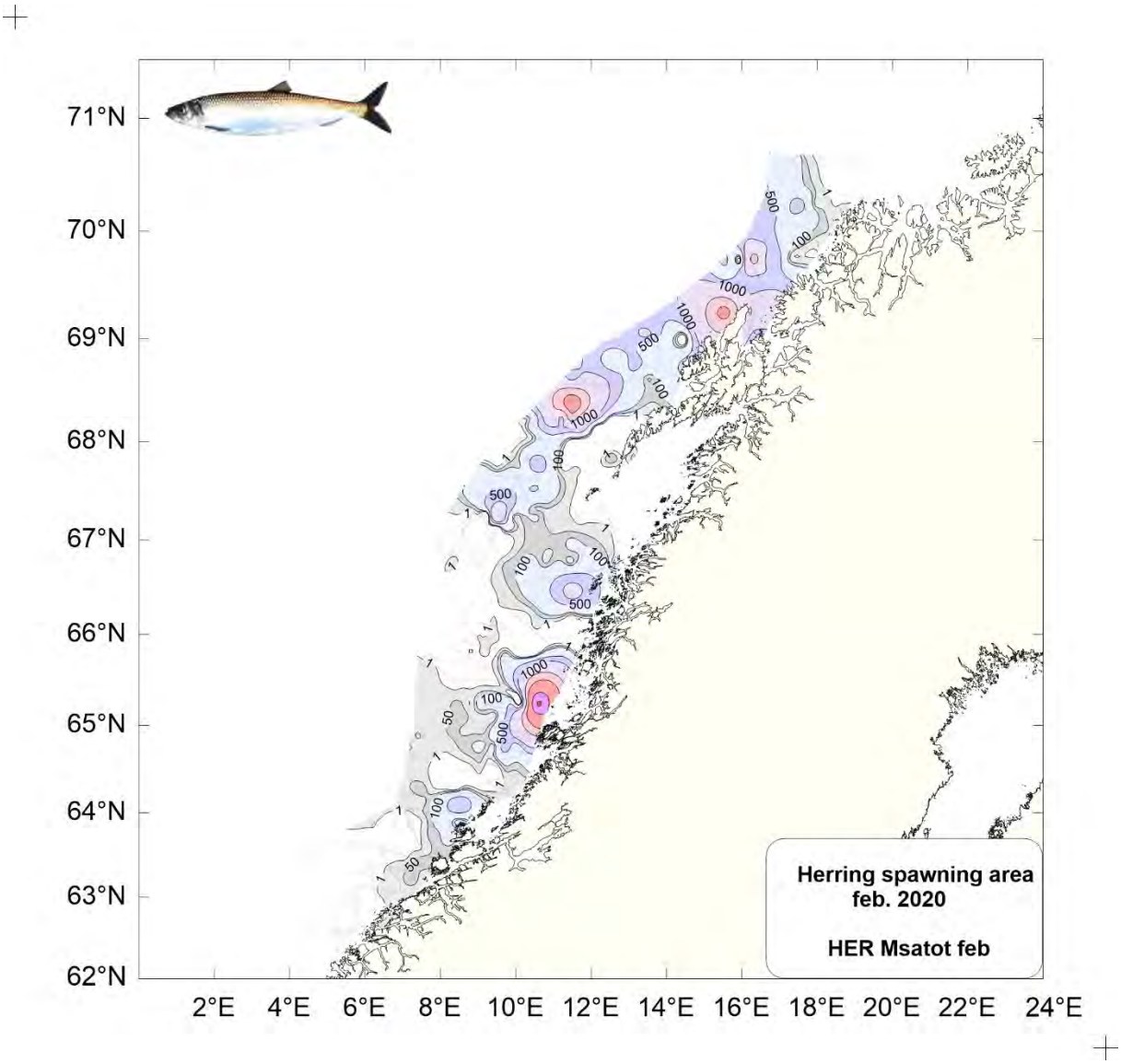

Figure 9. Contour plot of acoustic density (NASC) of herring recorded during 14.-26. February 2020.

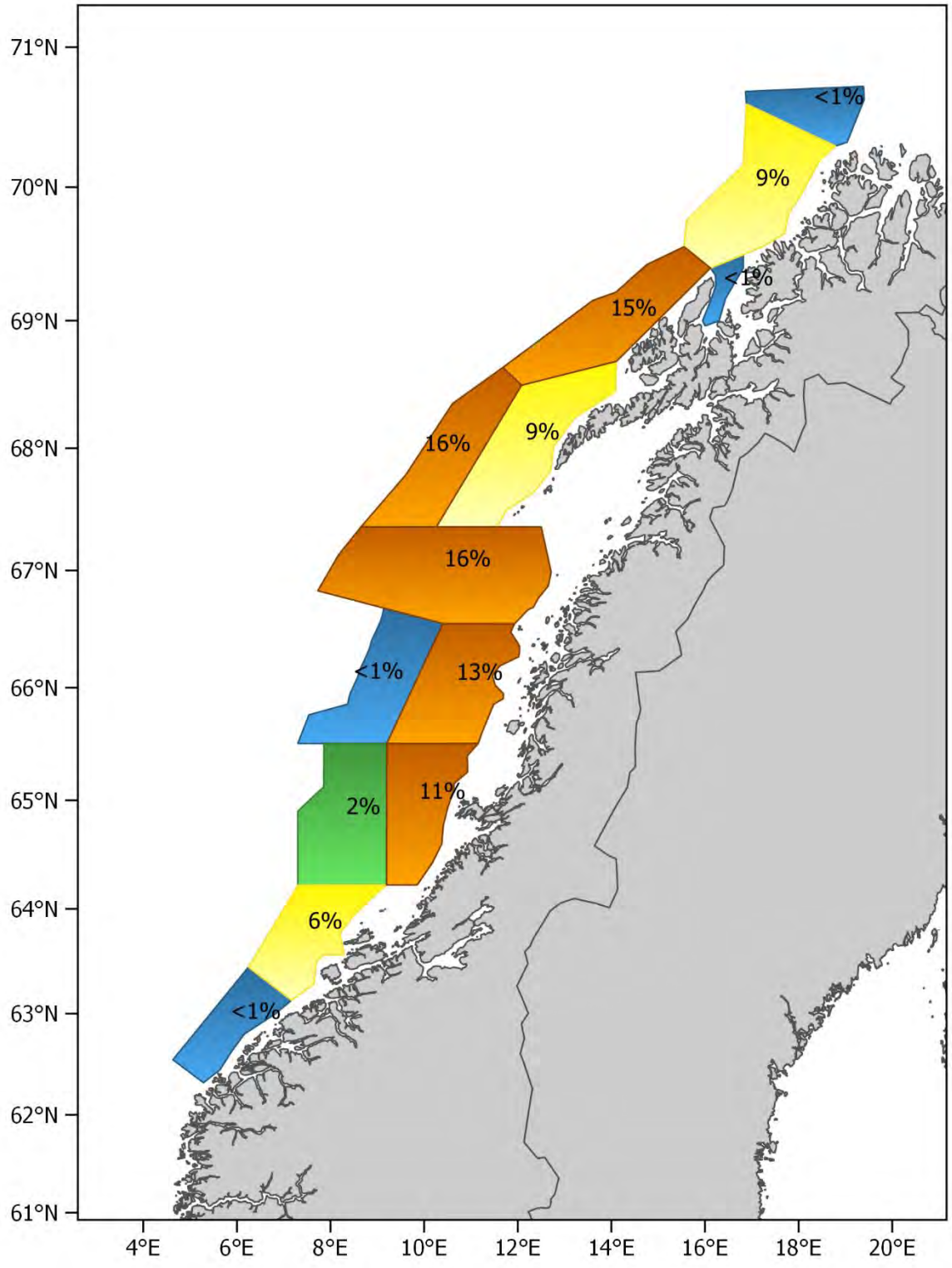

Figure. 10. Relative distribution by stratum of the biomass of herring (baseline estimates from StoX) 14.-26. February 2020. Strata numbers are given in Figure 2.

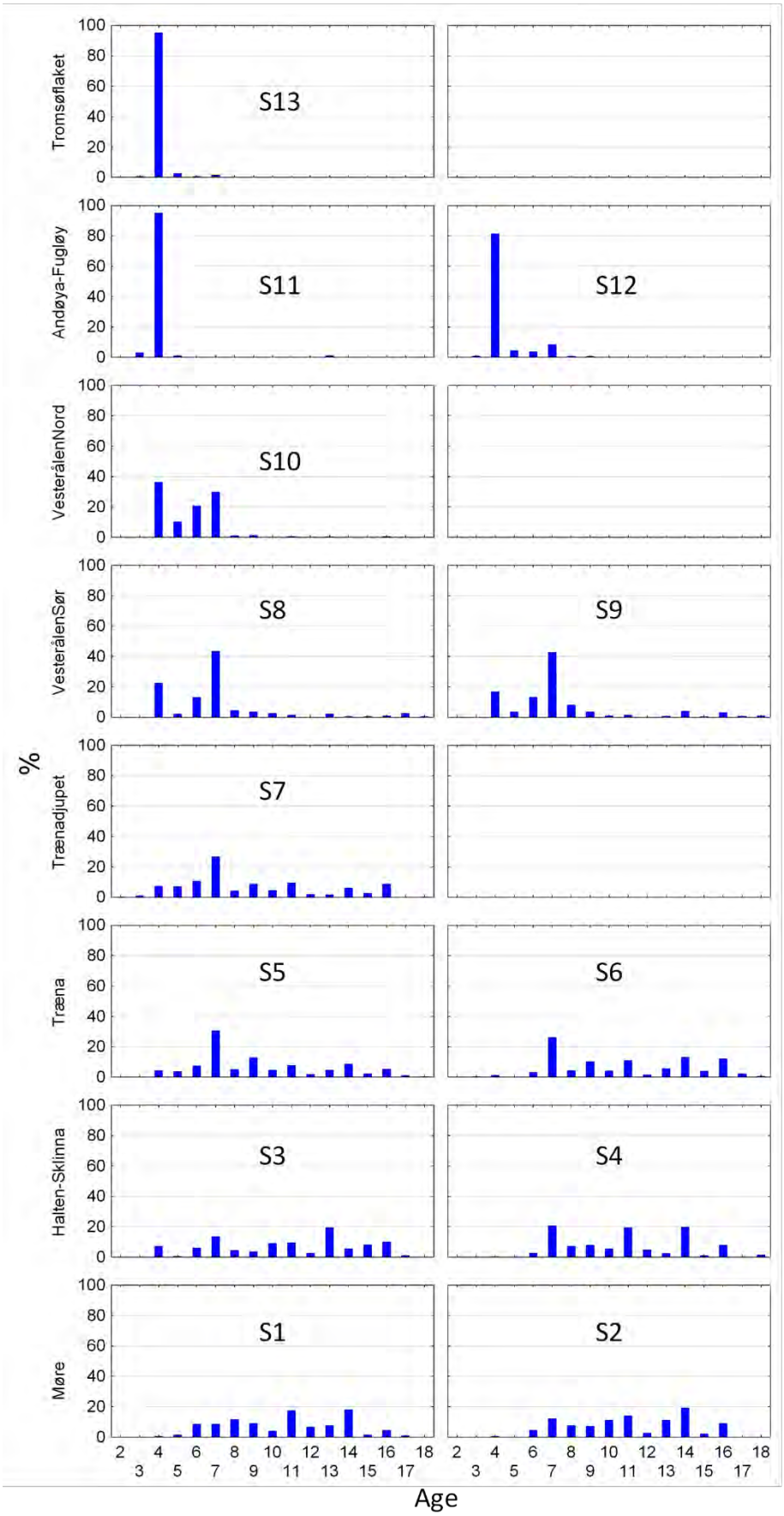

Figure 11. Comparison of age composition (%) estimated in different strata covered during 14.-26. February 2020. Strata numbers are given in Figure 2.

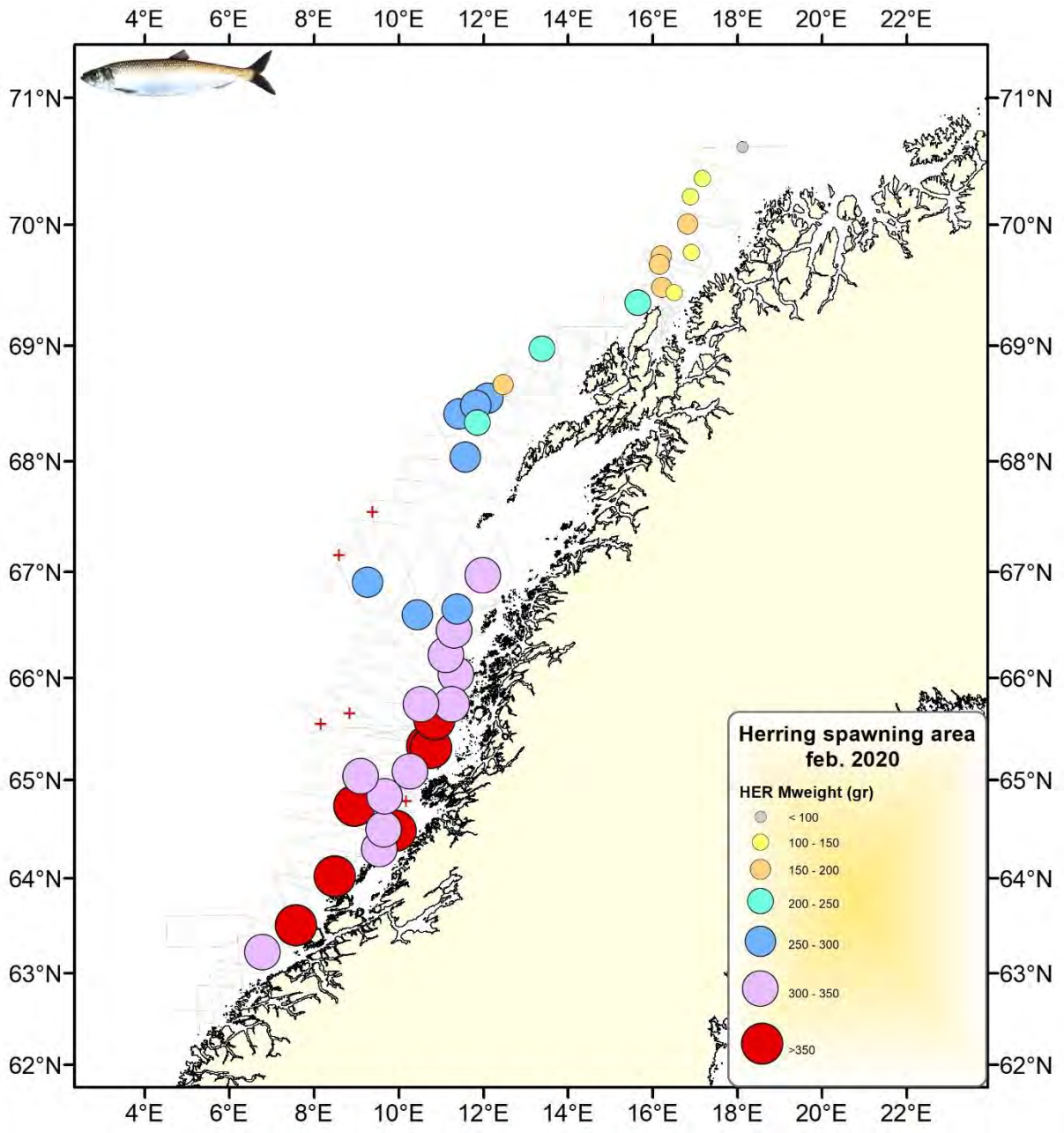

Figure 12. Mean weight (g) of herring by trawl station during the Norwegian spring-spawning herring survey 14.-26. February 2020.

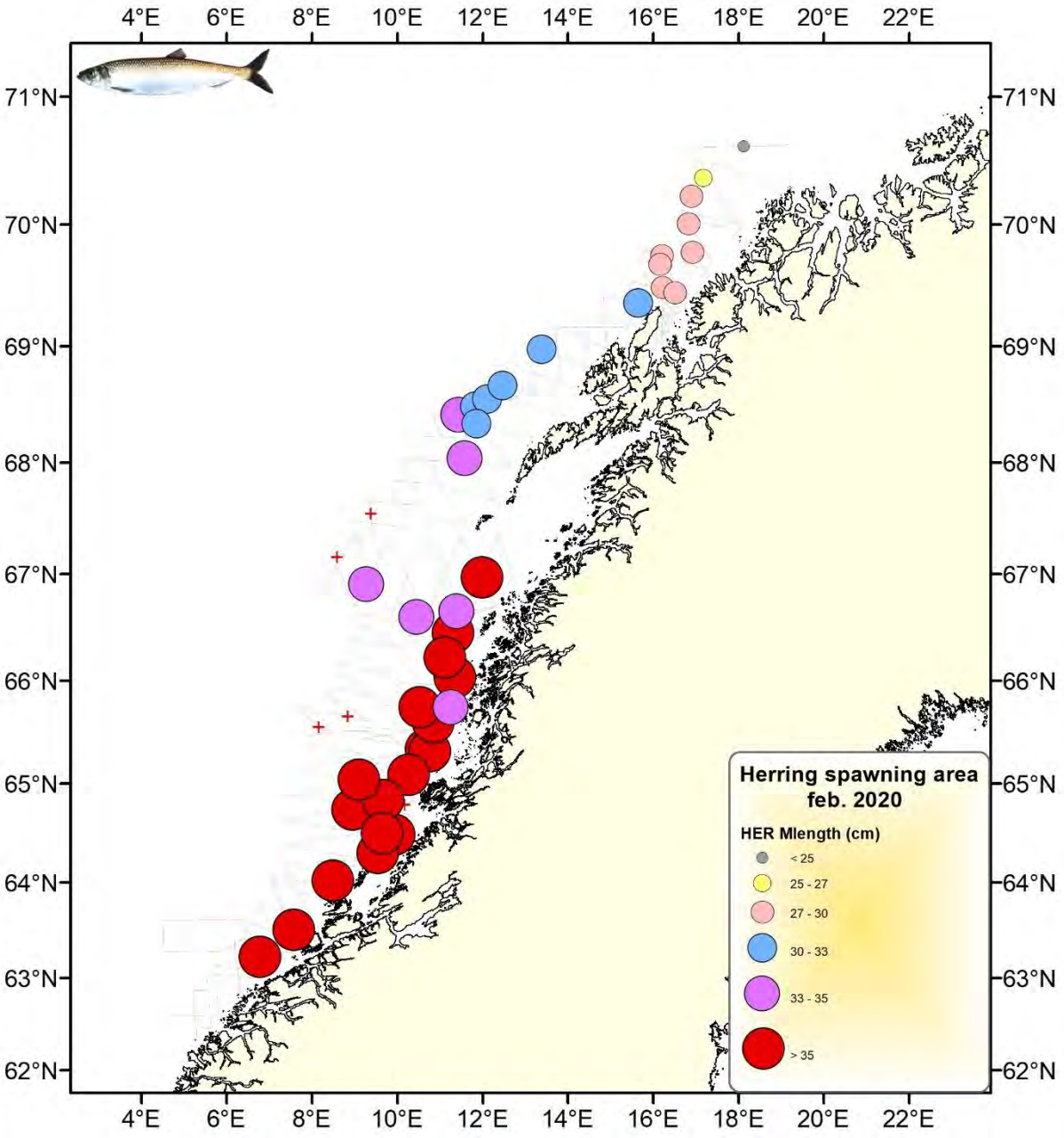

Figure 13. Mean length (cm) of herring by trawl station during the Norwegian spring-spawning herring survey14.-26. February 2020.

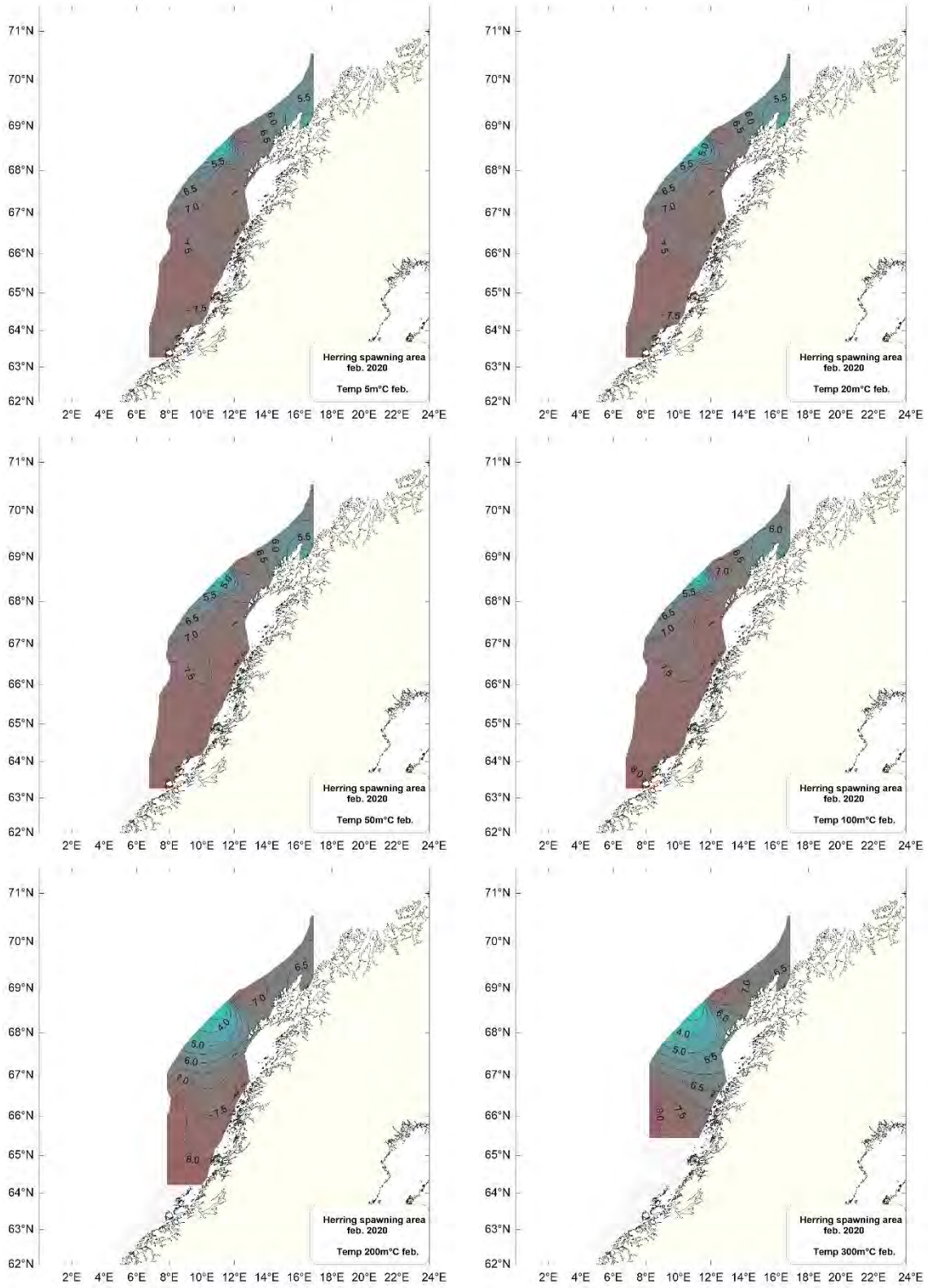

Figure 14. Temperature at 5, 20, 50, 100, 200, 300 m in the area covered during the Norwegian spring-spawning herring survey14.-26. February 2020.

Annex 1. Calibration results and settings

Table 1. Calibration data and parameter settings of the five echo sounders on each survey vessel in the survey, with the calibration done on February 14, 2020. Kings Bay has Simrad EK80 WBT's, while Vendla and EROS has Simrad EK60. EROS is running the EK80 software on the EK60 GPT's, while VENDLA runs the original EK60 software. The new WC57.2 calibration sphere was as target for all frequencies when calibrated at the tip of the fishery pier in Ålesund, with tabulated values for the sphere TS on EK60, and with the internally computed by the calibration program in EK80. After calibration was accepted, the new calibration parameters were entered into the echo sounders. The validity of the WC 57.2 calibration sphere against the original CU60 at 38 kHz was previously conducted on G.O.Sars in November 2018 with good results. The echo sounders calibration showed very good stability compared to 2017 and 2018. The 200 Khz echo sounder on Kings Bay was changed due to the failure discovered in 2018, and the 38 kHz system was changed due to a ripping of the old transducer cable. Otherwise, the systems are very stable, and as an example the calibration of the Vendla EK60 system gave values within 0.1 dB from previous February 2019 calibration except for 200 kHz, where the difference was 0.2 dB.

MS Kings Bay, Simrad EK80

Parameter					
	Survey data sample 2020818 1402: Simrad EK80, CW, 1 ms				
Transducer type	ES18	ES38-7	ES70-7C	ES120-7C	ES200-7C
Transmission frequency [kHz]	18	38	70	120	200
Transmission power [W]	2000	2000	750	250	150
Pulse duration [ms]	1.024	1.024	1.024	1.024	1.024
TS Transducer Gain [dB]	23.06	26.33	27.76	27.27	26.58
Sa Correction (dB)	0.009	0.000	0.16	-0.20	-0.33
Equivalent beam angle [dB]	-17.0	-20.7	-20.7	-20.7	-20.7
Absorption coefficient [dB km^{-1}]	2.9	10.1	20.9	31.8	52.15
Half power beam widths (along/athwart ship) [deg]	9.77/9.87	5.5/4.9	6.71/6.68	6.27/6.61	7.20/6.90
Transducer angle sensitivity (along ship and athwart ship)	15.5	23.0	23.0	23.0	23.0
Sound speed [m s^{-1}]	1473	1473	1473	1473	1473

M/S Vendla, Simrad EK60

Parameter					
	Calibration 20190218 Simrad EK60, CW narrow-band				
Transducer type	ES18	ES38B	ES70-7C	ES120-7C	ES200-7C
Transmission frequency [kHz]	18	38	70	120	200
Transmission power [W]	2000	2000	750	250	120
Pulse duration [ms]	1.024	1.024	1.024	1.024	1.024
TS Transducer Gain [dB]	22.84	25.46	26.53	27.09	27.25
Sa Correction (dB)	-0.57	-0.72	-0.35	-0.27	-0.27
Equivalent beam angle [dB]	-17.0	-20.6	-20.7	-21.0	-20.7
Absorption coefficient [dB km^{-1}]	2.8	9.6	20.3	31.3	44.5

Half power beam widths (along/athwart ship) [deg]	10.81/10.86	6.97/7.05	6.53/6.62	6.44/6.56	6.59/6.3|
Transducer angle sensitivity (along ship and athwart ship)	15.5	23.0	23.0	23.0	23.0
Sound speed [m s^{-1}]	1471	1471	1471	1471	1471

M/S EROS, Simrad EK60

Parameter					
	Calibration 20180218, Simrad EK60, CW narrow-band				
Transducer type	ES18	ES38B	ES70-7C	ES120-7C	ES200-7C
Transmission frequency [kHz]	18	38	70	120	200
Transmission power [W]	2000	2000	375	150	90
Pulse duration [ms]	1.024	1.024	1.024	1.024	1.024
TS Transducer Gain [dB]	22.25	25.84	26.52	26.67	26.53
SaCorrection (dB)	-0.23	0.00	-0.33	-0.36	-0.26
Equivalent beam angle [dB]	-17.0	-20.6	-20.7	-21.0	-20.7
Absorption coefficient [dB km^{-1}]	2.8	9.7	20.6	31.6	44.9
Half power beam widths (along/athwart ship) [deg]	10.15/10.32	6.99/6.80	6.86/6.92	6.97/6.70	6.03/5.79
Transducer angle sensitivity (along ship and athwart ship)	15.5	23.0	23.0	23.0	23.0
Sound speed [m s^{-1}]	1473	1473	1473	1473	1473

February 25. 2020, Egil Ona, M/S EROS, at Sea

Annex 2. Measuring the migration speed of herring

The spawning survey on NVG herring along the Norwegian coast is designed as a snap-shot survey over 12 days, covering a survey area of 30443 nmi^2. A zig zag survey design gives a higher mean progress speed than parallel transects (Harbiz, 2019). However, before spawning, the herring migrate against the prevailing current direction, and actively use the tidal variations in the current to adjust the migration speed. Vertical positioning therefore seems to be important. Simmonds and MacLennan (2005) writes: "The movements of fish can be conceived as having two components, random motion and migration. In the former case, the fish swim at a certain speed in directions that change randomly with time. In the latter case, the fish swim consistently in the same direction. Simmonds *et al*. (2002) used a fine-scale model of North Sea herring schools, based on a spatial grid covering 120 000 km^2 with a node spacing of 40 m, to study the effect of fish movements on the results of simulated surveys. They found that the random motion was unimportant, but the effect of systematic migration even at a modest speed could not be ignored. One factor in the survey design is the timing in relation to the migration cycle, which should ensure that the surveyed area includes the entire stock. But even if this condition is met, migration of the stock within the surveyed area can bias the abundance estimate. The extent of the bias depends on the direction of the migration in relation to the transects. Suppose the fish are migrating at speed vf , and vs is the speed at which the survey progresses in the direction of migration. If vs is positive, this means that the fish tend to follow the vessel as it travels along successive transects. If the cruise track were drawn on a map whose frame of reference moved with the fish, the transects would be closer together than those on the geostationary map. Thus the effective area applicable to the analysis is less than the actual area surveyed. The observed densities are unbiased, but since the abundance is the mean density multiplied by the effective area, the estimate ˆQ is biased. The expected value of ˆQ is:

$$E(\hat{Q}) = Q(1 + vf / vs)$$

Note that when the transects are long and perpendicular to the migration, vs is much smaller than the cruising speed of the vessel. For example, if the cruising speed is 5 ms−1, and the transect length is 10 times the spacing, then the survey progresses at vs = 0.5m s−1, a value which could well be comparable with vf . Harden Jones (1968) suggests that herring are capable of migration speeds up to 0.6m s−1. The swimming capability of fish depends on their size, but adult herring and mackerel can sustain speeds around 1.0m s−1 for long periods (He and Wardle 1988; Lockwood 1989). The bias is greatly reduced if the transects run alternately with and against the migration".

A rough model can be plotted using the equation suggested by Simmonds and MacLennan (2005), with the suggested bias in the survey on the z axis. The start of the survey, the progress speed is about 1.17 m s-1 in the North - direction, indicating that the bias could be from 0 to 50% with a constant fish migration speed of 0.2 m s-1, well within the swimming capacity of adult herring. Using fishery sonar on distinct schools have been tried for direct measurement of the migration speed on earlier surveys, (Slotte et al, 2015,2016), but in this particular spawning survey, only a small fraction of the herring is moving in distinct schools. The more typical situation is layers, either in the water column, or closer to the bottom, as shown in Figure 1, and a better way to measure the migration speed is to use a Doppler system, as realized in a scientific ADCP.

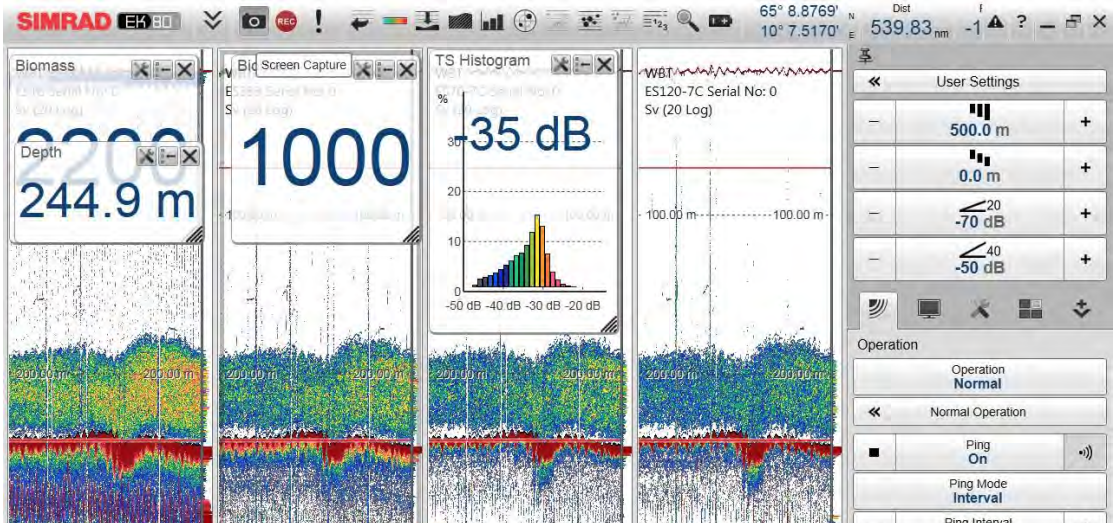

Fig 1. Typical herring layer in the NVG spawning survey (Slotte et al., 2019)

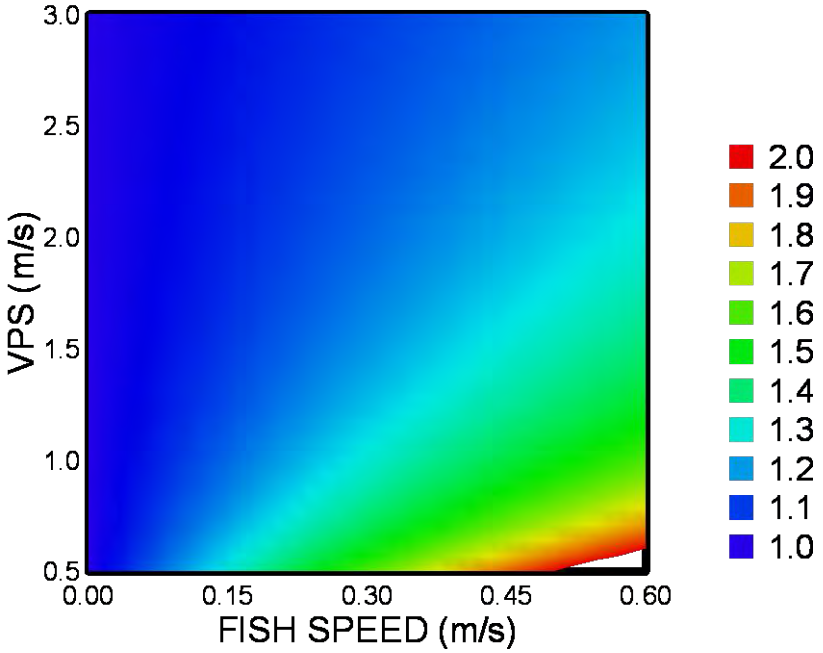

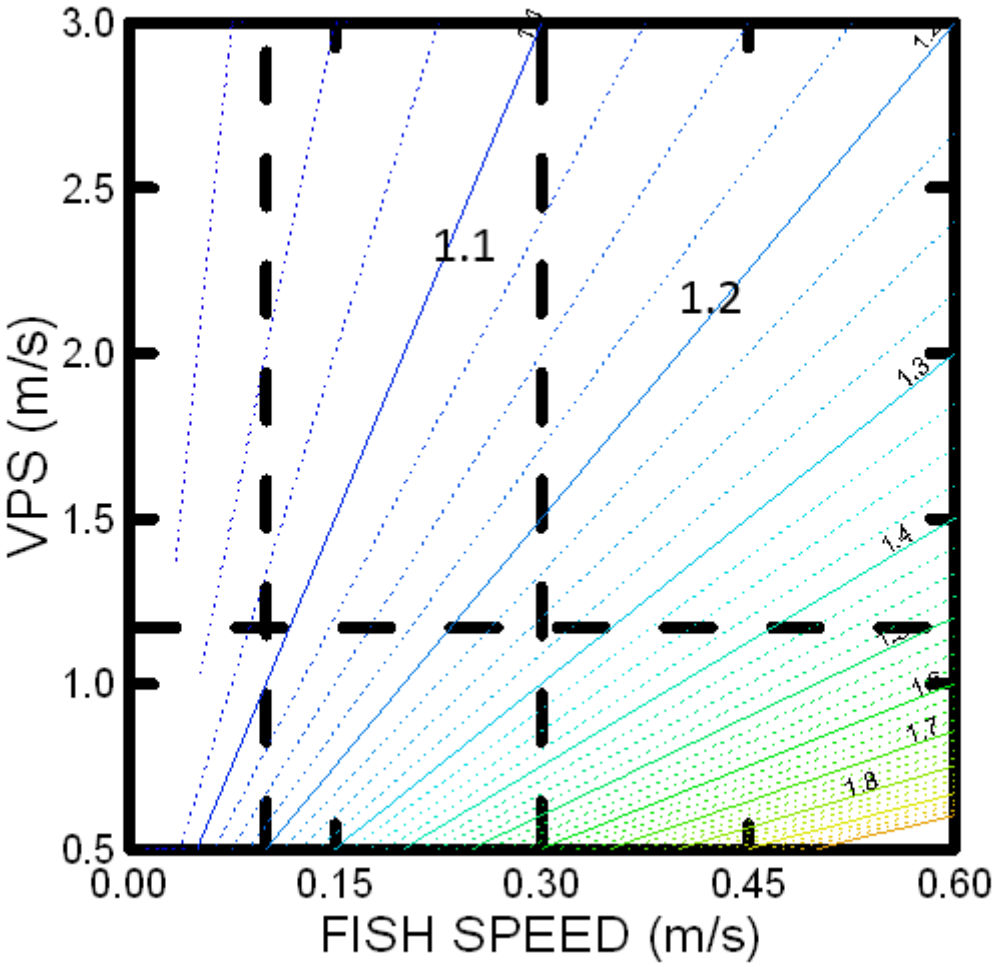

Fig 2. A, B, Overall figures for the migration error as a function of vessel progress speed, VPS (m s-1) and the herring migration speed. Error on Z axis, but with the mean vessel progress speed indicated for all strata 1.17 m s-1 as a vertical line. Observed migration speed for herring is between 0 and 0.3 m s-1, and the potential error can be evaluated to be maximum 1.2, or 20% in the worst case!

Material and methods

A Kongsberg Maritime ES150C EK80 ADCP system, with four acoustic beams transmitting a 150 kHz CW or FM signal installed on MS "EROS" in the dry dock at "Båtbygg", Måløy, Norway, prior to the survey. The flat array transducer with the EK80 WBT installed in the transducer was transmitting a 12.1 ms CW pulse for the selected settings using phased array steering of the beams in ADCP mode, and a split beam transducer with 3° beam width in broad band echo sounder mode. The system was tested and tried calibrated in Ålesund February 14, 2020. Vessel GPS and KM motion Reference Unit (MRU) were coupled to the instrument, logging raw data to disk on the ADCP system PC.

Fig. 3. ADCP Simrad EC150-3C transducer (and WBT) mounted in box keel in front of the fishery sonars on EROS.

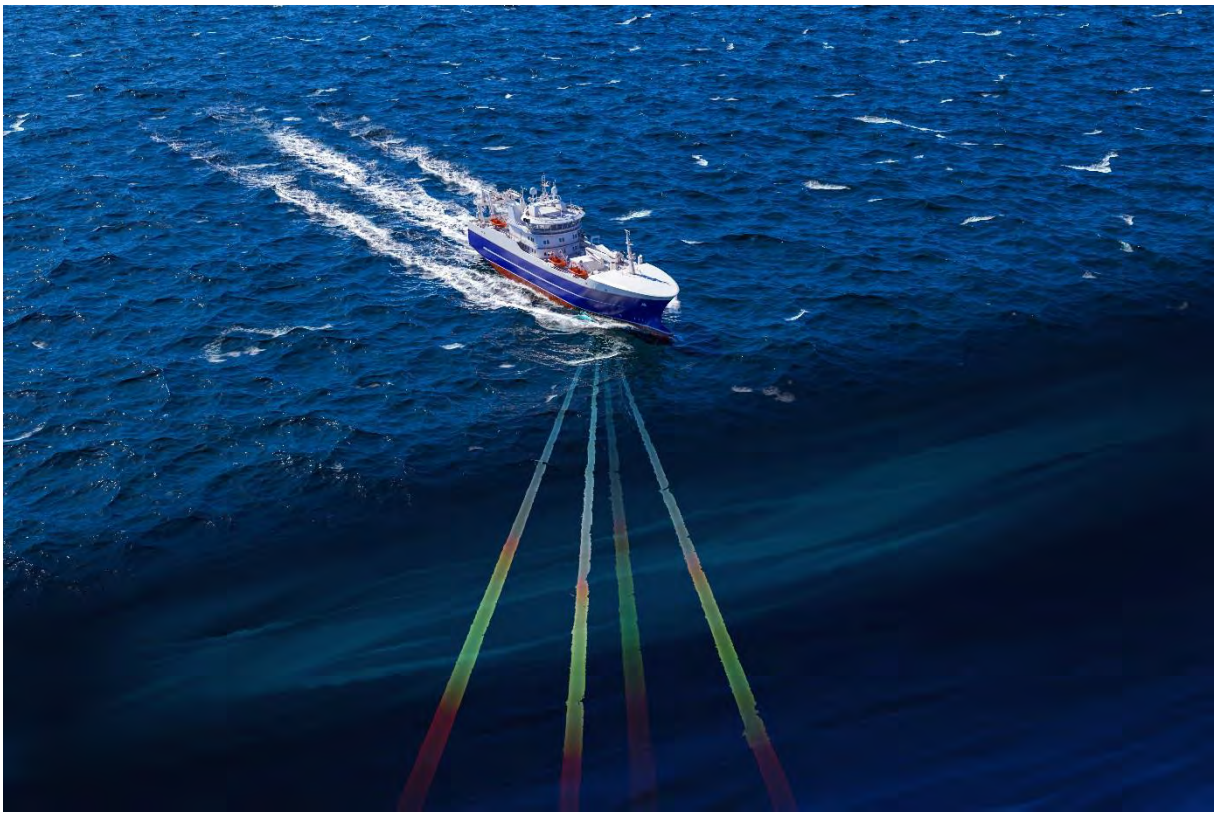

Fig 4. Principal sketch of the Simrad EC150-3C measuring system. (Figure: ®Tonny Algrøy, Kongsberg Maritime)

The ADCP system was run in parallel with the 5 EK60 GPT echo sounders and one SU90 sonar, as a stand-alone system, with no external triggering from the master echo sounder. Only weak interference was observed on the 120 kHz EK60 system, but not enough to disturb the abundance estimation of herring. GPS and a Kongsberg Motion Reference Unit, MRU 5 was connected to the ES150-C system.

The raw data was recorded, and the ADCP generated standard output current profile echograms on the screen, where both the movement of the water current and the herring movement could be monitored in real time.

For stability, averaging over 100 transmissions were used to generate preliminary real time current echograms, but could be re-run in echosounder replay using shorter averaging intervals needed for herring schools. Individual data sets were selected for further inspection and replayed locally on a secondary computer, based upon the scrutinizing results from the survey, using LSSS. During this process, the EK80 generated new processed data files, using standard output in NETCDF format. These were further read by a Phyton script, where further manipulation of the data could be done. Only preliminary analysis was done during the survey itself.

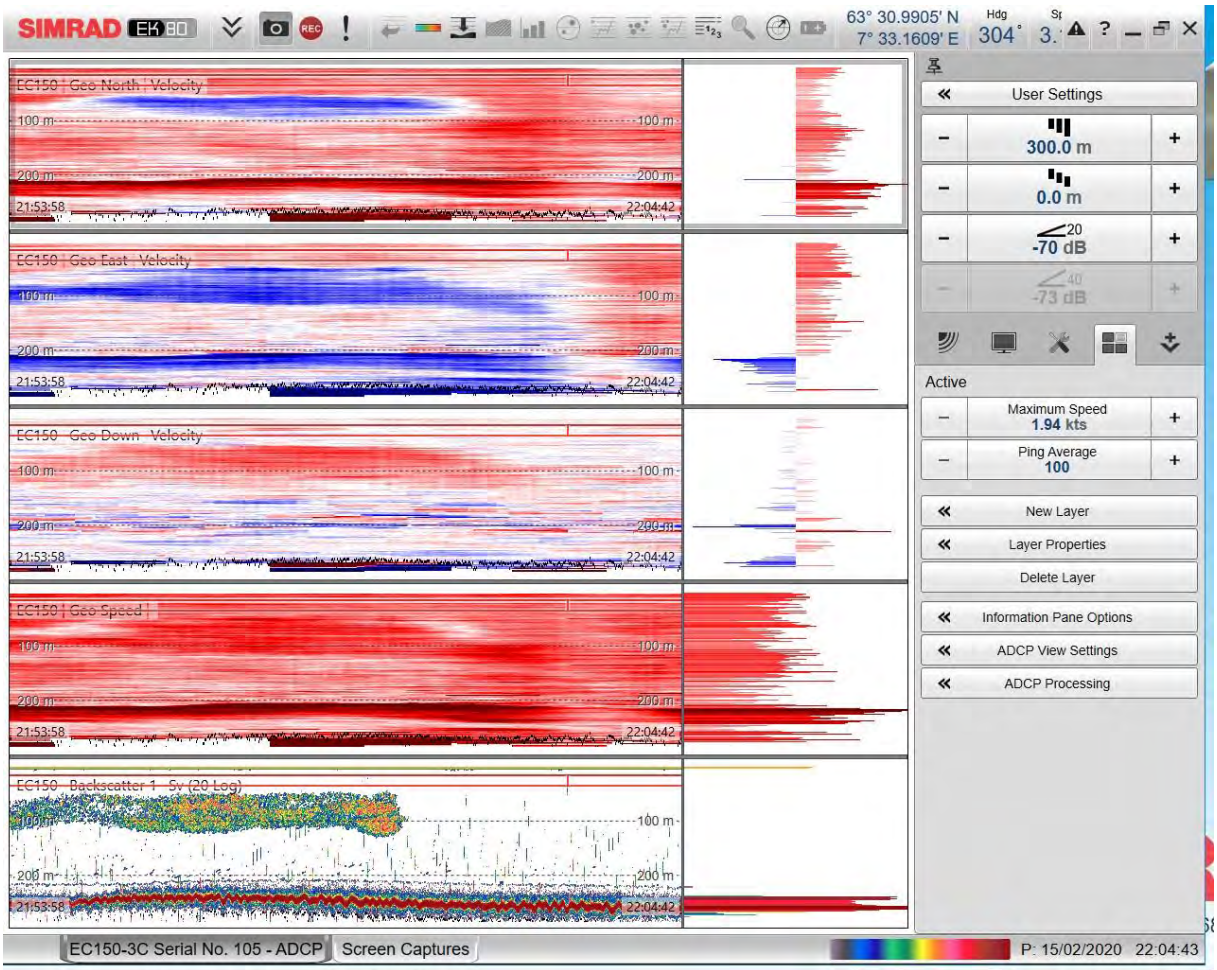

Fig 5. Example display of ADCP processed data. The screen is divided into 4 "echograms" horizontally, where the lower panel shows the backscattering in one of the ADCP beams. The upper panel shows the N/S component, here scaled to 0-2 knots, red is North, blue is South. The panel below the upper one is the E-W display, with similar settings, red is East, blue is West. Then, the third panel is the vertical speed measured, using the same scale, DOWN/ UP, with down as red, up as blue. Further, the last panel shows the sum of the vectors in the previous panels. All measurements here is geo-references, showing movement over ground. It is here clear that the herring swims against the relatively strong costal current.

Interpretation of example display:
First, the current in this transect is moving in a North direction at about 0.5 knots and slightly towards East. The current speed is similar across the entire whole water column.
The herring, however, is migrating in South direction at 0.5 knots, but also towards East with a similar swimming speed, 0.5 knots, i.e straight against the prevailing current. So, first the herring must compete and overcome the current, and exceeded the water speed with 0.5 knots. Relative to the surrounding water, it is actually swimming at 1 knot, 0.5 m s-1, or about 1.5 bl s-1, which according to Harden Jones (1968) is well within herring migration capacity.
During this first survey, there was no analyzing and processing tools available, and a manual selection of 10 values from the school and 10 values from the water column was selected and stored as separate variables.

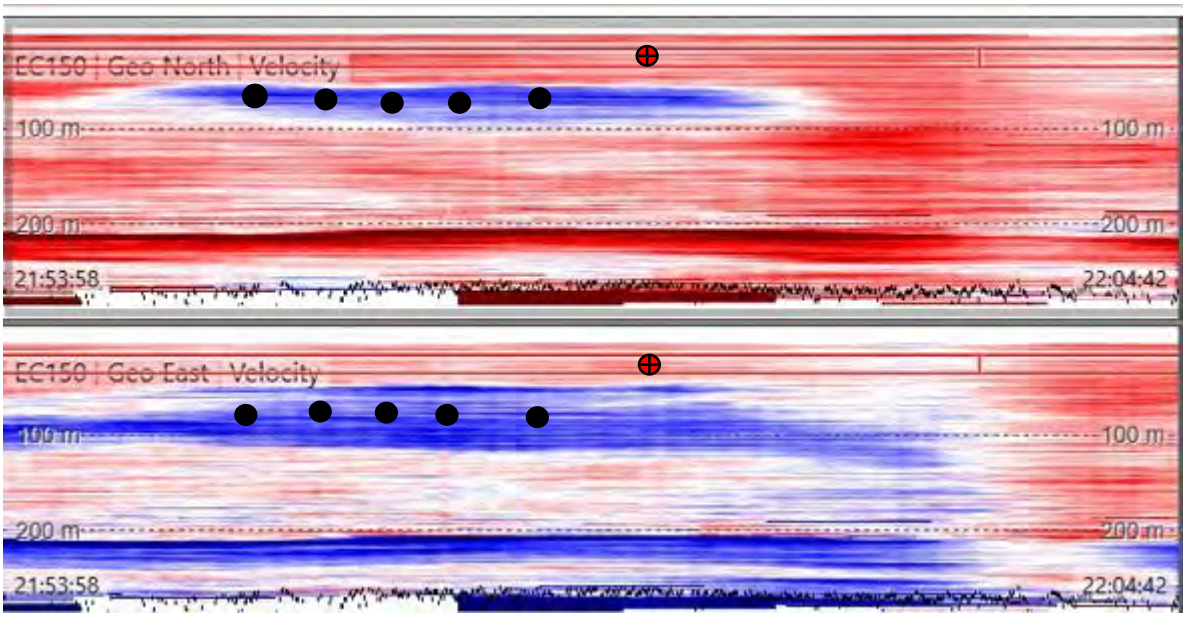

Fig 6. Manual selection of representative swimming speed and current speed, Version 1. In later versions of processing, a mask should be created using LSSS, and the mask transferred to the current echograms. Normal gridding output for both water and herring can then be computed and stored to normal user files.

About 39 data sets have been analyzed during the survey, where the herring swimming speed and current direction have been manually extracted. These data will be used to pair with the density data, either at transect level, or at stratum level.
One could either chose to weigh the speed with the acoustic density, either at transect level or at strata level:
Transect level:

$$h = \frac{\sum_n^i (v_i s_A)}{\sum_n^i s_A}$$

Then, compute the mean backscattered energy weighed speed to be used for the individual strata.
Or at strata level, h could be is the mean speed for all herring inside the strata, and the weight of migration could be the density inside the strata. (not yet decided).

The statistics of the mean survey progress (SPS) speed is shown in the Table 1.

stratum	Δt (H)	S (nmi)	VPS (knots)	VPS (m s-1)
1	14.39	67.65	4.70	2.42
2	24.64	65.67	2.67	1.37
3	55.74	77.42	1.39	0.71
4	50.55	77.10	1.53	0.78
5	38.02	70.56	1.86	0.95
6	37.32	62.56	1.68	0.86
7	38.45	48.70	1.27	0.65
8	36.66	79.48	2.17	1.12
9	30.21	76.62	2.54	1.30
10	25.53	63.60	2.49	1.28
11	11.01	32.40	2.94	1.51
12	45.78	72.00	1.57	0.81
13	9.01	25.54	2.84	1.46

Table 1. Vessel progress speed in North direction in the different strata of the survey. Delta h is the number of hours inside the strata, and the number of sailed nautical miles inside the strata is S 8nmi). Minimum 0.65 m s-1 and maximum 2.41 m s-1in strata 7 and 1 respectively. The overall mean progress speed is 1.17 m s-1 with a standard deviation of 0.47 m s-1.

We are now working on measuring the mean migration speed for each stratum, but already see that while the migration speed is high in the southern and middle strata, the migration is slower and less systematic further north.
Examples of processed data in Phyton, after replaying in local EK80 software, and generation of NETCDF output files, is shown below.
If we should make an educated guess at this point, correction for the migration effect on this survey would increase the biomass with 5 to 10%, which is still inside the uncertainty level of the survey estimate.

Egil Ona, At sea 26.2.2020, and home office 30.3.2020.

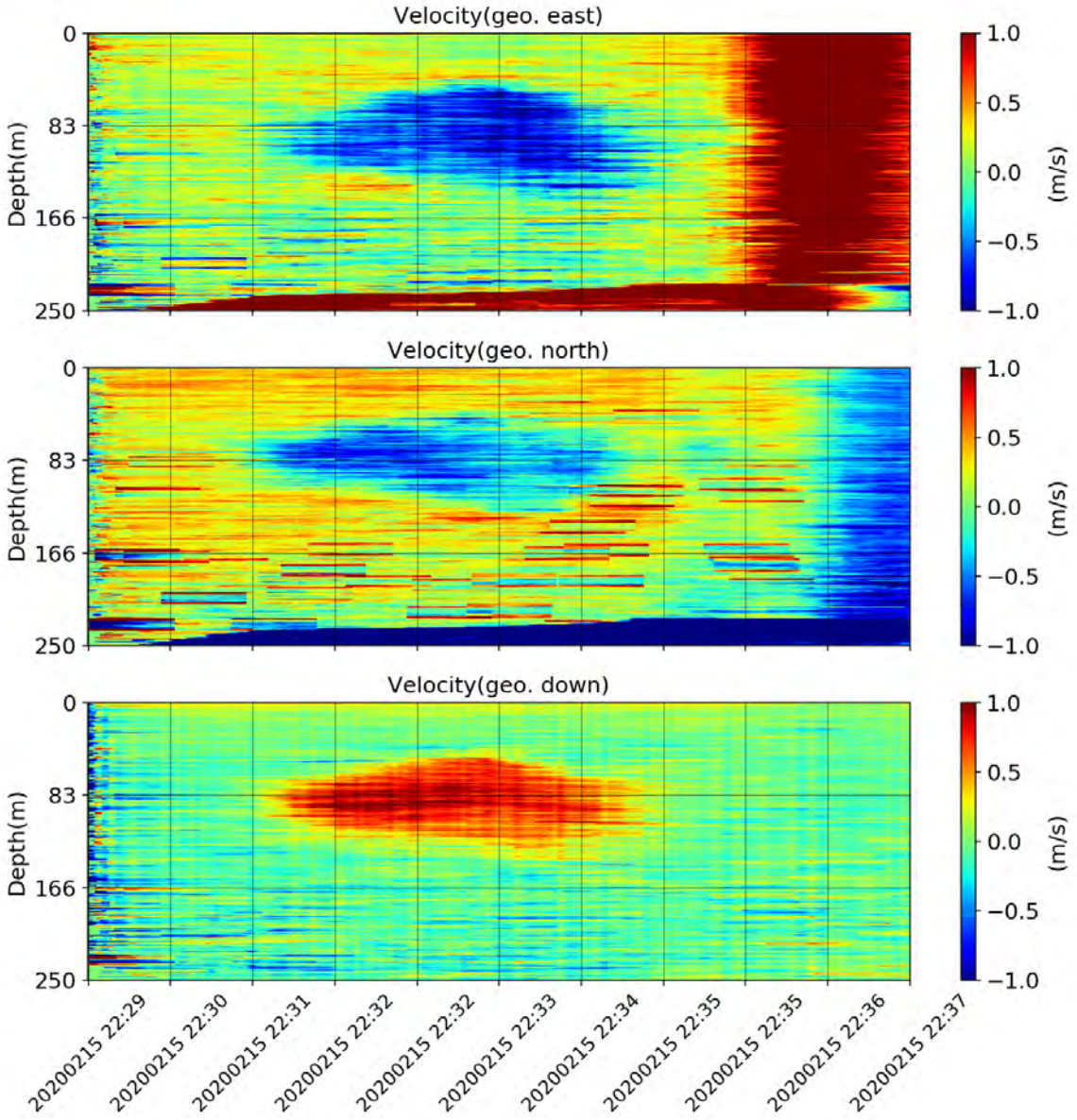

Figure 7. Phyton output of water and herring speed, georeferenced, i.e speed over ground, UPPER (East-West direction, MIDDLE (North-South direction) and LOWER : Vertical direction, Down-Up, with DOWN positive= Red. The dark red in the last part of the "echogram" is connected with a turning of the vessel, a movement which is not compensated for properly, the "sliding movement" of the ship while turning.

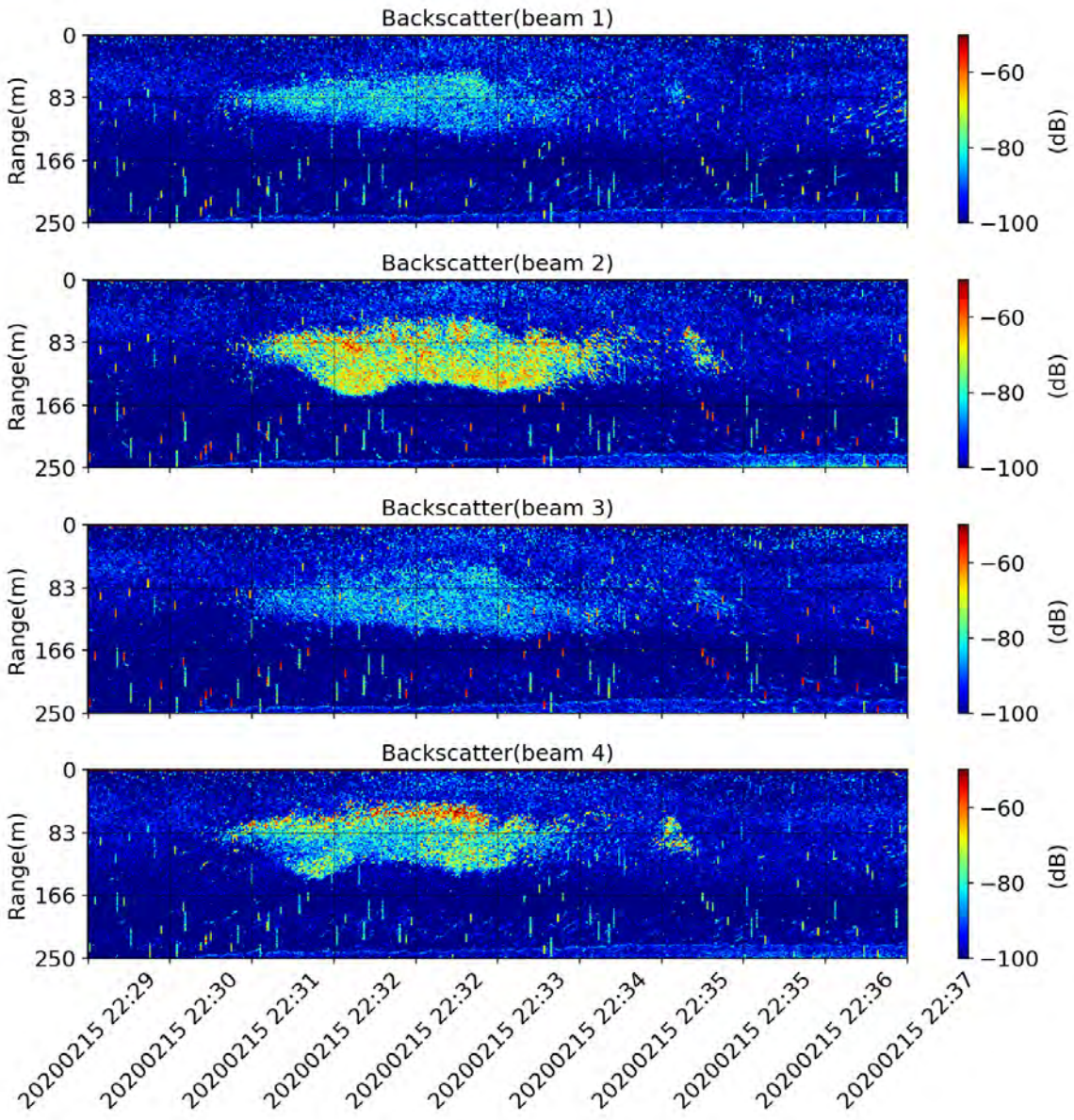

Figure 8. Echogram from the 4 ADCP beams where the Doppler is extracted.

Working document 07, WGWIDE 2020, 26 August-1 September 2020

Inventory of industry-acoustic data for potential application on blue whiting biomass estimates

Benoit Berges[1], Serdar Sakinan[1], Sytse Ybema[2], Gert-Jan Kooij[2], Martin Pastoors[3]

Abstract

Since 2012 the Dutch pelagic industry (PFA) has been engaged in the collection of acoustic data at a large scale. This working document presents an overview of the acoustic data with a focus on blue whiting. Further work will be carried out to (automatically) analyse the acoustic data and couple those results with the PFA self-sampling data. The ambition is to explore the development of an index of abundance from commercial acoustic data that could aid the blue whiting acoustic survey in case of missing surveys or bad weather conditions.

[1] Wageningen Marine Research, The Netherlands

[2] Sustainovate, Norway

[3] Pelagic Freezer-trawler Association, The Netherlands

1 Background

Since 2012 the Dutch pelagic industry (PFA) is engaged in the collection of acoustic data at a large scale. Through the years, this took the form of several projects serving abundance estimation [1]–[4] and species identification [5], [6] (SEAT project, unpublished[1],[2]). Through the course of the various projects, consistency in the type of data collected (using SIMRAD EK systems, EK60, ES70, EK80) and quality through regular calibration was ensured. Since, 2019, there is an effort to automate and standardize the data collection through the Ocean-Box system[3]. As a result, there is a wealth of quality acoustic data available that could be used to derive a range of indicators on various fish stocks in the North Sea. Since 2015, this is complemented by biological data collected through the self-sampling program put in place by PFA. This program expands the ongoing biological monitoring programs on board of pelagic freezer-trawlers by the specialized crew of the vessels [7], [8]. In the context of WGWIDE, the focus of the hereby report is on Blue Whiting and especially the inventory of data available to date for this fish species.

2 Overview of industry acoustic data available

Acoustic data on blue whiting collected by Dutch Freezer trawlers are composed of:

1. data collected and analysed through the course of two historical projects ([1], [2])
2. data collected systematically onboard specific vessels but not analysed to date.

2.1 Data from historical projects

Through the course of the two historical projects, acoustic data on blue whiting, herring and sprat has been collected. During both projects, substantial effort has been devoted to the calibration of the participating vessels.

Acoustic data collected during 2012 [1]

[1] https://sustainovate.com/portfolio/seat-phase-1/
[2] https://sustainovate.com/portfolio/seat-phase-2/
[3] https://sustainovate.com/portfolio/oceanbox/

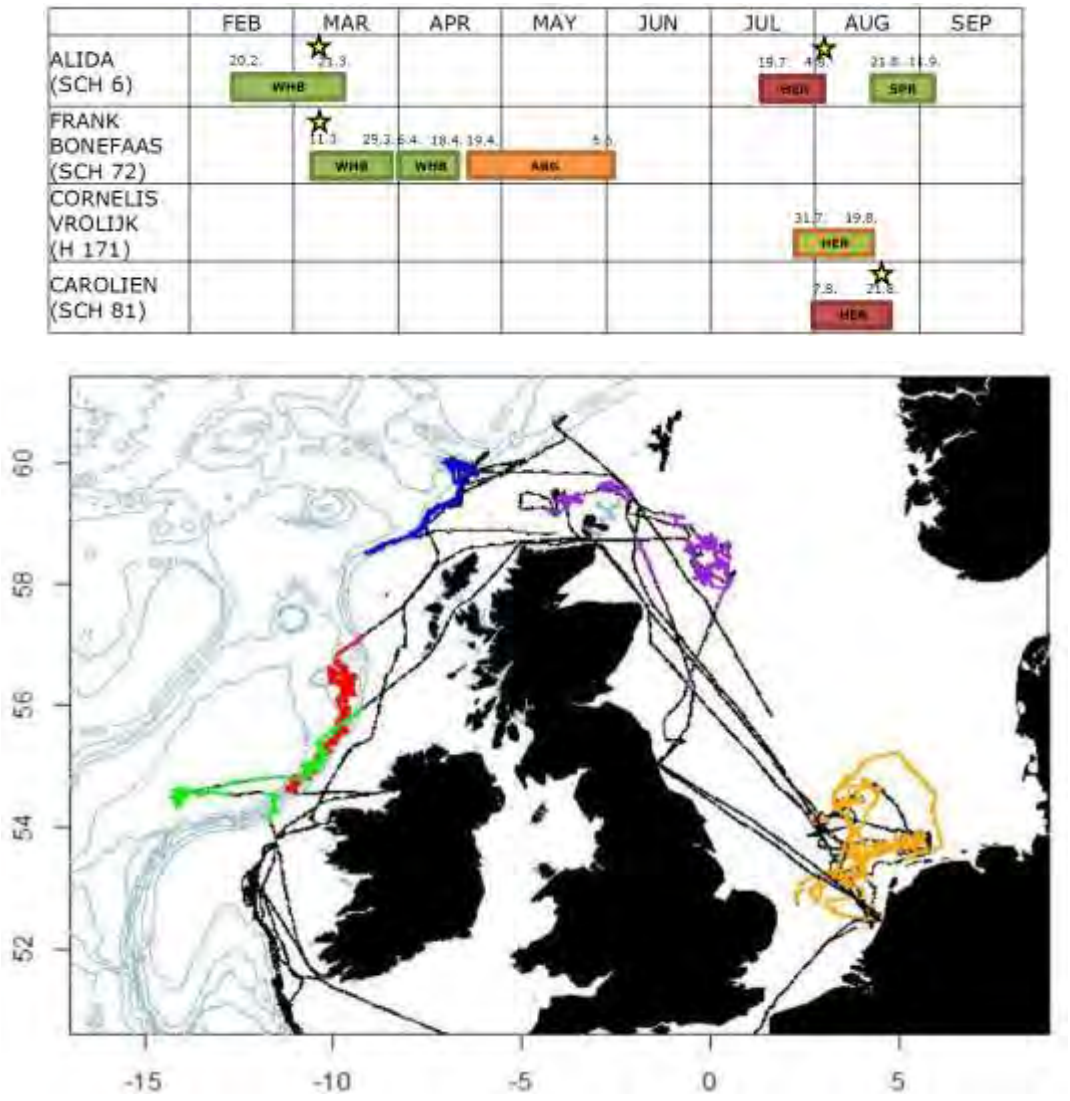

Figure 1 timing tracks of fishing trips on which acoustic data was collected during 2012. Coloured sections correspond to locations where acoustic density values of fish species were rec-orded: blue whiting (green, red and blue), herring (purple) and sprat (orange). Extracted from [1].

Acoustic data collected during 2013-2015 [2]

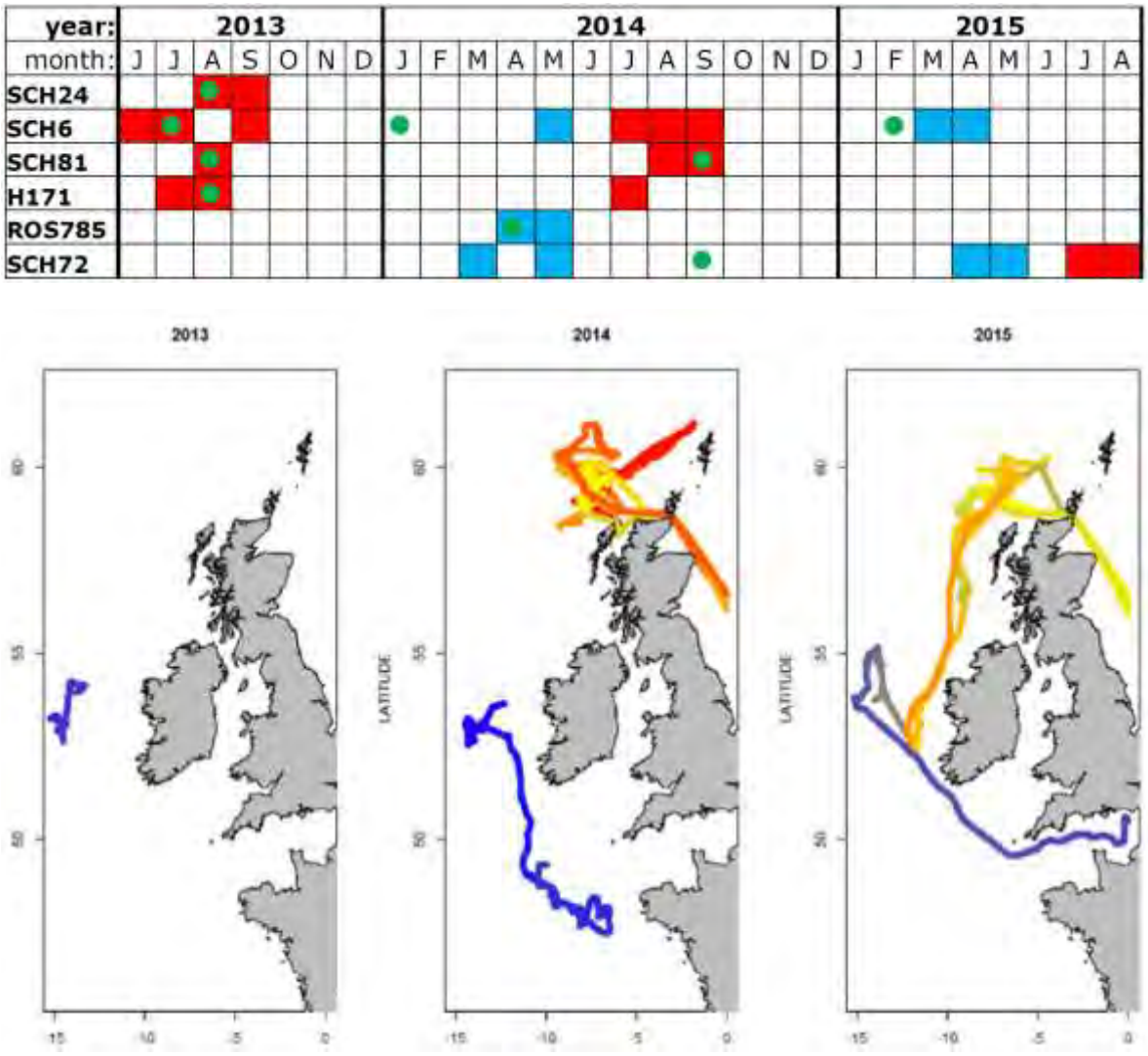

Figure 2 timing and tracks of the fishing trips during which the data was collected from 2012-2015 for blue whiting. Colouring represents the timeline of data collection (start in blue (3 March), end in red (28 May). Extracted from [2].

2.2 Data from other projects (not yet analysed)

During the course of several other projects, directed at acoustics species recognition or acoustic biomass estimation, acoustic data relevant to the blue whiting fisheries has been collected. An overview by year is presented in figure 3 and and overview by year and week in figure 4.

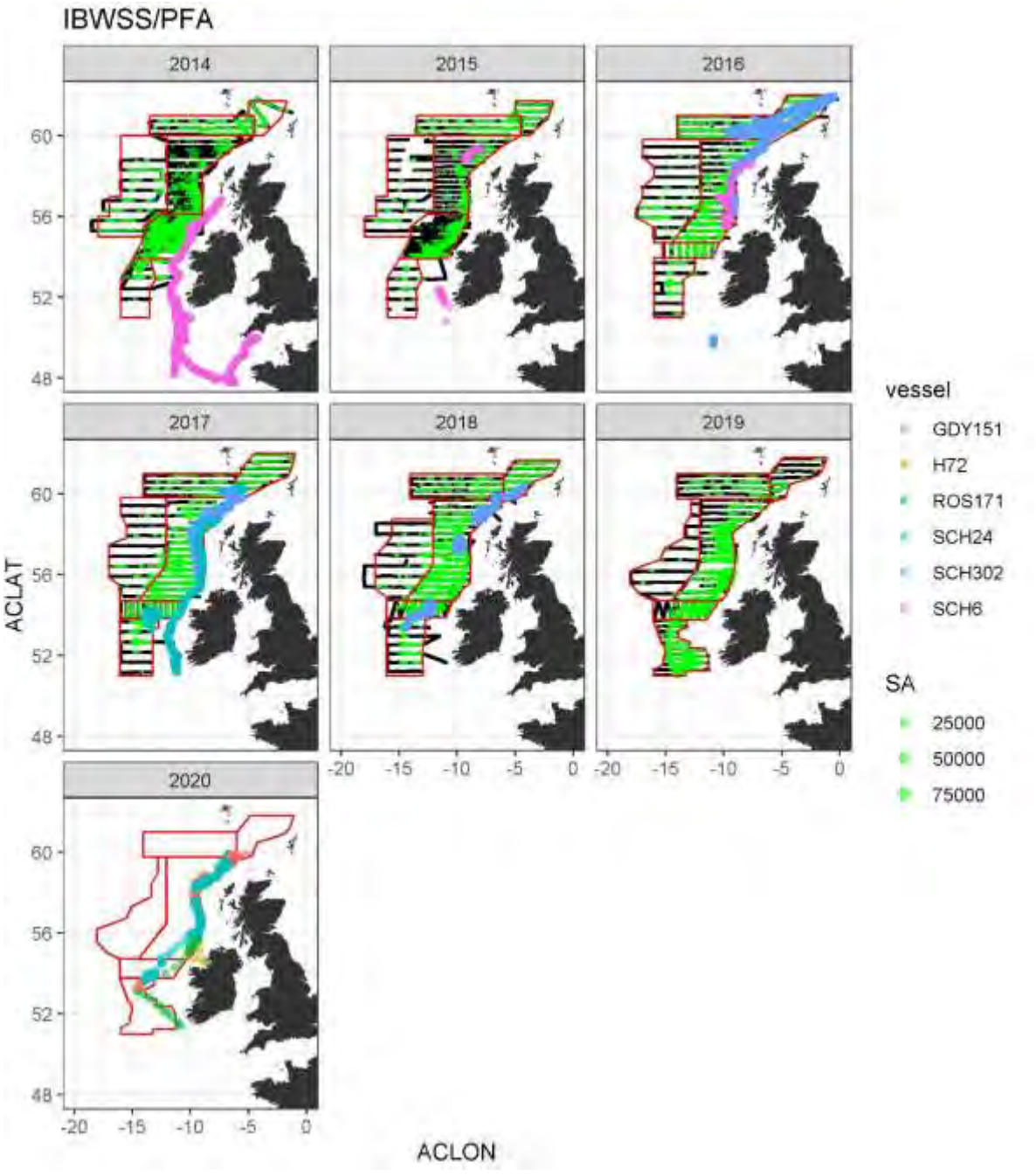

Figure 3 annual maps of acoustic data collected by PFA trawlers (associated to trips where WHB was caught) around the IBWSS surveys in the different years (March/April). Red boxes are the different strata used for the analysis of the IBWSS survey. The green circle markers are the WHB acoustic densities in 1 nmi intervals.

Figure 4 weekly maps of acoustic data collected by PFA trawlers (associated to trips where WHB was caught) around the IBWSS surveys in the different years (March/April). Red boxes are the different strata used for the analysis of the IBWSS survey. The green circle markers are the WHB acoustic densities in 1 nmi intervals.

3 Ambition and further work

In 2020, due to COVID-19 pandemics, the IBWSS survey was cancelled so that no survey index is available for 2020. Similarly, in 2010, the survey index was not used for the assessment because of disruptions in the survey. Our ambition is to explore whether data collected on board of commercial trawlers could potentially be used to derive an alternative index of abundance. The immediate ambition of this working document has been to present an overview of the data that has been collected on board of commercial trawlers since the start of the acoustic data collection projects. Currently, Wageningen Marine Research, Sustainovate and the Pelagic Freezer-trawler Association are working together to aggregate and analyse the acoustic data collected onboard freezer-trawlers in order to derive indicators blue whiting (and herring) stocks. This will be done in combination with the available self-sampling data [7].

The next steps in the project will be the analysis of the acoustic data (e.g. using automated processing) and the development of the methodology for deriving a relative abundance index over the 2012-2020 period. Of course these methods will need to deal with the biased data sampling that is implied by fishing operations. The intention is to present results of this work to WGWIDE 2021.

4 References

[1] T. Brunel, S. Gastauer, S. Fassler, and D. Burggraaf, “Using acoustic data from pelagic fishing vessels to monitor fish stocks,” IMARES (Report / IMARES Wageningen UR C021/13), p. 121, 2013.

[2] S. M. M. Fassler, T. Brunel, A. S. Couperus, S. Gastauer, and D. Burgraaf, “VIP report acoustic data collection : implementation of the structural use of acoustic data from pelagic trawlers in scientific stock estimates (PelAcousticII),” IJmuiden IMARES Wageningen UR (IMARES Rep. C178/15), p. 121, 2015.

[3] S. M. M. Fässler, T. Brunel, S. Gastauer, and D. Burggraaf, “Acoustic data collected on pelagic fishing vessels throughout an annual cycle: Operational framework, interpretation of observations, and future perspectives,” Fish. Res., vol. 178, pp. 39–46, Jun. 2016.

[4] M. Ybema and K. Johannsen, “Fish abundance estimates. A big data approach. Phase II - Pilot North Sea herring comparison,” Oslo, Sustainovate, 2020.

[5] S. M. M. Fassler et al., “VIP report ‘Use of new broadband echosounder’ : Techniques for improved ocean imaging and selectivity in pelagic fisheries,” IMARES Rep., vol. C171/15, p. 100, 2015.

[6] B. J. P. Berges et al., “Practical implementation of real-time fish classification from acoustic broadband echo sounder data,” IJmuiden Wageningen Mar. Res. (Wageningen Mar. Res. Rep. C076/19), 2019.

[7] M. Pastoors, “PFA self-sampling report 2015-2018,” PFA, vol. 03, 2019.

[8] M. Pastoors, “Self-sampling Manual v 2.12,” PFA2, vol. 05, 2019.

Working document 08, WGWIDE 2020, 26 August - 1 September 2020

Progress report on industry gonad research in the context of the “Year of the mackerel and horse mackerel 2019-2020”

Cindy van Damme, Ewout Blom, Martin Pastoors, 30/08/2020 16:52:02

Abstract

This Working Document summarizes the status of the industry-science collaboration aimed at improving the knowledge on gonad development of mackerel and horse mackerel. The work is based on samples taken by the fishing industry (PFA) on targeted or bycatches of mackerel and/of horse mackerel. The overall aim of the Year of the Mackerel project is to gain insight in the gonad devel-opment of female and male mackerel throughout the year in order to better understand the spawning strategy. For horse mackerel, the aim is to investigate when western horse mackerel spawning occurred in 2020. To date, 1365 mackerel have been sampled and 197 horse mackerel (horse mackerel only started in 2020). Preliminary results of the analysis on mackerel are presented in the working document. Final results for mackerel are expected in October 2020 and for horse mackerel in the first half of 2021.

1 Introduction

Mackerel

The stock of Northeast Atlantic mackerel has raised a lot of attention over the last number of years. The expansion of the area of distribution of mackerel has been very conspicuous, with mackerel now being caught much more westerly and northerly compared to the past. In recent years also changes in spawning are apparent, with changes in timing and centre of gravity of spawning. Dealing with a stock with such a wide area of distribution from the west of Portugal all the way to the Norwegian Sea is providing a continuous challenge to attempt to monitor the development of this stock. Unfortunately we have also witnessed some hick-ups in the scientific assessment and advisory system in recent years that have resulted in substantial revisions of the perception of stock size. This is a highly valuable stock and it is beyond question that getting the best available understanding of stock development and stock behaviour is in the interest of everyone involved with this stock.

Currently there are five main information sources to inform the stock assessment of mackerel:

1. Commercial catches reported by each country
2. Recruitment index based on coordinated international scientific survey 'IBTS'
3. Tagging time-series – with tags recovered from X factories
4. Scientific swept-area survey in the northern feeding area
5. Egg survey in the spawning areas every 3 years.

The fishing industry has been getting involved in providing data on mackerel through different means, such as the mackerel tagging program and providing vessels to conduct the swept-area survey and the mackerel egg survey. In all cases, understanding the spatial-temporal patterns of mackerel is key to making these sources reliable indicators for stock assessment. There is a need to improve understanding of how mackerel gonads develop ane when and where mackerel spawn (or do not) because this information could affect the design of the mackerel egg survey and possibly also how spawning stock biomass is calculated from the stock in numbers within the stock assessment model.

In order to follow the gonad development, it is necessary to prepare histological sections of the gonads to follow the growth of oocytes and spermatozoa. Ideally, gonads would be fixed in formaldehyde before they are sectioned. On commercial vessels, were fish is caught for human consumption, it is not allowed to have formaldehyde on board. Thus, samples from

commercial vessels will have to be frozen before being fixed in formaldehyde. During the spawning season tests have already been carried out with frozen samples to investigate the quality of the histological sections and the oocyte development. During a pilot project in 2018, it was tested if it is possible to prepare high quality histological sections from frozen mackerel gonads outside the spawning season.

The resulting photographs of these histological sections were discussed with international colleagues during the Workshop on egg staging, fecundity and atresia in horse mackerel and mackerel (WKFATHOM) in 2018. The report of the workshop is not yet available. The main conclusions of this discussion were:

1. The quality of the male and female gonad sections of the frozen fish is surprisingly good and enough to follow oocyte and spermatozoa development through time.
2. Staining of the male gonads needs to be improved at the start of the Year of the Mackerel project in order to be able to more easily see the development of the spermatozoa.
3. Working with fixed frozen mackerel gonads is possible.

Horse mackerel

Horse mackerel (Trachurus trachurus) is one of the most important pelagic species for the freezer-trawler fleet (https://www.pelagicfish.eu/species). At the moment the western horse mackerel spawning stock biomass (SSB) is low (ICES, 2019a). In 2017 SSB was estimated as the lowest in the time-series, below the limit reference point and just above in 2018 (ICES, 2019a). Currently there are four main information sources to inform the stock assessment of western horse mackerel:

1. Commercial catches reported by each country
2. Recruitment index based on coordinated international scientific survey 'IBTS'
3. Acoustic survey SSB estimate
4. Egg survey in the spawning areas every 3 years.

One of the indices used for the assessment is the annual egg production estimated from the mackerel and horse mackerel egg survey results. This survey is coordinated by the ICES Working Group for Mackerel and Horse mackerel Egg Surveys (WGMEGS). Once every three years this survey covers the spawning area of mackerel and horse mackerel during the spawning season (ICES, 2019b). To get an accurate estimate of the annual egg production of horse mackerel, the egg survey should sample the entire spawning area multiple times during the spawning season. Because horse mackerel is an indeterminate spawner the Daily Egg Production Method (DEPM; i.e. estimating batch fecundity and daily egg production)

should be used for converting egg production to SSB (Damme et al. 2013). WGMEGS is currently investigating the possible collecting of batch fecundity samples for the DEPM survey (ICES, in prep.). Therefore, WGMEGS currently provides only an egg production estimate for the horse mackerel assessment and not a SSB estimate.

Western horse mackerel spawns in the northern Bay of Biscay, Celtic Sea and west of Ireland (ICES, 2019b). In the past, horse mackerel spawning occurred in May-July, with peak spawning in June. This was overlapping with mackerel (Scomber scombrus) spawning from February till July (See WGMEGS reports). In the last decade the mackerel stock has increased, and the horse mackerel stock has decreased. This has coincided with horse mackerel gradually spawning later in the year (ICES, 2014, 2017, 2019b).

At the moment there are doubts whether the current time window of the mackerel and horse mackerel survey still covers the horse mackerel spawning season. In 2013 the peak of spawning of horse mackerel occurred in July, the last month of the mackerel and horse mackerel egg survey (ICES, 2014). WGMEGS could therefore not be certain if the actual spawning peak had been sampled that year. In 2016 an extra survey was added at the end of July, to check for continued spawning of horse mackerel (ICES, 2017). This survey showed that the peak of horse mackerel spawning occurred earlier in July 2016. In 2019 the egg survey last sampling period was in beginning July (ICES, 2019b). The numbers of eggs found in June and July were very low compared to previous surveys, with a very small peak at the beginning of July (ICES, 2019b). Investigating gonad samples of horse mackerel showed that only few horse mackerel had started spawning and a high percentage were still developing oocytes and did not show signs of spawning (ICES, in prep.). This was contrary to 2016 and 2013 surveys when horse mackerel gonads did show signs of spawning. Based on this WGMEGS concluded that it was highly likely that the egg survey of 2019 missed the peak of western horse mackerel spawning and that the egg production estimate was not a reliable index as before (ICES, in prep.). The question is: has the western horse mackerel spawning shifted to later in the year and when is the actual horse mackerel spawning occurring?

2 Research questions

Mackerel

The overall aim of the Year of the Mackerel project is to gain insight in the gonad development of female and male mackerel throughout the year in order to better understand the spawning strategy. On a monthly basis male and female mackerel will be collected by the pelagic industry throughout the distribution area of mackerel. Histological sections will be prepared of the gonads. Each gonad will be analysed to identify which development stages of oocytes and spermatozoa are present in the gonad. This will allow to follow the gonadal development over time and determine the timing when mackerel is ready for spawning.

Horse mackerel

For annual egg production to be an accurate index of SSB, it is necessary that the entire spawning area is sampled multiple times for eggs during the spawning season. As western horse mackerel spawning has gradually shifted to later in the year (ICES, 2019b) and the sampling periods have not been extended, it is unlikely that the results of the mackerel and horse mackerel egg surveys provided an accurate estimate of western horse mackerel in 2019 (ICES, in prep.). In this project we will investigate when western horse mackerel spawning occurred in 2020. This information can be used to inform WGMEGS for the planning of the 2022 mackerel and horse mackerel egg survey and try to improve horse mackerel sampling.

By collecting western horse mackerel gonad samples from May till November it is possible to follow the development of oocytes in the ovaries and sperm cells in the testis and to check for spawning activity. Hydrated oocytes, eggs and post-ovulatory follicles (POFs) in an ovary are signs of recent spawning. Motile spermatozoa are sings of male spawning activity. Such sampling would provide evidence of the actual spawning period and of a possible shift of spawning to later in the year.

3 Approach

Fish were collected on board the vessels, aim was to collect 25 fish, both females and males during each fishing trip. During an egg survey gonad samples are directly fixed in 3.6% buffered formaldehyde, but on fishing vessels formaldehyde is not allowed. It was decided to use frozen samples, which are shock-frozen on board and will be fixed in the laboratory before being defrosted. In November 2018 a test was run with 50 gonads to test if this method would work. Although we saw deterioration of the samples compared to freshly fixed gonads the samples were of good enough quality to do the required analyses on to be able to investigated development within the gonads.

The first sampling started in February 2019 and continued until February 2020. Mackerel were collected from the fishing hauls. Immediately after catch the gonads and guts were taken from the fish. The gonad was put in a small plastic bag, the fish in another plastic bag. The gonad was than added to the bag with the fish. The large bag containing fish and gonad was labelled and shock frozen as soon as possible. The shock freezing is important in this aspect as that produces less damage to the tissue inside the gonads compared to regular freezing.

The frozen fish and gonads arrived in the laboratory in Ijmuiden (Fig 3.1). Fish and gonad was measured in the lab and maturity stage determined. Without defrosting the gonad was put in 3.6% buffered formaldehyde, to defrost and fix at the same time (Fig 3.1). The fish was than left to defrost and the next day otoliths were collected for age estimation. After two weeks in formaldehyde the gonads were properly fixed and could be cut for preparation of histological slides.

From the fixed gonad a slice of about 0.5 cm is cut (Fig 3.1). For the males it is important that this part is taken from the middle of the testis to ensure the spermatoduct is part of the 0.5 cm section. For the females it has been tested and oocyte stages are homogeneous distributed throughout the gonad, thus the exact position of the cutting is less important. However to ensure enough material a section from the middle part of the ovary was taken as well, unless the ovary was damaged. In case of damage a section of the non-damaged part was taken.

The 0.5 cm section was put in a fine mesh cassette (Fig 3.2). The cassettes were put in ethanol for dehydration (Fig 3.2). There are multiple steps of dehydrating the samples in different ethanol solutions. After the dehydration the samples are infiltrated with historesin (Fig 3.2). Again in multiple steps increasing the historesin concentration. After infiltration

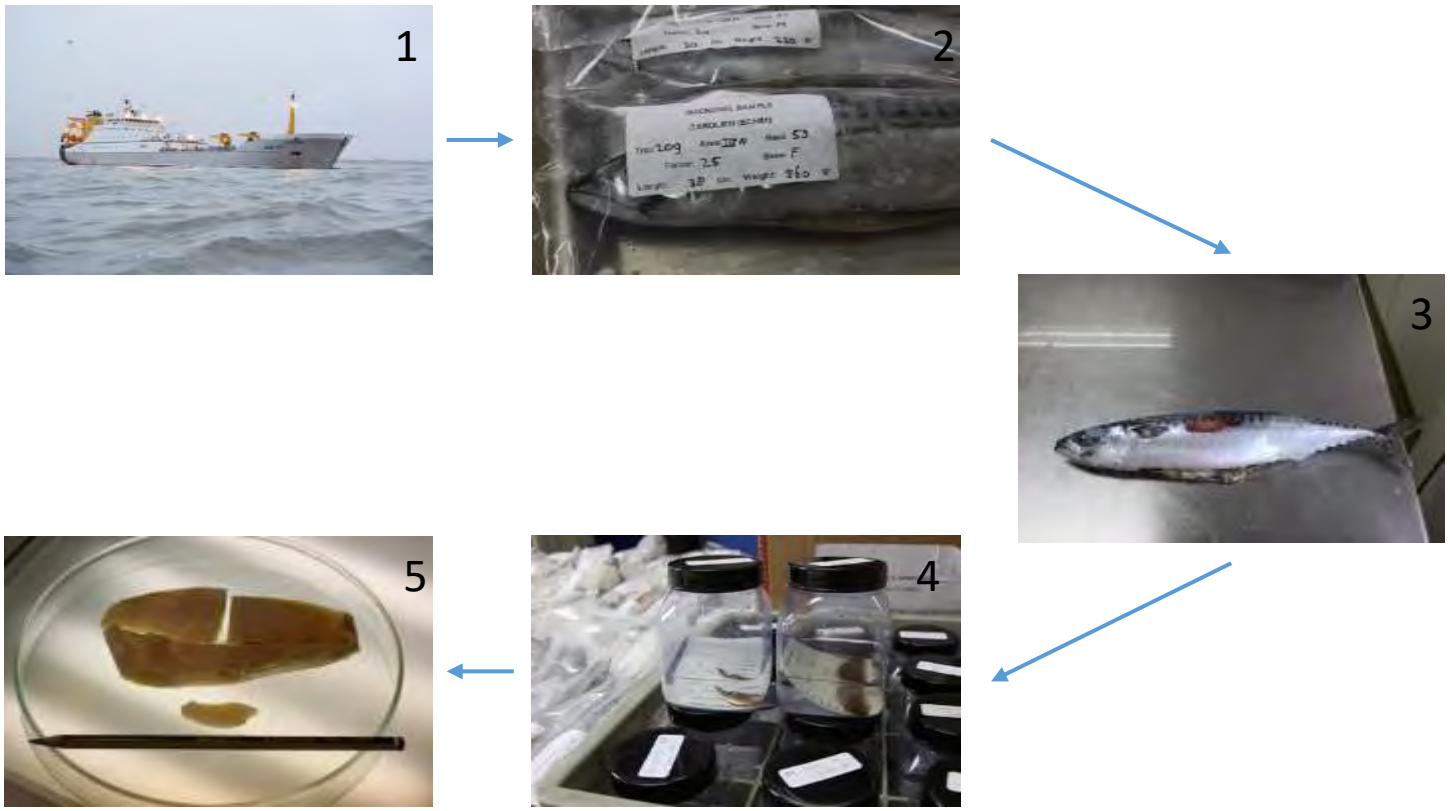

Figure 3.1. Fish was collected on board (1), gonads were dissected and frozen separately from the fish, and kept in the same large plastic bag with the fish (2). In the laboratory the frozen fish was measured and gonad weight taken (3) and the still frozen gonad was put in 3.6% buffered formaldehyde (4). After two weeks in formaldehyde the gonads are ready to be cut for the preparation of histological slides (5).

the samples are put in moulds and polymerised with clean historesin (Fig 3.2). The samples need to be cooled for a good polymerisation in the moulds. Afterwards the moulds are put in the fridge. The next day the samples are blocked up (Fig 3.2) and taken from the moulds. The blocks are kept in a box with high humidity to ensure the thin sections can be taken later on. This whole process takes about two weeks.

After some days in the humidity the samples are ready to be sectioned. Sections of 4 µm are cut and stained with haematoxylin and eosin. After mounting and covering the sections are ready for analyses (Fig 3.3).

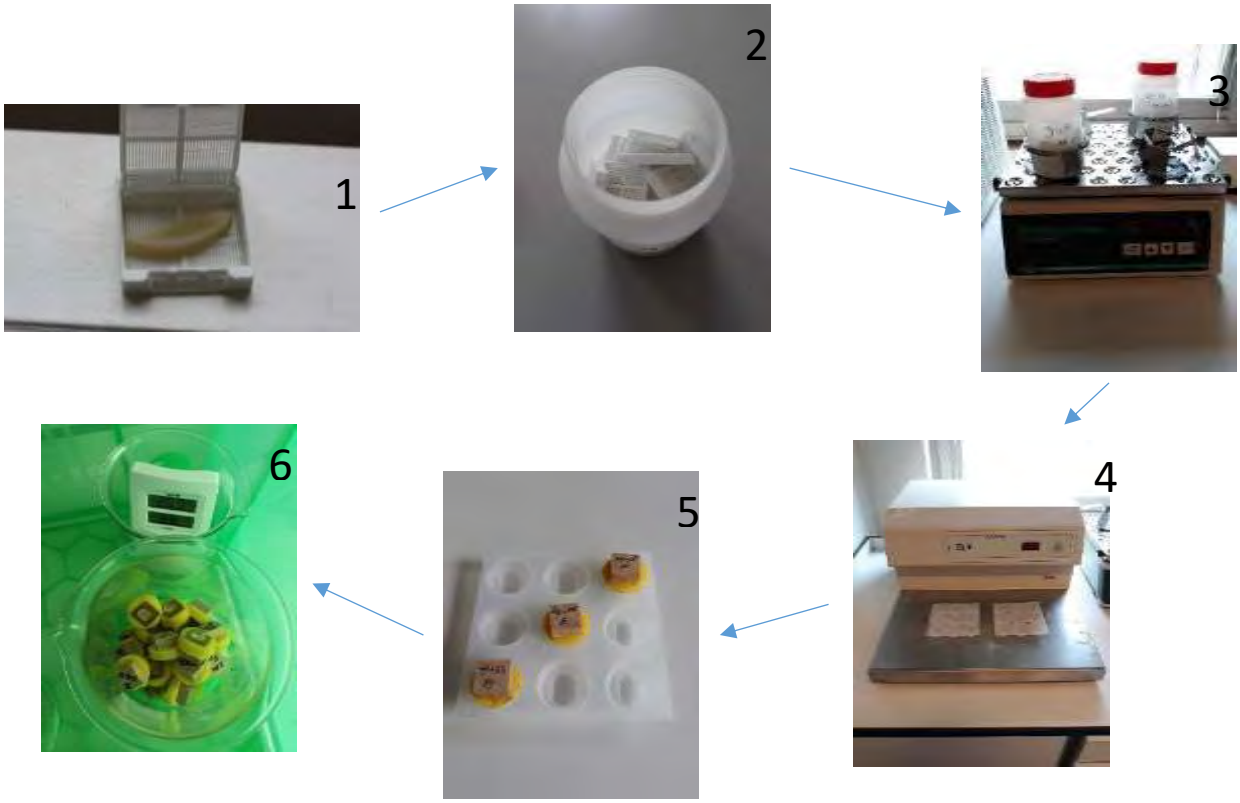

Figure 3.2. Preparation of the sample for sectioning. Gonad section of 0.5 cm is put in the cassette (1) and dehydrated in multiple ethanol steps (2). After dehydration samples are infiltrated with historesin (3) in multiple steps. Afterwards the samples are put in the moulds for polymerisation on a cooling plate (4). The samples are blocked up and marked (5) and kept in humid conditions (5) for later sectioning.

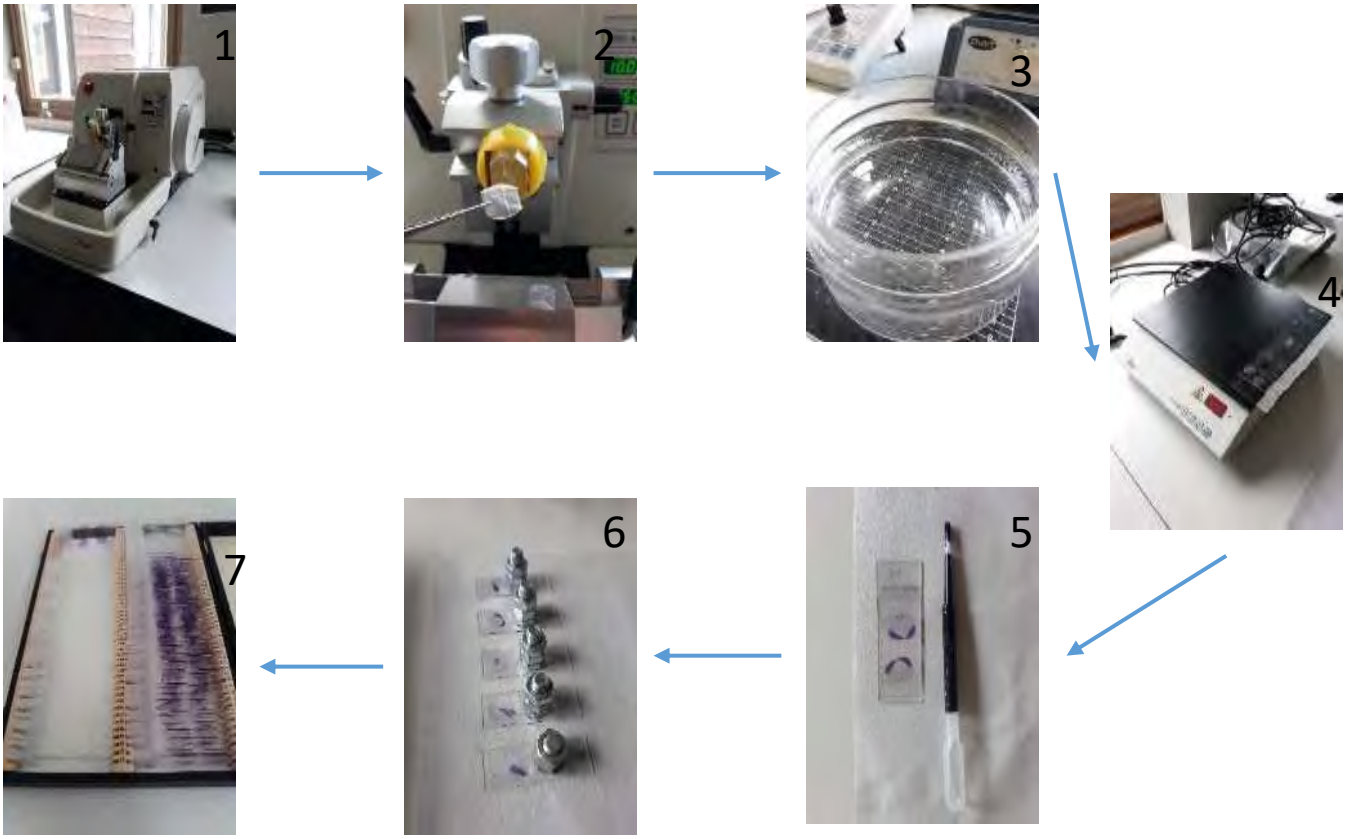

Figure 3.3. Preparation of the histological sections. On the microtome sections of 4 µm are cut (1 and 2). These are put in a water bath containing a few drops of ammonia (3). Samples are taking up on a glass slide and dried on a hot plate (4). The section is stained (5) and covered with a cover glass (6) and ready for analyses (7).

The female histological slides are scanned and images are examined in Hamamatsu NDP-viewer (Fig 3.4). Female ovaries sections are first screened for presence/absence of oocyte development stages. Afterwards two images at 5X magnification are selected. These images are analysed using a Weibel grid to estimate the area proportion of each of the oocyte development stages. On each image also the number of oocytes in each development stage is counted for an estimation of the oocytes in the gonad. The last step is the measurement of the oocyte diameter. In each 5X magnification image the 5 largest oocytes in each development stage are measured.

The male testis histological slides were only screened for presence/absence of the sperm cell development stages in the testis and in the spermatoduct.

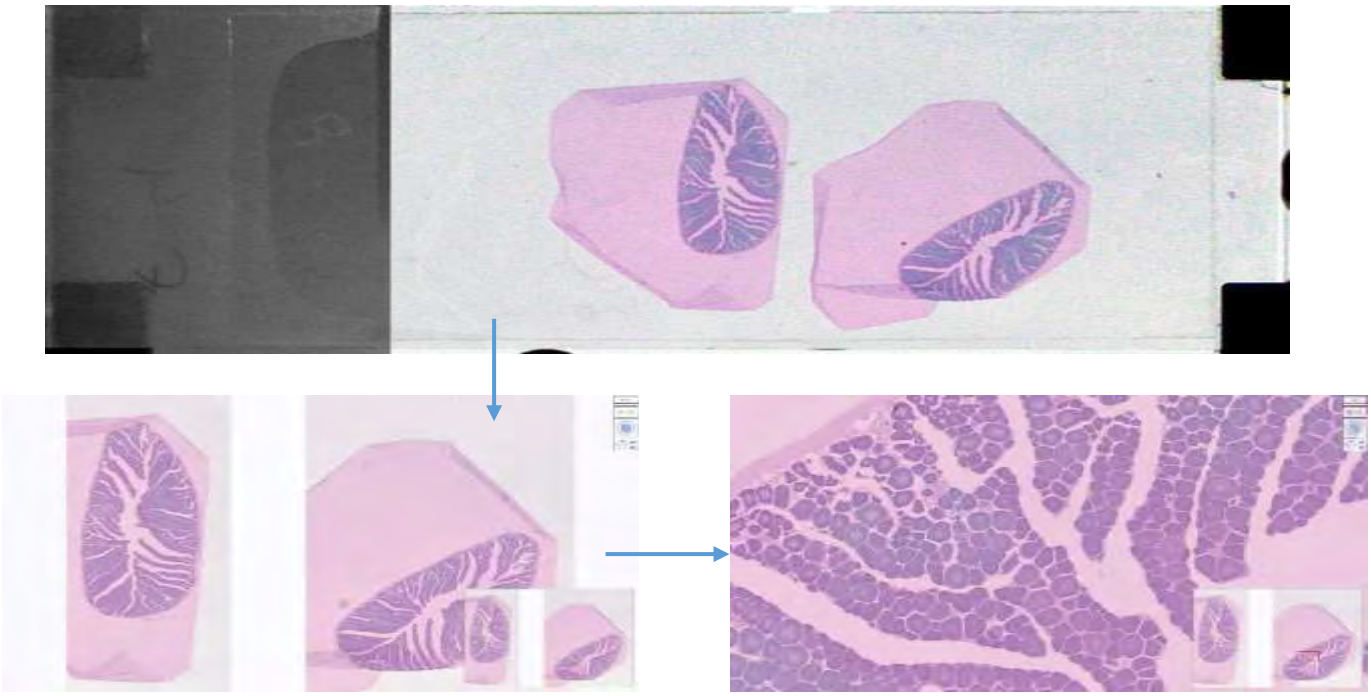

Figure 3.4. Histological section (top) zoomed in at 0.5X and 5X in NDP-viewer.

4 Samples collected

Overview of sampled hauls

year	month	nvessels	ntrips	nhauls	mac	hom
2019	2	3	3	30	51	0
2019	3	4	6	43	65	0
2019	4	4	5	24	40	0
2019	5	2	2	42	107	0
2019	6	1	1	8	28	0
2019	7	4	4	57	93	0
2019	8	4	7	93	131	0
2019	9	5	8	61	88	25
2019	10	5	6	49	73	0
2019	11	3	3	25	39	0
2019	12	4	4	39	66	0
2019	(all)		49	471	781	25
2020	1	5	7	52	132	0
2020	2	6	8	45	95	0
2020	3	6	8	86	169	0
2020	4	5	7	90	160	0
2020	5	3	5	40	28	21
2020	6	4	6	46	0	83
2020	7	2	2	21	0	66
2020	8	1	1	2	0	2
2020	(all)		44	382	584	172
(all)	(all)		93	853	1365	197

Table: Number of individuals

Haul positions

An overview of all self-sampled hauls in fisheries where mackerel or horse mackerel samples were taken.

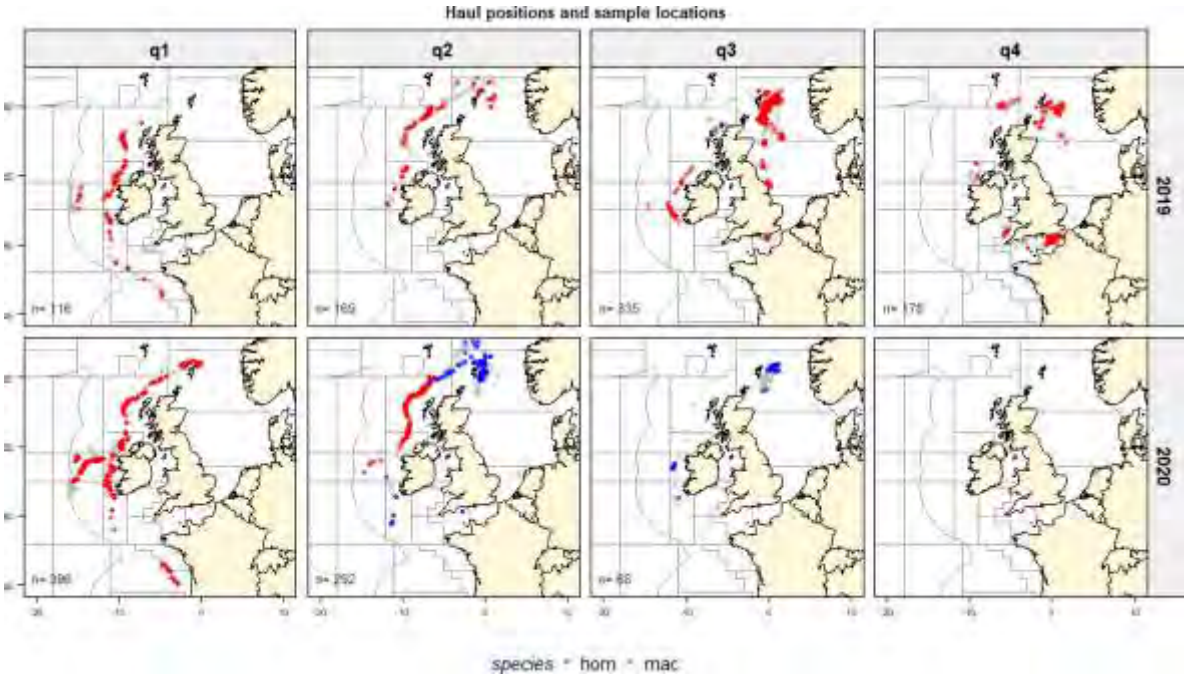

Figure 3.1: Haul positions in PFA self-sampled "Year of the Mackerel" (red). N indicates the number of sampled mackerel.

Length distributions by quarter

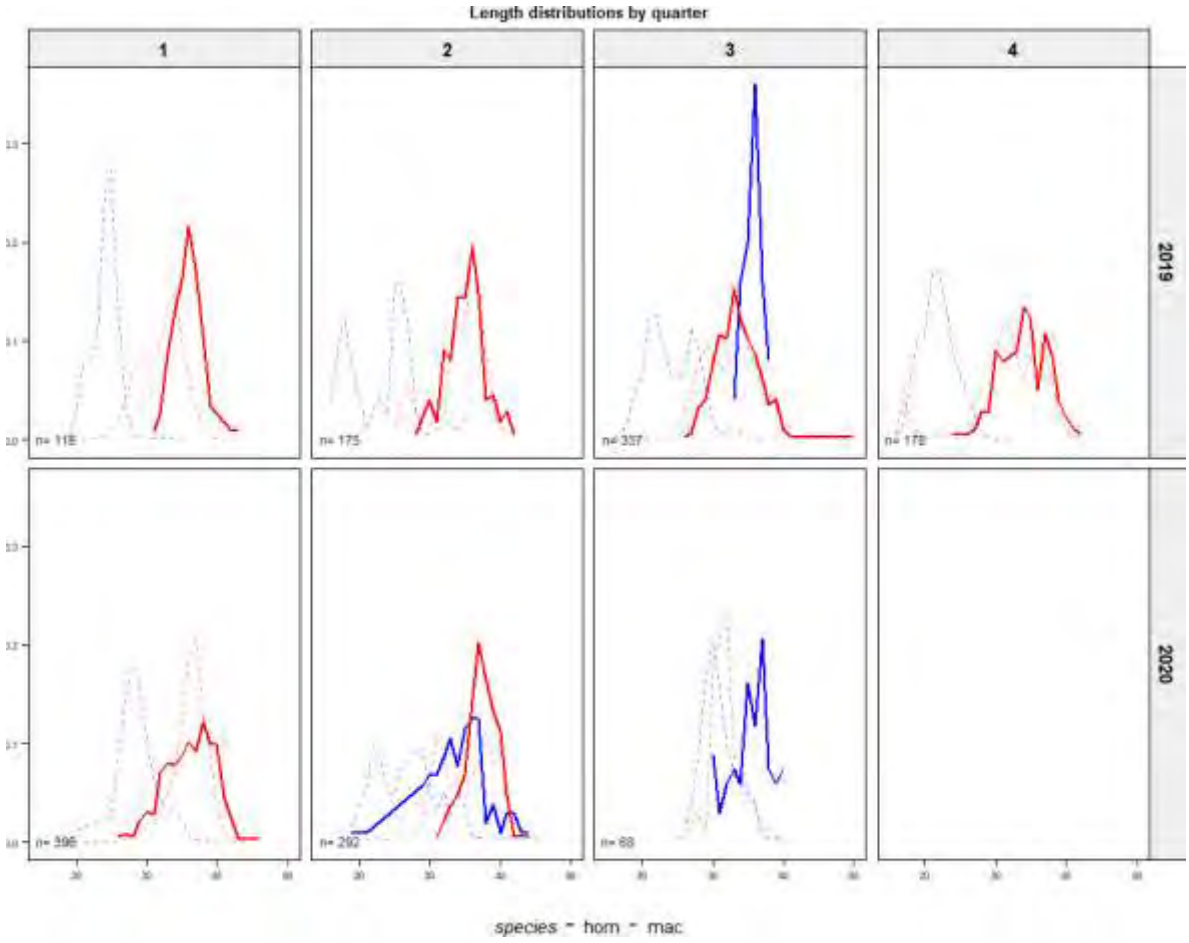

Figure 3.2: Comparing length compositions.

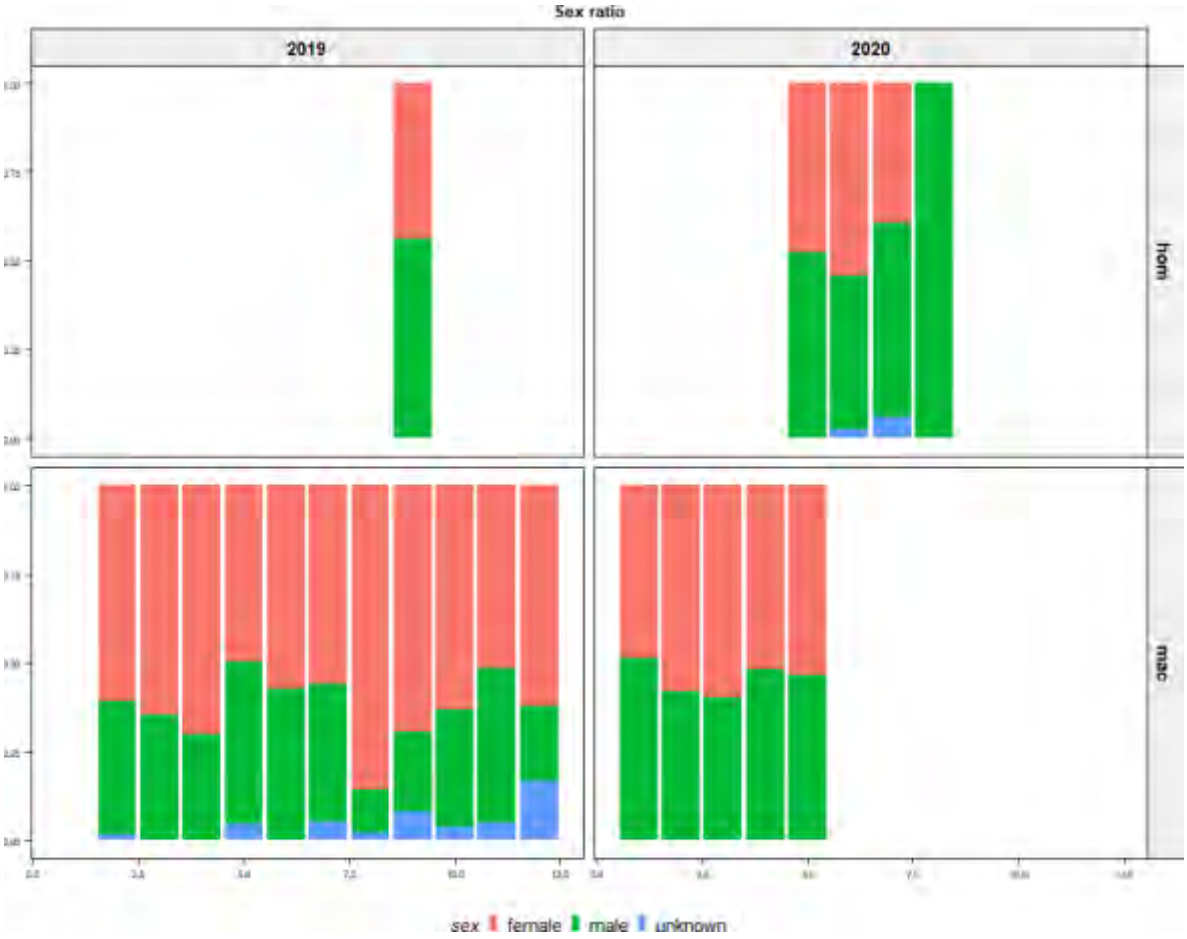

Figure 3.3: Sex ratio.

5 Results of analyses

[Ongoing]

Length of female mackerel analysed over the year did not vary much, although the mackerel in January to April are slightly larger compared to the other months (Fig 5.1). The variation in weight over the year is larger, with high weights in January to April, but also in September and October after the summer feeding period (Fig 5.1). Ovary weights were significantly higher in January to April compared to the other months (Fig 5.1). Highest ovary weights were found in February. The oldest fish were caught in the first four months of the year, which coincided with the slightly larger fish caught in this period (Fig. 5.1).

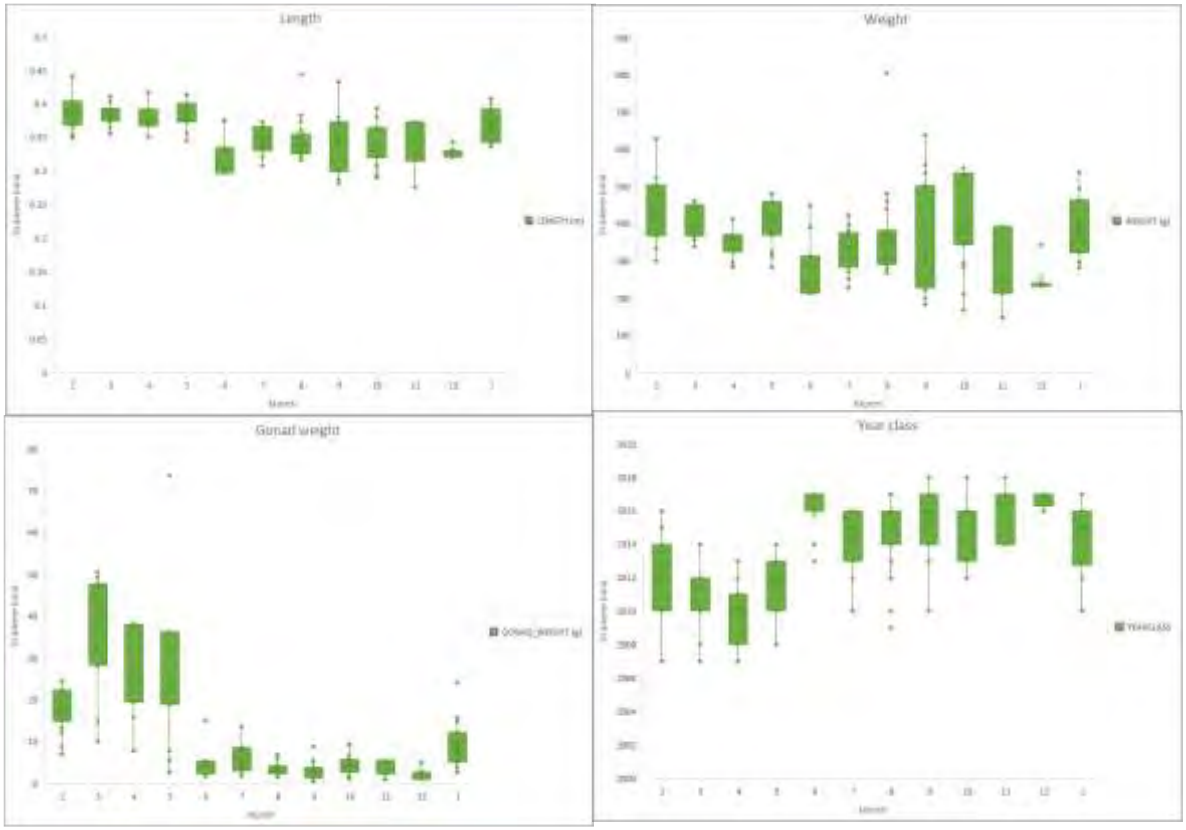

Figure 5.1. Length, weight, ovary weight and year class of the females analysed.

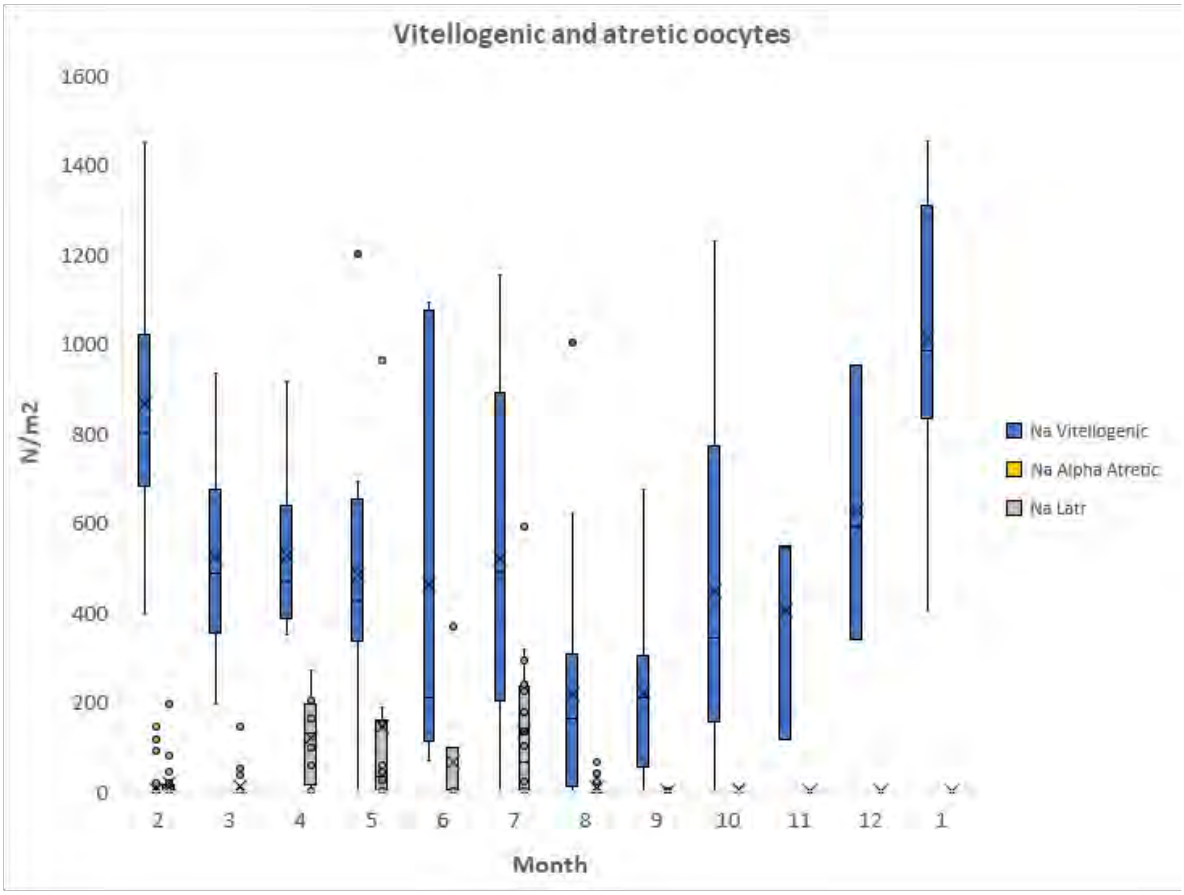

Figure 5.2. Number of vitellogenic and atretic oocytes in the ovaries per cm^2 over the year.

Vitellogenic oocytes were found in all months of the year, these are oocytes that are being developed. Higher numbers of vitellogenic oocytes were found in January-February, prior to spawning (Fig 5.2). Lower numbers of vitellogenic oocytes were found in July and August. This indicates that mackerel are always developing oocytes over the year and there is no resting period in the ovary between the actual spawning periods. Atretic oocytes are only found in February to July (Fig 5.2). This seems to suggest that from August to January the females are preparing oocytes for the next spawning season.

From August to January early vitellogenic oocytes dominate, while from February to July late vitellogenic oocytes are present (Fig 5.3). This supports the fact that the spawning season runs from February to July and females are only preparing oocytes for the next spawning season from August to January.

Few eggs were actually found in the samples (Fig 5.4), but post-ovulatory follicles (POFs) were present in higher numbers. POFs are the follicle that is left after the egg is spawned. POFs were also seen late in the year, indicating the long period it takes for POFs to be resorbed.

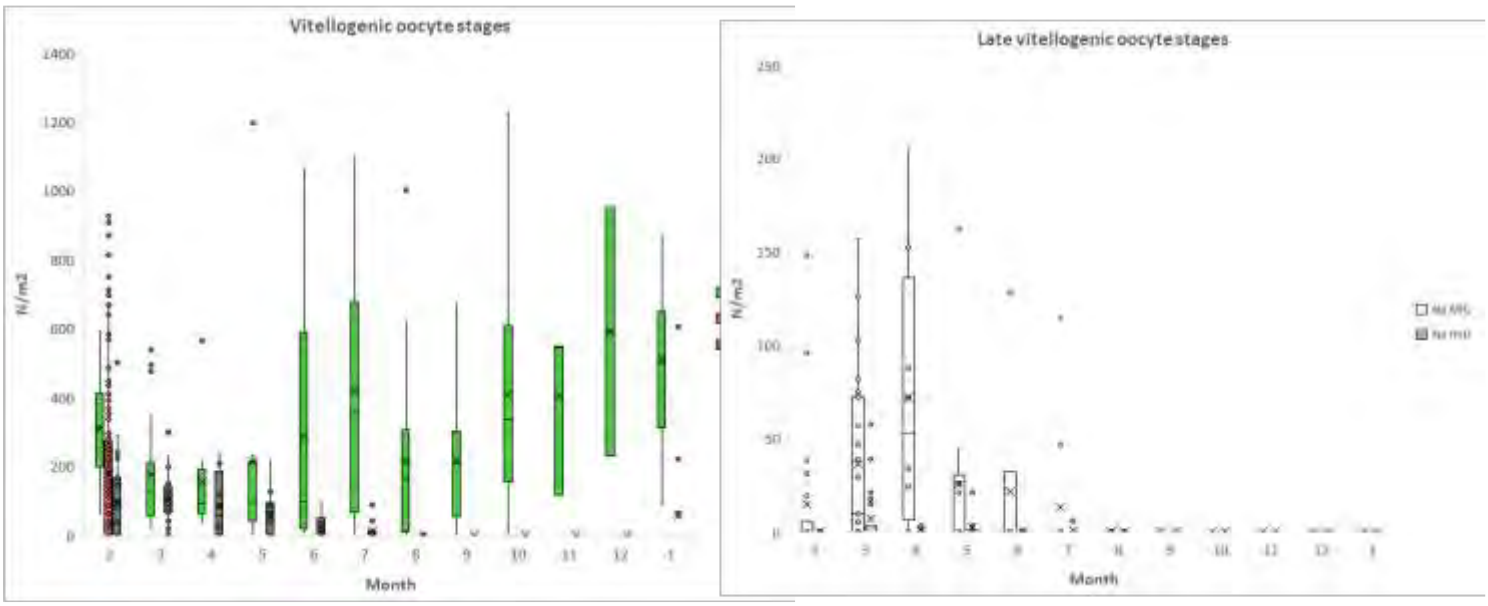

Figure 5.3. Early and late vitellogenic oocytes in the ovaries per cm^2 over the year.

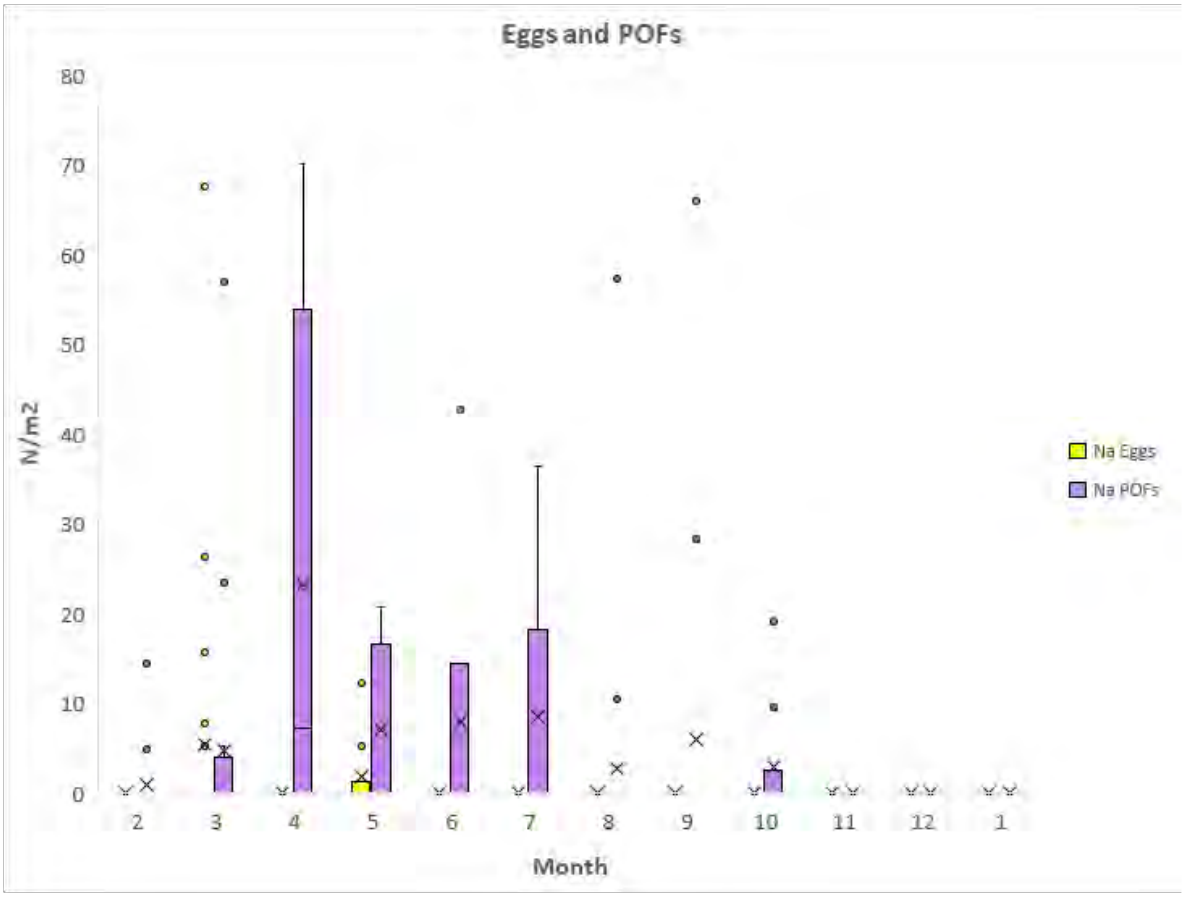

Figure 5.4. Number of eggs and POFs in the ovaries per cm^2 over the year.

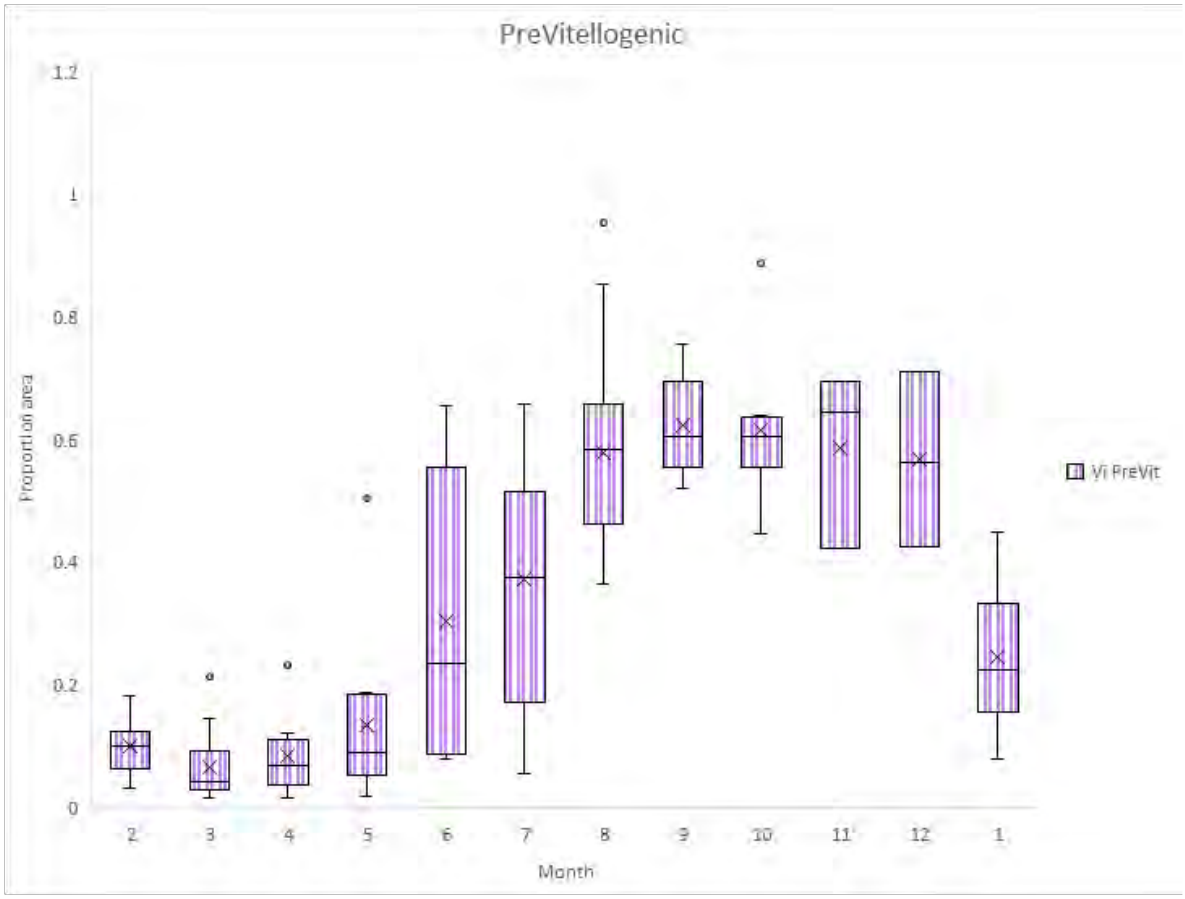

Figure 5.5. Proportion area of previtellogenic oocytes in the ovaries over the year.

Proportion area of previtellogenic oocytes (oocytes that are not being developed) was low January to May, increased June and July and was highest from August to December. This also shows that the spawning season runs from February till May, and June-July the spawning season is coming to an end (Fig 5.5).

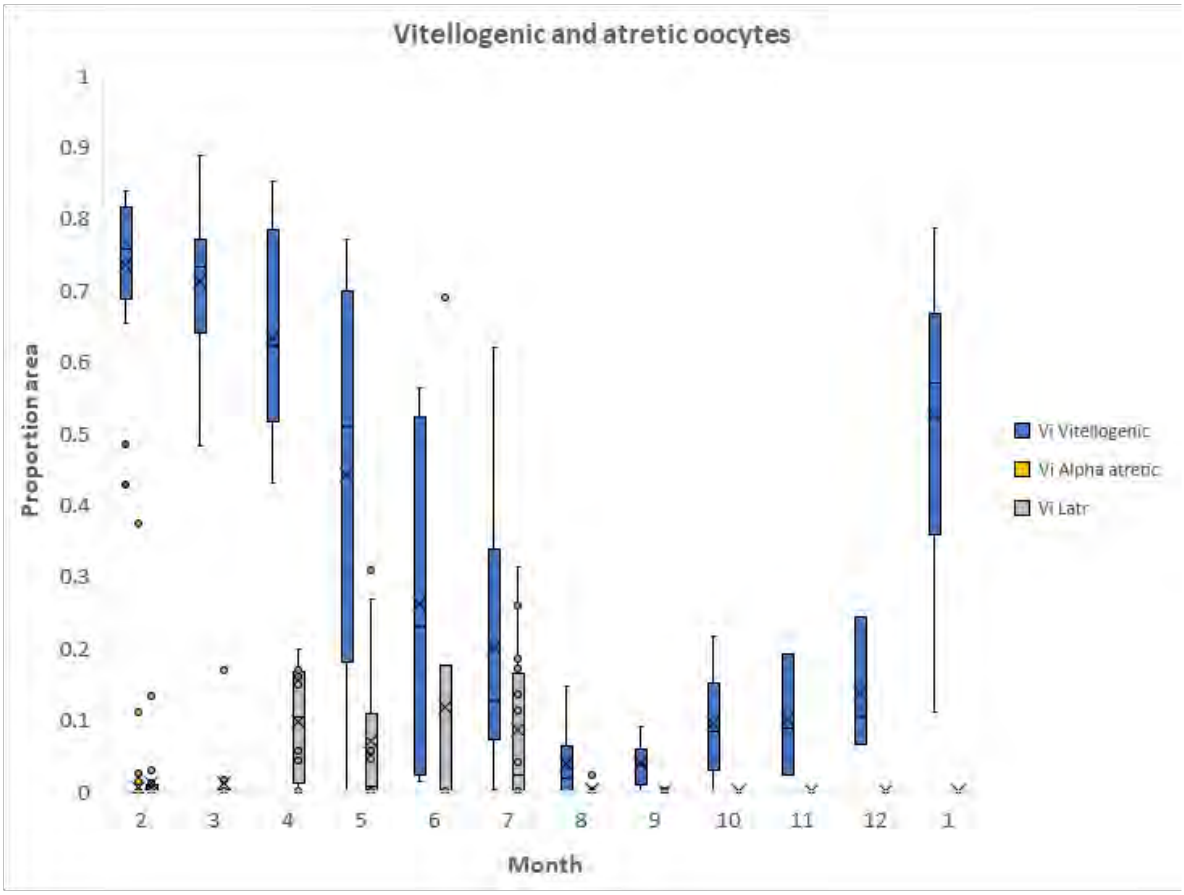

Figure 5.6. Proportion area of vitellogenic and atretic oocytes in the ovaries over the year.

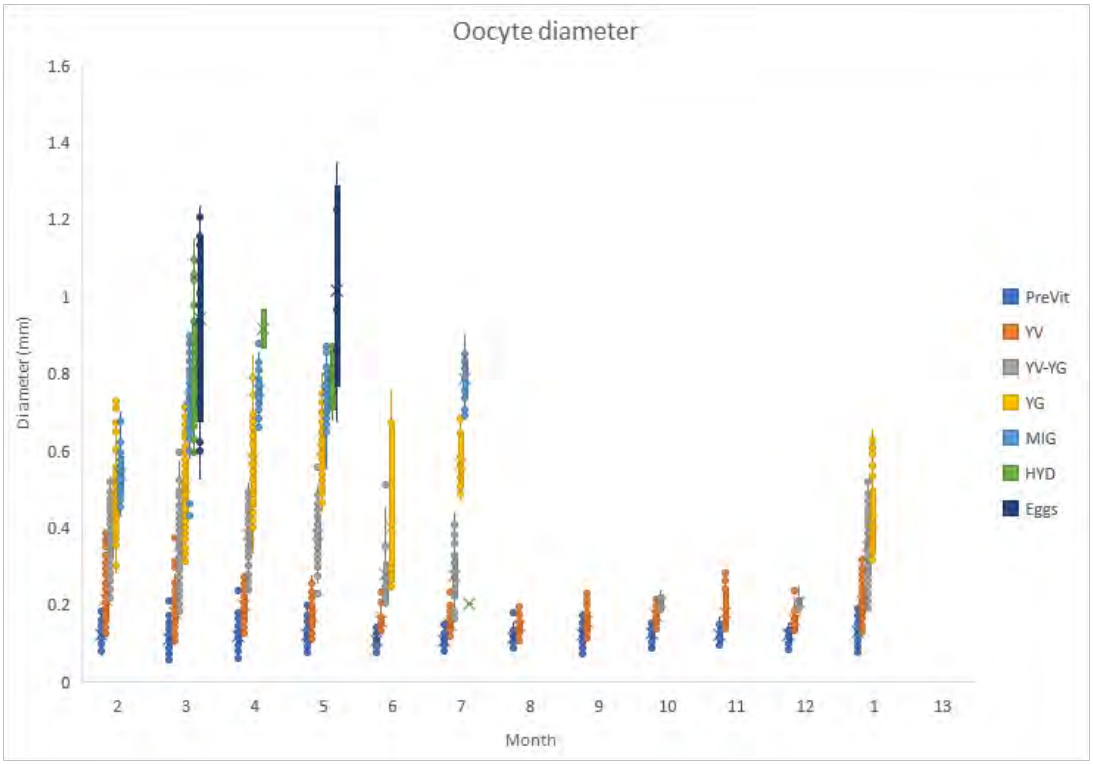

Figure 5.7. Diameters of vitellogenic oocytes and eggs in different development stage the ovaries over the year.

Oocyte diameters are small August to December, when oocytes are being prepared for the next spawning season (Fig 5.7). There is an increase in oocyte diameter in January just before spawning.

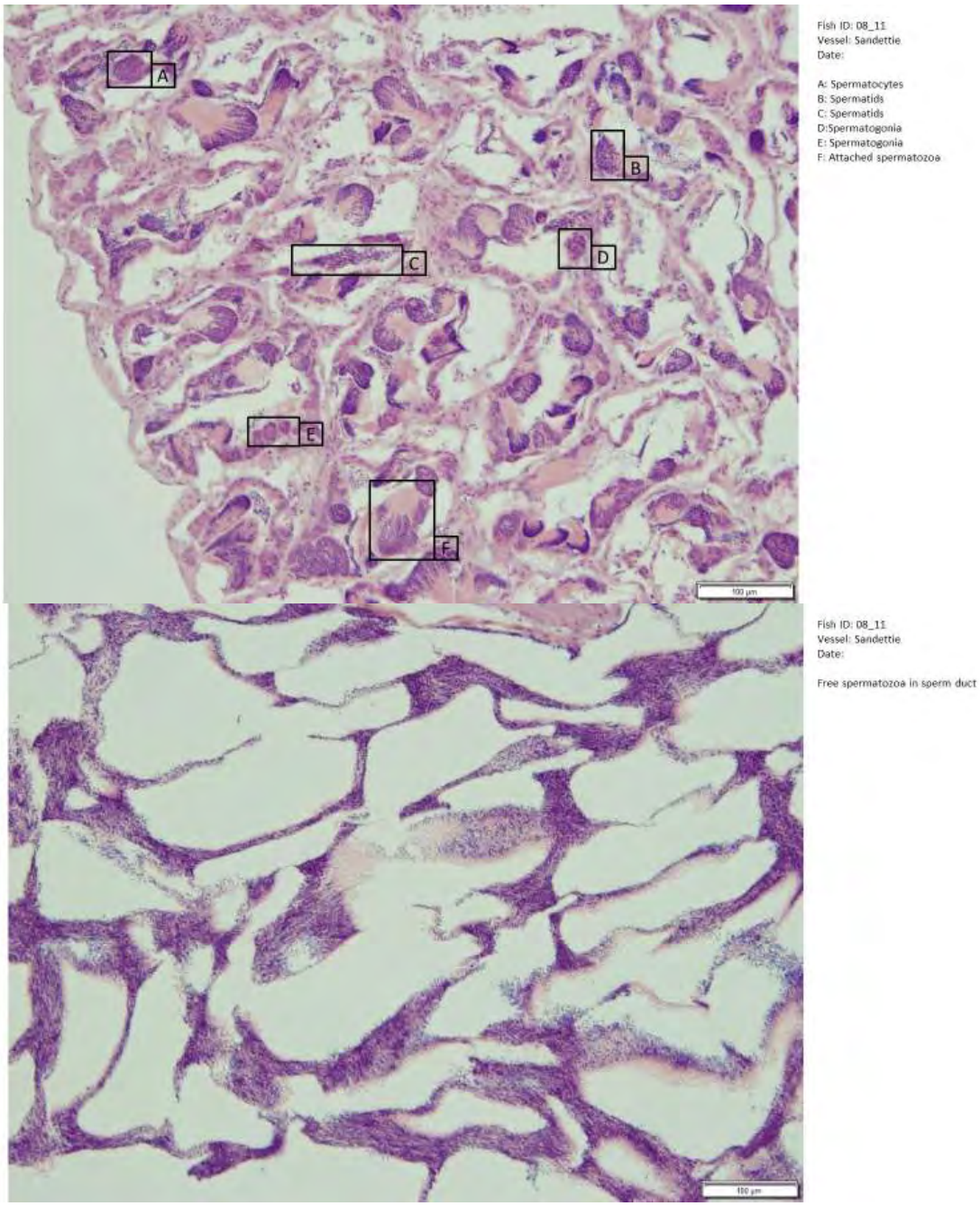

Figure 5.8. Evidence of spawning males. Top image shows various development stages of sperm cells. The bottom image shows the free spermatozoa in the spermatoduct, true sign of spawning.

Males were examined for the state of the testis, developing or actually spawning. Free spermatozoa can be present in the testis, but that is not a sign of actual spawning, because it was found that the spermatoduct was still empty. As soon as free spermatozoa were found in the spermatoduct these males were also running when the testis was pressed. Probably the movement from the testis to the spermatoduct takes a short time period and males keep developing sperm cells over the spawning season to be ready when

they meet a spawning female. There are signs that males show indeterminancy like females, i.e. keep recruting new sperm cells during the spawning season. But this needs to be investigated further.
An interesting find is that some males showed evidence of encapsulated eggs. This has been found in other fish species that were found in highly polluted waters, where the pollution stimulates the development of eggs in males. This will be investigated further.

6 references

Damme, C.J.G. van, A. Thorsen, M. Fonn, P. Alvarez, D. Garabana, B. O'Hea, J.R. Perez, M. Dickey-Collas, 2013. Fecundity regulation in horse mackerel, ICES J. Mar. Sci., 71(3): 546–558. https://doi.org/10.1093/icesjms/fst156.

ICES, 2014. Report of the Working Group on Mackerel and Horse Mackerel Egg Surveys (WGMEGS). ICES CM 2014/SSGESST:14.

ICES, 2017. Final Report of the Working Group on Mackerel and Horse Mackerel Egg Surveys. ICESCM 2017/SSGIEOM:18.

ICES, 2019a. Working Group on Widely Distributed Stocks (WGWIDE). ICES Scientific Reports. 1:36. 948 pp. http://doi.org/10.17895/ices.pub.5574

ICES, 2019a. Working Group on Mackerel and Horse Mackerel Egg Surveys (WGMEGS). ICES Scientific Reports. 1:66. 233 pp. http://doi.org/10.17895/ices.pub.5605

ICES, in prep. Working Group on Mackerel and Horse Mackerel Egg Surveys (WGMEGS). ICES Scientific Reports.

[Needs further updating]

NEA mackerel

Alternative assessment

Working Document #9 for WGWIDE 2020.

Höskuldur Björnsson

August 30st 2019

1 Introduction

The Mackerel assessment this year is as before based on 5 data sets.

1. Catch in numbers
2. Triannual Egg survey 1992-2019
3. Recruitment index from bottom trawl surveys in the Northsea and west of Ireland and Scotland.
4. Pelagic trawl survey in the North Atlantic.
5. Tagging data

4 different Muppet assessments are shown, all based on estimating a multiplier on the catches before 1998 and using catch in numbers since 1980 for tuning. None of the Muppet assessments uses the steel tag data. All (except VPA) use a seperable model with 2 selection periods. Where tag data are used tagloss is estimated. The difference between the assessments is.

1. All RFID tags where $RecaptureY > ReleaseY$.
2. VPA based on assessment 1.

3. No Tagging data.

4. Same tagging data as in the SAM assessment.

As before, results of the assessment are relatively strange and do not seem to follow main trends in the data. The SAM model utilizes process error in some strange way that is most likely a reflection of inconsistences in the data. In the Muppet model varying M lead to the conclusion that low or even negative M gives the best fit, probably an indication that the data are not perfect.

New egg survey was included last year but not this year. With increasing number of years that the pelagic survey has been conducted increases the weight of that survey in the Muppet assessment and the same can probably be said about the SAM assessment.

The recruitment index has been at very high level 2016-2019 and high since 2003 compared to the time before that (figure 2). As data on younger agegroups are scarce this index can have effect on adviced TAC if it is considered reliable.

The tuning data and 2 assessments, VPA and SAM are summarized in figure 1. The VPA assessment is used, as sufficiently far back in time the results are independent of the tuning data. B3+ is used instead of SSB for comparison with SAM as the Muppet model does not use exactly the same settings regarding proportion of F and M before spawning.

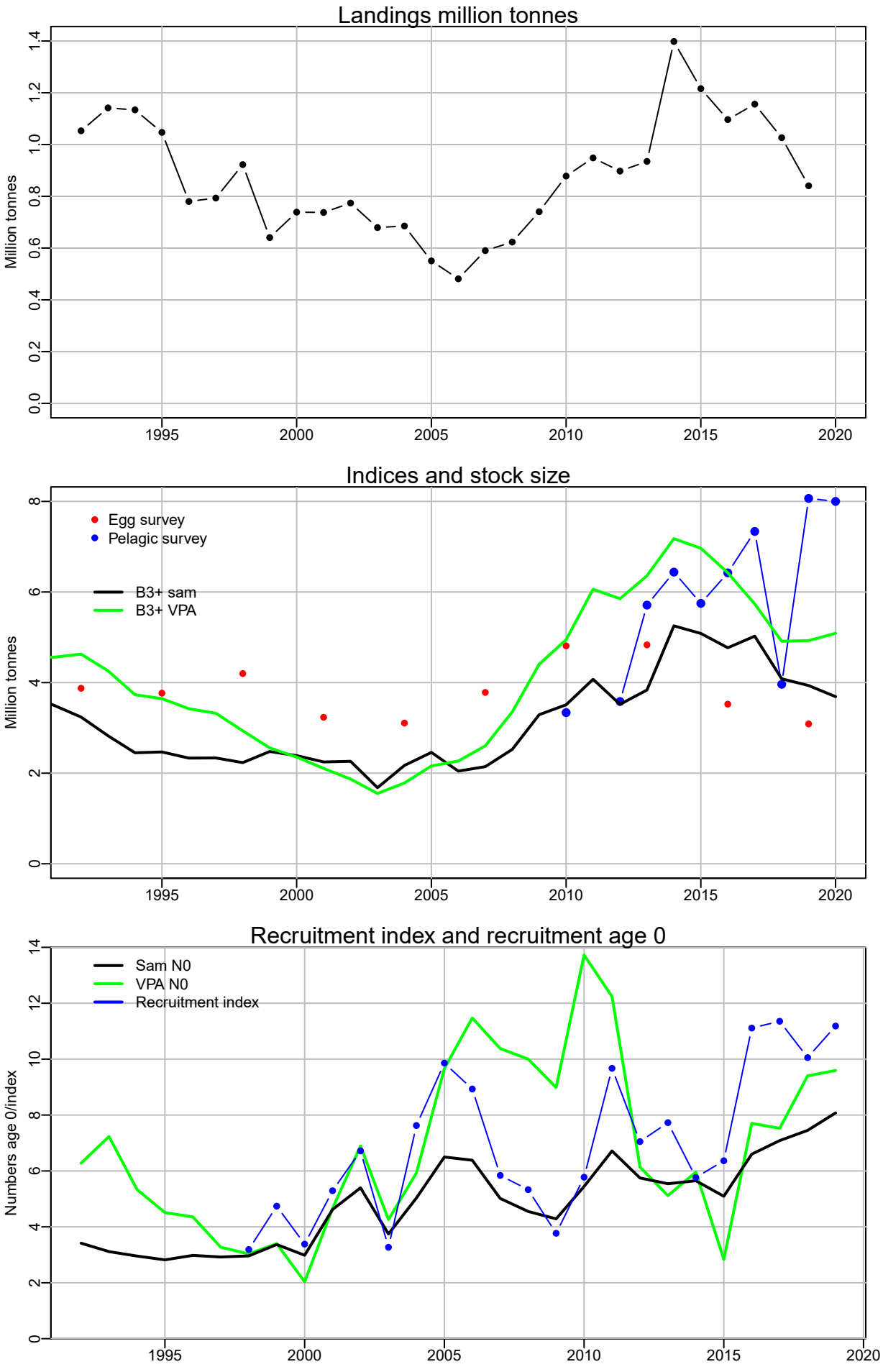

Figure 1: Summary of input data, SAM assessment and VPA assessment

The recruitment pattern from SAM is surpringly different from the VPA model. The development of the stock since 2014 is also somewhat in contrast with the pelagic survey thats indicate that the stock might be at very high level today (the egg survey 2019 is low). The variability in the pelagic survey in recent years will likely reduce the weight of this survey in the assessment.

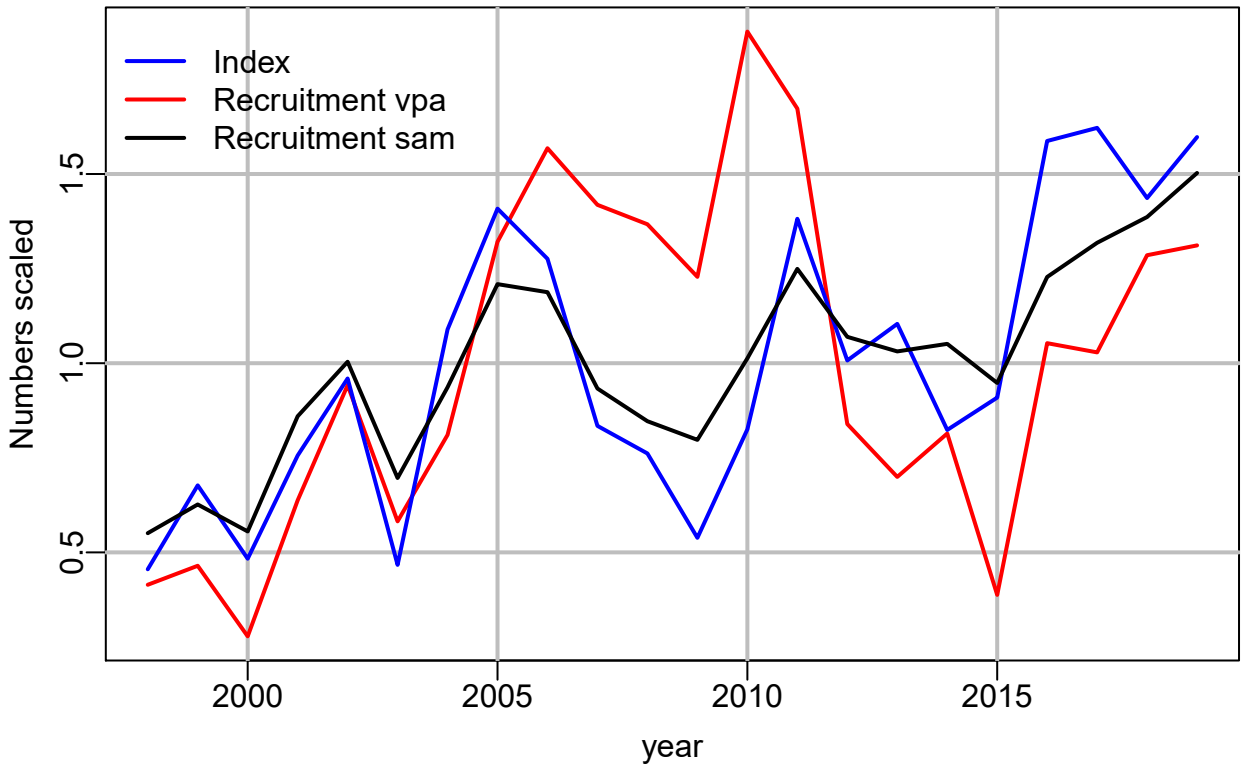

Figure 2: Recruitment index and recruitment (age 0) since 1998 , all values scaled to average of 1

Sam follows the recruitment much closer than muppet (figure 2). Estimated CV of this index in SAM is ≈ 0.2 but ≈ 0.4 in Muppet. The estimated CV in of the recruitment index in SAM is gradually increasing every new assessment year.

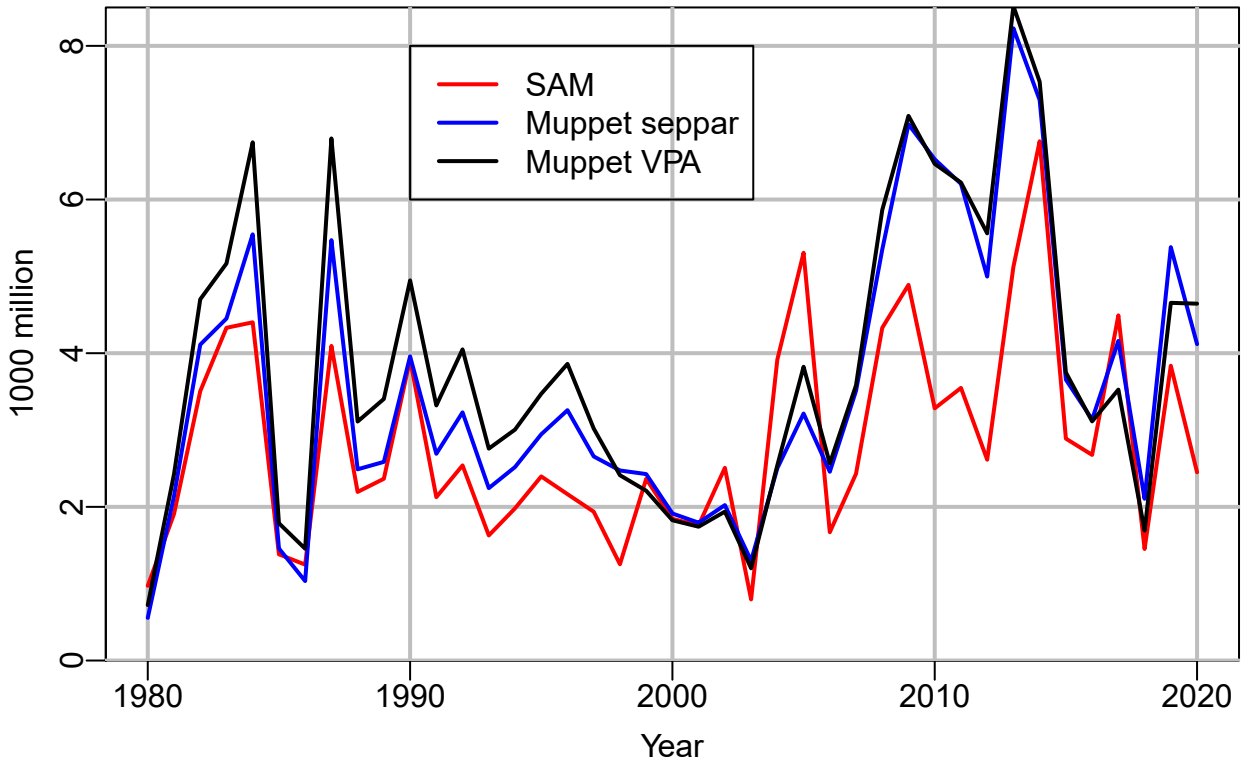

Figure 3: Number at age 3 from Muppet VPA and separable and Sam.

Looking at the comparison between age 3 from Muppet and SAM (figure 3) they are surprisingly similar before 2000 as the method and data used are very different in this period. After 2000 the number at age 3 are on the other hand surprisingly different. In the converged period VPA and Separable Muppet indicate similar numbers at age 3, the most notible difference is the 2002 yearclass. Before 1998 the estimated multplier in VPA is apparently a little higher than in the VPA model than the separable model.

Age 0 and age 3 from the Muppet model are very similar (figure 4). This is to be expected as fisheries on age 0-2 are limited.

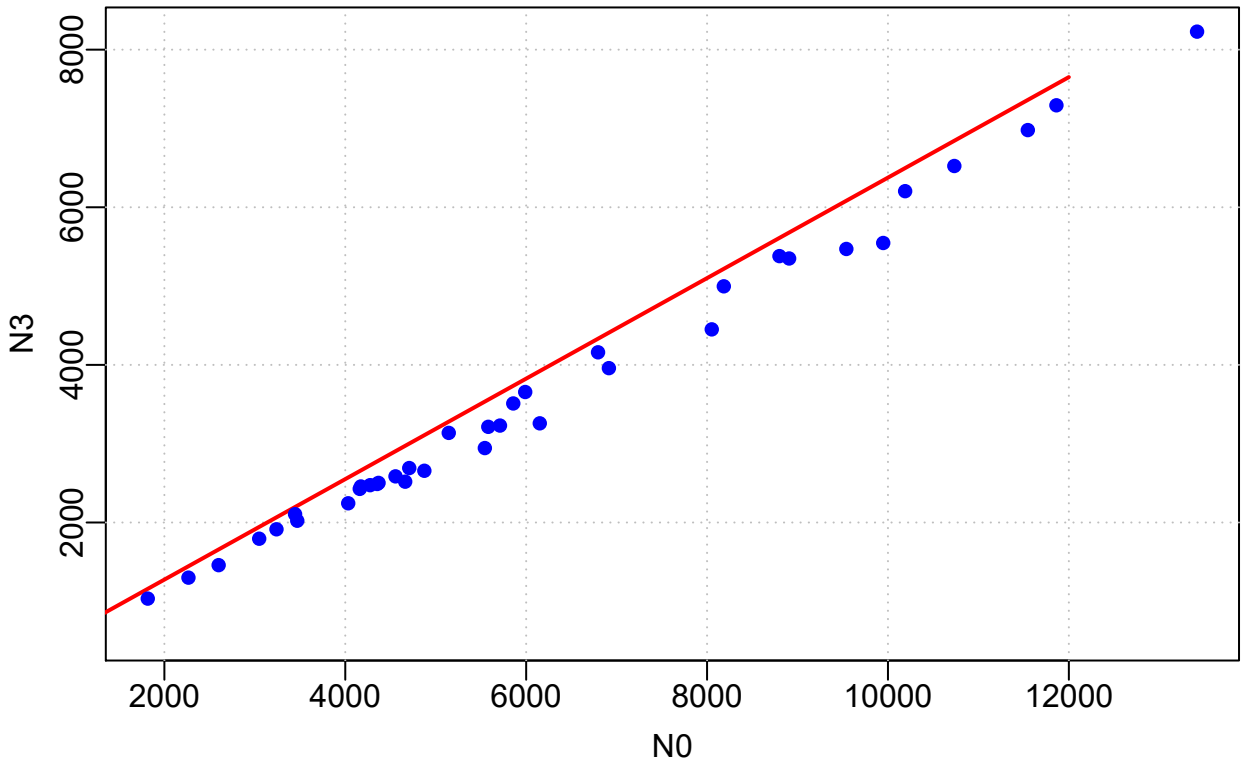

Figure 4: Muppet separable. Number at age 3 vs number at age 0. The red line has the slope $e^{-0.45}$

The relationship between n0 and n3 in SAM is on the other hand rather poor, $r^2 = 0.53$ on log scale (figure 5). The relationship between $n0$ and $n3$ is considerably worse than the relationship between $n0$ and the recruitment index (Important in HCR evaluations).

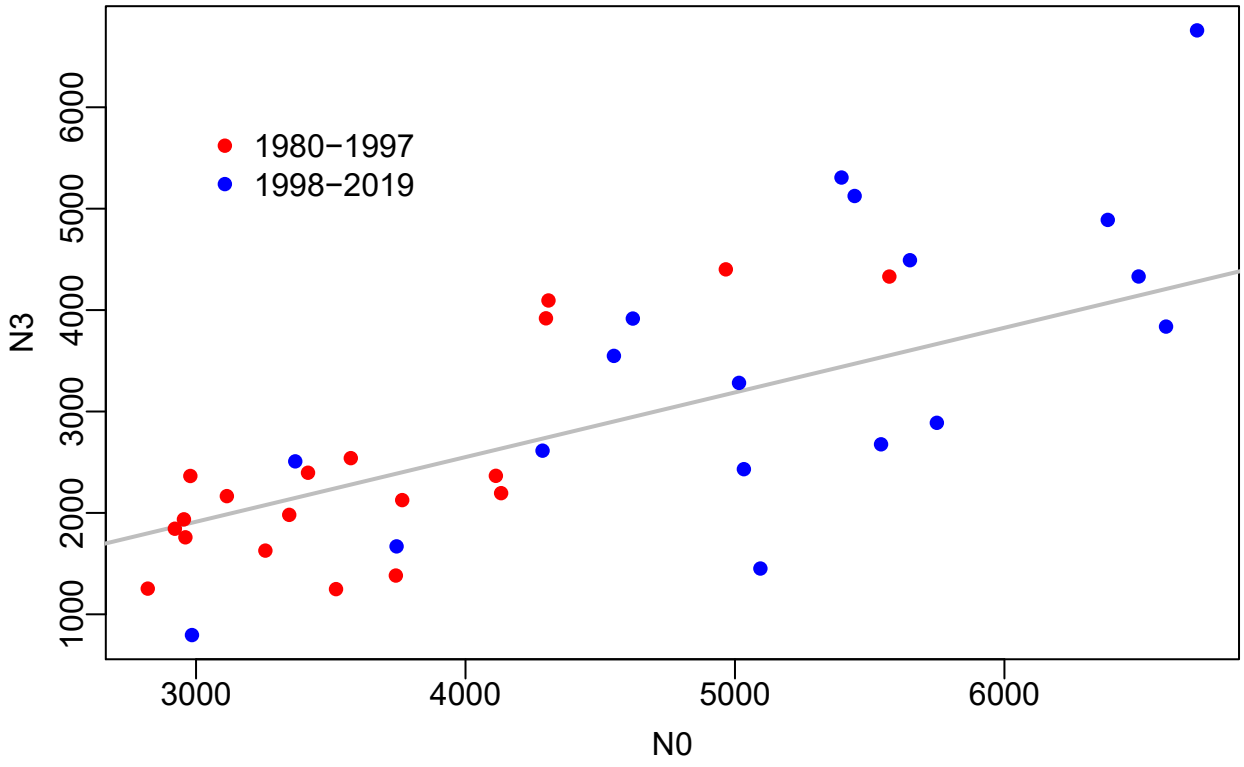

Figure 5: SAM. Number at age 3 vs number at age 0. The grey line has the slope $e^{-0.45}$

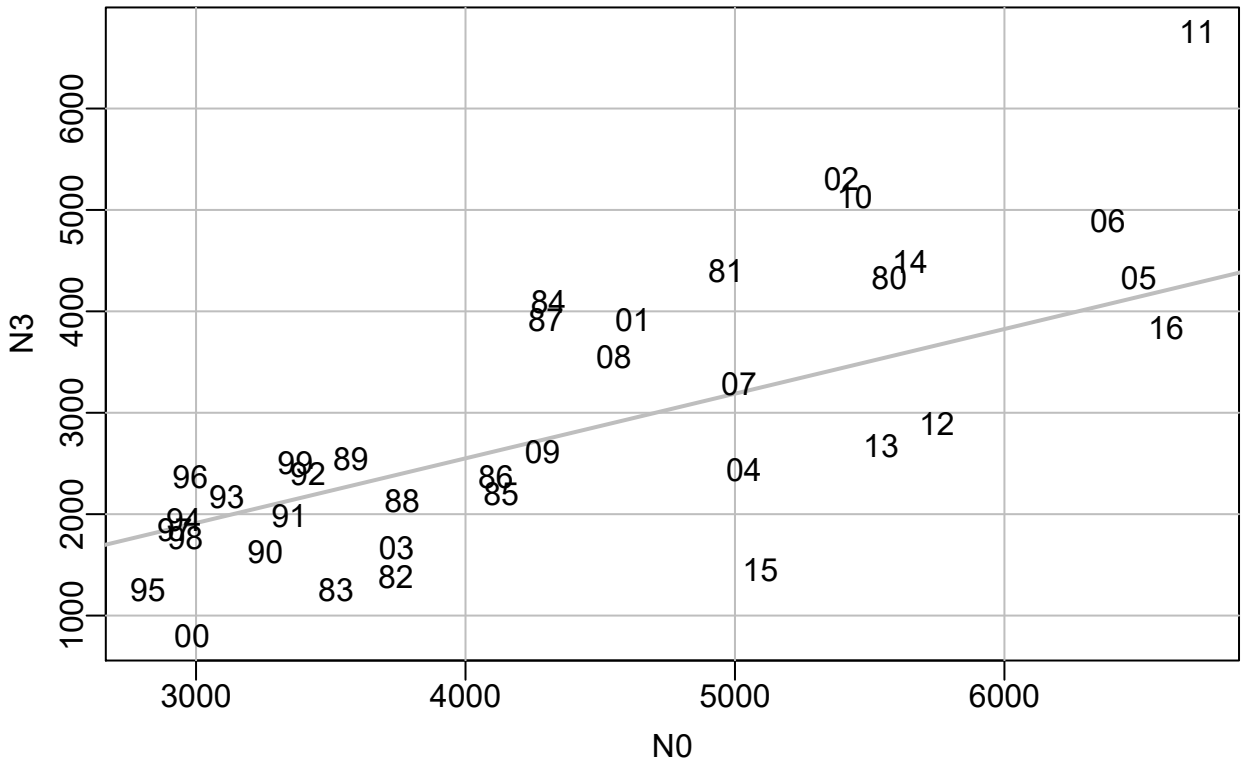

Figure 6: SAM. Number at age 3 vs number at age 0. The grey line has the slope $e^{-0.45}$. The text shows yearclass.

The pelagic survey might currently be the most important source of data in the assessment. The values from the pelagic survey are converted to biomass by multiplying the index by stock weights, summarizing over all the age groups. The stock weights are not the correct weights for this purpose but are probably sufficient for that is investigated here.

The pelagic index is at record high level in the years 2019 and 2020 while the stock assessment shows a downward trend since 2015 (figure 1). The Muppet and Sam assessments show somewhat different trends of biomass but do both have this "problem". In the figure predicted survey biomass and $B3+$ from Muppet are nearly identical ($q = 1$) but $B3+$ from SAM is lower but the trends are similar. The Muppet model limited to the same tags as the official assessment shows somewhat different trends (blue curve).

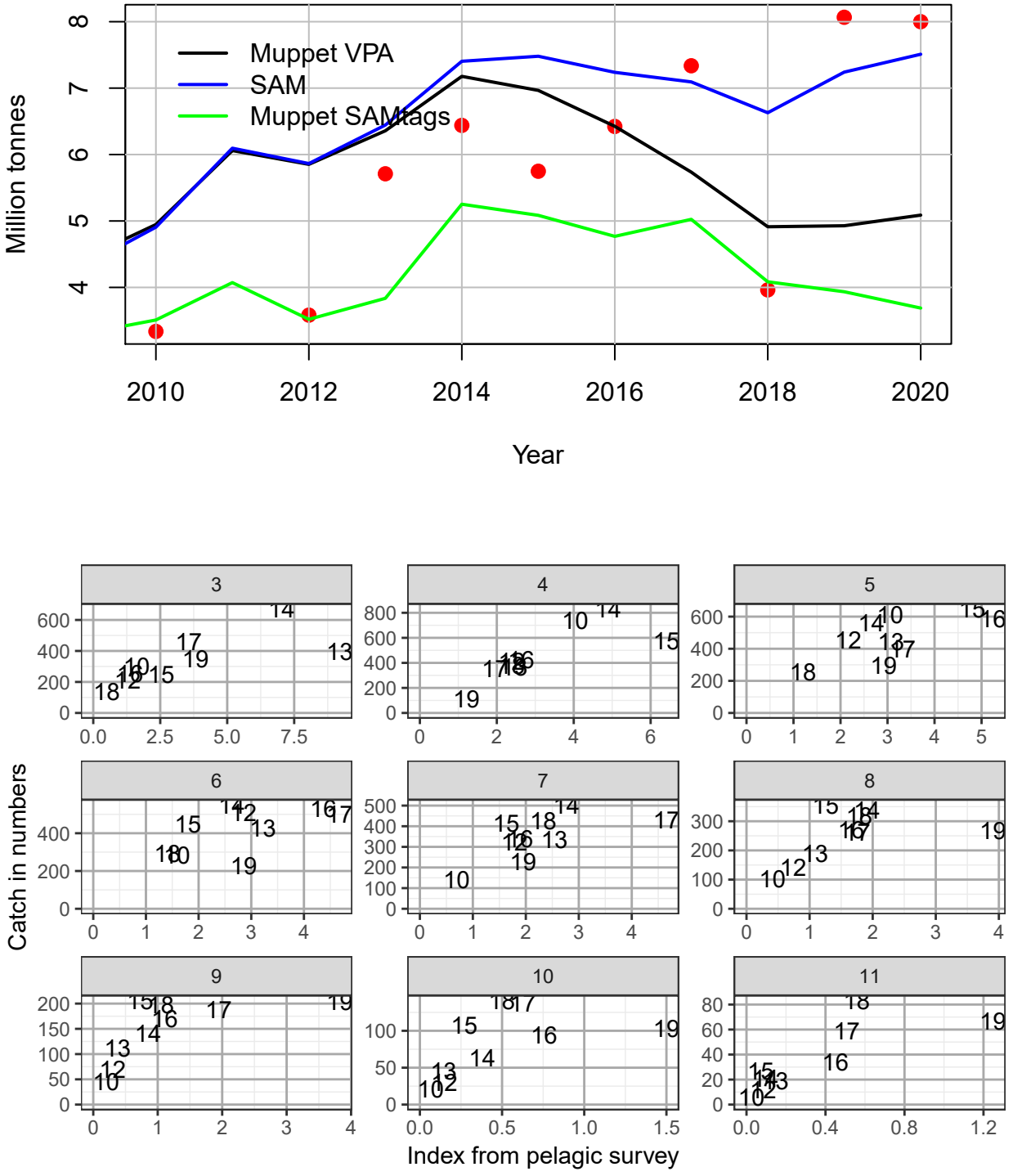

Figure 7: Catch in numbers by age vs indices from the Pelagic survey for the years 2010 and 2012:2019. The text indicate years.

Catch in numbers and index from the pelagic survey fit well for the older age groups but not as well for the younger age groups where contrast in data is less, especially in the catches. The plus group is missing in this plot but should be added.

Finally biomass 3+ and F_{4-8} from the 5 assessments listed above is shown (figure 8 and 9). The adopted assessment indicates the lowest biomass and highest fishing mortality. The range of results is probaly an indication of the uncertainty in the assessment that is probably even more than indicated by the range of results.

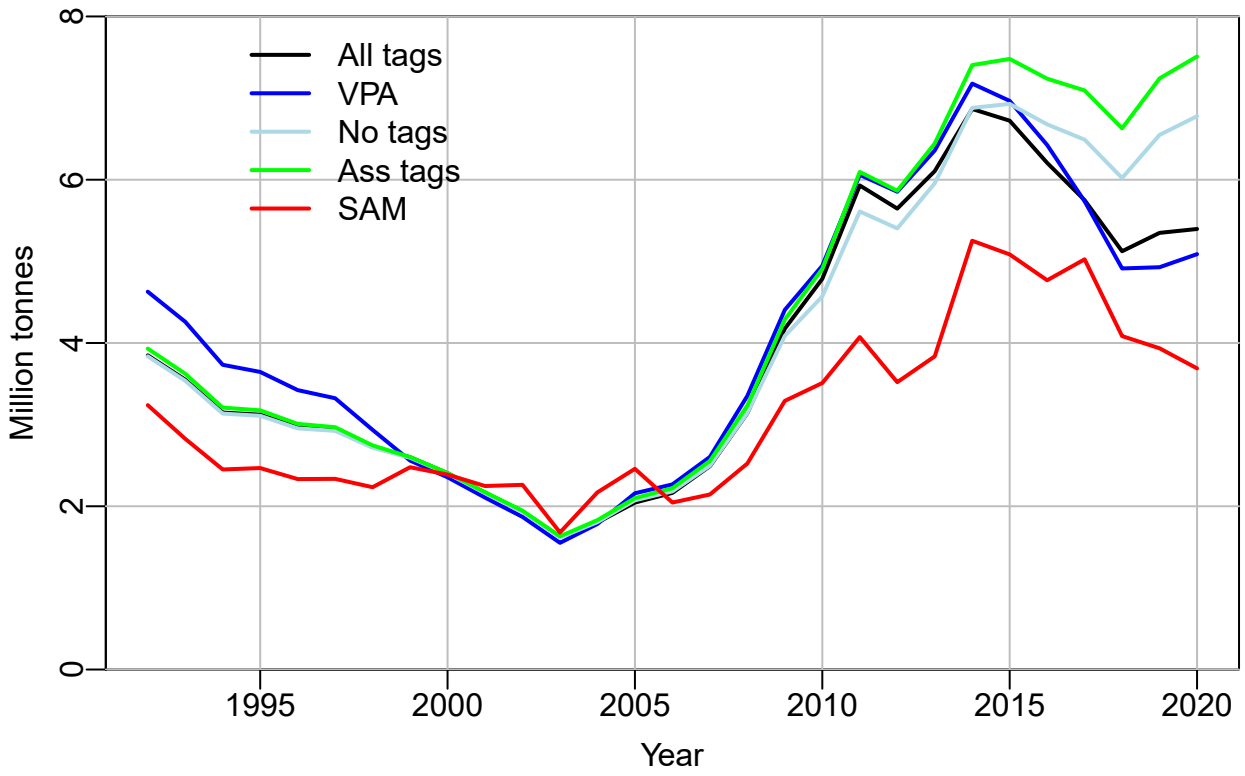

Figure 8: Development of B3+ from few diffent runs.

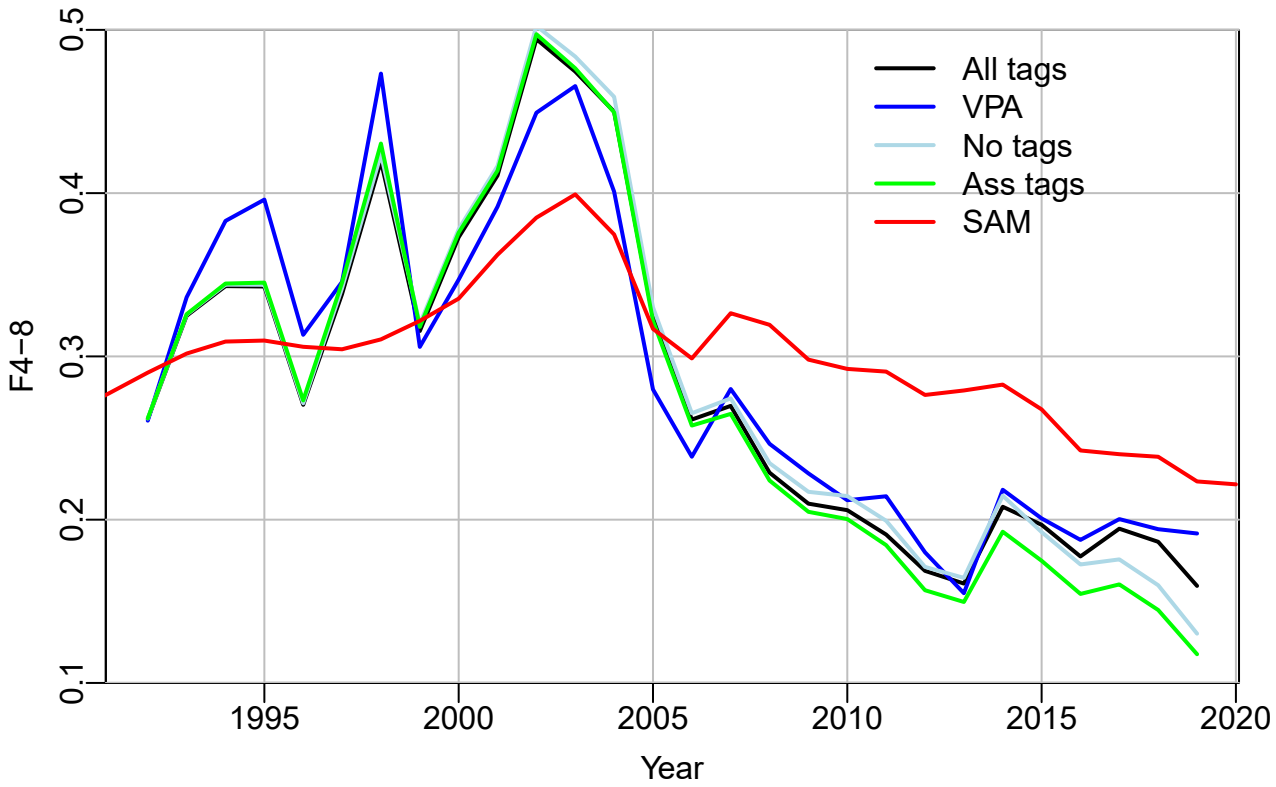

Figure 9: Development of F_{4-8} from few diffent runs.

Working Document to

Working Group on International Pelagic Surveys (WGIPS)
Belfast, 18 - 22 January 2021
and
Working Group on Widely Distributed Stocks (WGWIDE)
Copenhagen, 26 August - 1 September 2020

INTERNATIONAL ECOSYSTEM SURVEY IN NORDIC SEA (IESNS) in May – June 2020

Post-cruise meeting on Teams, 16-18 June 2020

Are Salthaug[1], Erling Kåre Stenevik[1], Sindre Vatnehol[1], Åge Høines[1], Valantine Anthonypillai[1], Kjell Arne Mork[1], Cecilie Thorsen Broms[1], Øystein Skagseth[1]
RV G.O. Sars

Kai Wieland[2], Karl-Johan Stæhr[2], Susan Mærsk Lusseau[2], Benoit Berges[3]
RV Dana

Sigurvin Bjarnason[4], Anna Heiða Ólafsdóttir[4]
RV Árni Friðriksson

Sólvá Káradóttir Eliasen[5], Jan Arge Jacobsen[5], Leon Smith[5]
RV Magnus Heinason

[1] Institute of Marine Research, Bergen, Norway
[2] DTU-Aqua, Denmark
[3] Wageningen Marine Research, IJmuiden, The Netherlands
[4] Marine and Freshwater Research Institute, Hafnarfjordur, Iceland
[5] Faroese Marine Research Institute, Tórshavn, Faroe Islands

Introduction

In May-June 2020, four research vessels; R/V Dana, Denmark (joined survey by Denmark, Germany, Ireland, The Netherlands, Sweden and UK. Due to the Covid19 situation in 2020 there was only participation from Denmark in the actual cruise), R/V Magnus Heinason, Faroe Islands, R/V Árni Friðriksson, Iceland and R/V G.O. Sars, Norway participated in the International ecosystem survey in the Nordic Seas (IESNS). The aim of the survey was to cover the whole distribution area of the Norwegian Spring-spawning herring with the objective of estimating the total biomass of the herring stock, in addition to collect data on plankton and hydrographical conditions in the area. The survey was initiated by the Faroes, Iceland, Norway and Russia in 1995. Since 1997 also the EU participated (except 2002 and 2003) and from 2004 onwards it was more integrated into an ecosystem survey. This report represents analyses of data from this International survey in 2020 that are stored in the PGNAPES database and supported by national survey reports from each survey (Dana: Cruise Report R/V Dana Cruise 04/2020. International Ecosystem survey in the Nordic Seas (IESNS) in 2020, Magnus Heinason: IESNS Cruise Report Magnus Heinasen, Eliasen et al, FAMRI 2020, Árni Friðriksson: Óskarsson et al. 2019).

As previous years, it was planned that Russia would cover the Barents Sea.
However, due to technical issues with the research vessel, Russia was not able to conduct the survey and thus no IESNS estimates from this area exist for 2020.

Material and methods

Coordination of the survey was done during the WGIPS meeting in January 2020 and by correspondence. Planning of the acoustic transects and hydrographic stations and plankton stations were carried out by using the recently developed survey planner function in the r-package Rstox version 1.11 (see www.imr.no/forskning/prosjekter/stox). The survey planner function generates the survey plan (transect lines) in a cartesian coordinate system, and transforms the positions to the geographical coordinate system (longitude, latitude) using the azimuthal equal distance projection, which ensures that distances, and also equal coverage, if the method used is designed with this prerequisite, are preserved in the transformation. Figure 1 shows the planned acoustic transects and hydrographic and plankton stations in each stratum. Only parallel transects were used this year, however, the transects now follow great circles instead of a constant latitude as before, so they appear bended in a Mercator projection. The participating vessels together with their effective survey periods are listed in the table below:

Vessel	Institute	Survey period
Dana	DTU Aqua - National Institute of Natural Resources, Denmark	01/5-25/5
G.O. Sars	Institute of Marine Research, Bergen, Norway	01/5-02/6
Magnus Heinason	Faroe Marine Research Institute, Faroe Islands	29/4- 11/5
Árni Friðriksson	Marine and Freshwater Research Institute, Iceland	10/5-28/5

Figure 2 shows the cruise tracks, Figure 3a the hydrographic and plankton stations and Figure 3b the pelagic trawl stations. Survey effort by each vessel is detailed in Table 1. Frequent contacts were maintained between the vessels during the course of the survey, primarily through electronic mail. The temporal progression of the survey is shown in Figure 4.

In general, the weather condition did not affect the survey even if there were some days that were not favourable and prevented for example WP2 and Multinet sampling at some stations. The survey was based on scientific echosounders using 38 kHz frequency. Transducers were calibrated with the standard sphere calibration (Foote *et al*., 1987) prior to the survey. Salient acoustic settings are summarized in the text table below.

Acoustic instruments and settings for the primary frequency (boldface).

	Dana	G.O. Sars	Arni Friðriksson	Magnus Heinason
Echo sounder	Simrad EK 60	Simrad EK 80	Simrad EK80	Simrad EK60
Frequency (kHz)	**38**	**38**, 18, 70, 120, 200, 333	**38**, 18, 70, 120, 200	**38**,200
Primary transducer	ES38BP	ES 38B	ES38-7	ES38B
Transducer installation	Towed body	Drop keel	Drop keel	Hull
Transducer depth (m)	5 - 7	8.5	8	3
Upper integration limit (m)	7 - 9	15	15	7
Absorption coeff. (dB/km)	10.1	10.1	10	10.1
Pulse length (ms)	1.024	1.024	1.024	1.024
Band width (kHz)	2.425	2.43	?	2.425
Transmitter power (W)	2000	2000	2000	2000
Angle sensitivity (dB)	21.9	21.9	18	21.9
2-way beam angle (dB)	-20.5	-20.7	-20.3	-20.8
Sv Transducer gain (dB)				
Ts Transducer gain (dB)	25.17	26.05	26.9	25.57
s_A correction (dB)	-0.50	-0.66	-0.02	-0.68
3 dB beam width (dg)				
alongship:	6.96	6.48	6.53	7.17
athw. ship:	6.98	6.22	6.5	7.06
Maximum range (m)	500	500	500	500
Post processing software	LSSS	LSSS	LSSS	LSSS

All participants used the same post-processing software (LSSS) and scrutinization was carried out according to an agreement at a PGNAPES scrutinizing workshop in Bergen in February 2009 (ICES 2009), and "Notes from acoustic Scrutinizing workshop in relation to the IESNS", Reykjavík 3.-5. March 2015 (Annex 4 in ICES 2015). Generally, acoustic recordings were scrutinized on daily basis and species identified and partitioned using catch information, characteristic of the recordings, and frequency between integration on 38 kHz and on other frequencies by a scientist

experienced in viewing echograms. All vessels used a large or medium-sized pelagic trawl as the main tool for biological sampling. The salient properties of the trawls are as follows:

	Dana	**G.O. Sars**	**Arni Friðriksson**	**Magnus Heinason**
Circumference (m)		**496**	**832**	**640**
Vertical opening (m)	**25-35**	**25-30**	**20–35**	**45–55**
Mesh size in codend (mm)	**16**	**24**	**20**	**40**
Typical towing speed (kn)	**3.5-4.0**	**3.0–4.5**	**3.1–5.0**	**3.0–3.5**

Catches from trawl hauls were sorted and weighed; fish were identified to species level, when possible, and other taxa to higher taxonomic levels. A subsample of herring, blue whiting and mackerel were sexed, aged, and measured for length and weight, and their maturity status was estimated using established methods. An additional sample of fish was measured for length. For the Norwegian, Icelandic and Faroese vessel, a smaller subsample of stomachs was sampled for further analyses on land. Salient biological sampling protocols for trawl catches are listed in the table below.

	Species	Dana	G.O. Sars	Arni Friðriksson	Magnus Heinason
Length measurements	Herring	200-300	100	300	100-200
	Blue whiting	200-300	100	50	100-200
	Mackerel	100-200	100	50	100-200
	Other fish sp.	100	30	30	30
Weighed, sexed and maturity determination	Herring	50	25-100	100	50-100
	Blue whiting	50	25-100	50	50-100
	Mackerel	0	25-100	50	50-100
	Other fish sp.	0	0	0	30*
Otoliths/scales collected	Herring	50	25-30	100	50-100
	Blue whiting	50	25-30	50	50-100
	Mackerel	0	25-30	50	50-100
	Other fish sp.	0	0	0	0
Stomach sampling	Herring	0	10	10	5-10
	Blue whiting	0	10	10	5-10
	Mackerel	0	10	10	5-10
	Other fish sp.	0	0	0	0

* Only weighed, not sexed or determination of maturity.

** Will be included in the final report

Acoustic data were analysed using the StoX software package which has been used for some years now for WGIPS coordinated surveys. A description of StoX can be found in Johnsen et al. (2019) and here: www.imr.no/forskning/prosjekter/stox. Estimation of abundance from acoustic surveys with StoX is carried out according to the stratified transect design model developed by Jolly and Hampton (1990). This

method requires pre-defined strata, and the survey area was therefore split into 6 strata with pre-defined acoustic transects as agreed during the WGIPS in January 2019. Within each stratum, parallel transects with equal distances were used. The distance between transects was based on available survey time, and the starting point of the first transect in each stratum was randomized. This approach allows for robust statistical analyses of uncertainty of the acoustic estimates. The strata and transects used in StoX are shown in Figure 1. All trawl stations within a given stratum with catches of the target species (either blue whiting or herring) were assigned to all transects within the stratum, and the length distributions were weighted equally within the stratum. The following target strength (TS)-to-fish length (L) relationships were used:

Blue whiting: $TS = 20 \log(L) - 65.2$ dB (ICES 2012)

Herring: $TS = 20.0 \log(L) - 71.9$ dB

The target strength for herring is the traditionally one used while this target strength for blue whiting was first applied in 2012 (ICES 2012).

The hydrographical and plankton stations by survey are shown in Figure 3a. Most vessels collected hydrographical data using a SBE 911 CTD. Maximum sampling depth was 1000 m. Zooplankton was sampled by a WPII on all vessels, according to the standard procedure for the surveys. Mesh sizes were 180 or 200 µm. The net was hauled vertically from 200 m to the surface or from the bottom whenever bottom depth was less than 200 m. All samples were split in two and one half was preserved in formalin while the other half was dried and weighed. The samples for dry weight were size fractionated before drying by sieving the samples through 2000 µm and 1000 µm sieves, giving the size fractions 180/200 – 1000 µm, 1000 – 2000 µm, and > 2000 µm. Data are presented as g total dry weight per m^2. For the zooplankton distribution map, all stations are presented. For the time series, stations in the Norwegian Sea delimited to east of 14°W and west of 20°E have been included. The zooplankton data were interpolated using objective analysis utilizing a Gaussian correlation function to obtain a time-series for four different areas. The results are given as inter-annual indexes of zooplankton abundance in May. This method was introduced at WGINOR in 2015 (ICES, 2016) and the results match the former used average index.

Results and Discussion

Hydrography

The temperature distributions in the ocean, averaged over selected depth intervals; 0-50 m, 50-200 m, and 200-500 m, are shown in Figures 5-7. The temperatures in the surface layer (0-50 m) ranged from below 0°C in the Greenland Sea to 9°C in the southern part of the Norwegian Sea (Figure 5). The Arctic front was encountered below 65°N east of Iceland extending eastwards towards about 2° West where it turned northeastwards to 65°N and then almost straight northwards. This front was

well-defined at 200-500 m depth while shallower it was unclear. Further to west at about 8° West another front runs northward to Jan Mayen, the Jan Mayen Front that was most distinct in the upper 200 m. The warmer North Atlantic water formed a broad tongue that stretched far northwards along the Norwegian coast with temperatures >6 °C to the Bear Island at 74,5° N in the surface layer.

Relative to a 25 years long-term mean, from 1995 to 2019, the temperatures at 0-50 m were 0-1 °C below the mean for almost the whole Norwegian Sea (Figure 5). Warmest region is in the eastern Greenland Sea with temperatures 2 °C higher than the mean. This warming can be observed at all depths. At 50-200 m the temperatures were also, in most regions, 0-1 °C lower than the long-term mean. An exception is for the southwestern Norwegian Sea, west of the 0 meridian, where the temperatures were about 0-0,5 °C higher than the mean (Figure 6). At 200-500 m depth, the pattern is more fragmented but in the southwestern region the temperatures were near the long-term mean while in more eastern areas the temperatures were in general lower than the mean (Figure 7).

The temperature, salinity and potential density in the upper 800 m at the Svinøy section in 26-28 April 2020 are shown in Figure 8. Atlantic water is lying over the colder and fresher intermediate layer and reach down to 500 m at the shelf edge and shallower westward. The warmest water, above 8 °C, is located near the shelf edge where the core of the inflowing Atlantic Water is located. Westward, temperature and salinity are reduced due to mixing with colder and less saline water. Compared to a 30 years long-term mean, from 1978 to 2007, the temperatures in 2020 were higher than the mean at the shelf edge but westward the temperatures were both lower and higher than the mean due to meandering or eddies. The salinity was however lower than the long-term mean for the whole section above 400 m with the exception in coastal water.

Two main features of the circulation in the Norwegian Sea, where the herring stock is grazing, are the Norwegian Atlantic Current (NWAC) and the East Icelandic Current (EIC). The NWAC with its offshoots forms the northern limb of the North Atlantic current system and carries relatively warm and salty water from the North Atlantic into the Nordic Seas. The EIC, on the other hand, carries Arctic waters. To a large extent this water derives from the East Greenland Current, but to a varying extent, some of its waters may also have been formed in the Iceland and Greenland Seas. The EIC flows into the southwestern Norwegian Sea where its waters subduct under the Atlantic waters to form an intermediate Arctic layer. While such a layer has long been known in the area north of the Faroes and in the Faroe-Shetland Channel, it is only in the last three decades that a similar layer has been observed all over the Norwegian Sea.

This circulation pattern creates a water mass structure with warm Atlantic Water in the eastern part of the area and more Arctic conditions in the western part. The NWAC is rather narrow in the southern Norwegian Sea, but when meeting the Vøring Plateau off Mid Norway it is deflected westward. The western branch of the NWAC reaches the area of Jan Mayen at about 71°N. Further northward in the Lofoten Basin the lateral extent of the Atlantic water gradually narrows again, apparently under topographic influence of the mid-ocean ridge. It has been shown that atmospheric forcing largely controls the distribution of the water masses in the Nordic Seas. Hence, the lateral extent of the NWAC, and consequently the position of the Arctic Front, that separates the warm North Atlantic waters from the cold Arctic waters, is correlated with the large-scale distribution of the atmospheric sea level pressure. The local air-sea heat flux in addition influence the upper layer and it is found that it can explain about half of the year to year variability of the ocean heat content in the Norwegian Sea.

Zooplankton

The zooplankton biomass (g dry weight m^{-2}) in the upper 200 m is shown in Figure 9. Sampling stations were evenly spread over the area, covering Atlantic water, Arctic water, and the Arctic frontal zone. The highest zooplankton biomasses were not concentrated in a specific area but spread over several locations in the northern part of the sampling area. High biomasses were found in northwestern parts of the central Norwegian Sea, northeast of Iceland and Jan Mayen, and in an area around Lofoten/Vesterålen and north of that area. Lower biomasses were found in the entire southern part of the sampling area, especially in southwest.

Figure 10 shows the zooplankton index given for the sampling area (delimited to east of 14°W and west of 20°E). To examine regional difference in the biomass, the total area where divided into 4 subareas 1) Southern Norwegian Sea including the Norwegian Sea Basin, 2) The Northern Norwegian Sea including the Lofoten Basin, 3) Jan Mayen Arctic front, and 4) East of Iceland. The mean index of subarea 1 and 2 is also given. The zooplankton biomass index for the Norwegian Sea and nearby areas in 2020 was 8.3 g dry weight m^{-2}, which is a decrease from last year. A similar decrease was observed in all sub-areas, except from East of Iceland where an increase was observed.

The zooplankton biomass index for the Norwegian Sea in May has been estimated since 1995. For the period 1995-2002 the plankton index was relatively high (mean 11.5 g) even if varying between years. From 2003-2006, the index decreased continuously and has been at lower levels since then, with a mean of 7.9 g for the period 2003-2020. An increase can be noted in the last part of the low-biomass period. This general pattern applies more or less to all the different sub-areas within the Norwegian Sea. The zooplankton biomass at the Jan Mayen Arctic front was high until 2007 but has since then been at the same level as the Norwegian Sea. The

zooplankton biomass East of Iceland was in general higher compared with the other sub-areas until 2015.

The reason for this fluctuation in the zooplankton biomass is not obvious to us. The unusually high biomass of pelagic fish feeding on zooplankton has been suggested to be one of the main causes for the reduction in zooplankton biomass. However, carnivorous zooplankton and not pelagic fish are the main predators of zooplankton in the Norwegian Sea (Skjoldal *et al.,* 2004), and we do not have good data on the development of the carnivorous zooplankton stocks. Timing effects, as match/mismatch with the phytoplankton bloom, can also affect the zooplankton abundance. It is also worth noting that the period with lower zooplankton biomass coincides with lower-than-average heat contents in the Norwegian Sea (ICES 2018) and reduced inflow of Arctic water into the southwestern Norwegian Sea (Kristiansen et al., 2019). More ecological and environmental research to reveal inter-annual variations and long-term trends in zooplankton abundance are recommended.

Norwegian spring-spawning herring

Survey coverage in the Norwegian Sea was considered adequate in 2020. The zero-line was believed to be reached for adult NSS herring in most of the areas. On some of the transects in stratum 2 and 4, however, aggregations of herring were recorded on the easternmost part indicating that the zero-line was not fully reached on those transect although some of the transect were extended. It is, however, recommended that the results from IESNS 2020 can be used for assessment purpose. The herring was primarily distributed in the south-western area where the 2013-year-class dominated, and in the eastern area where the 2016 year-class dominated (Figure 11). It is a commonly observed pattern that the older fish are distributed in the southwest while the younger fish are found closer to the nursery areas in the Barents Sea (Figure 12). The distribution of the recruiting 2016 year-class in the eastern part of the Norwegian Sea extends all the way from 70°N south to 64°N. This is different from earlier year-classes recruiting to the Norwegian Sea, which usually do not extend farther south than 69°N.

Four years old herring (year class 2016) dominated both in terms of number (57%) and biomass (41 %) on basis of the StoX baseline estimates for the Norwegian Sea (Tables 2-4). Its number at age 4 is higher than for the 2004 year class at same age (Figure 13), which puts the size of the 2016 year class into perspective. The large 2004 year class, which has dominated the stock together with the 2002 year class, has contributed significantly to the biomass of older age-groups (see paragraph on issues with age determination below). Herring aged 12-18 years old thus comprised 11% of the numbers and 19% of the biomass. Uncertainty estimates for number at age based on bootstrapping within StoX are shown in Figure 14 and Table 5. The relative standard error (CV) of the total biomass estimate is 15 % and 12 % for the

total numbers estimate, and the relative standard error for the dominating age groups is around 30 % (Figure 14 and Table 5).

The total estimate of herring in the Norwegian Sea from the 2020 survey was 22.8 billion in number and the biomass was 4.25 million tonnes. The biomass estimate is 0.62 million tonnes (13 %) lower than the 2019 survey estimate while the estimated number is 15 % higher in 2020. The biomass estimate decreased significantly from 2009 to 2012, and has since then been rather stable at 4.2 to 5.9 million tonnes with similar confidence interval (Figure 15), with the lowest abundance occurring in 2017. Although there is only little change in total abundance and biomass, there is a gradual shift in age and size composition with the 2016 year class becoming more dominant than the older year classes.

In the last 5 years, there have been concerns regarding age reading of herring, because the age distributions from the different participants have showed differences – particularly older specimens appear to have uncertain ages. A scale and otolith exchange has been ongoing for some period, where scales and otoliths for the same fish have been sampled. On basis of that work, a workshop was planned in the spring 2018 to discuss the results. This workshop was postponed indeterminately. The survey group emphasizes the necessity of having this workshop before next year's survey takes place.

With respect to age-reading concerns in the recent years, the comparison between the nations in this year's survey could not been done fully since restrictions on the cruise tracks due to COVID-19 prevented the Norwegian vessel to enter stratum 1 and 3. However, in stratum 2 and 4 there was overlap between the Norwegian vessel and the Danish vessel and the age distributions from those strata seems to be relatively similar between the two vessels (Figure 20).

In the IESNS survey in 2020 some differences regarding the acoustic scrutinizing between neighbouring vessels were observed and discussed. The data where re-scruitinized, and there was a better agreement between the vessel. Still, the difference between the original and the re-scrutinization where small, indicating that the difference where not caused by an scrutinization error. There is a need to further discuss the scrutinizing process before next year's survey. The survey group suggest to have a meeting before next year's survey to discuss the protocol for acoustic scrutinizing in the IESNS survey.

Recently concerns have been raised by the survey groups for the International ecosystem surveys in the Nordic Seas (IESNS and IESSNS) on mixing issues between Norwegian spring-spawning herring and other herring stocks (e.g. Icelandic summer-spawning, Faroese autumn-spawning, Norwegian summer-spawning and North Sea type autumn-spawning herring) occurring in some of the fringe regions in

the Norwegian Sea. Until now, fixed cut lines have been used by the survey group to exclude herring of presumed other types than NSS herring, however this simple procedure is thought to introduce some contamination of the stock indices of the target NSS herring.

In the IESNS 2020 survey, all herring in the Stratum 1 was allocated to NSSH, although the southernmost transect east of the Faroes (Figure 11) contained mainly autumn-spawning type herring, probably local Faroese autumn-spawners or North Sea type autumn-spawners. WGIPS noted in their 2019 report that the separation of different herring stock components is an issue in several of the surveys coordinated in WGIPS and the needs for development of standardized stock splitting methods was also noted in the WKSIDAC (ICES 2017).

Blue whiting

The spatial distribution of blue whiting in 2020 was similar to the years before, with the highest abundance estimates in the southern and eastern part of the Norwegian Sea, along the Norwegian continental slope. The main concentrations were observed in connections with the continental slopes of Norway and along the Scotland – Iceland ridge (Figure 16). Blue whiting was distributed similar as last year. The largest fish were found in the western and middle part of the survey area (Figure 17). It should be noted that the spatial survey design was not intended to cover the whole blue whiting stock during this period.

The total biomass index of blue whiting registered during the IESNS survey in 2020 was 0.39 million tonnes, which is a 26 % decrease from the biomass estimate in 2019 (0.53). The abundance index for 2020 was 4.9 billion, which is 21 % lower than in 2019. Age 1 is dominating the acoustic estimate (32.5 % of the biomass and 57% by number). Uncertainty estimates for numbers at age based on bootstrapping with StoX are shown in Figure 18 and Table 6. The relative standard error (CV) of total biomass estimate is 16 % and 17 % for total numbers (Table 6).

In this year's IESNS survey, one-year old blue whiting was at similar level as the estimate of one-year olds in 2019 and more numerous as compared to IESNS 2017 and 2018. The survey group compared age and length distributions by vessel and strata (Figure 20 and 21) and no clear differences were found compared to earlier years.

This year the blue whiting estimate was based on only three of the four vessels. Staffing constraints on Dana due to the Covid-19 situation meant that the survey data was scrutinised after the survey ended rather than during the cruise. This resulted in some discrepancy in the procedure used for scrutinization of blue whiting from Dana. Visual observation of significant inconsistencies between the neighbouring

transects of Dana and G. O. Sars lead the survey group to decide to omit the acoustic data from Dana this year. This resulted in a higher total estimate of blue whiting (~21%) but also higher uncertainty. The biological information from Dana was still used.

Mackerel

Trawl catches of mackerel are shown in Figure 22 Mackerel was present in the southern and eastern part of the Norwegian Sea (up to 69°N) in the beginning of May. No further quantitative information can be drawn from these data as this survey is not designed to monitor mackerel.

General recommendations and comments

RECOMMENDATION	ADRESSED TO
1. Continue the methodological research in distinguishing between Herring and blue whiting in the interpretation of echograms.	WGIPS
2. It is recommended that a workshop based on the ongoing otolith and scale exchange will take place before next year's IESNS survey.	WGBIOP, WGWIDE
3. It is recommended that the WGIPS meeting in 2021 includes a workshop on how to deal with stock components of herring in the IESNS-survey.	WGIPS
4. It is recommended that the WGIPS meeting in 2021 discusses the possible implementation of sonar observations in IESNS and other acoustic surveys.	WGIPS

Next year's post-cruise meeting

We will aim for next meeting in 15-17 June 2021. The final decision will be made at the next WGIPS meeting.

Concluding remarks

- The sea temperature in 2020 at 0-200 m depth was generally below the long-term mean (1995-2019) in the Norwegian Sea.
- The 2020 index of meso-zooplankton biomass in the Norwegian Sea and adjoining waters decreased a bit from last year.
- The total biomass estimate of NSSH in herring in the Norwegian Sea was 4.25 million tonnes, which is a 13 % decrease from the 2019 survey estimate. The estimate of total number of NSSH was 22.8 billion, which is a 15 % higher than in the 2019 survey. The survey followed the pre-planned protocol and the survey group recommends using the abundance estimates in the analytical assessment.

- The 2016 year class of NSSH dominated in the survey indices both in numbers (57%) and biomass (41%), and it is on the same level as the strong 2004 year class at the same age (in the 2008 survey).
- The biomass of blue whiting measured in the 2020 survey decreased by 26 % from last year's survey and 21 % in terms of numbers. Age 1 (2019 year class) is the dominating year class (32.5 % of the biomass and 57% by number)

References

Foote, K. G., Knudsen, H. P., Vestnes, G., MacLennan, D. N., and Simmonds, E. J. 1987. Calibration of acoustic instruments for fish density estimation: a practical guide. ICES Coop. Res. Rep. 144: 1–57.

ICES 2009. Report of the PGNAPES Scrutiny of Echogram Workshop (WKCHOSCRU) 17–19 February 2009, Bergen, Norway ICES CM 2009/RMC

ICES. 2012. Report of the Workshop on implementing a new TS relationship for blue whiting abundance estimates (WKTSBLUES), 23–26 January 2012, ICES Headquarters, Copenhagen, Denmark. ICES CM 2012/SSGESST:01. 27 pp.

ICES. 2015. Report of the Workshop on scrutinisation procedures for pelagic ecosystem surveys (WKSCRUT), 7-11 September 2015, Hamburg, Germany. ICES CM 2015/SSGIEOM:18. 107pp.

ICES. 2016. Report of the Working Group on the Integrated Assessments of the Norwegian Sea (WGINOR), 7-11 December 2015, Reykjavik, Iceland. ICES CM 2015/SSGIEA:10. 150 pp.

ICES. 2017. Workshop on Stock Identification and Allocation of Catches of Herring to Stocks (WKSIDAC). ICES WKSIDAC Report 2017 20-24 November 2017. Galway, Ireland. ICES CM 2017/ACOM:37. 99 pp.

ICES. 2018. Report of the Working Group on the Integrated Assessments of the Norwegian Sea (WGINOR), 26-30 November 2018, Reykjavik, Iceland. ICES CM 2018/IEASG:10. 123 pp.

ICES. 2019. Report of the Working Group on Integrated Ecosystem Assessments for the Norwegian Sea (WGINOR). ICES WGINOR REPORT 2018, 26-30 November 2018. Reykjavik, Iceland. ICES CM 2018/IEASG:10. 123 pp.

Johnsen, E., Totland, A., Skålevik, Å., Holmin, A.J., Dingsør, G.E., Fuglebakk, E., Handegard, N.O. 2019. StoX: An open source software for marine survey analyses. Methods Ecol Evol. 2019, 10:1523–1528.

Jolly, G. M., and I. Hampton. 1990. A stratified random transect design for acoustic surveys of fish stocks. Can.J. Fish. Aquat. Sci. 47: 1282-1291.

Kristiansen, I., Hátun H., Petursdottir, H., Gislason, A., Broms, C., Melle, W., Jacobsen, J.A., Eliasen S.K., Gaard E. 2019. Decreased influx of Calanus spp. into the south-western Norwegian Sea since 2003. Deep Sea Research, 149, 103048

Skjoldal, H.R., Dalpadado, P., and Dommasnes, A. 2004. Food web and trophic interactions. *In* The Norwegian Sea ecosystem. Ed. by H.R. Skjoldal. Tapir Academic Press, Trondheim, Norway: 447-506

Tables

Table 1. Survey effort by vessel for the International ecosystem survey in the Nordic Seas in May - June 2020.

Vessel	Effective survey period	Effective acoustic cruise track (nm)	Trawl stations	Ctd stations	Aged fish (HER)	Length fish (HER)	Plankton stations
Dana	01/05-25/05	1893	25	29	468	1866	34
Magnus Heinason	29/4-11/5	1319	15	22	394	775	22
Árni Fridriksson	12/5-26/5	3188	14	34	830	2758	30
G.O.Sars	01/5-02/6	3632	73	66	659	2065	60
Total		**10032**	**127**	**151**	**2351**	**7464**	**146**

Table 2. IESNS 2020 in the Norwegian Sea. Baseline estimates of abundance, mean weight and mean length of Norwegian spring-spawning herring.

	age																				
LenGrp	2	3	4	5	6	7	8	9	10	11	12	13	14	15	16	17	18	Unknown	Number (1E3)	Biomass (1E3kg)	Mean W (g)
14-15	15775	-	-	-	-	-	-	-	-	-	-	-	-	-	-	-	-	-	15775	276.1	17.50
15-16	-	-	-	-	-	-	-	-	-	-	-	-	-	-	-	-	-	-	-	-	-
16-17	-	-	-	-	-	-	-	-	-	-	-	-	-	-	-	-	-	-	-	-	-
17-18	-	-	-	-	-	-	-	-	-	-	-	-	-	-	-	-	-	2379	2379	-	-
18-19	-	-	-	-	-	-	-	-	-	-	-	-	-	-	-	-	-	-	-	-	-
19-20	-	-	-	-	-	-	-	-	-	-	-	-	-	-	-	-	-	8387	8387	385.8	46.00
20-21	20596	46719	-	-	-	-	-	-	-	-	-	-	-	-	-	-	-	-	67315	3942.2	58.56
21-22	-	42542	23662	-	-	-	-	-	-	-	-	-	-	-	-	-	-	-	66204	4583.0	69.23
22-23	-	124419	109173	-	-	-	-	-	-	-	-	-	-	-	-	-	-	-	233593	18657.3	79.87
23-24	-	63233	286786	-	-	-	-	-	-	-	-	-	-	-	-	-	-	-	350019	31906.0	91.16
24-25	-	63676	1122561	-	-	-	-	-	-	-	-	-	-	-	-	-	-	-	1186237	118331.1	99.75
25-26	-	26921	2767160	-	-	-	-	-	-	-	-	-	-	-	-	-	-	-	2794080	313130.6	112.07
26-27	-	24267	2575099	7327	-	30359	-	-	-	-	-	-	-	-	-	-	-	-	2637052	323632.1	122.72
27-28	-	96829	1389284	-	3530	24990	14119	-	-	3586	-	-	-	-	-	-	-	-	1532337	213322.6	139.21
28-29	-	5884	1927200	78548	47422	153158	41188	-	-	-	-	-	-	-	-	-	-	-	2253401	357169.5	158.50
29-30	-	-	1929251	84784	114419	415279	144971	45132	13717	-	9145	-	-	-	-	-	-	-	2756696	484901.5	175.90
30-31	-	-	731038	211152	282243	388372	287591	71245	39794	9036	8689	-	-	-	-	-	-	-	2029160	402964.2	198.59
31-32	-	-	89081	163380	260560	238699	50907	90121	78299	101878	27584	11822	-	-	-	-	-	-	1112330	248182.8	223.12
32-33	-	-	11658	22823	165992	404084	14312	30234	42153	49547	-	-	-	-	-	-	-	-	740803	179908.2	242.86
33-34	-	-	18429	2096	63689	517652	52388	40442	19271	2096	12573	-	-	-	-	-	-	-	728636	184875.2	253.73
34-35	-	-	9607	11823	64531	293609	125357	92216	28374	33103	7094	7094	4729	2365	9458	-	-	-	689359	193224.9	280.30
35-36	-	-	-	-	32093	81692	70022	164132	113785	163384	64187	140044	72939	35011	11670	-	-	-	948959	293187.8	308.96
36-37	-	-	-	-	-	25001	25001	44233	58296	211548	92913	180777	278740	115390	38463	17308	-	-	1087672	351837.7	323.48
37-38	-	-	-	-	-	-	2778	25002	27780	104176	57361	141679	255578	230576	137512	25002	-	-	1007445	340918.5	338.40
38-39	-	-	-	-	-	-	-	-	14787	11375	6825	44362	85311	109198	101236	32987	11375	-	417455	148142.6	354.87
39-40	-	-	-	-	-	-	-	-	-	-	-	19266	23799	-	36266	20400	5667	-	105398	39859.4	378.18
40-41	-	-	-	-	-	-	-	-	-	-	-	-	-	-	-	-	-	10205	10205	-	-
41-42	-	-	-	-	-	-	-	-	-	-	-	-	-	-	-	-	-	1136	1136	-	-
TSN(1000)	36371	494488	12989989	581932	1034479	2572896	828633	602757	436258	689729	286370	545043	721097	492539	334605	95697	17041	22107	22782032	-	-
TSB(1000 kg)	1471.2	47893.6	1755258.9	112070.0	232978.9	593613.9	192408.4	159723.7	119478.0	210165.6	90037.0	177472.5	238730.4	165718.0	116523.5	33343.8	6065.9	385.8	-	4253339.0	-
Mean length (cm)	17.81	23.76	26.86	30.19	31.15	31.50	31.37	33.21	33.68	34.82	35.10	36.18	36.60	36.83	37.25	37.59	38.33	29.75	-	-	-
Mean weight (g)	40.45	96.85	135.12	192.58	225.21	230.72	232.20	264.99	273.87	304.71	314.41	325.61	331.07	336.46	348.24	348.43	355.95	46.00	-	-	186.81

Table 4. IESNS 2020 in the Norwegian Sea. Estimates of abundance, mean weight and mean length of blue whiting.

	age											
LenGrp	1	2	3	4	5	6	7	8	10	Number (1E3)	Biomass (1E3kg)	Mean W (g)
16-17	3175	-	-	-	-	-	-	-	-	3175	69.8	22.00
17-18	56465	-	-	-	-	-	-	-	-	56465	1442.4	25.54
18-19	260128	-	-	-	-	-	-	-	-	260128	7978.6	30.67
19-20	895640	-	-	-	-	-	-	-	-	895640	33357.1	37.24
20-21	708352	39471	-	-	-	-	-	-	-	747823	33457.2	44.74
21-22	510440	49345	26468	-	-	-	-	-	-	586253	31207.9	53.23
22-23	267390	91340	18972	-	-	-	-	-	-	377703	23374.3	61.89
23-24	95144	105467	56782	-	-	-	-	-	-	257393	18312.6	71.15
24-25	24788	82626	122028	-	-	-	-	-	-	229442	19304.4	84.14
25-26	-	47957	171008	17439	10899	-	-	-	-	247304	23504.4	95.04
26-27	-	57515	154081	22617	19547	-	-	-	-	253760	26919.0	106.08
27-28	-	6822	31835	6822	9096	2656	11629	-	-	68860	8684.8	126.12
28-29	-	-	51237	24091	44665	79472	10325	9822	-	219613	32134.2	146.32
29-30	-	-	17933	73231	103619	39343	19603	-	-	253729	42296.7	166.70
30-31	-	-	30704	98407	120707	50174	27940	10235	-	338168	59325.9	175.43
31-32	-	-	-	13533	26074	45444	20141	-	-	105191	20992.3	199.56
32-33	-	-	-	-	17544	9029	2567	4695	-	33836	7113.2	210.23
33-34	-	-	-	-	-	2109	-	-	-	2109	493.6	234.00
34-35	-	-	-	-	-	-	-	-	-	-	-	-
36-37	-	-	-	-	-	-	-	-	382	382	113.9	298.20
TSN(1000)	2821522	480543	681050	256141	352152	228228	92204	24752	382	4936973	-	-
TSB(1000 kg)	126992.5	36024.1	68641.8	40862.5	57978.5	39223.4	16101.6	4143.9	113.9	-	390082.3	-
Mean length (cm)	20.09	23.27	25.44	28.95	29.36	29.55	29.59	29.63	36.00	-	-	-
Mean weight (g)	45.01	74.97	100.79	159.53	164.64	171.86	174.63	167.42	298.20	-	-	79.01

Table 5. IESNS 2020. Bootstrap estimates from StoX (based on 1000 replicates) of Norwegian spring-spawning herring. Numbers by age and total number (TSN) are in millions and total biomass (TSB) in thousand tons.

Age	5th percentile	Median	95th percentile	Mean	SD	CV
2	9.0	40.0	85.4	42.7	24.0	0.563
3	245.8	466.7	714.2	471.9	144.8	0.307
4	10156.8	13067.0	16037.7	13064.5	1826.4	0.140
5	216.9	512.5	808.0	512.7	175.7	0.343
6	528.3	977.8	1585.3	1009.2	317.5	0.315
7	1543.8	2446.6	3602.0	2492.2	633.2	0.254
8	404.4	758.2	1262.3	786.4	263.5	0.335
9	340.3	615.7	965.8	629.4	196.7	0.313
10	219.4	418.0	684.5	433.8	144.0	0.332
11	357.6	678.3	1071.4	694.2	223.6	0.322
12	152.4	311.2	528.3	323.8	113.2	0.349
13	231.7	484.8	843.4	505.1	192.8	0.382
14	356.1	698.5	1166.3	725.6	257.6	0.355
15	228.9	466.9	777.6	483.0	177.6	0.368
16	118.5	292.8	543.5	307.8	133.3	0.433
17	30.7	92.0	175.7	96.6	46.1	0.477
18	0.0	12.7	34.3	14.4	11.1	0.768
Unknown	9.0	21.7	40.8	22.8	10.0	0.439
TSN	18020.8	22708.0	27299.3	22615.9	2795.2	0.124
TSB	3161.1	4206.4	5296.1	4209.9	638.3	0.152

Table 6. IESNS 2020. Bootstrap estimates from StoX (based on 1000 replicates) of blue whiting. Numbers by age and total number (TSN) are in millions and total biomass (TSB) in thousand tons.

Age	5th percentile	Median	95th percentile	Mean	SD	CV
1	1931.0	2777.9	3834.2	2817.2	597.2	0.21
2	319.1	486.1	701.5	492.9	119.6	0.24
3	448.1	667.5	955.3	680.6	156.6	0.23
4	123.3	245.7	398.3	251.6	82.9	0.33
5	174.2	339.8	539.6	345.1	113.0	0.33
6	133.6	235.2	349.8	237.8	68.1	0.29
7	46.4	88.1	151.7	92.3	32.1	0.35
8	7.0	23.0	42.0	23.4	10.5	0.45
10	0.0	0.4	1.3	0.4	0.3	0.81
TSN	3682.9	4928.6	6231.0	4942.5	777.7	0.16
TSB	283.6	391.1	497.5	388.8	64.3	0.17

Figures

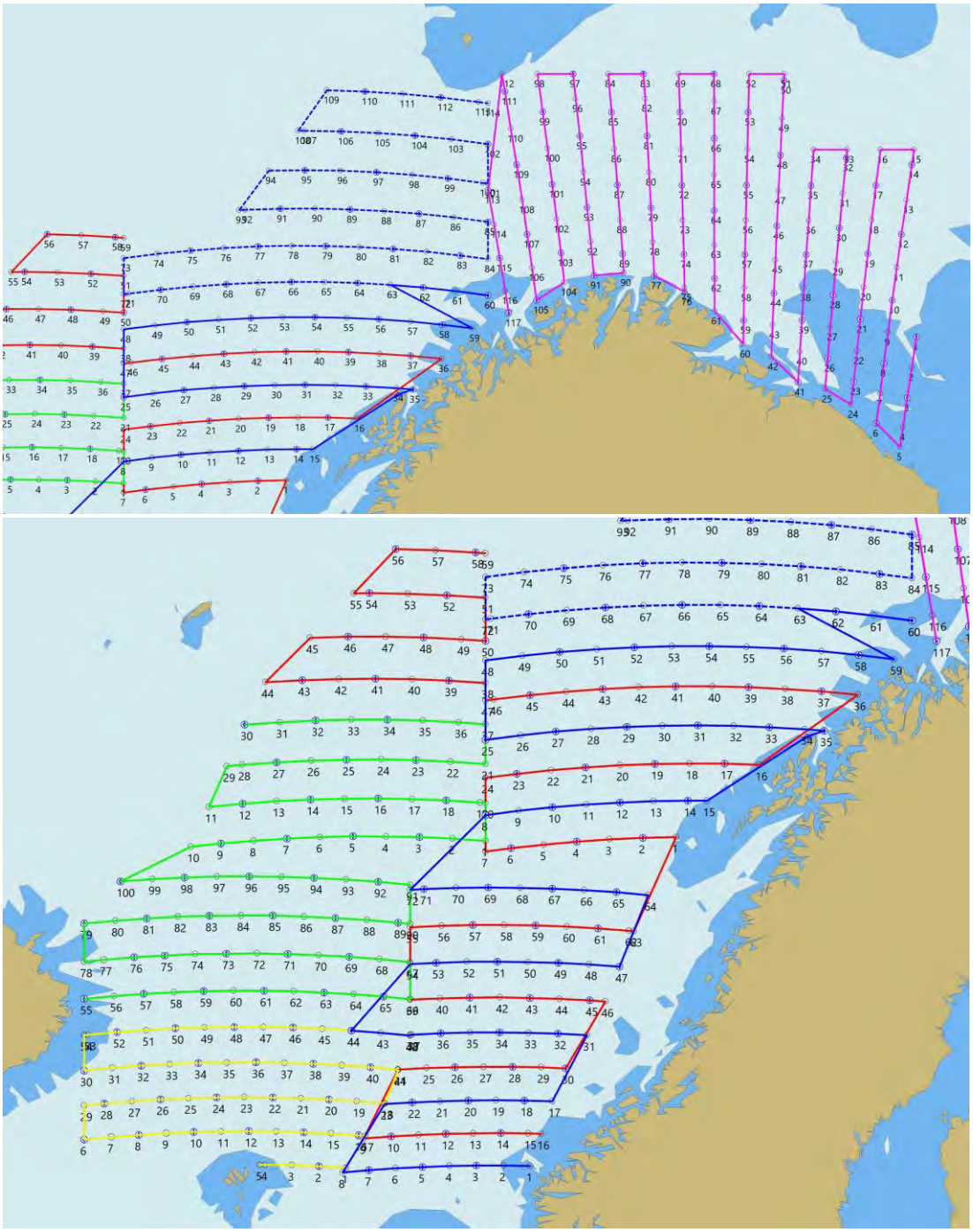

Figure 1. The pre-planned strata and transects for the IESNS survey in 2020 (red: EU, dark blue: Norway, yellow: Faroes Islands, violet: Russia, green: Iceland). Hydrographic stations and plankton stations are shown as blue circles with diamonds. All the transects have numbered waypoints for each 30 nautical mile and at the ends**.** **Note:** The Russian vessel was not able to conduct the survey planned in the Barents Sea.

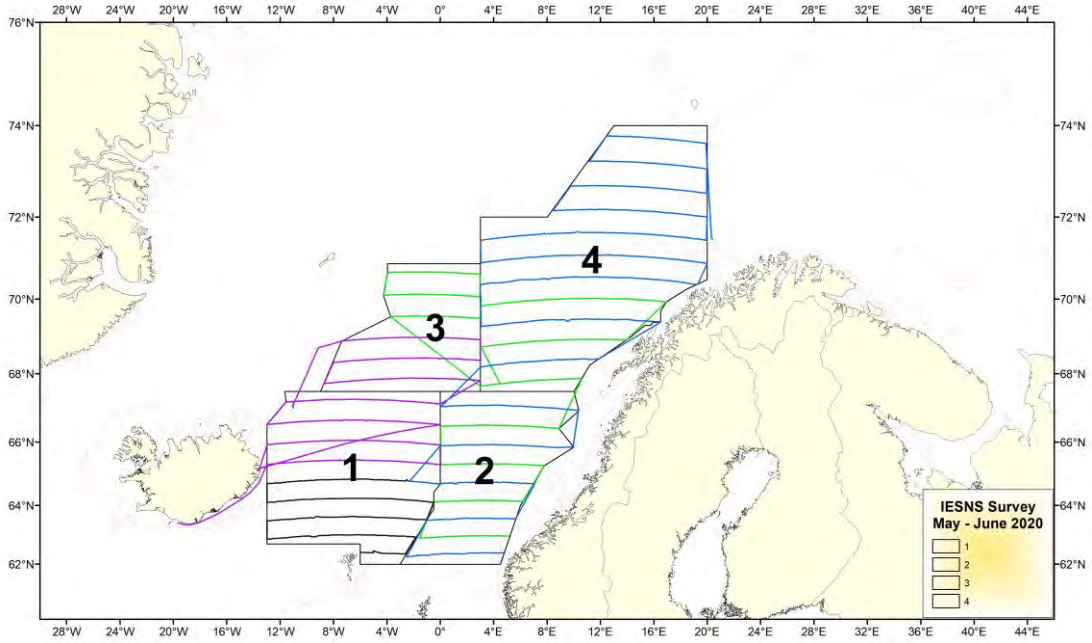

Figure 2. Cruise tracks and strata (with numbers) for the IESNS survey in May 2020.

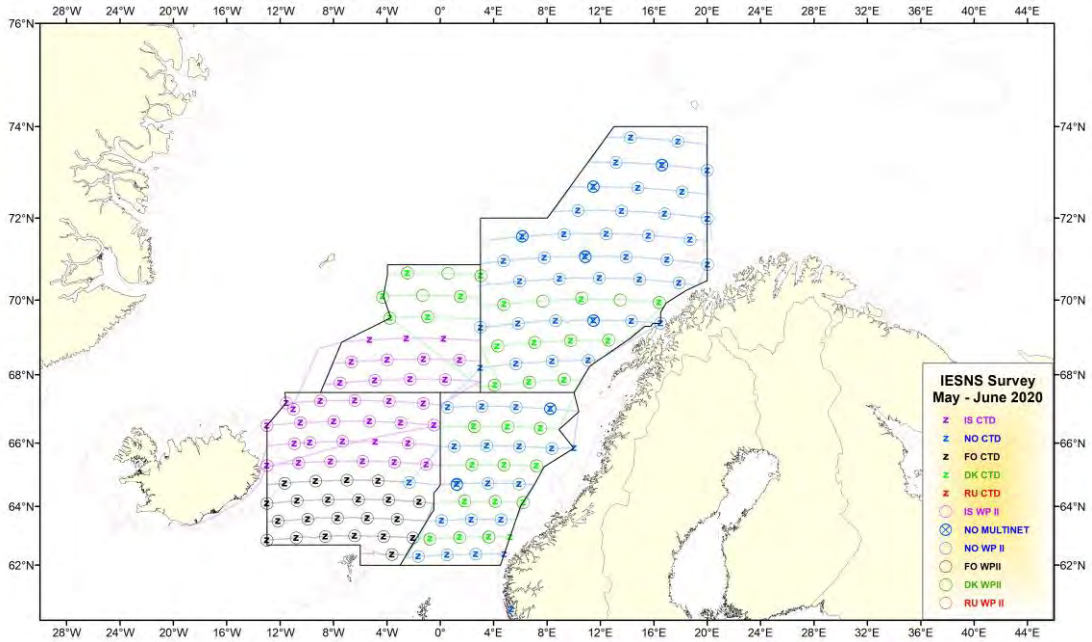

Figure 3a. IESNS survey in May 2020: location of hydrographic and plankton stations. The strata are shown.

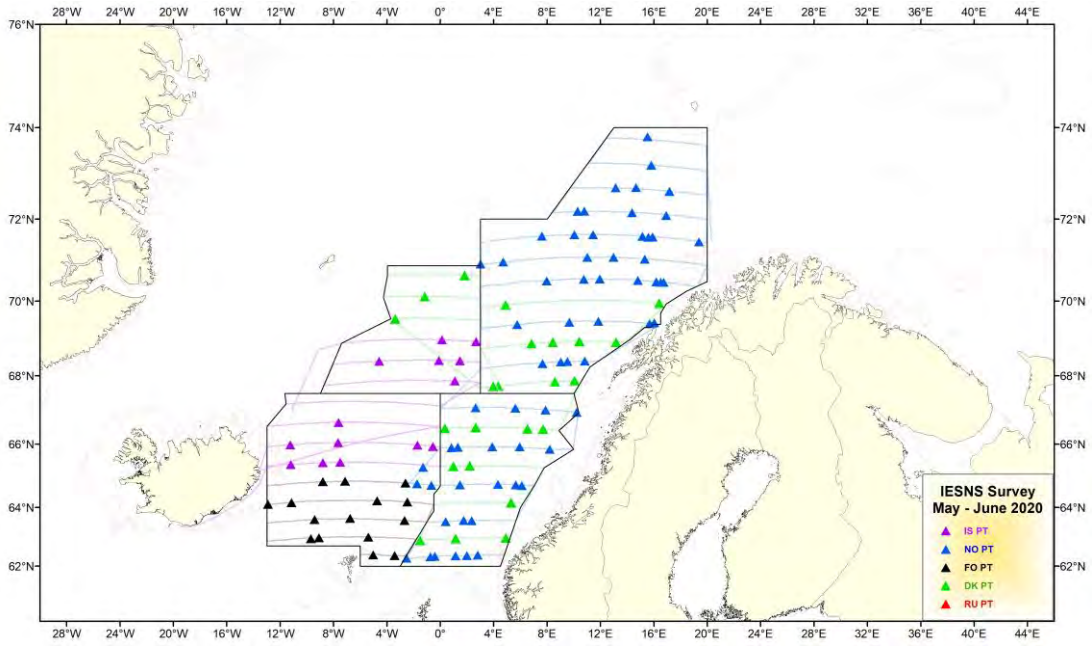

Figure 3b. IESNS survey in May 2020: location of pelagic trawl stations. The strata are shown.

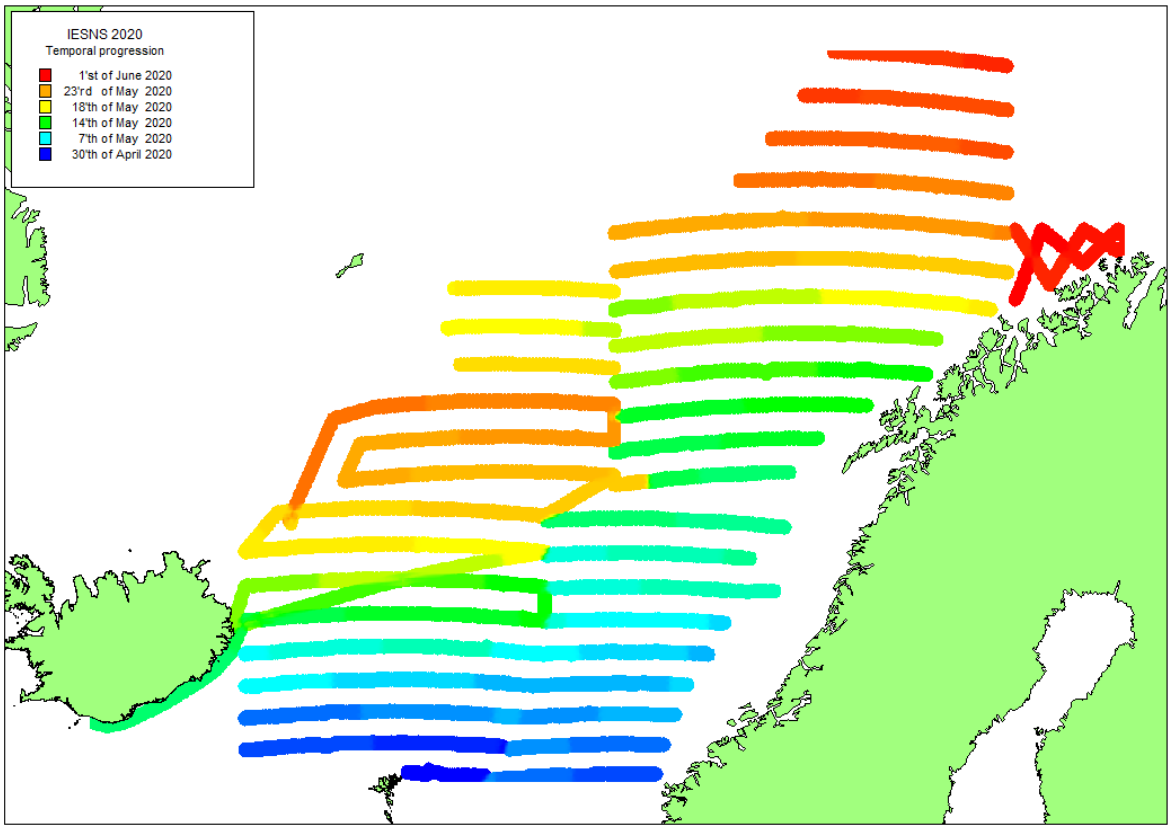

Figure 4. Temporal progression IESNS in May-June 2020.

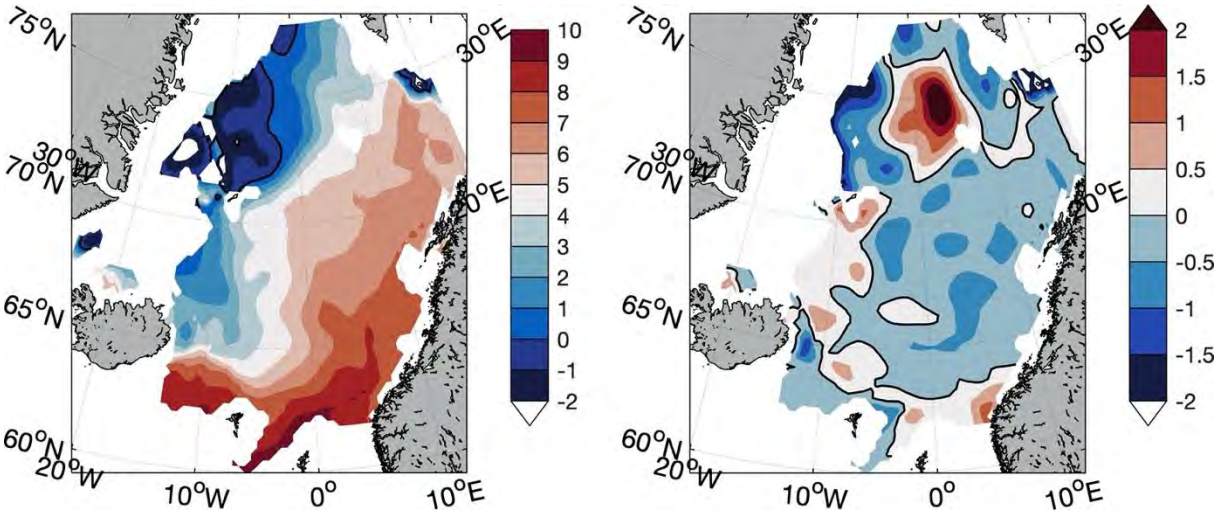

Figure 5. Temperature (left) and temperature anomaly (right) averaged over 0-50 m depth in May 2020. Anomaly is relative to the 1995-2019 mean.

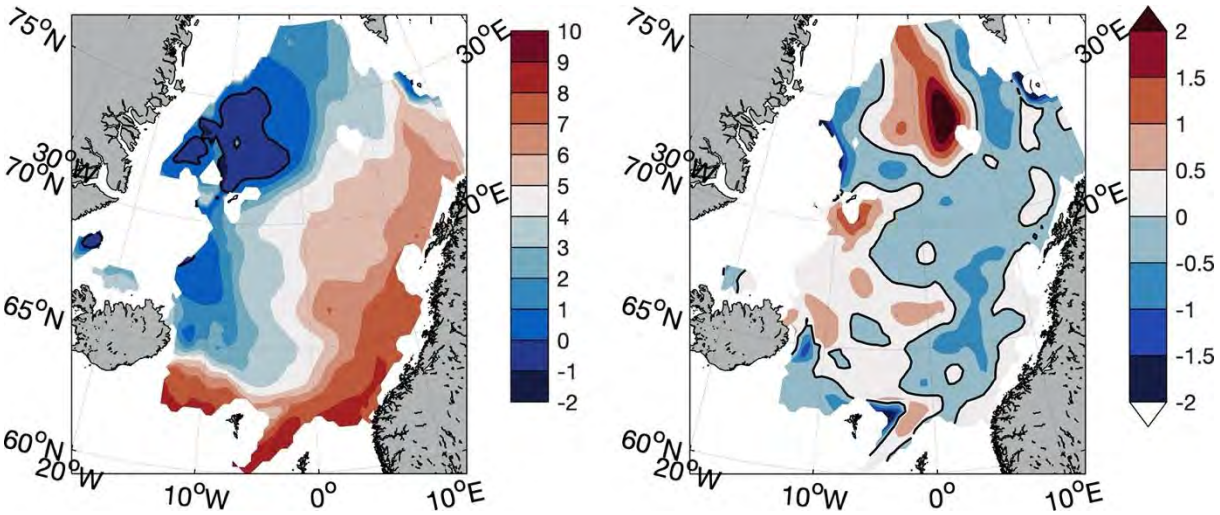

Figure 6. Same as above but averaged over 50-200 m depth.

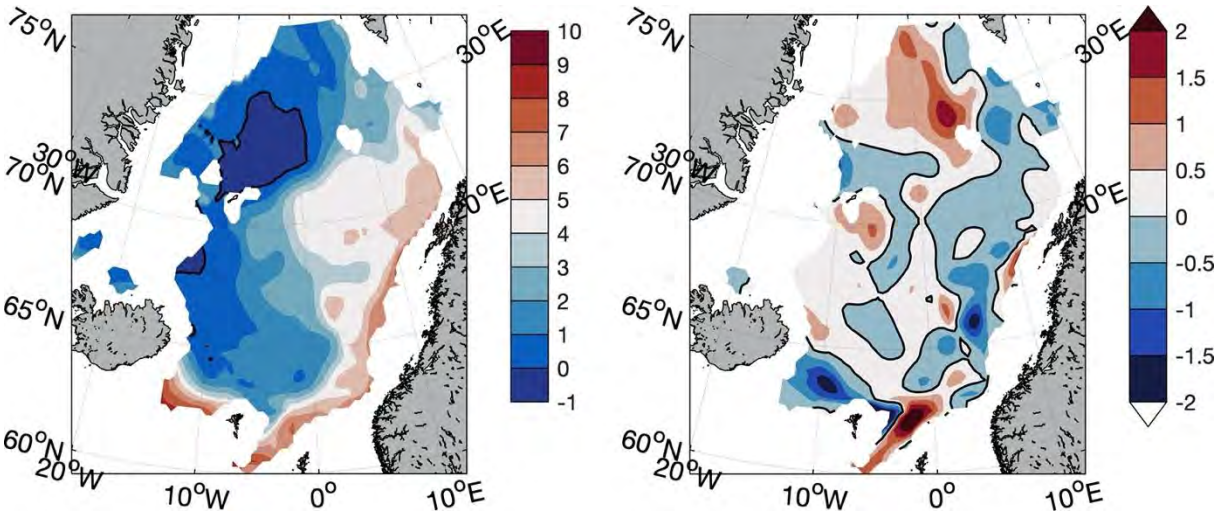

Figure 7. Same as above but averaged over 200-500 m depth.

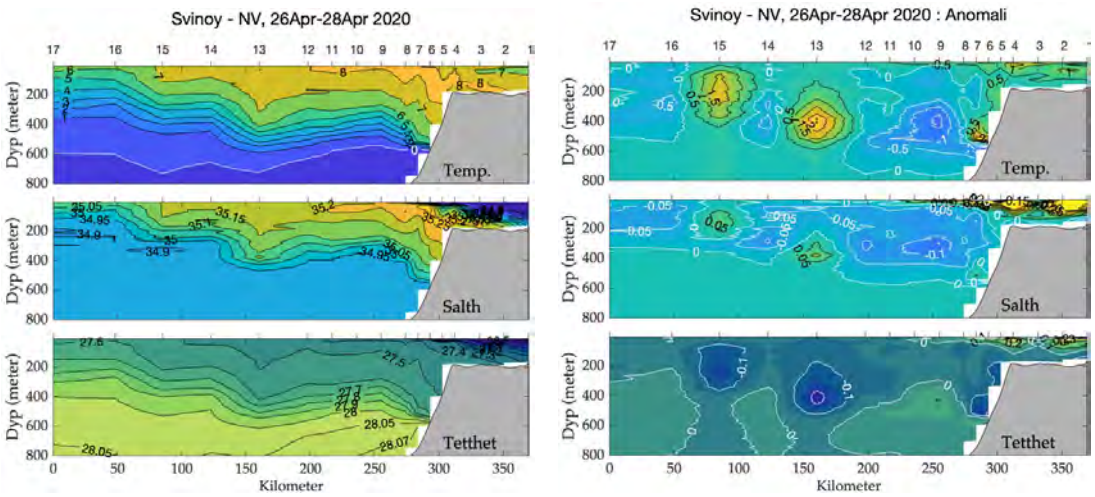

Figure 8. Temperature, salinity and potential density (sigma-t) (left figures) and anomalies (right figures) in the Svinøy section, 26-28 April 2020. Anomalies are relative to a 30 years long-term mean (1978-2007).

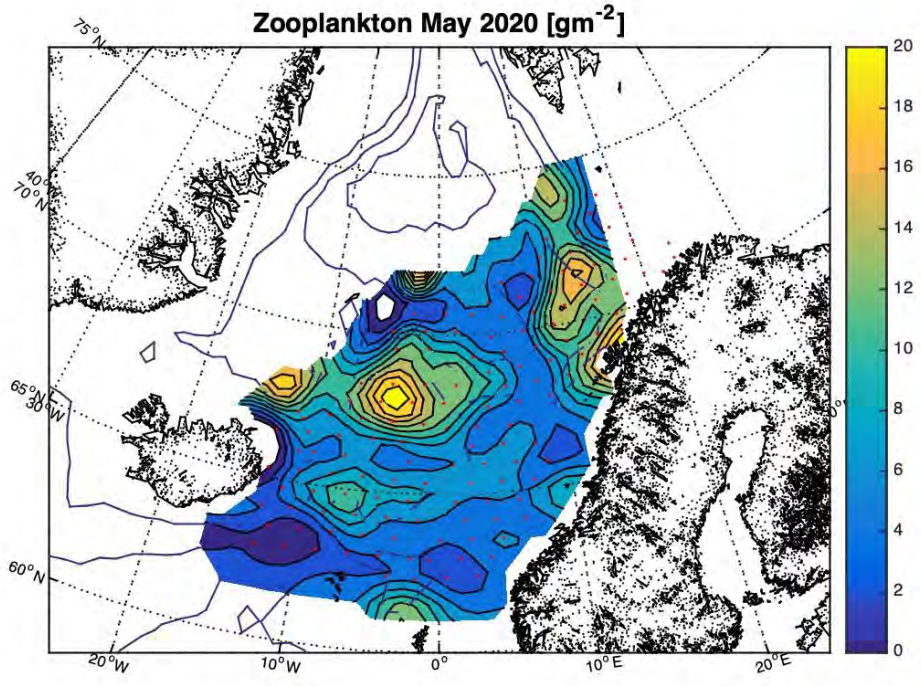

Figure 9. Representation of zooplankton biomass (g dry weight m^{-2}; at 0-200 m depth) in May 2020.

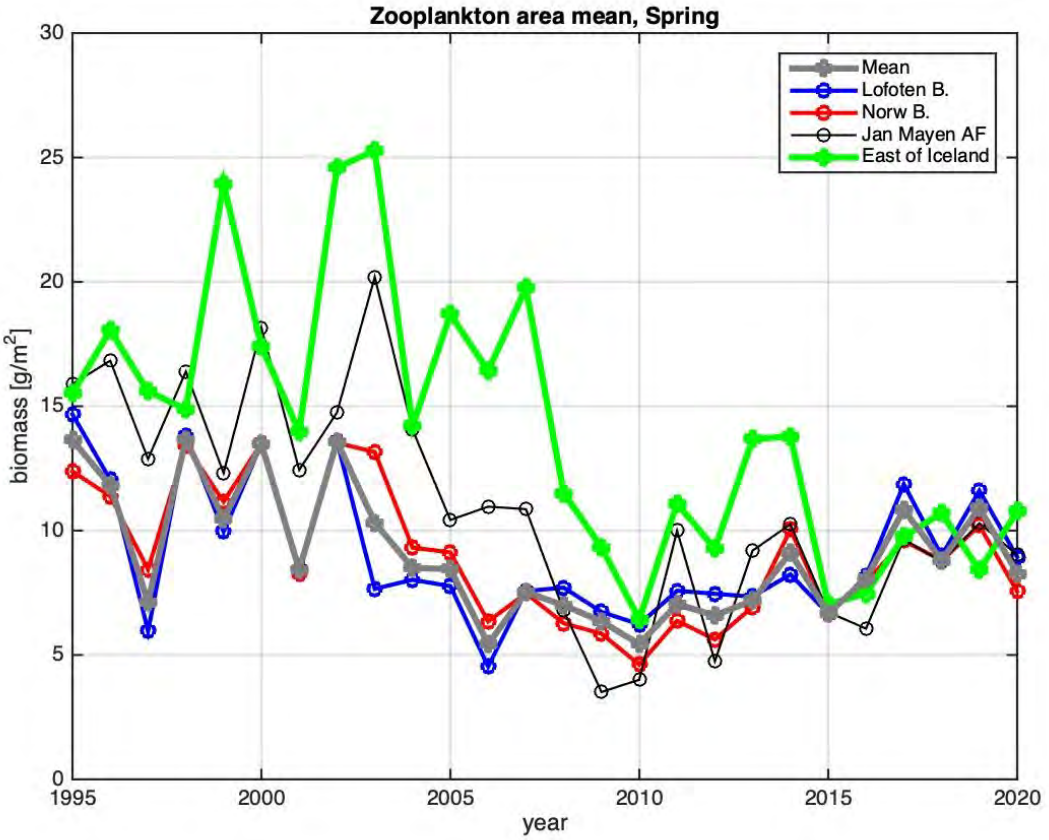

Figure 10. Indices of zooplankton dry weight (g m^{-2}) sampled by WP2 in May in (a) the different areas in and near Norwegian Sea from 1995 to 2020 as derived from interpolation using objective analysis utilizing a Gaussian correlation function (see details on methods and areas in ICES 2016).

(a)

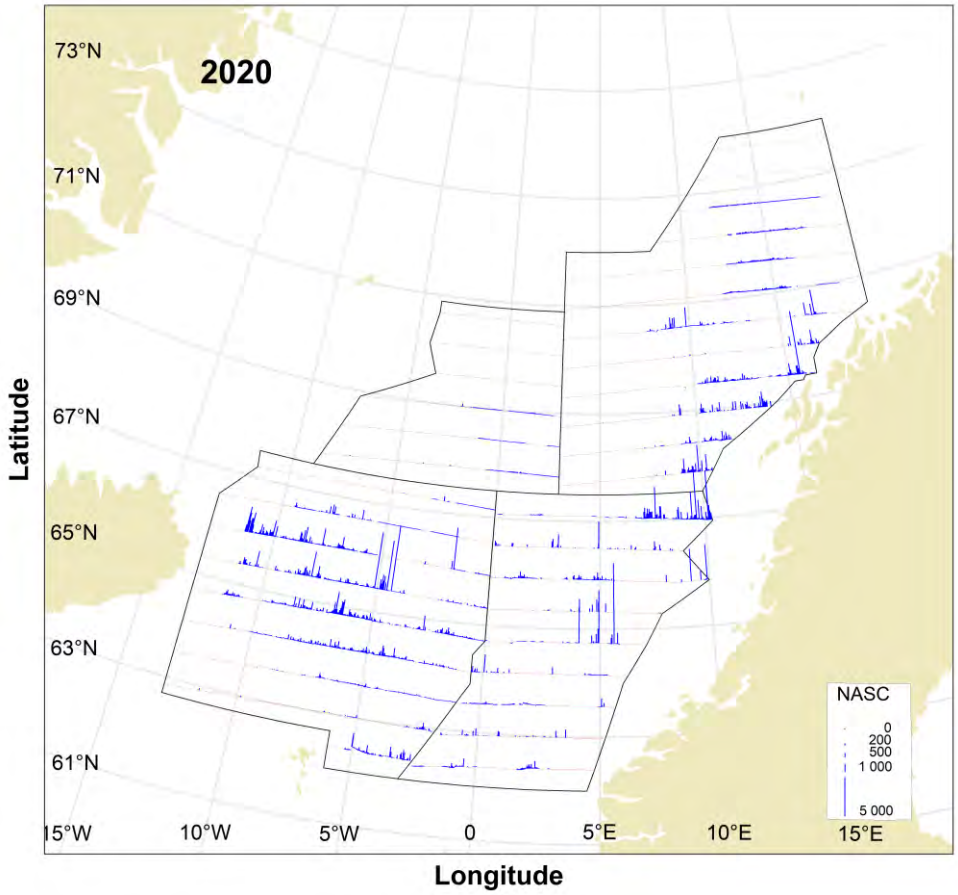

(b)

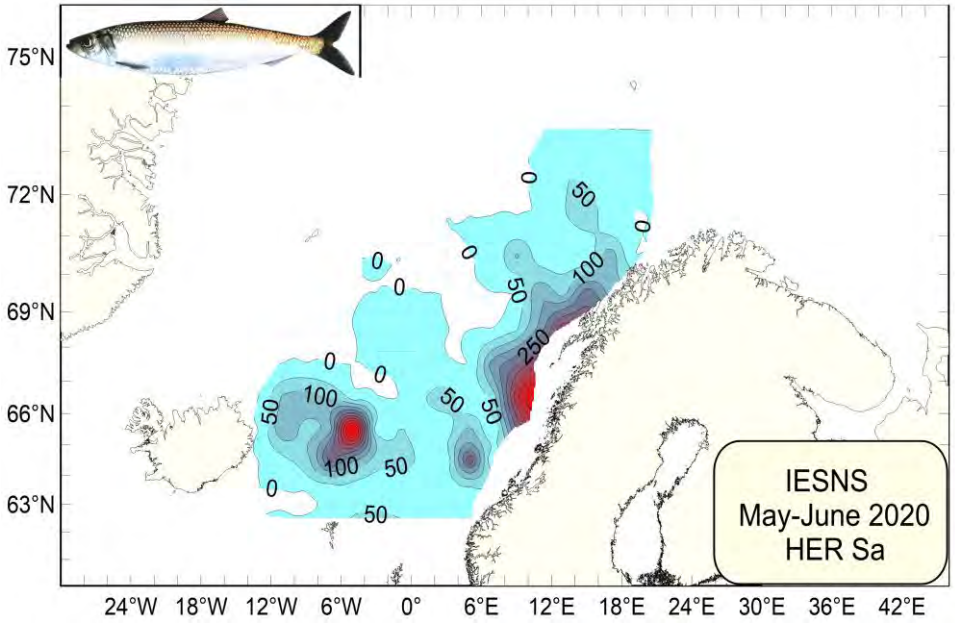

Figure 11. Distribution of Norwegian spring-spawning herring as measured during the IESNS survey in May 2020 in terms of NASC values (m^2/nm^2) averaged for every 1 nautical mile and (b) represented by a contour plot.

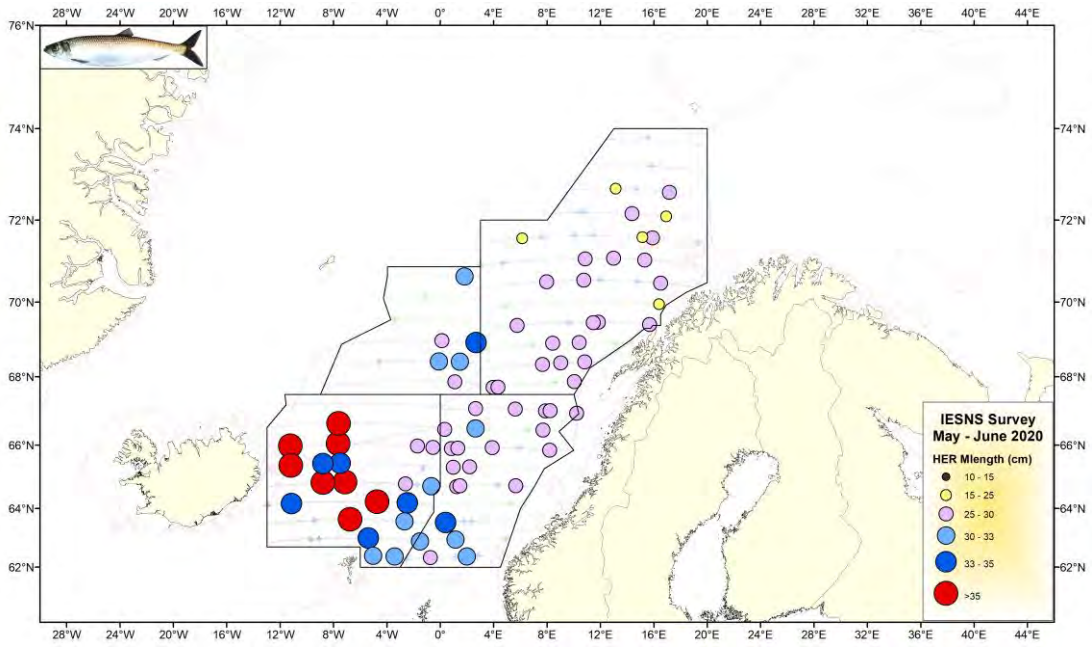

Figure 12. Mean length of Norwegian spring-spawning herring in all hauls in May 2020. The strata are shown.

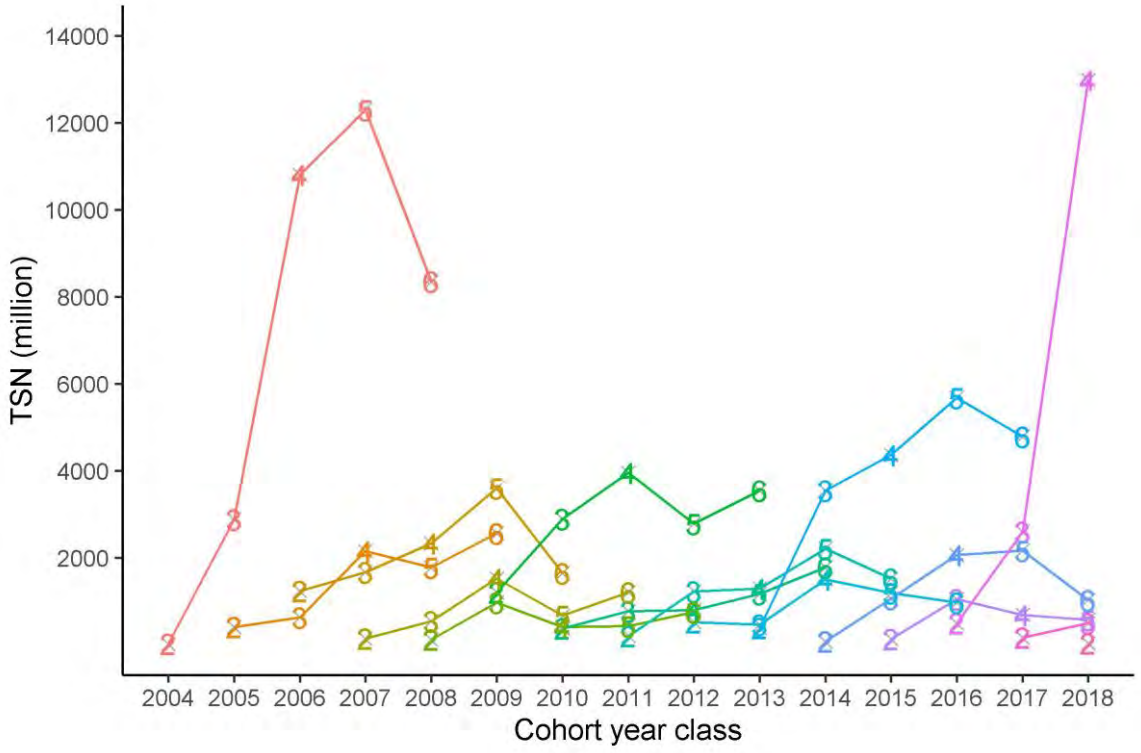

Figure 13. Tracking of the Total Stock Number (TSN, in millions) of Norwegian spring-spawning herring for each cohort since 2004 from age 2 to age 6. From 2008, stock is estimated using the StoX software. Prior to 2008, stock was estimated using BEAM.

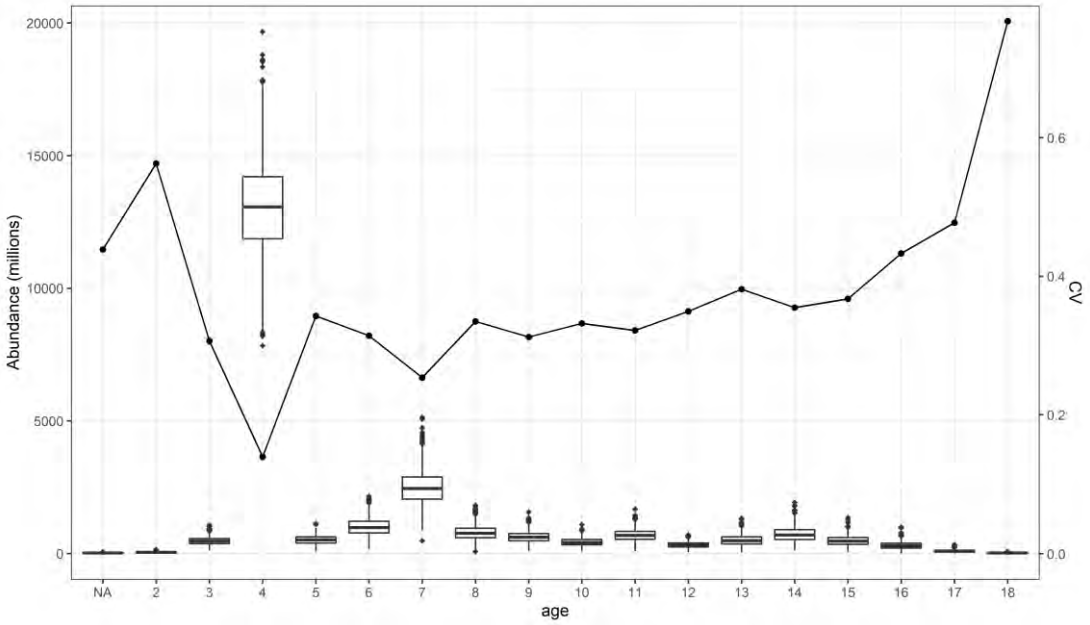

Figure 14. Norwegian spring-spawning herring in the Norwegian Sea: R boxplot of abundance and relative standard error (CV) obtained by bootstrapping with 1000 replicates using the StoX software.

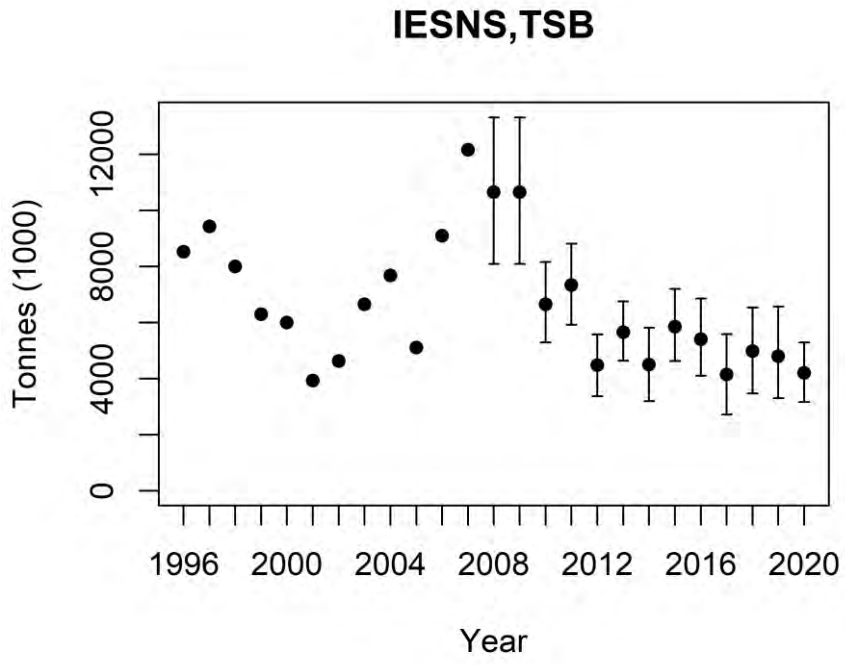

Figure 15. Biomass estimates of Norwegian-spring spawning herring in the IESNS survey (Barents Sea, east of 20°E, is excluded) from 1996 to 2020 as estimated using BEAM (1996-2007; calculated on basis of rectangles) and as estimated with the software StoX (2008-2020; boostrap means with 90% confidence interval; calculated on basis of standard stratified transect design).

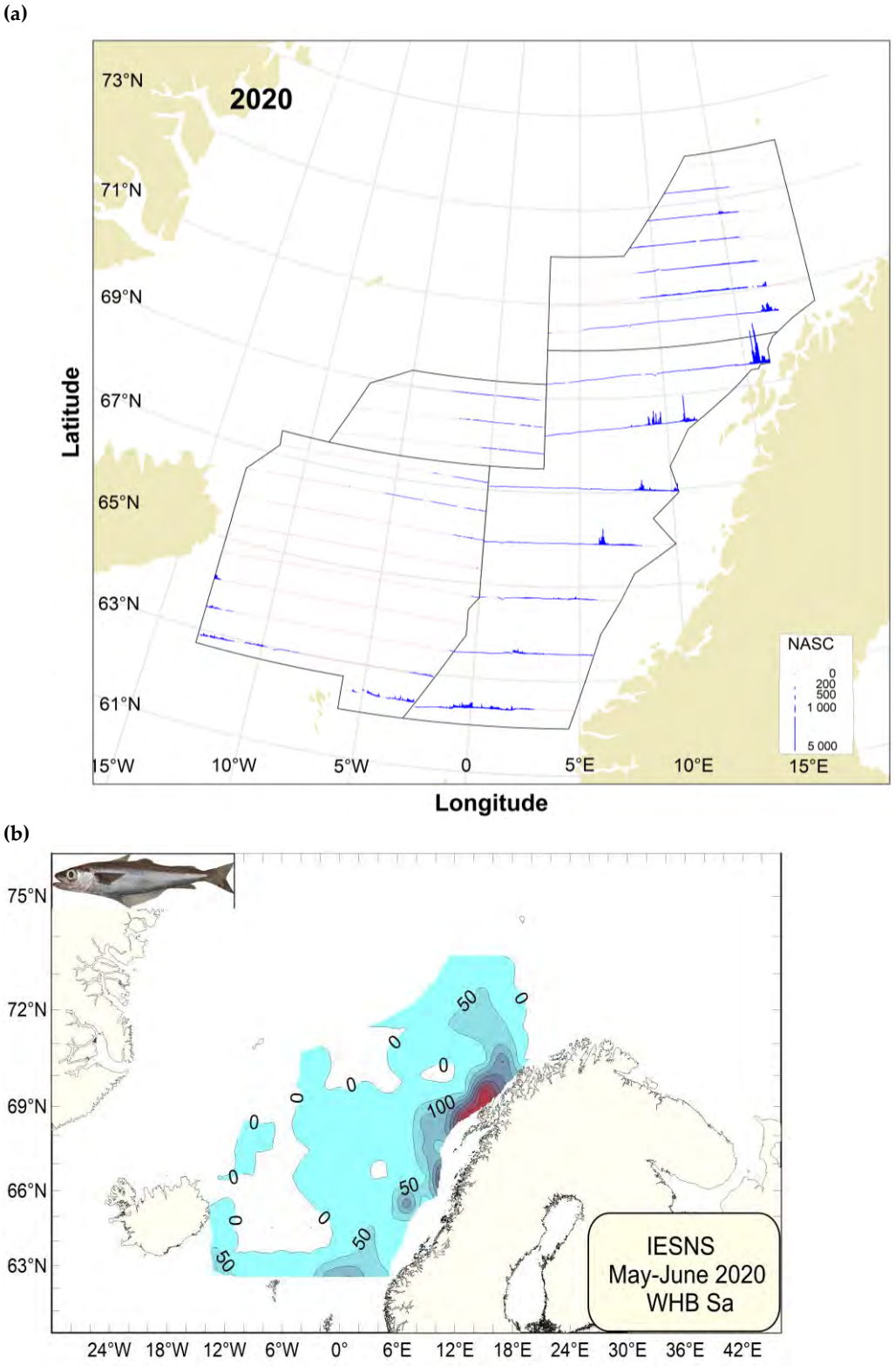

Figure 16. Distribution of blue whiting as measured during the IESNS survey in May 2020 in terms of NASC values (m^2/nm^2) (a) averaged for every 1 nautical mile and (b) represented by a contour plot.

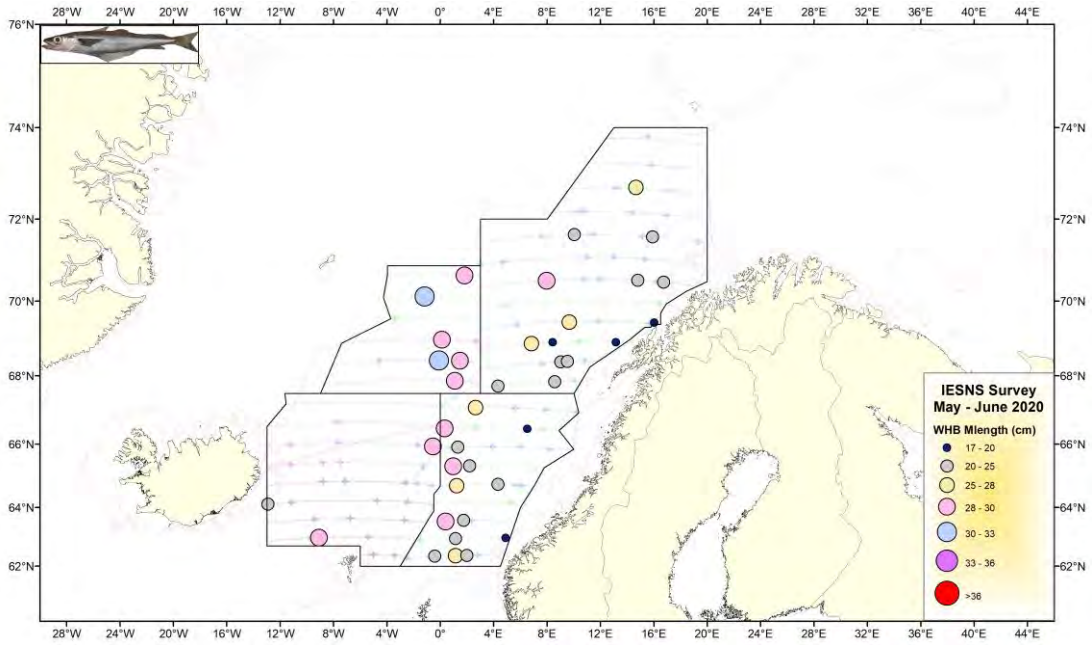

Figure 17. Mean length of blue whiting in all hauls in IESNS 2020. The strata are shown.

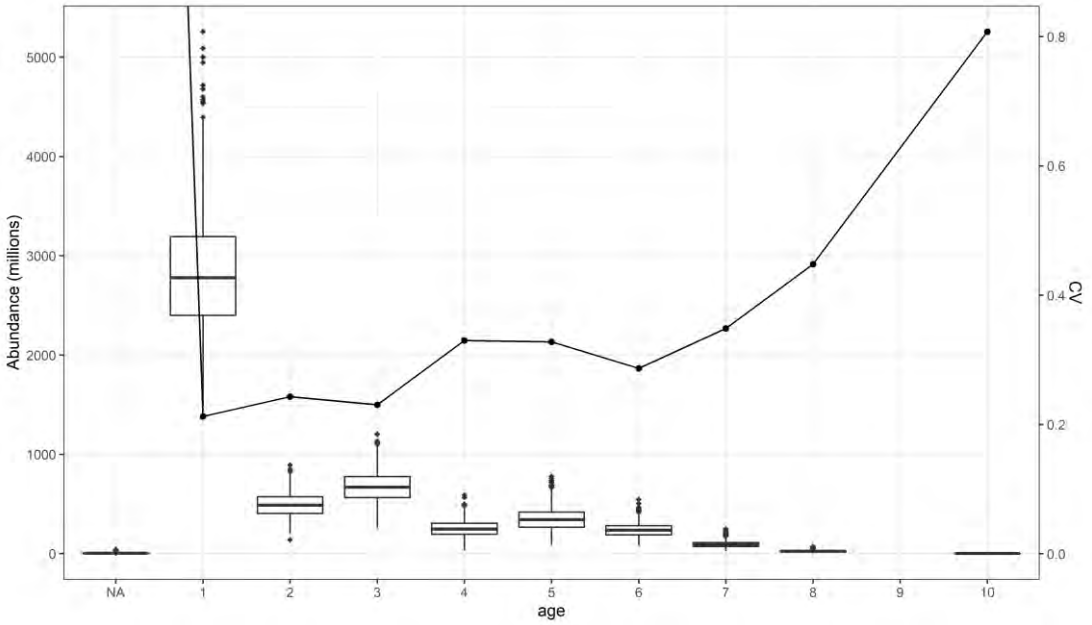

Figure 18. Blue whiting in the Norwegian Sea: R boxplot of abundance and relative standard error (CV) obtained by bootstrapping with 1000 replicates using the StoX software.

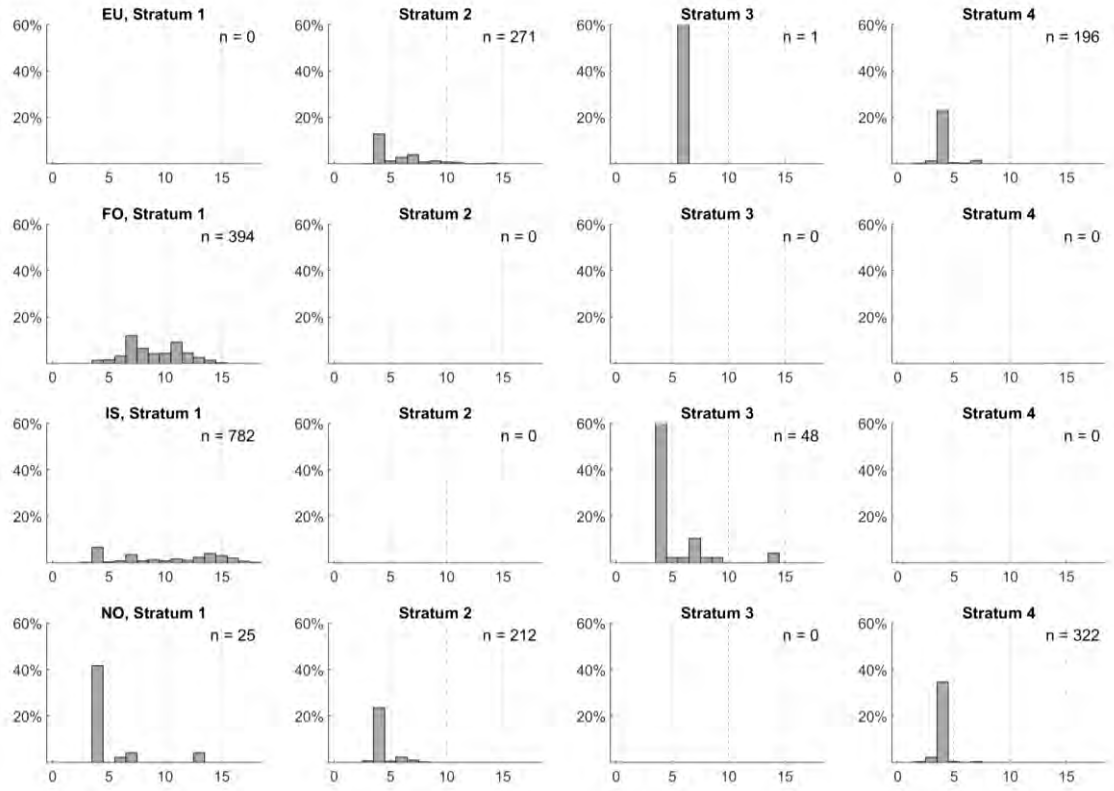

Figure 19. Comparison of the age distributions of NSS-herring by stratum and country in IESNS 2020. The strata are shown in Figure 3.

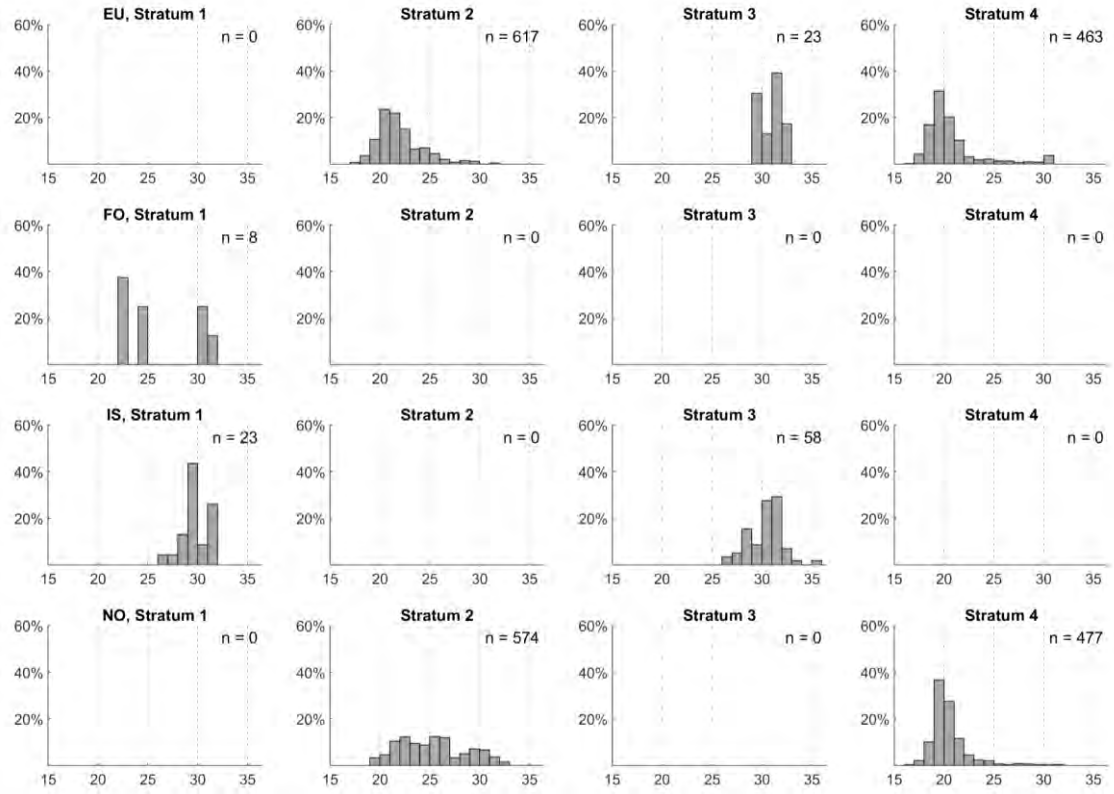

Figure 20. Comparison of the length distributions of blue whiting by stratum and country in IESNS 2020. The strata are shown in Figure 3.

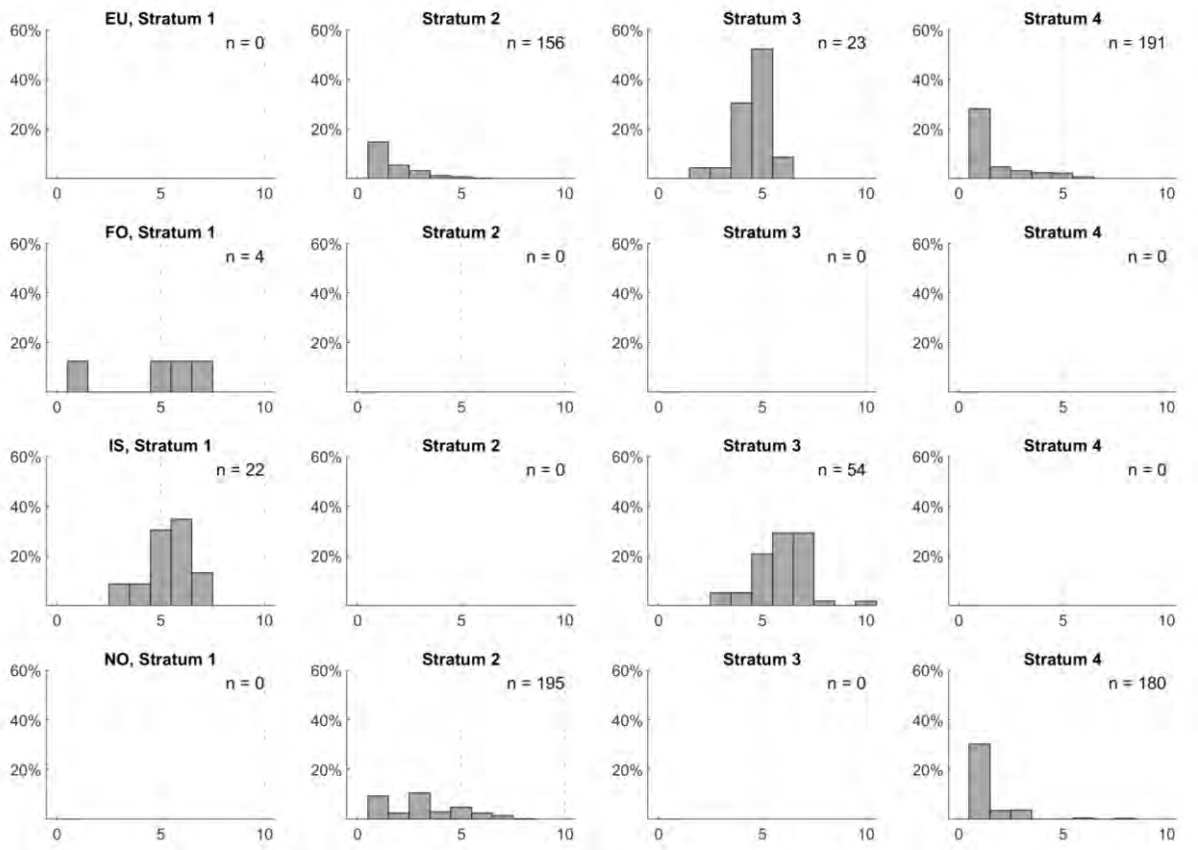

Figure 21. Comparison of the age distributions of blue whiting by stratum and country in IESNS 2020. The strata are shown in Figure 3.

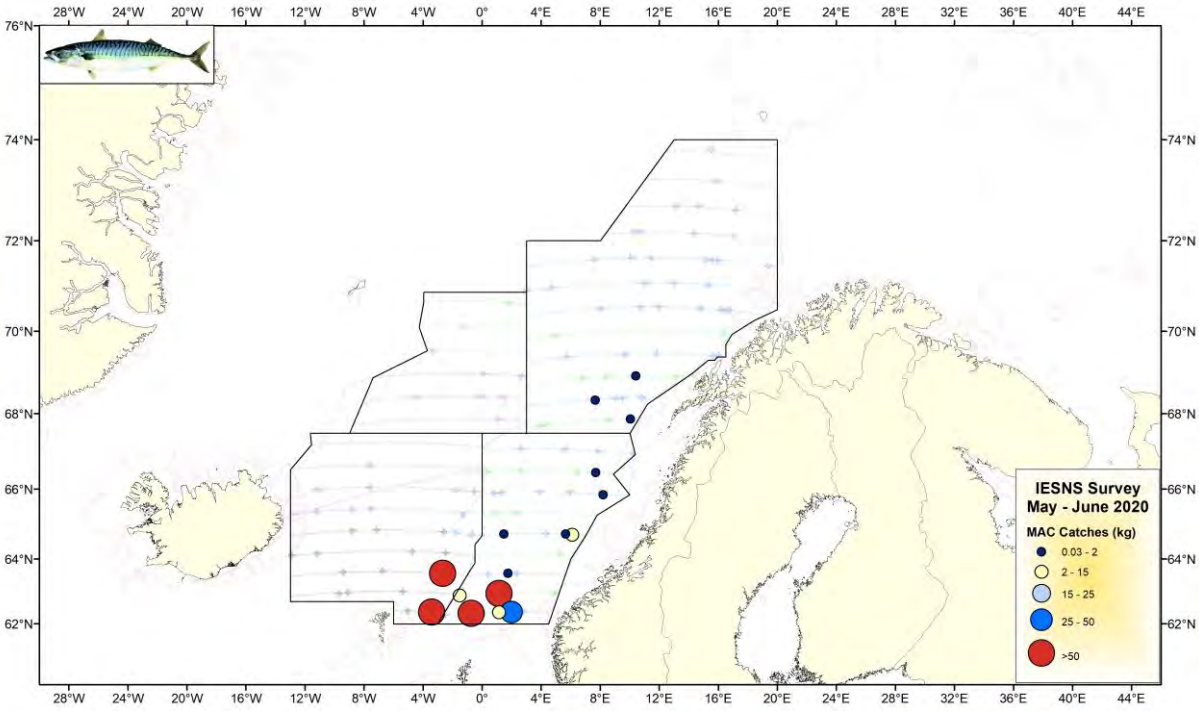

Figure 22. Pelagic trawl catches of mackerel in IESNS 2020. The strata are shown.

Appendix A

Distribution of NASC in the IESNS survey in the period 2014 – 2019.

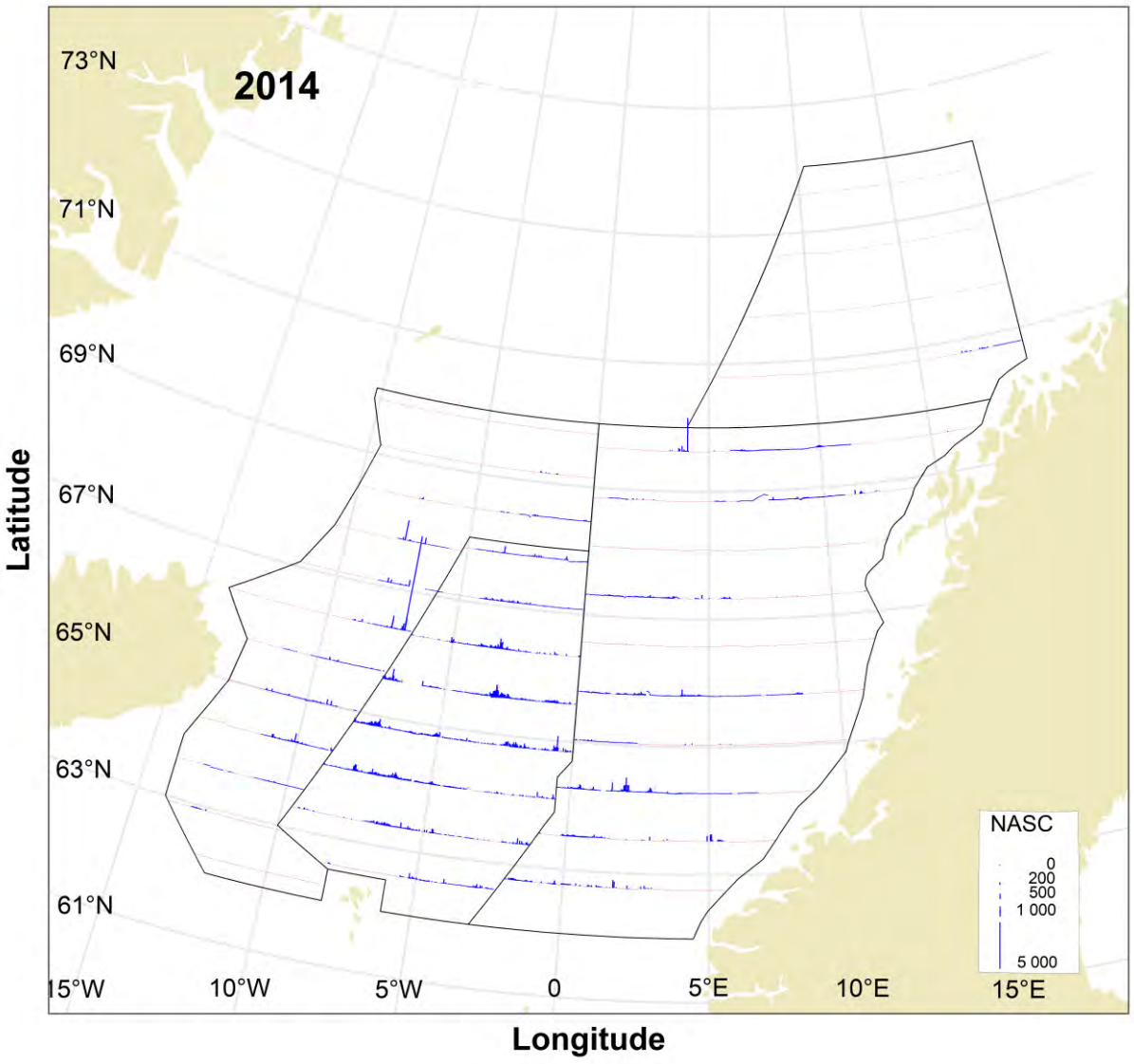

Figure A1. Distribution of Norwegian spring-spawning herring as measured during the IESNS survey in May 2014 in terms of NASC values (m^2/nm^2) (a) averaged for every 1 nautical mile

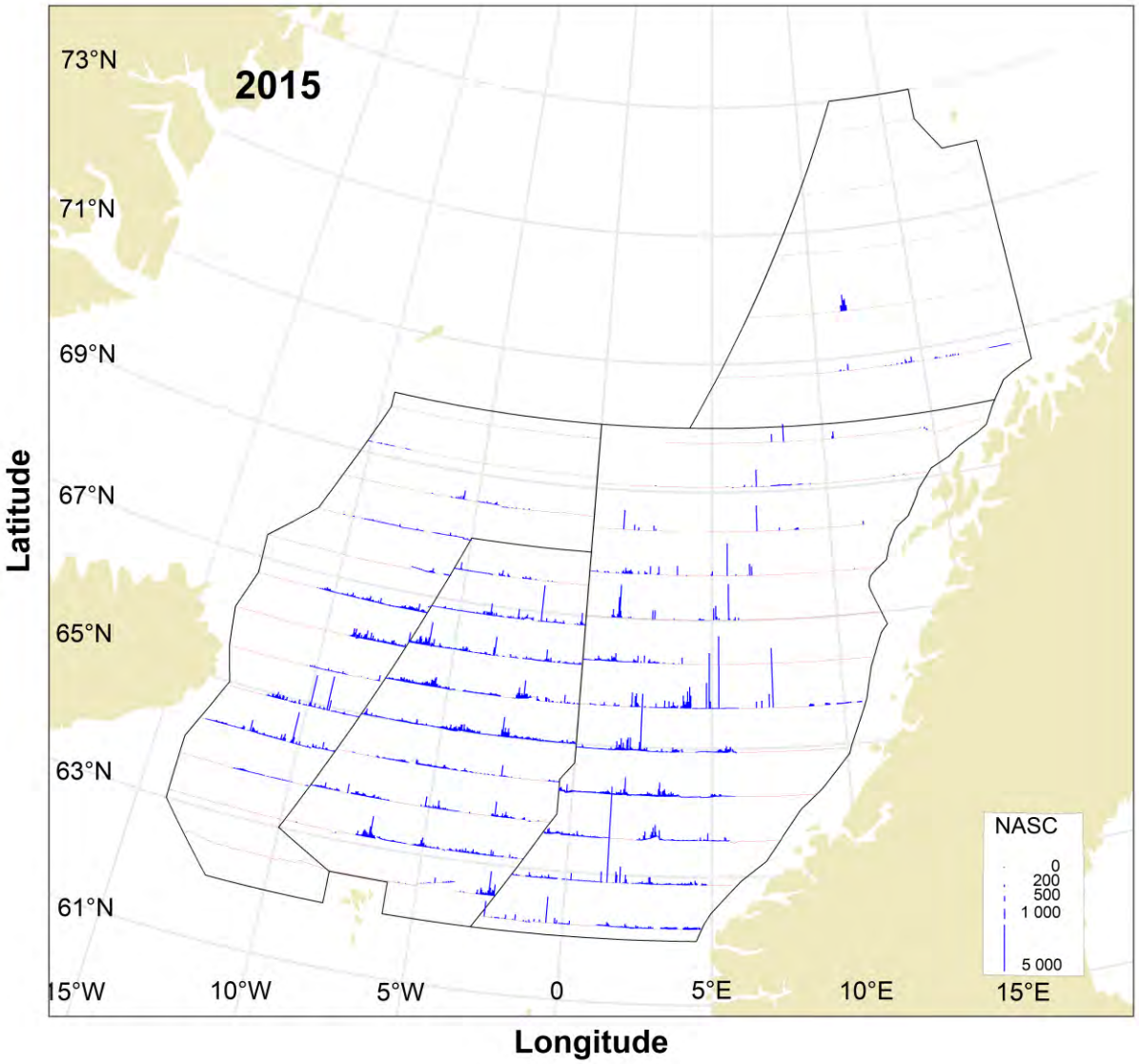

Figure A2. Distribution of Norwegian spring-spawning herring as measured during the IESNS survey in May 2015 in terms of NASC values (m^2/nm^2) (a) averaged for every 1 nautical mile

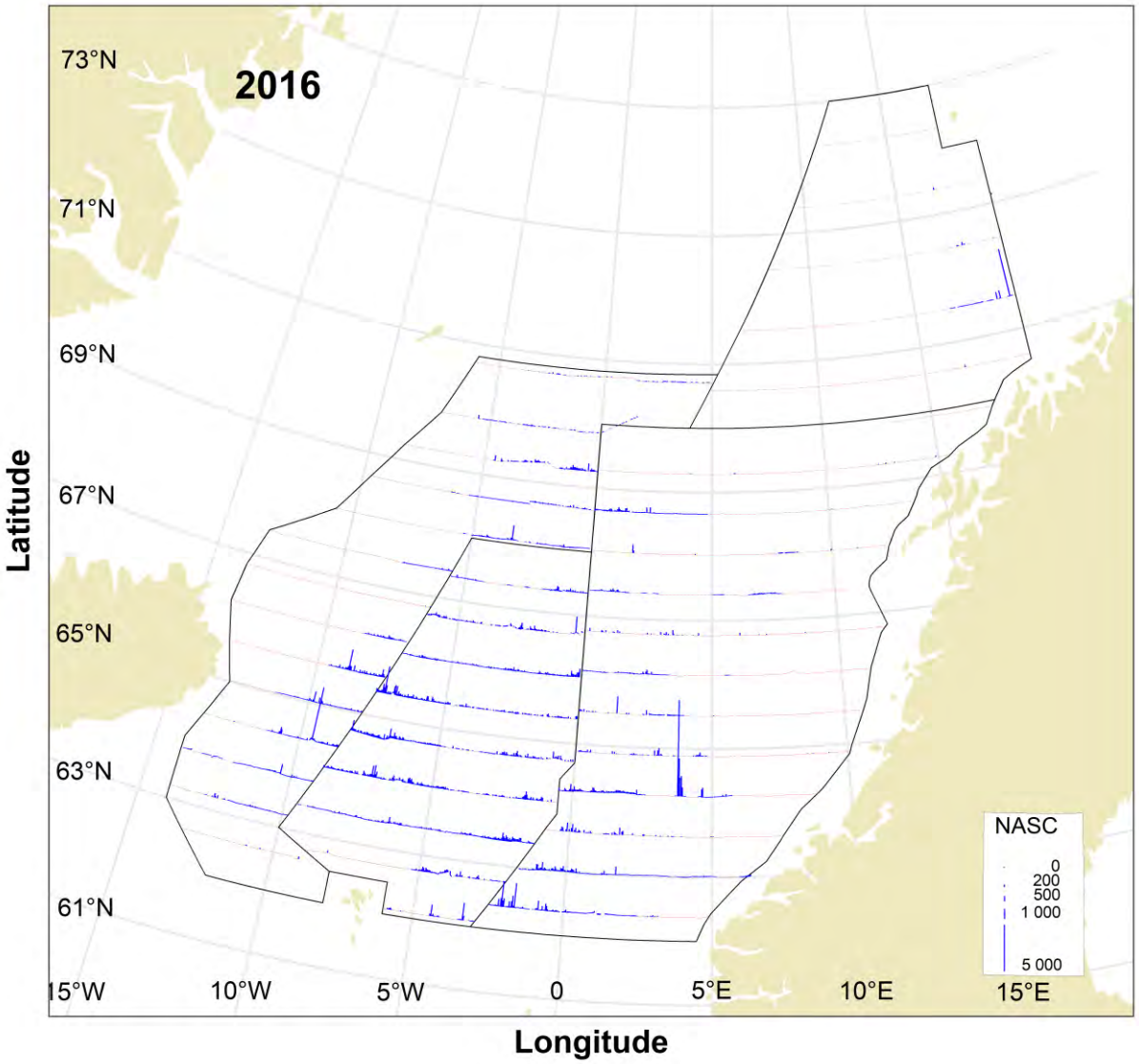

Figure A3. Distribution of Norwegian spring-spawning herring as measured during the IESNS survey in May 2016 in terms of NASC values (m^2/nm^2) (a) averaged for every 1 nautical mile

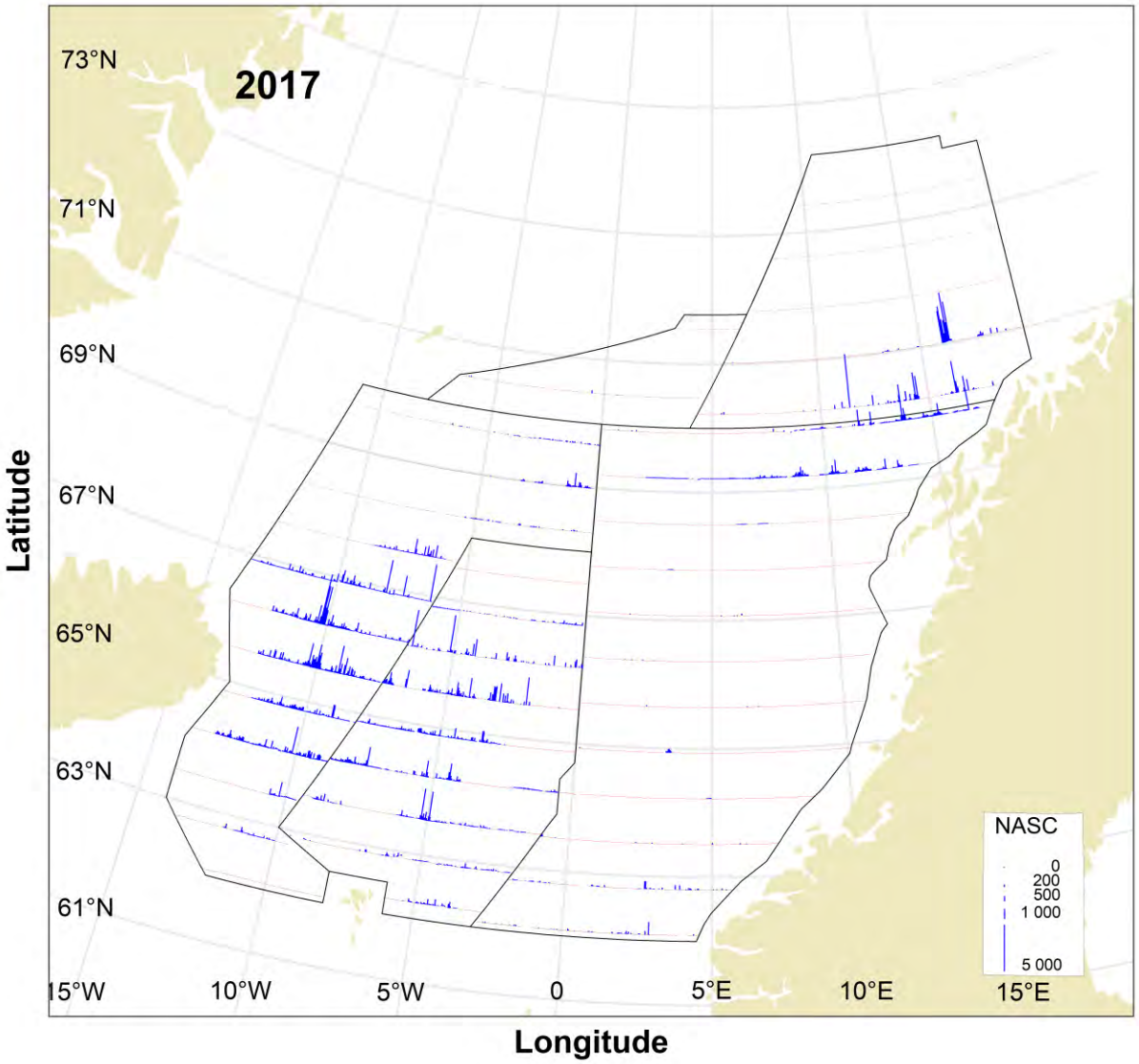

Figure A4. Distribution of Norwegian spring-spawning herring as measured during the IESNS survey in May 2017 in terms of NASC values (m^2/nm^2) (a) averaged for every 1 nautical mile

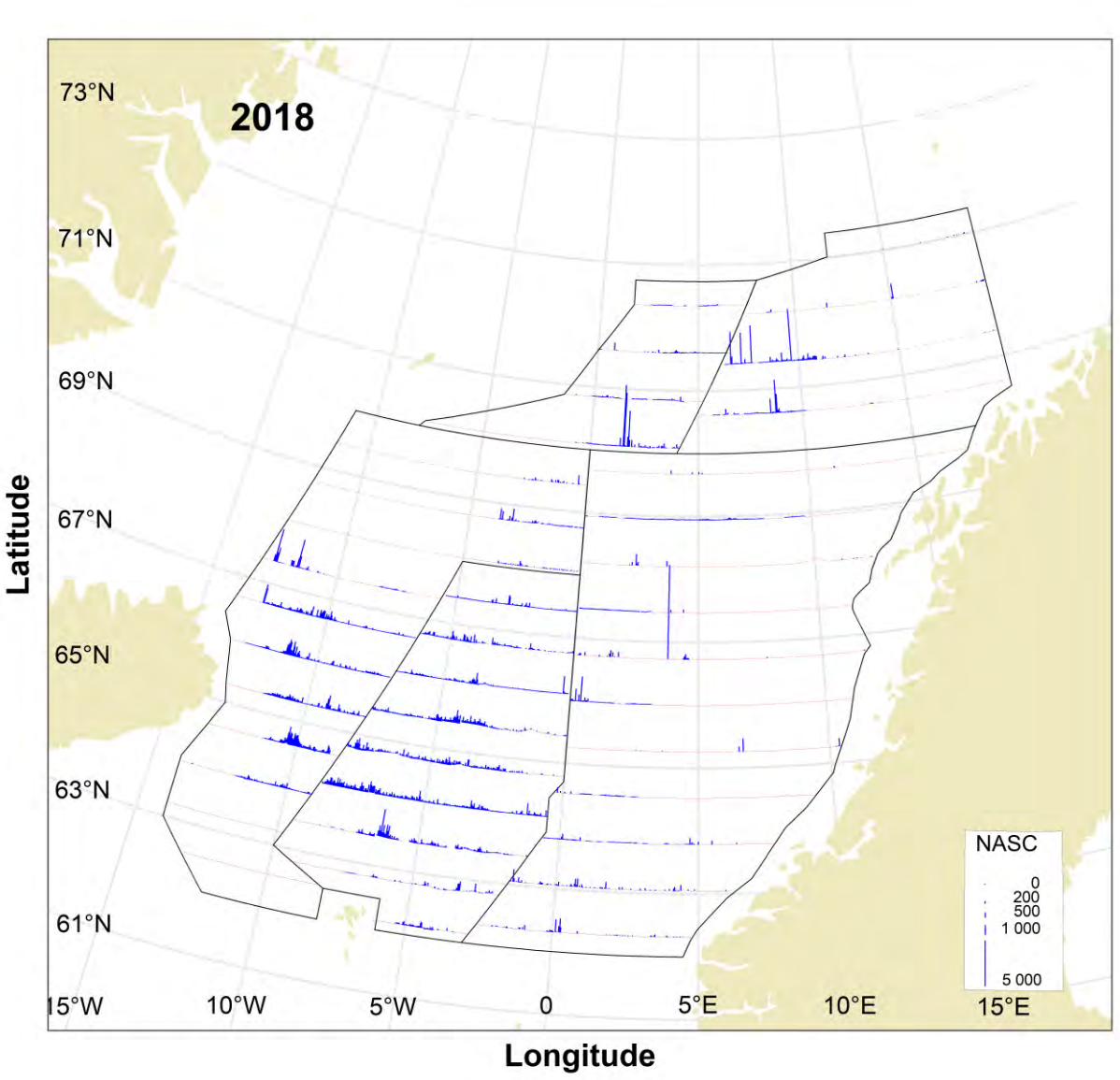

Figure A5. Distribution of Norwegian spring-spawning herring as measured during the IESNS survey in May 2018 in terms of NASC values (m^2/nm^2) (a) averaged for every 1 nautical mile

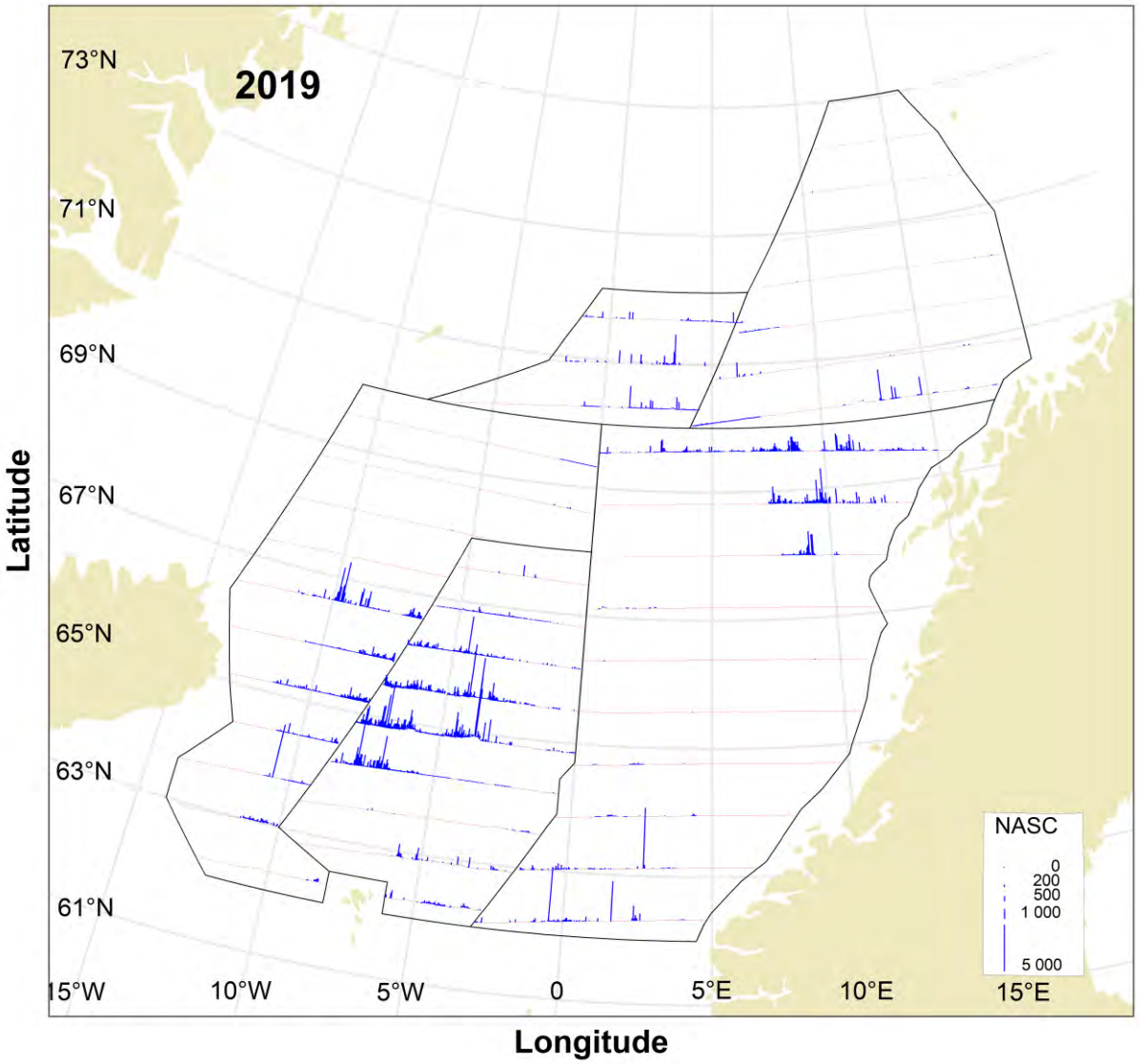

Figure A6. Distribution of Norwegian spring-spawning herring as measured during the IESNS survey in May 2019 in terms of NASC values (m^2/nm^2) (a) averaged for every 1 nautical mile.

Appendix B

Vertical distribution of herring from omni directional fisheries sonar during international ecosystem survey in Nordic SEA (IESNS) in May – June 2020

Héctor Peña
Marine ecosystem acoustic group
Institute of Marine Research, Bergen, Norway

Introduction

The biomass estimation method using hull mounted echo sounder has two sources of bias related to the collection of the acoustic backscattering of the target species: i) fish present in the echo sounder blind zone, and ii) fish avoidance to the surveying vessel. Omni directional fisheries sonars can potentially provide with data to investigate when these biases occur and its magnitude along an acoustic surveying.
Since 2017, the collection and scrutinizing of sonar data has been an additional activity in the IESNS survey carried out by the Institute of marine research. Experience gained will help to evaluate feasibility and benefits of using sonar in a routine basis during acoustic pelagic trawling surveys.
The main goal of the present study was to use the omni sonar SU90 onboard RV "G. O. Sars" to quantify the fraction of NSS herring in the upper 60 m during the IESNS survey in the Nordic sea. Sonar vertical distribution of fish abundance will be compared with the distribution from echo sounder.

Methods

Sonar set up

The horizontal beams from the sonar onboard RV "G. O. Sars" was previously calibrated prior to the survey on May 1st in Bergen bay. Calibration using a reference target was done at 26 kHz frequency, FM normal transmission mode and narrow beam. Attempt to calibrate vertical beams was unsuccessful because of high noise levels, which not allowed visualization the calibration sphere. Echoes from bottom may be the reason and in future is planned to perform calibration in deeper waters.
During the survey (1st May to 03rd June), the sonar was set up to achieve a high ping rate operating at a range of 600 m. The sonar was synchronized with the EK80 echo sounder and

MS70 scientific sonar to avoid interference, which resulted in a ping rate of the horizontal beams between 4 to 5 seconds.
A tilt of 5 deg was set for the horizontal beams with a theoretical upper depth of the beam of 8 m at 50 m range and lower depth of the beam of 90 m at the maximum operational range. Experienced showed that shallower tilt angles (i.e. 1 or 2 deg) can affect severely data acquisition, which is subject to noise produced by air bubbles swept down by waves, that in high winds (>25 knots) can reach up to 50 m below the surface. The vessel roll contained in the echo sounder data was used as an indicator of bad sonar conditions (high wind and high waves), not processing sonar data with absolute roll angles larger than 2.5 deg.
The 180° vertical beam fan was set perpendicular to the vessel track with a horizontal range of 600 m and a vertical range of 600 m.
All the sonar filters (AGC, RCG, Ping to ping) were set to the default values, except for the "Noise filter", which was disabled because it alters the values of exported raw data.

PROFOS settings
The Processing system for omni directional fisheries sonar (Profos) module of the LSSS software was used for the data replay and school segmentation. The automatic school detection functionality was used, with a posterior manual quality control of the segmented school. The segmentation settings most commonly used were: 12 dB above the background level, minimum surface of 300 m^2, maximum surface of 7000 m^2, two missing pings, at least 10 pings schools, and a ratio of 10 between length and school width. The output from LSSS contained school descriptors and vessel navigation information for each ping de the school was detected.

Vertical distribution of sonar and echo sounder
School descriptors from sonar data were used to compute the nautical area scattering coefficient (S_A, m^2 nmi^{-2}) by 1 nmi distance and depth channels of 10 m, from surface up to 60 m. Similar integration criteria was used with the echo sounder data resulted from the official survey scrutiny. Data was sorted by transects and vertical distributions of S_A were generated. A correlation analysis was done to compare the standardized NASC form sonar and echosounder by 10 m depth channels.
Because different ensonification angle of the two instruments used (vertical for echo sounder and horizontal for sonar) the S_A values are not directly comparable, and a conversion factor was used to upscale the lower sonar S_A values, and facilitate the visual comparison. The conversion factor used was 2.5. This value corresponds to the linear difference of 4 dB between the lower horizontal mean target strength compared with the mean vertical target strength.

Results

Predominant NSS herring from 2016-year class was found mostly as well defined small (ca. 10 m diameter) and medium size (ca. 100 m diameter) schools in the upper 100 m.

Conditions for sonar operation were optimal almost during the whole survey with few periods of bad weather which impeded good sonar data.

The sum of the herring NASC from 0 to 60 m depth by transects for sonar showed a similar spatial distribution as the NASC from the echo sounder from transect 1 to 8 (Figure 1). Only in the western part of transect 4, more schools were detected by the sonar. In the northern transects (9 to 12), herring was distributed disperse and not as schools or dense layers, and therefore only observed by the echo sounder. In transects with higher herring NASC values (i.e. transects 3 to 7), schools were observed in the eastern end towards the Norwegian coast.

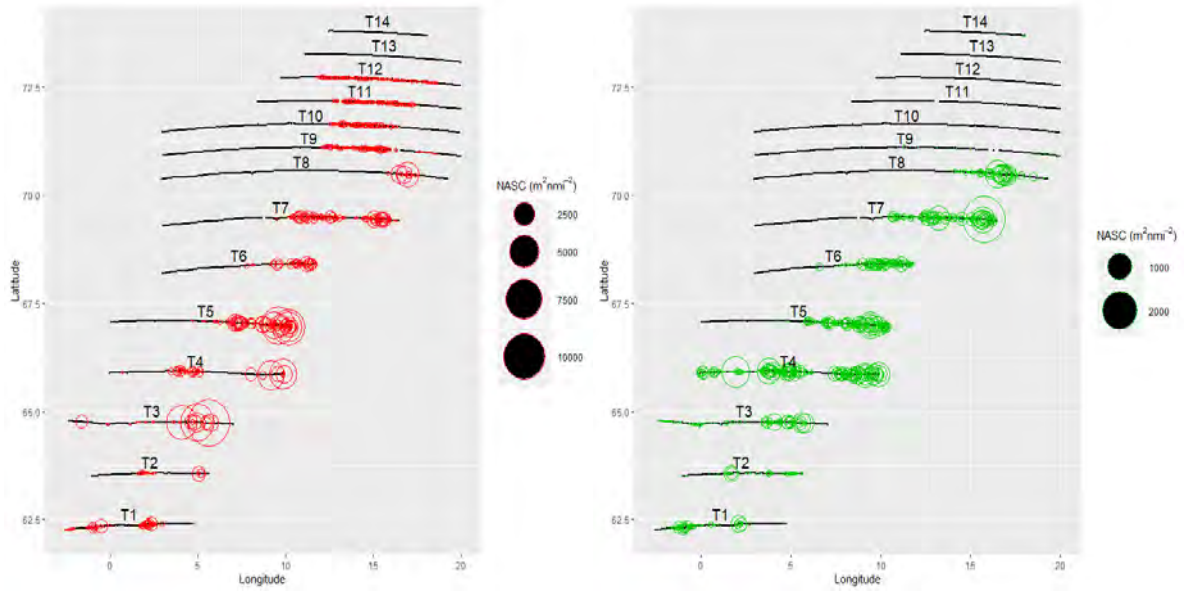

Figure 1. Herring NASC from 0 to 60 m by transects for echo sounder (left panel) and sonar (right panel).

In this region, presence of herring schools was found until the eastern border (end of transects 4 and 6, start of transect 5) of transects towards the coast, indicating that the zero line was not reached (Figure 2 and 3). Transects 4 and 5 were extended during the survey towards east from its original design, but not enough to reach areas with no herring. During surveying, sonar information was valuable to evaluate the presence of schools ahead of the vessel track, and the need to establish criteria to extend a transect (when zero line has not been reached), based in sonar observations, was suggested in the post-cruise meeting.

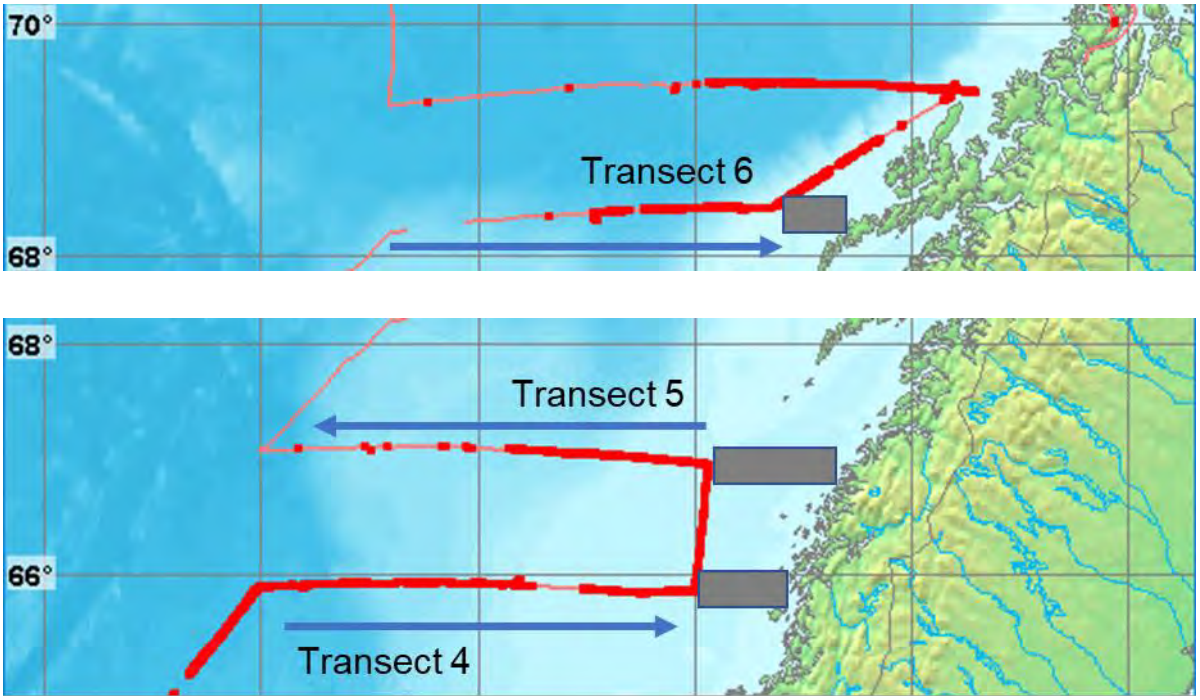

Figure 2. Detail of transects 4, 5 and 6 showing the schools detected by sonar as red dots along the survey pink line. Blue arrows indicate vessel direction and grey boxes regions towards the east that were not covered by the transects along the coast.

Examples of the different herring schools observed by echo sounder and sonar displayed in LSSS are shown in Figure 3. In general, larger schools were observed in transects 3 to 5, and smaller and denser in the region off Loffoten and Vesterålen (transects 6 to 8).

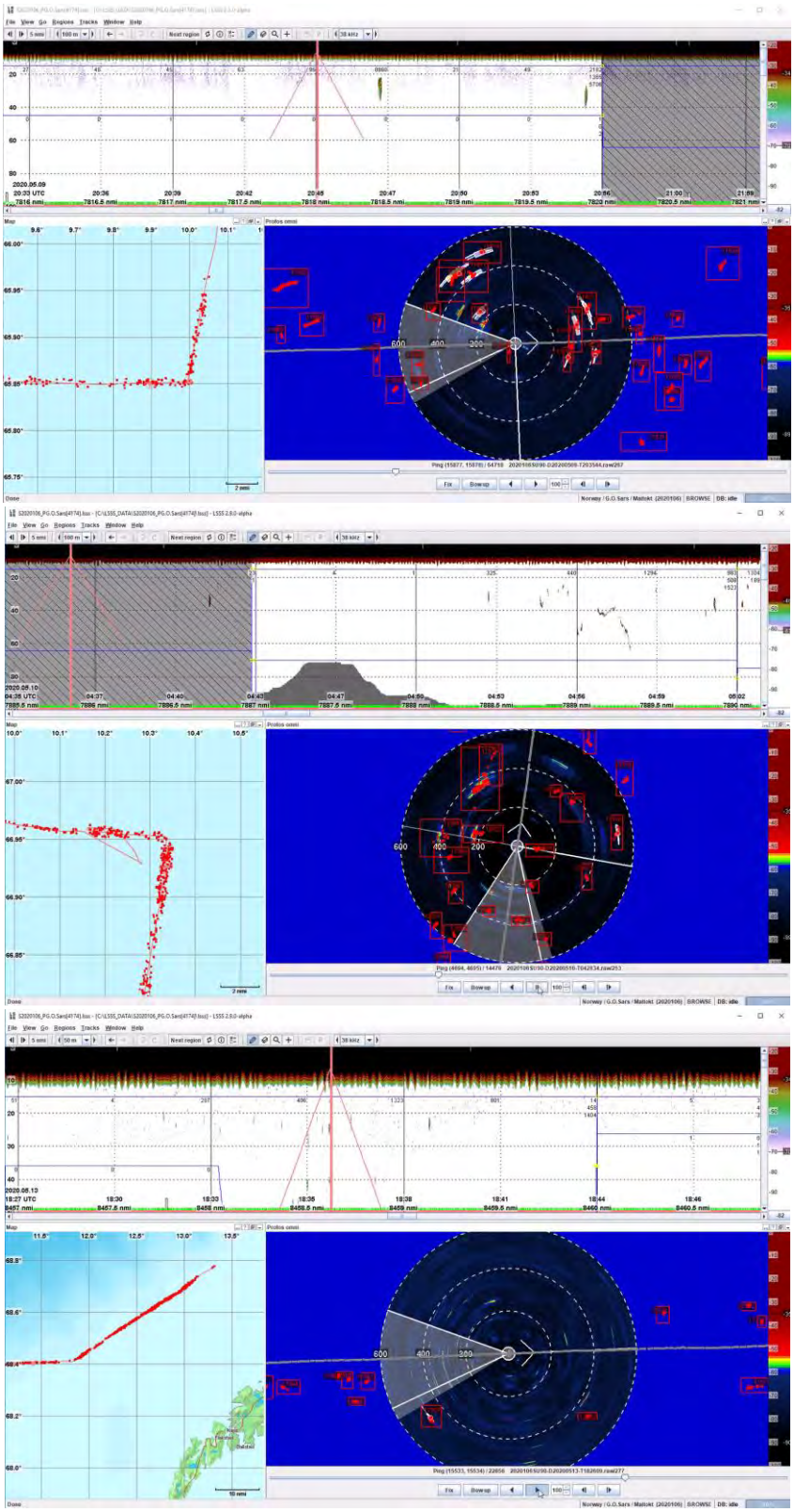

Figure 3. Image of LSSS display showing typical herring aggregations from echo sounder and sonar in transects 4 (Top), 5 (middle) and 6 (bottom). Larger and more distant schools in transect 4, smaller and more dense schools in transects 5 and 6.

No statistical differences were found between the standardized NASC by 10 m depth channels from echo sounder and sonar in any of the transects where herring was observed (*i.e.* transects 1 to 8) (Figure 4)

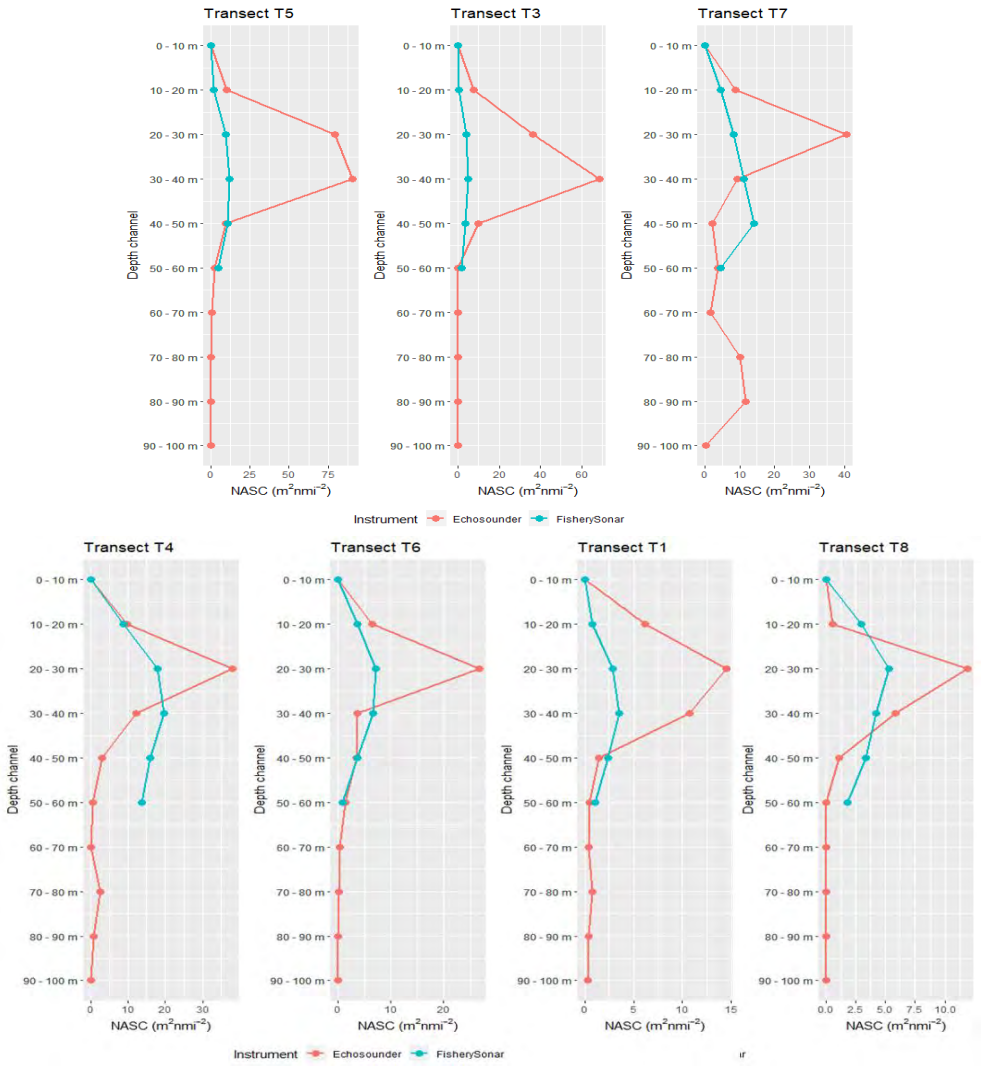

Figure 4. Vertical distribution of herring NASC values from echo sounder and sonar for transects in decreasing order of contribution of NASC from echo sounder measurements (top left to bottom right).

Discussion

NSS herring 2016-year class was predominant in the sonar measurements in the upper 60 m in the 2020 IESNS survey. Well defined schools and general good weather conditions conditioned good quality sonar data.

Abundant schools were measured with the sonar in the eastern end of transects 4 to 6, not reaching the zero line. Even though a reduced transect extension was implemented, it was not enough. The need to establish a criterion based in the sonar measurement, when these situations occurs, was indicated in the post-cruise meeting. For example, the absence of schools in the sonar for 10 nmi after the end of a transect could be a rule to decide stop surveying along that transect and continue with the next one.

The similar spatial distribution of herring from echo sounder and sonar is a good indicator that both acoustic systems are detecting the presence of herring in the layer up to 60 m depth, when herring was aggregated in schools (transect 1 to 8). In the northern area (transects 8 to 12), herring was present as disperse fish, and not detected by the sonar.

The analysis of the vertical distribution of herring between echo sounder and sonar indicate no statistical differences between distributions on depth and levels of NASC. The relative contribution of NASC by depth channels from the sonar data, don't show higher levels in the 10 to 20 m depth, similar observed in echo sounder distribution, which indicate no bias of the echo sounder in this depth layer.

Current analysis of data series from 2017 to 2020 aim to evaluate if the current scaling factor between the sonar and echo sounder NASC is appropriate or need to be modified.

In summary, the vertical distribution of herring from sonar indicates no bias from the measurements of the echo sounder from depths from 10 to 60 m during the IESNS 2020 survey. In three transects the zero line was not reached, and a procedure to use the sonar information to avoid this problem is indicated.

Appendix C

Vertical distribution of herring from sonars during international ecosystem survey in Nordic seas (IESNS) in May 2020

Rolf Korneliussen and Arne Johannes Holmin
Research group Ecosystem acoustics
Institute of Marine Research, Norway

Introduction

The biomass estimation method using hull mounted echosounders only, have at least two sources of bias related to the collection of the acoustic backscattering of the pelagic target species: i) fish present in the echosounder blind zone close to the sea surface, and ii) fish avoidance to the surveying vessel. Horizontally oriented sonars can potentially provide data to investigate those biases.

During the last three years, the collection and scrutinizing of sonar data has been an additional activity in the IESNS survey carried out by the Institute of Marine Research (IMR). Experience gained will help to evaluate feasibility and benefits of using sonar in a routine basis during acoustic pelagic trawling surveys.

Two classes of sonars were used; an omnidirectional fisheries sonar (SU90), and a scientific matrix sonar (MS70). The SU90 sonar can be run in two modes: either by measuring in a 360 degrees dish, or in a vertical slice. The SU90 is similar to sonars common on many fishing vessels and has the advantage of being available on many fishing vessels, while MS70 is currently only available onboard RV “G.O. Sars”. The MS70 points port and use a mesh containing 25 x 20 beams = 500 beams covering 60 degrees (horizontally) by 45 degrees (vertically) in. Thus, the MS70 sonar has a better spatial resolution, but a poorer horizontal coverage than SU90. MS70 provides data both at horizontal ranges from the ship and also vertically.

The main goal of the present study was to use the sonars onboard RV “G. O. Sars” to quantify the fraction of NSS herring in the upper depths of 60 m during the IESNS survey in the Nordic seas. SU90 can cover the upper 60 m, and MS70 was used to investigate the upper 200 m. The vertical distribution of fish abundance by means of SU90 and MS70 will be compared with the distribution from echo sounder. In this document we concentrate on the MS70 sonar, while the SU90 comparison is mainly covered in another document.

Methods

MS70 was calibrated at the survey operation mode with for the first time in 2019 with the highest frequency in the top fan. New integrated electronic cards were installed in MS70 in 2020, and MS70 sonar was calibrated prior to the 2020 survey.

The MS70 scientific matrix sonar

Setup

MS70 was set up to cover a horizontal distance of 250 m (i.e. range 410 m) and to ping at least every second EK80 ping (1 ping per 2 seconds). The highest frequency (112 kHz) closest to the surface with centre of beams parallel to the surface, and the lowest beams (75 kHz) was pointing 45 degrees down. The highest frequencies were used at the top to have the narrowest beams in the vertical direction in order to get as close to the surface as possible. The MS70 transducer were mounted on a protrudable instrument keel, with the centre of the transducer at 7.5 m below the sea surface.

Data preprocessing

The MS70 data were preprocessed by means of LSSS-PROMUS (Processing system for advanced multibeam sonar). A brief description of the preprocessing is as follows:

1) Spatial and temporal spikes were detected and replaced median of the surrounding data.
2) Ambient noise was estimated for each of the 500 beams and then each sample was corrected for ambient noise.
3) Data were collected to a range of 500 m. Data closer to the ship than 20 m were removed. Data at larger horizontal range from the ship than 250 m were removed.
4) Data closer to the surface than 2.5 m were removed. This implies that at least the two uppermost fans were cut at ranges where the upper edge of beam is closer to the surface than 2.5 m. The vertical extent of the fans is a source of uncertainty: we used the nominal vertical beamwidth multiplied by 1.65.
5) Data more than 200 m below the surface were removed. This implies that at least the two uppermost fans were cut at ranges where the upper edge of beam is closer to the surface than 2.5 m. The vertical extent of the fans is a source of uncertainty, but unlike the uppermost beams the lowermost beams were cut by using used the nominal vertical (i.e. the beamwidth multiplied by 1.0).
6) Data were thresholded, so that all S_v-samples weaker than -70 dB and stronger than -5 dB were removed (set to -120 dB).
7) Data were compressed by removing data where 20 samples in a row were weaker than -70 dB. This reduced the data volume by 85%.

Pre-scrutiny

School-candidates were automatically detected from preprocessed data according to specified criteria. The most important of those were:

1) The school seed-point needed to be between -30 and -60 dB.
2) The maximum grow-depth of the centre of the beam was 200 m (although the lower edge of the beam could be deeper). This means that at depths deeper than 200 m, the data are not trusthworthy.

3) The minimum grow-depth depended on the weather. It mostly varied between 2.5 and 15 m below the sea surface, but it could be as deep as 25 – 30 m.

Data interpretation (scrutiny)

The EK80 data were scrutinized by the cruise leader and the chief instrument engineer some hours after the data were collected. The MS70 data were scrutinized by a single scientist (Rolf Korneliussen). MS70-data collected after May 20 were scrutinized a few hours after the EK80 data. Data collected from May 1 were scrutinized after May 20. All scrutiny finished by the end of the survey.

No data with central axis deeper than 200 m was stored. Thus, the data deeper than 200 m is not representative

MS70 data were scrutinizing by first removing outliers of the school-candidates. Then the school-candidates were scrutinized in pretty much the same way as the EK80 data, i.e. by considering scattering strength, shape of school (in 4 dimensions), biological samples, and by conferring the results of the EK80-data scrutiny. Scrutinization of 24 hours of MS70 data took typically 20 minutes.

Data were stored in a database as volume backscattering data and were exported to files to be processed in external systems. The data were averaged to over the same distance (1 nmi) as the EK80 data, and in range-cells of 10 m, and at its native beam resolution. Thus, each database cell is an average of typically 4500 MS70-samples. Note that MS70-data and database storage cells are natively shaped as sphere-sectors, and that the data used here are converted to cartesian coordinates.

Scrutinization of the fishery sonar and MS70 sonar differ from that of the echosounder in that they consider schools of a minimum volume 250 m^3. This represents a potential source of bias in the comparison between the instruments, as a layer of small schools or individual fish can contribute significantly to the echosounder NASC while being excluded from the sonar NASC.

Results

Figure 1 shows the 2020106 survey. The cruise started in south. After the “official” cruise tracks shown, there was additional triangular shaped cruise-lines in north-west (not shown).

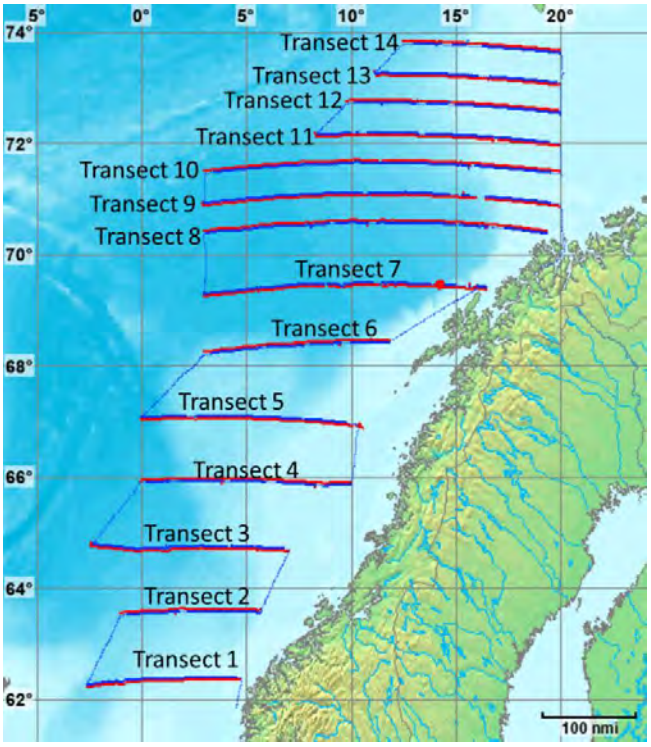

Figure 1. Cruise tracks of survey 2020106. Transects started in south and ended in north.

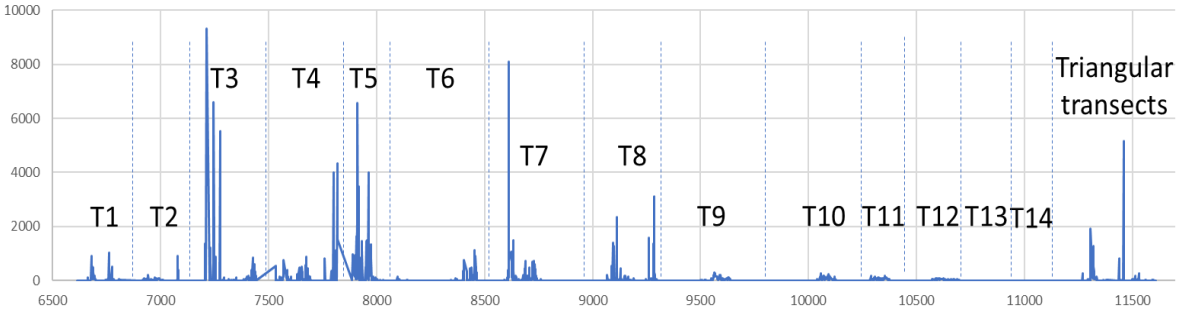

Figure 2. Herring scrutinized on survey 2020106, 38 kHz CW EK80 data. Transects are named "Transect N" or TN. After Transect 14, there were some triangular shaped cruise lines that was not a part of the official survey.

Comparison between echosounder and sonar cannot be done directly as the database contains NASC for the echosounder and s_V for the sonars. $s_V = 4\pi 1852^2 s_v$, so the difference between NASC = s_A and s_V is multiplication by the vertical extent of the depth channel, which in this case is 10 m for the EK80 data. Furthermore, the frequencies of the sonar MS70 is 75 – 112 kHz, i.e. approximately 90 kHz on average, while it is 38 kHz for EK80. For herring, measured frequency response measured by means of echosounder data indicate that NAASC is approximately 50% stronger at 38 kHz than at 90 kHz. In addition to this, dorsal tilt distribution is much smaller than the horizontal direction. Theoretical estimations indicate approximately 4.5 dB difference between herring measured dorsally and horizontally at the same frequency. Thus, the frequency and horizontal measurements is expected to be approximately a factor 4 (2.8 x 1.5 = 4.2 ≈ 4) weaker. In total, the s_V measured horizontally at 90 kHz by MS70 needs to be multiplied by (approximately) 10 (m) x 4 = 40. Figure 3 shows vertical distribution from the 2020 survey, and Figure 4 similar vertical distributions from three selected transects of the 2019 survey for comparison.

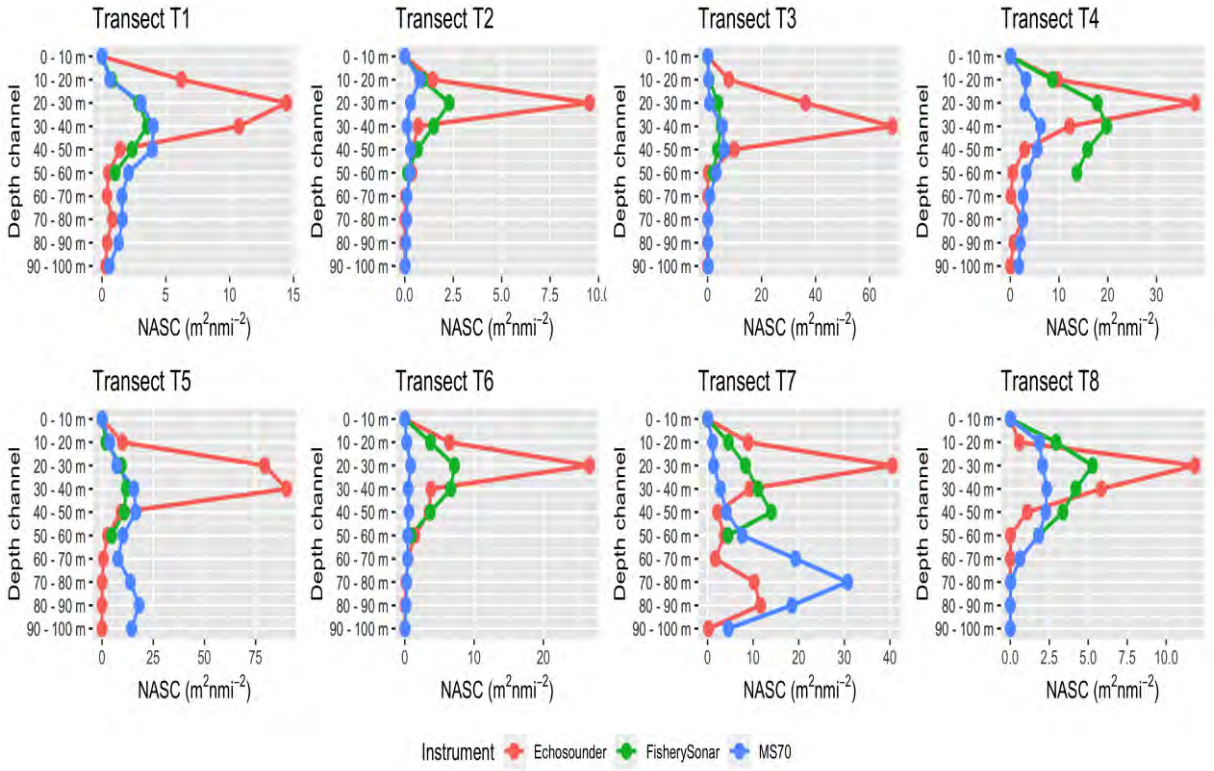

Figure 3. Vertical distribution of Transects T1 – T8 from the 2020106 Norwegian Sea ecosystem survey for echosounder (EK80 - red), fishery sonar (SU90 – green), matrix sonar (MS70 – blue).

Figure 2 was used to select transect with large herring abundance. Figure 4 shows the vertical distribution from surface down to 200 m depth. The horizontal distance from the ship is 50 – 200 m. The integrated acoustic abundance (integral under the curves) are not very different, but MS70 finds most of the abundance deeper than the EK80. This is somewhat surprising as the MS70 is designed to detect schools all the way up to the surface.

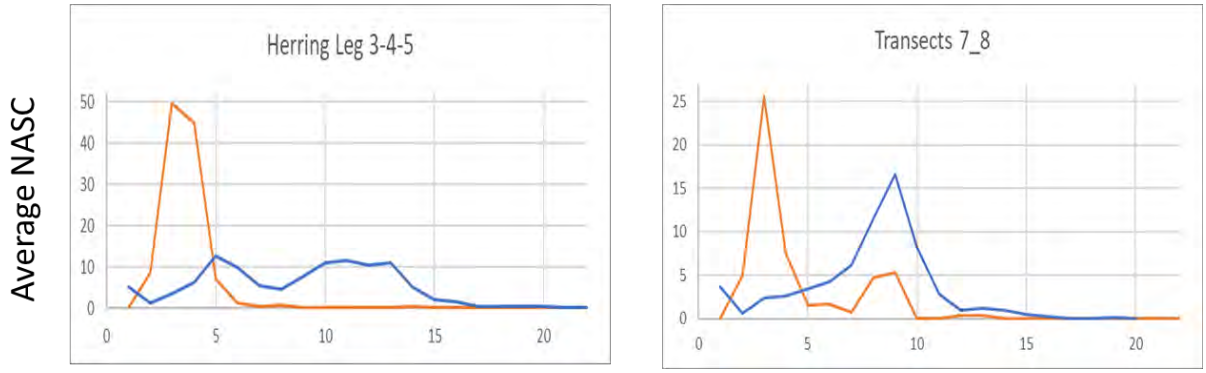

Figure 4. Survey 2020106. Vertical distribution of herring NASC values from echo sounder (red) and MS70 sonar (blue) for transects 3-5 (left panel), 7-8 (right panel). Depth channel 1 (horizontal axis) is 0 – 10 m below sea surface, depth channel 2 is 10 – 20 m (and so on). The MS70 data is based on data from 50 m – 200 m horizontally from the ship, and down to 200 m depth (centre beam).

As a reminder from previous Ecosystem surveys from the Norwegian Sea, Figure 5 shows the vertical distribution from 3 selected transects, and Figure 6 visualize an image from MS70. Figures 5 and 6 shows that MS70 should be able to see schools of fish close to the surface. As shown in Figure 5 (2019 survey), the surface noise on the MS70 sonar propagates below 20 m depth in transect S2019107-T10 (red layer in the lower panel, frame "MS70-Phantom"), intersecting with the large peak in the

vertical distribution of the echosounder. In transect S2019107-T8 the surface noise is negligible.

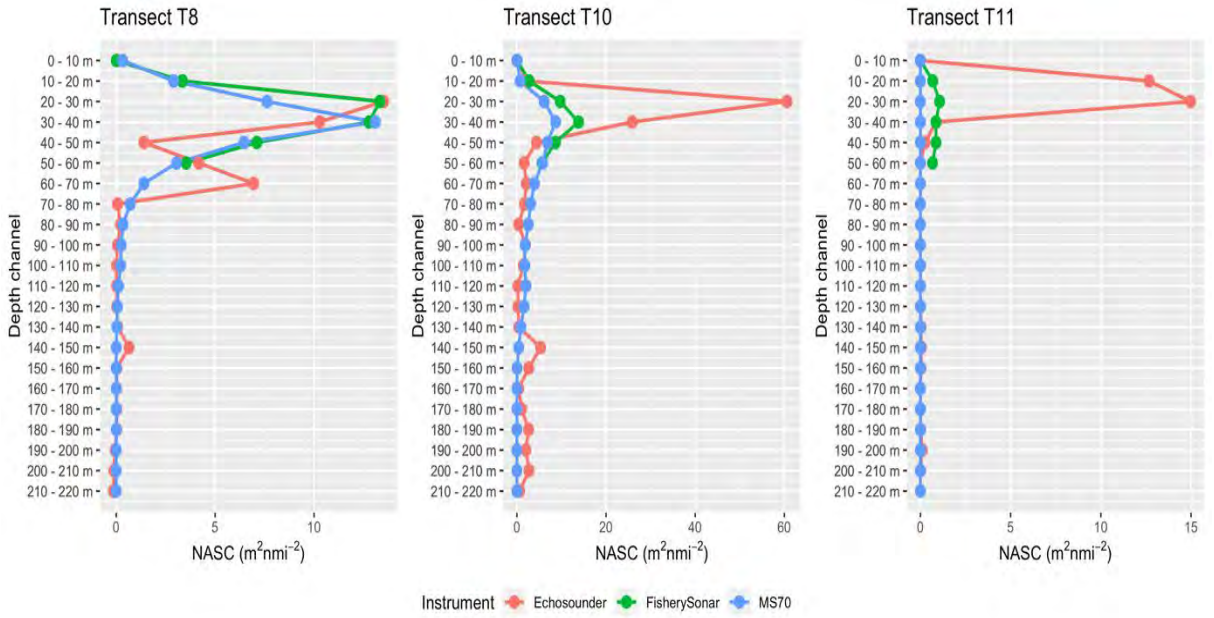

Figure 4. Survey 2019107. Vertical distribution of herring NASC values from echo sounder (red), fishery sonar (green) and MS70 sonar (blue) for transects 8 (left panel), 10 (middle panel), 11 (right panel).

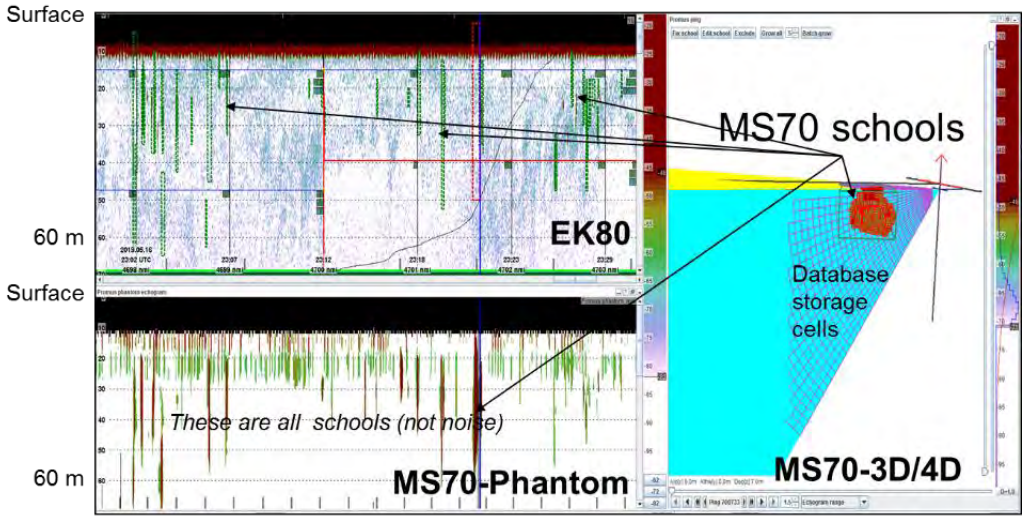

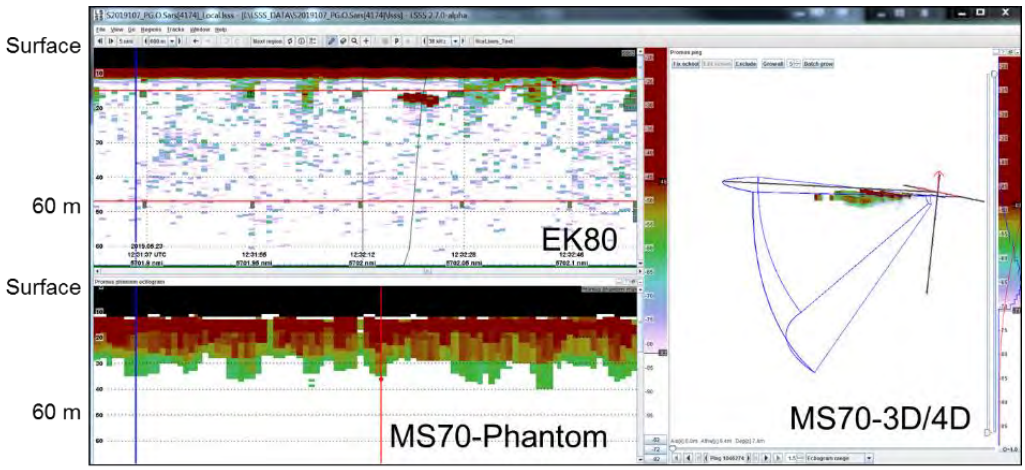

Figure 5. From survey S2019106. Screen dump from the Large Scale Survey System (LSSS), showing echosounder echogram (upper left frame), MS70 phantom echogram (lower left frame) and 3-D view of the MS70 sonar (right frame) of transect T8 (upper panel) and T10 (lower panel). In T8 there were some schools found in EK80, and many in MS70 (some "onto" the surface). In T10, the weather was bad, so the upper school detection depth was 20m. In T10, the weather was very bad, which explains very few detections of MS70.

Discussion

The vertical distribution from echosounder and the fishery sonar and MS70 sonar showed discrepancies in the level depending on the transects. On average the sonars fail to return a peak at the same level as the echosounder. This discrepancy illustrates a fundamental issue with sonar data, which is related to the width of the sonar beams. When observing a near surface school, separation of school and surface noise can be challenging, which could result in exclusion of these schools from the vertical distribution

The sonar data were scrutinized in terms of schools of a required size. The echosounder data can in contrast include all data down to single targets, as long as the data are categorized in acoustic categories representing species. If there are aggregations of individual fish and small schools at certain depths, this difference in post-processing can lead to bias in the vertical distribution from the sonars. This can in particular be a problem close to the surface, where small schools are more likely to be excluded from the sonar scrutinization than larger schools.

The vertical distribution from the echosounder did not show any strong signs of avoidance to the vessel in this survey, with a peak in the vertical distribution starting at 10 m depth and reaching a maximum in the interval 20 to 30 m depth. As such, these data serve as a useful example to comparing vertical distribution from the different instruments, as the avoidance, which is generally unknown, will not affect the comparison. Given that the echosounder performs equally well or better than the sonars as indicator of biomass in the upper 30 meters, there is no strong cause for using sonar to assist the survey estimation. Note, however, that the school depths found by the sonars are estimated from the centre of the beam. Although this is a good estimate of depth for most beams, it also prevents registering schools at the shallowest depths. For MS70, the two uppermost beams were cut at some range, so that a school on the surface 150 m from the transducer would be registered at 20 m depth. Results from calmer weather during this survey showed that MS70 could in fact measure schools onto the surface. Thus, methods to visualize shallow schools need to be developed.

The methods presented in this study for estimating vertical distribution from sonars can be applied to other surveys where reactions to the research vessel may be stronger than in the IESNS survey from 2019 used in this study. In calm weather the sonars appear to compare well to the echosounder in terms of vertical distribution. In rough weather scrutinization of sonar can however be challenging, and further development should focus on improving separation of fish and noise in these conditions.

Difference in scrutiny of EK80 and MS70

Is the difference in depth distribution close to the surface measured with EK80 and MS70 be due to how data are scrutinized or the ability to measure, or is there maybe another reason? Is the difference in depth distribution at depths 50 – 100 m as measured with EK80 and MS70 due to how data are scrutinized or the ability to measure? These are not easy questions to answer.

1) The EK80 data were scrutinized by the cruise-leader and the instrument engineer close to the time of data collection, all in accordance with procedure for interpreting acoustic data.
2) The MS70 data were scrutinized by one scientist. From May 20, the data were scrutinized shortly after collection, while data prior to May 20 were scrutinized after May 20.
3) Candidates for schools measured by means of MS70 was automatic detected. There were a set of criteria for detection of schools, e.g. a minimum size of schools. The data were inspected by the scrutinizer. Herring was expected to dominate the abundance of schools at shallow depths, and down to 200 m. A criterium for allocating acoustic values to herring was scattering strength, but it turned out to be surprisingly difficult to identify which schools were herring, from what was thought to be likely zooplankton. The sonar does not measure relative frequency response.
4) The EK80 data close to the surface were to a large extent layers, i.e. not schools. They were not seen clearly on the echogram but were still interpreted to be herring due to catches.
5) Catches could be directed by EK80, but in practice not by MS70.

WGWIDE 2020, Working document 11

Population structure of the Atlantic horse mackerel (*Trachurus trachurus*) revealed by whole-genome sequencing

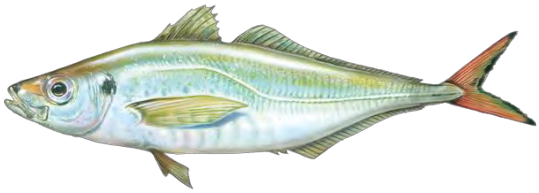

A report prepared for the members of the

Northern Pelagic Working Group

and

the Pelagic Advisory Council

by

Angela P. Fuentes-Pardo, Mats Pettersson, C. Grace Sprehn, Leif Andersson

Uppsala University, Sweden

&

Edward Farrell

EDF Scientific Limited, Ireland

July 2020

Executive Summary

The Atlantic horse mackerel, *Trachurus trachurus* (Linnaeus, 1758) is a species of jack mackerel distributed in the East Atlantic, from Norway to west Africa and the Mediterranean Sea. It is a pelagic shoaling species found on the continental shelf and it is one of the most widely distributed species in shelf waters in the northeast Atlantic, where it is targeted in pelagic fisheries. In the northeast Atlantic region, the species is assessed and managed as three stocks: the Western, the North Sea and the Southern. Despite the commercial importance of the horse mackerel, the accuracy of alignment of these stock divisions with biological units is still uncertain.

The aims of this study were to identify informative genetic markers for the stock identification of horse mackerel and to estimate the extent of genetic differentiation among populations distributed across the distribution range of the species. For this we used modern sequencing techniques that allowed us to assess genetic variants in the entire genome. We discovered that while the populations differ in a small fraction of their DNA (< 1.5%), such genetic differences are significant as they likely represent natural selection and might be involved in local adaptation. We validated a small fraction of these highly differentiated genetic variants by a SNP assay and demonstrated that they can be used as informative molecular markers for the genetic identification of the main stock divisions of the Atlantic horse mackerel.

The results, based on the analysed samples, indicated that the North Sea horse mackerel are a separate and distinct population. The samples from the Western stock, west of Ireland and the northern Spanish shelf, and the northern part of the Southern stock, northern Portugal, appear to form a genetically close group. There was significant genetic differentiation between the northern Portuguese samples and those collected in Southern Portuguese waters, with those in the south representing a separate population. The North African and Alboran Sea samples were distinct from each other and from all other samples.

These results indicate that a further large-scale analysis of samples, with a greater temporal and spatial coverage, with the newly identified molecular markers is required to test and reassess the current stock delineations.

Table of Contents

1. Background

1.1 Biology

The horse mackerel, *Trachurus trachurus* (Linnaeus, 1758) is a species of jack mackerel from the Carangidae family and is distributed in the East Atlantic from Norway to Western Africa and the Mediterranean Sea (Froese and Pauly, 2015). It is a pelagic shoaling species found on the continental shelf and is one of the most widely distributed species in shelf waters in the northeast Atlantic. The range of horse mackerel partially overlaps with four other *Trachurus* spp; *Trachurus picturatus* (Bowdich, 1825) and *Trachurus mediterraneus* (Steindachner, 1868) in Iberian, North African and Mediterranean waters, *Trachurus trecae* (Cadenat, 1949) in West African waters and the very closely related *Trachurus capensis* (Castelnau, 1861) in west and southwest African waters.

Horse mackerel are estimated to mature at c.20 cm total length and between 2 and 4 years of age (Abaunza et al., 2003). Waldron and Kerstan (2001) validated the age determination of horse mackerel otoliths, through marginal increment analysis of whole otoliths, up to age four. However, examination of subsequent growth zones indicated that false rings and annuli are often of a similar appearance and as such accurate ageing beyond four years of age year is difficult. Horse mackerel grow rapidly during the first years of life and more slowly after three years of age. The maximum estimated age is reported as 40 years (Abaunza et al., 2003). Both growth and age at maturity fluctuate, which is suggested to be a density-dependent response to the extremely large fluctuations in year-class strength (ICES, 1991).

Horse mackerel is considered to be an asynchronous batch spawner with an indeterminate fecundity (Gordo et al., 2008; Ndjaula et al., 2009). In the northeast Atlantic area, the horse mackerel population has an 8-month long spawning season (Abaunza et al., 2003; Dransfeld et al., 2005), although the duration of an individual's spawning period is unknown (Van Damme et al., 2014). Horse mackerel appear to undertake annual migrations to spawning, feeding and over-wintering area (Abaunza et al., 2003). The peak spawning in the northeast Atlantic west of Britain and Ireland is in June in shelf waters (ICES, 2017; van Damme et al., 2014). Peak spawning in the North Sea occurs in May and June (Macer, 1974), and spawning occurs in the coastal regions of the southern North Sea along the coasts of Belgium, the Netherlands, Germany, and Denmark. Peak spawning in Portuguese waters is earlier than the other regions being in February in shelf waters (Borges & Gordo, 1991), though it should be noted that there is significant overlap between these areas. In winter the North Sea spawning horse mackerel are believed to migrate to the Western English Channel, whilst those that spawn west of Ireland and Britain migrate from feeding grounds off Norway and the northern North Sea to the continental slope southwest of Ireland (Heessen et al., 2015).

1.2 Stock Identification

ICES has long considered horse mackerel in the northeast Atlantic to consist of three stocks (Figure 1). The southern stock was defined as that found in the Atlantic waters of the Iberian Peninsula (Division 9a), the North Sea stock in the eastern English Channel and southern North Sea area (Divisions 3a, 4b,c, and 7d), and the western stock on the northeast continental shelf of Europe, stretching from the Bay of Biscay in the south to Norway in the north (Subarea 8 and Divisions 2a, 4a, 5b, 6a, and 7a–c, e–k). This separation of horse mackerel was based on a variety of factors including the temporal and spatial distribution of the fishery, the observed egg and larval distributions, information from acoustic and trawl surveys and from parasite infestation rates (see ICES, 2015). A tagging programme was established in 1994 (ICES, 1995) and further studies based on genetic (allozyme) population structure and morphometric characteristics, were conducted in 1997 (ICES, 1998). Tagging studies failed to recover any tagged fish, and neither the genetic nor morphometric studies provided a basis for changing the stock separation as previously defined.

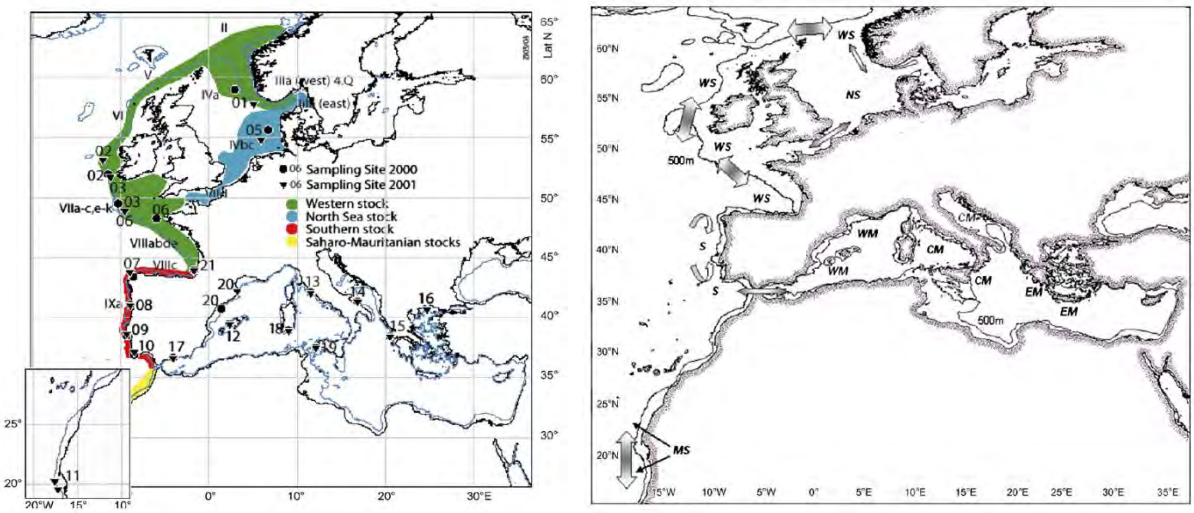

Figure 1. (Left panel) The suggested stocks of horse mackerel prior to the HOMSIR project. The sampling sites in the HOMSIR project in 2000 (circles) and 2001 (triangles). (Right panel) Proposed horse mackerel stocks according to the HOMSIR project. The arrows indicate possible migratory movements. WS: western stock; NS: North Sea stock; S: southern stock; MS: Saharo-Mauritanian stock; WM: western Mediterranean stock; CM: central Mediterranean stock; EM: eastern Mediterranean stock. From Abaunza *et al*. (2008).

Further refinements of the definitions of stock units were based on the results from the EU-funded HOMSIR project (2000-2003), which utilised a multidisciplinary approach including various genetic approaches (allozymes, mitochondrial DNA and microsatellites), the use of parasites as biological tags, body morphometrics, otolith shape analysis and the comparative study of life history traits (growth, reproduction and distribution) (Abaunza et al., 2008). The resulting stock structure was broadly similar to that previously considered by ICES (Figure 1). However, it was observed that the population structure in the western European coasts could be more complicated and that more research was needed to clarify the migration patterns within the Northeast Atlantic Ocean. This was especially relevant to the mixing areas between the North Sea stock and the Western stock (Northern North Sea and English Channel). The sampling in this region was relatively sparse whereas the southern regions had significantly better coverage (Figure 2). The genetic components of the project failed to resolve stock structure largely due to the low number (four microsatellites) and low power of the genetic markers employed (Kasapidis and Magoulas, 2008).

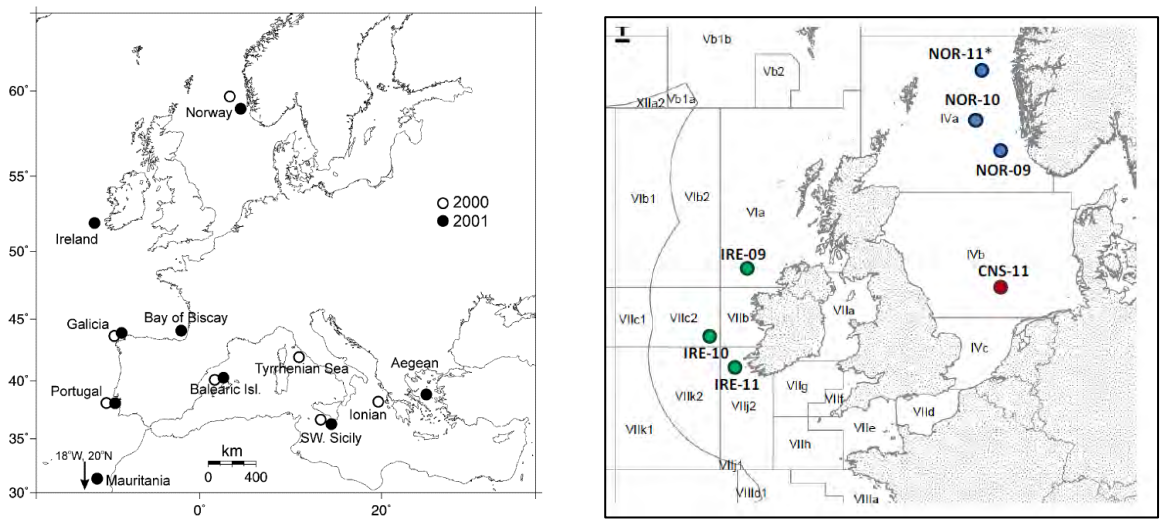

Figure 2. (Left Panel) The genetic samples collected and analysed in the Kasapidis and Magoulas (2008) study which was part of HOMSIR. (Right Panel) The genetic samples collected and analysed in the Mariani (2012) pilot study.

A recent preliminary study on western and North Sea horse mackerel employed 12 microsatellites (4 from horse mackerel, *Trachurus trachurus* and 8 from Chilean jack mackerel, *Trachurus murphyi* Nichols, 1920) to screen a small number of samples (n = 7 samples/339 individuals) from both putative stocks (Figure 2). The results indicated significant population structure within the samples from the western stock while no significant structure was observed between the samples collected west of Ireland and those collected in the central North Sea (Mariani, 2012). However, there were a number of issues related to the genetic markers employed being non species-specific and also the samples screened not being from spawning individuals.

The degree of separateness of the western and North Sea stocks is uncertain. It is known that the western stock spawns west of Ireland while the North Sea stock has a separate spawning ground in the North Sea. However, it is unclear if these spawning grounds are used interchangeably. Unlike herring (*Clupea harengus* Linnaeus, 1758), horse mackerel are not known to be faithful to their original spawning grounds. Therefore, without strong evidence to the contrary, it cannot be assumed that the two stocks are indeed separate. Treating these stocks as separate, if indeed they are not, is dangerous from a precautionary management perspective. Further research is needed to clarify the level of differentiation between the North Sea and Western stocks and also to define the boundary areas, if any, between them. The levels of mixing in the northern North Sea (area 4a) are also unclear and catches and survey data from this area are currently allocated to the North Sea stock in quarters 1 and 2 and to the western stock in quarters 3 and 4, highlighting the uncertainty in the assessments for these stocks.

1.3 Stage 1 - PFA/IMARES pilot study

In 2015 the Pelagic Freezer Trawler Association (PFA) contracted the Wageningen UR, Institute for Marine Resources and Ecosystem Studies, IJmuiden (IMARES) to undertake a study on North Sea Horse Mackerel (Brunel et al., 2016). The primary aim of the study was to improve the data quality used for an analytical stock assessment model of North Sea horse mackerel. The stock is currently classified by ICES as a data poor stock, for which the catch advice is based on the trend in an abundance index.

The management boundary between the western and North Sea stocks in the English Channel (corresponding to the separation between areas 7e, western Channel and 7d, eastern Channel) does not correspond to a real biological boundary, as mixing of the two stocks is known to occur in area 7d in autumn and winter (Brunel et al., 2016). The catches taken in 7d are officially considered as being North Sea horse mackerel and represent c.80% of the catches from this stock. An unknown proportion of this catch is likely from the western stock, which interferes with the cohort signal in the catch at age matrix, hampering the development of an age-structured assessment model for the North Sea stock. Developing methods to separate catches from the western stock from catches from the North Sea stock in area 7d are therefore necessary to improve the quality of the catch information for the North Sea stock. Within the project, two pilot studies, based on chemical fingerprint and genetics, were conducted to investigate new methods to determine stock structure and to develop techniques to identify the stock origin of the catches taken in the eastern English Channel.

The chemical fingerprint analysis was carried out by IMARES using two-dimensional gas chromatography (GCxGC-MS), in order to establish a full chemical fingerprint of the horse mackerel samples from both the western and North Sea stocks. Results were inconclusive but suggested that the chemical fingerprint approach was a potential tool to determine stock of origin, with a moderate risk of misclassification. However, more insight on the sources of variation of compound concentrations (seasonal changes, influence of sex, length, age, reproducibility of the results from year to year) is required before this method can be further developed.

IMARES, contracted University College Dublin (UCD) to undertake a pilot study to develop a method of genetic stock identification for discriminating North Sea and Western Horse mackerel (Brunel et al.,

2016). The aims of the pilot study were to firstly develop and validate at least 24 polymorphic microsatellites markers in horse mackerel and secondly to screen spawning fish collected in 2015 from the Western and North Sea stocks to establish a genetic baseline of the spawning stocks and test the presence of population structure. Recently developed Next Generation Sequencing (NGS) and Genotyping by Sequencing (GBS) based approaches, which were developed on cod (*Gadus morhua* Linnaeus, 1758), boarfish (*Capros aper* Lacépède, 1802) and 6a/7bc herring were used for marker development and screening of spawning samples (Carlsson *et al.*, 2013; Farrell *et al.*, 2016; Vartia *et al.*, 2014 & 2016). The pilot study successfully identified a large number of novel microsatellites, however initial data analyses were confounded by a poor-quality sequencing run and as such the discrimination power between the western and North Sea sample was low. This resulted in the pilot study being unable to separate the two stocks conclusively and unequivocally.

1.4 Stage 2 – Northern Pelagic Working Group (NPWG) genetic baseline project

In an effort to resolve these uncertainties the Northern Pelagic Working Group contracted EDF Scientific Limited and Jens Carlsson to undertake a comprehensive genetic stock identification study on Atlantic horse mackerel (Farrell & Carlsson, 2018). Sampling was conducted over three consecutive years and three spawning seasons and covered a large area of the distribution of the species including the Western, North Sea and Southern stock areas and also West African waters. In total 33 population samples, comprising 2,295 individual fish were collected from 2015 to 2017 across the study area (Figure 3). Total genomic DNA was extracted from 2,208 of these specimens. Spawning samples were analysed with a panel of 37 novel, putatively neutral microsatellite markers and statistical analyses (F_{ST}, structure, assignment testing, mixed stock analyses and FCA analyses) indicated that horse mackerel in the northeast Atlantic region does not represent a single biological unit. A high level of species misidentification in the West African samples was also observed. On the highest level there are mixed species catches in African waters, a clear separation of the southern North Sea from other regions and further, less pronounced, structure along the northeast Atlantic continental shelf. Exploratory assignment testing and mixed stock analysis of the western and North Sea baselines indicated a success rate of c.60-65% for self- assignment. This was considered relatively low and is due to the relatively low genetic differentiation between the populations at putatively neutral loci. Despite this, further exploratory assignment testing and mixed stock analysis of the fish caught outside spawning time in the northern North Sea and western English Channel (Figure 3) indicated that a large component of these fish belonged to the Western stock. No samples from the eastern English Channel were available for testing.

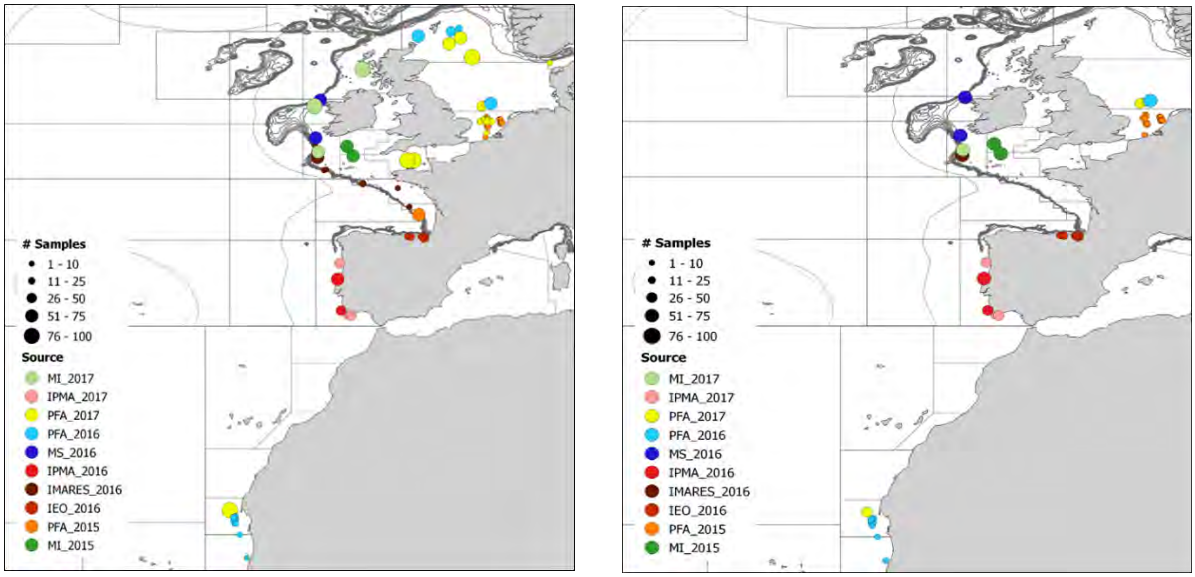

Figure 3. (Left Panel) The horse mackerel samples collected from 2015 to 2017 and (right panel) those included in the baseline dataset.

The results showed that the genetic information produced in the stage 2 study could be used for mixed stock analyses and that the information could be used to delineate the range of the North Sea stock – information that could be taken into account by fisheries management. However, it was suggested in the project report that further genetic analyses were warranted (full genome, RNA and RAD sequencing-based approaches) to increase the numbers and types of genetic markers available for this species. This would improve stock discrimination, mixed stock analyses and individual assignment capacity, similar to the approaches deployed for Baltic and Atlantic herring and other commercial fisheries species. This proposal by Dr Edward Farrell of EDF Scientific Limited, Ireland and Professor Leif Andersson, Uppsala University outlines one such approach.

1.5 Stage 3 & Stage 4 - Population genomics of horse mackerel and SNP validation

The current report presents the results of stages 3 and 4 of the horse mackerel project. To improve our ability to identify informative genetic markers, Dr Edward Farrell of EDF Scientific Limited, Ireland, and Professor Leif Andersson of Uppsala University, Sweden, proposed to undertake full genome sequencing of horse mackerel. This method provides the highest resolution of genetic variants with respect to the reference genome of the species', which was recently assembled by the Wellcome Sanger Institute, UK (website: https://vgp.github.io/genomeark/Trachurus_trachurus/). The Northern Pelagic Working Group funded stage 3, which involved the whole-genome pooled DNA sequencing of a subset of the populations sampled in stage 2 to identify population specific genetic markers. Further validation of potentially informative SNPs was undertaken as stage 4 and was funded by the Pelagic Advisory Council.

2. Materials and Methods

2.1 Sampling and DNA isolation

The samples included in the current study were a subset of the baseline samples analysed in stage 2 (Farrell and Carlsson, 2018). Sampling was organised by EDF Scientific and the Pelagic Freezer Trawler association (PFA). Samples were collected opportunistically, from 2015-2017, through existing fisheries surveys and from both target and non-target fisheries. One additional sample from the Alboran Sea in the Mediterranean Sea was provided by Dr Jens Carlsson from the ATLAS Project (https://www.eu-atlas.org/). The primary focus of sampling for the genetic analysis was collection of spawning fish, in order to ensure that samples could be considered to provide a valid baseline. However, due to the opportunistic nature of the sampling programme this was not always possible. Maturity stages were recorded by sample collectors using a number of different maturity keys. Therefore, these were standardised to the six-point international horse mackerel maturity scale (see Annex 1 Table S1; ICES, 2015). Each fish was measured for total length (TL) to the 0.5 cm below and total body weight (TW) to the nearest 1.0 g. Sex and maturity were also assessed and a 0.5 cm^3 piece of tissue was excised from the dorsal musculature of each specimen and stored at 4°C in absolute ethanol. Total genomic DNA (gDNA) was extracted from the majority of samples by Weatherbys Scientific Ltd, from c.30 mg of tissue from each fish using sbeadex™ magnetic bead-based extraction chemistry on the LGC Oktopure™ platform. The remaining samples were extracted using a Chelex and proteinase-K or CTAB based extraction protocol (Table 1). Extracted DNA was quantified on a NanoDrop® ND-1000 spectrophotometer (Nano-Drop Technologies, Wilmington, DE, USA) and laid out on 96-well PCR plates.

2.2 High-throughput sequencing, QC of raw reads, and read mapping

We performed whole-genome resequencing of pooled DNA (Pool-Seq) to assess the population-level genomic variation of the 12 fish aggregates sampled in this study. For this, individual DNA samples were combined into 12 pools by location and year in equal quantity to obtain at least 1.5 μg in 25-50 μL (Table 1). Between 30 and 96 individuals were included in each pool (Table 1). Pools were quantified in ng/μL using a Qubit Fluorometer (Thermo Fischer Scientific Inc) prior to submission to the SNP&SEQ Technology Platform in Uppsala, Sweden for library preparation and high-throughput sequencing. A PCR-free Illumina TruSeq library kit with a target insert size of 350 base pairs (bp) (Illumina Inc) was used for most pools, except for 6a and 6b, for which a Splinted Ligation Adapter Tagging (SPLAT) library preparation was used because their DNA was single-stranded (Raine et al., 2016). All libraries were paired-end sequenced on Illumina NovaSeq S4 flowcells with a read sequence length of 150 bp.

The quality of raw sequence reads for each pool was examined with *FastQC* v0.11.8 (Andrews, 2010), and jointly analysed in a single report with *MultiQC* v.1.7 (Ewels et al., 2016). Based on this initial sequence quality assessment, we removed low quality bases (Phred score < 15), Illumina adapters, and short reads (< 36 bp) with *Trimmomatic* v.0.36 (Bolger et al., 2014) (parameters: ILLUMINACLIP:adapters.fa:2:40:15:8:true SLIDINGWINDOW:4:15 LEADING:15 TRAILING:15 MINLEN:36). The quality of the resulting trimmed reads was assessed again with *FastQC* before further analysis.

Reads were mapped against the Atlantic horse mackerel (*Trachurus trachurus*) genome using *bwa-mem* 0.7.17 (Li, 2013) and default parameters. Read mapping quality statistics, including the number of aligned reads and the average read depth of coverage, were generated with *QualiMap* v.2.2.1 (Okonechnikov et al., 2015). Prior to variant calling, mapped reads were sorted using *SAMtools* v.1.10

(Li et al., 2009), duplicated reads were marked and read groups were added, both with *Picard* v2.20.4 (Broad Institute, 2018), and an index file was created with *SAMtools*.

2.3 Variant calling and filtering

Variant calling was performed with *GATK-UnifiedGenotyper* v3.8 (McKenna et al., 2010) because, in our experience, this algorithm works well and produces less false positives than the *GATK-HaplotypeCaller* when analysing pooled samples. The *GATK-UnifiedGenotyper* is a single-base caller that simultaneously identifies Single Nucleotide Polymorphisms (SNPs) and small indels (insertions and deletions). Since we aimed to characterize genome-wide variation based on biallelic SNPs, we extracted these genetic markers from the raw variant set using *GATK*.

To remove spurious markers and thus, retain the best quality ones for further analysis, we applied various filters to the raw SNP set. First, we performed hard-filtering by retaining SNPs that passed cut-off values that were set based on the genome-wide distribution of GATK variant quality annotations. The cut-off values used were: FisherStrand (FS) > 60.0, StrandOddsRatio (SOR) > 3.0, RMSMappingQuality (MQ) < 40.0, MappingQualityRankSumTest (MQRankSum) < -12.5, and ReadPosRankSumTest (ReadPosRankSum) < -8.0 (for more details on the GATK quality annotations, see *https://gatk.broadinstitute.org/hc/en-us/articles/360035890471-Hard-filtering-germline-short-variants*). Next, we retained SNPs with a genotype quality (GQ) greater than 20, allowed for a missing rate per locus of a maximum of 20%, kept loci with a minor allele count of at least 3 reads (MAC), and removed monomorphic loci with *BCFtools* v.1.10 (Li et al., 2009). Lastly, we applied a depth of coverage filter as follows. Based on the total read depth (DP) per locus and pool, we generated depth of coverage distributions for each pool with *R* (R Core Development Team, 2020) and the *R* package *ggplot2* (Wickham, 2016). We evaluated three different cut-off value ranges (listed from the most to the least stringent filter): mean $\pm$ 1 standard deviation, mode $\pm$ ½ the mode, and between 20x and 300x (300x corresponds to three times the mean coverage for all pools). We retained SNPs that fulfilled the depth of coverage requirement for all pools while excluding samples 6a, 6b and 7 (see results for details). The resulting high-quality SNP set was used in further analysis. A schematic summary of the data generation steps is illustrated in Figure S1.

2.4 Population genetic structure

The population-level allele frequencies computed from Pool-Seq data are derived from the read counts of a variant site. To control for potential technical artifacts inherent to Pool-Seq that could bias the allele frequency calculation, such random variation in read coverage and in chromosome representation across pools (Dohm et al., 2008; Kolaczkowski et al., 2011), we applied the n_{eff} allele count correction (Feder et al., 2012; Kolaczkowski et al., 2011) to the read counts of each SNP using a custom script implementing this formula $n_{\text{eff}} = \frac{(n*CT)-1}{n+CT}$ where *CT* corresponds to read depth and *n* to the number of chromosomes in a pool, being equal to 2*N* for diploid species like herring. Population allele frequencies were then calculated based on the n_{eff} corrected read counts and constituted the basis of subsequent population analysis.

To estimate the level of genetic differentiation among pools, we computed the unbiased pool-F_{ST} statistic ($\hat{F}_{\text{ST}}^{\text{pool}}$) for all possible paired comparisons with the R package *poolfstat* (Hivert et al., 2018). This statistic is equivalent to the (Weir & Cockerham, 1984) F_{ST} and accounts for random chromosome sampling characteristic of Pool-Seq experiments. The pool-F_{ST} statistic ranges between 0 and 1, where a value of 0 indicates no genetic differences exists between populations, while a value of 1 means complete genetic differentiation between populations. In addition, to assess clustering patterns of pool samples, we performed Principal Component Analysis (PCA) using the whole SNP set. In a pilot analysis samples 1b, 6a, and 6b appeared as outliers (Figure S4). Considering that technical biases might have affected these samples, they were excluded from subsequent analyses.

Table 1. Collection details of the Atlantic horse mackerel samples analysed in the current project.
Abbreviations: N: North, S: South, W: West, SW: Southwest, *N*: Number of individuals, Mag: Magnetic, Med: Mediterranean.

											Maturity Stage						
Stock	**Area**	**Sample**	**Year**	***N***	**Latitude**	**Longitude**	**Extraction method**	**Pool**	***N* per**	**Pool ID**	**1**	**2**	**3**	**4**	**5**	**6**	**NA**
Western	W Ireland	1a	2016	51	54.42	-10.62	Mag Bead	1a	51	1a-WIR-2016		31	19	1			
Western	SW Ireland	1b	2016	44	51.35	-10.98	Mag Bead	1b	44	1b-WIR-2016		32	12				
Western	SW Ireland	2a	2017	46	50.20	-10.79	Mag Bead	2	62	2-WIR-2017			44	2			
Western	W Ireland	2b	2017	16	53.93	-11.09	Mag Bead	2					16				
N Sea	S North Sea	3	2016	96	54.15	3.30	Mag Bead	3	96	3-SNS-2016		88		8			
N Sea	S North Sea	4a	2017	18	54.07	2.85	Mag Bead	4	70	4-SNS-2017				18			
N Sea	S North Sea	4b	2017	21	54.03	2.90	Mag Bead	4						21			
N Sea	S North Sea	4c	2017	31	53.93	2.55	Mag Bead	4						31			
Southern	N Portugal	5a	2016	64	39.83	-9.20	Mag Bead	5a	64	5a-NPT-2016		64					
Southern	S Portugal	5b	2016	30	37.26	-8.92	Mag Bead	5b	30	5b-SPT-2016	22	5	3				
Southern	N Portugal	6a	2017	48	41.14	-9.03	Chelex	6a	47	6a-NPT-2017		47	1				
Southern	S Portugal	6b	2017	23	36.84	-8.38	Chelex	6b	48	6b-SPT-2017		18	2	3			
Southern	S Portugal	6c	2017	25	36.84	-8.10	Chelex	6b				19	6				
N African	Mauritania	7a	2016	4	20.20	-17.50	Mag Bead	7	57	7-NAF-2016		1		3			
N African	Mauritania	7b	2016	4	19.00	-17.20	Mag Bead	7						4			
N African	Mauritania	7c	2016	8	19.90	-17.60	Mag Bead	7				1		7			
N African	Mauritania	7d	2016	1	17.10	-16.60	Mag Bead	7				1					
N African	Mauritania	7e	2016	7	20.10	-17.70	Mag Bead	7					1	6			
N African	Mauritania	7f	2016	4	20.40	-17.70	Mag Bead	7				1		3			
N African	Mauritania	7g	2016	8	20.50	-17.50	Mag Bead	7				1		7			
N African	Mauritania	7h	2016	9	20.50	-17.6	Mag Bead	7				4		5			
N African	Mauritania	7j	2016	7	20.30	-17.7	Mag Bead	7						7			
N African	Mauritania	7k	2016	5	20.40	-17.7	Mag Bead	7				1		4			
Western	N Spanish Shelf	8a	2016	22	43.31	-3.46	Mag Bead	8	96	8-NSP-2016		9	12				1
Western	N Spanish Shelf	8b	2016	23	43.27	-3.21	Mag Bead	8				5	18				
Western	N Spanish Shelf	8c	2016	3	43.27	-2.42	Mag Bead	8					3				
Western	N Spanish Shelf	8d	2016	44	43.22	-2.14	Mag Bead	8				15	28	1			
Western	N Spanish Shelf	8e	2016	4	43.20	-2.10	Mag Bead	8					4				
Med	Alboran Sea	9a	2018	10	36.36	-5.12	CTAB	9	49	9-MED-2018				10			
Med	Alboran Sea	9b	2018	10	36.56	-4.55	CTAB	9						10			
Med	Alboran Sea	P9c	2018	10	36.49	-4.42	CTAB	9						10			
Med	Alboran Sea	P9d	2018	10	36.6865	-4.28	CTAB	9						10			
Med	Alboran Sea	P9e	2018	10	36.70	-3.56	CTAB	9						10			

2.5 Detection of loci putatively under selection

To identify regions of the genome with elevated genetic differences, generally interpreted as candidate signatures of natural selection, we calculated the absolute delta allele frequency (dAF) of each SNP between paired contrasts of single or grouped pools. In specific, we first calculated the mean allele frequency per SNP within each proposed group, and after, the absolute difference between the two groups. The contrasts and groupings examined were established taking in consideration geographic closeness, PCA clustering patterns, and stock divisions. The paired contrasts evaluated were:

- Each pool against all other samples
- Southern North Sea (3 and 4) vs. others (1a, 8, 5a, 5b, 9)
- Western Ireland (1a) vs. other northern samples (2, 3, 4, 8, 5a)
- Western Ireland (1a, 2) vs. other northern samples (3, 4, 8, 5a)
- Northern Spanish shelf (8) vs. other northern samples (2, 3, 4, 8, 5a)
- Southern Portugal and Alboran Sea (5b, 9) vs. all others (1a, 3, 4, 8, 5a)
- Southern Portugal and northern Africa (5b, 7) vs. all others (1a, 3, 4, 8, 5a, 9)
- "North" (1a, 2, 3, 4, 8, 5a) vs. "South" (5b, 7) groupings
- Northern Africa (7) vs. others (1a, 3, 4, 8, 5a, 5b, 9)

To identify genomic regions with consistent differentiation across various markers, we also calculated the moving (or rolling) mean of dAF values in windows of 100 SNPs for each contrast. In this way, we ruled out single SNPs that could be influenced by random effects of Pool-Seq experiments. We further explored the allele frequency pattern of the most highly differentiated SNPs at each locus and contrast across the 12 pool samples. We included here samples 1b, 6a, and 6b as it was focused on loci that were well supported in other samples. All the analyses were performed using *R* and plotting was done with the *ggplot2* package.

2.6 Individual validation of informative markers for stock assessment

The primary aim of this study was to identify a reduced and highly informative set of SNP markers that could be used for genetic stock identification. For this purpose and to validate the main findings with the Pool-Seq data, we screened a subset of the 100 most differentiated SNPs in a total of 160 individuals. In addition to confirming the allele frequencies observed in the Pool-Seq data it was also possible to undertake a preliminary analyses of population structure between the main sampling areas.

The loci included in the SNP panel were selected as follows. We started from a list of candidate SNPs with the highest dAF values from the major genomic regions of divergence in each of the main contrasts. In most cases we selected SNPs with dAF $\geq$ 0.35, but when a large number of SNPs passed this threshold we set a higher cut-off value, so we could obtain a reduced number of SNPs representative of that locus. We required that SNPs had a coverage $\geq$ 20x, a base quality $\geq$ 20, a mapping quality $\geq$ 20; that they were at least 10 bp away from an indel, more than 100 bp far from repetitive sequences, and more than 1 kb from the closest informative SNP; that alleles were equally supported by forward and reverse reads (no strand bias); that several chromosomes would be represented when that was the case; and that enough flanking sequence of good quality was available for primer design ($\pm$ 120 bp). The genomic context of target SNPs was further examined using the genome browser *IGV* (Robinson et al., 2011; Thorvaldsdóttir et al., 2013). We additionally chose a set of SNPs that were lowly undifferentiated (or "neutral") and a few SNPs that were distinctive of sample 1b, to test whether this sample was actually unique as it behaved as an outlier in pilot analysis. The

neutral SNPs were randomly selected from the chromosomes underrepresented in the paired contrasts. We required these SNPs had a depth of coverage between 40x and 200x; were at least 10 bp away from nearby SNPs and indels; had an average allele frequency between 0.4 and 0.7; and had enough flanking sequence (± 120 bp) of good quality for primer design, which was visually evaluated with *IGV*. The final split of loci per region in the 100-SNP panel was: southern North Sea (n = 28), neutral loci (n = 24), north-south break (n = 13), 1b-western Ireland (n = 10), Alboran Sea (n = 13), southern Portugal (n = 4), 1a-western Ireland (n = 4), northern Africa (n = 4) (Figure S6).

A subset of 20 individuals each was selected from 8 of the 12 samples included in the Pool-Seq analyses (Table 2) for the SNP validation. Three or four individuals per sample were genotyped twice in order to test for genotyping errors. DNA extraction and SNP genotyping was undertaken by IdentiGEN, Dublin, Ireland using their proprietary IdentiSNP genotyping assay chemistry. The protocol utilises target specific primers and universal hydrolysis probes. Following the endpoint PCR reaction different genotypes are detected using a fluorescence reader.

Only individuals with >80% genotyping success and SNPs with >80% genotyping success were retained in the analyses. Deviations from Hardy–Weinberg equilibrium and linkage disequilibrium were tested with *Genepop* 4.2 – default settings (Rousset, 2008). *Microsatellite Analyzer* (*MSA*) 4.05 was used, under default settings, to calculate pairwise F_{ST} estimates (Dieringer & Schlötterer, 2003). In all cases with multiple tests, significance levels were adjusted using the sequential Bonferroni technique (Rice 1989). Discriminant Analysis of Principal Components (DPCA) and clustering analyses were performed in *R* using the *adegenet* package for the multivariate analysis of genetic markers (Jombart, 2008). It should be noted that sample sizes were small and therefore the results of the analyses presented in section 3.6 should be viewed as preliminary until further large-scale screening is undertaken. To illustrate the potential of the markers for individual assignment for stock identification, an exploratory assignment was also conducted in *GeneClass2* (Piry et al., 2004) and the *R* package *geneplot* (McMIllan & Fewster, 2017) with the Bayesian method of Rannala and Mountain (1997).

Table 2. The horse mackerel samples included in the SNP validation analyses

Stock	Area	Sample	Pool	Year	#individuals	# repeated
Western	West of Ireland	1a	1a	2016	20	4
Western	Southwest of Ireland	1b	1b	2016	20	4
North Sea	Southern North Sea	3	3	2016	20	4
North Sea	Southern North Sea	4b	4	2017	20	4
Southern	Northern Portugal	5a	5a	2016	20	4
Southern	Southern Portugal	5b	5b	2016	20	4
North African	Mauritania	7a	7	2016	4	0
North African	Mauritania	7b	7	2016	4	1
North African	Mauritania	7c	7	2016	8	1
North African	Mauritania	7e	7	2016	4	1
Western	Northern Spanish Shelf	8d	8	2016	20	3

3. Results

3.1 Sampling and DNA Isolation

A total of 33 collections comprising 716 individual fish were included in this study (Figure 4 and Table 1). Samples were aggregated into 12 pools based on spatial and temporal proximity, thus broadly representing most of the geographical range of the species in the northeast Atlantic and the western part of the Mediterranean Sea.

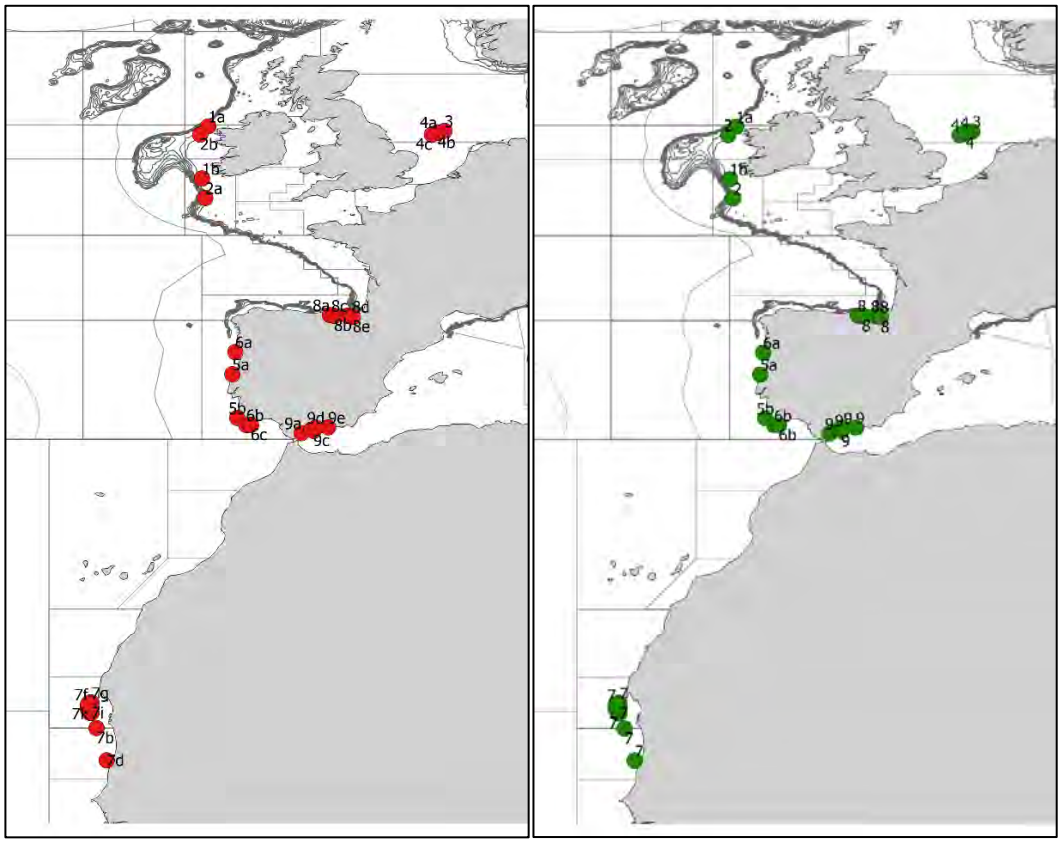

Figure 4. Sampling locations of the Atlantic horse mackerel included in this study. (Left) Sample batches collected at each location, (right) Pooled samples.

Four of the available samples corresponded to temporal replicates collected one year apart, which allowed us to examine the short-term stability of the genetic composition at these sites. Pool 2 was a mix of the replicates of the two samples collected in western Ireland (1a and 1b); pools 6a and 6b were temporal replicates of pools 5a and 5b from Northern and Southern Portugal, respectively; and pool 4 was the replicate of pool 3 from southern North Sea).

3.2 High-throughput sequencing, QC of raw reads, and read mapping

A total of 490-764 million high-quality reads were obtained for each pool. Mean read depth of coverage per pool ranged between 25.7x and 46.3x, mean mapping quality (MQ) was larger than 35 for all pools, and GC content was ~42% for most samples except for the African pool (46.6%) (Table S2).

A comparison of the mapping statistics of all pools showed that three of them (6a, 6b, 7) might be affected by technical artefacts. The two temporal replicates from Portugal (6a, 6b), which were extracted with Chelex and had a SPLAT library preparation, had a smaller mean coverage and shorter insert size (~245 bp vs. ~400-465 bp) than the other pools (Figure S2). The sample from Africa had a

flatter and wider coverage distribution, higher GC content, and higher missing rate (Figure S2) with respect to the other pools, which could be the result of certain degradation of the starting genetic material that was noticeable during DNA quantification. Given the difficulty to rule out the effect of technical biases from biological variation in these samples, they were excluded from some analyses.

3.3 Variant calling and filtering

From the three depth of coverage thresholds tested (Figure S3), we chose the range of 20x-300x because in a pilot analysis it provided a large number of SNPs and similar genetic patterns as the more stringently filtered sets. A total of ~12.8 million polymorphic biallelic SNPs passed all the quality filters and were used in the population analysis.

3.4 Population genetic structure

The large set of genetic variants here analysed indicated that overall, there are low levels of genetic differentiation among Atlantic horse mackerel populations distributed across the broad geographic area here represented (Figure 5) (global mean pool-F_{ST} = 0.007, pairwise pool-F_{ST} values ranged between 0.001 and 0.015). The genetic differences among populations constituted less than 1.5% of their entire genome.

The pairwise pool-F_{ST} values revealed a north-south genetic break along mid Portugal, distinguishing a “north” group comprising southern North Sea (3, 4), western Ireland (1a, 2), northern Spanish shelf (8) and northern Portugal (5a), from a “south” group including southern Portugal (5b), northern Africa (7), and the Alboran Sea (9) samples (Figure 5). These statistics also showed that the sample from the Alboran Sea (pool 9) was the most genetically distinct of all (pool-F_{ST} 0.01-0.015), followed by Southern Portugal (5b) and northern Africa (7), respectively (pool-F_{ST} 0.005-0.007). In contrast, the two samples collected one year apart from southern North Sea (pools 3 and 4) were the most genetically similar of all (pool-F_{ST} 0.001).

For the PCA we excluded samples 1b, 6a and 6b, as in a pilot analysis they appeared as outliers. The PCA agreed with the previous observations of a north-south break and it additionally revealed sub-structuring within the “north” and “south” groupings. The first two PCs show that the genetic differences among the samples within the “north” group (1a, 2, 3, 4, 5a, 8) are very small (all cluster together near the centre) with respect to the differences between the three samples in the “south” group (5b, 7, 9). PC1 shows that within the “south” group, genetic differences exist between the Alboran Sea (9), southern Portugal (5b) and northern Africa (7). PC2 indicates that differences also occur between northern Africa (7) and the Alboran Sea (9) and southern Portugal (5b). PC3 separates the “north” and “south” groups, being southern Portugal (5b) closer to the “north” group than northern Africa (7) and the Alboran Sea (9). PC4 distinguishes western Ireland (1a) and northern Portugal (5a) and also shows the high genetic similarity (tight clustering) between the two samples from the southern North Sea (3, 4).

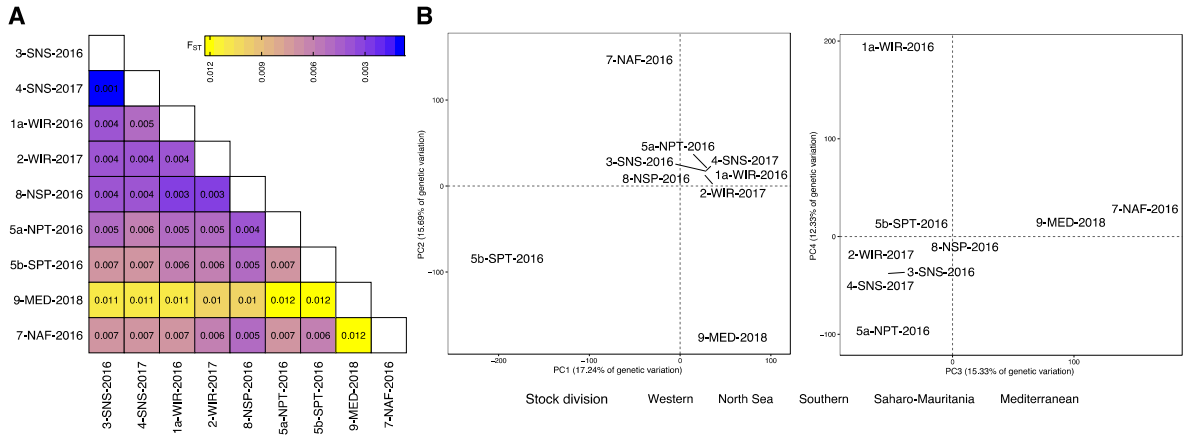

Figure 5. Population genetic structure of the 9 pool samples analysed. **A**. Pairwise pool-F_{ST} statistics, **B**. PCA of 9 pools; (left) PC1-2, (right) PC3-4.

3.5 Detection of loci putatively under selection

The genome-wide scans for the identification of candidate loci under selection revealed a number of genomic regions with elevated allele frequency differences for three contrasts: i) "north" vs. "south" groupings; ii) southern North Sea vs. others; and iii) Alboran Sea (9) vs. others.

The comparison between the "north" and "south" groups disclosed that a single large locus, likely corresponding to a chromosome structural variation (SV), underlies the north-south genetic break (Figure 6). This locus on chromosome 21 appears as a large block of SNPs with elevated allele frequency differences spanning 9.9 Mb. The large genomic size and abrupt change in allele frequencies (well-defined edges) at this locus are common characteristics of SVs with suppressed recombination (e.g. inversions). A further exploration of the allele frequency patterns of some of the most differentiated SNPs at this locus (dAF ≥ 0.72) showed that one allele occurs at high frequency among all northern samples and in the Alboran Sea; at intermediate frequencies in southern Portugal (Figure 6, inset box); and the alternative allele occurs at high frequency in northern Africa, the southernmost sample studied.

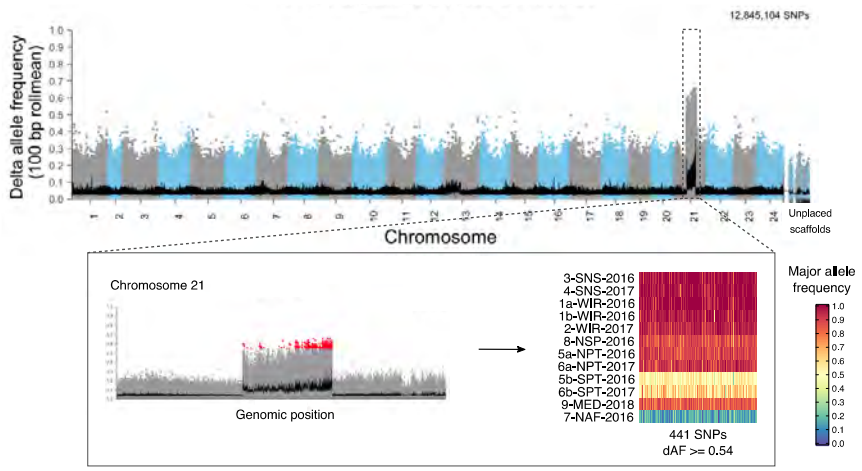

Figure 6. Manhattan plot representing the dAF of each SNPs along the genome for the north-south contrast. Each dot corresponds to a single SNP, the x-axis shows its genomic position, and the y-axis indicates its dAF frequency value for a given contrast. The line in black corresponds to the rolling mean of dAF calculated over 100 SNPs. The inset box shows a zoom-in of the putative chromosomal structural variant found in chromosome 21. The red dots correspond to the SNPs with a dAF ≥ 0.72. The heatmap plot at the right-hand side of the inset

shows the major allele frequencies of these top SNPs. In the heatmap plot, rows correspond to pool samples, and columns to SNP variants.

The comparison of the southern North Sea samples against all others disclosed that seven genomic regions distinguish this population. Two of these regions are located on chromosome 1, and the others are on chromosomes 4, 7, 11, 20, and 21 (Figure 7); they stand out as a "peak" or aggregate of SNPs with elevated differences in allele frequencies in respect to the neighbouring variants. Further examination of the allele frequencies of some of the most divergent SNPs at each locus show the large agreement in allele frequency patterns that exists between the two southern North Sea temporal replicates, and that they are distinctive of this population (Figure 7, inset boxes).

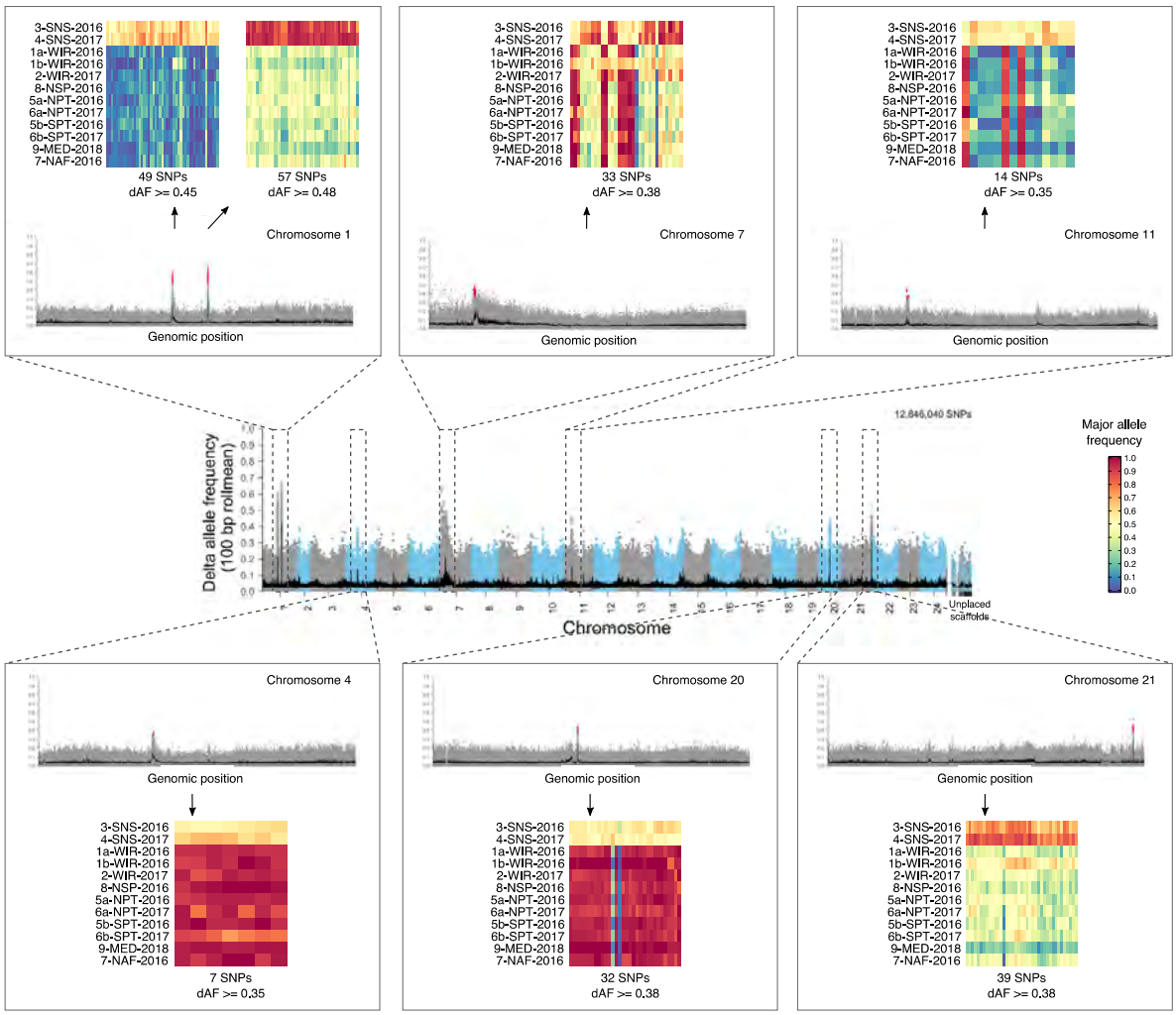

Figure 7. Manhattan plot of the dAF of each SNPs along the genome for the contrast distinguishing the southern North Sea samples. Each dot is a single SNP. The line in black corresponds to the rolling mean of dAF over 100 SNPs. The inset boxes show a zoom-in into the 7 genomic regions across chromosomes 1, 4, 7, 11, 20, and 21, characteristics of the North Sea samples. The red dots in the zoomed dAF profile of each chromosome correspond to the most highly differentiated SNPs per genomic region. The heatmap plot at the right-hand side of the inset shows the major allele frequencies of these top SNPs. In the heatmap plot, rows correspond to pool samples, and columns to SNP variants.

The contrast of the Alboran Sea sample against all others showed that two regions, one on chromosome 5 and another on chromosome 21, distinguish this sample from other samples (Figure 8). In this case the "peaks" of divergence were not as evident as in the other contrasts, for which it was necessary to focus more on the patterns shown by the rolling mean in dAF values. The

examination of allele frequencies of the most differentiated SNPs showed that the Alboran Sea sample had a characteristic allele frequency pattern.

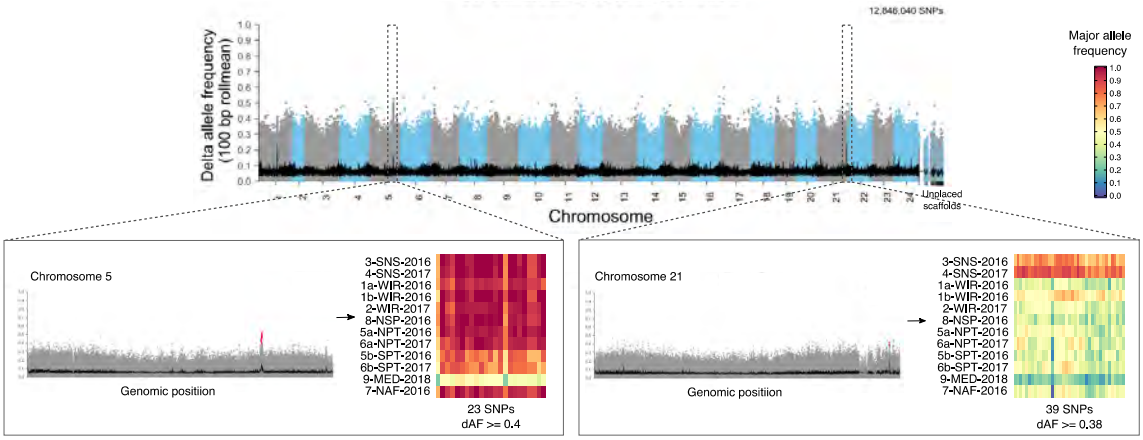

Figure 8. Manhattan plot of the dAF of each SNPs along the genome for the contrast distinguishing the Alboran Sea (from the western part of the Mediterranean Sea) sample. Each dot is a single SNP. The line in black corresponds to the rolling mean of dAF over 100 SNPs. The inset boxes show a zoom-in into the two genomic regions in chromosomes 5 and 21 showing high differentiation between the Alboran Sea sample and other samples. The red dots in the zoomed dAF profile of each chromosome correspond to the most highly differentiated SNPs per genomic region. The heatmap plot at the right-hand side of the inset shows the major allele frequencies of these top SNPs. In the heatmap plot, rows correspond to pool samples, and columns to SNP variants.

3.6 Individual validation of informative markers for stock assessment

The strong correlation between population allele frequencies obtained with individual genotyping and with Pool-Seq confirms the main genomic regions of divergence discovered with Pool-Seq (Figure S5). A total of 72 out of the 100 SNPs included in the panel had a genotyping success >80% (Table 3). Of these, six SNPs had indication of deviation from Hardy-Weinberg Equilibrium (HWE), two markers (12_3119866 and 17_972744) were not polymorphic and one had evident scoring errors (24_5252083). After removing these nine markers, the resulting dataset had 63 SNPs and 157 out of 160 individuals with a genotyping success >80%.

Table 3. Details of the 100 SNPs tested in the validation analyses. The SNPs highlighted in red did not reach the 80% genotyping success threshold or failed to amplify. The SNPs highlighted in orange deviated from HWE, were not polymorphic or had scoring errors and were removed from the analyses. '*LD*' indicates significant linkage disequilibrium between samples and '*Assumed*' indicates assumed LD based on chromosome position. * indicates SNPs that were included in the 17 SNP dataset.

SNP Name	>80% success	Chromosome	Position	Contrast	LD Group	Comment
1_17504018*	Yes	1	17504018	Southern North Sea	Assumed	
1_17506941	Yes	1	17506941	Southern North Sea	LD	
1_17510324	Yes	1	17510324	Southern North Sea	LD	
1_17517550	Yes	1	17517550	Southern North Sea	LD	
1_17521852	Yes	1	17521852	Southern North Sea	LD	
1_17523218	Yes	1	17523218	Southern North Sea	LD	
1_17525646	Yes	1	17525646	Southern North Sea	Assumed	
1_17558501	Yes	1	17558501	Southern North Sea	LD	
1_22046469	Yes	1	22046469	Southern North Sea	LD	
1_22046756	Yes	1	22046756	Southern North Sea	LD	
1_22047461	Yes	1	22047461	Southern North Sea	LD	
1_22049353	Yes	1	22049353	Southern North Sea	LD	
1_22053057*	Yes	1	22053057	Southern North Sea	LD	
1_22081696	No	1	22081696	Southern North Sea	Assumed	
3_2811572	No	3	2811572	Neutral markers		
3_18949602	No	3	18949602	Neutral markers		
3_18951336	Yes	3	18951336	Neutral markers		
3_33715024	No	3	33715024	Neutral markers		
4_13086614*	Yes	4	13086614	Southern North Sea	LD	
4_13088818	Yes	4	13088818	Southern North Sea	LD	
4_13098092	Yes	4	13098092	Southern North Sea	LD	
5_22983273	No	5	22983273	Western Ireland (1a)		
5_28197435	Yes	5	28197435	Med and/or S Portugal		
5_28205448	Yes	5	28205448	Med and/or S Portugal		
5_28240764	Yes	5	28240764	Med and/or S Portugal		
5_28240785	Yes	5	28240785	Med and/or S Portugal		
5_28241356*	Yes	5	28241356	Med and/or S Portugal		
5_28242757	No	5	28242757	Med and/or S Portugal		
5_28243095	Yes	5	28243095	Med and/or S Portugal		
5_28274875	No	5	28274875	Med and/or S Portugal		
6_18368752*	Yes	6	18368752	Neutral markers		
6_24275858	No	6	24275858	Neutral markers		
6_33295851*	Yes	6	33295851	Neutral markers		
7_5053296*	Yes	7	5053296	Southern North Sea		
7_5108289	Yes	7	5108289	Southern North Sea		
8_2410897	No	8	2410897	Neutral markers		
8_3426603*	Yes	8	3426603	Neutral markers		
11_6942036	Yes	11	6942036	Southern North Sea		Out of HWE in 2 pops
12_3119866	Yes	12	3119866	Neutral markers		Not polymorphic
12_10994158	No	12	10994158	Neutral markers		
12_27660258	Yes	12	27660258	Neutral markers		Out of HWE in 3 pops
13_4844455	No	13	4844455	Western Ireland (1b)		
13_4874422	Yes	13	4874422	Western Ireland (1b)	LD	
13_4874692	Yes	13	4874692	Western Ireland (1b)	LD	
13_4874725	Yes	13	4874725	Western Ireland (1b)	LD	
13_5015377*	Yes	13	5015377	Western Ireland (1b)		
13_5092546	Yes	13	5092546	Western Ireland (1b)		
16_22440492	No	16	22440492	Africa		
17_955542	No	17	955542	Western Ireland (1b)		
17_955717	Yes	17	955717	Western Ireland (1b)		Out of HWE in 1 pop
17_961283	No	17	961283	Western Ireland (1b)		
17_972744	Yes	17	972744	Western Ireland (1b)		Not polymorphic
18_4093892*	Yes	18	4093892	Africa		
19_4188265	No	19	4188265	Neutral markers		
19_4189387	No	19	4189387	Neutral markers		
19_4194438	No	19	4194438	Neutral markers		
19_13550308	No	19	13550308	Neutral markers		
20_11636865	Yes	20	11636865	Southern North Sea	LD	
20_11638825*	Yes	20	11638825	Southern North Sea	LD	
20_11640406	Yes	20	11640406	Southern North Sea	LD	
20_11643211	Yes	20	11643211	Southern North Sea	LD	
20_11644062	Yes	20	11644062	Southern North Sea	LD	
20_11647497	Yes	20	11647497	Southern North Sea	LD	
20_11647537	Yes	20	11647537	Southern North Sea	LD	
20_11649644	Yes	20	11649644	Southern North Sea	LD	
21_13901383	Yes	21	13901383	North-South pattern		
21_15195721	Yes	21	15195721	Southern Portugal		
21_15619806*	Yes	21	15619806	North-South pattern		
21_16093398	Yes	21	16093398	North-South pattern		
21_18106603	Yes	21	18106603	North-South pattern		
21_19507025	Yes	21	19507025	Southern Portugal		Out of HWE in 1 pop
21_20477335	Yes	21	20477335	North-South pattern		

Table 3. *Continuation*.

SNP Name	>80% success	Chromosome	Position	Contrast	LD Group	Comment
21_20646321	Yes	21	20646321	North-South pattern	LD	
21_20838721	Yes	21	20838721	North-South pattern	LD	
21_21340446	Yes	21	21340446	North-South pattern	LD	
21_21591928	Yes	21	21591928	North-South pattern		
21_21801450	Yes	21	21801450	North-South pattern		
21_22552517	Yes	21	22552517	North-South pattern		
21_23412586*	Yes	21	23412586	North-South pattern	LD	
21_23420067	Yes	21	23420067	North-South pattern	LD	
21_34276436	No	21	34276436	Southern Portugal		
21_34279224	No	21	34279224	Southern Portugal		
21_34570675	Yes	21	34570675	Med and/or S Portugal	LD	
21_34571601	No	21	34571601	Med and/or S Portugal		
21_34571721	Yes	21	34571721	Med and/or S Portugal	LD	
21_34573582*	Yes	21	34573582	Med and/or S Portugal	LD	
21_34578009	No	21	34578009	Med and/or S Portugal		
22_253248	No	22	253248	Africa		
22_29332559	Yes	22	29332559	Western Ireland (1a)		Out of HWE in 5 pops
22_29369048*	Yes	22	29369048	Western Ireland (1a)		
22_29400293	Yes	22	29400293	Western Ireland (1a)		
24_2630784	No	24	2630784	Neutral markers		
24_2631095	No	24	2631095	Neutral markers		
24_3769194	No	24	3769194	Neutral markers		
24_5252083	Yes	24	5252083	Africa		Scoring error
24_5255627	No	24	5255627	Neutral markers		
24_10305770*	Yes	24	10305770	Neutral markers		
24_10306442	Yes	24	10306442	Neutral markers		Out of HWE in 1 pop
24_14507474	No	24	14507474	Neutral markers		
24_19228299*	Yes	24	19228299	Neutral markers		

As expected, analyses of linkage disequilibrium (LD) indicated significant linkage between a number of SNPs located in close proximity on the same chromosomes (Table 3). Though LD was not statistically significant in some cases (e.g. SNPs on chromosome 5), these were considered to be linked due to the closeness of the SNPs. In order to identify the most informative SNPs for discriminating the samples, the F_{ST} per locus was analysed by marker and by population (Figure 9). The most informative SNP (highest average F_{ST}) per linkage group was retained, yielding a 17 SNP dataset comprising 155 out of 160 individuals with a genotyping success >80%. Further analyses were conducted with both the 63_SNP and the 17_SNP datasets (individual genotypes in each SNP set are shown in Figure S7).

There was no significant genetic differentiation between the North Sea temporal replicates or between the two west of Ireland samples (Table 4). There was also no significant genetic differentiation between the northern Spanish shelf sample, the northern Portugal sample and the two west of Ireland samples (Table 4). Discriminant Analysis of Principal Components (DAPC) and clustering analyses of the 63_SNP and 17_SNP datasets indicated the same pattern as the F_{ST} analyses with the North Sea temporal replicates clustering together, the west of Ireland, northern Spanish shelf and northern Portugal samples clustering together and the southern Portugal and northern African samples forming two separate clusters (Figure 10). Due to the lack of genetic differentiation, the two North Sea samples were combined into one sample and the two west of Ireland samples were combined into one sample for further analyses.

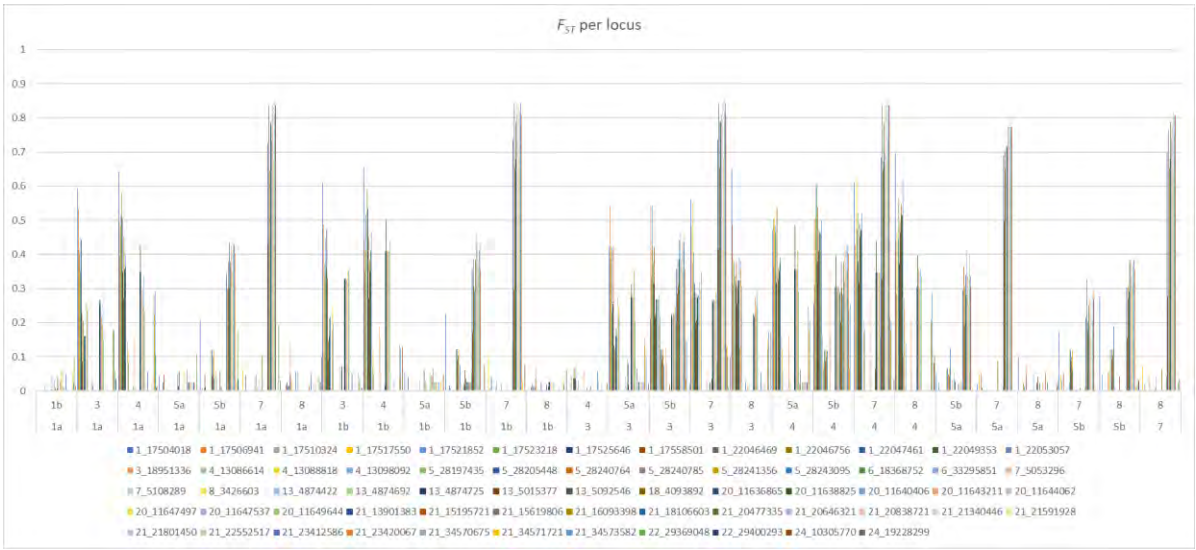

Figure 9. The pairwise F_{ST} per locus for the 63_SNP dataset

Table 4. Pairwise multi-locus F_{ST} (above the diagonal) and associated *P*-values (below the diagonal) for the 63_SNP dataset (top panel) 17_SNP dataset (bottom panel). *P*-values highlighted in red were still significant after sequential Bonferroni correction.

	1a	1b	3	4	5a	5b	7	8
1a		0.004	0.195	0.260	-0.004	0.135	0.361	0.004
1b	0.28		0.198	0.265	-0.006	0.124	0.352	-0.003
3	0.00	0.00		-0.006	0.180	0.243	0.417	0.218
4	0.00	0.00	0.60		0.241	0.287	0.446	0.286
5a	0.61	0.71	0.00	0.00		0.101	0.323	-0.002
5b	0.00	0.00	0.00	0.00	0.00		0.080	0.111
7	0.00	0.00	0.00	0.00	0.00	0.00		0.334
8	0.29	0.54	0.00	0.00	0.51	0.00	0.00	

	1a	1b	3	4	5a	5b	7	8
1a		0.016	0.138	0.196	0.004	0.088	0.241	0.009
1b	0.09		0.121	0.190	0.003	0.075	0.221	-0.002
3	0.00	0.00		-0.002	0.102	0.137	0.297	0.168
4	0.00	0.00	0.53		0.154	0.187	0.340	0.233
5a	0.32	0.35	0.00	0.00		0.033	0.183	0.006
5b	0.00	0.00	0.00	0.00	0.01		0.055	0.068
7	0.00	0.00	0.00	0.00	0.00	0.00		0.209
8	0.17	0.52	0.00	0.00	0.26	0.00	0.00	

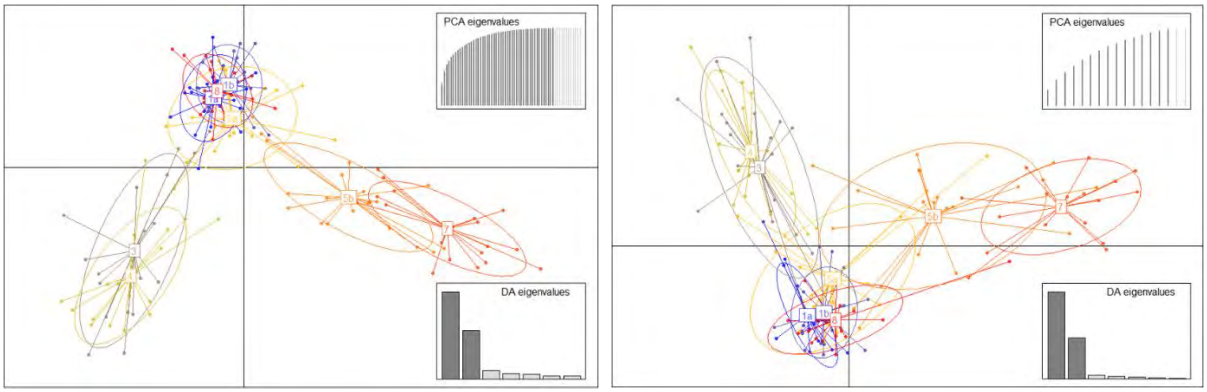

Figure 10. Discriminant Analysis of Principal Components of the 63_SNP dataset (left panel) and the 17_SNP dataset (right panel).

Membership probability plots of the two datasets also indicated the close affinity between the west of Ireland samples and the northern Spanish shelf and northern Portugal samples. A degree of mixing or admixture is evident in a small number of individuals (3-4) in the North Sea sample that have a high probability of originating from the western group. Similarly, the southern Portugal sample had a number of outliers which appear to originate from the western group (n=3) or from the African group (n=2).

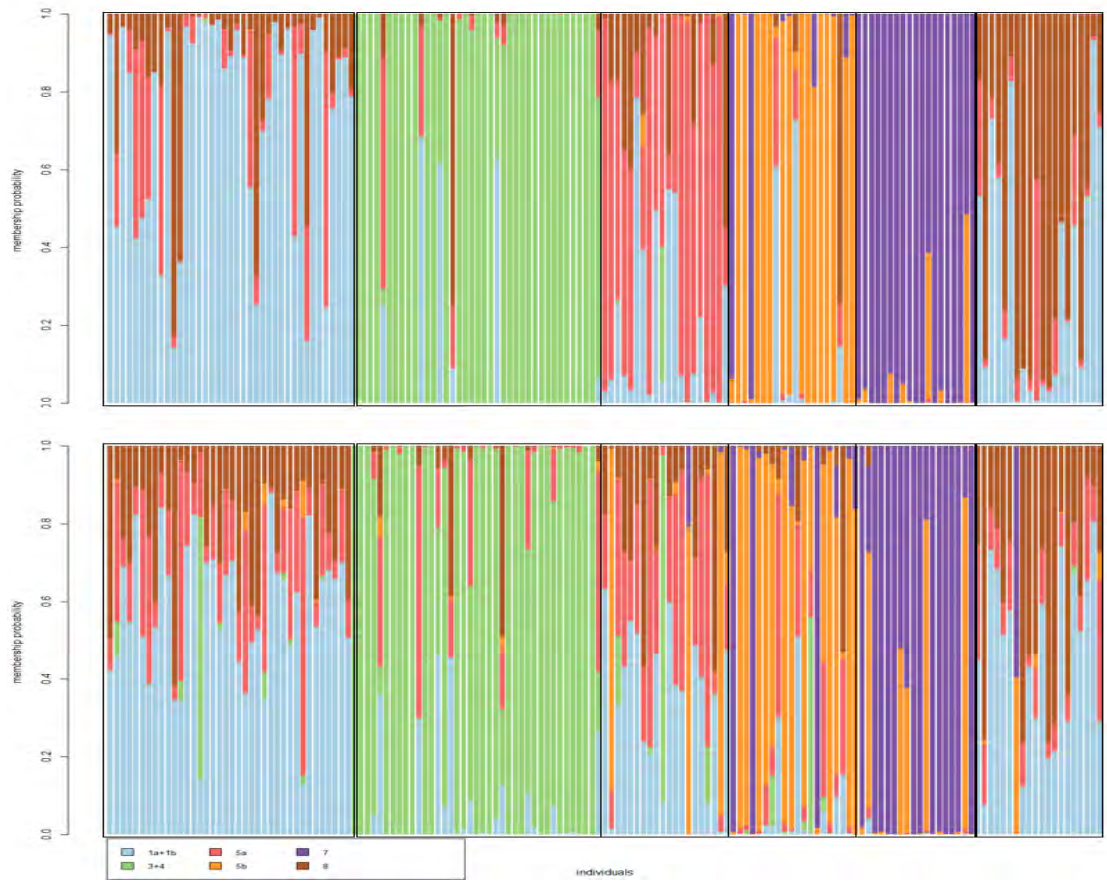

Figure 11. Membership probability plots the 63_SNP dataset (top panel) and the 17_SNP dataset (bottom panel). Samples 1a and 1b are combined into one sample and samples 3 and 4 are combined into one sample. Samples are delineated by the black boxes.

An exploratory assignment was conducted for illustration purposes using a combined 1a, 1b, 8 sample to represent what is currently considered to be the Western Stock and a combined 3, 4 sample to represent the North Sea. Only the 17_SNP dataset was used in order to avoid the violation of the assumption of independent markers, which is a prerequisite of the Rannala and Mountain approach. *Geneplot* indicated a self-assignment rate of 93% and *geneclass2* a self-assignment rate of 95%, indicating significant power to discriminate between mixed samples from these areas.

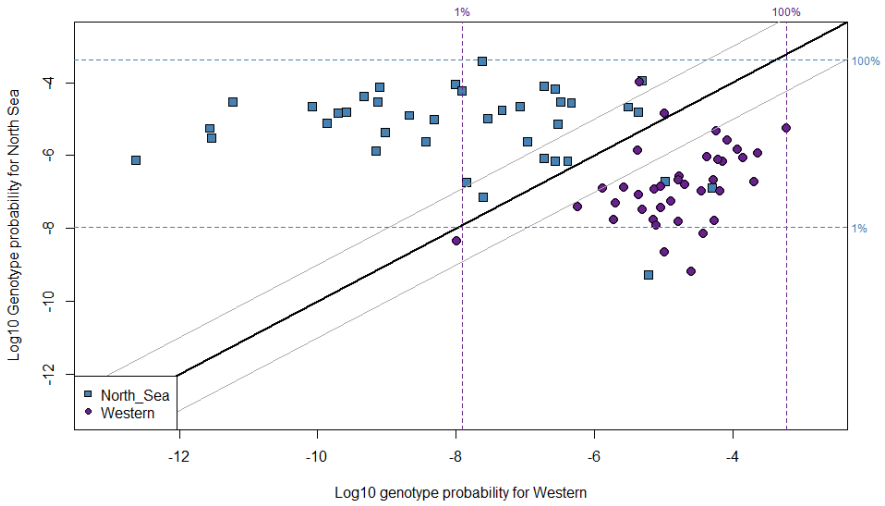

Figure 12. Plot generated with *genePlot* based on the 17_SNP dataset of the Western and North Sea stock samples. Each point represents an individual. The horizontal axis shows the posterior log-probability of obtaining each individual's genotype from the Western stock; the vertical axis shows the same, but with respect to the North Sea stock. The thick diagonal line shows equal probability with respect to Western and the North Sea. The vertical dashed lines shows the 0% and 100% percentile lines, that is, the minimum and maximum log-genotype probability, for the Western stock; the horizontal lines show the 0% and 100% percentile lines for the North Sea population.

4. Discussion

This study represents the largest and most comprehensive genetic assessment of the Atlantic horse mackerel to date. The combination of extensive geographic sampling and analysis of a large number of SNP markers derived from whole-genome sequencing, provided a powerful dataset that allowed us to discover, for the first time, genomic regions supporting population subdivision within the species. The genetic differences largely separate five groups: i) southern North Sea, ii) western Ireland - northern Spanish shelf - northern Portugal, iii) southern Portugal, iv) Alboran Sea/Mediterranean, and v) northern Africa. With the exception of the Southern stock, these genetic-based subdivisions are in agreement with the main horse mackerel stocks proposed by the HOMSIR project using morphometry, parasites, and life history traits (Abaunza et al., 2008). Our genetic data suggest that the samples from the southern stock in Portuguese waters do not come from a single biological population. The samples from northern Portugal appear to be genetically closer to the Western stock, while samples from southern Portugal form their own group. Further wide scale sampling is required to confirm these findings and assess the spatial and temporal trends in mixing between these areas. We additionally demonstrated that 63 of the most genetically differentiated SNP markers tag the genetic subdivisions and, thus, could be used as a genetic tool to inform the appropriate level of data collation for fisheries stock assessment. In fact, using a reduced panel of 17 markers, we demonstrated that it is possible to differentiate between individuals collected in the North Sea and Western stocks with a potential accuracy up to 95%.

Population structuring detected at loci putatively under selection

Genetic analysis of horse mackerel revealed that populations distributed across the broad geographic area spanning from the North Sea to northern Africa (Figure 5) differ by less than 1.5% of their DNA (Global mean pool-F_{ST} = 0.007, pairwise pool-F_{ST} values ranged between 0.001 and 0.015). This result indicates that gene flow occurs across the distribution range of the species. The observed genetic differences, despite representing a small fraction of the genome, are highly significant as they correspond to outlier SNPs putatively under selection and support population structuring within the species. A pattern of low genome-wide differentiation at neutral loci and high differentiation at adaptive loci is becoming a relatively common observation among various highly dispersive marine species inhabiting heterogeneous environments [e.g. Atlantic cod (Clucas et al., 2019); Atlantic herring (Lamichhaney et al., 2017)]. Many of these species, including the horse mackerel (Abaunza et al., 2008; Bozano et al., 2015; Cimmaruta et al., 2008; Farrell & Carlsson, 2018; Healey et al., 2020), were previously assumed to be panmictic, largely because prior genetic techniques did not provide enough genomic resolution. New genomic sequencing techniques enable the thorough examination of the genetic variation of non-model species and are revealing unprecedented levels of structuring, as we accomplished here for the horse mackerel. The large population sizes and high dispersal and gene flow presumed to be characteristic of numerous marine species may explain the low levels of genome-wide structuring observed, as the role of genetic drift in population structuring becomes negligible in these circumstances. The presence of well-defined parts of the genome showing high differentiation, so called “genomic islands of divergence or speciation” are generally associated with ecological adaptation or reproductive isolation (Seehausen et al., 2014; Turner et al., 2005). Theory predicts that when genetic variants are advantageous in a local environment, natural selection would favour their frequency in the local population (Yeaman & Whitlock, 2011). Thus, when different populations are locally adapted to heterogenous environments, it would be expected to see large differences in allele frequencies between them. This scenario goes in line with the fact that the horse mackerel exhibits a broad spatial distribution encompassing heterogeneous environments, for which, populations should be exposed to diverse selective pressures that can promote genetic differentiation, and thus, local adaptation.

Indeed, we hypothesize that the large chromosomal structural variant (9.9 Mb) underlying the cryptic north-south genetic break discovered here for the horse mackerel along mid Portugal, is associated with differential responses of populations to contrasting environmental conditions. Interestingly, a similar genetic pattern has also been observed in the boarfish (*Capros aper*) (Farrell et al., 2016), a pelagic fish with overlapping distribution and similar life-history characteristics in the northeast Atlantic. This suggests that a major biogeographic barrier may exist in Portugal waters, which could be leading to differentiation of biota inhabiting this area.

The structural variant exhibits high frequency of homozygotes for one allele among populations from the "north" (southern North Sea, west of Ireland, northern Spanish shelf, northern Portugal) and the Alboran Sea; heterozygotes are predominant in southern Portugal; and homozygotes for the alternative allele are in high frequency in the "south", at coastal areas near Mauritania, northern Africa. These contrasting allele frequency patterns are in concordance with differences in sea water conditions at the local spawning peak in each area. For example, oceanographic data collected in previous horse mackerel egg surveys (ICES, 2019) suggest that reproduction along the west of Ireland and the northern Spanish shelf may occur at temperatures around 12.5-14°C. Similarly, reproduction at the northern coast of Portugal may occur at sea water temperatures around 12.5° and also at lower salinities associated with freshwater discharge from rivers. In contrast, reproduction at the southern coast of Portugal may happen at warmer sea water temperatures around 17° and higher salinity with to respect to the northern coast of Portugal (ICES, 2019).

Out of the 12 samples included in this study, the sample from the Alboran Sea, at the western part of the Mediterranean Sea, was the most genetically distinct of all. This result may be explained by the ecological (Coll et al., 2010; Emig & Geistdoerfer, 2004) and geological (Garcia-Castellanos et al., 2009) differences existing between the Mediterranean Sea and the Atlantic Ocean. Moreover, the genetic data supports the consideration of the Mediterranean Sea as a separate stock, as proposed by the HOMSIR project based on morphometry, otoliths, and life history traits (Abaunza et al., 2008). The genetic distinctiveness of the Alboran Sea sample suggests that it likely constitutes a separate population, although its genetic closeness with the sample from southern Portugal indicates that gene flow may occur between these two areas. This observation is also in agreement with data collected in the HOMSIR project, indicating the mixed nature of the Alboran Sea populations (Abaunza et al., 2008).

Our genetic analysis provides evidence that the North Sea stock represents a distinct population. As many as 7 specific genomic regions distinguished the southern North Sea samples. The allele frequency patterns at these genomic regions were nearly identical between the 1-year temporal replicates, which also showed the smallest genome-wide differentiation of the 12 samples analysed (pool-F_{ST} 0.001). The North Sea samples were the northeastern most samples included in this study. Thus, we hypothesize that the observed genetic differentiation may be associated with local adaptation to colder sea water conditions experienced during spawning or at early life-history stages. We expect that further gene annotation of the novel horse mackerel genome, will help understand the putative role of these genomic regions in the differentiation of the North Sea stock. Regardless, a subset of the top outlier SNPs distinguishing the North Sea samples could be used for conservation and management purposes, as these genetic markers could help elucidate the extent of mixing between the Western and North Sea stocks along the English Channel and in ICES area 4a in the northern North Sea.

The samples from the Western stock, west of Ireland and the northern Spanish shelf, and the northern part of the Southern stock, northern Portugal, appear to form a genetically close group. This result

lends support to the inclusion of the Spanish shelf in the Western stock as proposed by the HOMSIR project, and also points to the need of an extended genetic study along the Spanish shelf and northern Portugal to determine whether the southern boundary of the Western stock should be extended.

Individual genotyping confirms Pool-Seq findings and constitute an informative SNP panel

The individual genotype data for the subset of samples corroborate the main results of the Pool-Seq analyses (Figure S4). The same pattern of sample clustering was observed with temporally stable samples in the North Sea that were distinct from all others. The two samples collected west of Ireland did not display any significant genetic differentiation between themselves or the northern Spanish Shelf sample. The northern Portuguese sample was also closely affiliated with these western samples and could not be robustly separated based on the reduced marker panels. The southern Portuguese samples formed a separate cluster, however there was evidence of mixing between this and the northern Portuguese group. As expected, the outlier group consisting of the African samples was significantly differentiated to all other samples but most closely related to the most geographically close sample in southern Portugal. Whilst these results should be treated with caution, as the sample sizes were small and temporal stability was not tested in all populations, they do prove the potential for using the reduced marker panels to investigate the population structure of horse mackerel on a larger scale.

Limitations and recommendations

While this study made important contributions to our understanding of the population structuring of the horse mackerel, we acknowledge there is room for improvement and emphasize the importance of follow-up studies. Firstly, the sampling, conducted over three consecutive years and three spawning seasons, while it covered a large area of the distribution of the species, is spatially and temporally limited. A more extensive spatial sampling within each stock area could, for instance, help identify the boundaries between the Western and Southern stocks, and between the Western and North Sea stocks. Repeated genetic monitoring (e.g. every one or two years) are necessary to assess the long-term stability of genetic sub-divisions. The Mediterranean Sea was a notable exclusion, as only a single sample from the Alboran Sea was studied. Whilst analysis of this sample indicates limited connectivity with the adjacent southern Portuguese samples, it does not enable any further conclusions the be drawn regarding population structure within the Mediterranean Sea. Secondly, whilst every effort was made to collect spawning fish from each putative stock this proved to be difficult in some areas and as such the best available alternative samples were included. Future sampling efforts should focus both on the collection of spawning baseline samples from each of the putative populations and also the collection of potentially mixed samples outside of the spawning season. Lastly, while the Pool-Seq approach is a powerful method to perform genome scans, it is sensitive to poor DNA sample quality, and variation in laboratory procedures such as pooling and library preparation. Thus, high quality DNA and standard laboratory procedures among samples are highly recommended to minimize technical biases.

5. Acknowledgements

The authors would like to thank Martin Pastoors, Maria Manuel Angélico, Finlay Burns, Gersom Costas, Cindy Van Damme, Cristina Nunes, Brendan O'Hea, Ciaran O'Donnell, Michael O'Malley and all scientists and crew on the survey and commercial vessels involved in sampling. We thank to the SNP&SEQ Technology Platform and to UPPMAX in Uppsala for the provided service in high-throughput sequencing and computational infrastructure under the SNIC projects 2020/5-36 and 2020/16-14. These facilities are part of the National Genomics Infrastructure (NGI) of Sweden and Science for Life

Laboratory. The SNP&SEQ Platform is also supported by the Swedish Research Council and the Knut and Alice Wallenberg Foundation.

6. References

Abaunza, P., Gordo, L., Karlou-Riga, C., Murta, A., Eltink, A.T.G.W., Santamaria, M.T.G., Zimmermann, C., Hammer, C., Lucio, P., Iversen, S.A., Molloy, J., and Gallo, E. 2003. Growth and Reproduction of Horse Mackerel, *Trachurus trachurus* (Carangidae). Fish Biology and Fisheries, 13:27–61.

Abaunza, P., Murta, A. G., Campbell, N., Cimmaruta, R., Comesaña, A. S., Dahle, G., García Santamaría, M. T., Gordo, L. S., Iversen, S. A., MacKenzie, K., Magoulas, A., Mattiucci, S., Molloy, J., Nascetti, G., Pinto, A. L., Quinta, R., Ramos, P., Sanjuan, A., Santos, A. T., … Zimmermann, C. (2008). Stock identity of horse mackerel (Trachurus trachurus) in the Northeast Atlantic and Mediterranean Sea: Integrating the results from different stock identification approaches. *Fisheries Research*, *89*(2), 196–209. https://doi.org/10.1016/j.fishres.2007.09.022

Andrews, S. (2010). *FastQC: a quality control tool for high throughput sequence data.* http://www.bioinformatics.babraham.ac.uk/projects/fastqc

Bolger, A. M., Lohse, M., & Usadel, B. (2014). Trimmomatic: a flexible trimmer for Illumina sequence data. *Bioinformatics*, *30*(15), 2114–2120. https://doi.org/10.1093/bioinformatics/btu170

Borges, M.F. and Gordo, L.S. 1991. Spatial distribution by season and some biological parameters of horse mackerel (*Trachurus trachurus*) in the Portuguese continental waters (Division IXa). ICES Document CM 1991/H: 54. 16 pp.

Bozano, Mariani, Barratt, Sacchi, Boufana, & Coscia. (2015). Spatio-temporal variability in the population structure in North-east Atlantic stocks of horse mackerel (Trachurus trachurus). *Biology and Environment: Proceedings of the Royal Irish Academy*, *115B*(3), 211. https://doi.org/10.3318/bioe.2015.20

Broad Institute. (2018). *Picard tools*. http://broadinstitute.github.io/picard/

Brunel, T., Farrell, E.D., Kotterman, M., Kwadijk, C., Verkempynck, R., Chen, C and Miller, D. 2016. Improving the knowledge basis for advice on North Sea horse mackerel. Developing new methods to get insight on stock boundaries and abundance. Wageningen, IMARES Wageningen UR (University & Research centre), Wageningen Marine Research report C092/16 57 pp.

Cimmaruta, R., Bondanelli, P., Ruggi, A., & Nascetti, G. (2008). Genetic structure and temporal stability in the horse mackerel (Trachurus trachurus). *Fisheries Research*, *89*(2), 114–121. https://doi.org/10.1016/j.fishres.2007.09.030

Clucas, G. V., Lou, R. N., Therkildsen, N. O., & Kovach, A. I. (2019). Novel signals of adaptive genetic variation in northwestern Atlantic cod revealed by whole-genome sequencing. *Evolutionary Applications*, *12*(10), 1971–1987. https://doi.org/10.1111/eva.12861

Coll, M., Piroddi, C., Steenbeek, J., Kaschner, K., Ben Rais Lasram, F., Aguzzi, J., Ballesteros, E., Bianchi, C. N., Corbera, J., Dailianis, T., Danovaro, R., Estrada, M., Froglia, C., Galil, B. S., Gasol, J. M., Gertwagen, R., Gil, J., Guilhaumon, F., Kesner-Reyes, K., … Voultsiadou, E. (2010). The Biodiversity of the Mediterranean Sea: Estimates, Patterns, and Threats. *PLoS ONE*, *5*(8), e11842. https://doi.org/10.1371/journal.pone.0011842

Dieringer, D. & Schlötterer, C. 2003 Microsatellite Analyser (MSA): a platform independent analysis tool for large microsatellite data sets. Molecular Ecology Resources, 3: 167–169.

Dohm, J. C., Lottaz, C., Borodina, T., & Himmelbauer, H. (2008). Substantial biases in ultra-short read data sets from high-throughput DNA sequencing. *Nucleic Acids Research*, *36*(16), e105–e105. https://doi.org/10.1093/nar/gkn425

Dransfeld, L., Dwane, O., Molloy, J., Gallagher, S., and Reid, D. G. 2005. Estimation of mackerel (*Scomber scombrus* L., 1758) and horse mackerel (*Trachurus trachurus* L., 1758) daily egg production outside the standard ICES survey area. ICES Journal of Marine Science, 62: 1705–1710.

Emig, C. C., & Geistdoerfer, P. (2004). The Mediterranean deep-sea fauna: historical evolution, bathymetric variations and geographical changes. *Carnets de Géologie (Notebooks on Geology)*, *Articles*. https://doi.org/10.4267/2042/3230

Ewels, P., Magnusson, M., Lundin, S., & Käller, M. (2016). MultiQC: summarize analysis results for multiple tools and samples in a single report. *Bioinformatics*, *32*(19), 3047–3048.

https://doi.org/10.1093/bioinformatics/btw354

Farrell, E. D., & Carlsson, J. (2018). *Genetic stock Identification of Northeast Atlantic Horse mackerel, Trachurus trachurus*. A report prepared for the members of the Northern Pelagic Working Group. 40pp.

Farrell, E. D., Carlsson, J. E. L., & Carlsson, J. (2016). Next Gen Pop Gen: implementing a high-throughput approach to population genetics in boarfish (Capros aper). *Royal Society Open Science*, *3*(12), 160651. https://doi.org/10.1098/rsos.160651

Feder, A. F., Petrov, D. A., & Bergland, A. O. (2012). LDx: Estimation of Linkage Disequilibrium from High-Throughput Pooled Resequencing Data. *PLoS ONE*, *7*(11), e48588. https://doi.org/10.1371/journal.pone.0048588

Garcia-Castellanos, D., Estrada, F., Jiménez-Munt, I., Gorini, C., Fernàndez, M., Vergés, J., & De Vicente, R. (2009). Catastrophic flood of the Mediterranean after the Messinian salinity crisis. *Nature*, *462*(7274), 778–781. https://doi.org/10.1038/nature08555

Gordo, L.S., Costa, A., Abaunza, P., Lucio, P., Eltink, A.T.G.W. and Figueiredo, I. 2008. Determinate versus indeterminate fecundity in horse mackerel. Fisheries Research, 89: 181–185.

Healey, A. J. E., Farthing, M. W., Nunoo, F. K. E., Potts, W. M., Sauer, W. H. H., Skujina, I., King, N., Becquevort, S., Shaw, P. W., & McKeown, N. J. (2020). Genetic analysis provides insights into species distribution and population structure in East Atlantic horse mackerel (Trachurus trachurus and T. capensis). *Journal of Fish Biology*, *96*(3), 795–805. https://doi.org/10.1111/jfb.14276

Heessen, H.J.L., Daan, N. and Ellis JR. 2015. Fish atlas of the Celtic Sea, North Sea, and Baltic Sea. Heessen HJL, Daan N, Ellis JR, editors. Wageningen Academic Publishers; 2015. 572 p.

Hivert, V., Leblois, R., Petit, E. J., Gautier, M., & Vitalis, R. (2018). Measuring Genetic Differentiation from Pool-Seq Data. *Genetics*, *210*(1), genetics.300900.2018. https://doi.org/10.1534/genetics.118.300900

ICES. 1991. Report of the Horse Mackerel (Scad) Otolith Reading Workshop. Lisbon, 21–27 November 1990. ICES C.M. 1991/H:59, 59 pp.

ICES. 1995. Report of the Working Group on the assessment of mackerel, horse mackerel, sardine and anchovy. 21 June-1 July 1994, ICES Headquarters, Copenhagen. ICES CM 1995/Assess:2: Part 1: 165pp.

ICES. 1998. Report of the Working Group on the assessment of mackerel, horse mackerel, sardine and anchovy. 9-18 September 1997, ICES Headquarters, Copenhagen. ICES CM 1998/Assess:6: Part 1: 176pp.

ICES. 2015. Report of the Workshop on Maturity Staging of Mackerel and Horse Mackerel (WKMSMAC2), 28 September–2 October 2015, Lisbon, Portugal. ICES CM 2015/SSGIEOM:17. 93 pp.

ICES. 2017. Final Report of the Working Group on Mackerel and Horse Mackerel Egg Surveys. WGMEGS Report 2017 24-28 April 2017. Vigo, Spain. ICES CM 2017/SSGIEOM:18. 134 pp.

ICES. (2019). Working Group on Mackerel and Horse Mackerel Egg Surveys (WGMEGS). In *ICES Scientific Reports: Vol. 1:66*. https://doi.org/http://doi.org/10.17895/ices.pub.5605

Jombart, T. 2008. adegenet: a R package for the multivariate analysis of genetic markers. Bioinformatics, 24: 1403-1405.

Kasapidis, P. and Magoulas, A. 2008. Development and application of microsatellite markers to address the population structure of the horse mackerel *Trachurus trachurus*. Fisheries Research, 89: 132–135.

Kolaczkowski, B., Kern, A. D., Holloway, A. K., & Begun, D. J. (2011). Genomic Differentiation Between Temperate and Tropical Australian Populations of Drosophila melanogaster. *Genetics*, *187*(1), 245–260. https://doi.org/10.1534/genetics.110.123059

Lamichhaney, S., Fuentes-Pardo, A. P., Rafati, N., Ryman, N., McCracken, G. R., Bourne, C., Singh, R., Ruzzante, D. E., & Andersson, L. (2017). Parallel adaptive evolution of geographically distant herring populations on both sides of the North Atlantic Ocean. *Proceedings of the National*

Academy of Sciences, *114*(17), E3452–E3461. https://doi.org/10.1073/pnas.1617728114

Li, H. (2013). Aligning sequence reads, clone sequences and assembly contigs with BWA-MEM. *ArXiv Preprint ArXiv*, *00*(00), 3. https://doi.org/arXiv:1303.3997 [q-bio.GN]

Li, H., Handsaker, B., Wysoker, A., Fennell, T., Ruan, J., Homer, N., Marth, G., Abecasis, G., & Durbin, R. (2009). The Sequence Alignment/Map format and SAMtools. *Bioinformatics*, *25*(16), 2078–2079. https://doi.org/10.1093/bioinformatics/btp352

Macer, C.T. 1974. The reproductive biology of the horse mackerel *Trachurus trachurus* (L.) in the North Sea and English Channel. Journal of Fish Biology, 6: 415-438.

Mariani, S. 2012. Genetic identification of horse mackerel (*Trachurus trachurus*) in the North-East Atlantic. Results of the service provided to the Pelagic Freezer-Trawler Association, between 2010 and 2012. Work carried out by the Mariani labs at UCD Dublin and Salford University. 12pp.

McMillan, L.F. and Fewster, R.M. 2017. Visualizations for Genetic Assignment Analyses using the Saddlepoint Approximation Method. Biometrics 73, 1029–1041.

Ndjaula, H.O.N., Hansen, T., Kruger-Johnsen, M. and Kjesbu, O. S. 2009. Oocyte development in captive Atlantic horse mackerel *Trachurus trachurus*. ICES Journal of Marine Science, 66: 623–630.

Okonechnikov, K., Conesa, A., & García-Alcalde, F. (2015). Qualimap 2: advanced multi-sample quality control for high-throughput sequencing data. *Bioinformatics*, *32*(2), btv566. https://doi.org/10.1093/bioinformatics/btv566

Piry, S., Alapetite, A., Cornuet, J-M., Paetkau, D., Baudouin, L., Estoup, A. 2004. geneclass2: a software for genetic assignment and first-generation migrant detection. Journal of Heredity, 95: 536–539.

R Core Development Team. (2020). *R: A language and environment for statistical computing. Vienna, Austria: R Foundation for Statistical Computing*.

Rannala, B. and Mountain, J. L. 1997. Detecting immigration by using multilocus genotypes. Proc. Natl. Acad. Sci. USA 94: 9197-9221.

Rice, W.R. 1989. Analyzing tables of statistical tests. Evolution, 43: 223–225.

Robinson, J. T., Thorvaldsdóttir, H., Winckler, W., Guttman, M., Lander, E. S., Getz, G., & Mesirov, J. P. (2011). Integrative genomics viewer. *Nature Biotechnology*, *29*(1), 24–26. https://doi.org/10.1038/nbt.1754

Rousset, F. 2008 Genepop'007: a complete reimplementation of the Genepop software for Windows and Linux. Molecular Ecology Resources, 8: 103-106.

Seehausen, O., Butlin, R. K., Keller, I., Wagner, C. E., Boughman, J. W., Hohenlohe, P. A., Peichel, C. L., Saetre, G.-P., Bank, C., Brännström, Å., Brelsford, A., Clarkson, C. S., Eroukhmanoff, F., Feder, J. L., Fischer, M. C., Foote, A. D., Franchini, P., Jiggins, C. D., Jones, F. C., … Widmer, A. (2014). Genomics and the origin of species. *Nature Reviews Genetics*, *15*(3), 176–192. https://doi.org/10.1038/nrg3644

Thorvaldsdóttir, H., Robinson, J. T., & Mesirov, J. P. (2013). Integrative Genomics Viewer (IGV): High-performance genomics data visualization and exploration. *Briefings in Bioinformatics*, *14*(2), 178–192. https://doi.org/10.1093/bib/bbs017

Turner, T. L., Hahn, M. W., & Nuzhdin, S. V. (2005). Genomic Islands of Speciation in Anopheles gambiae. *PLoS Biology*, *3*(9), e285. https://doi.org/10.1371/journal.pbio.0030285

Van Damme, C.J.G., Thorsen, A., Fonn, M., Alvarez, P., Garabana, D., O'Hea, B., Perez, J.R. et al. 2014. Fecundity regulation in horse mackerel. ICES Journal of Marine Science, 71: 546–558.

Vartia, S., Collins, P.C., Cross, T.F., FitzGerald, R.D., Gauthier, D.T., McGinnity, P., Mirimin, L. & Carlsson J. 2014. Multiplexing with three-primer PCR for rapid and economical microsatellite validation. Hereditas, 151: 43–54.

Vartia, S., Villanueva, J.L., ., Finarelli, J., Farrell, E.D., Hughes, G., Carlsson, J.E.L., Collins, P.C., Gauthier, D.T., McGinnity, P., Cross, T.F., FitzGerald, R.D., Mirimin, L., Cotter, P. & Carlsson, J. 2016. A

novel method of microsatellite genotyping-by-sequencing using individual combinatorial barcoding. Royal Society Open Science, 3 DOI: 10.1098/rsos.150565.

Waldron, M.E. and Kerstan, M. 2001. Age validation in horse mackerel (*Trachurus trachurus*) otoliths. ICES Journal of Marine Science, 58: 806-813.

Weir, B. S., & Cockerham, C. C. (1984). Estimating F-Statistics for the Analysis of Population Structure. *Evolution*, *38*(6), 1358. https://doi.org/10.2307/2408641

Wickham, H. (2016). *ggplot2: Elegant Graphics for Data Analysis*. Springer-Verlag New York. https://ggplot2.tidyverse.org

Yeaman, S., & Whitlock, M. C. (2011). The genetic architecture of adaptation under migration-selection balance. *Evolution*, *65*(7), 1897–1911. https://doi.org/10.1111/j.1558-5646.2011.01269.x

7. Annex

Table S1. The international maturity scale for horse mackerel, *Trachurus trachurus.*

Stage	Name	Female	Male
1	Immature	Ovaries small. Ovaries wine red and clear, torpedo shaped.	Testes small, when fresh pale flattened and transparent. When frozen it may be opaque.
2	Developing	Ovaries occupying 1/4 to almost filling body cavity. Opaque eggs visible in ovaries giving pale pink to yellow to orange coloration. Largest oocytes may have oil globules.	Gonads occupying 1/4 to to almost filing body cavity. Testes off-white to creamy white., milt not running. When frozen testes can be bleuish.
3	Spawning	Ovaries characterized by externally visible hyaline oocytes no matter how few or how early the stage of hydration. Ovary size variable from full to < 1/4 of body cavity. Ovaries can be bloodshot.	Testes from filling to < 1/4 of body cavity, milt freely running. Testes can be shrivelled (wrinkled and contracted) at anus. When frozen there might be a change of structure and the testes needs a little pushing before running.
4	Regressing Regenerating	Ovaries occupying 1/4 or less of body cavity. Ovaries reddish and often murky (dark and gloomy) in appearance, sometimes with a scattering or patch of opaque eggs. The empty ovaries will ripple when pushed together.	Ovaries occupying 1/4 or less of body cavity. Testes opaque with brownish tint and no trace of milt. When frozen testes can be bleuish ore purple.
5	Omitted spawning	No evidence of omitted spawning	No evidence of omitted spawning
6	Abnormal	No evidence of abnormal ovaries	No evidence of abnormal testes

Table S2. Read mapping summary statistics of the Pool-Seq data of 12 horse mackerel samples included in this study. Abbreviations: W: Western, SW: Southwestern, S: South, N: North, MQ: Mapping quality, cov.: coverage.

Area	Sample	Total reads	% reads aligned	%GC	Median insert size	Mean MQ	Median cov.	Mean cov.
W Ireland	1a-WIR-2016	496686692	99.0	42.4	405	39.05	83	30.7
SW Ireland	1b-WIR-2016	594538427	99.1	42.2	416	38.97	99	35.2
SW Ireland	2-WIR-2017	573044377	99.0	42.4	465	38.95	96	35.5
S North Sea	3-SNS-2016	724017069	99.1	42.3	416	39	122	45.1
S North Sea	4-SNS-2017	764658923	99.1	42.3	419	38.97	128	46.3
N Portugal	5a-NPT-2016	571274302	99.2	42.4	404	38.9	95	35.2
S Portugal	5b-SPT-2016	494209199	99.1	42.9	426	39.13	83	29.0
N Portugal	6a-NPT-2017	490808045	98.1	41.8	*248*	39.32	75	26.1
S Portugal	6b-SPT-2017	514732597	99.2	42.3	*245*	39.12	79	27.5
Africa Mauritania	7-NAF-2016	714009211	98.5	*46.6*	425	38.49	91	25.7
N Spanish Shelf	8-NSP-2016	720020789	98.9	43.3	438	38.96	122	41.0
Mediterranean - Alboran Sea	9-MED-2018	671149600	98.8	42.5	422	35.13	112	41.5

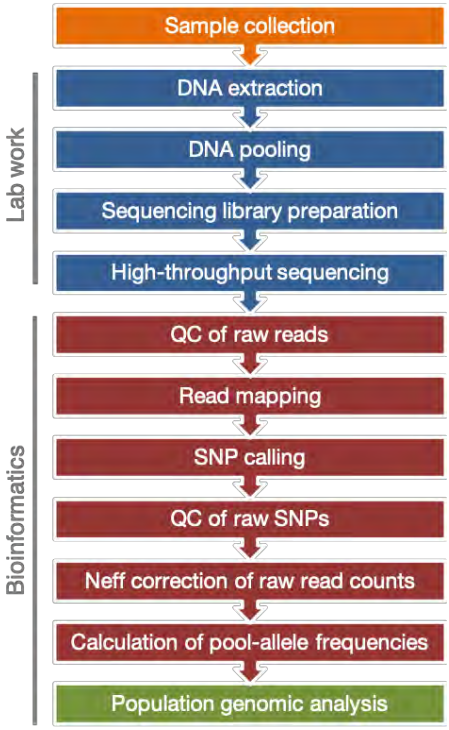

Figure S1. Schematic summary of steps followed for data generation.

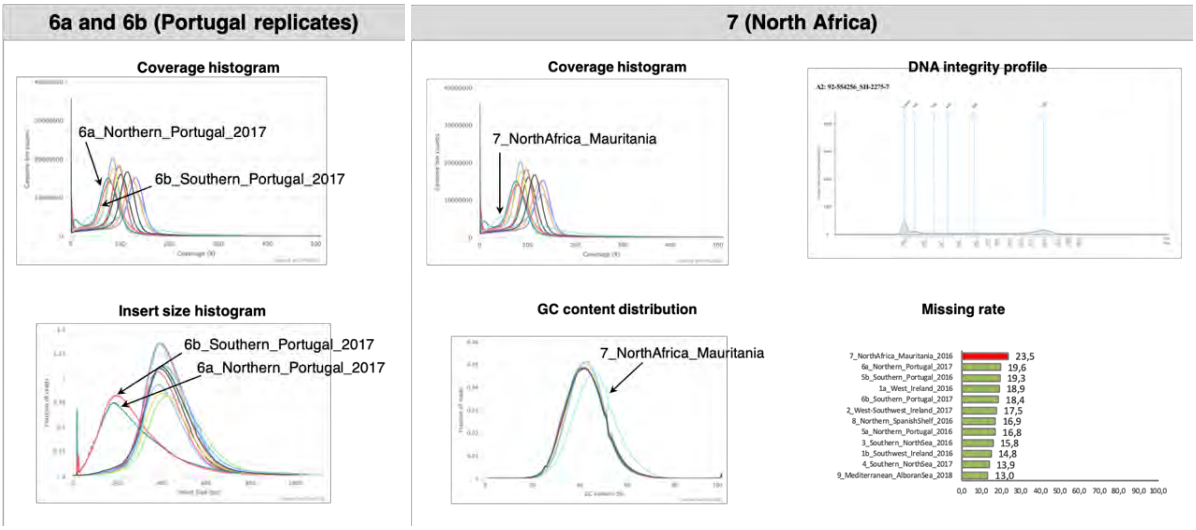

Figure S2. Read mapping statistics supporting that samples 6a, 6b, 7 were likely affected by technical artefacts. Plots obtained with *MultiQC*. (Left) Coverage and insert size distribution plots for the 12 samples, denoting the lines corresponding to samples 6a and 6b. (Right) Left, coverage and GC content distribution for all 12 samples, sample 7 is highlighted. Right, DNA integrity profile for the African sample and comparison of missing rate percentage for all 12 samples, the African sample is denoted in red.

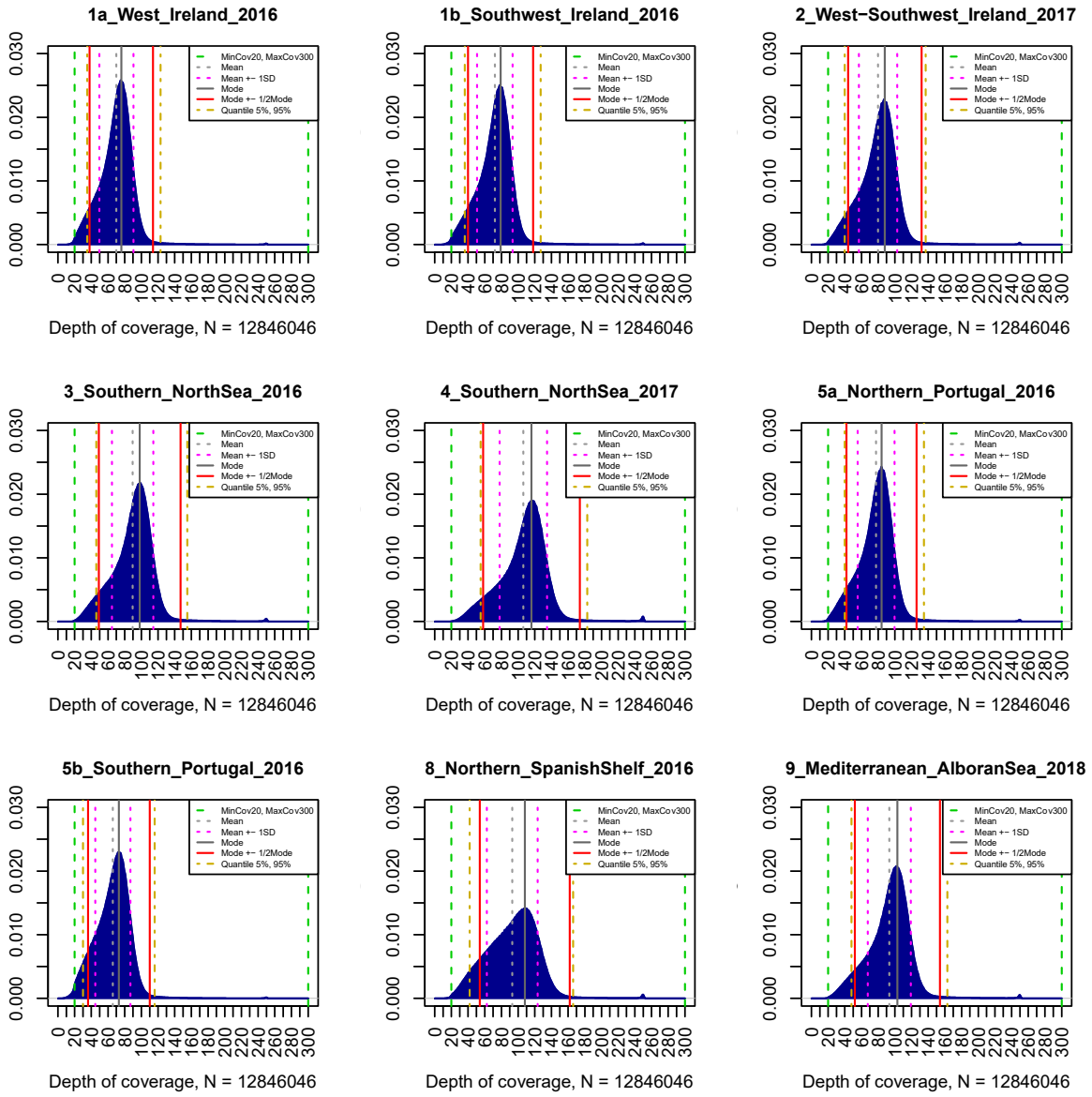

Figure S3. Depth of coverage distribution of 9 horse mackerel pools based on the SNPs that passed quality filters (~12 million). The different vertical lines correspond to the various lower and upper depth of coverage cut-off values examined.

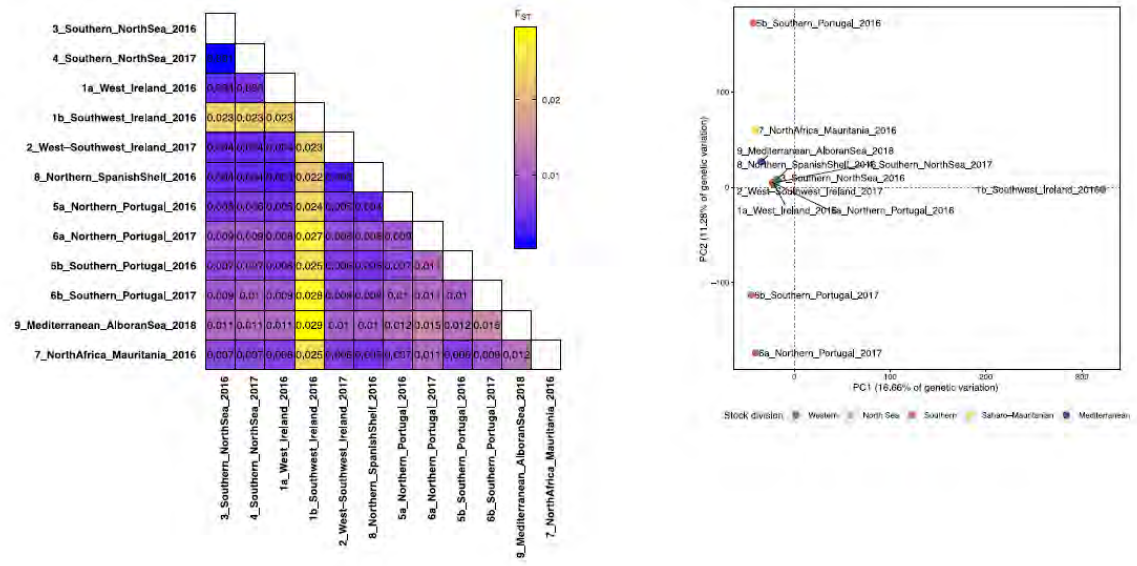

Figure S4. Exploratory population structure analysis for the 12 pools of the horse mackerel showing that samples 1b, 6a, and 6b correspond to outlier samples. (Left) Pairwise F_{ST}. (Right) PCA.

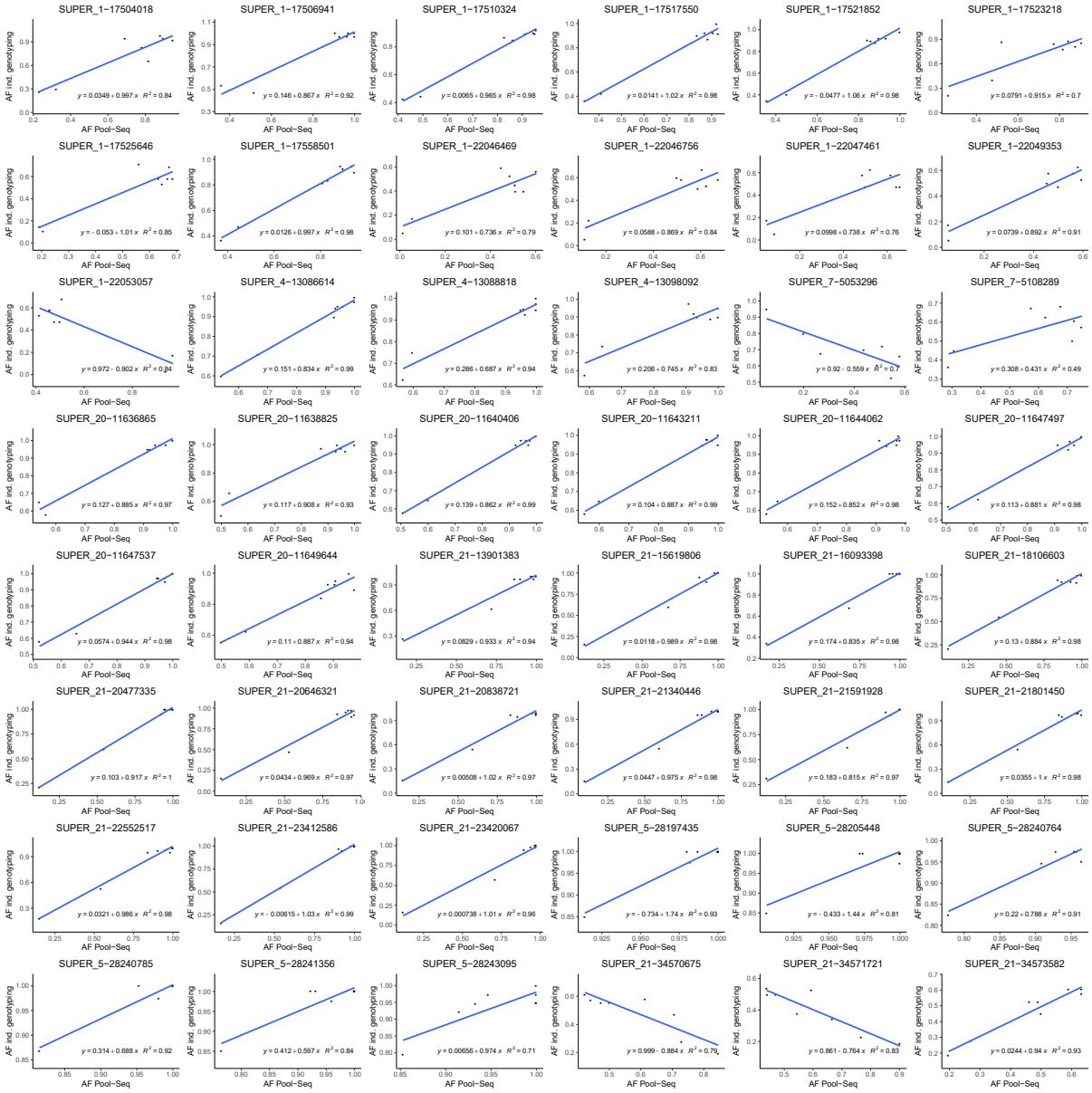

Figure S5. Comparison of population allele frequencies obtained with Pool-Seq and individual genotyping for the 48 SNPs putatively under selection.

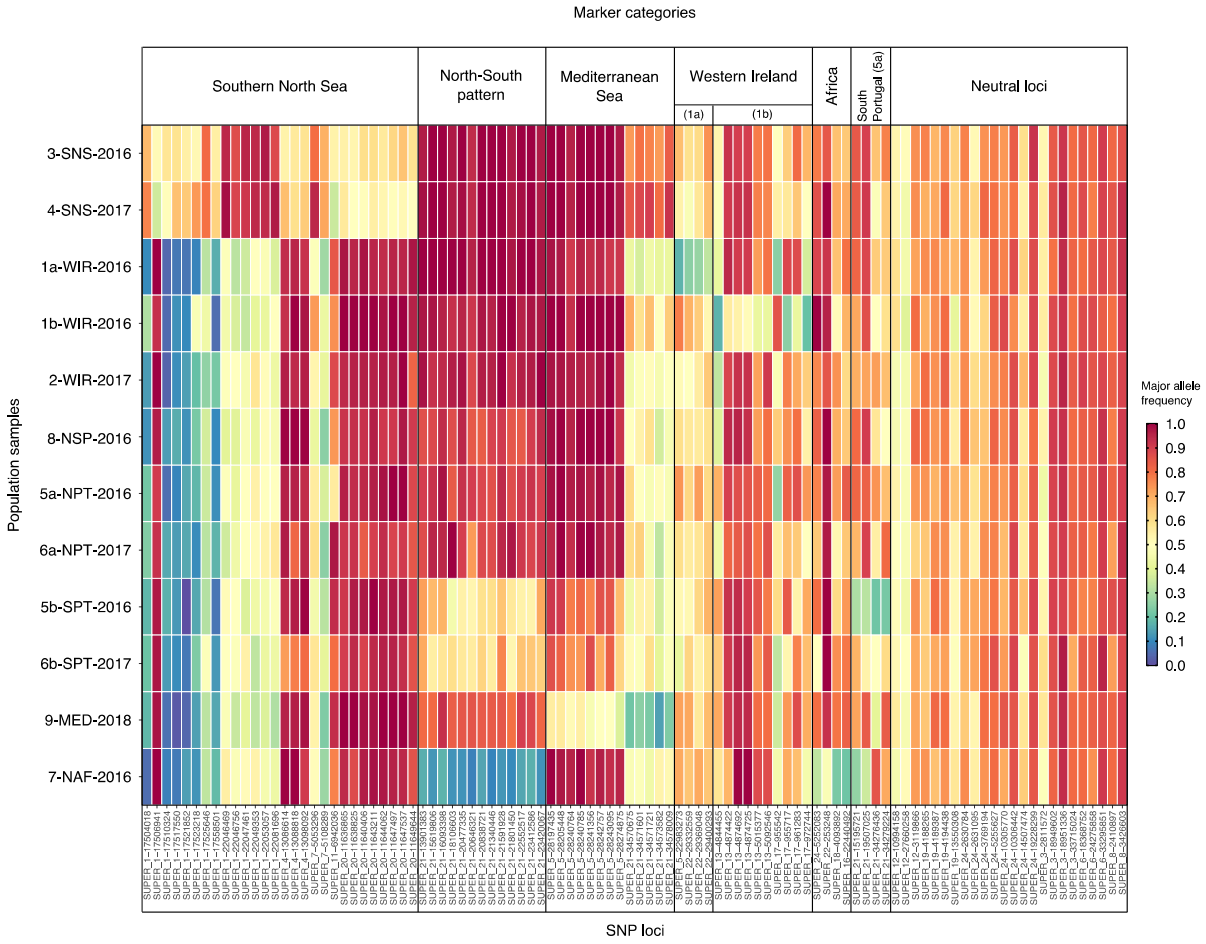

Figure S6. Heatmap plot representing the population allele frequencies of the 100 genetic markers included in the SNP panel. Rows correspond to samples and columns to SNP loci.

Figure S7. Heatmap plot representing the genotype of 157 individuals screened in 63 of the most informative SNPs for the horse mackerel. Squares in blue highlight the genotypes distinguishing the southern North Sea and the north-south genetic break.